The Role of NADPH Oxidase-2 in Chronic Intermittent Hypoxia-induced Respiratory System Dysfunction

Sarah E. Drummond, BSc (Hons)

Department of Physiology

Thesis submitted to National University of Ireland, University College Cork, for the award of Doctor of Philosophy

Under the supervision of:

Prof. Ken D. O'Halloran (Head of Department)
& Dr. Vincent Healy

December 2020

Declaration

This is to certify that the work I am submitting is my own and has not been submitted for another degree, either at University College Cork or elsewhere. The contribution of others through collaboration has been acknowledged. All external references and sources are clearly acknowledged and identified within the contents. I have read and understood the regulations of University College Cork concerning plagiarism.

Sarah Drummond
December 2020

List of Figures

List of Tables

List of Abbreviations

1/2 RT	Half-relaxation time
4-HNE	4-hydroxynoneal
5-HIAA	5-hydroxyindole acetic acid
5-HT	Serotonin
AA	Arachidonic acid
AEBSF	4-(2-aminoethyl)benzenesulfonyl fluoride hydrochloride
AHI	Apnoea-hypopnoea index
Akt	Protein kinase B
ALS	Amyotrophic lateral sclerosis
Ang-II	Angiotensin-II
APO	Apocynin
ATP	Adenosine triphosphate
Atrogin-1	Muscle atrophy Fbox
BB_n	Breath-breath interval
BB_{n+1}	Subsequent breath-breath interval
BCA	Bicinchoninic acid
BNIP3	Bcl-2 nineteen-kilodalton interacting protein 3
BSO	Buthionine sulfoxamine
Ca^{2+}	Calcium
CAT	Catalase
cDNA	Complementary DNA
CHF	Chronic heart failure
CICR	Calcium induced calcium release
CIH	Chronic intermittent hypoxia
CNS	Central nervous system
CO_2	Carbon dioxide
COPD	Chronic obstructive pulmonary disease
COX	Cyclooxygenase
CPAP	Continuous positive airway pressure

CPG	Central pattern generator
Cq	Quantification cycle
CSA	Cross-sectional area
CT	Contraction time
DHPR	Dihydropyridine receptor
DMD	Duchenne muscular dystrophy
DNA	Deoxyribonucleic acid
DPI	Diphenyleneiodonium
DTNB	5,5'-dithiobis-(2-nitrobenzoic acid
DTT	Dithiothreitol
DUOX	Dual oxidase
EC	Excitation-contraction
ECF	Extracellular fluid
ECL	Enhanced chemiluminescence
ECM	Extracellular matrix
EDL	Extensor digitorum longus
EDTA	Ethylenediamine tetra acetic acid
EMG	Electromyography
ERK 1/2	Extracellular regulated kinases 1/2
ETC	Electron transport chain
$FADH_2$	Flavin adenine dinucleotide
Fmax	Peak tetanic force
FOXO	Forkhead box O
f_R	Breathing frequency
GABARAPL1	Gamma-aminobutyric acid receptor-associated protein-like 1
GI	Gastrointestinal
GPDH	Glycerol-3-phosphate
GPX	Glutathione peroxidase
GR	Glutathione reductase
GSH	Glutathione
GSK3β	Glycogen synthase kinase 3 beta

GSSG	Glutathione disulfide
H_2O	Water
H_2O_2	Hydrogen peroxide
Hct	Haematocrit
HCVR	Hypercapnic ventilatory response
HIF	Hypoxia inducible factor
HPLC	High performance liquid chromatography
Hprt1	Hypoxanthine-guanine phosphoribosyltransferase-1
HRE	Hypoxia response element
HRP	Horse radish peroxidase
HVR	Hypoxic ventilatory response
IGF1	Insulin-like growth factor-1
IH	Intermittent hypoxia
JNK	c-Jun NH_2-terminal kinase
KO	Knock-out
LC3B	Microtubule-associated proteins 1A/1B light chain 3B
L_o	Optimum length
LOX	Lipoxygenase
LTF	Long term facilitation
LV	Left ventricle
MAD	Mandibular advancement device
MAPK	Mitogen activated protein kinase
MDA	Malondialdehyde
MEF2C	MADS box transcription enhancer factor 2 C
MHC	Myosin heavy chain
MRFs	Myogenic regulatory factors
mRNA	Messenger RNA
MSD	Mesoscale discovery
mTOR	Mammalian target of rapamycin
MurF1	Muscle RING finger protein 1
MyoD	Myoblast determination protein 1

NAC	N-acetylcysteine
NADH	Nicotinamide adenine dinucleotide
NADPH	Nicotinamide adenine dinucleotide phosphate
NAFLD	Non-alcoholic fatty liver disease
NaOH	Sodium hydroxide
NEB	Neuroepithelial body
NOX	NADPH oxidase
Noxa1	NOX activator 1
Noxo1	NOX organiser 1
NRF2	Nuclear factor erythroid 2-related factor 2
NTS	Nucleus tractus solitarius
O_2	Oxygen
O_2^-	Superoxide
OAA	Oxaloacetate
OH^-	Hydroxyl
OSAS	Obstructive sleep apnoea syndrome
p70S6K	p70S6 kinase
$PaCO_2$	Partial pressure of carbon dioxide
PARK2	Parkin
Pcrit	Critical closing pressure of the pharynx
PD	Parkinson's disease
Pdi	Transdiaphragmatic pressure
PEF	Peak expiratory flow
PI3K	Phosphoinositide 3-kinase
PIF	Peak inspiratory flow
PINK1	PTEN-induced kinase
PKA	Protein kinase A
PKC	Protein kinase C
PLA2	Phospholipase A2
Pmax	Maximum mechanical power
PMSF	Phenylmethylsulfonyl fluoride

PO_2	Partial pressure of oxygen
Poldip2	Polymerase delta-interacting protein
preBötC	Pre-Bötzinger complex
PRG	Parafacial respiratory group
P_t	Isometric twitch force
PTEN	Phosphatase and tensin homolog
PTP	Protein tyrosine phosphatase
PVN	Paraventricular nucleus of the hypothalamus
qRT-PCR	Quantitative reverse transcription polymerase chain reaction
RDI	Respiratory disturbance index
RER	Respiratory exchange ratio
RIPA	Radioimmunoprecipitation assay
RMANOVA	Repeated measures two-way ANOVA
RNA	Ribonucleic acid
ROS	Reactive oxygen species
RPM	Revolutions per minute of rotor
RTK	Receptor tyrosine kinase
RV	Right ventricle
RVLM	Rostral ventrolateral medulla
RyR	Ryanodine receptor
SCI	Spinal cord injury
SD	Standard deviation
SD1	Short-term variability of breathing
SD2	Long-term variability of breathing
SDB	Sleep disordered breathing
SDH	Succinate dehydrogenase
SDS	Sodium dodecyl sulfate
SERCA	Sarco/endoplasmic reticulum Ca^{2+}-ATPase
SIDS	Sudden infant death syndrome
SIRT1	Silent mating type information regulation 2 homologue 1
Smax	Maximum shortening

SOD	Superoxide dismutase
SOL	Soleus
SR	Sarcoplasmic reticulum
TA	Tibialis anterior
TBARS	Thiobarbituric acid reactive substances
TBST	Tris-buffered saline tween
TCA	Tricarboxylic acid
T_e	Expiratory duration
TEMED	Tetramethylethylenediamine
TGFβ	Transforming growth factor β
T_i	Inspiratory duration
TRK5	Tyrosine kinase substrate 5
T_{tot}	Total breath duration
UA	Upper airway
UCP-3	Mitochondrial uncoupling protein-3
VAIH	Ventilatory adaptation to intermittent hypoxia
$\dot{V}CO_2$	Carbon dioxide production
$\dot{V}_I$	Minute ventilation
$\dot{V}_I/\dot{V}CO_2$	Ventilatory equivalent for carbon dioxide
$\dot{V}_I/\dot{V}O_2$	Ventilatory equivalent for oxygen
Vmax	Maximum shortening velocity
$\dot{V}O_2$	Oxygen consumption
VSMC	Vascular smooth muscle cell
V_T	Tidal volume
WBP	Whole-body plethysmography
Wmax	Maximum mechanical work
XO	Xanthine oxidase
ΔΔCT	Double-delta threshold cycle method

Conference Proceedings

Royal Academy of Medicine in Ireland Biomedical Sciences Meeting 2021 (Virtual, IRL). Drummond SE, Burns DP, Healy V & O'Halloran KD (2021) "The role of NADPH oxidase 2 in chronic intermittent hypoxia-induced respiratory system dysfunction in adult male mice: insights from pharmacological and transgenic approaches" (Oral).

Experimental Biology (San Diego, USA). American Physiological Society. Drummond SE, Burns DP, Ziegler O, El Maghrani S, Healy V & O'Halloran KD (2020) "NADPH oxidase 2 knockout prevents chronic intermittent hypoxia-induced diaphragm muscle weakness but not increased propensity for apnoea in a mouse model of obstructive sleep apnoea syndrome" (Poster).

New Horizons in Medical Research UCC (Cork, IRL). Drummond SE, Burns DP, Ziegler O, El Maghrani S, Healy V & O'Halloran KD (2019) "Role of NADPH oxidase in chronic intermittent hypoxia-induced diaphragm muscle dysfunction: Insights from pharmacological and transgenic approaches" (Oral).

Experimental Biology (Orlando, USA). American Physiological Society. Burns DP, Drummond SE, Bolger D, Murphy KH, Coiscaud A, Edge D & O'Halloran KD (2019) "N-Acetyl cysteine improves dystrophic (*mdx*) mouse diaphragm muscle quality and strength" (Poster).

Experimental Biology (Orlando, USA). American Physiological Society. Drummond SE, Burns DP, Ziegler O, El Maghrani S, Healy V & O'Halloran KD (2019) "Role of NADPH oxidase in chronic intermittent hypoxia-induced respiratory dysfunction: Insights from pharmacological and transgenic approaches" (Poster).

New Horizons in Medical Research UCC (Cork, IRL). Burns DP, Drummond SE, Bolger D, Murphy KH, Coiscaud A, Edge D & O'Halloran KD (2018) "N-Acetyl cysteine improves dystrophic (*mdx*) mouse diaphragm muscle quality and strength" (Poster).

Europhysiology 2018 (London, UK). The Physiological Society. Burns DP, Drummond SE, Sheeran L, Coiscaud A, O'Hehir C, Edge D & O'Halloran KD (2018) "Chronic intermittent hypoxia enhances respiratory muscle weakness in dystrophin-deficient *mdx* mice" (Poster).

Europhysiology 2018 (London, UK). The Physiological Society. Drummond SE, Burns DP, Healy V & O'Halloran KD (2018) "NADPH oxidase 2 is necessary for

chronic intermittent hypoxia-induced respiratory muscle weakness in adult male mice" (Poster).

Europhysiology 2018 (London, UK). The Physiological Society. Drummond SE, Burns DP, Healy V & O'Halloran KD (2018) "Apocynin reduced apnoea index in a mouse model of chronic intermittent hypoxia in a non-NADPH oxidase 2 dependent manner" (Poster).

Experimental Biology 2018 (San Diego, USA). American Physiological Society. Drummond SE, Burns DP, Healy V & O'Halloran KD (2018) "NADPH oxidase 2 knockout prevents chronic intermittent hypoxia induced sternohyoid muscle weakness in adult male mice" (Poster).

New Horizons in Medical Research UCC (Cork, IRL). Drummond SE, Burns DP, Healy V & O'Halloran KD (2018) "Chronic intermittent hypoxia induced respiratory muscle dysfunction in adult male mice: a role for NADPH oxidase" (Poster).

Physiology 2016 (Dublin, IRL). Drummond SE, Burns DP, Healy V & O'Halloran KD (2016) "Effects of chronic intermittent hypoxia on breathing, metabolism and diaphragm muscle contractile properties in adult male mice" (Poster).

Royal Academy of Medicine in Ireland Biomedical Sciences Meeting 2016 (Cork, IRL). Drummond SE, Burns DP, Healy V & O'Halloran KD (2016) "Effects of chronic intermittent hypoxia on breathing, metabolism, and diaphragm contractile properties in adult male mice" (Poster).

Oral Communications

Royal Academy of Medicine in Ireland (RAMI) Biomedical Sciences Meeting (2021).

New Horizons in Medical Research Conference, UCC, Cork, Ireland (2019).

Early Careers Symposium at Europhysiology, a meeting of The Physiological Society, the Scandinavian Physiological Society, the Deutsche Physiologische Gesellschaft and the Federation of European Physiological Societies, London, UK (2018).

Control of Breathing Symposium, UCC, Cork, Ireland (2018) – Visiting Professor Gordon Mitchell, University of Florida, USA.

Hypoxia Research Symposium, UCC, Cork, Ireland (2016) – Visiting Professor Trevor Day, Mount Royal University, Calgary, Canada.

Department of Physiology Annual Research Day, UCC, Cork, Ireland (2015-2020 inclusive).

Publications

Published:

Burns DP, Drummond SE, Bolger D, Murphy KH, Coiscaud A, Edge D & O'Halloran KD "N-acetylcysteine decreases fibrosis and increases force-generating capacity of *mdx* diaphragm" *Antioxidants* 2019, 8(12), 581.

O'Neill J, Jasionek G, Drummond SE, Brett O, Lucking EF, Abdulla MA, O'Halloran KD "Renal oxygen homeostasis is perturbed following exposure to long-term but not short-term intermittent hypoxia in the rat" *American Journal of Physiology-Renal Physiology 2019,* 316(4), F635-F645.

Burns DP, Canavan L, Rowland J, O'Flaherty R, Brannock M, Drummond SE, O'Malley D, Edge D & O'Halloran KD "Recovery of respiratory function in *mdx* mice co-treated with neutralizing interleukin-6 receptor antibodies and Urocortin-2". *The Journal of Physiology* 2018, 596(21), 5175-5197.

O'Leary AJ, Drummond SE, Edge D, O'Halloran KD "Diaphragm muscle weakness following acute sustained hypoxic stress in the mouse is prevented by pre-treatment with N-acetyl cysteine". *Oxidative Medicine and Cellular Longevity* 2018, 4805493.

In review:

Drummond SE, Burns DP, O'Connor KM, Clarke G, O'Halloran KD "The role of NADPH oxidase in chronic intermittent hypoxia-induced respiratory plasticity in adult male mice". *Respiratory Physiology and Neurobiology (RPNB).*

O'Connor KM, Bastiaanssen TFS, Lucking EF, Cabrera Rubio R, Crispie F, Drummond SE, Cotter P, Clarke G, Golubeva AV, Cryan JF, O'Halloran KD "Strategies for effective gut microbiota recolonisation after chronic broad-spectrum antibiotic administration in adult male rats". *The ISME Journal: Multidisciplinary Journal of Microbial Ecology.*

In preparation:

Drummond SE, Burns DP, Healy V & O'Halloran KD "NADPH oxidase-2 knockout prevents chronic intermittent hypoxia-induced sternohyoid muscle weakness in adult male mice".

Drummond SE, Burns DP, Healy V & O'Halloran KD "NADPH oxidase-2 knockout prevents chronic intermittent hypoxia-induced diaphragm muscle weakness in adult male mice".

Burns DP, Drummond SE, Sheeran L, Coisaud A, O'Hehir C, Edge D & O'Halloran KD "Effects of chronic intermittent hypoxia on respiratory control in the *mdx* mouse model of Duchenne muscular dystrophy".

Slyne AD, Drummond SE, Cussen D, O'Halloran KD & Burns DP "Respiratory muscle dysfunction in the *mdx* mouse model of muscular dystrophy: Role of NADPH oxidase (NOX)?".

Burns DP, Drummond SE, Woelfel S, Mackrill JJ, O'Halloran KD "Selenium deficiency impairs upper airway muscle performance in the rat".

Acknowledgements

First and foremost, I want to express my sincere gratitude to my PhD supervisors. Prof. Ken O'Halloran, I am truly grateful for the wealth of opportunities you have provided me during my time in the Department of Physiology. From my BSc to an MSc and then with one last minute turn of events... a PhD! Thank you for your guidance and tutelage which has hugely shaped my PhD experience and professional development. Thank you for always supporting and encouraging me to present my research at scientific meetings, at home and abroad. I feel very fortunate to have carried out this research under your supervision and I look forward to working with you into the future. Dr. Vincent Healy, thank you for giving me my first insight into research in the Department of Physiology as a 4th year student. Since then, thank you for the kindness and support you have shown me throughout my PhD endeavours.

Dr. David Burns, thank you for being a good colleague and a great friend. I truly appreciate your friendship, support, enthusiasm and contribution to this project. I look forward to continuing our collaborations into the future… I'm sure that whiteboard is already jam-packed and ready to go!

I would like to express my sincere thanks to the academic, technical and administrative staff in the Department of Physiology, University College Cork, for your assistance in, and contribution to, my PhD training. Thank you to the members of my PRP panel, Dr. John Mackrill and Dr. Therese Ruane-O'Hora, for your support and encouragement over the last few years. Thank you to the staff at the Biological Services Unit, University College Cork. Finally, thank you to my thesis examiners, Dr. Brian McDonagh, Prof. Mai ElMallah and Dr. John Mackrill.

To my fellow postgraduate students in the Department of Physiology, to those who are still here and those who have flown the WGB nest! From the coffees in Cork to the cocktails in Vegas. From having 'one' in Tom's to dancing in Chambers! Thank you for your friendship and camaraderie over these past few years. It's been a journey!

To my friends outside of science, thank you for being the best mates anyone could wish for. I feel extremely lucky to have a crew like you. For all the staycays, vacays and spa days! I cannot wait for what the notions of 2021 and beyond will bring... everyone will be asking!

To my siblings, Niall, Finbar and Ciara. Ye're simply the best! Thank you for your love, friendship and encouragement throughout my PhD and throughout all the years growing up together. Thank you for paving the way, making it a little easier for me to come along behind! Most importantly, Niall, I still finished first!

To my parents, Joe and Sheila. Nothing we do would be possible without you. I think I speak for all 4 of us when I say that words cannot describe how much your endless support, encouragement and love has led us to be where we are in life today. I am eternally grateful for everything you have done for me over the past 28 years. As a wise woman once said, we weren't spoiled… we were just well taken care of!

Mam and Dad, I dedicate this thesis to you.

Abstract

Obstructive sleep apnoea syndrome (OSAS) is characterised by exposure to chronic intermittent hypoxia (CIH) as a consequence of repetitive occlusions of the upper airway in patients during sleep. Exposure to CIH evokes redox changes which culminate in impaired upper airway and diaphragm muscle function. Excessive reactive oxygen species (ROS) are also associated with aberrant respiratory plasticity, which manifests as destabilised breathing during sleep. There is a paucity of information regarding the molecular mechanisms underlying these effects. We sought to investigate the putative role of the superoxide-generating NADPH oxidase-2 (NOX2) enzyme in CIH-induced respiratory muscle dysfunction and respiratory mal-adaptation.

A mouse model of CIH was generated by the cycling of gas from normoxia (21% O_2) for 210 seconds to hypoxia (5% O_2 at the nadir) over 90 seconds for 8hr/day for 2 weeks. Adult male (C57BL/6J) mice were assigned to one of 5 groups: normoxic controls, CIH-exposed, CIH + apocynin (NOX2 inhibitor, 2mM) given in the drinking water throughout the exposure to CIH, and NOX2 null (B6.129S-*Cybb*^{tm1Din}/J) assigned to a sham or CIH exposure. On day 15, whole body plethysmography (WBP) was used to measure breathing parameters on a breath-by-breath basis in room air and in response to chemostimulation. An apnoea was defined as ≥ 2 missed breaths. Sternohyoid and diaphragm muscle contractile function was examined *ex vivo.* Gene expression was examined by quantitative reverse transcription polymerase chain reaction (qRT-PCR). Western blot was used to measure protein expression. NOX enzyme activity and indices of oxidative stress were determined using spectrophotometric assays.

Basal minute ventilation ($\dot{V}_I$) was unchanged following 2 weeks of exposure to CIH, however the number of apnoeas per hour was significantly increased compared with sham-exposed mice. Apocynin intervention significantly reduced the frequency of apnoeas compared with the CIH-exposed group. Apnoea index was increased in NOX2 null mice exposed to CIH, reminiscent of that observed in wild-type mice.

Exposure to CIH resulted in severe sternohyoid and diaphragm muscle weakness, evidenced by a ~45% reduction in the force-generating capacity of these respiratory muscles compared with sham. Exposure to CIH increased NOX enzyme activity in the sternohyoid, with no alteration to the gene or protein expression of NOX subunits. In contrast, exposure to CIH increased the protein and mRNA expression of NOX4 in the diaphragm, while NOX activity and expression of all other NOX subunits remained unchanged. No indication of overt oxidative stress was observed in the diaphragm or sternohyoid muscle following exposure to CIH. Apocynin treatment and NOX2 gene knock-out completely prevented CIH-induced diaphragm and sternohyoid muscle weakness. Exposure to CIH increased the mRNA expression of genes relating to autophagy, atrophy and muscle differentiation in the diaphragm in a NOX2-dependent manner; these CIH-induced responses were not observed in the sternohyoid.

Mice show signs of profound respiratory muscle dysfunction following exposure to a mild-to-moderate paradigm of CIH. The putative NOX inhibitor, apocynin, prevents CIH-induced respiratory muscle weakness. Moreover, studies in NOX2 null mice reveal that NOX2 is obligatory for CIH-induced respiratory muscle weakness. The mechanisms underpinning CIH-induced muscle weakness likely differ between sternohyoid and diaphragm muscle, evidenced by varied molecular responses to CIH, which may relate to differences in fibre-type expression. CIH-induced respiratory muscle weakness may contribute to upper airway obstruction and impaired swallow and cough, relevant to OSAS. The reduction in apnoea frequency following treatment with apocynin, but not NOX2 knock-out, implicates ROS (that are not NOX2-derived) in the manifestation of CIH-induced respiratory disturbances. CIH-induced increase in the propensity for apnoea may be of clinical relevance as it may underpin progression in the severity of OSAS pathology (i.e. mild-to-moderate-to-severe OSAS). Our results have implications for human OSAS and point to antioxidant intervention, potentially targeting NOX2 blockade, as a potential therapeutic strategy.

Chapter 1. Introduction.

1.1 The respiratory control system

1.1.1 The control of breathing

Breathing represents a complex neuro-mechanical process that relies on the coordinated activity of the muscles of respiration and control centres in the brain. Adequate ventilation is pivotal in the maintenance of blood gas homeostasis to support the metabolic demands of the body. The respiratory system is an integrated system involving a multiplicity of components including the central nervous system (CNS), motor nerves, skeletal musculature and the lungs and conducting airways. An important characteristic of the respiratory control system lies in its ability to adjust breathing patterns in response to physiological perturbations in situations of both health and disease.

Control of the respiratory system is maintained by a central respiratory oscillatory network located within the medulla of the brainstem, from which neural output travels through cranial and spinal motoneurons to the muscles of respiration. Changes are effected through two groups of muscles, inspiratory and expiratory, whose coordinated activity serves to meet physiological demands. Breathing is a state-dependent process with the automatic control of breathing originating from distinct sites of the brainstem, the central pattern generators (CPGs), which comprise rhythm-generating sites including the Pre-Bötzinger complex (Pre-BötzC) and the parafacial respiratory group (PRG) (Feldman and Del Negro, 2006, Smith et al., 2009).

The respiratory control system responds to various perturbations by altering its output in order to maintain respiratory homeostasis. Sensory cues from receptors located throughout the upper airway (irritant, temperature and pressure-sensitive receptors), the respiratory muscles (muscle spindles) and the lungs (e.g. pulmonary stretch receptors) are relayed to the respiratory centres of the brain. In addition to this, the respiratory control system alters its output based on sensory cues from chemoreceptors, which relay information regarding the gas composition and pH of the blood. These chemoreceptors are located in the peripheral and central nervous systems. The aortic and carotid bodies are the principal peripheral chemoreceptors

(Prabhakar and Peng, 2004). The carotid body is the primary oxygen (O_2) sensor, comprised of a collection of O_2-sensitive glomus cells, located at the bifurcations of the common carotid arteries. The carotid body is pivotal for eliciting the ventilatory and cardiovascular responses to periods of hypoxaemia. Central chemoreceptors respond to alterations in the hydrogen ion content in the surrounding environment of the brain, such as changes in brain extracellular fluid (ECF) carbon dioxide (CO_2) and pH. The central chemoreceptors are located in diffuse sites throughout the brainstem including: the ventrolateral medulla (Okada et al., 2002), within the raphé serotonergic system (Corcoran et al., 2009), the retrotrapezoid nucleus (Guyenet et al., 2009) and the locus coeruleus (Gargaglioni et al., 2010). Collectively, the respiratory control system maintains respiratory homeostasis, that is, the maintenance of appropriate levels of arterial O_2, CO_2 and pH.

1.1.2 Respiratory plasticity

Respiratory plasticity has been described as a persistent change in the neural control system, which manifests as structural and/or functional alterations, based on prior experience (Mitchell and Johnson, 2003). The respiratory control system has the ability to induce adaptive plastic changes to accommodate short-term perturbations, such as walking, exercising, vocalization, or may relate to environmental stressors, such as ascent to and descent from high altitude. The control system also exhibits the capacity to adapt over longer periods, for example during pregnancy, as well as throughout growth, development and ageing (Mitchell and Johnson, 2003). These alterations in respiratory output are considered beneficial, adaptive changes to maintain respiratory homeostasis in the face of increased demand.

Sleep poses a significant challenge for the respiratory control system. Although sleep is a natural and essential process, this state results in a reduction in eupnoeic ventilation (Douglas et al., 1982a) and diminished hypoxic and hypercapnic responsiveness (Douglas et al., 1982a, Douglas et al., 1982b). During wakefulness, an increase in upper airway (UA) resistance leads to mechanical loading of the airway and a concomitant increase in pharyngeal dilator muscle activity, serving to prevent the occurrence of apnoea (respiratory pause) and hypopnoea (inadequate

ventilation) (Fogel et al., 2001). However, a loss of the 'wakefulness stimulus' during sleep leaves ventilation under metabolic control. This, coupled with a reduction in respiratory muscular tone during sleep, renders the respiratory control system sensitive to a reduction in the partial pressure of CO_2 ($PaCO_2$), thus predisposing those with low CO_2 reserve or high upper airway collapsibility to apnoeic events (Skatrud and Dempsey, 1983, Dempsey et al., 2010).

The phenotypical response of the respiratory system to a perturbation is largely based on the pattern, duration and intensity of the stimulus (Baker and Mitchell, 2000, Peng and Prabhakar, 2004) as well as the timing of the perturbation throughout the life cycle (Reeves and Gozal, 2006). Hypoxia-induced respiratory plasticity, which has a wide scope for clinical relevance, is one of the best-studied forms of plasticity. Hypoxia refers to the condition wherein tissues are inadequately oxygenated to meet the demand necessary to carry out physiological functions. A reduced level of O_2 appears in many situations, including exposure to high altitude (West, 1987), physical exercise (Richardson et al., 1995) and multiple disease states (Semenza, 2014). While hypoxia initiates rapid and robust increases in respiratory motor output to defend against hypoxaemia, it also triggers persistent changes in chemosensory neurons and integrative pathways that transmit brainstem respiratory activity to respiratory motor neurons (MacFarlane et al., 2008). The ventilatory response to sustained hypoxia is a well characterised mechanism known as ventilatory acclimatization to hypoxia (VAH) (Powell et al., 1998). The classic example of VAH is the prototypical response upon ascent to high altitude, exhibited as a progressive increase in ventilation, sustained beyond the initial hypoxic exposure. However, when hypoxia is experienced intermittently, unique forms of respiratory plasticity occur. Intermittent hypoxia (IH) is a feature of many respiratory disorders, notably obstructive sleep apnoea syndrome (OSAS), as a result of repetitive upper airway collapse. Of interest, both adaptive and mal-adaptive forms of respiratory plasticity have been reported following IH exposure (Bradford et al., 2005, Mahamed and Mitchell, 2008).

IH-induced plasticity occurs at multiple levels of the respiratory control system and has been shown to manifest impaired motor control of the upper airway (O'Halloran et al., 2002, Veasey et al., 2004, Ray et al., 2007), discordant respiratory rhythm and pattern generation culminating in increased apnoea index (Edge et al., 2012, Donovan et al., 2014, Zanella et al., 2014, Souza et al., 2015, Elliot-Portal et al., 2018), facilitation of breathing or altered chemoreflex control of breathing (Reeves and Gozal, 2006, Skelly et al., 2012b, Morgan et al., 2016b, Elliot-Portal et al., 2018) and respiratory muscle weakness (McGuire et al., 2002a, McGuire et al., 2002b, Liu et al., 2005, Pae et al., 2005, Dunleavy et al., 2008, Liu et al., 2009, Jia and Liu, 2010, Skelly et al., 2012b, Wang et al., 2013b, Zhou and Liu, 2013, McDonald et al., 2015). Thus, the mechanisms underlying IH-induced plasticity are of great interest in the context of diseases characterised by IH, such as OSAS.

1.2 Respiratory musculature

Respiratory muscles are striated skeletal muscles made up of many bundles of cells from the fusion of developmental myoblasts to produce long, cylindrical, multi-nucleated structures called fibres (Frontera and Ochala, 2015). The functional unit of skeletal muscle, the motor unit, constitutes a single motor neuron and the bundle of muscle fibres it innervates, all of which have similar structural and functional properties (Hoppeler, 2014). Upon firing, a motor neuron stimulates all fibres within that motor unit to contract simultaneously, thus creating the appropriate muscle response. The size of motor units varies depending on their role, with motor units in the eye containing a small number of target fibres producing precise movements, whereas motor units containing a large number of fibres, for example in the leg, yield more powerful movements (Sherwood, 2001).

1.2.1 Respiratory muscle structure

Respiratory muscle structure encompasses a high degree of sophistication as it comprises a variety of fibre types, enabling different functional properties. The myosin heavy chain (MHC) is the motor protein of muscle thick filaments after which a classification system subdividing skeletal muscle fibres into 4 major groups is

named. Fibres are classed as type 1, type 2a, type 2x or type 2b determined by the isoform of MHC they express (Schiaffino et al., 1989). Type 1 muscle fibres are red in colour due to a high myoglobin composition. They are slow contractile fibres, specialised for continuous low-level contractions and resemble a fatigue-resistant phenotype. These fibres are endowed with a high mitochondrial content and a resultant large oxidative capacity. Type 2a fibres are fast oxidative fibres that also appear red due to large myoglobin content. They too are rich in mitochondrial density and yield fast, medium-powered contractions with good resistance to fatigue, albeit less than that of type1 fibres. Type 2a fibres hold the capacity for both oxidative and glycolytic metabolism. Type 2x fibres are fast contractile fibres, with high power production and intermediate resistance to fatigue. They possess low myoglobin content, medium mitochondrial density and oxidative capacity, and high glycolytic capacity. Type 2b fibres are white in colour due to low myoglobin concentration and mitochondria density. These fibres are very fast contracting with the greatest power production of the 4 subtypes; however, they have a low resistance to fatigue. They constitute the most glycolytic fibre, with a low oxidative capacity. The functional capacity of a respiratory muscle is determined by its MHC composition, which essentially regulates the metabolic make up and thus, force generation and fatigability of that muscle (Torgan and Daniels, 2001). Alterations to MHC composition can have diverse consequences for muscle physiology, as evidenced in a range of different rodent models of disease (Mathur et al., 2014, Talbot and Maves, 2016, Chaillou, 2018).

1.2.2 Respiratory muscle function

Skeletal muscle plays a vital role in multiple bodily functions widely categorised into mechanical and metabolic roles. It is primarily important for converting chemical energy into mechanical energy, thus generating force and power, maintaining posture and producing movement. Additionally, it contributes to basal energy metabolism, the maintenance of core temperature and the utilisation of large amounts of O_2 and fuel during physical activity and exercise (Frontera and Ochala, 2015). Muscle fibres are hugely adaptable and malleable in response to an array of stimuli including exercise, injury/disease and environmental stimuli such as hypoxia

(Hoppeler and Vogt, 2001). Adaptations can manifest as alterations in the metabolic capacity, contractile apparatus and cell signalling-mediated regulation of the muscle (Fluck and Hoppeler, 2003). While adaptation is a necessary and appropriate response in the face of perturbations, skeletal muscle can also succumb to mal-adaptive tendencies following persistent stimulation (Cutlip et al., 2006).

The mechanism of excitation–contraction (EC) coupling was first defined by Alexander Sandow as the series of events occurring from the generation of an action potential in skeletal muscle fibres to the production of force (Sandow, 1952). The propagation of an action potential along the sarcolemma of a muscle fibre results in a rapid depolarisation. This depolarisation extends into invaginations of the sarcolemma called t-tubules inducing a conformational change in the L-type calcium (Ca^{2+}) channel, dihydropyridine receptors (DHPRs). By direct protein-protein interactions, DHPRs open ryanodine receptors (RyRs) enabling the efflux of Ca^{2+} into the myoplasm. RyRs reside in close proximity to the sarcoplasmic reticulum (SR), a pivotal intracellular Ca^{2+} store. The SR stores Ca^{2+} at high concentrations and so the opening of RyRs produces a favourable concentration gradient, promoting the outflow of Ca^{2+} from the SR into the myoplasm. This increase in intracellular Ca^{2+} encourages the binding of actin and myosin to yield a contractile twitch. Ca^{2+} released from the SR binds to troponin C, causing tropomyosin to move away from the active site of actin. Myosin attaches to actin's now vacant binding site forming a cross-bridge. The breakdown of adenosine triphosphate (ATP) releases energy which enables the myosin to pull the actin filaments inwards and shorten the muscle, generating a power stroke. ATP binding to myosin eventually breaks the cross-bridge by detaching it from actin. This process of muscular contraction can continue to repeat, as long as there are adequate stores of ATP and Ca^{2+}. Once a stimulus has ceased, the muscle relaxes as Ca^{2+} is taken back into the SR, a process facilitated by sarco/endoplasmic reticulum Ca^{2+}-ATPase pumps (SERCAs) (Lamboley et al., 2014).

1.2.3 Respiratory pump muscle

The diaphragm muscle is a thin, dome-shaped, striated skeletal muscle with fibres extending radially from its central tendon to insertion points on the ribcage. The diaphragm displays remarkable adaptability and plasticity owing to its mixed fibre-type composition, which encompasses a mixture of all 4 MHC subtypes. This mixed fibre-type composition is essential in befitting the physiological role of the diaphragm muscle. Type 1 fibres support the diaphragm's primary function as an inspiratory pump muscle through the preservation of a high degree of endurance, essential for providing substantial muscle stamina. This function is fundamental in supporting adequate ventilation on a breath-by-breath basis throughout life. Additionally, the diaphragm exhibits a large force reserve capacity owing to type 2a and 2x/2b fibres. These fibres generate large amounts of force to facilitate non-respiratory functions such as airway clearance manoeuvres (Gransee et al., 2012). During restful breathing, the diaphragm contracts increasing volume in the thoracic cavity, generating subatmospheric pressure within the thorax, thus allowing the lungs to fill with air from the external environment. Expiration is predominantly a passive process, as the diaphragm relaxes back to its resting position allowing the thoracic cavity to recover to its pre-inspiratory volume. The lungs have a natural tendency to recoil inwardly, thus also facilitating a return to their resting volume. Accessory muscles, such as the external intercostals, parasternal intercostals, and scalenes are active during quiet breathing and as such are considered obligatory muscles of inspiration (De Troyer and Estenne, 1984). During active periods of breathing, such as during exercise and forced-breathing manoeuvres, accessory muscles of inspiration including the sternocleidmastoids, serratus and pectoralis are recruited to aid the diaphragm by raising the upper ribs and sternum (De Troyer et al., 1987, Fujiwara et al., 1999). This also holds true for the process of expiration during active breathing, as accessory expiratory muscles including the internal intercostals, rectus abdominis, external and internal obliques and transversus abdominis contract to forcibly expel air from the lungs. Impaired diaphragm function is well described in a plethora of disease states characterised by respiratory morbidity including OSAS, Duchenne muscular dystrophy (DMD), chronic heart failure (CHF), chronic obstructive pulmonary disease

(COPD) and amyotrophic lateral sclerosis (ALS) (Chien et al., 2010a, Ahn et al., 2017, Burns et al., 2018, Sharma and Singh, 2019, de Carvalho et al., 2019).

1.2.4 Upper airway musculature

The UA consists of a complex arrangement of soft tissue, cartilage, bone and skeletal muscle subserving a multiplicity of functions. It operates as more than simply a conduit for air, food and drink, with vital respiratory and non-respiratory functions, such as phonation, also described (Morris, 1988, Fregosi and Ludlow, 2014). The pattern of muscle control in the UA must have the ability to rapidly alternate between different system requirements for non-respiratory and respiratory functions to ensure the maintenance of UA calibre. This requires the co-ordinated activity of more than 20 UA muscles, which contract and dilate, stiffen, or constrict the airway under voluntary or involuntary control, circumstantially. The paired sternohyoid muscles provide an example of a muscle which exhibits low activity during basal ventilation, with an increased activation upon airway occlusion, highlighting their role in maintaining airway patency as well as re-establishing airway patency following collapse (Roberts et al., 1984). The sternohyoid is a thin, narrow muscle attaching the hyoid bone to the sternum and is structurally composed of mainly type 2b fibres enabling large force generation. The sternohyoid has been the focus of a wealth of research regarding upper airway stability in recent years (Skelly et al., 2013, O'Connell et al., 2013, Shortt and O'Halloran, 2014, Williams et al., 2015a) with its ease of accessibility and fibres which run in a uniform direction making it a good candidate for *ex vivo* experimental approaches. These airway muscles regulate airway patency and collectively decrease resistance to airflow during inspiration, facilitating in concert with the thoracic muscles, the matching of ventilation of alveoli to their perfusion (gas exchange), and they prevent aspiration of foreign objects or noxious material into the lungs. Respiratory muscles in the upper airway exhibit activation patterns that are coordinated with the diaphragm muscle in order to effectively couple low airway resistance to air inflow into the lungs during periods of reduced intrathoracic pressure (Gransee et al., 2012). When the dilating force produced by the upper airway muscles in insufficient to counterbalance

the collapsing force produced by the inspiratory pump muscles, UA collapse ensues leading to occlusive events and subsequent hypopnoea and apnoea, characteristic of OSAS (Brouillette and Thach, 1979b).

1.3 Cell signalling mediated regulation of skeletal muscle

Skeletal muscle relies on the complex interplay between a multitude of signalling pathways in order to function normally and maintain homeostasis in response to changes in demand of a muscle. Many of these pathways have reactive oxygen species (ROS)-sensitive components (e.g. protein tyrosine phosphatases; PTPs), making them viable targets controlling alterations in growth, metabolic activity, fibre-type and contractile abilities of muscles during periods of exercise or exposure to hypoxia.

1.3.1 Atrophy/Hypertrophy

The balance between protein synthesis and degradation, or hypertrophy and atrophy, is pivotal in determining muscle mass, thereby directly affecting its contractile performance. Atrophy of skeletal muscle is a major consequence of many disease states (Lecker et al., 2006). Studies examining gene expression in models of muscle atrophy has led to the identification of a category of genes that are routinely up- or downregulated in atrophying muscle, commonly termed atrogenes (Sandri et al., 2004, Sandri, 2008). The ubiquitin-proteasome system and autophagy-lysosomal system are the predominant mechanisms by which the cell breaks down proteins, both of which are transcriptionally controlled by the Forkhead box O (FOXO) family of transcription factors.

1.3.2 The ubiquitin-proteasome system

The ubiquitin-proteasome system is a protein degradation system whereby proteins are tagged for poly-ubiquitination and subsequent degradation. This regulatory system preferentially recognises and degrades oxidised proteins, thus preventing their potentially cytotoxic build up which has been implicated in various human disease states including neurodegenerative disorders and cancer (Aiken et al., 2011).

Muscle wasting has been associated with an increase in proteolysis through increased ubiquitin conjugation to muscle proteins with a concomitant increase in the key muscle specific ubiquitin ligases; muscle RING finger protein 1 (MurF1) and muscle atrophy Fbox (MAFbx/Atrogin-1) (Lecker et al., 2006). Additionally, inflammation has been shown to cause an up-regulation in the mRNA expression of MurF1 and/or MAFbx/Atrogin-1 in incidences of muscle wasting in a range of conditions including cancer, COPD, severe head trauma and ALS (Narici and Maffulli, 2010).

1.3.3 The autophagy-lysosomal system

The autophagy-lysosomal system represents a lysosomally-mediated proteolytic process, commonly activated by ROS in periods of oxidative stress. Whether this system functions to mediate atrophy or facilitate cell survival remains a highly complex subject and appears to be largely stimulus-dependent (Mammucari et al., 2007). Basal levels of autophagy are necessary for the homeostatic maintenance of muscle mass. Knock-out mice for the critical Atg7 gene to block autophagy, specifically in skeletal muscle, demonstrate muscle atrophy, weakness and several features of myopathy (Masiero et al., 2009). Conversely, autophagy genes (LC3B, GABARAPL1 and BNIP3) are among the upregulated atrogenes, which encode for proteins that are degraded when autophagosomes fuse with lysosomes (Zhao et al., 2007). Oxidative stress, induced by expression of mutant $SOD1^{G93A}$ specifically in skeletal muscle, results in loss of muscle mass and weakness mainly via autophagy activation (Dobrowolny et al., 2008). This muscle atrophy was prevented by the inhibition of microtubule-associated proteins 1A/1B light chain 3B (LC3B), highlighting the interplay between autophagy and atrophy pathways (Dobrowolny et al., 2008).

A specialised form of autophagy, described as mitophagy, functions to remove damaged mitochondria and maintain mitochondrial integrity and quality. Receptor-mediated mitophagy is one of the primary mechanisms of mitochondrial quality control essential for cell survival (Wu et al., 2014). Mitophagy receptors are commonly found on the outer and inner mitochondrial membrane and certain outer

mitochondrial membrane receptors of mitophagy have been identified, including BNIP3, Nip3-like protein X (NIX), and the FUN14 domain-containing protein 1 (FUNDC1) (Lazarou, 2015). These mitophagy receptors contain motifs that indicate their direct interaction with LC3B to enable the engulfment of defective mitochondria (Gkikas et al., 2018). The expression and activity of BNIP3 on the outer mitochondrial membrane was initially shown to be involved in cell death processes (Liu et al., 2014a). BNIP3-deficient mammalian cells exhibit PINK1 proteolysis activation which resulted in a subsequent inability to induce mitophagy (Zhang et al., 2016b). Additionally, upon exposure to hypoxia, BNIP3 expression is increased in a HIF-1 dependent manner, which subsequently inhibits the cleavage of PINK1 proteolysis, thus promoting mitophagy (Zhang et al., 2016b). The PTEN-induced kinase (PINK1)-Parkin (PARK2)-dependent pathway has emerged as a principal regulator of mitochondrial degradation in a range of biological systems (Narendra and Youle, 2011). The majority of research into this pathway focuses on mutations in PINK1 and PARK2 genes associated with an increase in mitophagy in hereditary early onset Parkinson disease (PD) (Ashrafi and Schwarz, 2015). Similar to observations in the traditional autophagy pathway, mitophagy holds an essential homeostatic function in skeletal muscle as evidenced by the observation that PARK2-deficient mice exhibit a mild impairment in muscle contractility and severe impairment in mitochondrial function evidenced by a decrease in mitochondrial respiration rates, uncoupling and electron transport chain (ETC) complex functioning (Gouspillou et al., 2018). Additionally, physical inactivity and thus skeletal muscle unloading is known to contribute to loss of muscle mass and function. Studies have revealed molecular marker patterns indicative of increased mitophagy and decreased regulation of mitochondrial biogenesis, preceding a loss in mitochondrial content, which may underlie muscle dysfunction (Leermakers et al., 2019).

1.3.4 PI3K/AKT

Protein kinase B (Akt) is a serine/threonine protein kinase capable of acting as pro-hypertrophic or pro-atrophic in skeletal muscle, dependent upon its phosphorylation state. Akt is a pivotal component in the process of regulating skeletal muscle fibre size and promoting hypertrophy through the activation of downstream signalling

components involved in protein synthesis including mammalian target of rapamycin (mTOR) and glycogen synthase kinase 3 beta (GSK3β). Negative genetic perturbations of Akt, mTOR and p70S6 Kinase (p70S6K) (downstream target of mTOR) have resulted in a significantly reduced cell size, thus highlighting their importance and central role in the integration of a variety of growth signals for protein synthesis to occur (Glass, 2005). Studies in myotubes have suggested that the pharmacological activation of any one of these components may provide a therapeutic intervention in diseases characterised by muscle atrophy (Rommel et al., 2001).

GSK3β has been shown to modulate hypertrophy upon its phosphorylation by Akt. This inhibits its catabolic activity as the expression of a dominant negative kinase inactive form induces dramatic hypertrophy in skeletal muscles (Rommel et al., 2001). While there are independent atrophy systems, skeletal muscle atrophy pathways can also function as the converse of hypertrophy pathways. Indeed, the inhibition of Akt has been shown to be pro-atrophic in a burn model of atrophy (Sugita et al., 2005). Similarly, the activation of the phosphoinositide 3-kinase (PI3K)-Akt-FOXO pathway can elicit cell growth, with its inhibition associated with reduced cell survival.

Atrophy, associated with a specific increased expression of ubiquitin ligases, MuRF1 and MAFbx, is antagonised by treatment with insulin-like growth factor-1 (IGF1) through the PI3K-Akt pathway in myotubes and in a diabetic model of atrophy (Sandri et al., 2004, Lee et al., 2004). This affirms that Akt holds the capacity to inhibit atrophy, as well as stimulate hypertrophy. The mechanism underlying this inhibition was shown to involve the FOXO family of transcription factors. When phosphorylated by Akt, FOXO is excluded from the nucleus, rendering it unable to translocate and upregulate the transcription of MuRF1 and MAFbx (Sandri et al., 2004).

1.3.5 FOXO

The FOXO proteins are a subgroup of the Forkhead family of transcription factors characterised by a conserved DNA-binding domain, 'the forkhead box'. In mammals, there are four FOXO genes, FOXO1, 3, 4 and 6, all of which are expressed in skeletal

muscle and encompass a central role in skeletal muscle plasticity. FOXO factors are evolutionarily conserved mediators of insulin and growth factor signalling, which are found at the interface of essential cellular processes including the regulation of gene expression that controls apoptosis, cell cycle progression and oxidative resistance. FOXO3 and FOXO1 are involved in the modulation of the activity of certain components in the ubiquitin-proteasome and the autophagy-lysosome proteolytic pathways, culminating in muscle atrophy (Accili and Arden, 2004). FOXO factors can initiate apoptosis by activating the transcription of ubiquitin ligases, and also FasL, the ligand of the Fas-dependent cell death pathway. However, they are also involved in stress resistance by upregulating catalase and MnSOD in periods of oxidative stress. While it appears paradoxical that FOXO proteins can regulate both apoptosis and cell survival mechanisms, a possible explanation has been suggested in that it is stress-resistant under mild conditions and pro-apoptotic when the intensity of a stimulus increases beyond that of a certain threshold (Carter and Brunet, 2007).

1.3.6 mTOR

mTOR is a highly conserved serine/threonine kinase of the phosphatidylinositol kinase-related family. A number of signal transduction pathways result in the simulation of mTOR, primarily involved in pathways responsible for the upregulation of protein synthesis. It plays a key role in the co-ordination of important homeostatic mechanisms including cell growth, metabolism and the inhibition of apoptotic signalling with its best understood targets including the translation regulators ribosomal protein S6 kinase (P70S6K), S6K1 and 4E-BP1 (Marini and Veicsteinas, 2010). The function of mTOR differs amongst tissues and so while pharmacological inhibition may prove beneficial in one, it may have detrimental effects in another, making the therapeutic targeting of mTOR a complex issue. mTOR is activated by a wide range of stimuli including growth factors, mechanotransduction signals and the energetic state of the cell. A decrease in ATP levels inhibits mTOR through the activation of 5'AMP-activated protein kinase (AMPK). Therefore, under hypoxic conditions, the downregulation of mTOR facilitates pro-atrophic signalling and predisposes muscle to its detrimental effects (Vadysirisack and Ellisen, 2012).

1.3.7 MAPK

The mitogen activated protein kinases (MAPKs) are a family of serine/threonine protein kinases composed of 3 distinct signalling molecules in skeletal muscle: extracellular regulated kinases 1 & 2 (ERK 1/2), p38 MAPK and c-Jun NH_2-terminal kinases (JNK). These MAPK branches are activated by MEK 1/2, MKK 3/6 and MKK 4/7 following stimulation by cytokines, growth factors and cellular stress to elicit their effects intracellularly to regulate cell proliferation, differentiation, inflammation, cell survival and apoptosis. A putative role of stimulated MAPKs includes the transcriptional regulation of the cellular redox status. They have been suggested to mediate adaptive antioxidant defence systems in skeletal muscle in response to oxidative stress. Hydrogen peroxide (H_2O_2) has been shown to induce a strong activation of ERKs, JNKs and p38 in a dose- and time-dependent manner in skeletal myoblasts (Kefaloyianni et al., 2006). Whether MAPKs are pro-hypertrophic or pro-atrophic remains largely controversial, as the specific activity of these individual paths are dependent on the type, duration and intensity of a contractile stimulus in skeletal muscle, as well as their interaction with other signalling mechanisms. However, ERK 1/2 appears to be largely pro-hypertrophic, and p38 and JNK, termed the stress kinases, are predominantly pro-atrophic.

1.3.8 Muscle differentiation/regeneration

The process of generating muscle, myogenesis, can be divided into several distinct phases, which occur during embryonic development (Tajbakhsh, 2009). However, adult skeletal muscle can also undergo regenerative myogenesis, which depends on the activation of satellite cells that have the potential to differentiate into newly functional muscle fibres (Yin et al., 2013). The most extensively studied form of regenerative myogenesis takes place when mature muscle undergoes damage, which stimulates large cohorts of satellite cells to expand mitotically and differentiate to repair the tissue and re-establish homeostasis (Rudnicki et al., 2008). It is well documented that skeletal muscle regeneration shares some similarities with myogenesis, including several molecular mechanisms including common transcription factors and signalling molecules, as well as having encompassing similar cellular events such as the activation and proliferation of myogenic cells, and the

formation of myotubes (Yusuf and Brand-Saberi, 2012). Skeletal muscle regeneration is finely orchestrated by several cellular and molecular events leading to the restoration of muscle mass, muscle vascularization, innervation, as well as the recovery of contractile and metabolic properties of the muscle (Chargé and Rudnicki, 2004). However, in the face of chronic muscle damage or insult, a progressive process of fibrosis may ensue as successive rounds of degeneration and regeneration can result in the incomplete remodelling of the extracellular matrix (ECM) and consequently, an accumulation of matrix components (Smith and Barton, 2018). Thus, the ECM replaces functional muscle with resultant large amount of fibrosis and scar tissue rather than contractile tissue yielding a muscle with a lower force-generating capacity (Smith and Barton, 2018). Two of the principal molecular pathways in the regulation of muscle hypertrophy involve myogenic regulatory factors (MRFs) and IGF-I (Asfour et al., 2018, Bikle et al., 2015).

Briefly, myoblast determination protein 1 (MyoD) is predominantly upregulated during the proliferation of satellite cells, which yields the formation of myoblasts (Sharman et al., 2001). The upregulation of the MRF, myogenin, is widely suggested to signify the subsequent myoblast differentiation (Smith et al., 1994). The contribution of other MRFs to myogenesis is unsettled in the literature, however, the deletion of MADS box transcription enhancer factor 2 C (MEF2C) has been shown to prevent muscle differentiation in satellite cells, through a failure to differentiate, highlighting its importance in the process (Liu et al., 2014b). Silent mating type information regulation 2 homologue 1 (SIRT1) is a sensitive modulator of metabolic processes and indeed, has been shown to regulate metabolic processes during myogenesis (Nedachi et al., 2008). An inhibition of SIRT1 activity yields a reduced myofibre size and attendant decrease in gene expression central to muscle development (Ryall et al., 2015). Myostatin is a key endogenous, negative regulator of muscle growth with a principal function in the determination of both muscle fibre number and size with the disruption of the myostatin gene resulting in skeletal muscle hypertrophy and hyperplasia with a resultant two-fold increase in muscle mass in mouse models (McPherron et al., 1997). Moreover, myostatin inhibitors have shown therapeutic potential in disease models characterised by muscle

degeneration (Smith and Lin, 2013). The inhibition of myostatin in the *mdx* mouse model of DMD results in greater muscle mass, increased functional strength, and decreased fibrosis and fatty infiltration of muscles, culminating in a reduction in the severity of muscular dystrophy (Wagner et al., 2002).

In addition to these MRFs, it has been demonstrated that IGF-I is involved in the induction of anabolism through the stimulation of satellite cells to proliferate and differentiate during the process of compensatory hypertrophy (Adams and McCue, 1998), while also activating a cascade of signalling pathways via PI3K/Akt/ mTOR/ p70S6K, resulting in the downstream activation of targets required for protein synthesis (Glass, 2003). Thus, the pivotal role of IGF-1 in the regulation of muscle hypertrophy has been demonstrated in numerous animal models, which report an increase in IGF-1 expression in concert with increased muscle mass (Phelan and Gonyea, 1997, Musarò et al., 2001). Interestingly, an IGF-1-induced increase in muscle mass has been shown in both human (Bamman et al., 2001) and animal models (DeVol et al., 1990) in response to mechanical load, suggesting that the activation of this pathway may have relevance to disorders characterised by load-induced hypertrophy.

1.3.9 Hypoxia inducible factor

The hypoxia inducible factor (HIF) family is made up of HIF-1, HIF-2 and HIF-3 and it represents the cell's primary response system to hypoxia, achieved through orchestrating an appropriate cellular response during periods of low partial pressure of oxygen (PO_2). First sequenced and purified in 1995, HIF is a heterodimeric protein belonging to the basic helix-loop-helix PAS family of transcription factors (Wang and Semenza, 1995). Of the isoforms in this family, HIF-1 is the most ubiquitously expressed and best characterised, with it widely recognised as a master regulator of hypoxia signaling, due to its general and diverse role in the cell. HIF-1 undergoes continuous degradation through its hydroxylation, which enables its recognition by E3 ubiquitin ligases (Epstein et al., 2001). However, during periods of hypoxia, this degradation is decreased and HIF-1α stabilises, accumulates and complexes with the HIF-1β subunit to form a functional transcription complex. This activates a plethora

of hypoxia inducible genes through binding at the respective hypoxia response element (HRE). The HIF family also comprises HIF-2 and HIF-3. HIF-2 protein is regulated in a similar manner to HIF-1 and is also implicated in the hypoxia response, as it is suggested to confer muscle resistance to ischaemia (Aragones et al., 2008). Very little data exists concerning HIF-3 function, with no studies to date examining its expression or role in skeletal muscle.

The HIF α/β heterodimeric transcription factor controls more than 100 genes with functions in erythropoiesis/iron metabolism, vascular tone, angiogenesis, matrix metabolism, cell proliferation and apoptosis (Ke and Costa, 2006). The stabilisation of HIF-1 is largely organ- and stimulus-dependent with evidence that brain tissue begins to accumulate HIF-1α when inspired oxygen drops to 18%, whereas organs such as the liver and kidneys require a more severe drop in PO_2 before the accumulation of HIF-1α ensues (Stroka et al., 2001). Similarly, normoxic HIF-1α stability has been demonstrated at higher levels in type 2 fast glycolytic fibres, than in type 1 slow oxidative fibres, suggesting that HIF activity is also muscle fibre-type specific (Pisani et al., 2005).

1.4 Reactive oxygen species (ROS)

ROS is the collective term for a variety of reactive entities derived from molecular O_2. These include oxygen radicals, superoxide (O_2^-) and hydroxyl (OH^-), as well as non-radical substances such as hydrogen peroxide (H_2O_2). The structure and function of many biomolecules is subject to modification by oxidation-reduction (redox) reactions facilitated by these ROS. The univalent reduction of O_2 yields the formation of O_2^-, the precursor of most forms of ROS and an imperative mediator of oxidative chain events. O_2^- can spontaneously degrade or be dismutated by superoxide dismutase (SOD) to form H_2O_2. Unlike O_2^-, H_2O_2 holds the capacity to cross the cell membrane easily, enabling its implication in more widespread effects. O_2^- and H_2O_2 have a relatively low reactivity. However, when H_2O_2 is not fully reduced to water (H_2O), its partial reduction yields the strongest and most potent oxidant, the hydroxyl radical (OH^-), which exerts detrimental effects on a broad range of non-specific

targets. ROS react with a large range of biomolecules, albeit to alternating degrees, dependent upon the type of ROS present, the source of ROS, the stimulus evoking ROS production, the subcellular location and antioxidant defence capacity in a particular tissue or organ (Steinbacher and Eckl, 2015).

1.4.1 Physiological role of ROS in skeletal muscle function

Davies et al., (1982) were the first group to demonstrate that specific ROS, O_2^- and H_2O_2, are generated in skeletal muscle at rest and at increased levels during contraction. It has since been well established that skeletal muscle continuously produces ROS, with the contractile apparatus of muscle fibres proving highly sensitive to alterations in cellular redox state (Powers, 2011). Skeletal muscle experiences varying effects of ROS, with the force generated by muscle largely determined by redox balance (Figure 1.1). The application of antioxidants or a reducing agent, thus eliminating ROS, yields a muscle force-generating capacity significantly below that of its maximum ability (Figure 1.1; Point 1). In a similar manner, when the cell is in a highly oxidised state, muscle force is production is severely compromised (Figure 1.1; Point 4). In its basal state, muscle force is produced at approximately half of its potential capacity (Figure 1.1; Point 2) when compared to maximal force production observed at an optimal redox state (Figure 1.1; Point 3). This suggests that under basal conditions, ROS exert a powerful tonic inhibition on skeletal muscle contractile performance. Indeed, it has been demonstrated that superoxide scavengers and NOX2 inhibitors are powerful inotropic agents in diaphragm and representative UA muscles (Skelly et al., 2010, Skelly et al., 2012b, Williams et al., 2015b). By extension, it could be posited that ROS associated with stimuli, such as hypoxia, which also reflexly serves to enhance muscle activity, impair muscle contractile performance.

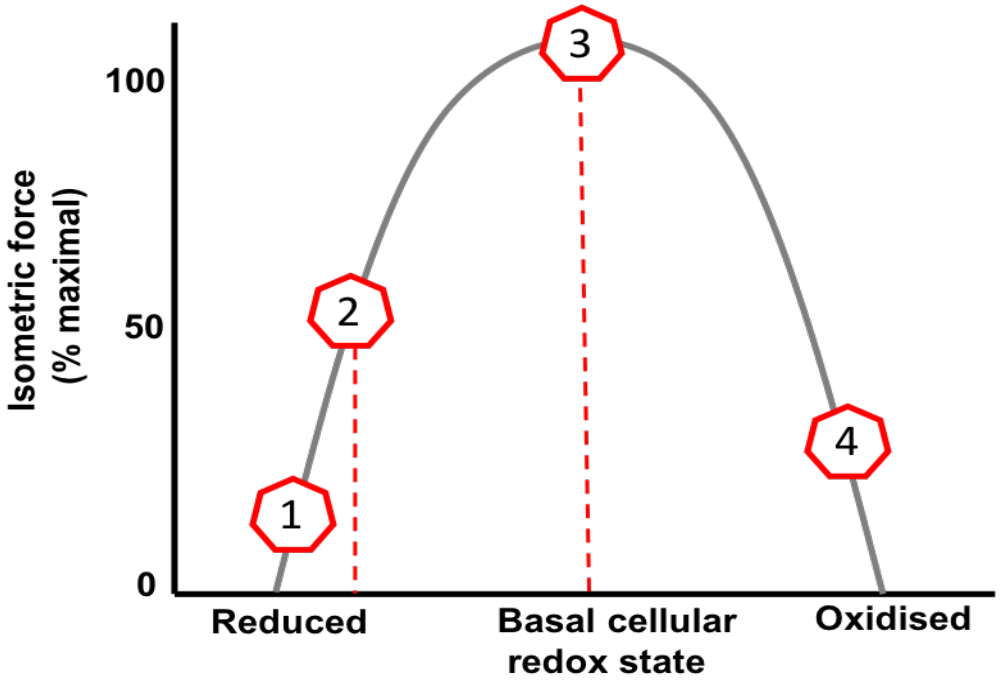

Figure 1.1 Redox balance in skeletal muscle. A theoretical model proposed by (Reid et al., 1993) displaying the biphasic effects of ROS on skeletal muscle force production. Schematic adapted from review by (Powers, 2011).

Studies examining the underlying mechanisms pertaining to ROS-dependent alterations to muscle function have largely suggested that ROS elicit complex redox alterations to Ca^{2+} release apparatus and/or increase the sensitivity of myofibrillar contractile proteins to Ca^{2+}. ROS have been shown to activate ryanodine 1 receptors (RyR1) via s-glutathionylation of cysteine residues producing an increase in calcium-induced calcium release (CICR) in the t-tubules of skeletal muscle (Hidalgo et al., 2006). It has also been demonstrated that thiol groups on the sarcoplasmic reticulum are a critical target of oxidative modification by O_2^-, culminating in an increase in Ca^{2+} release, with thiol reducing agents successfully closing the channel (Abramson and Salamaz, 1988). In contrast, various studies have reported a down-regulation and impaired Ca^{2+} channel functioning in skeletal muscle upon exposure to ROS (Guerra et al., 1996). This apparent dichotomy may be attributed to varying levels of ROS, which are known to have divergent effects in skeletal muscle. Additionally, ROS can potentially alter the sensitivity of myofibrillar contractile proteins to Ca^{2+} or affect

muscle at the level of cross-bridge cycling (Powers, 2011). Positive inotropic effects observed in a pharyngeal dilator muscle following administration of the superoxide scavenger, tempol, were reported to be due to an increased Ca^{2+} sensitivity of myofibrillar contractile apparatus, as contractile kinetics were unaffected (Skelly et al., 2010).

1.4.2 ROS reactions with protein

ROS are well renowned for eliciting their effects through cysteine residues in proteins, which act as redox switches. This results in the oxidation of these residues, inducing a conformational change that alters a protein's activity and manifests as a change in metabolic processes, homeostasis and contractile performance (Zuo and Clanton, 2005, Marin-Corral et al., 2009, Klomsiri et al., 2011). Excessive levels of ROS, culminating in oxidative stress, results in tissues exhibiting higher levels of carbonylated proteins, ultimately leading to protein loss of function (Moller and Kristensen, 2004). Amino acids differ in their susceptibility to ROS with thiol and sulphur containing amino acids showing the greatest susceptibility, as the oxidation of iron-sulphur centres by O_2^- is largely irreversible and renders enzymes inactive. Excessive ROS results in site-specific modifications of amino acids, fragmentation of peptide chains and an increased susceptibility to proteolysis. Studies have suggested that oxidised proteins are more likely to be tagged for ubiquitination and subsequent proteasomal degradation (Cabiscol et al., 2000). Interestingly, the muscle-specific ubiquitin ligase, MuRF1, has been shown to bind the MHC complex in skeletal muscle resulting in its degradation, with siRNA blockage of MuRF1 preventing this loss (Clarke et al., 2007).

Increased levels of protein oxidation with concomitant alterations to antioxidant responses have been reported in poorly functioning respiratory and limb muscles of COPD (Barreiro et al., 2017), DMD (Petrillo et al., 2017) and CHF (Ahn et al., 2017) patients. The effect of hypoxia on redox alterations, in the form of protein oxidation, in murine models of respiratory disease is varied. Models which utilise sustained hypoxia, typically report increases in protein oxidation in skeletal muscle, exemplified by increased carbonyl and/or decreased free thiol content (Lewis et al.,

2015, Lewis et al., 2016). In contrast, the effects of intermittent hypoxia on skeletal muscle largely depend on the severity of the IH stimulus, which will be discussed in more detail below (1.10.3). Indeed, increased levels of protein oxidation and the subsequent role this plays in alterations to muscle contractile capacity appears to be correlated with disease or stimulus severity.

1.4.3 ROS reactions with DNA

ROS are a major source of DNA damage that have the potential to affect both nuclear and mitochondrial DNA. Oxidative alterations to purine or pyrimidine bases and the deoxyribose backbone of DNA generally involve a reaction with OH^-. OH^- favourably oxidises guanine to produce 8-hydroxyguanine, making it a routinely used biomarker of DNA oxidative damage (Tsuboi et al., 1998). Unrepaired oxidative modifications of DNA bases on a single strand results in a mismatch in nucleotides. This forms the basis for ROS-induced DNA mutations with the subsequent translation yielding malfunctioning or inactive proteins. Mitochondrial DNA appears to be more susceptible to oxidative damage than nuclear DNA, possibly owing to its low level of protective proteins and histones and as well as its significantly closer localisation to the main ROS-producing system within the cell (Richter, 1992). An accumulation of mitochondrial DNA mutations has been shown to predispose the mitochondria to oxidative stress through an increased build-up and leakage of electrons from the ETC. This culminates in dysfunctional mitochondria and a resultant shift from oxidative to glycolytic metabolism in certain tumorous cancers, a theory first proposed by Otto Warburg in the 1920s (Koppenol et al., 2011).

Furthermore, similar ROS-induced metabolic adaptations that may have implications for skeletal muscle contractile function have been identified in patients and models encompassing hypoxia as a core feature of disease. Slow-to-fast fibre-type transitions in patients with COPD and CHF is commonly reported in limb muscle, resulting in a more fatigable muscle (Kitzman et al., 2014, Ausín et al., 2017). Interestingly, an opposite adaptation in fibre-type composition from fast-to-slow is evident in the diaphragm of these patients, culminating in a weaker muscle (Doucet et al., 2004, Bowen et al., 2017). While there are a multitude of possible stimuli for

these transitions, the former is suggested to be a product of chronic muscle inactivity, with the latter explained by the large contractile activity necessary by the diaphragm to sustain breathing pattern in these diseases. A shift towards a faster fibre-type has also been demonstrated in the UA muscles of patients with OSAS, with the mechanism and cause-result relationship in this instance remaining less clear (Chen et al., 2016), but probably related to loading due to airway obstruction.

1.4.4 ROS reactions with lipids

Lipid peroxidation is among the most detrimental processes of ROS-induced stress, by enhancing pre-existing oxidative stress, through the production of radicals that hold the capacity to further react with proteins and DNA. This initiates a cyclical chain of events resulting in a plethora of mal-adaptive effects including loss of membrane fluidity and elasticity, impaired cell function and rupture. Direct products of lipid peroxidation include malondialdehyde (MDA), isoprostanes and 4-hydroxynoneal (4-HNE), which harbour mutagenic and carcinogenic properties, rendering them highly cytotoxic substances. MDA levels have been shown to be significantly higher in the plasma of patients with breast and lung cancer (Gonenc et al., 2001). Similarly, an increase in levels of F-2 isoprostane has been observed in the early stages of patients with Alzheimer's disease (Montine et al., 2002) and hepatic cirrhosis (Pratico et al., 1998). Lipid peroxidation is most well documented in the skeletal muscle of patients with diabetes. It has been demonstrated that 4-HNE adducts directly related to the severity of insulin resistance through the modification of mitochondrial proteins and essential components of the insulin signalling pathway (Ingram et al., 2012). Stressors, including sustained and intermittent hypoxia, have also been shown to induce lipid peroxidation in weakened skeletal muscle (Shortt et al., 2014, O'Leary et al., 2018).

1.4.5 ROS reactions with residues of cell signalling components

While ROS oxidise a vast array of biomolecules directly, they may also exert their effects through the alteration of various elements of cell signalling pathways. PTPs have a vital role in dephosphorylating receptor tyrosine kinases (RTKs), thus

regulating the downstream signalling cascade they control (Truong and Carroll, 2013). The reversible oxidation of the catalytic site in the cysteine residue to sulfenic acid in these phosphatases results in a sustained activation of the associated pathway (Lim et al., 2008). However, when further oxidation to sulfinic or sulfonic acid occurs, the process is irreversible (Lim et al., 2008).

ROS have been shown to inhibit PTPs, which regulate pathways associated with protein synthesis and degradation, such as the MAPK pathway (Zhang et al., 2016a). Sustained activation of ERK 1/2 results in an unregulated proliferation of cells associated with tumorigenesis in a range of cancers (Feitelson et al., 2015), while sustained activation of p38 and JNK is associated with unregulated cell death and neuronal apoptosis in patients with Alzheimer's and PD (Kim and Choi, 2010). Similarly, phosphatase and tensin homolog (PTEN), which regulates the PI3K pathway, has also been shown to be subject to redox regulation by H_2O_2 in humans (Lee et al., 2002). Indeed, an inhibition or loss of PTEN activity has been described as a central mechanism in an array of cancers and rare syndromes (Hollander et al., 2011).

The difficulty in defining the contribution of ROS to signalling lies with the fact that they exert their effects at multiple stages of signalling (upstream or downstream) and sometimes in opposing fashions (inhibitory or stimulatory). In addition, transcription factors have also been shown to be redox-sensitive (Haddad, 2002). Nuclear factor kappa B (NF-κB) is a family of transcription factors associated with a wide range of functions in inflammation, immunity, cell proliferation, apoptosis and tumorigenesis (Oeckinghaus and Ghosh, 2009). ROS can inhibit NF-κB directly by binding at the specific p50 cysteine, which inhibits its DNA binding ability (Morgan and Liu, 2011). In contrast, ROS can also activate NF-κB by phosphorylating its inhibitor 1-κB, thus highlighting the complexity of the role that ROS play in the control of cell signalling with their effects like to be circumstantially defined (Morgan and Liu, 2011).

1.5 Endogenous antioxidant systems

Oxidative stress was first described by (Sies, 1991) as "a disturbance in the pro-oxidant to antioxidant balance, in favour of the former, leading to potential damage". This occurs due to an accumulation of ROS, a depletion of antioxidant defences, or a culmination of both. All forms of life maintain a reducing environment in cells with the body employing a number of enzymatic and non-enzymatic defence systems in order to maintain levels of ROS at an optimal level necessary for a range of homeostatic functions. Skeletal muscle is endowed with this sophisticated defence system, rendering it remarkably flexible in response to changes in the redox milieu that can occur both in health and disease (Kozakowska et al., 2015). A principal mechanism essential for cellular defence against redox imbalance is the activation of the transcription factor, nuclear factor erythroid 2-related factor 2 (NRF2). The NRF2-antioxidant response element signalling pathway controls the expression of genes whose protein products are responsible for the elimination of reactive oxidants by enhancing cellular antioxidant capacity (Nguyen et al., 2009). The most predominant antioxidant systems which function in this manner include superoxide dismutase (SOD), catalase (CAT), the glutathione (GSH) system and peroxiredoxins (PRDXs).

1.5.1 Superoxide dismutase

SOD is pivotal in neutralising the primary form of ROS, O_2^-. Three SOD isoenzymes exist which catalyse the conversion of O_2^- to H_2O_2, using a transition metal incorporated into its active site. Of these isoenzymes, SOD-1 incorporates copper-zinc and is located in the cytosol and mitochondrial intermembrane, SOD-2 uses manganese with its localisation exclusive to the mitochondrial matrix and SOD-3 also uses copper-zinc with its highest expression reported in the extracellular space. ALS is a neurological disorder resulting in the death of motor neurons in the brain and spinal cord leading to muscular paralysis (Bruijn et al., 2004). In humans, SOD-1 mutations underlie apoptosis of spinal neurons, revealing its central role in the pathogenesis of ALS (Fridovich, 1995). The pivotal role of SOD-1 in the pathogenesis of ALS has since been exemplified and well examined in a wide range of models

harbouring SOD-1 mutations (Nagahisa et al., 2016, Crown et al., 2019, Bakavayev et al., 2019).

SOD isoforms have been shown throughout skeletal muscle fibres, with 15%-35% of total SOD activity attributed to the mitochondria and the remaining activity in the cytosol (Powers et al., 1994). Furthermore, higher SOD activity has been reported in oxidative (type 1) fibres, compared to glycolytic (type 2b) muscle fibres in rodent models (Criswell et al., 1993). Skeletal muscle from SOD-1 deficient mice exhibit muscle atrophy with concomitant oxidative damage, resembling that of an accelerated age-related sarcopenia (Muller et al., 2006). This was suggested to be as a result of excess O_2^- and its secondary product, highlighting the pivotal physiological role of SOD-1 as a ROS buffer in skeletal muscle. Furthermore, an increase in the mRNA of embryonic myosin heavy chain (MyHC-emb), paired box protein-7 (Pax7) and myogenin, characteristic of the early phase of muscle regeneration, were significantly increased in skeletal muscle of SOD-1 null mice (Nagahisa et al., 2016). This reveals the capacity for excessive ROS, due to the absence of SOD-1, to initiate skeletal muscle damage and resultant structural alterations that can present as mal-adaptive to muscle function. Interestingly, the accelerated age-related muscle loss and weakness in whole-body SOD1 KO mice (Muller et al., 2006) is considerably less severe when SOD1 is specifically deleted in skeletal muscle or neurons of mice (Sakellariou et al., 2018). Findings from the latter study demonstrate that neuromuscular integrity, redox mechanisms, and pathways are differentially altered in nerve and muscle of whole-body and muscle-specific SOD1 deficient mice (Sakellariou et al., 2018). These results point to impaired redox signalling, rather than oxidative damage, in peripheral nerves as a key contributor to muscle loss in whole-body SOD1 deficient mice and thus, potentially sarcopenia during aging.

1.5.2 Catalase

CAT is a heme-dependent enzyme responsible for catalysing the conversion of H_2O_2 to H_2O and O_2 utilising iron as a co-factor attached to its active site. It exhibits a wide distribution throughout the cell with an extremely high turnover rate. Mice lacking CAT exhibit a diminished rate of removal of H_2O_2 and increased susceptibility to

oxidant tissue injury (Ho et al., 2004). As a result, a deficiency in CAT has been linked to ROS-induced accelerated diabetic renal injury (Hwang et al., 2012) and non-alcoholic fatty liver disease (NAFLD) (Hwang et al., 2020).

CAT is also localised to skeletal muscle and similar to SOD, its activity is reportedly highest in oxidative fibres compared to those with a low mitochondrial density (Laughlin et al., 1990). Increased levels of H_2O_2 with an attendant decrease in CAT have been demonstrated in a mouse model of sarcopenia (Sullivan-Gunn and Lewandowski, 2013). It is suggested that the increased level of ROS and decline in CAT-dependent antioxidant capacity may be a contributing factor to the development of muscle weakness that is characteristic of sarcopenia.

1.5.3 Glutathione system

8 isoforms of GPX (GPX 1-8) have been reported in mammals which catalyse the reduction of H_2O_2 to H_2O, through the utilisation of reduced glutathione (GSH). GSH is readily oxidised to form glutathione disulfide (GSSG) through this reaction. Therefore, this demands that cells possess a pathway to continuously replenish GSH stores and maintain a reduced environment. Expression of GPX in skeletal muscle varies across fibres types, with oxidative fibres exhibiting the highest activity when compared with muscle fibres of low oxidative capacity (Lawler et al., 1994). Oxidative fibres also incorporate 4-5 times the amount of GSH that glycolytic fibres do (Leeuwenburgh et al., 1997). GSH encompasses a range of functions including direct reactions with several ROS through acting as a substrate for the elimination of H_2O_2. GSH also participates in the reduction of other antioxidants, thus aiding their activity e.g. vitamin E & C. The administration of GSH precursors, such as N-acetylcysteine (NAC), have shown efficacy in preventing respiratory muscle weakness in murine models which exhibit oxidative stress (O'Leary et al., 2018, Burns et al., 2019). This highlights the importance of a balanced GSH/GSSG ratio in ensuring a homeostatic redox state to support optimal skeletal muscle function.

SOD, CAT, GPX and GSH display a sensitivity to exercise in rat skeletal muscle, in that the alterations to the activity of these antioxidants is largely determined by the

intensity and duration of exercise (Powers et al., 1994, Leeuwenburgh et al., 1997). In a similar manner, hypoxia holds the capacity to alter antioxidant capacity dependent upon the pattern, duration and intensity of the hypoxia paradigm employed. Hypoxia-induced decreases in antioxidant status are believed to represent instances of oxidative stress based on an overwhelming depletion of antioxidant capacity (Jackson et al., 1996, Williams et al., 2015b, Debevec et al., 2017). In contrast, hypoxia-induced increases in antioxidant defences has also been demonstrated, which may serve as an early protective mechanism to combat an increase in ROS levels to maintain redox balance (White et al., 1988). Similarly, the administration of antioxidants to boost antioxidant defence systems and prevent against deleterious effects of hypoxia-induced ROS have been demonstrated (Ding and Liu, 2011, Shortt et al., 2014).

1.5.4 Peroxiredoxins

Peroxiredoxins (PRDXs) are a highly abundant ubiquitous family of cysteine-dependent peroxidase enzymes which have a central role in regulating peroxide levels within cells, and as such represent an important antioxidant defence mechanism (Perkins et al., 2015). In humans, six different isoforms of PRDX are present (PRDX 1-6) , four PRDX1 subtypes, one PRDX5 subtype and one PRDX6 subtype (Dammeyer and Arnér, 2011). PRDX1, PRDX2, PRDX3, PRDX5 and PRDX6 are localized in the cytosol, in the mitochondria, in the nuclei and in the peroxisomes (Kang et al., 1998, Seo et al., 2000, Rhee et al., 2005), whereas PRDX4 is mainly present in the endoplasmic reticulum, or it is secreted (Fujii et al., 2015). This family of enzymes represents one of the most important and widespread peroxide and peroxynitrite scavenging enzymes (Karplus, 2015), with their role previously overshadowed by well-studied antioxidant enzymes such as catalase and GPX, considered for a long time to be the major enzymes responsible for protecting cells against hydroperoxides. PRDXs have a key role in the control of various physiological functions, including cell growth, differentiation, apoptosis, embryonic development, lipid metabolism, the immune response, as well as cellular homeostasis (Nicolussi et al., 2017).

PRDXs are expressed in multiple cellular compartments and have the ability to scavenge and react with H_2O_2 in cells at very low physiological concentrations and are several orders of magnitude more reactive with H_2O_2 than many other proteins reported to be redox regulated (Manta et al., 2009). PRDX1, 2 & 3 are rapidly and reversibly oxidised following treatment with H_2O_2 and in response to repeated isometric contraction in isolated muscle fibres (Stretton et al., 2020). These findings suggest that PRDXs are likely candidates to link contraction-induced H_2O_2 generation in skeletal muscle with activation of redox-regulated signalling proteins and transcription factors (Stretton et al., 2020). PRX3 has also been suggested to function as a regulator of mitochondrial function, thus having implications in skeletal muscle performance (Lee et al., 2014). Mice deficient in PRX3 exhibit deregulated mitochondrial networks and membrane potential of myotubes, in which ROS levels were significantly increased. A concomitant increase in skeletal muscle fatigability was also reported, suggested to be a result of disrupted mitochondrial homeostasis (Lee et al., 2014). Interestingly, proteomic screening of EDL muscle from dystrophin deficient *mdx* mice has revealed an 80% reduction in PRDX2, suggested to be due to proteolytic degradation following hyperoxidation by NOX2 (Olthoff et al., 2018). Muscle force loss due to eccentric contractions was exacerbated by PRDX2 ablation and improved by PRDX2 overexpression, highlighting the pivotal role of this antioxidant in protection against oxidant induced muscle injury in this model (Olthoff et al., 2018).

1.6 Sources of ROS

1.6.1 Mitochondria

ATP synthesis is an energetically unfavourable reaction with the energy necessary for its occurrence dependent on the oxidation of nicotinamide adenine dinucleotide (NADH) and flavin adenine dinucleotide ($FADH_2$). This is achieved by the four complexes of the ETC in a process of aerobic metabolism. The differential electrical charge established throughout this cycle drives ATP synthesis with ROS produced as normal intermediate molecules. Electron leakage occurs as electrons exit the ETC prematurely, most commonly at complexes 1 and 3, prior to O_2 being terminally

reduced at cytochrome C oxidase. This accounts for ~1-2% of O_2 consumption as these electrons react with molecular O_2 to form ROS, which function in their homeostatic role under resting conditions (Jastroch et al., 2010). Mitochondria have been deemed the primary location of oxygen consumption and ROS production and as a result, they are becoming key players in O_2 sensing (Taylor, 2008).

Hypoxia has been described as the PO_2 where the mitochondrial ETC is more reduced, considered a sentinel for insufficient O_2 availability at the level of mitochondrial flow (Clanton, 2007). Skeletal muscle is an example of a tissue that adapts to local reductions in PO_2 during hypoxia by inducing a hypometabolic state to sustain O_2 delivery and ensure adequate tissue oxygenation (Lewis and O'Halloran, 2016). Adaptations of skeletal muscle to sustained periods of hypoxia include a loss of mitochondrial content, thus a reduced oxidative capacity (Gamboa and Andrade, 2010). This loss of mitochondrial content is proportional to muscle fatigue, suggesting a shift to a more glycolytic muscle phenotype.

Given the pivotal role of O_2 as an electron acceptor in the ETC, hypoxia induces a build-up of electrons in this cycle. This ultimately leads to an increase in electron leakage and subsequent ROS formation, serving to exacerbate mitochondrial dysfunction (Waypa et al., 2016). It has been suggested that mitochondrial membrane potential regulates the production of mitochondrial ROS and that uncoupling oxidative phosphorylation from the ETC in mitochondrial membrane may decrease mitochondrial superoxide production (O'Leary and O'Halloran, 2016). An increase in the mRNA expression of a mitochondrial uncoupling protein, UCP-3, in respiratory muscle following sustained hypoxia exposure may represent a protective mechanism against ROS overproduction. However, this would also yield an associated decrease in ATP synthesis, highlighting the possible implication of ROS-induced alterations to mitochondrial capacity in diaphragm muscle weakness.

1.6.2 Xanthine Oxidase

Xanthine Oxidase (XO) is an isoform of xanthine oxidoreductase belonging to the molybdenum hydroxylase flavoprotein family. It holds a primary function in

catalysing the oxidation of hypoxanthine to xanthine, and further to uric acid in the process of purine catabolism. These reactions utilise molecular O_2 as an electron acceptor resulting in the formation of O_2^- (Volek et al., 2002). It has been demonstrated that XO plays a role in exercise-induced stress in the diaphragm muscle of COPD patients. An increase in MDA and GSSG in the diaphragm of patients with COPD following strenuous exercise was absent in patients treated with a XO inhibitor, allopurinol (Heunks et al., 1999). Treatment with allopurinol has also been shown to attenuate endothelial dysfunction in rats following exposure to CIH (Dopp et al., 2011). Similarly, allopurinol prevents IH-induced hypertension, oxidative stress and XO activation in the adrenal medulla of rats exposed to CIH, affirming its potential role in CIH-induced ROS production (Nanduri et al., 2013a).

1.6.3 Phospholipase A2

The importance of lipids in cell signalling and tissue physiology can be appreciated by the array of pathologies associated with dysregulated lipid metabolism (Bang and Dyerberg, 1980, Adibhatla and Hatcher, 2008, Musso et al., 2009). An important event in lipid metabolism involves the activation of phospholipase A2 (PLA2) enzymes which hydrolyse membrane phospholipids. PLA2 enzymes cleave fatty acids at the sn-2 position of glycerophospholipids to yield free fatty acids and lysopholipids. This reaction is of particular importance when arachidonic acid (AA) is released as it serves as a primary substrate for ROS-generating enzyme systems including lipooxygenases (LOXs) and cyclooxygenases (COXs) (Adibhatla and Hatcher, 2008). Both Ca^{2+}-dependent and independent forms of PLA2 have been identified in skeletal muscle, which both exhibit the capacity to produce ROS (Powers, 2011). Of interest, hypoxia-induced activation of PLA2 has been observed in the left myocardium of male rats, highlighting its possible role as a source of CIH-induced ROS (Micova et al., 2016).

1.7 NADPH oxidase (NOX)

Skeletal muscle fibres produce ROS on a continuous basis throughout different subcellular localisations in response to physiological and pathological stimuli

(Moldovan and Moldovan, 2004). The mitochondria have long been considered the predominant source of ROS in skeletal muscle. Ten years after the discovery of O_2^- superoxide production in isolated skeletal muscle fibres (Reid et al., 1992), the presence of the NOX enzyme complex in ventilatory skeletal muscle was described (Javeshghani et al., 2002). While ROS are continuously produced, by sources such as the mitochondria, the discovery of the NOX enzyme complex demonstrated that ROS can also be produced by enzymatic systems in a controlled manner in response to various stimuli. The NOX family of enzymes is the only known system whose sole purpose is to produce ROS, with their function governed by alterations in gene expression as well as acute regulation. There are seven members of the NOX family: NOX1-5 and DUOX1-2. These isoforms differ in their level of expression, regulation of expression, organ-specific expression, the specific type of ROS they produce and in the control of their enzymatic activity (Brandes et al., 2014).

1.7.1 NOX1

NOX1 is primarily considered to be a colonic NOX system as it is highly expressed in epithelial cells of the gastrointestinal (GI) tract. In concert with this, NOX1-derived O_2^- demonstrate their principal function in GI host defence. However, the overexpression of NOX1 and subsequent overproduction of ROS has been reported in the pathogenesis of inflammation-associated tumour development through an increase in the resistance of tumour cells to cell death mechanisms (Rokutan et al., 2006). NOX1 is expressed at marginal levels in cardiomyocytes, where it is suggested to play a protective role against hypoxia-induced bradycardia (Kojima et al., 2015). It has been demonstrated that NOX1 expression is upregulated by myostatin in differentiating C2C12 muscle cells (Sriram et al., 2011). However, its levels in skeletal muscle are relatively low compared with other NOX isoforms and thus, its physiological role in this instance has not yet been well discerned.

The majority of NOX isoforms require the association of the catalytic subunit with accessory cytosolic subunits for successful enzymatic activation. NOX1 is found complexed with the cytosolic subunit, p22phox, with its ROS production dependent on its co-expression with regulatory subunits, p47phox and p67phox, as increased

superoxide production is abolished in their absence (Bánfi et al., 2003). Additionally, in the search for other NOX1 interacting proteins, its preferential activation by NOX activator 1 (Noxa1) and NOX organiser 1 (Noxo1) proteins has been reported, leading to high stimulus-independent increases in ROS (Schröder et al., 2017). These results suggest that NOX1 activity is differentially activated depending upon the stimulus present. Like the majority of NOX isoforms, NOX1 is Rac-dependent, with its activation pivotal in the assembly of accessory subunits to the catalytic subunit, thus enabling their association and subsequent activation (Cheng et al., 2006).

1.7.2 NOX2

NOX2 (gp91phox) was originally discovered in phagocytes and neutrophils as a pivotal component of the 'respiratory burst' enabling its specialised function in host defence against invading pathogens and microorganisms. While NOX2 is still widely considered to have a phagocytic specific tissue expression, studies now suggest that it is actually the most widely expressed NOX isoform. NOX2 mRNA has been identified in the thymus, small intestine, colon, spleen, pancreas, ovary, placenta, prostate, and testis, with this wide tissue distribution thought to be a result of the infiltration of phagocytes and/or blood (Cheng et al., 2001). However, an increasing body of evidence is emerging which reveals the expression of NOX2 in a large range of non-phagocytic tissues including neurons (Serrano et al., 2003), hepatocytes (Reinehr et al., 2005), cardiomyocytes (Heymes et al., 2003) and skeletal muscle myocytes (Javeshghani et al., 2002).

The NOX2 enzyme complex is composed of the catalytic subunit, gp91phox, and p22phox, which together form a mutually stabilising complex, flavocytochrome$_{b558}$, in the plasma membrane. The activity of NOX2 can be induced by specific agonists such as angiotensin II (AngII), growth factors and by mechanical stress including that of muscle contractions (Loureiro et al., 2016). Upon stimulation, accessory cytosolic subunits including p47phox, p67phox, p40phox and Rac assemble the complex in its entirety. This enables and regulates its enzymatic activity to initiate the electron transfer from NADPH on the cytosolic side to O_2 across the cell membrane to generate O_2^-. While all subunits have been shown to be involved in NOX2-derived O_2^-

generation, the relative contribution of each subunit is highly complex and remains largely inconclusive. Nevertheless, the phosphorylation of p47phox and activation of Rac appear to be among the pivotal regulators of O_2^- production by NOX2 in skeletal muscle. Significantly impaired diaphragm contractile function with an attendant increase in p47phox mRNA in a mouse model of CHF are notably absent in p47phox null mice (Ahn et al., 2015). The authors suggest that NOX2-dependent ROS production was inhibited in the absence of the activator subunit, p47phox. Similarly, an increase in Rac activity has been reported in the skeletal muscle of *mdx* dystrophic mice (Pal et al., 2014). Interestingly, Rac inhibitors result in a decrease in the phosphorylation state of p47phox and markers of H_2O_2 production, suggesting a role for Rac in NOX2-induced oxidative stress in *mdx* skeletal muscle. Additionally, Rac associated with microtubules has been shown to activate NOX2 enzymes following contraction, with the stretch-induced increase in ROS prevented in skeletal muscle fibres lacking NOX2 or Rac (Sylow et al., 2015).

All NOX2-related subunits have been identified in skeletal muscle (Javeshghani et al., 2002), highlighting the possibility of their role in ROS-dependent alterations to EC coupling mechanisms. Skeletal muscle SR has been shown to contain NOX, which reduces molecular O_2 to generate O_2^- (Xia et al., 2003). O_2^- generated by NOX present in the SR increases RyR activity, due to an increase in RyR binding and thus Ca^{2+} release (Xia et al., 2003). Additionally, this group have confirmed that the increase in NOX activity was associated with increased O_2^- generation that originated in the SR, not in the mitochondria (Xia et al., 2003). The expression of NOX2 subunits including gp91phox, p47phox, p22phox and p67phox has also been shown in intact and isolated t-tubules and triads of mammalian skeletal muscle (Hidalgo et al., 2006). NOX2 increased O_2^- and H_2O_2 production and enhanced the activity of RyRs, confirmed by their significantly increased s-glutathionylation. NOX2 expression and activity are higher in skeletal muscle exhibiting predominantly type-1 fibres, encompassing a high oxidative capacity compared to type-2 fast twitch fibres, which comprise a more glycolytic phenotype. Therefore, the differences regarding NOX2 expression among fibre types may have relevance to the contractile characteristics of that fibre (Loureiro et al., 2016). Studies in isolated fibres from mouse flexor

digitorum have demonstrated that NOX2 is a major contributor of ROS which regulates muscle force production at rest and during contractions (Sakellariou et al., 2013). NOX2 has also been shown to be activated during moderate-intensity exercise in mouse and human skeletal muscle, representing the primary source of ROS under these conditions (Henríquez-Olguin et al., 2019). Additionally, mice lacking regulatory NOX2 subunits showed that lack of ROS generation during exercise strongly impaired muscle glucose uptake and GLUT4 translocation during exercise (Henríquez-Olguin et al., 2019). These findings suggest that NOX2 is a major source of ROS production during exercise and that NOX2-dependent ROS production is an important signal for increasing muscle glucose uptake during exercise. As well as the respiratory musculature, the expression of NOX2 has been documented throughout sites of the respiratory control network, including peripheral chemoreceptors (carotid body) (Dinger et al., 2007, Peng et al., 2009), central pattern generating and integrative sites (Glass et al., 2007), and motor neurons (MacFarlane et al., 2008). Thus, NOX2-dependent ROS may exert their effects at multiple levels of the respiratory system, which culminates in alterations to the system's phenotypic response that manifests as adaptive or mal-adaptive.

Hypoxia is a potent activator of NOX2 (Williams et al., 2015b, Nanduri et al., 2015). NOX2-derived ROS have been implicated in a wide range of CIH-induced morbidities across organs and systems including the brain (Zhan et al., 2005), heart (Hayashi et al., 2008) and testes (Zhang et al., 2013). Interestingly, CIH has been shown to exacerbate respiratory muscle dysfunction in DMD by reducing diaphragm strength by a further 30% (Farkas et al., 2007). Moreover, inhibiting NOX2-dependent ROS production increases force and respiratory function in dystrophic diaphragm (Loehr et al., 2018). This highlights a potential role for NOX2 blockade in the prevention of CIH-induced diaphragm muscle weakness. The role of NOX2 in CIH-induced respiratory system dysfunction is discussed in detail below.

1.7.3 NOX3

The vestibular system of the inner ear is central for the perception of motion and gravity with otoconia being the key organs of this system. NOX3 expression is limited

to the plasma membrane of vesicles in the inner ear where O_2^- is thought to trigger a conformational change in the binding of otoconin to phospholipids of the vesicle membrane, thus promoting its formation. A clear enzymatic function of NOX3 has been exhibited in otoconia morphogenesis as mutations affecting otoconia formation result in mutations in the gene for NOX3 (Paffenholz et al., 2004). NOX3 complexes with p22phox, but other subunit regulation differs depending on species. Association with Noxo1 alone markedly stimulates ROS production in humans (Cheng et al., 2004), whereas mouse models appear to require Noxo1 and Noxa1 (Banfi et al., 2004a). However, Noxo1 may be considered the most physiologically relevant regulator of NOX3 in the context of our present knowledge, as NOX3-dependent ocotonia formation has shown to be impaired following Noxo1 inactivation mutations (Kiss et al., 2006). This suggests a constructive developmental role for NOX3-derived ROS. Contradictory results exist regarding the involvement of Rac in NOX3 activation (Ueyama et al., 2006, Miyano et al., 2006) affirming the complexity in the regulation of NOX enzymes.

1.7.4 NOX4

The NOX4 isoform was first discovered in the kidney and it is the tissue with the highest expression, with lower levels reported in skeletal muscle, endocrine tissue and lungs (Bedard and Krause, 2007). The catalytic component of NOX4 requires the binding of p22phox for successful ROS generation, independent of other conventional NOX subunits. NOX4 has been shown to preferentially produce H_2O_2, as approximately 90% of the electron flux through isolated Nox4 produces H_2O_2 and only 10% forms O_2^- (Nisimoto et al., 2014). NOX4 exhibits constitutive activity, enabling NOX4-derived ROS to elicit long-lasting and adaptive effects. As a result, it has long been thought to be predominantly regulated by transcription, although there is evidence to suggest that it may be subject to acute activation by a range of stimuli also (Manea et al., 2015). While NOX4 does not rely on conventional NOX subunits for its activity, some modulators of NOX4 have been suggested including polymerase delta-interacting protein (Poldip2), tyrosine kinase substrate 5 (TRK5) and Rac.

Poldip2 is highly expressed in skeletal muscle and may function to stabilise and regulate the NOX4-p22phox complex (Lyle et al., 2009). The interaction of Poldip2 with p22phox results in a 3-fold increase in NOX4 activity in vascular smooth muscle cells (VSMCs) (Lyle et al., 2009). TSK5 has also been suggested to be a regulatory protein required for ROS production by NOX4 in certain cells. NOX4 contains a p47phox binding domain and TSK5 is structurally similar to p47phox, deducing its possible interaction with the enzyme complex (Diaz et al., 2009). The information regarding Rac is controversial, however there is potential for its role in NOX4 activation as an inhibition of Rac by knockdown in mesangial cells prevents a NOX4-dependent increase in ROS (Gorin et al., 2003). Additionally, reports suggest that since there is no Rac binding site on NOX4 it may function through an alternative mechanism. An increase in ROS, with a concomitant increase in NOX4 and Rac in VSMCs is prevented by knockdown of NOX4 or inactivation of Rac (Meng et al., 2008). Additionally, there was no evidence for a direct interaction between NOX4 and Rac, suggesting that Rac may function through alterations to the cytoskeleton, which change the supply of NADPH to NOX4 or alter its intracellular location.

NOX4 contains a mitochondria localisation sequence and as such, has been identified in the mitochondria of cardiac (Ago et al., 2010) and skeletal muscle (Sakellariou et al., 2013), more specifically in the SR and t-tubules of the latter (Loureiro et al., 2016). The expression and activity of NOX4 have been shown to be induced by cytokines, transforming growth factor β (TGFβ), angiotensin and hypoxia. NOX4 plays a pivotal role in the response to hypoxia by functioning as an O_2 sensor as it possesses an unusually high Km for oxygen (~18%). This is similar to that of known oxygen-sensing enzymes which enables it to generate H_2O_2 as a function of PO_2 (Nisimoto et al., 2014). Hypoxia rapidly enhanced the mRNA and protein expression of NOX4 in pulmonary vessels, an effect which was abrogated following mutation of the hypoxic response element of NOX4 (Diebold et al., 2010). Hypoxia-induced vascular remodelling and pulmonary hypertension have been shown to be associated with increased levels of NOX4 and p22phox (Nisbet et al., 2009). NOX4 expression has also been shown to be positively regulated by O_2 tension. An increase in NOX4-derived H_2O_2 has been shown to be coupled to an increased oxidation of cysteine residues of

RyRs in isolated SRs, cultured myofibres and intact muscle. This produced an increase in Ca^{2+} release and enhanced muscle contraction, thus implicating a role for NOX4 in muscle performance in response to changes in PO_2 (Sun et al., 2011b). Additionally, it has recently been demonstrated that NOX4 can be regulated by ATP levels due to its ATP-binding motif (Shanmugasundaram et al., 2017). ATP has the capacity to directly bind and negatively regulate NOX4 activity, suggesting that NOX4 can serve as a metabolic sensor and become activated with decreased mitochondrial ATP levels, which may be important in the response to exercise. Indeed, studies in NOX4 deficient mice demonstrates that H_2O_2 and NOX4 are necessary to promote the immediate response to exercise in skeletal muscle as glucose and fatty acid oxidation were notably blunted in NOX4 deficient mice, possibly through the regulation of UCP3 (Specht et al., 2021). This study points to NOX4 as a major source of ROS responsible for initiating metabolic signalling, pivotal in skeletal muscle adaptation to exercise (Specht et al., 2021).

Similar to NOX2, higher NOX4 expression and activity has been identified in slow twitch fibres compared to fast twitch fibres (Loureiro et al., 2016). Furthermore, higher levels of NOX4 have been observed in the diaphragm compared to limb muscles (Frye et al., 2012). NOX4 abundance and activity may therefore be based on muscle fibre-type composition or the recruitment pattern of specific muscles. However, exercise-induced adaptations of skeletal muscle, including alterations to muscle metabolism or muscle fibre-type composition occur independently of NOX4 (Vogel et al., 2015). Diaphragm muscle dysfunction is a key component of the ventilatory abnormalities that are part of the integrative pathophysiology of CHF. An increase in NOX4-related subunits and levels of protein carbonyls have been implicated in diaphragm muscle weakness in patients with CHF (Ahn et al.). Additionally, spinal cord injury (SCI) results in marked atrophied and dysfunctional skeletal muscle. An increase in NOX4 mRNA and protein in limb muscle has been shown to be associated with enhanced binding of Nox4 to RyR1, increased oxidation and nitrosylation of RyR1, culminating in reduced muscle force in SCI rats (Liu et al., 2017). Indeed, NOX4 has been reported to increase oxidative stress on skeletal

muscle RyRs in metastases, thus inducing skeletal muscle weakness in breast cancer (Regan et al., 2017).

1.7.5 NOX5

NOX5 is a O_2^- generating enzyme that is structurally unique and deemed distantly related to other members of the NOX family, as it contains NH_2-terminal EF-hand motifs, which possess four Ca^{2+} binding sites that are essential for its activation. Therefore, this isoform of NOX requires no association with additional subunits for its activation, but rather is Ca^{2+}-dependent. An increase in Ca^{2+} binding induces a conformational change in the EF-hand motifs, exposing its catalytic site and enabling the transfer of electrons from NADPH to O_2 to form O_2^- (Banfi et al., 2004b). It is the most recent of the conventional NOX enzymes to be identified and was first located in human testes, lymph nodes and spleen (Bánfi et al., 2001). The absence of NOX5 from the rodent genome has significantly impaired the understanding of its structure and mechanism of action and as a result most of the knowledge surrounding this isoform comes from human tissues and overexpression studies.

NOX5 expression has been demonstrated in the vasculature, heart and kidneys highlighting its possible implication in cardiovascular disease, as renal function is impaired and blood pressure elevated in mice expressing human NOX5 (Chatterjee et al., 2015). Oxidative stress associated with hypertension can affect vascular function through the post-translational oxidative modification of cysteine residues in proteins central to vascular redox signalling (Montezano et al., 2015). Therefore, this is suggested to influence the cellular response to oxidative stimuli by promoting a proliferative rather than contractile phenotype as an example of vascular remodelling, eventually predisposing the system to dysfunction. The mechanisms of NOX5-derived ROS are only newly emerging, but it is plausible to suggest that it may have implications for oxidative stress-induced hypertension commonly observed in a range of disease states.

1.7.6 DUOX1 and DUOX2

Dual oxidase 1 (DUOX1) and dual oxidase 2 (DUOX2) both encompass the traditional catalytic core subunit associated with NOX enzymes, but also have an intracellular domain containing two EF-hand motifs comprising of Ca^{2+} binding sites. DUOX1 and DUOX2 are activated independent of an association with other cytosolic subunits. However, they do require the maturation proteins DUOXA1 and DUOXA2 to enable their preferential localisation to the plasma membrane from the endoplasmic reticulum (Rigutto et al., 2009). Both DUOXs were initially identified as a source of H_2O_2 necessary for thyroid hormone biosynthesis with Ca^{2+} shown to trigger an increased ROS production in human thyroid cells and bronchial epithelial cells (De Deken et al., 2000, De Deken et al., 2002). Bi-allelic inactivating mutations in the DUOX2 gene results in a complete disruption of thyroid hormone synthesis characterised by severe and permanent hypothyroidism in patients, confirming the pivotal contribution of DUOX2 to homeostatic thyroid function (Moreno et al., 2002). However, the overexpression of DUOX1 in the thyroid yielded a delayed but sustained increase in ROS in response to ionising radiation with evidence of DNA damage (Ameziane-El-Hassani et al., 2015), an effect that may promote secondary malignancies following radiation treatment. Interestingly, pre-treatment with catalase abrogated these effects.

Transfection of skeletal muscle myoblasts with DUOXA1 has been shown to increase levels of H_2O_2 and apoptosis, with siRNA knockdown ameliorating this effect (Sandiford et al., 2014). Additionally, both dual oxidases have been characterised in hind leg skeletal muscle of rats, with their physiological function in this instance unknown (Sun et al., 2011a). DUOXs have been located at the apical side of the airway and digestive tract suggesting that these enzymes also function in the traditional NOX role of innate host defence against pathogens (Rigutto et al., 2009). While incorporating similar homologies, DUOX1 and DUOX2 appear to function differentially, possibly due to a divergence in their regulation. It has been reported that DUOX1 is positively regulated by cAMP-dependent protein kinase A (PKA) while DUOX2 is highly induced by protein kinase C (PKC) (Rigutto et al., 2009).

1.7.7 NOX inhibitors

The most promising approach in the development of therapeutic strategies against oxidative stress is by identifying disease-relevant enzymatic sources of ROS, targeting these selectively, while leaving physiological ROS signalling through other sources intact. NOX enzymes have been identified as the main potential drug-target candidates in diseases associated with dysfunction in ROS signalling. NOX enzymes stand out as their sole function is to produce ROS, whereas the majority of enzymatic sources produce ROS as a by-product or upon biochemical uncoupling or damage.

A range of small molecules have long been thought to inhibit NOX activity, however, the majority have been identified as non-specific due to off-target effects. The most traditional and well-studied of these molecules include, diphenyleneiodonium (DPI) and apocynin. DPI is a flavoprotein inhibitor and thus inhibits many other enzymes besides NOX, which may result in an over-scavenging of ROS. Similarly, while apocynin is reported to inhibit the translocation of p47phox to the plasma membrane, thus inhibiting NOX2 activity, non-specific ROS scavenging properties have also been observed (Altenhöfer et al., 2015). However, even the most advanced NOX inhibitors in development, setanaxib and GKT136901, have been shown to exhibit ROS scavenging activities (Augsburger et al., 2019, Dao et al., 2020). Thus, it has been suggested that a panelled approach may be beneficial in assessing the target specificity of NOX inhibitors given the importance of NOX-dependent redox signalling in physiological homeostasis across tissues (Dao et al., 2020).

The World Health Organisation (WHO) has recently recognised NOX inhibitors as a new therapeutic class, which hold significant potential for the treatment of fibrotic, inflammatory, neurodegenerative and oncological disorders. GKT137831 (setanaxib or GKT-831), claimed to be a NOX1/4 dual inhibitor and a partial NOX5 inhibitor, was the first NOX inhibitor to reach the clinical trial stage (Wiesel et al., 2012). Phase II clinical trials using GKT137831 are ongoing for the treatment of idiopathic pulmonary fibrosis and kidney disease in patients with type 1 diabetes. Additionally, Ewha-18278 (APX-115) has been shown to inhibit NOX1, NOX2, and NOX4 in pre-clinical studies

(Cha et al., 2017). Moreover, this NOX inhibitor is currently moving from Phase I to II in clinical trials for patients with diabetic kidney disease (Lee et al., 2020).

NOX inhibitors have also shown some efficacy in other pre-clinical models of disease. GKT137831 induced favourable effects in models of ischaemic retina disease and diabetic retinopathy (Appukuttan et al., 2018, Jiao et al., 2019), hypertensive cardiac remodelling and hypertrophy (Zeng et al., 2019) and liver fibrosis (Sun et al., 2017). VAS2870, a pan NOX inhibitor, has demonstrated vascular protective effects in models of pulmonary hypertension (Li et al., 2019) and Alzheimer's disease (Abubaker et al., 2019). Additionally, ML090, which has preferential activity toward NOX5, was beneficial in models of stroke (Casas et al., 2019, Dao et al., 2020). Collectively, NOX inhibition seems to represent a promising therapeutic strategy with a wide scope of clinical applications.

1.8 Obstructive sleep apnoea syndrome (OSAS)

OSAS is a common respiratory disorder affecting at least 4% of men and 2% of women worldwide (Lee et al., 2008). It represents the most prevalent form of sleep disordered breathing (SDB) recorded in ~85% of all SDB cases (Ho and Brass, 2011). Predisposition to OSAS is multifactorial, however abnormal airway anatomy remains a central feature of this disorder, with both congenital and acquired factors affecting the size of the pharyngeal airway. Although OSAS can affect individuals indiscriminately, numerous risk factors including obesity (BMI > 30) (Romero-Corral et al., 2010), family history, age, hypertension (Al Lawati et al., 2009) and smoking (Lin et al., 2012) have been identified.

1.8.1 Pathophysiology of OSAS

More than 20 UA muscles work harmoniously to regulate UA patency and prevent airway collapse. The pharynx lacks bony and cartilaginous support resulting in greater susceptibility to collapse (White and Younes, 2012). This is especially true during inspiration, as the diaphragm and accessory inspiratory muscles contract to produce a sub-atmospheric (negative) pressure in the UA. This results in reflex activation of

pharyngeal dilator muscles to ensure protection of airway patency on a breath-by-breath basis, as well as functioning to restore airflow following pharyngeal collapse. However, when the negative pressure produced by the diaphragm exceeds the dilative force-generating capacity of the UA muscles, airway occlusion occurs. The resultant apnoea is described as a cessation of external breathing (airflow) for more than 10 seconds (Eckert et al., 2009). The severity of OSAS is clinically quantified by the apnoea-hypopnoea index (AHI) i.e. the number of apnoeas and hypopneas per hour of sleep due to recurrent collapse of the upper airway, with severe OSAS patients experiencing more than 30 apnoeic events per hour during sleep (Olson et al., 2003, Crummy et al., 2008).

Upon airway collapse, a fall in PO_2 and increase in PCO_2 is sensed by the carotid body and central chemoreceptors, respectively, to produce an increased ventilatory effort. However, arousal from sleep is typically necessary to re-establish airway patency and normal ventilation, resulting in hazardous levels of daytime hypersomnolence (Ward et al., 2013). The repetitive collapse of the UA begets recurrent waves of hypoxia (with concomitant arterial oxygen desaturation) and subsequent re-oxygenation upon airway re-opening. This results in the hallmark feature of OSAS, chronic intermittent hypoxia (CIH). CIH is widely considered to be the driving force behind the development and maintenance of a range of morbidities reported in patients presenting with OSAS. The detrimental effects are likely attributable to CIH-induced oxidative stress, extensively shown to be produced following repeated hypoxia/re-oxygenation cycles throughout the night cycle (Lavie, 2003).

UA collapse in OSAS is likely to be multifactorial as CIH-induced mal-adaptation presents at multiple levels of the respiratory control system. This includes respiratory muscle weakness and fatigue (Clanton et al., 2001, McGuire et al., 2002a, McGuire et al., 2002b, McGuire et al., 2003a, Liu et al., 2005, Pae et al., 2005, Liu et al., 2009, Skelly et al., 2012b, Skelly et al., 2013, Shortt et al., 2014, Shortt and O'Halloran, 2014, McDonald et al., 2015) impaired motor control of the upper airway (O'Halloran et al., 2002, Veasey et al., 2004, Ray et al., 2007) and discordant respiratory rhythm and pattern generation (Peng et al., 2003, Reeves and Gozal, 2006, Edge et al., 2012,

Moraes et al., 2013, Donovan et al., 2014, Souza et al., 2015, Elliot-Portal et al., 2018, Joseph et al., 2020). This highlights the potential for CIH-induced oxidative stress to exacerbate OSAS, perpetuating a vicious cycle of respiratory morbidity. OSAS is a highly underdiagnosed disease associated with a plethora of co-morbidities beyond that of the respiratory system, thus elevating its status to that of a major public health risk (Lavie, 2009). The range of maladies is widespread with evidence for neurocognitive (Al Lawati et al., 2009), metabolic (Drager et al., 2011), cardiovascular (Dumitrascu et al., 2013), testicular (Torres et al., 2014), hepatic (Savransky et al., 2007), renal (Rosas, 2011) and pancreatic (Wang et al., 2013a) disorders.

1.8.2 Current treatments

At present, the gold standard treatment for severe OSAS is the application of continuous positive airway pressure (CPAP) during sleep, which pneumatically stabilises the upper airway (Becker et al., 2003). However, there is only ~50% compliance with this current line of treatment, as patients frequently report claustrophobia, facial discomfort, throat dryness, nasal and eye pain (Wolkove et al., 2008). Oral appliances, categorised into tongue retaining devices and mandibular advancement devices (MADs), are commonly used and more efficacious in patients with a mild-to-moderate form of OSAS, but are also utilised in instances of severe OSAS when CPAP is poorly tolerated. These appliances aim to improve UA patency during sleep by enlarging the UA or by decreasing UA collapsibility (Gagnadoux et al., 2009). Surgical treatments aimed at reducing the obstruction caused by anatomical features that may predispose to OSA such as the retroposition of the mandible, enlarged pharyngeal fat pads, enlarged soft palate, enlarged tongue, narrow posterior airway space, and UA hypotonia have shown some success, but may not represent a true clinical cure (Pavwoski and Shelgikar, 2017). Experiments utilising hypoglossal nerve stimulation, to protrude the tongue, thus opening the pharyngeal airway and ensuring patency have shown some promise (Kezirian et al., 2014). Hypoglossal nerve stimulation has been shown to successfully reduce the AHI index by 68% (Strollo et al., 2014), with this magnitude of improvement persisting for 3 years post-treatment in patients with moderate-to-severe OSAS (Woodson et al., 2016). However, hypoglossal nerve stimulation is not deemed a viable treatment

option for patients with a BMI > 32 and those with concentric retropalatal collapse (Strollo et al., 2014). Transcranial magnetic stimulation has also shown some early signs of promise as a drug-free treatment (Bradford, 2013), but this may only hold true for a subset of OSAS patients. Studies investigating the role of drug therapy in reducing the severity of OSAS by increasing UA muscle tone, ventilatory drive, cholinergic tone, arousal threshold or reduction in the proportion of paradoxical (REM) sleep remain largely inconclusive (Mason et al., 2013). Thus, the development of specific antioxidants which may serve as an adjunct therapy by ameliorating excessive levels of ROS, central to respiratory morbidity in OSAS, are of great interest.

1.9 Animal models of OSAS

1.9.1 Spontaneous models

The English bulldog represents the first natural model of sleep disordered breathing (Hendricks et al., 1987). This model is characterised by abnormal upper airway anatomy encompassing an enlarged soft palate, narrow oropharynx and innate tendency to snore. The relative area of fast fibres is increased in the UA musculature of this model (Petrof et al., 1994), similar to observations in human OSAS patients (Smirne et al., 1991), consistent with airway dilator muscle fatigue. Studies examining this model reveal disordered ventilation, O_2 desaturations to less than 90% and central and obstructive apnoeas during REM sleep, leading to daytime hypersomnolence at levels ~10 times greater than those observed in controls. The understanding of the effect of SDB on respiratory muscle activation was significantly increased arising from experiments utilising this model, which demonstrate a significantly reduced respiratory drive to the diaphragm (suppressed to 42% of its original drive) and sternohyoid (suppressed to 17% of its original drive) muscles at the onset of SDB during REM sleep (Hendricks et al., 1991). Serotonin (5-HT) has been implicated in the pathogenesis of OSAS. At high doses, ondansetron, a 5-HT antagonist, reduced the respiratory disturbance index (RDI) in the English bulldog model during REM sleep, with no observable effect on sleep efficiency or oxyhaemoglobin saturation (Veasey et al., 2001). Studies in extremely obese Yucatan miniature pigs have shown oxyhaemoglobin desaturations with concomitant

obstructive and central apnoeas during REM sleep, thus highlighting the central role of obesity as a major risk factor in the elaboration of severity of OSAS (Lonergan et al., 1998). Similarly, a smaller pharyngeal airway cross-sectional area during both inspiration and expiration and a reduction in the increase in airway area during inspiration has been observed in obese Zucker rats (Brennick et al., 2006). These mechanical abnormalities were attributed to fat infiltration in the tongue, similar to that observed in OSAS patients.

1.9.2 Surgical models

Animal models of OSAS can also be experimentally induced through surgical methods, by mechanically occluding or altering the UA. Studies utilising this model of OSAS have been used in a range of animals including dogs (Kimoff et al., 1997), baboons (White et al., 1995), pigs (Chen and Scharf, 2000) and rats (Fletcher et al., 1992). Typically, this involves the use of tracheotomy with intermittently occluding endotracheal tubes. A computer controls the sequence of events which begins with an UA obstruction due to the valve of the tracheotomy closing at the onset of sleep. Once the animal is aroused from sleep, the valve opens, and the pharyngeal collapse is recovered. These models are highly valuable as they are widely accepted to closely mimic the events of OSAS in humans and enable the precise control of the frequency of apnoea occurrence as well as their relative severity i.e. duration. These models allow the analysis of a comprehensive range of factors critical for understanding the underlying pathology of OSAS including arousal from sleep, intrathoracic pressure, length of apnoeas and oxygen desaturations. However, these models are labour-intensive, with concomitant low throughput, rendering them quite demanding for use in the study of OSAS.

1.9.3 Intermittent hypoxia models

IH is a central feature of OSAS and so the exposure of animals to repetitive intermittent cycles of hypoxia interspersed with normoxia, modelling the arterial hypoxaemia experienced by OSAS patients due to airway collapse, has become one of the most widely used models of SDB. IH is widely considered to be one of the most

noxious stimuli of OSAS, as well as being easily adjusted to induce varying degrees of severity of OSAS (Mesarwi et al., 2015). A system to deliver hypoxic gases to rodents in a cyclical pattern reminiscent of the oxygen profile observed in severe OSAS was developed in the early 90s (Fletcher et al., 1992), resulting in rats developing hypertension through a mechanism reliant upon reflex sympathetic overactivity following IH exposure for 3 weeks during their sleep phase. IH models minimise the invasive aspect of surgical experimental models while also enabling a higher experimental throughput. IH-reoxygenation paradigms have been employed in humans (Tamisier et al., 2009) and more extensively in rodents (Farré et al., 2018). Rodents are exposed to IH during the diurnal period during sleep and are subsequently returned to normoxic room air for night hours during wakefulness, in an attempt to mimic the pattern of human exposure in OSAS.

The pattern, duration and intensity of IH exposure is pivotal in determining phenotypical responses in the respiratory and other systems (Reeves and Gozal, 2006, Morgan et al., 2016a). Interestingly, several experiments have demonstrated beneficial effects of IH. Animals exposed to acute bouts of IH become more resistant to damage associated with exposure to severe hypoxic paradigms (Almendros et al., 2014). Mice treated with acute and brief episodes of IH, lasting for several hours and/or days with mild hypoxia (>12% F_iO_2) survive longer when subsequently exposed to severe IH, characterised by <12% F_iO_2. This suggests that by utilising a mild hypoxia paradigm, animals develop protective and adaptive mechanisms. This form of preconditioning is based on the principle that applying potentially deleterious stimuli near or just below the threshold of damage enables tissues and organs to become resistant to the same noxious stimuli, thus reducing or even preventing IH-induced injury (Peng et al., 2003). Short-term exposure to IH comprising of 3-10 cycles for 1-2 hours/day results in a form of respiratory motor plasticity, known as long-term facilitation (LTF) and results in an increase in the strength of respiratory muscle contractions and ventilation (Dale et al., 2014). Additionally, these acute hypoxia paradigms have been shown to upregulate hypoxia-sensitive growth/tropic factors within respiratory motor neurons resulting in an increased phrenic, hypoglossal and carotid sinus nerve discharge both in humans (Xing et al., 2013) and

animals (Mahamed and Mitchell, 2007). Thus, acute bouts of mild hypoxia may have relevance as a therapeutic strategy in certain disease states (Navarrete-Opazo and Mitchell, 2014).

However, OSAS is a chronic condition and when IH is administered over a long period of time it is termed CIH. The conventional settings used for applying IH to animals include two major parameters: the frequency and severity of hypoxic events. When IH is administered over a chronic period, at a moderate-to-severe dose and at a high frequency, mal-adaptative outcomes tend to occur, with deleterious consequences for integrative body systems. Typically, animals are subjected to CIH involving the cyclical change of the oxygen fraction (FiO_2) in the gas breathed by the animals from room air (F_IO_2 - 21%) to nadir values ranging from F_IO_2 of 4 to 15%, over a time period of days, weeks, or months, which results in a concomitant decrease in O_2 saturation ranging from 60-80%, values comparable to humans presenting with moderate-to-severe OSAS (Lim and Pack, 2014).

These models produce different degrees of hypoxia severity, yielding dose-response effects (Lim et al., 2016, Gallego-Martin et al., 2017, Docio et al., 2018). Additionally, setting the frequency of IH allows a calibration, albeit possibly loose, to the clinical AHI observed in polysomnographic studies of patients with OSAS. Studies in animal models have utilised varying rates of hypoxic events, to mimic a wide range of AHI, e.g., from the high event rates in severe OSAS patients (60 events/h) to occasional events in patients with a mild form of the disorder (2 events/h) (Gozal et al., 2001, Almendros et al., 2013). There is extensive experimental and epidemiological evidence that the oxidative stress and inflammatory response generated at both systemic and tissue levels by the recurrent hypoxia-reoxygenation events over a longer period of time are major drivers underlying clinically-relevant morbid consequences of OSAS (Lavie, 2015). These include, but are not confined to, increased risk of cardiovascular, metabolic, neurocognitive and malignant diseases (Lévy et al., 2015). Evidence from experimental models for the role of CIH-induced mal-adaptation at multiple levels of the respiratory control is discussed in detail in the next section.

1.10 Chronic Intermittent hypoxia and the respiratory control system

Exposure to CIH drives a pro-oxidant state resulting in aberrant plasticity at multiple levels of the respiratory control system, thus accounting for the devastating clinical consequences of OSAS. Mal-adaptive remodelling culminates in alterations to respiratory rhythm and pattern generation (Peng et al., 2003, Reeves and Gozal, 2006, Edge et al., 2012, Moraes et al., 2013, Donovan et al., 2014, Souza et al., 2015, Elliot-Portal et al., 2018, Joseph et al., 2020), impaired motor control of the upper airway (O'Halloran et al., 2002, Veasey et al., 2004, Ray et al., 2007) and respiratory muscle weakness (Clanton et al., 2001, McGuire et al., 2002a, McGuire et al., 2002b, McGuire et al., 2003a, Liu et al., 2005, Pae et al., 2005, Liu et al., 2009, Skelly et al., 2012b, Skelly et al., 2013, Shortt et al., 2014, Shortt and O'Halloran, 2014, McDonald et al., 2015). Therefore, specific antioxidant strategies may have application as an adjunctive treatment in OSAS and other respiratory conditions characterised by exposure to CIH.

1.10.1 CIH and impaired motor control of the upper airway

Muscles of the UA play a critical role in the maintenance of airway calibre and in the alleviation of obstructive events. However, in certain instances, this control is compromised and the airway becomes unstable (O'Halloran et al., 2002). O'Halloran et al. (2002) were the first to show that exposure to CIH impairs reflex control of UA muscle activity *in vivo*. Exposure to CIH significantly reduced sternohyoid EMG responsiveness during acute hypoxic and asphyxic challenges, with no alteration to diaphragm EMG responses. This selective impairment of motor drive to the UA muscle may perpetuate a vicious cycle of events to exacerbate the likelihood of further airway collapse. An assessment of the critical closing pressure of the pharynx (Pcrit) is considered a clinically relevant 'gold standard' measurement of airway collapsibility. 12 weeks of exposure to CIH in rats has been shown to cause a more positive pharyngeal pressure associated with collapse (Pcrit) (Ray et al., 2007). This increased collapsibility of the airway was not attributable to changes in musculature of the UA as measured by MHC composition. Rather, it is suggested to be due to an alteration in the neurological mechanisms controlling the UA, and specifically the

serotonergic system. Exposure to CIH has been shown to reduce the excitability of the hypoglossal motor nerve which innervates dilator muscles of the pharynx. Administration of tempol, a superoxide dismutase mimetic, ameliorated CIH-induced impairment (Veasey et al., 2004). However, 7 days of exposure to CIH was insufficient to alter genioglossus electromyograph (EMG) responses to airway occlusion in rats (Edge et al., 2014). Interestingly, the same CIH paradigm induced breathing instability in sleeping rats as evidenced by an increased spontaneous apnoea index (Edge et al., 2012). Administration of the superoxide dismutase mimetic, tempol, or the NOX inhibitor, apocynin, prevented the CIH-induced increase in the propensity for apnoea. This further highlights the role of oxidative stress, which may be NOX2-derived, in CIH-induced respiratory plasticity.

1.10.2 CIH and impaired respiratory control

The respiratory control system has the ability to exhibit considerable plasticity, similar to that observed in many other neural networks. Plasticity can be defined as a persistent change in a neural control system based on a prior experience, which may involve structural and/or functional alterations (Mitchell and Johnson, 2003). Challenges to the respiratory control system elicit alterations which are adaptive in nature in order to maintain respiratory homeostasis i.e. optimal blood gas and pH levels. However, the determination of whether neuroplasticity presents as adaptative or mal-adaptive is largely based on the pattern, duration and intensity of the stimulus (Baker and Mitchell, 2000, Peng and Prabhakar, 2004), as well as the timing of the perturbation throughout life (Gozal et al., 2001). Hypoxia-induced plasticity, which has clinical relevance to OSAS, is one of the best studied forms of respiratory plasticity. Indeed, both adaptive and mal-adaptive alterations in respiratory control have been demonstrated following intermittent hypoxic exposure in humans and animal studies (Bradford et al., 2005, Mahamed and Mitchell, 2008).

Long-term facilitation is characterised by a progressive increase in respiratory motor output during or following exposure to IH (Baker and Mitchell, 2000, Mahamed and Mitchell, 2007). Sensory and motor plasticity is well described in rodents following

exposure to CIH (Peng et al., 2001, Peng et al., 2003, MacFarlane and Mitchell, 2008, MacFarlane et al., 2009, Edge et al., 2009, Edge et al., 2012). Exposure to CIH can evoke sensory long-term facilitation within the carotid body (Peng et al., 2003), and induce facilitation of breathing or altered chemoreflex control of breathing (Reeves and Gozal, 2006, Skelly et al., 2012b, Morgan et al., 2016b, Elliot-Portal et al., 2018). Recent evidence highlights the role of NOX2 as a potential source of ROS underlying sensory and motor plasticity at multiple sites of the respiratory control network (Peng et al., 2006a, Peng et al., 2009, MacFarlane et al., 2009, Peng et al., 2011, MacFarlane et al., 2014, Perim et al., 2018).

Ventilatory adaptation is a form of respiratory plasticity described as a persistent increase in normoxic ventilation following exposure to IH. This likely represents a chemoreflex-driven increase in sympathetic outflow and breathing that contributes to systemic hypertension and respiratory instability in OSAS patients (Marcus et al., 2010). Ventilatory adaptation following exposure to CIH has been demonstrated in rats (Reeves and Gozal, 2006, Skelly et al., 2012b). In contrast, exposure to CIH had no effect on resting ventilation in guinea pigs (Lucking et al., 2018), rats (McGuire et al., 2003b, Edge et al., 2012, Souza et al., 2015, Joseph et al., 2020) and mice (Elliot-Portal et al., 2018). This may be explained by variations in the intensity of the IH stimulus employed. Indeed, ventilatory adaptation to intermittent hypoxia (VAIH) has been reported in rats following 30 (Reeves and Gozal, 2006) and 21 days of treatment (Morgan et al., 2016a), with the duration and paradigm of IH exposure appearing pivotal in determining the phenotypical respiratory response. Exposure to CIH has been shown to result in a decrease in metabolic rate in rat models (Morgan et al., 2016a, Joseph et al., 2020). Morgan et al., (2016a) emphasise the importance of assessing metabolic rate in concert with respiratory recordings, to account for the decrease in metabolic rate that occurs when small mammals are acutely exposed to hypoxia (Frappell et al., 1992). This is an especially crucial consideration in mouse models, as mice exhibit greater hypometabolic effects of hypoxia than rats (Jochmans-Lemoine et al., 2015). A failure to report on metabolic measures can potentially result in an over- or under-estimation of ventilatory responsiveness (Morgan et al., 2016a). These observations stress the importance of incorporating

metabolic measures when examining ventilation in animal models of OSAS and other diseases characterised by respiratory disturbance such as DMD (Burns et al., 2017).

Exposure to CIH has been shown to modulate respiratory chemoreflex responses to hypoxia and hypercapnia (Greenberg et al., 1999, Peng et al., 2003, Morgan et al., 2016a, Elliot-Portal et al., 2018, O'Connor et al., 2019), consistent with observations in OSAS. The functional significance of altered responses to these acute challenges is divergent. Respiratory mal-adaptation may present in an apnoeic patient when an inability to respond to a perturbation with an appropriate ventilatory response results in chemoreflexes not holding the essential capability to terminate apnoeic events. Conversely, an 'overshoot' or exaggerated ventilatory response may serve to create respiratory instability by excessively removing CO_2, thus reducing the CO_2 reserve toward the apnoeic threshold during sleep (Dempsey et al., 2010). Ventilatory responsiveness to hypoxia varies greatly depending on the pattern and duration of hypoxic exposure. Augmented hypoxic ventilatory responses and concomitant oxidative stress have been observed in healthy individuals following exposure to CIH (Pialoux et al., 2009) and in patients with OSAS (Narkiewicz et al., 1999). The ability for exposure to CIH to stimulate carotid body sensory facilitation is a well described phenomenon (Peng et al., 2001, Rey et al., 2004, Peng et al., 2006b). An enhancement (Reeves et al., 2003, Reeves and Gozal, 2004, Peng et al., 2006b, Julien et al., 2008, Morgan et al., 2016a, Elliot-Portal et al., 2018), depression (Reeves et al., 2006, Gonzalez-Martín et al., 2011, Olea et al., 2014, Lucking et al., 2018) or unchanged (Edge et al., 2009, Skelly et al., 2012b) hypoxic ventilatory response in intact animals has been reported across a range of species following treatment with a variety of IH paradigms.

There is increasing interest in the role of oxidative stress in enhancing hypoxic chemosensitivity, but evidence surrounding the culpable source of ROS remains largely inconclusive. NOX subunits including p22phox, gp91phox, p47phox, and p67phox have been localised to type I cells of guinea pig, rat, and human carotid bodies (Kummer and Acker, 1995). Exposure to CIH significantly increases the mRNA expression of NOX1, NOX2 and NOX3 in peripheral chemoreceptors (Peng et al.,

2009, Khan et al., 2011, Prabhakar et al., 2015). Moreover, there is ample evidence to suggest that CIH-induced sensory plasticity of the carotid body is NOX2-dependent (Peng et al., 2006a, Peng et al., 2009, Yuan et al., 2011, Nanduri et al., 2013b, Nanduri et al., 2015) CIH-induced increases in ventilatory responsiveness to hypoxia are attenuated in rats treated with apocynin, as evidenced by a reduction in $\dot{V}_E/\dot{V}CO_2$ (Morgan et al., 2016b). This implicates ROS, which may be NOX2-derived in altered chemoreflex sensitivity following exposure to CIH. However, p47phox, but not gp91phox, knock-out alters the O_2 sensing capability of the carotid body seen as a potentiated ventilatory and chemoreceptor response to hypoxia (Sanders et al., 2002). This suggests that NOX subunits significantly differ in their complex regulatory function of respiratory control. Patch-clamp studies have demonstrated that intact neuroepithelial bodies (NEBs) in lung slice preparations from mice deficient in gp91phox, failed to respond to a hypoxic stimulus (Fu et al., 2000). This provides evidence indicating that the dysfunction of NOX disrupts the O_2 sensing capability of the NEBs. Interestingly, no difference in the response to hypoxia between wild-type and gp91phox null mice has also been reported (Roy et al., 2000). This is attributed to no alteration in glomus cell functioning and a conclusion that although NOX is a major source of ROS, it does not function as an oxygen sensor in the carotid body.

Although CO_2 has a pivotal role in ventilatory control during sleep, there is a paucity of information examining the effects of exposure to CIH on hypercapnic sensitivity. Chemoreflexes are essential during sleep as a protective mechanism to stimulate arousal and subsequent termination of apnoeic events. Failure to do so may contribute to an increased propensity of apnoeic events, thus leading to an increased severity of OSAS. Conversely, an exaggerated response to CO_2 contributes to ventilatory instability by reducing the CO_2 reserve towards apnoeic threshold (Dempsey et al., 2010). An increase in the hypercapnic ventilatory response (HCVR) has been observed in OSAS patients, as a result of episodic hypoxia (Appelberg and Sundström, 1997, Khodadadeh et al., 2006). Indeed, a CIH-induced increase in the ventilatory response to hypercapnia has been reported in mice (Elliot-Portal et al., 2018) and dogs (Katayama et al., 2007). Conversely, evidence supports an unaltered

hypercapnic ventilatory response following CIH in other rodents including guinea pigs (Lucking et al., 2018) and rats (Greenberg et al., 1999, Edge et al., 2012).

Whilst obstructive apnoeas are the predominant apnoea type in OSAS patients due to collapse of the upper airway, central or spontaneous apnoeas also occur in patients due to a lack of ventilatory drive. This reveals a common overlap in obstructive and central sleep apnoea. OSAS patients receiving CPAP treatment regularly present with periodic breathing and central apnoeas, with some patients consequentially being diagnosed with complex apnoea (Morgenthaler et al., 2006). Complex apnoea in OSAS patients may be a result of CIH-induced remodelling in the central respiratory network governing respiration, serving to perpetuate the severity of OSAS (O'Halloran, 2016). It is well documented that exposure to CIH contributes to reduced respiratory stability that can manifest in rodents as increased apnoea index and increased variability of breathing (Edge et al., 2012, Souza et al., 2015, Elliot-Portal et al., 2018, Joseph et al., 2020). Exposure to CIH causes an increase in the propensity for central apnoea in neonatal rat pups (Julien et al., 2008), adult rats (Edge et al., 2012, Souza et al., 2015, Joseph et al., 2020) and mice (Elliot-Portal et al., 2018). Moreover, the CIH-induced increase in the frequency of spontaneous apnoeas in rats has been shown to be ameliorated by the administration of apocynin, thus implicating NOX2-derived ROS in the manifestation of increased apnoea index (Edge et al., 2012).

A degree of breathing variability is normal and essential to enable the respiratory control system to be malleable enough to respond to various perturbations (Wuyts et al., 2011). Sighs, reportedly generated in the preBötC, hold an essential function in the normal respiratory cycle, by monitoring brain states, stimulating arousal and resetting breathing variability (Ramirez, 2014). An increase in sigh frequency during respiratory perturbations, such as hypoxia, stimulates an arousal, highlighting their critical role in survival. Failure to sigh or arouse has been implicated in sudden infant death syndrome (Garcia et al., 2013). However, an increase in sigh frequency can manifest as pathological when there is persistent and excessive breathing variability. In an attempt to regularise breathing variability, increased sigh generation could

further increase irregularity through the generation of post-sigh apnoeas. An increase in the frequency of post-sigh apnoeas can create conditions of IH and oxidative stress upon frequent sighing (Garcia et al., 2013, Ramirez et al., 2013), further exacerbating the severity of OSAS. Indeed, exposure to CIH has also been shown to increase the frequency of sighs and post-sigh apnoeas in rat models (Edge et al., 2012, Souza et al., 2015, Joseph et al., 2020). Additional assessments of respiratory stability through Poincaré plot analysis of respiratory timing in adult rats suggests that exposure to CIH produces an increase in short- and long-term breathing variability, resulting in changes in respiratory pattern (Souza et al., 2015). Conversely, studies in guinea pigs, which have hypoxia-insensitive carotid bodies, reveal a CIH-induced decrease in indices of breathing variability (Lucking et al., 2018). This apparent dichotomy in results may relate to differences in sex, species and IH intensity and duration between experimental approaches, as well as actions at multiple sites of the respiratory control network.

Respiratory neurons at multiple brainstem sites have key roles in generating homeostatic respiratory rhythm, with inspiratory neurons at the preBötC coming to the fore as key players in this process. Exposure to CIH has been shown to alter the electrophysiological properties of these neurons (Moraes et al., 2013) and respiratory circuits at the level of the preBötC, in turn affecting transmission to the hypoglossal motor nucleus leading to increased transmission failure to the hypoglossal nerve (Garcia et al., 2016). Furthermore, complete ablation of the preBötC increases the propensity for apnoea in sleeping rats (McKay and Feldman, 2008). ROS are implicated in multiple forms of IH-induced plasticity, with H_2O_2 capable of modulating rhythmogenesis by the preBötC (Garcia et al., 2011). Notably, antioxidant therapy has been shown to successfully reduce CIH-mediated irregularities of the network rhythm and improve transmission to the hypoglossal nerve (Garcia et al., 2016). Thus, exposure to CIH may promote a pro-oxidant state which destabilises rhythmogenesis originating from the preBötC. This may represent part of a central mechanism that promotes apnoea and respiratory instability.

1.10.3 CIH and respiratory muscle weakness

UA dilator muscles are pivotal in the maintenance of airway patency. Impaired function of these striated muscles is a well-described contributor to perpetuated respiratory pathology in OSAS (Petrof et al., 1996, Bradford et al., 2005). The structure and function of UA muscles is altered in patients with OSAS, with these functional deficits subsequently contributing to upper airway collapse (Sérlès et al., 1996, Carrera et al., 1999). It was first demonstrated in the early 2000s that CIH, the hallmark feature of OSAS, alters respiratory muscle function. Studies examining the contractile function of the geniohyoid, a representative upper airway muscle, in rats revealed a CIH-induced increase in muscle fatigue (McGuire et al., 2002a, McGuire et al., 2002b, Bradford et al., 2005). A plethora of studies demonstrating CIH-induced muscle weakness and/or fatigue in representative UA muscles including the geniohyoid, genioglossus and sternohyoid, have since come to the fore (Liu et al., 2005, Pae et al., 2005, Dunleavy et al., 2008, Liu et al., 2009, Jia and Liu, 2010, Ding and Liu, 2011, Skelly et al., 2012b, Wang et al., 2013b, Zhou and Liu, 2013, McDonald et al., 2015). Perhaps not surprisingly, outcomes are variable, with notable differences in the pattern and duration of the CIH employed in the studies, as well as differences in the sex and age used across models.

CIH-induced UA muscle dysfunction has been demonstrated both in male and female rat pups (McDonald et al., 2015). However, there is evidence to suggest that the effects of exposure to CIH in adults are sex-specific, as sternohyoid muscle weakness has been demonstrated in male, but not female rats (Skelly et al., 2012b). If this CIH-induced UA muscle weakness translates into an increased propensity for airway collapse, it may be reflective of the human condition, as male sex is an independent risk factor for the development of OSAS (Lin et al., 2008). Moreover, the administration of oestrogen prevents against CIH-induced genioglossus dysfunction in female rats. This highlights that female hormones may have a protective role against the deleterious effects of exposure to CIH on respiratory muscle function (Liu et al., 2009, Jia and Liu, 2010, Zhou and Liu, 2013). In addition, age-specific effects of exposure to CIH on respiratory muscle function have been described. The exposure of aged male rats to CIH revealed no effect on sternohyoid muscle force or endurance

(Skelly et al., 2012a). As this group have previously exhibited CIH-induced sternohyoid muscle weakness in adult male rats using the same CIH paradigm (Skelly et al., 2012b), the lack of an effect on contractile function in this instance was deemed a justified age effect, perhaps related to the confirmed increased glycolytic capacity in the upper airway muscles of aged rats. Exposure to CIH during neonatal development has also been shown to cause sternohyoid muscle weakness in male and female rats (McDonald et al., 2015). Moreover, this muscle dysfunction persists into young adult life following the return to normoxia, suggesting that there is a critical window during development where UA muscles are most susceptible to impairment, perhaps related to epigenetic modifications. The latter findings may have relevance to long-term cardiorespiratory outcomes in human infants with disordered breathing (e.g. apnoea of prematurity).

There remains a paucity of information pertaining to the mechanisms underlying CIH-induced UA muscle dysfunction. Shifts in the structural phenotype of UA muscles have been described in OSAS patients, which may underlie alterations to the functional output of these muscles (Sérlès et al., 1996, Ferini-Strambi et al., 1998). Indeed, fibre-type transitions from a slow-to-fast phenotype have been observed in human OSAS (Smirne et al., 1991), as well as in the English bulldog model of this disorder (Petrof et al., 1994). A relatively short duration of exposure to CIH has been shown to be sufficient to induce a fibre-type transition to predominantly type 2b fibres in the geniohyoid and sternohyoid muscles, thus yielding a more fatigable muscle phenotype (Pae et al., 2005). While these fibre-type transitions may initially be adaptive in order to generate large forces necessary to maintain a patent airway in patients with compromised airway patency, it will eventually manifest as mal-adaptive as UA muscles are more prone to fatigue, which likely contributes to recurring occlusive events. However, structural alterations to UA muscles, manifesting as fibre-type transitions and/or atrophy, are not obligatory for the development of CIH-induced muscle dysfunction. This is evident through a multitude of studies which report little to no alteration to UA muscle fibre-type composition or cross-sectional area following exposure to CIH (McGuire et al., 2002a, Skelly et al., 2012b, McDonald et al., 2015). Succinate dehydrogenase (SDH), citrate synthase and

glycerol-3-phosphate (GPDH) activity, indices of oxidative and glycolytic capacity respectively, also remain unchanged in UA muscles following exposure to CIH (Skelly et al., 2012b, Skelly et al., 2012a, McDonald et al., 2015, Williams et al., 2015b). This provides further affirmation that some paradigms of CIH, sufficient to cause muscle weakness, result in no major alteration to the metabolic profile of the muscle, an effect that that is commonly seen following sustained hypoxia and may contribute to the deficits in the contractile function of muscle in this instance (O'Leary and O'Halloran, 2016, Lewis and O'Halloran, 2016).

OSAS is widely considered to be an oxidative stress disorder with a strong link emerging between CIH-induced increases in ROS and impaired muscle function. A decrease in enzymes relating to antioxidant status including aconitase, glutathione reductase (GR), glutathione peroxidase (GPX), CAT and SOD have been reported in UA muscles following exposure to CIH (Ding and Liu, 2011, Williams et al., 2015b). This decrease in antioxidant capacity is suggestive of a modest oxidative stress or an imbalance in redox status, which may have mal-adaptive consequences for the force-generating capacity of muscle. ROS-dependent UA muscle dysfunction occurs in the absence of overt oxidative stress, which is typically observed as increased protein oxidation or lipid peroxidation. Indeed, unaltered levels of protein thiols, carbonyls and 4-HNE have been reported in the UA muscles of various models of CIH (Williams et al., 2015b, McDonald et al., 2015), notwithstanding evidence of muscle dysfunction. While sustained hypoxia appears to enable the stabilisation of HIF-1α (Nguyen et al., 2016), fewer studies have observed HIF-1α stabilisation in skeletal muscle during IH. This is possibly due to transient stabilisation as a result of alternating periods of hypoxia followed by re-oxygenation. Indeed, exposure to CIH yielded no change in HIF-1α protein content in the sternohyoid muscle (Williams et al., 2015a).

Antioxidant supplementation ameliorates or prevents UA muscle dysfunction following exposure to CIH in rat models (Liu et al., 2005, Dunleavy et al., 2008, Skelly et al., 2012b, Skelly et al., 2013). Disruption of the endogenous glutathione antioxidant system using buthionine sulfoxamine (BSO) results in an exacerbation of

CIH-induced sternohyoid muscle fatigue (Dunleavy et al. 2008). Moreover, administration of the glutathione precursor, NAC, throughout the exposure to CIH prevented muscle dysfunction, highlighting the protective effect of the glutathione system against excessive ROS (Dunleavy et al., 2008). Similarly, the administration of the superoxide scavenger, tempol, has proved efficacious in preventing CIH-induced sternohyoid muscle dysfunction. Interestingly, the application of tempol acutely, also reverses CIH-induced muscle weakness (Skelly et al., 2012b). This suggests that the mechanism underpinning CIH-induced UA muscle dysfunction is likely to be a subtle, reversible stimulus such as the redox modulation of EC coupling and thus alterations to muscle contractile proteins, as opposed to muscle weakness due to structural changes or severe oxidative damage. By extension, a recent study by the same group proposes that NOX2-dependent ROS may be implicated in CIH-induced UA muscle dysfunction. A CIH-induced increase in the protein expression of NOX2 and the activator subunit, p47phox, was observed in sternohyoid muscle in the absence of overt oxidative stress, supporting the notion that altered redox signalling is sufficient to drive muscle dysfunction (Williams et al., 2015b).

Diaphragm muscle dysfunction has been also reported in OSAS patients (Griggs et al., 1989, Chien et al., 2010b), and animals exposed to tracheal occlusion (Smith et al., 2012). Conversely, there is also evidence that diaphragm dysfunction does not present in OSAS patients (Montserrat et al., 1997). These divergences are likely due to differences in the severity of OSAS in patients or varied paradigms of hypoxia utilised in animal models. During inspiration, the contraction of the diaphragm plays an essential role in the determination of UA patency. A fine balance between the dilating and stabilising forces produced by UA muscles and the sub-atmospheric, collapsing pressure of the diaphragm ensures that UA calibre remains patent (Brouillette and Thach, 1979a). During OSAS, the diaphragm is under considerable stress, as a consequence of heavy and prolonged contractions during hypoxic periods. This may culminate in tissue hypoxia and disordered energy balance, rendering it more susceptible to further damage, stress and dysfunction (Clanton et al., 2001). It has also been suggested that the diaphragm is susceptible to fatigue during apnoeic episodes in OSAS patients (Vincken et al., 1987). Diaphragm fatigue

may represent a reduction in the collapsing force during apnoeas, thereby functioning to offset the effect of UA muscle dysfunction on OSAS pathology. CIH-induced muscle plasticity has been shown to extend to the diaphragm, however the underlying mechanisms are largely underexplored.

The effects of exposure to CIH are largely reliant on the duration and intensity of exposure and thus, varied effects of exposure to IH on diaphragm muscle function have been reported (Clanton et al., 2001, McGuire et al., 2003a, Pae et al., 2005, Shortt et al., 2014, Giordano et al., 2015). A relatively short duration of IH (hours), previously shown to induce UA muscle fatigue, was insufficient to cause an alteration to the force-generating capacity of the diaphragm. Similarly, this IH exposure resulted in no observable effect on diaphragm fibre-type composition (Pae et al., 2005). However, 4 days of IH has been shown to cause diaphragm muscle fatigue. Following IH exposure, the diaphragm demonstrated significant atrophy with a concomitant increase in the mRNA expression of autophagy markers, LC3B, GABA(A) receptor-associated-protein-like 3 (GABARAPL1) and BCL2 interacting protein 3 (BNIP3), with no alteration to the levels of MuRF1 or Atrogin-1. Additionally, a fibre-type shift towards type-1 fibres was exhibited, suggestive of a compensatory metabolic adaptation associated with fatigue resistance (Giordano et al., 2015). Elevated diaphragm force with improved anoxic tolerance and no alteration to fatigue or fibre-type composition has been observed following a longer IH treatment (10 days) in rats. It is postulated that this paradigm of IH evokes adaptive responses in the diaphragm that preserve its function in anoxia (Clanton et al., 2001). These time- and intensity-dependent effects of IH on the contractile properties of the diaphragm are well demonstrated in a study by (Shortt et al., 2014). Diaphragm muscle contractile properties were unaltered following exposure to 1 week of IH, while 2 weeks was sufficient to significantly decrease diaphragm force and endurance. A CIH-induced increase in the density of type 2b fibres was reported (Shortt et al., 2013, Shortt et al., 2014), suggestive of a shift to a more fatigable phenotype. CIH-induced diaphragm dysfunction occurred in the absence of an alteration to SDH or GPDH activity (Shortt et al., 2013, Shortt et al., 2014), thus an alteration to metabolic enzymes is not likely to underlie the increase in diaphragm

muscle fatigue. Similarly, diaphragm fatigue has also been reported following exposure to 5 weeks of CIH with attendant increase in the proportion of type 2b fibres (McGuire et al., 2003a). Additionally, many patients with DMD are diagnosed with SDB and of particular interest, exposure to CIH has been shown to exacerbate respiratory muscle dysfunction in DMD by reducing diaphragm strength by a further 30% (Farkas et al., 2007).

Similar to studies in UA musculature, increased ROS production has been implicated in diaphragm muscle dysfunction and indeed, antioxidants have been efficacious in preventing diaphragm weakness and fatigue (Shortt et al., 2014). The latter study demonstrated that 2 weeks of exposure to CIH resulted in no alteration to levels of malondialdehyde or 4-HNE (markers of lipid peroxidation), however exposure to CIH did significantly increase DNA oxidation and the GSSG/GSH ratio, indicative of modest oxidative stress. Administration of tempol, apocynin and NAC each prevented CIH-induced diaphragm muscle fatigue, with NAC proving most efficacious since it also prevented CIH-induced muscle weakness, likely through increased levels of GSH and reduced levels of GSSG. While atrophy and fibre-type transitions have been described in the diaphragm following IH (Shortt et al., 2014, Giordano et al., 2015), aberrant diaphragm function is not likely to be underpinned by these structural alterations as muscle contractile properties were fully recovered following antioxidant supplementation in the absence of amelioration or prevention of a CIH-induced increase in the areal density of 2b muscle fibres (Shortt et al., 2014). Collectively, these observations suggest that, similar to the UA musculature, altered redox signalling may underlie alterations in the contractile function of the diaphragm due to the lack of an apparent overt redox signature and metabolic remodelling, which are seen in models of chronic sustained hypoxia (Lewis et al., 2016). Interestingly, inhibiting NOX2-dependent ROS production increases force and respiratory function in dystrophic diaphragm (Loehr et al., 2018), further highlighting a potential role for apocynin and NOX2 blockade in the prevention of CIH-induced diaphragm muscle weakness.

1.11 Thesis aims and structure

The overarching aim of this thesis was to examine the role of NOX2 in chronic intermittent hypoxia (CIH)-induced respiratory system plasticity in a mouse model of obstructive sleep apnoea syndrome (OSAS).

Specific aims:

- To characterise the effects of exposure to CIH on respiratory muscle (sternohyoid and diaphragm) function in adult male mice.

- To characterise the effects of exposure to CIH on respiratory control in adult male mice.

- To examine the efficacy of the putative NOX2 inhibitor/antioxidant, apocynin, on respiratory muscle function and respiratory control in mice exposed to CIH.

- To examine the specific role of NOX2 in CIH-induced respiratory muscle weakness and apnoea, through the use of transgenic NOX2 null mice.

1.12 References

ABRAMSON, J. J. & SALAMAZ, G. 1988. Sulfhydryl oxidation and Ca2+ release from sarcoplasmic reticulum. *Molecular and Cellular Biochemistry,* 82**,** 81-84.

ABUBAKER, A. A., VARA, D., VISCONTE, C., EGGLESTON, I., TORTI, M., CANOBBIO, I. & PULA, G. 2019. Amyloid Peptide β1-42 Induces Integrin αIIbβ3 Activation, Platelet Adhesion, and Thrombus Formation in a NADPH Oxidase-Dependent Manner. *Oxid Med Cell Longev,* 2019**,** 1050476.

ACCILI, D. & ARDEN, K. C. 2004. FoxOs at the crossroads of cellular metabolism, differentiation, and transformation. *Cell,* 117**,** 421-6.

ADAMS, G. R. & MCCUE, S. A. 1998. Localized infusion of IGF-I results in skeletal muscle hypertrophy in rats. *J Appl Physiol (1985),* 84**,** 1716-22.

ADIBHATLA, R. M. & HATCHER, J. F. 2008. Altered Lipid Metabolism in Brain Injury and Disorders. *In:* QUINN, P. J. & WANG, X. (eds.) *Lipids in Health and Disease.* Dordrecht: Springer Netherlands.

AGO, T., KURODA, J., PAIN, J., FU, C., LI, H. & SADOSHIMA, J. 2010. Upregulation of Nox4 by hypertrophic stimuli promotes apoptosis and mitochondrial dysfunction in cardiac myocytes. *Circ Res,* 106**,** 1253-64.

AHN, B., BEHARRY, A. W., COBLENTZ, P. D., PATEL, N., JUDGE, A. R., BONNELL, M. R. & HOOPES, C. W. Diaphragm Abnormalities in Heart Failure Patients: Upregulation of NAD(P)H Oxidase Subunits and Heightened Protein Oxidation. *C73. OXIDANTS.*

AHN, B., BEHARRY, A. W., FRYE, G. S., JUDGE, A. R. & FERREIRA, L. F. 2015. NAD(P)H oxidase subunit p47phox is elevated, and p47phox knockout prevents diaphragm contractile dysfunction in heart failure. *Am J Physiol Lung Cell Mol Physiol,* 309**,** L497-505.

AHN, B., COBLENTZ, P. D., BEHARRY, A. W., PATEL, N., JUDGE, A. R., MOYLAN, J. S., HOOPES, C. W., BONNELL, M. R. & FERREIRA, L. F. 2017. Diaphragm Abnormalities in Patients with End-Stage Heart Failure: NADPH Oxidase Upregulation and Protein Oxidation. *Frontiers in Physiology,* 7.

AIKEN, C. T., KAAKE, R. M., WANG, X. & HUANG, L. 2011. Oxidative Stress-Mediated Regulation of Proteasome Complexes. *Molecular & Cellular Proteomics,* 10.

AL LAWATI, N. M., PATEL, S. R. & AYAS, N. T. 2009. Epidemiology, risk factors, and consequences of obstructive sleep apnea and short sleep duration. *Prog Cardiovasc Dis,* 51**,** 285-93.

ALMENDROS, I., MONTSERRAT, J. M., TORRES, M., DALMASES, M., CABAÑAS, M. L., CAMPOS-RODRÍGUEZ, F., NAVAJAS, D. & FARRÉ, R. 2013. Intermittent hypoxia increases melanoma metastasis to the lung in a mouse model of sleep apnea. *Respir Physiol Neurobiol,* 186**,** 303-7.

ALMENDROS, I., WANG, Y. & GOZAL, D. 2014. The polymorphic and contradictory aspects of intermittent hypoxia. *Am J Physiol Lung Cell Mol Physiol,* 307**,** L129-40.

ALTENHÖFER, S., RADERMACHER, K. A., KLEIKERS, P. W., WINGLER, K. & SCHMIDT, H. H. 2015. Evolution of NADPH Oxidase Inhibitors: Selectivity and Mechanisms for Target Engagement. *Antioxid Redox Signal,* 23**,** 406-27.

AMEZIANE-EL-HASSANI, R., TALBOT, M., DE SOUZA DOS SANTOS, M. C., AL GHUZLAN, A., HARTL, D., BIDART, J. M., DE DEKEN, X., MIOT, F., DIALLO, I., DE VATHAIRE, F., SCHLUMBERGER, M. &

DUPUY, C. 2015. NADPH oxidase DUOX1 promotes long-term persistence of oxidative stress after an exposure to irradiation. *Proc Natl Acad Sci U S A,* 112**,** 5051-6.

APPELBERG, J. & SUNDSTRÖM, G. 1997. Ventilatory response to CO2 in patients with snoring, obstructive hypopnoea and obstructive apnoea. *Clin Physiol,* 17**,** 497-507.

APPUKUTTAN, B., MA, Y., STEMPEL, A., ASHANDER, L. M., DELIYANTI, D., WILKINSON-BERKA, J. L. & SMITH, J. R. 2018. Effect of NADPH oxidase 1 and 4 blockade in activated human retinal endothelial cells. *Clin Exp Ophthalmol,* 46**,** 652-660.

ARAGONES, J., SCHNEIDER, M., VAN GEYTE, K., FRAISL, P., DRESSELAERS, T., MAZZONE, M., DIRKX, R., ZACCHIGNA, S., LEMIEUX, H., JEOUNG, N. H., LAMBRECHTS, D., BISHOP, T., LAFUSTE, P., DIEZ-JUAN, A., HARTEN, S. K., VAN NOTEN, P., DE BOCK, K., WILLAM, C., TJWA, M., GROSFELD, A., NAVET, R., MOONS, L., VANDENDRIESSCHE, T., DEROOSE, C., WIJEYEKOON, B., NUYTS, J., JORDAN, B., SILASI-MANSAT, R., LUPU, F., DEWERCHIN, M., PUGH, C., SALMON, P., MORTELMANS, L., GALLEZ, B., GORUS, F., BUYSE, J., SLUSE, F., HARRIS, R. A., GNAIGER, E., HESPEL, P., VAN HECKE, P., SCHUIT, F., VAN VELDHOVEN, P., RATCLIFFE, P., BAES, M., MAXWELL, P. & CARMELIET, P. 2008. Deficiency or inhibition of oxygen sensor Phd1 induces hypoxia tolerance by reprogramming basal metabolism. *Nat Genet,* 40**,** 170-80.

ASFOUR, H. A., ALLOUH, M. Z. & SAID, R. S. 2018. Myogenic regulatory factors: The orchestrators of myogenesis after 30 years of discovery. *Exp Biol Med (Maywood),* 243**,** 118-128.

ASHRAFI, G. & SCHWARZ, T. L. 2015. PINK1- and PARK2-mediated local mitophagy in distal neuronal axons. *Autophagy,* 11**,** 187-9.

AUGSBURGER, F., FILIPPOVA, A., RASTI, D., SEREDENINA, T., LAM, M., MAGHZAL, G., MAHIOUT, Z., JANSEN-DÜRR, P., KNAUS, U. G., DOROSHOW, J., STOCKER, R., KRAUSE, K. H. & JAQUET, V. 2019. Pharmacological characterization of the seven human NOX isoforms and their inhibitors. *Redox Biol,* 26**,** 101272.

AUSÍN, P., MARTÍNEZ-LLORENS, J., SABATÉ-BRESCO, M., CASADEVALL, C., BARREIRO, E. & GEA, J. 2017. Sex differences in function and structure of the quadriceps muscle in chronic obstructive pulmonary disease patients. *Chron Respir Dis,* 14**,** 127-139.

BAKAVAYEV, S., CHETRIT, N., ZVAGELSKY, T., MANSOUR, R., VYAZMENSKY, M., BARAK, Z., ISRAELSON, A. & ENGEL, S. 2019. Cu/Zn-superoxide dismutase and wild-type like fALS SOD1 mutants produce cytotoxic quantities of H2O2 via cysteine-dependent redox short-circuit. *Scientific Reports,* 9**,** 10826.

BAKER, T. L. & MITCHELL, G. S. 2000. Episodic but not continuous hypoxia elicits long-term facilitation of phrenic motor output in rats. *J Physiol,* 529 Pt 1**,** 215-9.

BAMMAN, M. M., SHIPP, J. R., JIANG, J., GOWER, B. A., HUNTER, G. R., GOODMAN, A., MCLAFFERTY, C. L., JR. & URBAN, R. J. 2001. Mechanical load increases muscle IGF-I and androgen receptor mRNA concentrations in humans. *Am J Physiol Endocrinol Metab,* 280**,** E383-90.

BANFI, B., MALGRANGE, B., KNISZ, J., STEGER, K., DUBOIS-DAUPHIN, M. & KRAUSE, K. H. 2004a. NOX3, a superoxide-generating NADPH oxidase of the inner ear. *J Biol Chem,* 279**,** 46065-72.

BANFI, B., TIRONE, F., DURUSSEL, I., KNISZ, J., MOSKWA, P., MOLNAR, G. Z., KRAUSE, K. H. & COX, J. A. 2004b. Mechanism of Ca2+ activation of the NADPH oxidase 5 (NOX5). *J Biol Chem,* 279**,** 18583-91.

BANG, H. O. & DYERBERG, J. 1980. Lipid Metabolism and Ischemic Heart Disease in Greenland Eskimos. *In:* DRAPER, H. H. (ed.) *Advances in Nutritional Research.* Boston, MA: Springer US.

BECKER, H. F., JERRENTRUP, A., PLOCH, T., GROTE, L., PENZEL, T., SULLIVAN, C. E. & PETER, J. H. 2003. Effect of nasal continuous positive airway pressure treatment on blood pressure in patients with obstructive sleep apnea. *Circulation,* 107**,** 68-73.

BEDARD, K. & KRAUSE, K.-H. 2007. The NOX family of ROS-generating NADPH oxidases: physiology and pathophysiology. *Physiol Rev,* 87.

BIKLE, D. D., TAHIMIC, C., CHANG, W., WANG, Y., PHILIPPOU, A. & BARTON, E. R. 2015. Role of IGF-I signaling in muscle bone interactions. *Bone,* 80**,** 79-88.

BOWEN, T. S., BRAUER, D., ROLIM, N. P. L., BÆKKERUD, F. H., KRICKE, A., ORMBOSTAD BERRE, A. M., FISCHER, T., LINKE, A., DA SILVA, G. J., WISLOFF, U. & ADAMS, V. 2017. Exercise Training Reveals Inflexibility of the Diaphragm in an Animal Model of Patients With Obesity-Driven Heart Failure With a Preserved Ejection Fraction. *J Am Heart Assoc,* 6.

BRADFORD, A. 2013. Transcranial magnetic stimulation--a potential unobtrusive, non-invasive and drug-free treatment for obstructive sleep apnoea. *Exp Physiol,* 98**,** 882.

BRADFORD, A., MCGUIRE, M. & O'HALLORAN, K. D. 2005. Does episodic hypoxia affect upper airway dilator muscle function? Implications for the pathophysiology of obstructive sleep apnoea. *Respir Physiol Neurobiol,* 147**,** 223-34.

BRANDES, R. P., WEISSMANN, N. & SCHRODER, K. 2014. Nox family NADPH oxidases: Molecular mechanisms of activation. *Free Radic Biol Med,* 76**,** 208-26.

BRENNICK, M. J., PICKUP, S., CATER, J. R. & KUNA, S. T. 2006. Phasic respiratory pharyngeal mechanics by magnetic resonance imaging in lean and obese zucker rats. *Am J Respir Crit Care Med,* 173**,** 1031-7.

BROUILLETTE, R. T. & THACH, B. T. 1979a. A neuromuscular mechanism maintaining extrathoracic airway patency. *J Appl Physiol Respir Environ Exerc Physiol,* 46**,** 772-9.

BROUILLETTE, R. T. & THACH, B. T. 1979b. A neuromuscular mechanism maintaining extrathoracic airway patency. *Journal of Applied Physiology,* 46**,** 772-779.

BRUIJN, L. I., MILLER, T. M. & CLEVELAND, D. W. 2004. Unraveling the mechanisms involved in motor neuron degeneration in ALS. *Annu Rev Neurosci,* 27**,** 723-49.

BURNS, D. P., CANAVAN, L., ROWLAND, J., O'FLAHERTY, R., BRANNOCK, M., DRUMMOND, S. E., O'MALLEY, D., EDGE, D. & O'HALLORAN, K. D. 2018. Recovery of respiratory function in mdx mice co-treated with neutralizing interleukin-6 receptor antibodies and urocortin-2. *J Physiol,* 596**,** 5175-5197.

BURNS, D. P., DRUMMOND, S. E., BOLGER, D., COISCAUD, A., MURPHY, K. H., EDGE, D. & O'HALLORAN, K. D. 2019. N-acetylcysteine Decreases Fibrosis and Increases Force-Generating Capacity of mdx Diaphragm. *Antioxidants (Basel),* 8.

BURNS, D. P., ROY, A., LUCKING, E. F., MCDONALD, F. B., GRAY, S., WILSON, R. J., EDGE, D. & O'HALLORAN, K. D. 2017. Sensorimotor control of breathing in the mdx mouse model of Duchenne muscular dystrophy. *J Physiol,* 595**,** 6653-6672.

BÁNFI, B., CLARK, R. A., STEGER, K. & KRAUSE, K.-H. 2003. Two Novel Proteins Activate Superoxide Generation by the NADPH Oxidase NOX1. *Journal of Biological Chemistry,* 278**,** 3510-3513.

BÁNFI, B., MOLNÁR, G., MATURANA, A., STEGER, K., HEGEDÛS, B., DEMAUREX, N. & KRAUSE, K.-H. 2001. A Ca2+-activated NADPH Oxidase in Testis, Spleen, and Lymph Nodes. *Journal of Biological Chemistry,* 276**,** 37594-37601.

CABISCOL, E., PIULATS, E., ECHAVE, P., HERRERO, E. & ROS, J. 2000. Oxidative stress promotes specific protein damage in Saccharomyces cerevisiae. *J Biol Chem,* 275**,** 27393-8.

CARRERA, M., BARBÉ, F., SAULEDA, J., TOMÁS, M., GÓMEZ, C. & AGUSTÍ, A. G. 1999. Patients with obstructive sleep apnea exhibit genioglossus dysfunction that is normalized after treatment with continuous positive airway pressure. *Am J Respir Crit Care Med,* 159**,** 1960-6.

CARTER, M. E. & BRUNET, A. 2007. FOXO transcription factors. *Current biology : CB,* 17**,** R113-R114.

CASAS, A. I., KLEIKERS, P. W., GEUSS, E., LANGHAUSER, F., ADLER, T., BUSCH, D. H., GAILUS-DURNER, V., DE ANGELIS, M. H., EGEA, J., LOPEZ, M. G., KLEINSCHNITZ, C. & SCHMIDT, H. H. 2019. Calcium-dependent blood-brain barrier breakdown by NOX5 limits postreperfusion benefit in stroke. *J Clin Invest,* 129**,** 1772-1778.

CHA, J. J., MIN, H. S., KIM, K. T., KIM, J. E., GHEE, J. Y., KIM, H. W., LEE, J. E., HAN, J. Y., LEE, G., HA, H. J., BAE, Y. S., LEE, S. R., MOON, S. H., LEE, S. C., KIM, G., KANG, Y. S. & CHA, D. R. 2017. APX-115, a first-in-class pan-NADPH oxidase (Nox) inhibitor, protects db/db mice from renal injury. *Lab Invest,* 97**,** 419-431.

CHAILLOU, T. 2018. Skeletal Muscle Fiber Type in Hypoxia: Adaptation to High-Altitude Exposure and Under Conditions of Pathological Hypoxia. *Frontiers in Physiology,* 9.

CHARGÉ, S. B. & RUDNICKI, M. A. 2004. Cellular and molecular regulation of muscle regeneration. *Physiol Rev,* 84**,** 209-38.

CHATTERJEE, S., FUJIWARA, K., PEREZ, N. G., USHIO-FUKAI, M. & FISHER, A. B. 2015. Mechanosignaling in the vasculature: emerging concepts in sensing, transduction and physiological responses. *Am J Physiol Heart Circ Physiol,* 308**,** H1451-62.

CHEN, H. H., LU, J., GUAN, Y. F., LI, S. J., HU, T. T., XIE, Z. S., WANG, F., PENG, X. H., LIU, X., XU, X., ZHAO, F. P., YU, B. L. & LI, X. P. 2016. Estrogen/ERR-α signaling axis is associated with fiber-type conversion of upper airway muscles in patients with obstructive sleep apnea hypopnea syndrome. *Sci Rep,* 6**,** 27088.

CHEN, L. & SCHARF, S. M. 2000. Effects of aortic nerve on hemodynamic response to obstructive apnea in sedated pigs. *J Appl Physiol (1985),* 89**,** 1455-61.

CHENG, G., CAO, Z., XU, X., VAN MEIR, E. G. & LAMBETH, J. D. 2001. Homologs of gp91phox: cloning and tissue expression of Nox3, Nox4, and Nox5. *Gene,* 269**,** 131-40.

CHENG, G., DIEBOLD, B. A., HUGHES, Y. & LAMBETH, J. D. 2006. Nox1-dependent Reactive Oxygen Generation Is Regulated by Rac1. *Journal of Biological Chemistry,* 281**,** 17718-17726.

CHENG, G., RITSICK, D. & LAMBETH, J. D. 2004. Nox3 Regulation by NOXO1, p47phox, and p67phox. *Journal of Biological Chemistry,* 279**,** 34250-34255.

CHIEN, M.-Y., WU, Y.-T., LEE, P.-L., CHANG, Y.-J. & YANG, P.-C. 2010a. Inspiratory muscle dysfunction in patients with severe obstructive sleep apnoea. *European Respiratory Journal,* 35**,** 373-380.

CHIEN, M. Y., WU, Y. T., LEE, P. L., CHANG, Y. J. & YANG, P. C. 2010b. Inspiratory muscle dysfunction in patients with severe obstructive sleep apnoea. *Eur Respir J,* 35**,** 373-80.

CLANTON, T. L. 2007. Hypoxia-induced reactive oxygen species formation in skeletal muscle. *J Appl Physiol (1985),* 102**,** 2379-88.

CLANTON, T. L., WRIGHT, V. P., REISER, P. J., KLAWITTER, P. F. & PRABHAKAR, N. R. 2001. Selected Contribution: Improved anoxic tolerance in rat diaphragm following intermittent hypoxia. *Journal of Applied Physiology,* 90**,** 2508-2513.

CLARKE, B. A., DRUJAN, D., WILLIS, M. S., MURPHY, L. O., CORPINA, R. A., BUROVA, E., RAKHILIN, S. V., STITT, T. N., PATTERSON, C., LATRES, E. & GLASS, D. J. 2007. The E3 Ligase MuRF1 degrades myosin heavy chain protein in dexamethasone-treated skeletal muscle. *Cell Metab,* 6**,** 376-85.

CORCORAN, A. E., HODGES, M. R., WU, Y., WANG, W., WYLIE, C. J., DENERIS, E. S. & RICHERSON, G. B. 2009. Medullary serotonin neurons and central CO2 chemoreception. *Respir Physiol Neurobiol,* 168**,** 49-58.

CRISWELL, D., POWERS, S., DODD, S., LAWLER, J., EDWARDS, W., RENSHLER, K. & GRINTON, S. 1993. High intensity training-induced changes in skeletal muscle antioxidant enzyme activity. *Med Sci Sports Exerc,* 25**,** 1135-40.

CROWN, A. M., ROBERTS, B. L., CROSBY, K., BROWN, H., AYERS, J. I., HART, P. J. & BORCHELT, D. R. 2019. Experimental Mutations in Superoxide Dismutase 1 Provide Insight into Potential Mechanisms Involved in Aberrant Aggregation in Familial Amyotrophic Lateral Sclerosis. *G3 (Bethesda),* 9**,** 719-728.

CRUMMY, F., PIPER, A. J. & NAUGHTON, M. T. 2008. Obesity and the lung: 2. Obesity and sleep-disordered breathing. *Thorax,* 63**,** 738-46.

CUTLIP, R. G., BAKER, B. A., GERONILLA, K. B., MERCER, R. R., KASHON, M. L., MILLER, G. R., MURLASITS, Z. & ALWAY, S. E. 2006. Chronic exposure to stretch-shortening contractions results in skeletal muscle adaptation in young rats and maladaptation in old rats. *Appl Physiol Nutr Metab,* 31**,** 573-87.

DALE, E. A., BEN MABROUK, F. & MITCHELL, G. S. 2014. Unexpected benefits of intermittent hypoxia: enhanced respiratory and nonrespiratory motor function. *Physiology (Bethesda),* 29**,** 39-48.

DAMMEYER, P. & ARNÉR, E. S. 2011. Human Protein Atlas of redox systems - what can be learnt? *Biochim Biophys Acta,* 1810**,** 111-38.

DAO, V. T., ELBATREEK, M. H., ALTENHÖFER, S., CASAS, A. I., PACHADO, M. P., NEULLENS, C. T., KNAUS, U. G. & SCHMIDT, H. 2020. Isoform-selective NADPH oxidase inhibitor panel for pharmacological target validation. *Free Radic Biol Med,* 148**,** 60-69.

DE CARVALHO, M., SWASH, M. & PINTO, S. 2019. Diaphragmatic Neurophysiology and Respiratory Markers in ALS. *Frontiers in Neurology,* 10.

DE DEKEN, X., WANG, D., DUMONT, J. E. & MIOT, F. 2002. Characterization of ThOX Proteins as Components of the Thyroid H2O2-Generating System. *Experimental Cell Research,* 273**,** 187-196.

DE DEKEN, X., WANG, D., MANY, M. C., COSTAGLIOLA, S., LIBERT, F., VASSART, G., DUMONT, J. E. & MIOT, F. 2000. Cloning of two human thyroid cDNAs encoding new members of the NADPH oxidase family. *J Biol Chem,* 275**,** 23227-33.

DE TROYER, A. & ESTENNE, M. 1984. Coordination between rib cage muscles and diaphragm during quiet breathing in humans. *J Appl Physiol Respir Environ Exerc Physiol,* 57**,** 899-906.

DE TROYER, A., NINANE, V., GILMARTIN, J. J., LEMERRE, C. & ESTENNE, M. 1987. Triangularis sterni muscle use in supine humans. *J Appl Physiol (1985),* 62**,** 919-25.

DEBEVEC, T., MILLET, G. P. & PIALOUX, V. 2017. Hypoxia-Induced Oxidative Stress Modulation with Physical Activity. *Frontiers in Physiology,* 8.

DEMPSEY, J. A., VEASEY, S. C., MORGAN, B. J. & O'DONNELL, C. P. 2010. Pathophysiology of sleep apnea. *Physiol Rev,* 90**,** 47-112.

DEVOL, D. L., ROTWEIN, P., SADOW, J. L., NOVAKOFSKI, J. & BECHTEL, P. J. 1990. Activation of insulin-like growth factor gene expression during work-induced skeletal muscle growth. *Am J Physiol,* 259**,** E89-95.

DIAZ, B., SHANI, G., PASS, I., ANDERSON, D., QUINTAVALLE, M. & COURTNEIDGE, S. A. 2009. Tks5-dependent, nox-mediated generation of reactive oxygen species is necessary for invadopodia formation. *Sci Signal,* 2**,** ra53.

DIEBOLD, I., PETRY, A., HESS, J. & GORLACH, A. 2010. The NADPH oxidase subunit NOX4 is a new target gene of the hypoxia-inducible factor-1. *Mol Biol Cell,* 21**,** 2087-96.

DING, W. & LIU, Y. 2011. Genistein attenuates genioglossus muscle fatigue under chronic intermittent hypoxia by down-regulation of oxidative stress level and up-regulation of antioxidant enzyme activity through ERK1/2 signaling pathway. *Oral Dis,* 17**,** 677-84.

DINGER, B., HE, L., CHEN, J., LIU, X., GONZALEZ, C., OBESO, A., SANDERS, K., HOIDAL, J., STENSAAS, L. & FIDONE, S. 2007. The role of NADPH oxidase in carotid body arterial chemoreceptors. *Respir Physiol Neurobiol,* 157**,** 45-54.

DOBROWOLNY, G., AUCELLO, M., RIZZUTO, E., BECCAFICO, S., MAMMUCARI, C., BONCOMPAGNI, S., BELIA, S., WANNENES, F., NICOLETTI, C., DEL PRETE, Z., ROSENTHAL, N., MOLINARO, M., PROTASI, F., FANÒ, G., SANDRI, M. & MUSARÒ, A. 2008. Skeletal muscle is a primary target of SOD1G93A-mediated toxicity. *Cell Metab,* 8**,** 425-36.

DOCIO, I., OLEA, E., PRIETO, L. J., GALLEGO-MARTIN, T., OBESO, A., GOMEZ-NIÑO, A. & ROCHER, A. 2018. Guinea Pig as a Model to Study the Carotid Body Mediated Chronic Intermittent Hypoxia Effects. *Front Physiol,* 9**,** 694.

DONOVAN, L. M., LIU, Y. & WEISS, J. W. 2014. Effect of endothelin antagonism on apnea frequency following chronic intermittent hypoxia. *Respir Physiol Neurobiol,* 194**,** 6-8.

DOPP, J. M., PHILIPPI, N. R., MARCUS, N. J., OLSON, E. B., BIRD, C. E., MORAN, J. J., MUELLER, S. W. & MORGAN, B. J. 2011. Xanthine oxidase inhibition attenuates endothelial dysfunction caused by chronic intermittent hypoxia in rats. *Respiration,* 82**,** 458-67.

DOUCET, M., DEBIGARÉ, R., JOANISSE, D. R., CÔTÉ, C., LEBLANC, P., GRÉGOIRE, J., DESLAURIERS, J., VAILLANCOURT, R. & MALTAIS, F. 2004. Adaptation of the diaphragm and the vastus lateralis in mild-to-moderate COPD. *Eur Respir J,* 24**,** 971-9.

DOUGLAS, N. J., WHITE, D. P., WEIL, J. V., PICKETT, C. K., MARTIN, R. J., HUDGEL, D. W. & ZWILLICH, C. W. 1982a. Hypoxic ventilatory response decreases during sleep in normal men. *Am Rev Respir Dis,* 125**,** 286-9.

DOUGLAS, N. J., WHITE, D. P., WEIL, J. V., PICKETT, C. K. & ZWILLICH, C. W. 1982b. Hypercapnic ventilatory response in sleeping adults. *Am Rev Respir Dis,* 126**,** 758-62.

DRAGER, L. F., LI, J., REINKE, C., BEVANS-FONTI, S., JUN, J. C. & POLOTSKY, V. Y. 2011. Intermittent Hypoxia Exacerbates Metabolic Effects of Diet-Induced Obesity. *Obesity (Silver Spring, Md.),* 19**,** 2167-2174.

DUMITRASCU, R., HEITMANN, J., SEEGER, W., WEISSMANN, N. & SCHULZ, R. 2013. Obstructive sleep apnea, oxidative stress and cardiovascular disease: lessons from animal studies. *Oxid Med Cell Longev,* 2013**,** 234631.

DUNLEAVY, M., BRADFORD, A. & O'HALLORAN, K. D. 2008. Oxidative stress impairs upper airway muscle endurance in an animal model of sleep-disordered breathing. *Adv Exp Med Biol,* 605**,** 458-62.

ECKERT, D. J., MALHOTRA, A. & JORDAN, A. S. 2009. Mechanisms of apnea. *Prog Cardiovasc Dis,* 51**,** 313-23.

EDGE, D., BRADFORD, A. & O'HALLORAN, K. D. 2012. Chronic intermittent hypoxia increases apnoea index in sleeping rats. *Adv Exp Med Biol,* 758**,** 359-63.

EDGE, D., MCDONALD, F. B., JONES, J. F. X., BRADFORD, A. & O'HALLORAN, K. D. 2014. Effect of chronic intermittent hypoxia on the reflex recruitment of the genioglossus during airway obstruction in the anesthetized rat. *Progress in brain research,* 209**,** 147-168.

EDGE, D., SKELLY, J. R., BRADFORD, A. & O'HALLORAN, K. D. 2009. Ventilatory drive is enhanced in male and female rats following chronic intermittent hypoxia. *Adv Exp Med Biol,* 648**,** 337-44.

ELLIOT-PORTAL, E., LAOUAFA, S., ARIAS-REYES, C., JANES, T. A., JOSEPH, V. & SOLIZ, J. 2018. Brain-derived erythropoietin protects from intermittent hypoxia-induced cardiorespiratory dysfunction and oxidative stress in mice. *Sleep,* 41.

EPSTEIN, A. C. R., GLEADLE, J. M., MCNEILL, L. A., HEWITSON, K. S., O'ROURKE, J., MOLE, D. R., MUKHERJI, M., METZEN, E., WILSON, M. I., DHANDA, A., TIAN, Y.-M., MASSON, N., HAMILTON, D. L., JAAKKOLA, P., BARSTEAD, R., HODGKIN, J., MAXWELL, P. H., PUGH, C. W., SCHOFIELD, C. J. & RATCLIFFE, P. J. 2001. C. elegans EGL-9 and Mammalian Homologs Define a Family of Dioxygenases that Regulate HIF by Prolyl Hydroxylation. *Cell,* 107**,** 43-54.

FARKAS, G. A., MCCORMICK, K. M. & GOSSELIN, L. E. 2007. Episodic hypoxia exacerbates respiratory muscle dysfunction in DMD(mdx) mice. *Muscle Nerve,* 36**,** 708-10.

FARRÉ, R., MONTSERRAT, J. M., GOZAL, D., ALMENDROS, I. & NAVAJAS, D. 2018. Intermittent Hypoxia Severity in Animal Models of Sleep Apnea. *Front Physiol,* 9**,** 1556.

FEITELSON, M. A., ARZUMANYAN, A., KULATHINAL, R. J., BLAIN, S. W., HOLCOMBE, R. F., MAHAJNA, J., MARINO, M., MARTINEZ-CHANTAR, M. L., NAWROTH, R., SANCHEZ-GARCIA, I., SHARMA, D., SAXENA, N. K., SINGH, N., VLACHOSTERGIOS, P. J., GUO, S., HONOKI, K., FUJII, H., GEORGAKILAS, A. G., BILSLAND, A., AMEDEI, A., NICCOLAI, E., AMIN, A., ASHRAF, S. S., BOOSANI, C. S., GUHA, G., CIRIOLO, M. R., AQUILANO, K., CHEN, S., MOHAMMED, S. I., AZMI, A. S., BHAKTA, D., HALICKA, D., KEITH, W. N. & NOWSHEEN, S. 2015. Sustained proliferation in cancer: Mechanisms and novel therapeutic targets. *Semin Cancer Biol,* 35 Suppl**,** S25-s54.

FELDMAN, J. L. & DEL NEGRO, C. A. 2006. Looking for inspiration: new perspectives on respiratory rhythm. *Nat Rev Neurosci,* 7**,** 232-42.

FERINI-STRAMBI, L. J., SMIRNE, S., MOZ, U., SFERRAZZA, B. & IANNACCONE, S. 1998. Muscle fibre type and obstructive sleep apnea. *Sleep Res Online,* 1**,** 24-7.

FLETCHER, E. C., LESSKE, J., QIAN, W., MILLER, C. C., 3RD & UNGER, T. 1992. Repetitive, episodic hypoxia causes diurnal elevation of blood pressure in rats. *Hypertension,* 19**,** 555-61.

FLUCK, M. & HOPPELER, H. 2003. Molecular basis of skeletal muscle plasticity--from gene to form and function. *Rev Physiol Biochem Pharmacol,* 146**,** 159-216.

FOGEL, R. B., MALHOTRA, A., PILLAR, G., EDWARDS, J. K., BEAUREGARD, J., SHEA, S. A. & WHITE, D. P. 2001. Genioglossal activation in patients with obstructive sleep apnea versus control subjects. Mechanisms of muscle control. *Am J Respir Crit Care Med,* 164**,** 2025-30.

FRAPPELL, P., LANTHIER, C., BAUDINETTE, R. V. & MORTOLA, J. P. 1992. Metabolism and ventilation in acute hypoxia: a comparative analysis in small mammalian species. *Am J Physiol,* 262**,** R1040-6.

FREGOSI, R. F. & LUDLOW, C. L. 2014. Activation of upper airway muscles during breathing and swallowing. *J Appl Physiol (1985),* 116**,** 291-301.

FRIDOVICH, I. 1995. Superoxide radical and superoxide dismutases. *Annu Rev Biochem,* 64**,** 97-112.

FRONTERA, W. R. & OCHALA, J. 2015. Skeletal muscle: a brief review of structure and function. *Calcif Tissue Int,* 96**,** 183-95.

FRYE, G., AHN, B., BRANDES, R. P., SCHRÖDER, K. & FERREIRA, L. F. 2012. Skeletal muscle force is preserved in NOX4 deficient mice. *The FASEB Journal,* 26**,** 1075.12.

FU, X. W., WANG, D., NURSE, C. A., DINAUER, M. C. & CUTZ, E. 2000. NADPH oxidase is an O2 sensor in airway chemoreceptors: evidence from K+ current modulation in wild-type and oxidase-deficient mice. *Proc Natl Acad Sci U S A,* 97**,** 4374-9.

FUJII, J., IKEDA, Y., KURAHASHI, T. & HOMMA, T. 2015. Physiological and pathological views of peroxiredoxin 4. *Free Radic Biol Med,* 83**,** 373-9.

FUJIWARA, T., HARA, Y. & CHINO, N. 1999. Expiratory function in complete tetraplegics: study of spirometry, maximal expiratory pressure, and muscle activity of pectoralis major and latissimus dorsi muscles. *Am J Phys Med Rehabil,* 78**,** 464-9.

GAGNADOUX, F., FLEURY, B., VIELLE, B., PÉTELLE, B., MESLIER, N., N'GUYEN, X. L., TRZEPIZUR, W. & RACINEUX, J. L. 2009. Titrated mandibular advancement versus positive airway pressure for sleep apnoea. *Eur Respir J,* 34**,** 914-20.

GALLEGO-MARTIN, T., FARRÉ, R., ALMENDROS, I., GONZALEZ-OBESO, E. & OBESO, A. 2017. Chronic intermittent hypoxia mimicking sleep apnoea increases spontaneous tumorigenesis in mice. *Eur Respir J,* 49.

GAMBOA, J. L. & ANDRADE, F. H. 2010. Mitochondrial content and distribution changes specific to mouse diaphragm after chronic normobaric hypoxia. *Am J Physiol Regul Integr Comp Physiol,* 298**,** R575-83.

GARCIA, A. J., 3RD, KHAN, S. A., KUMAR, G. K., PRABHAKAR, N. R. & RAMIREZ, J. M. 2011. Hydrogen peroxide differentially affects activity in the pre-Bötzinger complex and hippocampus. *J Neurophysiol,* 106**,** 3045-55.

GARCIA, A. J., 3RD, KOSCHNITZKY, J. E. & RAMIREZ, J. M. 2013. The physiological determinants of sudden infant death syndrome. *Respir Physiol Neurobiol,* 189**,** 288-300.

GARCIA, A. J., 3RD, ZANELLA, S., DASHEVSKIY, T., KHAN, S. A., KHUU, M. A., PRABHAKAR, N. R. & RAMIREZ, J. M. 2016. Chronic Intermittent Hypoxia Alters Local Respiratory Circuit Function at the Level of the preBötzinger Complex. *Front Neurosci,* 10**,** 4.

GARGAGLIONI, L. H., HARTZLER, L. K. & PUTNAM, R. W. 2010. The locus coeruleus and central chemosensitivity. *Respir Physiol Neurobiol,* 173**,** 264-73.

GIORDANO, C., LEMAIRE, C., LI, T., KIMOFF, R. J. & PETROF, B. J. 2015. Autophagy-associated atrophy and metabolic remodeling of the mouse diaphragm after short-term intermittent hypoxia. *PLoS One,* 10**,** e0131068.

GKIKAS, I., PALIKARAS, K. & TAVERNARAKIS, N. 2018. The Role of Mitophagy in Innate Immunity. *Front Immunol,* 9**,** 1283.

GLASS, D. J. 2003. Molecular mechanisms modulating muscle mass. *Trends Mol Med,* 9**,** 344-50.

GLASS, D. J. 2005. Skeletal muscle hypertrophy and atrophy signaling pathways. *The International Journal of Biochemistry & Cell Biology,* 37**,** 1974-1984.

GLASS, M. J., CHAN, J., FRYS, K. A., OSELKIN, M., TARSITANO, M. J., IADECOLA, C. & PICKEL, V. M. 2007. Changes in the subcellular distribution of NADPH oxidase subunit p47phox in dendrites of rat dorsomedial nucleus tractus solitarius neurons in response to chronic administration of hypertensive agents. *Exp Neurol,* 205**,** 383-95.

GONENC, A., OZKAN, Y., TORUN, M. & SIMSEK, B. 2001. Plasma malondialdehyde (MDA) levels in breast and lung cancer patients. *J Clin Pharm Ther,* 26**,** 141-4.

GONZALEZ-MARTÍN, M. C., VEGA-AGAPITO, M. V., CONDE, S. V., CASTAÑEDA, J., BUSTAMANTE, R., OLEA, E., PEREZ-VIZCAINO, F., GONZALEZ, C. & OBESO, A. 2011. Carotid body function and ventilatory responses in intermittent hypoxia. Evidence for anomalous brainstem integration of arterial chemoreceptor input. *J Cell Physiol,* 226**,** 1961-9.

GORIN, Y., RICONO, J. M., KIM, N. H., BHANDARI, B., CHOUDHURY, G. G. & ABBOUD, H. E. 2003. Nox4 mediates angiotensin II-induced activation of Akt/protein kinase B in mesangial cells. *Am J Physiol Renal Physiol,* 285**,** F219-29.

GOUSPILLOU, G., GODIN, R., PIQUEREAU, J., PICARD, M., MOFARRAHI, M., MATHEW, J., PURVES-SMITH, F. M., SGARIOTO, N., HEPPLE, R. T., BURELLE, Y. & HUSSAIN, S. N. A. 2018. Protective role of Parkin in skeletal muscle contractile and mitochondrial function. *J Physiol,* 596**,** 2565-2579.

GOZAL, D., DANIEL, J. M. & DOHANICH, G. P. 2001. Behavioral and anatomical correlates of chronic episodic hypoxia during sleep in the rat. *J Neurosci,* 21**,** 2442-50.

GRANSEE, H. M., MANTILLA, C. B. & SIECK, G. C. 2012. Respiratory muscle plasticity. *Compr Physiol,* 2**,** 1441-62.

GREENBERG, H. E., SICA, A., BATSON, D. & SCHARF, S. M. 1999. Chronic intermittent hypoxia increases sympathetic responsiveness to hypoxia and hypercapnia. *J Appl Physiol (1985),* 86**,** 298-305.

GRIGGS, G. A., FINDLEY, L. J., SURATT, P. M., ESAU, S. A., WILHOIT, S. C. & ROCHESTER, D. F. 1989. Prolonged relaxation rate of inspiratory muscles in patients with sleep apnea. *Am Rev Respir Dis,* 140**,** 706-10.

GUERRA, L., CERBAI, E., GESSI, S., BOREA, P. A. & MUGELLI, A. 1996. The effect of oxygen free radicals on calcium current and dihydropyridine binding sites in guinea-pig ventricular myocytes. *British Journal of Pharmacology,* 118**,** 1278-1284.

GUYENET, P. G., BAYLISS, D. A., STORNETTA, R. L., FORTUNA, M. G., ABBOTT, S. B. & DEPUY, S. D. 2009. Retrotrapezoid nucleus, respiratory chemosensitivity and breathing automaticity. *Respir Physiol Neurobiol,* 168**,** 59-68.

HADDAD, J. J. 2002. Science review: Redox and oxygen-sensitive transcription factors in the regulation of oxidant-mediated lung injury: role for nuclear factor-kappaB. *Crit Care,* 6**,** 481-90.

HAYASHI, T., YAMASHITA, C., MATSUMOTO, C., KWAK, C.-J., FUJII, K., HIRATA, T., MIYAMURA, M., MORI, T., UKIMURA, A., OKADA, Y., MATSUMURA, Y. & KITAURA, Y. 2008. Role of gp91^{phox}-containing NADPH oxidase in left ventricular remodeling induced by intermittent hypoxic stress. *American Journal of Physiology - Heart and Circulatory Physiology,* 294**,** H2197-H2203.

HENDRICKS, J. C., KLINE, L. R., KOVALSKI, R. J., O'BRIEN, J. A., MORRISON, A. R. & PACK, A. I. 1987. The English bulldog: a natural model of sleep-disordered breathing. *J Appl Physiol (1985),* 63**,** 1344-50.

HENDRICKS, J. C., KOVALSKI, R. J. & KLINE, L. R. 1991. Phasic respiratory muscle patterns and sleep-disordered breathing during rapid eye movement sleep in the English bulldog. *Am Rev Respir Dis,* 144**,** 1112-20.

HENRÍQUEZ-OLGUIN, C., KNUDSEN, J. R., RAUN, S. H., LI, Z., DALBRAM, E., TREEBAK, J. T., SYLOW, L., HOLMDAHL, R., RICHTER, E. A., JAIMOVICH, E. & JENSEN, T. E. 2019. Cytosolic ROS production by NADPH oxidase 2 regulates muscle glucose uptake during exercise. *Nat Commun,* 10**,** 4623.

HEUNKS, L. M., VINA, J., VAN HERWAARDEN, C. L., FOLGERING, H. T., GIMENO, A. & DEKHUIJZEN, P. N. 1999. Xanthine oxidase is involved in exercise-induced oxidative stress in chronic obstructive pulmonary disease. *Am J Physiol,* 277**,** R1697-704.

HEYMES, C., BENDALL, J. K., RATAJCZAK, P., CAVE, A. C., SAMUEL, J. L., HASENFUSS, G. & SHAH, A. M. 2003. Increased myocardial NADPH oxidase activity in human heart failure. *J Am Coll Cardiol,* 41**,** 2164-71.

HIDALGO, C., SANCHEZ, G., BARRIENTOS, G. & ARACENA-PARKS, P. 2006. A transverse tubule NADPH oxidase activity stimulates calcium release from isolated triads via ryanodine receptor type 1 S -glutathionylation. *J Biol Chem,* 281**,** 26473-82.

HO, M. L. & BRASS, S. D. 2011. Obstructive sleep apnea. *Neurol Int,* 3**,** e15.

HO, Y. S., XIONG, Y., MA, W., SPECTOR, A. & HO, D. S. 2004. Mice lacking catalase develop normally but show differential sensitivity to oxidant tissue injury. *J Biol Chem,* 279**,** 32804-12.

HOLLANDER, M. C., BLUMENTHAL, G. M. & DENNIS, P. A. 2011. PTEN loss in the continuum of common cancers, rare syndromes and mouse models. *Nat Rev Cancer,* 11**,** 289-301.

HOPPELER, H. 2014. *Eccentric Exercise: Physiology and application in sport and rehabilitation*, Taylor & Francis.

HOPPELER, H. & VOGT, M. 2001. Muscle tissue adaptations to hypoxia. *J Exp Biol,* 204**,** 3133-9.

HWANG, I., LEE, J., HUH, J. Y., PARK, J., LEE, H. B., HO, Y.-S. & HA, H. 2012. Catalase Deficiency Accelerates Diabetic Renal Injury Through Peroxisomal Dysfunction. *Diabetes,* 61**,** 728-738.

HWANG, I., UDDIN, M. J., PAK, E. S., KANG, H., JIN, E. J., JO, S., KANG, D., LEE, H. & HA, H. 2020. The impaired redox balance in peroxisomes of catalase knockout mice accelerates nonalcoholic fatty liver disease through endoplasmic reticulum stress. *Free Radic Biol Med,* 148**,** 22-32.

INGRAM, K. H., HILL, H., MOELLERING, D. R., HILL, B. G., LARA-CASTRO, C., NEWCOMER, B., BRANDON, L. J., INGALLS, C. P., PENUMETCHA, M., RUPP, J. C. & GARVEY, W. T. 2012. Skeletal muscle lipid peroxidation and insulin resistance in humans. *J Clin Endocrinol Metab,* 97**,** E1182-6.

JACKSON, R. M., PARISH, G. & HO, Y. S. 1996. Effects of hypoxia on expression of superoxide dismutases in cultured ATII cells and lung fibroblasts. *Am J Physiol,* 271**,** L955-62.

JASTROCH, M., DIVAKARUNI, A. S., MOOKERJEE, S., TREBERG, J. R. & BRAND, M. D. 2010. Mitochondrial proton and electron leaks. *Essays Biochem,* 47**,** 53-67.

JAVESHGHANI, D., MAGDER, S. A., BARREIRO, E., QUINN, M. T. & HUSSAIN, S. N. 2002. Molecular characterization of a superoxide-generating NAD(P)H oxidase in the ventilatory muscles. *Am J Respir Crit Care Med,* 165**,** 412-8.

JIA, S. S. & LIU, Y. H. 2010. Down-regulation of hypoxia inducible factor-1alpha: a possible explanation for the protective effects of estrogen on genioglossus fatigue resistance. *Eur J Oral Sci,* 118**,** 139-44.

JIAO, W., JI, J., LI, F., GUO, J., ZHENG, Y., LI, S. & XU, W. 2019. Activation of the Notch-Nox4-reactive oxygen species signaling pathway induces cell death in high glucose-treated human retinal endothelial cells. *Mol Med Rep,* 19**,** 667-677.

JOCHMANS-LEMOINE, A., VILLALPANDO, G., GONZALES, M., VALVERDE, I., SORIA, R. & JOSEPH, V. 2015. Divergent physiological responses in laboratory rats and mice raised at high altitude. *J Exp Biol,* 218**,** 1035-43.

JOSEPH, V., LAOUAFA, S., MARCOUILLER, F., ROUSSEL, D., PIALOUX, V. & BAIRAM, A. 2020. Progesterone decreases apnoea and reduces oxidative stress induced by chronic intermittent hypoxia in ovariectomized female rats. *Exp Physiol,* 105**,** 1025-1034.

JULIEN, C., BAIRAM, A. & JOSEPH, V. 2008. Chronic intermittent hypoxia reduces ventilatory long-term facilitation and enhances apnea frequency in newborn rats. *Am J Physiol Regul Integr Comp Physiol,* 294**,** R1356-66.

KANG, S. W., BAINES, I. C. & RHEE, S. G. 1998. Characterization of a mammalian peroxiredoxin that contains one conserved cysteine. *J Biol Chem,* 273**,** 6303-11.

KARPLUS, P. A. 2015. A primer on peroxiredoxin biochemistry. *Free Radic Biol Med,* 80**,** 183-90.

KATAYAMA, K., SMITH, C. A., HENDERSON, K. S. & DEMPSEY, J. A. 2007. Chronic intermittent hypoxia increases the CO2 reserve in sleeping dogs. *J Appl Physiol (1985),* 103**,** 1942-9.

KE, Q. & COSTA, M. 2006. Hypoxia-inducible factor-1 (HIF-1). *Mol Pharmacol,* 70**,** 1469-80.

KEFALOYIANNI, E., GAITANAKI, C. & BEIS, I. 2006. ERK1/2 and p38-MAPK signalling pathways, through MSK1, are involved in NF-kappaB transactivation during oxidative stress in skeletal myoblasts. *Cell Signal,* 18**,** 2238-51.

KEZIRIAN, E. J., GODING, G. S., MALHOTRA, A., O'DONOGHUE, F. J., ZAMMIT, G., WHEATLEY, J. R., CATCHESIDE, P. G., SMITH, P. L., SCHWARTZ, A. R., WALSH, J. H., MADDISON, K. J., CLAMAN, D. M., HUNTLEY, T., PARK, S. Y., CAMPBELL, M. C., PALME, C. E., IBER, C., EASTWOOD, P. R., HILLMAN, D. R. & BARNES, M. 2014. Hypoglossal Nerve Stimulation Improves Obstructive Sleep Apnea: 12 Month Outcomes. *Journal of sleep research,* 23**,** 77-83.

KHAN, S. A., NANDURI, J., YUAN, G., KINSMAN, B., KUMAR, G. K., JOSEPH, J., KALYANARAMAN, B. & PRABHAKAR, N. R. 2011. NADPH oxidase 2 mediates intermittent hypoxia-induced mitochondrial complex I inhibition: relevance to blood pressure changes in rats. *Antioxid Redox Signal,* 14**,** 533-42.

KHODADADEH, B., BADR, M. S. & MATEIKA, J. H. 2006. The ventilatory response to carbon dioxide and sustained hypoxia is enhanced after episodic hypoxia in OSA patients. *Respir Physiol Neurobiol,* 150**,** 122-34.

KIM, E. K. & CHOI, E.-J. 2010. Pathological roles of MAPK signaling pathways in human diseases. *Biochimica et Biophysica Acta (BBA) - Molecular Basis of Disease,* 1802**,** 396-405.

KIMOFF, R. J., BROOKS, D., HORNER, R. L., KOZAR, L. F., RENDER-TEIXEIRA, C. L., CHAMPAGNE, V., MAYER, P. & PHILLIPSON, E. A. 1997. Ventilatory and arousal responses to hypoxia and hypercapnia in a canine model of obstructive sleep apnea. *Am J Respir Crit Care Med,* 156**,** 886-94.

KISS, P. J., KNISZ, J., ZHANG, Y., BALTRUSAITIS, J., SIGMUND, C. D., THALMANN, R., SMITH, R. J., VERPY, E. & BANFI, B. 2006. Inactivation of NADPH oxidase organizer 1 results in severe imbalance. *Curr Biol,* 16**,** 208-13.

KITZMAN, D. W., NICKLAS, B., KRAUS, W. E., LYLES, M. F., EGGEBEEN, J., MORGAN, T. M. & HAYKOWSKY, M. 2014. Skeletal muscle abnormalities and exercise intolerance in older patients with heart failure and preserved ejection fraction. *Am J Physiol Heart Circ Physiol,* 306**,** H1364-70.

KLOMSIRI, C., KARPLUS, P. A. & POOLE, L. B. 2011. Cysteine-Based Redox Switches in Enzymes. *Antioxidants & Redox Signaling,* 14**,** 1065-1077.

KOJIMA, A., MATSUMOTO, A., NISHIDA, H., REIEN, Y., IWATA, K., SHIRAYAMA, T., YABE-NISHIMURA, C. & NAKAYA, H. 2015. A protective role of Nox1/NADPH oxidase in a mouse model with hypoxia-induced bradycardia. *J Pharmacol Sci,* 127**,** 370-6.

KOPPENOL, W. H., BOUNDS, P. L. & DANG, C. V. 2011. Otto Warburg's contributions to current concepts of cancer metabolism. *Nat Rev Cancer,* 11**,** 325-37.

KOZAKOWSKA, M., PIETRASZEK-GREMPLEWICZ, K., JOZKOWICZ, A. & DULAK, J. 2015. The role of oxidative stress in skeletal muscle injury and regeneration: focus on antioxidant enzymes. *Journal of Muscle Research and Cell Motility,* 36**,** 377-393.

KUMMER, W. & ACKER, H. 1995. Immunohistochemical demonstration of four subunits of neutrophil NAD(P)H oxidase in type I cells of carotid body. *J Appl Physiol (1985),* 78**,** 1904-9.

LAMBOLEY, C. R., MURPHY, R. M., MCKENNA, M. J. & LAMB, G. D. 2014. Sarcoplasmic reticulum Ca(2+) uptake and leak properties, and SERCA isoform expression, in type I and type II fibres of human skeletal muscle. *The Journal of Physiology,* 592**,** 1381-1395.

LAUGHLIN, M. H., SIMPSON, T., SEXTON, W. L., BROWN, O. R., SMITH, J. K. & KORTHUIS, R. J. 1990. Skeletal muscle oxidative capacity, antioxidant enzymes, and exercise training. *J Appl Physiol (1985),* 68**,** 2337-43.

LAVIE, L. 2003. Obstructive sleep apnoea syndrome--an oxidative stress disorder. *Sleep Med Rev,* 7**,** 35-51.

LAVIE, L. 2009. Oxidative stress--a unifying paradigm in obstructive sleep apnea and comorbidities. *Prog Cardiovasc Dis,* 51**,** 303-12.

LAVIE, L. 2015. Oxidative stress in obstructive sleep apnea and intermittent hypoxia--revisited--the bad ugly and good: implications to the heart and brain. *Sleep Med Rev,* 20**,** 27-45.

LAWLER, J. M., POWERS, S. K., VAN DIJK, H., VISSER, T., KORDUS, M. J. & JI, L. L. 1994. Metabolic and antioxidant enzyme activities in the diaphragm: effects of acute exercise. *Respir Physiol,* 96**,** 139-49.

LAZAROU, M. 2015. Keeping the immune system in check: a role for mitophagy. *Immunol Cell Biol,* 93**,** 3-10.

LECKER, S. H., GOLDBERG, A. L. & MITCH, W. E. 2006. Protein degradation by the ubiquitin-proteasome pathway in normal and disease states. *J Am Soc Nephrol,* 17**,** 1807-19.

LEE, K. P., SHIN, Y. J., CHO, S. C., LEE, S. M., BAHN, Y. J., KIM, J. Y., KWON, E. S., JEONG, D. Y., PARK, S. C., RHEE, S. G., WOO, H. A. & KWON, K. S. 2014. Peroxiredoxin 3 has a crucial role in the contractile function of skeletal muscle by regulating mitochondrial homeostasis. *Free Radic Biol Med,* 77**,** 298-306.

LEE, S. R., AN, E. J., KIM, J. & BAE, Y. S. 2020. Function of NADPH Oxidases in Diabetic Nephropathy and Development of Nox Inhibitors. *Biomol Ther (Seoul),* 28**,** 25-33.

LEE, S. R., YANG, K. S., KWON, J., LEE, C., JEONG, W. & RHEE, S. G. 2002. Reversible inactivation of the tumor suppressor PTEN by H2O2. *J Biol Chem,* 277**,** 20336-42.

LEE, S. W., DAI, G., HU, Z., WANG, X., DU, J. & MITCH, W. E. 2004. Regulation of muscle protein degradation: coordinated control of apoptotic and ubiquitin-proteasome systems by phosphatidylinositol 3 kinase. *J Am Soc Nephrol,* 15**,** 1537-45.

LEE, W., NAGUBADI, S., KRYGER, M. H. & MOKHLESI, B. 2008. Epidemiology of Obstructive Sleep Apnea: a Population-based Perspective. *Expert Rev Respir Med,* 2**,** 349-64.

LEERMAKERS, P. A., KNEPPERS, A. E. M., SCHOLS, A., KELDERS, M., DE THEIJE, C. C., VERDIJK, L. B., VAN LOON, L. J. C., LANGEN, R. C. J. & GOSKER, H. R. 2019. Skeletal muscle unloading results in increased mitophagy and decreased mitochondrial biogenesis regulation. *Muscle Nerve,* 60**,** 769-778.

LEEUWENBURGH, C., HOLLANDER, J., LEICHTWEIS, S., GRIFFITHS, M., GORE, M. & JI, L. L. 1997. Adaptations of glutathione antioxidant system to endurance training are tissue and muscle fiber specific. *Am J Physiol,* 272**,** R363-9.

LEWIS, P. & O'HALLORAN, K. D. 2016. Diaphragm Muscle Adaptation to Sustained Hypoxia: Lessons from Animal Models with Relevance to High Altitude and Chronic Respiratory Diseases. *Frontiers in Physiology,* 7**,** 623.

LEWIS, P., SHEEHAN, D., SOARES, R., COELHO, A. V. & O'HALLORAN, K. D. 2016. Redox Remodeling Is Pivotal in Murine Diaphragm Muscle Adaptation to Chronic Sustained Hypoxia. *Am J Respir Cell Mol Biol,* 55**,** 12-23.

LEWIS, P., SHEEHAN, D., SOARES, R., VARELA COELHO, A. & O'HALLORAN, K. D. 2015. Chronic sustained hypoxia-induced redox remodeling causes contractile dysfunction in mouse sternohyoid muscle. *Frontiers in Physiology,* 6.

LI, T., LUO, X. J., WANG, E. L., LI, N. S., ZHANG, X. J., SONG, F. L., YANG, J. F., LIU, B. & PENG, J. 2019. Magnesium lithospermate B prevents phenotypic transformation of pulmonary arteries in rats with hypoxic pulmonary hypertension through suppression of NADPH oxidase. *Eur J Pharmacol,* 847**,** 32-41.

LIM, D. C., BRADY, D. C., SOANS, R., KIM, E. Y., VALVERDE, L., KEENAN, B. T., GUO, X., KIM, W. Y., PARK, M. J., GALANTE, R., SHACKLEFORD, J. A. & PACK, A. I. 2016. Different cyclical intermittent hypoxia severities have different effects on hippocampal microvasculature. *J Appl Physiol (1985),* 121**,** 78-88.

LIM, D. C. & PACK, A. I. 2014. Obstructive sleep apnea and cognitive impairment: Addressing the blood–brain barrier. *Sleep medicine reviews,* 18**,** 10.1016/j.smrv.2012.12.003.

LIM, J. C., CHOI, H. I., PARK, Y. S., NAM, H. W., WOO, H. A., KWON, K. S., KIM, Y. S., RHEE, S. G., KIM, K. & CHAE, H. Z. 2008. Irreversible oxidation of the active-site cysteine of peroxiredoxin to

cysteine sulfonic acid for enhanced molecular chaperone activity. *J Biol Chem,* 283**,** 28873-80.

LIN, C. M., DAVIDSON, T. M. & ANCOLI-ISRAEL, S. 2008. Gender differences in obstructive sleep apnea and treatment implications. *Sleep Med Rev,* 12**,** 481-96.

LIN, Y. N., LI, Q. Y. & ZHANG, X. J. 2012. Interaction between smoking and obstructive sleep apnea: not just participants. *Chin Med J (Engl),* 125**,** 3150-6.

LIU, L., SAKAKIBARA, K., CHEN, Q. & OKAMOTO, K. 2014a. Receptor-mediated mitophagy in yeast and mammalian systems. *Cell Res,* 24**,** 787-95.

LIU, N., NELSON, B. R., BEZPROZVANNAYA, S., SHELTON, J. M., RICHARDSON, J. A., BASSEL-DUBY, R. & OLSON, E. N. 2014b. Requirement of MEF2A, C, and D for skeletal muscle regeneration. *Proc Natl Acad Sci U S A,* 111**,** 4109-14.

LIU, S. S., LIU, H. G., XIONG, S. D., NIU, R. J., XU, Y. J. & ZHANG, Z. X. 2005. [Effects of Shen-Mai injection on sternohyoid contractile properties in chronic intermittent hypoxia rat]. *Zhonghua Jie He He Hu Xi Za Zhi,* 28**,** 611-4.

LIU, X. H., HARLOW, L., GRAHAM, Z. A., BAUMAN, W. A. & CARDOZO, C. 2017. Spinal Cord Injury Leads to Hyperoxidation and Nitrosylation of Skeletal Muscle Ryanodine Receptor-1 Associated with Upregulation of Nicotinamide Adenine Dinucleotide Phosphate Oxidase 4. *J Neurotrauma,* 34**,** 2069-2074.

LIU, Y. H., HUANG, Y. & SHAO, X. 2009. Effects of estrogen on genioglossal muscle contractile properties and fiber-type distribution in chronic intermittent hypoxia rats. *Eur J Oral Sci,* 117**,** 685-90.

LOEHR, J. A., WANG, S., CULLY, T. R., PAL, R., LARINA, I. V., LARIN, K. V. & RODNEY, G. G. 2018. NADPH oxidase mediates microtubule alterations and diaphragm dysfunction in dystrophic mice. *Elife,* 7.

LONERGAN, R. P., WARE, J. C., ATKINSON, R. L., WINTER, W. C. & SURATT, P. M. 1998. Sleep apnea in obese miniature pigs. *Journal of Applied Physiology,* 84**,** 531-536.

LOUREIRO, A. C. C., DO RÊGO-MONTEIRO, I. C., LOUZADA, R. A., ORTENZI, V. H., DE AGUIAR, A. P., DE ABREU, E. S., CAVALCANTI-DE-ALBUQUERQUE, J. P. A., HECHT, F., DE OLIVEIRA, A. C., CECCATTO, V. M., FORTUNATO, R. S. & CARVALHO, D. P. 2016. Differential Expression of NADPH Oxidases Depends on Skeletal Muscle Fiber Type in Rats. *Oxidative Medicine and Cellular Longevity,* 2016**,** 6738701.

LUCKING, E. F., O'CONNOR, K. M., STRAIN, C. R., FOUHY, F., BASTIAANSSEN, T. F. S., BURNS, D. P., GOLUBEVA, A. V., STANTON, C., CLARKE, G., CRYAN, J. F. & O'HALLORAN, K. D. 2018. Chronic intermittent hypoxia disrupts cardiorespiratory homeostasis and gut microbiota composition in adult male guinea-pigs. *EBioMedicine,* 38**,** 191-205.

LYLE, A. N., DESHPANDE, N. N., TANIYAMA, Y., SEIDEL-ROGOL, B., POUNKOVA, L., DU, P., PAPAHARALAMBUS, C., LASSEGUE, B. & GRIENDLING, K. K. 2009. Poldip2, a novel regulator of Nox4 and cytoskeletal integrity in vascular smooth muscle cells. *Circ Res,* 105**,** 249-59.

LÉVY, P., KOHLER, M., MCNICHOLAS, W. T., BARBÉ, F., MCEVOY, R. D., SOMERS, V. K., LAVIE, L. & PÉPIN, J. L. 2015. Obstructive sleep apnoea syndrome. *Nat Rev Dis Primers,* 1**,** 15015.

MACFARLANE, P. M. & MITCHELL, G. S. 2008. Respiratory long-term facilitation following intermittent hypoxia requires reactive oxygen species formation. *Neuroscience,* 152**,** 189-97.

MACFARLANE, P. M., SATRIOTOMO, I., WINDELBORN, J. A. & MITCHELL, G. S. 2009. NADPH oxidase activity is necessary for acute intermittent hypoxia-induced phrenic long-term facilitation. *J Physiol,* 587**,** 1931-42.

MACFARLANE, P. M., VINIT, S. & MITCHELL, G. S. 2014. Spinal nNOS regulates phrenic motor facilitation by a 5-HT2B receptor- and NADPH oxidase-dependent mechanism. *Neuroscience,* 269**,** 67-78.

MACFARLANE, P. M., WILKERSON, J. E., LOVETT-BARR, M. R. & MITCHELL, G. S. 2008. Reactive oxygen species and respiratory plasticity following intermittent hypoxia. *Respir Physiol Neurobiol,* 164**,** 263-71.

MAHAMED, S. & MITCHELL, G. S. 2007. Is there a link between intermittent hypoxia-induced respiratory plasticity and obstructive sleep apnoea? *Exp Physiol,* 92**,** 27-37.

MAHAMED, S. & MITCHELL, G. S. 2008. Respiratory long-term facilitation: too much or too little of a good thing? *Adv Exp Med Biol,* 605**,** 224-7.

MAMMUCARI, C., MILAN, G., ROMANELLO, V., MASIERO, E., RUDOLF, R., DEL PICCOLO, P., BURDEN, S. J., DI LISI, R., SANDRI, C., ZHAO, J., GOLDBERG, A. L., SCHIAFFINO, S. & SANDRI, M. 2007. FoxO3 controls autophagy in skeletal muscle in vivo. *Cell Metab,* 6**,** 458-71.

MANEA, S. A., CONSTANTIN, A., MANDA, G., SASSON, S. & MANEA, A. 2015. Regulation of Nox enzymes expression in vascular pathophysiology: Focusing on transcription factors and epigenetic mechanisms. *Redox Biol,* 5**,** 358-366.

MANTA, B., HUGO, M., ORTIZ, C., FERRER-SUETA, G., TRUJILLO, M. & DENICOLA, A. 2009. The peroxidase and peroxynitrite reductase activity of human erythrocyte peroxiredoxin 2. *Arch Biochem Biophys,* 484**,** 146-54.

MARCUS, N. J., LI, Y. L., BIRD, C. E., SCHULTZ, H. D. & MORGAN, B. J. 2010. Chronic intermittent hypoxia augments chemoreflex control of sympathetic activity: role of the angiotensin II type 1 receptor. *Respir Physiol Neurobiol,* 171**,** 36-45.

MARIN-CORRAL, J., MINGUELLA, J., RAMÍREZ-SARMIENTO, A. L., HUSSAIN, S. N. A., GEA, J. & BARREIRO, E. 2009. Oxidised proteins and superoxide anion production in the diaphragm of severe COPD patients. *European Respiratory Journal,* 33**,** 1309-1319.

MARINI, M. & VEICSTEINAS, A. 2010. The exercised skeletal muscle: a review. *2010,* 20**,** 16.

MASIERO, E., AGATEA, L., MAMMUCARI, C., BLAAUW, B., LORO, E., KOMATSU, M., METZGER, D., REGGIANI, C., SCHIAFFINO, S. & SANDRI, M. 2009. Autophagy is required to maintain muscle mass. *Cell Metab,* 10**,** 507-15.

MASON, M., WELSH, E. J. & SMITH, I. 2013. Drug therapy for obstructive sleep apnoea in adults. *Cochrane Database Syst Rev***,** Cd003002.

MATHUR, S., BROOKS, D. & CARVALHO, C. R. 2014. Structural alterations of skeletal muscle in copd. *Front Physiol,* 5**,** 104.

MCDONALD, F. B., WILLIAMS, R., SHEEHAN, D. & O'HALLORAN, K. D. 2015. Early life exposure to chronic intermittent hypoxia causes upper airway dilator muscle weakness, which persists into young adulthood. *Exp Physiol,* 100**,** 947-66.

MCGUIRE, M., MACDERMOTT, M. & BRADFORD, A. 2002a. Effects of chronic episodic hypoxia on rat upper airway muscle contractile properties and fiber-type distribution. *Chest,* 122**,** 1012-7.

MCGUIRE, M., MACDERMOTT, M. & BRADFORD, A. 2002b. The effects of chronic episodic hypercapnic hypoxia on rat upper airway muscle contractile properties and fiber-type distribution. *Chest,* 122**,** 1400-6.

MCGUIRE, M., MACDERMOTT, M. & BRADFORD, A. 2003a. Effects of chronic intermittent asphyxia on rat diaphragm and limb muscle contractility. *Chest,* 123**,** 875-81.

MCGUIRE, M., ZHANG, Y., WHITE, D. P. & LING, L. 2003b. Chronic intermittent hypoxia enhances ventilatory long-term facilitation in awake rats. *J Appl Physiol (1985),* 95**,** 1499-508.

MCKAY, L. C. & FELDMAN, J. L. 2008. Unilateral ablation of pre-Botzinger complex disrupts breathing during sleep but not wakefulness. *Am J Respir Crit Care Med,* 178**,** 89-95.

MCPHERRON, A. C., LAWLER, A. M. & LEE, S. J. 1997. Regulation of skeletal muscle mass in mice by a new TGF-beta superfamily member. *Nature,* 387**,** 83-90.

MENG, D., LV, D. D. & FANG, J. 2008. Insulin-like growth factor-I induces reactive oxygen species production and cell migration through Nox4 and Rac1 in vascular smooth muscle cells. *Cardiovasc Res,* 80**,** 299-308.

MESARWI, O. A., SHARMA, E. V., JUN, J. C. & POLOTSKY, V. Y. 2015. Metabolic dysfunction in obstructive sleep apnea: A critical examination of underlying mechanisms. *Sleep Biol Rhythms,* 13**,** 2-17.

MICOVA, P., HAHNOVA, K., HLAVACKOVA, M., ELSNICOVA, B., CHYTILOVA, A., HOLZEROVA, K., ZURMANOVA, J., NECKAR, J., KOLAR, F., NOVAKOVA, O. & NOVOTNY, J. 2016. Chronic intermittent hypoxia affects the cytosolic phospholipase A2alpha/cyclooxygenase 2 pathway via beta2-adrenoceptor-mediated ERK/p38 stimulation. *Mol Cell Biochem,* 423**,** 151-163.

MITCHELL, G. S. & JOHNSON, S. M. 2003. Neuroplasticity in respiratory motor control. *J Appl Physiol (1985),* 94**,** 358-74.

MIYANO, K., UENO, N., TAKEYA, R. & SUMIMOTO, H. 2006. Direct involvement of the small GTPase Rac in activation of the superoxide-producing NADPH oxidase Nox1. *J Biol Chem,* 281**,** 21857-68.

MOLDOVAN, L. & MOLDOVAN, N. I. 2004. Oxygen free radicals and redox biology of organelles. *Histochem Cell Biol,* 122**,** 395-412.

MOLLER, I. M. & KRISTENSEN, B. K. 2004. Protein oxidation in plant mitochondria as a stress indicator. *Photochem Photobiol Sci,* 3**,** 730-5.

MONTEZANO, A. C., TSIROPOULOU, S., DULAK-LIS, M., HARVEY, A., CAMARGO, L. D. L. & TOUYZ, R. M. 2015. Redox signaling, Nox5 and vascular remodeling in hypertension. *Current Opinion in Nephrology and Hypertension,* 24**,** 425-433.

MONTINE, T. J., NEELY, M. D., QUINN, J. F., BEAL, M. F., MARKESBERY, W. R., ROBERTS, L. J. & MORROW, J. D. 2002. Lipid peroxidation in aging brain and Alzheimer's disease. *Free Radic Biol Med,* 33**,** 620-6.

MONTSERRAT, J. M., KOSMAS, E. N., COSIO, M. G. & KIMOFF, R. J. 1997. Lack of evidence for diaphragmatic fatigue over the course of the night in obstructive sleep apnoea. *Eur Respir J,* 10**,** 133-8.

MORAES, D. J., DA SILVA, M. P., BONAGAMBA, L. G., MECAWI, A. S., ZOCCAL, D. B., ANTUNES-RODRIGUES, J., VARANDA, W. A. & MACHADO, B. H. 2013. Electrophysiological properties of

rostral ventrolateral medulla presympathetic neurons modulated by the respiratory network in rats. *J Neurosci,* 33**,** 19223-37.

MORENO, J. C., BIKKER, H., KEMPERS, M. J., VAN TROTSENBURG, A. S., BAAS, F., DE VIJLDER, J. J., VULSMA, T. & RIS-STALPERS, C. 2002. Inactivating mutations in the gene for thyroid oxidase 2 (THOX2) and congenital hypothyroidism. *N Engl J Med,* 347**,** 95-102.

MORGAN, B. J., ADRIAN, R., WANG, Z. Y., BATES, M. L. & DOPP, J. M. 2016a. Chronic intermittent hypoxia alters ventilatory and metabolic responses to acute hypoxia in rats. *J Appl Physiol (1985),* 120**,** 1186-95.

MORGAN, B. J., BATES, M. L., RIO, R. D., WANG, Z. & DOPP, J. M. 2016b. Oxidative stress augments chemoreflex sensitivity in rats exposed to chronic intermittent hypoxia. *Respir Physiol Neurobiol,* 234**,** 47-59.

MORGAN, M. J. & LIU, Z.-G. 2011. Crosstalk of reactive oxygen species and NF-κB signaling. *Cell Research,* 21**,** 103-115.

MORGENTHALER, T. I., KAGRAMANOV, V., HANAK, V. & DECKER, P. A. 2006. Complex sleep apnea syndrome: is it a unique clinical syndrome? *Sleep,* 29**,** 1203-9.

MORRIS, I. R. 1988. Functional anatomy of the upper airway. *Emergency medicine clinics of North America,* 6**,** 639-669.

MULLER, F. L., SONG, W., LIU, Y., CHAUDHURI, A., PIEKE-DAHL, S., STRONG, R., HUANG, T. T., EPSTEIN, C. J., ROBERTS, L. J., 2ND, CSETE, M., FAULKNER, J. A. & VAN REMMEN, H. 2006. Absence of CuZn superoxide dismutase leads to elevated oxidative stress and acceleration of age-dependent skeletal muscle atrophy. *Free Radic Biol Med,* 40**,** 1993-2004.

MUSARÒ, A., MCCULLAGH, K., PAUL, A., HOUGHTON, L., DOBROWOLNY, G., MOLINARO, M., BARTON, E. R., SWEENEY, H. L. & ROSENTHAL, N. 2001. Localized Igf-1 transgene expression sustains hypertrophy and regeneration in senescent skeletal muscle. *Nat Genet,* 27**,** 195-200.

MUSSO, G., GAMBINO, R. & CASSADER, M. 2009. Recent insights into hepatic lipid metabolism in non-alcoholic fatty liver disease (NAFLD). *Progress in Lipid Research,* 48**,** 1-26.

NAGAHISA, H., OKABE, K., IUCHI, Y., FUJII, J. & MIYATA, H. 2016. Characteristics of Skeletal Muscle Fibers of SOD1 Knockout Mice. *Oxidative Medicine and Cellular Longevity,* 2016**,** 9345970.

NANDURI, J., VADDI, D. R., KHAN, S. A., WANG, N., MAKARENKO, V., SEMENZA, G. L. & PRABHAKAR, N. R. 2015. HIF-1α activation by intermittent hypoxia requires NADPH oxidase stimulation by xanthine oxidase. *PLoS One,* 10**,** e0119762.

NANDURI, J., VADDI, D. R., KHAN, S. A., WANG, N., MAKERENKO, V. & PRABHAKAR, N. R. 2013a. Xanthine oxidase mediates hypoxia-inducible factor-2alpha degradation by intermittent hypoxia. *PLoS One,* 8**,** e75838.

NANDURI, J., VADDI, D. R., KHAN, S. A., WANG, N., MAKERENKO, V. & PRABHAKAR, N. R. 2013b. Xanthine oxidase mediates hypoxia-inducible factor-2α degradation by intermittent hypoxia. *PLoS One,* 8**,** e75838.

NARENDRA, D. P. & YOULE, R. J. 2011. Targeting mitochondrial dysfunction: role for PINK1 and Parkin in mitochondrial quality control. *Antioxid Redox Signal,* 14**,** 1929-38.

NARICI, M. V. & MAFFULLI, N. 2010. Sarcopenia: characteristics, mechanisms and functional significance. *Br Med Bull,* 95**,** 139-59.

NARKIEWICZ, K., VAN DE BORNE, P. J., PESEK, C. A., DYKEN, M. E., MONTANO, N. & SOMERS, V. K. 1999. Selective potentiation of peripheral chemoreflex sensitivity in obstructive sleep apnea. *Circulation,* 99**,** 1183-9.

NAVARRETE-OPAZO, A. & MITCHELL, G. S. 2014. Therapeutic potential of intermittent hypoxia: a matter of dose. *Am J Physiol Regul Integr Comp Physiol,* 307**,** R1181-97.

NEDACHI, T., KADOTANI, A., ARIGA, M., KATAGIRI, H. & KANZAKI, M. 2008. Ambient glucose levels qualify the potency of insulin myogenic actions by regulating SIRT1 and FoxO3a in C2C12 myocytes. *Am J Physiol Endocrinol Metab,* 294**,** E668-78.

NGUYEN, D. D., KIM, G. & PAE, E.-K. 2016. Modulation of Muscle Fiber Compositions in Response to Hypoxia via Pyruvate Dehydrogenase Kinase-1. *Frontiers in Physiology,* 7**,** 604.

NGUYEN, T., NIOI, P. & PICKETT, C. B. 2009. The Nrf2-antioxidant response element signaling pathway and its activation by oxidative stress. *J Biol Chem,* 284**,** 13291-5.

NICOLUSSI, A., D'INZEO, S., CAPALBO, C., GIANNINI, G. & COPPA, A. 2017. The role of peroxiredoxins in cancer. *Mol Clin Oncol,* 6**,** 139-153.

NISBET, R. E., GRAVES, A. S., KLEINHENZ, D. J., RUPNOW, H. L., REED, A. L., FAN, T. H., MITCHELL, P. O., SUTLIFF, R. L. & HART, C. M. 2009. The role of NADPH oxidase in chronic intermittent hypoxia-induced pulmonary hypertension in mice. *Am J Respir Cell Mol Biol,* 40**,** 601-9.

NISIMOTO, Y., DIEBOLD, B. A., COSENTINO-GOMES, D. & LAMBETH, J. D. 2014. Nox4: a hydrogen peroxide-generating oxygen sensor. *Biochemistry,* 53**,** 5111-20.

O'CONNELL, R. A., CARBERRY, J. & O'HALLORAN, K. D. 2013. Sternohyoid and diaphragm muscle form and function during postnatal development in the rat. *Exp Physiol,* 98**,** 1386-400.

O'CONNOR, K. M., LUCKING, E. F., GOLUBEVA, A. V., STRAIN, C. R., FOUHY, F., CENIT, M. C., DHALIWAL, P., BASTIAANSSEN, T. F. S., BURNS, D. P., STANTON, C., CLARKE, G., CRYAN, J. F. & O'HALLORAN, K. D. 2019. Manipulation of gut microbiota blunts the ventilatory response to hypercapnia in adult rats. *EBioMedicine,* 44**,** 618-638.

O'HALLORAN, K. D. 2016. Chronic intermittent hypoxia creates the perfect storm with calamitous consequences for respiratory control. *Respir Physiol Neurobiol,* 226**,** 63-7.

O'HALLORAN, K. D., MCGUIRE, M., O'HARE, T. & BRADFORD, A. 2002. Chronic intermittent asphyxia impairs rat upper airway muscle responses to acute hypoxia and asphyxia. *Chest,* 122**,** 269-75.

O'LEARY, A. J., DRUMMOND, S. E., EDGE, D. & O'HALLORAN, K. D. 2018. Diaphragm Muscle Weakness Following Acute Sustained Hypoxic Stress in the Mouse Is Prevented by Pretreatment with N-Acetyl Cysteine. *Oxid Med Cell Longev,* 2018**,** 4805493.

O'LEARY, A. J. & O'HALLORAN, K. D. 2016. Diaphragm muscle weakness and increased UCP-3 gene expression following acute hypoxic stress in the mouse. *Respir Physiol Neurobiol,* 226**,** 76-80.

OECKINGHAUS, A. & GHOSH, S. 2009. The NF-kappaB family of transcription factors and its regulation. *Cold Spring Harb Perspect Biol,* 1**,** a000034.

OKADA, Y., CHEN, Z., JIANG, W., KUWANA, S. & ELDRIDGE, F. L. 2002. Anatomical arrangement of hypercapnia-activated cells in the superficial ventral medulla of rats. *J Appl Physiol (1985),* 93**,** 427-39.

OLEA, E., AGAPITO, M. T., GALLEGO-MARTIN, T., ROCHER, A., GOMEZ-NIÑO, A., OBESO, A., GONZALEZ, C. & YUBERO, S. 2014. Intermittent hypoxia and diet-induced obesity: effects on oxidative status, sympathetic tone, plasma glucose and insulin levels, and arterial pressure. *J Appl Physiol (1985),* 117**,** 706-19.

OLSON, E. J., MOORE, W. R., MORGENTHALER, T. I., GAY, P. C. & STAATS, B. A. 2003. Obstructive sleep apnea-hypopnea syndrome. *Mayo Clin Proc,* 78**,** 1545-52.

OLTHOFF, J. T., LINDSAY, A., ABO-ZAHRAH, R., BALTGALVIS, K. A., PATRINOSTRO, X., BELANTO, J. J., YU, D. Y., PERRIN, B. J., GARRY, D. J., RODNEY, G. G., LOWE, D. A. & ERVASTI, J. M. 2018. Loss of peroxiredoxin-2 exacerbates eccentric contraction-induced force loss in dystrophin-deficient muscle. *Nat Commun,* 9**,** 5104.

PAE, E. K., WU, J., NGUYEN, D., MONTI, R. & HARPER, R. M. 2005. Geniohyoid muscle properties and myosin heavy chain composition are altered after short-term intermittent hypoxic exposure. *J Appl Physiol (1985),* 98**,** 889-94.

PAFFENHOLZ, R., BERGSTROM, R. A., PASUTTO, F., WABNITZ, P., MUNROE, R. J., JAGLA, W., HEINZMANN, U., MARQUARDT, A., BAREISS, A., LAUFS, J., RUSS, A., STUMM, G., SCHIMENTI, J. C. & BERGSTROM, D. E. 2004. Vestibular defects in head-tilt mice result from mutations in Nox3, encoding an NADPH oxidase. *Genes & Development,* 18**,** 486-491.

PAL, R., PALMIERI, M., LOEHR, J. A., LI, S., ABO-ZAHRAH, R., MONROE, T. O., THAKUR, P. B., SARDIELLO, M. & RODNEY, G. G. 2014. Src-dependent impairment of autophagy by oxidative stress in a mouse model of Duchenne muscular dystrophy. *Nature communications,* 5**,** 4425-4425.

PAVWOSKI, P. & SHELGIKAR, A. V. 2017. Treatment options for obstructive sleep apnea. *Neurol Clin Pract,* 7**,** 77-85.

PENG, Y., KLINE, D. D., DICK, T. E. & PRABHAKAR, N. R. 2001. Chronic intermittent hypoxia enhances carotid body chemoreceptor response to low oxygen. *Adv Exp Med Biol,* 499**,** 33-8.

PENG, Y. J., NANDURI, J., YUAN, G., WANG, N., DENERIS, E., PENDYALA, S., NATARAJAN, V., KUMAR, G. K. & PRABHAKAR, N. R. 2009. NADPH oxidase is required for the sensory plasticity of the carotid body by chronic intermittent hypoxia. *J Neurosci,* 29**,** 4903-10.

PENG, Y. J., OVERHOLT, J. L., KLINE, D., KUMAR, G. K. & PRABHAKAR, N. R. 2003. Induction of sensory long-term facilitation in the carotid body by intermittent hypoxia: implications for recurrent apneas. *Proc Natl Acad Sci U S A,* 100**,** 10073-8.

PENG, Y. J. & PRABHAKAR, N. R. 2004. Effect of two paradigms of chronic intermittent hypoxia on carotid body sensory activity. *J Appl Physiol (1985),* 96**,** 1236-42; discussion 1196.

PENG, Y. J., RAGHURAMAN, G., KHAN, S. A., KUMAR, G. K. & PRABHAKAR, N. R. 2011. Angiotensin II evokes sensory long-term facilitation of the carotid body via NADPH oxidase. *J Appl Physiol (1985),* 111**,** 964-70.

PENG, Y. J., YUAN, G., JACONO, F. J., KUMAR, G. K. & PRABHAKAR, N. R. 2006a. 5-HT evokes sensory long-term facilitation of rodent carotid body via activation of NADPH oxidase. *J Physiol,* 576**,** 289-95.

PENG, Y. J., YUAN, G., RAMAKRISHNAN, D., SHARMA, S. D., BOSCH-MARCE, M., KUMAR, G. K., SEMENZA, G. L. & PRABHAKAR, N. R. 2006b. Heterozygous HIF-1alpha deficiency impairs carotid body-mediated systemic responses and reactive oxygen species generation in mice exposed to intermittent hypoxia. *J Physiol,* 577**,** 705-16.

PERIM, R. R., FIELDS, D. P. & MITCHELL, G. S. 2018. Cross-talk inhibition between 5-HT(2B) and 5-HT(7) receptors in phrenic motor facilitation via NADPH oxidase and PKA. *Am J Physiol Regul Integr Comp Physiol,* 314**,** R709-r715.

PERKINS, A., NELSON, K. J., PARSONAGE, D., POOLE, L. B. & KARPLUS, P. A. 2015. Peroxiredoxins: guardians against oxidative stress and modulators of peroxide signaling. *Trends Biochem Sci,* 40**,** 435-45.

PETRILLO, S., PELOSI, L., PIEMONTE, F., TRAVAGLINI, L., FORCINA, L., CATTERUCCIA, M., PETRINI, S., VERARDO, M., D'AMICO, A., MUSARÒ, A. & BERTINI, E. 2017. Oxidative stress in Duchenne muscular dystrophy: focus on the NRF2 redox pathway. *Human Molecular Genetics,* 26**,** 2781-2790.

PETROF, B. J., HENDRICKS, J. C. & PACK, A. I. 1996. Does upper airway muscle injury trigger a vicious cycle in obstructive sleep apnea? A hypothesis. *Sleep,* 19**,** 465-71.

PETROF, B. J., PACK, A. I., KELLY, A. M., EBY, J. & HENDRICKS, J. C. 1994. Pharyngeal myopathy of loaded upper airway in dogs with sleep apnea. *J Appl Physiol (1985),* 76**,** 1746-52.

PHELAN, J. N. & GONYEA, W. J. 1997. Effect of radiation on satellite cell activity and protein expression in overloaded mammalian skeletal muscle. *Anat Rec,* 247**,** 179-88.

PIALOUX, V., HANLY, P. J., FOSTER, G. E., BRUGNIAUX, J. V., BEAUDIN, A. E., HARTMANN, S. E., PUN, M., DUGGAN, C. T. & POULIN, M. J. 2009. Effects of exposure to intermittent hypoxia on oxidative stress and acute hypoxic ventilatory response in humans. *Am J Respir Crit Care Med,* 180**,** 1002-9.

PISANI, D. F., LECLERC, L., JARRETOU, G., MARINI, J.-F. & DECHESNE, C. A. 2005. SMHS1 is involved in oxidative/glycolytic-energy metabolism balance of muscle fibers. *Biochemical and Biophysical Research Communications,* 326**,** 788-793.

POWELL, F. L., MILSOM, W. K. & MITCHELL, G. S. 1998. Time domains of the hypoxic ventilatory response. *Respir Physiol,* 112**,** 123-34.

POWERS, S. K. 2011. REACTIVE OXYGEN SPECIES: IMPACT ON SKELETAL MUSCLE. 1**,** 941-69.

POWERS, S. K., CRISWELL, D., LAWLER, J., JI, L. L., MARTIN, D., HERB, R. A. & DUDLEY, G. 1994. Influence of exercise and fiber type on antioxidant enzyme activity in rat skeletal muscle. *Am J Physiol,* 266**,** R375-80.

PRABHAKAR, N. R. & PENG, Y. J. 2004. Peripheral chemoreceptors in health and disease. *J Appl Physiol (1985),* 96**,** 359-66.

PRABHAKAR, N. R., PENG, Y. J., KUMAR, G. K. & NANDURI, J. 2015. Peripheral chemoreception and arterial pressure responses to intermittent hypoxia. *Compr Physiol,* 5**,** 561-77.

PRATICO, D., IULIANO, L., BASILI, S., FERRO, D., CAMASTRA, C., CORDOVA, C., FITZGERALD, G. A. & VIOLI, F. 1998. Enhanced lipid peroxidation in hepatic cirrhosis. *J Investig Med,* 46**,** 51-7.

RAMIREZ, J. M. 2014. The integrative role of the sigh in psychology, physiology, pathology, and neurobiology. *Prog Brain Res,* 209**,** 91-129.

RAMIREZ, J. M., GARCIA, A. J., 3RD, ANDERSON, T. M., KOSCHNITZKY, J. E., PENG, Y. J., KUMAR, G. K. & PRABHAKAR, N. R. 2013. Central and peripheral factors contributing to obstructive sleep apneas. *Respir Physiol Neurobiol,* 189**,** 344-53.

RAY, A. D., MAGALANG, U. J., MICHLIN, C. P., OGASA, T., KRASNEY, J. A., GOSSELIN, L. E. & FARKAS, G. A. 2007. Intermittent hypoxia reduces upper airway stability in lean but not obese Zucker rats. *Am J Physiol Regul Integr Comp Physiol,* 293**,** R372-8.

REEVES, S. R. & GOZAL, D. 2004. Platelet-activating factor receptor modulates respiratory adaptation to long-term intermittent hypoxia in mice. *Am J Physiol Regul Integr Comp Physiol,* 287**,** R369-74.

REEVES, S. R. & GOZAL, D. 2006. Changes in ventilatory adaptations associated with long-term intermittent hypoxia across the age spectrum in the rat. *Respir Physiol Neurobiol,* 150**,** 135-43.

REEVES, S. R., GOZAL, E., GUO, S. Z., SACHLEBEN, L. R., JR., BRITTIAN, K. R., LIPTON, A. J. & GOZAL, D. 2003. Effect of long-term intermittent and sustained hypoxia on hypoxic ventilatory and metabolic responses in the adult rat. *J Appl Physiol (1985),* 95**,** 1767-74.

REEVES, S. R., MITCHELL, G. S. & GOZAL, D. 2006. Early postnatal chronic intermittent hypoxia modifies hypoxic respiratory responses and long-term phrenic facilitation in adult rats. *Am J Physiol Regul Integr Comp Physiol,* 290**,** R1664-71.

REGAN, J. N., MIKESELL, C., REIKEN, S., XU, H., MARKS, A. R., MOHAMMAD, K. S., GUISE, T. A. & WANING, D. L. 2017. Osteolytic Breast Cancer Causes Skeletal Muscle Weakness in an Immunocompetent Syngeneic Mouse Model. *Frontiers in Endocrinology,* 8.

REID, M. B., KHAWLI, F. A. & MOODY, M. R. 1993. Reactive oxygen in skeletal muscle. III. Contractility of unfatigued muscle. *J Appl Physiol (1985),* 75**,** 1081-7.

REID, M. B., SHOJI, T., MOODY, M. R. & ENTMAN, M. L. 1992. Reactive oxygen in skeletal muscle. II. Extracellular release of free radicals. *J Appl Physiol (1985),* 73**,** 1805-9.

REINEHR, R., BECKER, S., EBERLE, A., GRETHER-BECK, S. & HÄUSSINGER, D. 2005. Involvement of NADPH Oxidase Isoforms and Src Family Kinases in CD95-dependent Hepatocyte Apoptosis. *Journal of Biological Chemistry,* 280**,** 27179-27194.

REY, S., DEL RIO, R., ALCAYAGA, J. & ITURRIAGA, R. 2004. Chronic intermittent hypoxia enhances cat chemosensory and ventilatory responses to hypoxia. *J Physiol,* 560**,** 577-86.

RHEE, S. G., CHAE, H. Z. & KIM, K. 2005. Peroxiredoxins: a historical overview and speculative preview of novel mechanisms and emerging concepts in cell signaling. *Free Radic Biol Med,* 38**,** 1543-52.

RICHARDSON, R. S., NOYSZEWSKI, E. A., KENDRICK, K. F., LEIGH, J. S. & WAGNER, P. D. 1995. Myoglobin O2 desaturation during exercise. Evidence of limited O2 transport. *J Clin Invest,* 96**,** 1916-26.

RICHTER, C. 1992. Reactive oxygen and DNA damage in mitochondria. *Mutat Res,* 275**,** 249-55.

RIGUTTO, S., HOSTE, C., GRASBERGER, H., MILENKOVIC, M., COMMUNI, D., DUMONT, J. E., CORVILAIN, B., MIOT, F. & DE DEKEN, X. 2009. Activation of Dual Oxidases Duox1 and Duox2: DIFFERENTIAL REGULATION MEDIATED BY cAMP-DEPENDENT PROTEIN KINASE AND PROTEIN KINASE C-DEPENDENT PHOSPHORYLATION. *The Journal of Biological Chemistry,* 284**,** 6725-6734.

ROBERTS, J. L., REED, W. R. & THACH, B. T. 1984. Pharyngeal airway-stabilizing function of sternohyoid and sternothyroid muscles in the rabbit. *Journal of Applied Physiology,* 57**,** 1790-1795.

ROKUTAN, K., KAWAHARA, T., KUWANO, Y., TOMINAGA, K., SEKIYAMA, A. & TESHIMA-KONDO, S. 2006. NADPH oxidases in the gastrointestinal tract: a potential role of Nox1 in innate immune response and carcinogenesis. *Antioxid Redox Signal,* 8**,** 1573-82.

ROMERO-CORRAL, A., CAPLES, S. M., LOPEZ-JIMENEZ, F. & SOMERS, V. K. 2010. Interactions Between Obesity and Obstructive Sleep Apnea: Implications for Treatment. *Chest,* 137**,** 711-9.

ROMMEL, C., BODINE, S. C., CLARKE, B. A., ROSSMAN, R., NUNEZ, L., STITT, T. N., YANCOPOULOS, G. D. & GLASS, D. J. 2001. Mediation of IGF-1-induced skeletal myotube hypertrophy by PI(3)K/Akt/mTOR and PI(3)K/Akt/GSK3 pathways. *Nat Cell Biol,* 3**,** 1009-13.

ROSAS, S. E. 2011. Sleep apnea in individuals with chronic kidney disease: a wake-up call. *Clin J Am Soc Nephrol,* 6**,** 954-6.

ROY, A., ROZANOV, C., MOKASHI, A., DAUDU, P., AL-MEHDI, A. B., SHAMS, H. & LAHIRI, S. 2000. Mice lacking in gp91 phox subunit of NAD(P)H oxidase showed glomus cell [Ca(2+)](i) and respiratory responses to hypoxia. *Brain Res,* 872**,** 188-93.

RUDNICKI, M. A., LE GRAND, F., MCKINNELL, I. & KUANG, S. 2008. The molecular regulation of muscle stem cell function. *Cold Spring Harb Symp Quant Biol,* 73**,** 323-31.

RYALL, J. G., DELL'ORSO, S., DERFOUL, A., JUAN, A., ZARE, H., FENG, X., CLERMONT, D., KOULNIS, M., GUTIERREZ-CRUZ, G., FULCO, M. & SARTORELLI, V. 2015. The NAD(+)-dependent SIRT1 deacetylase translates a metabolic switch into regulatory epigenetics in skeletal muscle stem cells. *Cell Stem Cell,* 16**,** 171-83.

SAKELLARIOU, G. K., MCDONAGH, B., PORTER, H., GIAKOUMAKI, II, EARL, K. E., NYE, G. A., VASILAKI, A., BROOKS, S. V., RICHARDSON, A., VAN REMMEN, H., MCARDLE, A. & JACKSON, M. J. 2018. Comparison of Whole Body SOD1 Knockout with Muscle-Specific SOD1 Knockout Mice Reveals a Role for Nerve Redox Signaling in Regulation of Degenerative Pathways in Skeletal Muscle. *Antioxid Redox Signal,* 28**,** 275-295.

SAKELLARIOU, G. K., VASILAKI, A., PALOMERO, J., KAYANI, A., ZIBRIK, L., MCARDLE, A. & JACKSON, M. J. 2013. Studies of mitochondrial and nonmitochondrial sources implicate nicotinamide adenine dinucleotide phosphate oxidase(s) in the increased skeletal muscle superoxide generation that occurs during contractile activity. *Antioxid Redox Signal,* 18**,** 603-21.

SANDERS, K. A., SUNDAR, K. M., HE, L., DINGER, B., FIDONE, S. & HOIDAL, J. R. 2002. Role of components of the phagocytic NADPH oxidase in oxygen sensing. *J Appl Physiol (1985),* 93**,** 1357-64.

SANDIFORD, S. D., KENNEDY, K. A., XIE, X., PICKERING, J. G. & LI, S. S. 2014. Dual Oxidase Maturation factor 1 (DUOXA1) overexpression increases reactive oxygen species production and inhibits murine muscle satellite cell differentiation. *Cell Communication and Signaling,* 12**,** 5.

SANDOW, A. 1952. Excitation-contraction coupling in muscular response. *Yale J Biol Med,* 25**,** 176-201.

SANDRI, M. 2008. Signaling in muscle atrophy and hypertrophy. *Physiology (Bethesda),* 23**,** 160-70.

SANDRI, M., SANDRI, C., GILBERT, A., SKURK, C., CALABRIA, E., PICARD, A., WALSH, K., SCHIAFFINO, S., LECKER, S. H. & GOLDBERG, A. L. 2004. Foxo transcription factors induce the atrophy-related ubiquitin ligase atrogin-1 and cause skeletal muscle atrophy. *Cell,* 117**,** 399-412.

SAVRANSKY, V., NANAYAKKARA, A., VIVERO, A., LI, J., BEVANS, S., SMITH, P. L., TORBENSON, M. S. & POLOTSKY, V. Y. 2007. Chronic intermittent hypoxia predisposes to liver injury. *Hepatology,* 45**,** 1007-13.

SCHIAFFINO, S., GORZA, L., SARTORE, S., SAGGIN, L., AUSONI, S., VIANELLO, M., GUNDERSEN, K. & LØMO, T. 1989. Three myosin heavy chain isoforms in type 2 skeletal muscle fibres. *Journal of Muscle Research & Cell Motility,* 10**,** 197-205.

SCHRÖDER, K., WEISSMANN, N. & BRANDES, R. P. 2017. Organizers and activators: Cytosolic Nox proteins impacting on vascular function. *Free Radic Biol Med,* 109**,** 22-32.

SEMENZA, G. L. 2014. Oxygen sensing, hypoxia-inducible factors, and disease pathophysiology. *Annu Rev Pathol,* 9**,** 47-71.

SEO, M. S., KANG, S. W., KIM, K., BAINES, I. C., LEE, T. H. & RHEE, S. G. 2000. Identification of a new type of mammalian peroxiredoxin that forms an intramolecular disulfide as a reaction intermediate. *J Biol Chem,* 275**,** 20346-54.

SERRANO, F., KOLLURI, N. S., WIENTJES, F. B., CARD, J. P. & KLANN, E. 2003. NADPH oxidase immunoreactivity in the mouse brain. *Brain Res,* 988**,** 193-8.

SHANMUGASUNDARAM, K., NAYAK, B. K., FRIEDRICHS, W. E., KAUSHIK, D., RODRIGUEZ, R. & BLOCK, K. 2017. NOX4 functions as a mitochondrial energetic sensor coupling cancer metabolic reprogramming to drug resistance. *Nat Commun,* 8**,** 997.

SHARMA, B. B. & SINGH, V. 2019. Diaphragmatic dysfunction in chronic obstructive pulmonary disease. *Lung India,* 36**,** 285-287.

SHARMAN, M. J., NEWTON, R. U., TRIPLETT-MCBRIDE, T., MCGUIGAN, M. R., MCBRIDE, J. M., HÄKKINEN, A., HÄKKINEN, K. & KRAEMER, W. J. 2001. Changes in myosin heavy chain composition with heavy resistance training in 60- to 75-year-old men and women. *Eur J Appl Physiol,* 84**,** 127-32.

SHERWOOD, L. 2001. *Human physiology: from cells to systems*, Brooks/Cole.

SHORTT, C. M., FREDSTED, A., BRADFORD, A. & O'HALLORAN, K. D. 2013. Diaphragm Muscle Remodeling in a Rat Model of Chronic Intermittent Hypoxia. *Journal of Histochemistry & Cytochemistry,* 61**,** 487-499.

SHORTT, C. M., FREDSTED, A., CHOW, H. B., WILLIAMS, R., SKELLY, J. R., EDGE, D., BRADFORD, A. & O'HALLORAN, K. D. 2014. Reactive oxygen species mediated diaphragm fatigue in a rat model of chronic intermittent hypoxia. *Exp Physiol,* 99**,** 688-700.

SHORTT, C. M. & O'HALLORAN, K. D. 2014. Hydrogen peroxide alters sternohyoid muscle function. *Oral Dis,* 20**,** 162-70.

SIES, H. 1991. Oxidative stress: from basic research to clinical application. *Am J Med,* 91**,** 31s-38s.

SKATRUD, J. B. & DEMPSEY, J. A. 1983. Interaction of sleep state and chemical stimuli in sustaining rhythmic ventilation. *J Appl Physiol Respir Environ Exerc Physiol,* 55**,** 813-22.

SKELLY, J. R., BRADFORD, A., JONES, J. F. & O'HALLORAN, K. D. 2010. Superoxide scavengers improve rat pharyngeal dilator muscle performance. *Am J Respir Cell Mol Biol,* 42**,** 725-31.

SKELLY, J. R., EDGE, D., SHORTT, C. M., JONES, J. F., BRADFORD, A. & O'HALLORAN, K. D. 2012a. Respiratory control and sternohyoid muscle structure and function in aged male rats: decreased susceptibility to chronic intermittent hypoxia. *Respir Physiol Neurobiol,* 180**,** 175-82.

SKELLY, J. R., EDGE, D., SHORTT, C. M., JONES, J. F., BRADFORD, A. & O'HALLORAN, K. D. 2012b. Tempol ameliorates pharyngeal dilator muscle dysfunction in a rodent model of chronic intermittent hypoxia. *Am J Respir Cell Mol Biol,* 46**,** 139-48.

SKELLY, J. R., ROWAN, S. C., JONES, J. F. & O'HALLORAN, K. D. 2013. Upper airway dilator muscle weakness following intermittent and sustained hypoxia in the rat: effects of a superoxide scavenger. *Physiol Res,* 62**,** 187-96.

SMIRNE, S., IANNACCONE, S., FERINI-STRAMBI, L., COMOLA, M., COLOMBO, E. & NEMNI, R. 1991. Muscle fibre type and habitual snoring. *Lancet,* 337**,** 597-9.

SMITH, B. K., MARTIN, A. D., VANDENBORNE, K., DARRAGH, B. D. & DAVENPORT, P. W. 2012. Chronic intrinsic transient tracheal occlusion elicits diaphragmatic muscle fiber remodeling in conscious rodents. *PLoS One,* 7**,** e49264.

SMITH, C. K., 2ND, JANNEY, M. J. & ALLEN, R. E. 1994. Temporal expression of myogenic regulatory genes during activation, proliferation, and differentiation of rat skeletal muscle satellite cells. *J Cell Physiol,* 159**,** 379-85.

SMITH, J. C., ABDALA, A. P., RYBAK, I. A. & PATON, J. F. 2009. Structural and functional architecture of respiratory networks in the mammalian brainstem. *Philos Trans R Soc Lond B Biol Sci,* 364**,** 2577-87.

SMITH, L. R. & BARTON, E. R. 2018. Regulation of fibrosis in muscular dystrophy. *Matrix Biol,* 68-69**,** 602-615.

SMITH, R. C. & LIN, B. K. 2013. Myostatin inhibitors as therapies for muscle wasting associated with cancer and other disorders. *Curr Opin Support Palliat Care,* 7**,** 352-60.

SOUZA, G. M., BONAGAMBA, L. G., AMORIM, M. R., MORAES, D. J. & MACHADO, B. H. 2015. Cardiovascular and respiratory responses to chronic intermittent hypoxia in adult female rats. *Exp Physiol,* 100**,** 249-58.

SPECHT, K. S., KANT, S., ADDINGTON, A. K., MCMILLAN, R. P., HULVER, M. W., LEARNARD, H., CAMPBELL, M., DONNELLY, S. R., CALIZ, A. D., PEI, Y., REIF, M. M., BOND, J. M., DEMARCO, A., CRAIGE, B., KEANEY, J. F., JR. & CRAIGE, S. M. 2021. Nox4 mediates skeletal muscle metabolic responses to exercise. *Mol Metab,* 45**,** 101160.

SRIRAM, S., SUBRAMANIAN, S., SATHIAKUMAR, D., VENKATESH, R., SALERNO, M. S., MCFARLANE, C. D., KAMBADUR, R. & SHARMA, M. 2011. Modulation of reactive oxygen species in skeletal muscle by myostatin is mediated through NF-kappaB. *Aging Cell,* 10**,** 931-48.

STEINBACHER, P. & ECKL, P. 2015. Impact of Oxidative Stress on Exercising Skeletal Muscle. *Biomolecules,* 5**,** 356-377.

STRETTON, C., PUGH, J. N., MCDONAGH, B., MCARDLE, A., CLOSE, G. L. & JACKSON, M. J. 2020. 2-Cys peroxiredoxin oxidation in response to hydrogen peroxide and contractile activity in skeletal muscle: A novel insight into exercise-induced redox signalling? *Free Radic Biol Med,* 160**,** 199-207.

STROKA, D. M., BURKHARDT, T., DESBAILLETS, I., WENGER, R. H., NEIL, D. A., BAUER, C., GASSMANN, M. & CANDINAS, D. 2001. HIF-1 is expressed in normoxic tissue and displays an organ-specific regulation under systemic hypoxia. *Faseb j,* 15**,** 2445-53.

STROLLO, P. J., JR., SOOSE, R. J., MAURER, J. T., DE VRIES, N., CORNELIUS, J., FROYMOVICH, O., HANSON, R. D., PADHYA, T. A., STEWARD, D. L., GILLESPIE, M. B., WOODSON, B. T., VAN DE HEYNING, P. H., GOETTING, M. G., VANDERVEKEN, O. M., FELDMAN, N., KNAACK, L. & STROHL, K. P. 2014. Upper-airway stimulation for obstructive sleep apnea. *N Engl J Med,* 370**,** 139-49.

SUGITA, H., KANEKI, M., SUGITA, M., YASUKAWA, T., YASUHARA, S. & MARTYN, J. A. 2005. Burn injury impairs insulin-stimulated Akt/PKB activation in skeletal muscle. *Am J Physiol Endocrinol Metab,* 288**,** E585-91.

SULLIVAN-GUNN, M. J. & LEWANDOWSKI, P. A. 2013. Elevated hydrogen peroxide and decreased catalase and glutathione peroxidase protection are associated with aging sarcopenia. *BMC Geriatrics,* 13**,** 104.

SUN, Q., ZHANG, W., ZHONG, W., SUN, X. & ZHOU, Z. 2017. Pharmacological inhibition of NOX4 ameliorates alcohol-induced liver injury in mice through improving oxidative stress and mitochondrial function. *Biochim Biophys Acta Gen Subj,* 1861**,** 2912-2921.

SUN, Q.-A., HESS, D. T., NOGUEIRA, L., YONG, S., BOWLES, D. E., EU, J., LAURITA, K. R., MEISSNER, G. & STAMLER, J. S. 2011a. Oxygen-coupled redox regulation of the skeletal muscle ryanodine receptor-Ca(2+) release channel by NADPH oxidase 4. *Proceedings of the National Academy of Sciences of the United States of America,* 108**,** 16098-16103.

SUN, Q. A., HESS, D. T., NOGUEIRA, L., YONG, S., BOWLES, D. E., EU, J., LAURITA, K. R., MEISSNER, G. & STAMLER, J. S. 2011b. Oxygen-coupled redox regulation of the skeletal muscle ryanodine receptor-Ca2+ release channel by NADPH oxidase 4. *Proc Natl Acad Sci U S A,* 108**,** 16098-103.

SYLOW, L., MOLLER, L. L., KLEINERT, M., RICHTER, E. A. & JENSEN, T. E. 2015. Stretch-stimulated glucose transport in skeletal muscle is regulated by Rac1. *J Physiol,* 593**,** 645-56.

SÉRLÈS, F., CÔTÉ, C., SIMONEAU, J.-A., PIERRE, S. S. & MARC, I. 1996. Upper airway collapsibility, and contractile and metabolic characteristics of musculus uvulae. *The FASEB Journal,* 10**,** 897-904
.

TAJBAKHSH, S. 2009. Skeletal muscle stem cells in developmental versus regenerative myogenesis. *J Intern Med,* 266**,** 372-89.

TALBOT, J. & MAVES, L. 2016. Skeletal muscle fiber type: using insights from muscle developmental biology to dissect targets for susceptibility and resistance to muscle disease. *Wiley Interdiscip Rev Dev Biol,* 5**,** 518-34.

TAMISIER, R., GILMARTIN, G. S., LAUNOIS, S. H., PEPIN, J. L., NESPOULET, H., THOMAS, R., LEVY, P. & WEISS, J. W. 2009. A new model of chronic intermittent hypoxia in humans: effect on ventilation, sleep, and blood pressure. *J Appl Physiol (1985),* 107**,** 17-24.

TAYLOR, C. T. 2008. Mitochondria, oxygen sensing, and the regulation of HIF-2α. Focus on “Induction of HIF-2α is dependent on mitochondrial O₂ consumption in an O₂-sensitive adrenomedullary chromaffin cell line”. *American Journal of Physiology - Cell Physiology,* 294**,** C1300-C1302.

TORGAN, C. E. & DANIELS, M. P. 2001. Regulation of Myosin Heavy Chain Expression during Rat Skeletal. *Mol Biol Cell,* 12**,** 1499-508.

TORRES, M., LAGUNA-BARRAZA, R., DALMASES, M., CALLE, A., PERICUESTA, E., MONTSERRAT, J. M., NAVAJAS, D., GUTIERREZ-ADAN, A. & FARRÉ, R. 2014. Male Fertility Is Reduced by Chronic Intermittent Hypoxia Mimicking Sleep Apnea in Mice. *Sleep,* 37**,** 1757-1765.

TRUONG, T. H. & CARROLL, K. S. 2013. Redox regulation of protein kinases. *Crit Rev Biochem Mol Biol,* 48**,** 332-56.

TSUBOI, H., KOUDA, K., TAKEUCHI, H., TAKIGAWA, M., MASAMOTO, Y., TAKEUCHI, M. & OCHI, H. 1998. 8-hydroxydeoxyguanosine in urine as an index of oxidative damage to DNA in the evaluation of atopic dermatitis. *Br J Dermatol,* 138**,** 1033-5.

UEYAMA, T., GEISZT, M. & LETO, T. L. 2006. Involvement of Rac1 in activation of multicomponent Nox1- and Nox3-based NADPH oxidases. *Mol Cell Biol,* 26**,** 2160-74.

VADYSIRISACK, D. D. & ELLISEN, L. W. 2012. mTOR activity under hypoxia. *Methods Mol Biol,* 821**,** 45-58.

VEASEY, S. C., CHACHKES, J., FENIK, P. & HENDRICKS, J. C. 2001. The effects of ondansetron on sleep-disordered breathing in the English bulldog. *Sleep,* 24**,** 155-60.

VEASEY, S. C., ZHAN, G., FENIK, P. & PRATICO, D. 2004. Long-term intermittent hypoxia: reduced excitatory hypoglossal nerve output. *Am J Respir Crit Care Med,* 170**,** 665-72.

VINCKEN, W., GUILLEMINAULT, C., SILVESTRI, L., COSIO, M. & GRASSINO, A. 1987. Inspiratory muscle activity as a trigger causing the airways to open in obstructive sleep apnea. *Am Rev Respir Dis,* 135**,** 372-7.

VOGEL, J., FIGUEIREDO DE REZENDE, F., ROHRBACH, S., ZHANG, M. & SCHRODER, K. 2015. Nox4 Is Dispensable for Exercise Induced Muscle Fibre Switch. *PLoS One,* 10**,** e0130769.

VOLEK, J. S., KRAEMER, W. J., RUBIN, M. R., GOMEZ, A. L., RATAMESS, N. A. & GAYNOR, P. 2002. L-Carnitine L-tartrate supplementation favorably affects markers of recovery from exercise stress. *Am J Physiol Endocrinol Metab,* 282**,** E474-82.

WAGNER, K. R., MCPHERRON, A. C., WINIK, N. & LEE, S. J. 2002. Loss of myostatin attenuates severity of muscular dystrophy in mdx mice. *Ann Neurol,* 52**,** 832-6.

WANG, G. L. & SEMENZA, G. L. 1995. Purification and Characterization of Hypoxia-inducible Factor 1. *Journal of Biological Chemistry,* 270**,** 1230-1237.

WANG, N., KHAN, S. A., PRABHAKAR, N. R. & NANDURI, J. 2013a. Impairment of pancreatic beta-cell function by chronic intermittent hypoxia. *Exp Physiol,* 98**,** 1376-85.

WANG, W. J., LU, G., DING, N., HUANG, H. P., DING, W. X. & ZHANG, X. L. 2013b. Adiponectin alleviates contractile dysfunction of genioglossus in rats exposed to chronic intermittent hypoxia. *Chin Med J (Engl),* 126**,** 3259-63.

WARD, K. L., HILLMAN, D. R., JAMES, A., BREMNER, A. P., SIMPSON, L., COOPER, M. N., PALMER, L. J., FEDSON, A. C. & MUKHERJEE, S. 2013. Excessive Daytime Sleepiness Increases the Risk of Motor Vehicle Crash in Obstructive Sleep Apnea. *Journal of Clinical Sleep Medicine : JCSM : Official Publication of the American Academy of Sleep Medicine,* 9**,** 1013-1021.

WAYPA, G. B., SMITH, K. A. & SCHUMACKER, P. T. 2016. O2 sensing, mitochondria and ROS signaling: The fog is lifting. *Mol Aspects Med,* 47-48**,** 76-89.

WEST, J. B. 1987. Alexander M. Kellas and the physiological challenge of Mt. Everest. *J Appl Physiol (1985),* 63**,** 3-11.

WHITE, C. W., JACKSON, J. H., MCMURTRY, I. F. & REPINE, J. E. 1988. Hypoxia increases glutathione redox cycle and protects rat lungs against oxidants. *J Appl Physiol (1985),* 65**,** 2607-16.

WHITE, D. P. & YOUNES, M. K. 2012. Obstructive sleep apnea. *Compr Physiol,* 2**,** 2541-94.

WHITE, S. G., FLETCHER, E. C. & MILLER, C. C., 3RD 1995. Acute systemic blood pressure elevation in obstructive and nonobstructive breath hold in primates. *J Appl Physiol (1985),* 79**,** 324-30.

WILLIAMS, R., LEMAIRE, P., LEWIS, P., MCDONALD, F. B., LUCKING, E., HOGAN, S., SHEEHAN, D., HEALY, V. & O'HALLORAN, K. D. 2015a. Chronic intermittent hypoxia increases rat sternohyoid

muscle NADPH oxidase expression with attendant modest oxidative stress. *Front Physiol,* 6**,** 15.

WILLIAMS, R., LEMAIRE, P., LEWIS, P., MCDONALD, F. B., LUCKING, E., HOGAN, S., SHEEHAN, D., HEALY, V. & O'HALLORAN, K. D. 2015b. Chronic intermittent hypoxia increases rat sternohyoid muscle NADPH oxidase expression with attendant modest oxidative stress. *Frontiers in Physiology,* 6.

WOLKOVE, N., BALTZAN, M., KAMEL, H., DABRUSIN, R. & PALAYEW, M. 2008. Long-term compliance with continuous positive airway pressure in patients with obstructive sleep apnea. *Canadian Respiratory Journal : Journal of the Canadian Thoracic Society,* 15**,** 365-369.

WOODSON, B. T., SOOSE, R. J., GILLESPIE, M. B., STROHL, K. P., MAURER, J. T., DE VRIES, N., STEWARD, D. L., BASKIN, J. Z., BADR, M. S., LIN, H. S., PADHYA, T. A., MICKELSON, S., ANDERSON, W. M., VANDERVEKEN, O. M. & STROLLO, P. J., JR. 2016. Three-Year Outcomes of Cranial Nerve Stimulation for Obstructive Sleep Apnea: The STAR Trial. *Otolaryngol Head Neck Surg,* 154**,** 181-8.

WU, H., XUE, D., CHEN, G., HAN, Z., HUANG, L., ZHU, C., WANG, X., JIN, H., WANG, J., ZHU, Y., LIU, L. & CHEN, Q. 2014. The BCL2L1 and PGAM5 axis defines hypoxia-induced receptor-mediated mitophagy. *Autophagy,* 10**,** 1712-25.

WUYTS, R., VLEMINCX, E., BOGAERTS, K., VAN DIEST, I. & VAN DEN BERGH, O. 2011. Sigh rate and respiratory variability during normal breathing and the role of negative affectivity. *Int J Psychophysiol,* 82**,** 175-9.

XIA, R., WEBB, J. A., GNALL, L. L., CUTLER, K. & ABRAMSON, J. J. 2003. Skeletal muscle sarcoplasmic reticulum contains a NADH-dependent oxidase that generates superoxide. *Am J Physiol Cell Physiol,* 285**,** C215-21.

XING, T., FONG, A. Y., BAUTISTA, T. G. & PILOWSKY, P. M. 2013. Acute intermittent hypoxia induced neural plasticity in respiratory motor control. *Clin Exp Pharmacol Physiol,* 40**,** 602-9.

YIN, H., PRICE, F. & RUDNICKI, M. A. 2013. Satellite cells and the muscle stem cell niche. *Physiol Rev,* 93**,** 23-67.

YUAN, G., KHAN, S. A., LUO, W., NANDURI, J., SEMENZA, G. L. & PRABHAKAR, N. R. 2011. Hypoxia-inducible factor 1 mediates increased expression of NADPH oxidase-2 in response to intermittent hypoxia. *J Cell Physiol,* 226**,** 2925-33.

YUSUF, F. & BRAND-SABERI, B. 2012. Myogenesis and muscle regeneration. *Histochem Cell Biol,* 138**,** 187-99.

ZANELLA, S., DOI, A., GARCIA, A. J., 3RD, ELSEN, F., KIRSCH, S., WEI, A. D. & RAMIREZ, J. M. 2014. When norepinephrine becomes a driver of breathing irregularities: how intermittent hypoxia fundamentally alters the modulatory response of the respiratory network. *J Neurosci,* 34**,** 36-50.

ZENG, S. Y., YANG, L., YAN, Q. J., GAO, L., LU, H. Q. & YAN, P. K. 2019. Nox1/4 dual inhibitor GKT137831 attenuates hypertensive cardiac remodelling associating with the inhibition of ADAM17-dependent proinflammatory cytokines-induced signalling pathways in the rats with abdominal artery constriction. *Biomed Pharmacother,* 109**,** 1907-1914.

ZHAN, G., SERRANO, F., FENIK, P., HSU, R., KONG, L., PRATICO, D., KLANN, E. & VEASEY, S. C. 2005. NADPH Oxidase Mediates Hypersomnolence and Brain Oxidative Injury in a Murine Model of Sleep Apnea. *American Journal of Respiratory and Critical Care Medicine,* 172**,** 921-929.

ZHANG, G.-L., DAI, D.-Z., ZHANG, C. & DAI, Y. 2013. Apocynin and raisanberine alleviate intermittent hypoxia induced abnormal StAR and 3β-HSD and low testosterone by suppressing endoplasmic reticulum stress and activated p66Shc in rat testes. *Reproductive Toxicology,* 36**,** 60-70.

ZHANG, J., WANG, X., VIKASH, V., YE, Q., WU, D., LIU, Y. & DONG, W. 2016a. ROS and ROS-Mediated Cellular Signaling. *Oxid Med Cell Longev,* 2016**,** 4350965.

ZHANG, T., XUE, L., LI, L., TANG, C., WAN, Z., WANG, R., TAN, J., TAN, Y., HAN, H., TIAN, R., BILLIAR, T. R., TAO, W. A. & ZHANG, Z. 2016b. BNIP3 Protein Suppresses PINK1 Kinase Proteolytic Cleavage to Promote Mitophagy. *J Biol Chem,* 291**,** 21616-21629.

ZHAO, J., BRAULT, J. J., SCHILD, A., CAO, P., SANDRI, M., SCHIAFFINO, S., LECKER, S. H. & GOLDBERG, A. L. 2007. FoxO3 coordinately activates protein degradation by the autophagic/lysosomal and proteasomal pathways in atrophying muscle cells. *Cell Metab,* 6**,** 472-83.

ZHOU, J. & LIU, Y. 2013. Effects of genistein and estrogen on the genioglossus in rats exposed to chronic intermittent hypoxia may be HIF-1α dependent. *Oral Dis,* 19**,** 702-11.

ZUO, L. & CLANTON, T. L. 2005. Reactive oxygen species formation in the transition to hypoxia in skeletal muscle. *American Journal of Physiology-Cell Physiology,* 289**,** C207-C216.

Chapter 2. Materials and Methods.

2.1 Ethical approval

Procedures on live animals were performed under licence from the Government of Ireland Department of Health (B100/4498) in accordance with National and European legislation (2010/63/EU) following approval by University College Cork Animal Research Ethics Committee (AEEC no. 2013/035) and conform to the principles and regulations described by (Grundy, 2015).

2.2 Chronic intermittent hypoxia animal model

C57BL/6J male mice (9 weeks old) were purchased from Envigo, UK, and assigned to one of 3 groups: normoxic control (sham; n = 20), chronic intermittent hypoxia (CIH)-exposed (CIH; n = 20) and CIH + apocynin (CIH + APO; n = 20). Exposure to CIH consisted of the cycling of gas from normoxia (21% O_2) for 210 seconds to hypoxia (5% O_2 at the nadir) over 90 seconds for 8hr/day during light hours for 14 consecutive days as previously described (Lucking et al., 2014). CIH + APO group also received the NADPH oxidase 2 inhibitor, apocynin, in the drinking water (2mM) for the duration of the exposure to CIH. The drug solution was made up fresh and changed daily for the 14 days. The sham group was exposed to 21% O_2 in parallel. In separate studies, 9-week-old NOX2 null male mice (B6.129S-Cybb^{tm1Din}/J) were purchased from the Jackson Laboratory (Bar Harbor, ME, USA) and assigned to a sham (NOX2 KO sham; n=12) or CIH (NOX2 KO CIH; n=12) exposure. Mice were housed in standard cages placed in commercially designed hypoxia chambers (Oxycyler™, Biospherix, Lacona, NY, USA) for daily gas treatment. Ambient O_2 concentration within the hypoxia chambers was continuously monitored and deviations from the desired O_2 concentration were automatically rectified by altering nitrogen gas flow to the chambers under the control of specialised software (Biospherix). Animals were conventionally housed in temperature- and humidity-controlled rooms, operating on a 12h light/ 12h dark cycle with food and water available *ad libitum*. Due to the immunocompromised nature of NOX2 null mice, these mice were housed in individually ventilated chambers when not undergoing exposure to CIH. Exposure to normoxia or CIH began at 11 weeks of age and all mice were studied the day after 14 consecutive days of exposure. Mice were weighed daily to monitor for any

substantial deleterious effects of exposure to CIH on body mass. On 'day 15', a subset of mice was subject to respiratory recordings using whole-body plethysmography (WBP; 2.3). Mice were subsequently anaesthetised with 5% isoflurane in air and euthanised humanely via cervical spinal dislocation. Brainstem tissue was collected from these mice, snap frozen in liquid nitrogen and stored at -80°C for subsequent analysis of monoamine concentrations using high performance liquid chromatography (HPLC; 2.4). An additional subset of mice was euthanised humanely as previously described. Sternohyoid (representative upper airway dilator muscle) and diaphragm (inspiratory pump muscle) muscles were excised and used for *ex vivo* muscle function analysis (2.5) or snap frozen in liquid nitrogen and stored at -80°C for further tissue processing prior to gene (2.6) and protein analysis (2.7, 2.8 & 2.9).

2.3 Whole-body plethysmography (WBP)

Respiratory flow recordings were examined in awake, unrestrained and unanaesthetised mice during quiet rest using WBP. Mice were introduced into plethysmograph chambers (Model PLY4211; volume 600ml, Buxco Research Systems, Wilmington, NC, USA) with room air flowing through to ensure adequate O_2 and CO_2 environmental conditions. Mice were allowed 60 minutes to acclimate to the chamber environment. Following exploration and grooming behaviours during this period, mice were considered settled and baseline recordings commenced. Multiple baseline measurements consisting of 15-minute bins were averaged to increase the length and power of the baseline period represented in table 3.2. Respiratory variables including respiratory frequency (f_R), tidal volume (V_T), minute ventilation ($\dot{V}_I$) inspiratory time (T_i), expiratory time (T_e), peak inspiratory flow (PIF) and peak expiratory flow (PEF) were recorded every 2 seconds for analysis offline. Levels of O_2 and CO_2 gas entering and exiting the plethysmograph chambers were measured on a minute-by-minute basis (O_2 and CO_2 analyser; AD Instruments, Colorado Springs, CO, USA) allowing O_2 consumption ($\dot{V}O_2$) and CO_2 production ($\dot{V}CO_2$) in mice to be determined (Burns et al., 2017, Burns et al., 2018). From this, the ventilatory equivalent for CO_2 ($\dot{V}_I$ / $\dot{V}CO_2$) and O_2 ($\dot{V}_I$/ $\dot{V}O_2$) were calculated.

2.3.1 Respiratory stability

Respiratory flow recordings for sham (n = 12), CIH (n = 12), CIH + APO (n = 12), NOX2 KO sham (n = 12) and NOX2 KO CIH (n =12) mice during normoxia (21% O2) were examined for the measurement of respiratory stability and apnoea scoring. The breath-to-breath (BB_n) and subsequent interval (BB_{n+1}) of 200 breaths were analysed as previously described (Peng et al., 2011, Souza et al., 2015). Poincaré plots expressing BB_n *versus* BB_{n+1} for 200 consecutive breaths were plotted for expiratory time (T_e) and total breath duration (T_{tot}) for all groups outlined above. Short-term variability (SD1) and long-term variability (SD2) were calculated as indices of breathing variability. Respiratory flow signals were visually analysed for the frequency of sigh events (augmented breaths), which was defined as an increase in tidal volume to at least twice the amplitude observed during a eupnoeic breath. Additionally, the frequency and duration of spontaneous and post-sigh apnoeic events were determined. The criterion for apnoea was defined as a cessation in breathing greater than two missed breaths and the criterion for a post-sigh apnoea was an apnoeic event occurring within 20s following an augmented breath, as previously described (Edge et al., 2012, O'Connor et al., 2019).

2.3.2 Ventilatory responsiveness to chemostimulation

Following baseline recordings, ventilatory responsiveness to chemostimulation was examined for all groups. A 10-minute hypoxic challenge (F_iO_2 = 0.1) was elicited in which mice were challenged with reduced levels of O_2 before returning flow to room air for 20 minutes. Once baseline was established, a 10-minute hypercapnic (F_iCO_2 = 0.05, F_iO_2 = 0.95) challenge was performed. Ventilatory parameters were also recorded every 2 seconds during hypoxic and hypercapnic challenges. These data were subsequently averaged and expressed on a minute-by-minute basis. Metabolic parameters ($\dot{V}O_2$ and $\dot{V}CO_2$) were recorded on a minute-by-minute basis. Peak ventilation for each individual animal was determined during hypoxia and hypercapnia and compared with the baseline normoxic period. Ventilatory responsiveness to hypoxia and hypercapnia was expressed as a change from baseline

(Δ $\dot{V}_I$). The corresponding $\dot{V}CO_2$ value for each peak response was then used to calculate Δ $\dot{V}_I$ / $\dot{V}CO_2$.

2.4 High performance liquid chromatography

Monoamines and metabolites important in the neurochemical control of breathing, including 5-hydroxytryptamine (5-HT) and 5-hydroxyindoleacetic acid (5-HIAA), were quantified in brainstem samples from all groups using high performance liquid chromatography (HPLC), as previously described (Clarke et al., 2013). Frozen samples were thawed in 500 μl of chilled homogenising buffer spiked with 2ng/20μl of N-Methyl 5-HT (Sigma, UK) as internal standard, sonicated for 2 x 4 s bursts (Bandelin Sonoplus HD 2070) and centrifuged at 14,000 RPM for 20 mins at 8^{o}C (MIKRO 22 R refrigerated centrifuge). 20 μl of supernatant was injected onto the HPLC system (Electrochemical Detection). The mobile phase contained 0.1M citric acid, 0.1M sodium dihydrogen phosphate, 0.01mM EDTA (Fisher Scientific Ireland), 5.6mM octane-1-sulphonic acid (Sigma) and 11% (v/v) HPLC-grade methanol (Fisher Scientific, Ireland), and was adjusted to pH 2.8 using 4N sodium hydroxide (Alkem/Reagecon). A reverse-phase column (Kinetex 2.6u C18 100 x 4.6mm, Phenomenex, UK) maintained at 30^{o}C was employed in the separation (flow rate 0.9ml/min), the glassy carbon working electrode combined with an Ag/AgCl reference electrode (Shimdazu) was operated a +0.8V and the chromatograms generated were analysed using Class-VP 5 software (Shimadzu, Corporation, Kyoto, Japan). Monoamines and their metabolites were identified by their characteristic retention times as determined by standard injections which were run at regular intervals during the sample analysis. The chromatograms were processed using Class 5-VP software (Shimadzu Corporation, Kyoto, Japan). Analyte: Internal standard peak height ratios were measured and compared with standard injections and results were expressed as ng of analyte per g tissue weight.

2.5 Ex vivo muscle function analysis

2.5.1 Muscle dissection and preparation

Animals were euthanised as described in section 2.2 and sternohyoid and diaphragm muscles were excised carefully, but quickly to minimise damage. Briefly, a ventral incision was made from the genu of the mandible to the sternum. A closed forceps was delicately placed under the paired sternohyoid muscles to gently tease them away from the trachea. The muscles were then cut at the rostral and caudal boundaries and were immediately placed in a storage bath of hyperoxic (95% O_2, 5% CO_2) Krebs solution (NaCl 120mM, KCl 5mM, Ca^{2+} gluconate 2.5 mM, $MgSO_4$ 1.2 mM, NaH_2PO_4 1.2 mM, $NaHCO_3$ 25 mM, glucose 11.5 mM and d-tubocurarine 25 µM) to allow the muscles to recover from dissection at room temperature. For removal of the diaphragm muscle, the ventral incision was extended from the neck to the abdomen, inferior to the lower ribcage. By firmly gripping the central tendon and cutting around the rib cage, the whole diaphragm muscle was excised and subsequently added to the storage bath of hyperoxic Krebs solution. For functional analysis, muscles were cut into strips of appropriate size. The sternohyoid was cut longitudinally along its natural midline, separating the two paired muscles (~2mm each) whereas a strip of diaphragm was cut longitudinally in the direction of its muscle fibres (~2mm in diameter). Muscles were returned to the hyperoxic Krebs solution for 10-15 minutes to recover from dissection. Following this, muscles were suspended vertically in a water-jacketed organ bath maintained at 35^{o}C. Using non-elastic string, one sternohyoid muscle was attached to an immobile hook on the bottom and a dual-mode lever transducer on top (Aurora Scientific Inc., Canada) with platinum plate electrodes flanking either side of the muscle. Similarly, a strip of diaphragm muscle was attached with non-elastic string at the rib end to the immobile hook and the central tendon to the dual-mode lever transducer, with platinum plate electrodes flanking either side of the muscle. The bath was filled with Krebs solution and constantly bubbled with carbogen (95% O_2, 5% CO_2) to maintain a hyperoxic environment. Muscles were allowed an equilibration time of 15 minutes in the muscle bath before the experimental protocol was initiated.

2.5.2 Isometric protocol

Muscle function was examined by employing a range of protocols extensively used by our group (O'Leary and O'Halloran, 2016, Burns et al., 2017, Burns et al., 2018, O'Leary et al., 2018, Burns et al., 2019). Sternohyoid and diaphragm muscles from all experimental groups (sham, CIH, CIH + APO, NOX2 KO sham & NOX2 KO CIH; n = 8-10 per group) were examined. When assessing isometric muscle contractions, the force transducer remained at maximum tension (>100% load). Muscle strips were stimulated at supramaximal voltage via the platinum plate electrodes. The optimal length (L_o), the length which produces the maximum twitch force, was obtained by stimulating the muscle supra-maximally for 1ms. The length of the muscle was adjusted using a micro-positioner between each of these stimulations and once the L_o was achieved, the muscle remained at this length for the duration of the protocol. The L_o (mm) encompasses the muscle between the knot attaching it to the immobile hook and the knot attaching it to the force transducer, therefore ensuring that only actively contracting muscle fibres are accounted for. A single twitch stimulation was applied from which twitch force and contractile kinetics including contraction time (CT; time to peak force) and half-relaxation time (1/2 RT; time for force to decay by 50%) were determined. Following this, an isometric tetanic contraction was evoked by supramaximal stimulation at a frequency of 100Hz for 300ms to determine the peak tetanic force (F_{max}). Specific force was calculated in N/cm^2 of estimated muscle cross sectional area (CSA). The CSA of each strip was determined by dividing the muscle mass (weight in grams) by the product of muscle L_o (cm) and muscle density (assumed to be $1.06g/cm^3$).

2.5.3 Isotonic protocol

Throughout the isotonic protocol, the force transducer was set to varying degrees of tension (0-100% load). Initially, the force transducer was set to its minimum tension (0%) and the muscle was stimulated to contract against a load that equated to 0% of its Fmax. This load was then increased in a step-like manner (5%, 10%, 20%, 30%, 40%, 60%, 80%, 100%) % of Fmax. A contraction was elicited at each step and 30 seconds was allowed between each contraction to allow the muscle to fully return to L_o. The length of shortening was defined as the maximum distance of shortening

during the contraction and shortening velocity was derived from the distance of shortening during the first 30ms of shortening during a contraction (when velocity is maximal). Peak shortening length and velocity were achieved at 0% of Fmax. Peak specific shortening (Smax) was defined as the length of shortening per optimal length (L/Lo). Peak specific shortening velocity (Vmax) was defined as Lo/s. From this protocol, we were able to calculate the work (force x shortening) and power-generating capacity (force x shortening velocity) of the sternohyoid muscle at each step. From the work-load and power-load relationships achieved through this protocol, peak work and peak power were extrapolated. Peak specific mechanical work (Wmax) was calculated as Joules/cm^2 and peak specific mechanical power (Pmax) as Watts/cm^2.

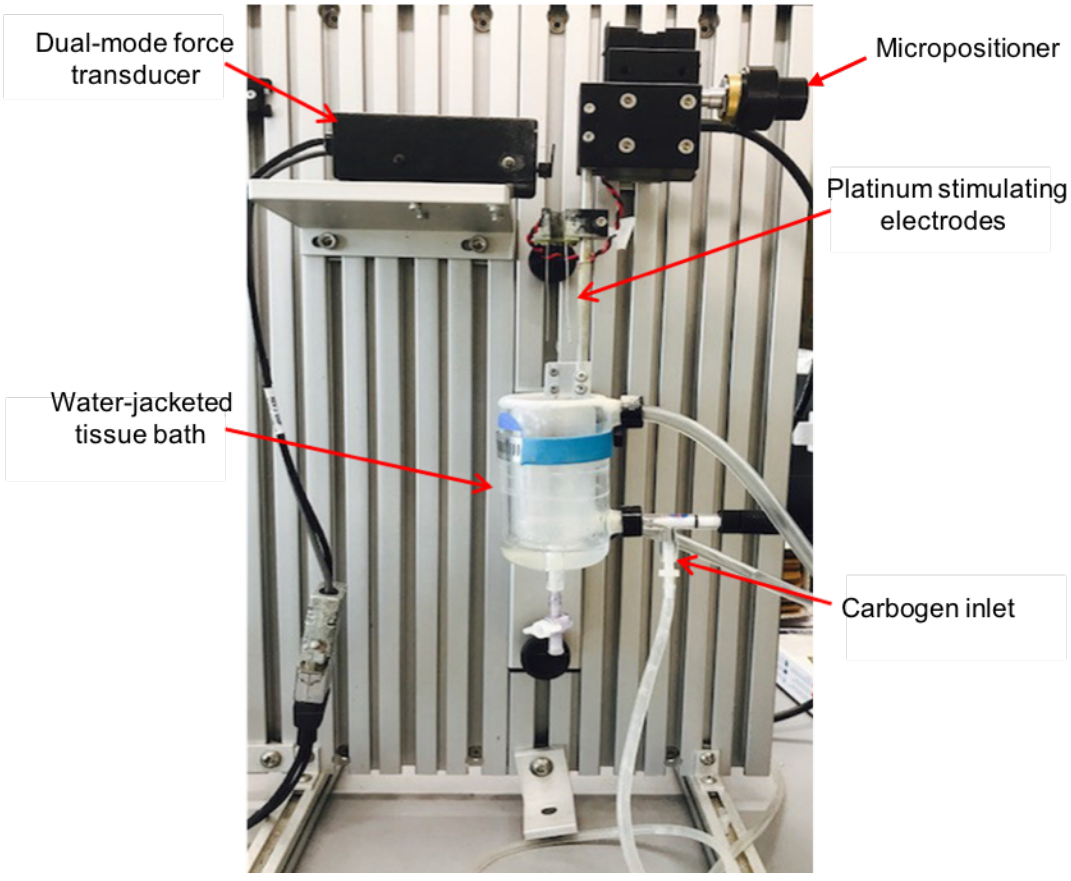

Figure 2.1 *Ex vivo* muscle bath set-up.

2.6 Quantitative reverse transcription polymerase chain reaction (qRT-PCR)

2.6.1 Tissue homogenisation

Equipment, gloves and surfaces were sprayed with RNase*Zap*® (Thermo Fisher Scientific, Ireland) to ensure a thoroughly decontaminated environment, pivotal for carrying out RNA preparation. Sternohyoid and diaphragm muscle samples from all experimental groups (sham, CIH, CIH + APO, NOX2 KO sham & NOX2 KO CIH; n = 6-9 per group) were removed from storage at -80°C and immediately weighed. Samples ranging from 20-40mg were homogenised in 1ml of Tripure Isolating Reagent (Roche Diagnostics Ltd., West Sussex, UK) on ice for 3 x 10 second bursts. Homogenates remained on ice for 20 minutes with intermittent vortexing to enable cell lysis and maximal RNA yield from muscle tissue. RNA was then either immediately isolated from the homogenised samples or samples were stored at -80°C until required.

2.6.2 RNA extraction

200μl of chloroform was added to each sample and following a 5-minute incubation period at room temperature, samples were centrifuged for 15 minutes at 4°C at 12,380 RPM (U-320R centrifuge, Boeckel + Co, Hamburg, Germany). Following this, three phases were observed, the upper aqueous phase containing RNA, the middle milky phase containing DNA and the lower pink phase containing proteins and lipids. The clear upper aqueous solution containing RNA was transferred to a fresh eppendorf and the lower phases were discarded. An additional chloroform step, as previously described, was repeated with 700μl added to the recovered supernatant. Following this, two clear phases were observed; the upper clear phase containing RNA and the lower clear phase contained nucleic acids and salts. 700μl of isopropanol was then added to each eppendorf containing the recovered upper RNA phase. Eppendorfs were inverted twice, incubated for 5 minutes at room temperature and centrifuged at 4°C at 12,380 RPM for 10 minutes to precipitate the RNA. Following this, a clear gel pellet of RNA was adhered to the side of the eppendorf as RNA is insoluble in isopropanol. Isopropanol was carefully poured off and ethanol (70%) was added to the pellet which was gently vortexed to ensure

thorough washing and removal of any salts and contaminants in RNA samples. Samples were then centrifuged at 4°C at 14,000 RPM for 10 minutes to adhere the pellet to the eppendorf once again. The ethanol was subsequently discarded, and the pellet was allowed to air dry. The RNA pellet was then re-dissolved in 20-60µl of RNase free water (Sigma Aldrich, Arklow, Wicklow, Ireland), depending on the mass of the muscle sample. RNA was treated with a TURBO DNA-free kit where necessary (Life Technologies, Biosciences, Dun Laoghaire, Ireland), as per the manufacturer's instructions, to ensure the complete digestion of any contaminating DNA that may be present within the sample. The purity and quantity of RNA was determined by spectrophotometry using a Nanodrop 1000 (Thermo Scientific, Wilmington, Delaware, USA) (Fig. 2.2; A). The 260/280 value measures protein and DNA contamination. The normal range for 260/280 values is between 1.8-2.0. The 260/230 value measures ethanol and isopropanol contamination. The normal range for 260/230 values is 1.8-2.2. The integrity of the RNA was also assessed using an agarose gel electrophoresis system (E-gel, Life Technologies) in which samples were loaded against a DNA ladder (E-gel, Life Technologies) to visualise clear 28S and 18S ribosomal RNA bands (Fig. 2.2; B).

(A)

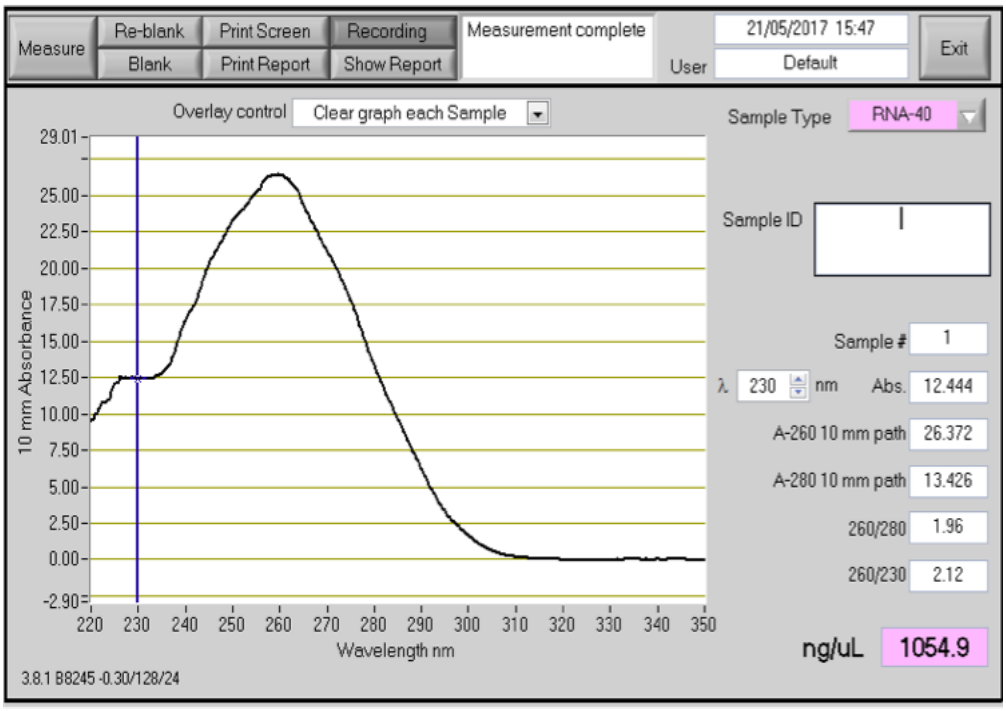

(B)

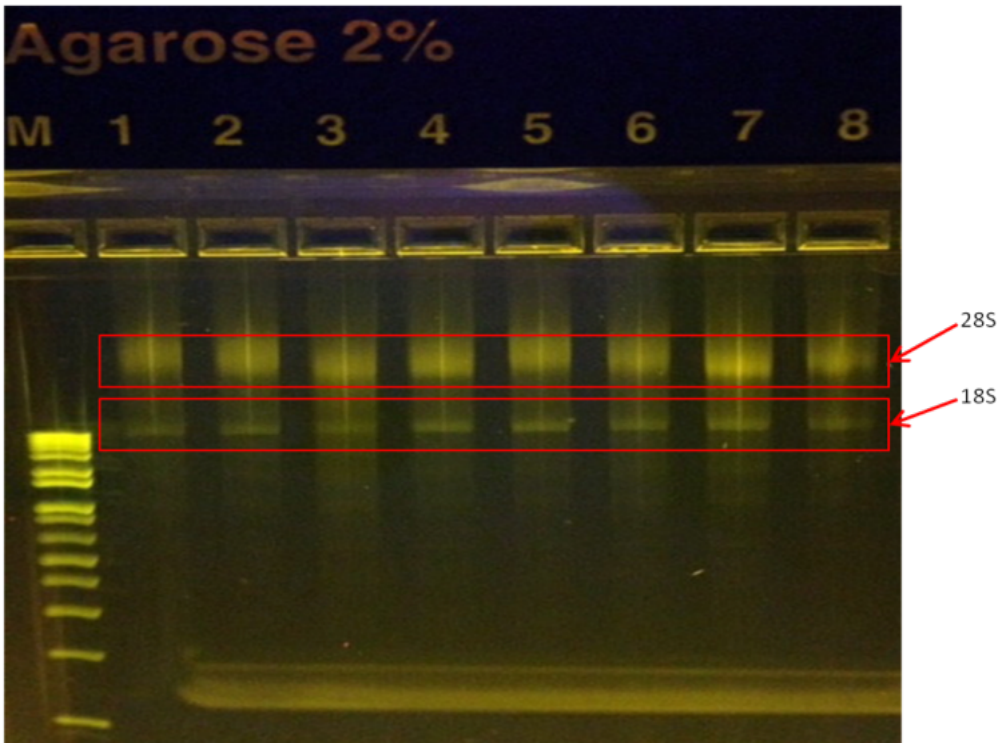

Figure 2.2 RNA purity & integrity screening. (A) An absorbance curve from the Nanodrop 1000 including the RNA concentration (ng/µl) of the sample being tested, 260/280 and 260/230 ratios and a single peak at 260nm, indicating good sample purity. (B) Representative image of an RNA sample run on an e-gel, showing distinctly separate 28S and 18S ribosomal RNA bands, indicating preservation of RNA integrity following isolation.

2.6.3 cDNA synthesis

RNA was reverse transcribed using a Transcriptor First Strand cDNA Synthesis Kit (Roche Diagnostics Ltd.). Briefly, the concentration of RNA was normalised across all samples, utilising concentrations (ng/μl) obtained from the nanodrop. Samples from all experimental groups (10μl) were then plated on a 96-well plate with an equal amount of master mix containing essential components (reverse transcriptase, random hexamer primers, anchored oligo$(dT)_{18}$ primer and protector RNase inhibitor) for the reverse transcription of RNA to cDNA. The 96-well plate was sealed and placed in the LightCycler 96 (Roche Diagnostics Ltd.) and exposed to three incubation periods, 10 minutes at 25°C (pre-incubation), 60 minutes at 50°C (reaction) and 5 minutes at 85°C (inactivation). The resultant cDNA was diluted 1:10 in RNase free water and stored at -20°C until required for further experimentation. A reverse transcription negative (RT negative) was also required for each sample, which contained 10μl of sample and 10μl of water. These were all subsequently tested against a PCR probe to confirm that there was no cDNA created without the addition of cDNA reaction mix. Thus, no non-specific PCR amplification could occur from the RNA alone or any traces of genomic DNA that may have been present in the sample. One RT negative representative of each group was used on every PCR plate thereafter.

2.6.4 qRT-PCR

cDNA was amplified using Realtime ready Catalog or Custom Assays (Roche Diagnostics Ltd.) and Fast Start Essential DNA Probe Master (Roche Diagnostics Ltd.). Reactions were carried out as per the manufacturer's instructions in 20μl (5μl cDNA and 15μl master mix). All reactions were carried out in duplicate along with appropriate positive and negative controls including reverse transcription negatives, RNA negatives, cDNA negatives (no template) and calibrators, as shown in Fig. 2.3. Once plated and sealed, the 96-well plate was placed in the LightCycler 96 (Roche Diagnostics Ltd.) and subjected to a pre-incubation period (1 cycle), 3 step amplification (45 cycles) and cooling (1 cycle). Quantification cycle (Cq) values obtained from experiments for our genes of interest (Table 2.1) were normalised to

that of a reference gene, *hypoxanthine-guanine phosphoribosyltransferase-1* (*hprt1)*. This allows a level of correction for any variation in the amount of RNA inputted or cDNA recovered following reverse transcription. Previous work in our laboratory (O'Leary and O'Halloran, 2016) has shown that *hprt1* was considered the most stable reference gene when tissue type (respiratory muscles) and gas exposure (hypoxia) was considered. We confirm this finding by showing that *hprt1* was stable across all experimental groups in the current study (Fig. 2.4). Relative gene expression was calculated using the ΔΔCT method to normalise the expression of genes of interest to that of the stable reference gene, *hprt1*, with a change in mRNA shown as a fold change over the controls (sham).

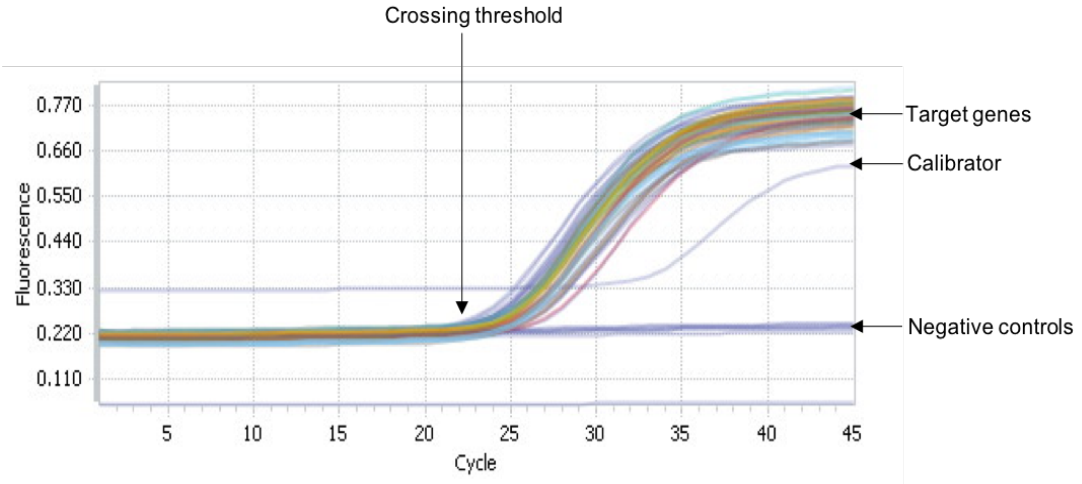

Figure 2.3 PCR amplification. Representative image of a PCR amplification curve obtained from the Lightcycler96.

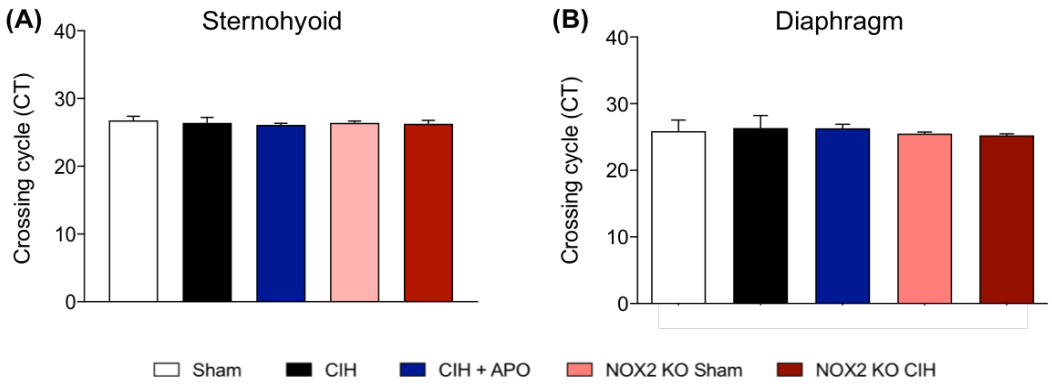

Figure 2.4 Reference gene for qRT-PCR. Stability of *hprt1* across all groups in (A) sternohyoid and (B) diaphragm muscle**.**

Gene name	Gene Symbol	Assay ID
NOX enzymes		
NOX1	NOX1	310986
NOX2	Cybb	317885
NOX4	NOX4	300795
p22phox	Cyba	317890
p47phox	Ncf1	301105
p67phox	Ncf2	317897
p40phox	Ncf4	317894
Rac	Racgap1	310907
Duox1	Duox1	317891
Duox2	Duox2	317888
Atrophy		
Atrogin-1	Fbxo32	317844
MuRF-1	Trim63	317843
Autophagy		
BNIP3	Bnip3	311465
LC3B	Map1lc3b	317920
GABARAPL1	Gabarapl1	317923
Mitophagy		
PINK-1	Pink1	331846
PARK-2	Park2	317264
Inflammation		
NFκB	Nfkb1	300085
Antioxidant		
SOD1	Sod1	310738
SOD2	Sod2	310295
Catalase	Cat	310718
Nrf2	Nfe2l2	313377
Muscle differentiation		
Myogenin	Myog	313501
Myostatin	Mstn	318626
MyoD	Myod1	313570
MEF2C	Mef2c	318629
IGF1	Igf1	313359
Sirtuin-1	Sirt1	310480
Reference		
HPRT1	Hprt1	307879

Table 2.1 Assay details for genes of interest. Real-time ready catalog and custom assays used for cDNA amplification.

2.7 Western blotting

2.7.1 Protein extraction and quantification

Sternohyoid and diaphragm muscles were removed from storage at -80°C and allowed to defrost on ice for 2 minutes. Muscles were weighed and homogenised with 8 x 10 second bursts using a general laboratory homogeniser (Omni-Inc., Kennesaw, Georgia, USA) in modified ice cold radioimmunoprecipitation assay buffer (RIPA buffer) containing: RIPA (25 mM Tris-HCl pH 7.6, 150 mM sodium chloride, 1% NP-40, 1% sodium deoxycholate, 0.1% SDS), deionised water, protease inhibitor cocktail (104 mM AEBSF, 80µM aprotinin, 4mM bestatin, 1.4mM E-64, 2mM leupeptin, 1.5mM pepstatin A) phosphatase inhibitor cocktail (200mM sodium fluoride, 5mM sodium orthovanadate) and 100mM PMSF (Sigma Aldrich, Arklow, Wicklow, Ireland) using a 10% w/v ratio. Homogenates were allowed 20 minutes lyse time on ice with intermittent vortexing at 4-minute intervals. Samples were centrifuged (U-320R centrifuge Boeckel + Co, Hamburg, Germany) for 20 minutes at 4°C at 14,000 RPM to separate insoluble cell fractions from protein homogenates. The clear protein containing supernatant was recovered from each sample and transferred to a fresh eppendorf. The protein concentration of each sample was determined using a bicinchoninic acid (BCA) protein quantification assay (Pierce Biotechnology, Ireland). A standard curve was generated using a serial dilution of stock (2mg/ml) bovine serum albumin (BSA) solution. Diluted standards and samples (1:10) were loaded in triplicate with 200µl working reagent and incubated at 37°C for 30 minutes. Absorbance was measured at 562nm using a SpectraMax-M3 spectrophotometer (Molecular Devices, Sunnyvale, California, USA) and protein concentrations were ascertained based on values from the standard curve. Homogenates were subsequently stored at -80°C until further use.

2.7.2 Gel electrophoresis

Western blot analysis was carried out on sternohyoid and diaphragm muscle homogenates from CIH-exposed and sham mice (n = 5-7 per group). Samples were diluted with deionised water, based on their protein concentration and mixed with an equivalent volume of SDS-PAGE loading buffer (4% SDS (sodium dodecyl sulfate),

200mM DTT (dithiothreitol), 20% glycerol, 100mM TRIS-CL (pH 6.8), 0.2% Bromophenol blue). Samples were subsequently boiled at 100°C for 5 minutes on a dry heating block (Techne, UK). Bio-Rad gel plates (Bio-Rad, Hertfordshire, UK) were set up in a clamped bracket apparatus in order to pour and set an acrylamide gel. 10% resolving gel (deionised water, 30% acrylamide, 1.5M TRIS pH 8.8, 10% SDS, 10% ammonium persulfate) was prepared with 5µl of tetramethylethylenediamine (TEMED) added immediately before use. Isopropanol was added along the surface of the resolving gel to ensure a level gel and to prevent air bubbles from inhibiting polymerisation. This was allowed to set for ~1 hour, following which isopropanol was rinsed off. A 5% stacking gel (deionised water, 30% acrylamide, 1.5M TRIS pH 6.8, 10% SDS, 10% ammonium persulfate) was made up and 5µl of TEMED was added immediately before use. The solution was poured on top of the resolving gel and a 15-well comb was placed into the gel to create even spaces for the sample addition. Once set, the comb was carefully removed and the gel was fitted into an electrophoretic chamber (Bio-Rad, Hertfordshire, UK) and electrophoresis running buffer (25 mM Tris, 192 mM glycine, 0.1% SDS, pH 8.3) was added. Specialised loading tips were used to add pre-stained molecular weight marker (Sigma Aldrich, Arklow, Wicklow, Ireland) to the first well followed by 15-20µg muscle homogenates into each of the wells thereafter. The chamber was connected to a power pack (Bio-Rad, Hertfordshire, UK) and a current of 200V was applied for 50-60 minutes, depending on the time required to resolve proteins of interest.

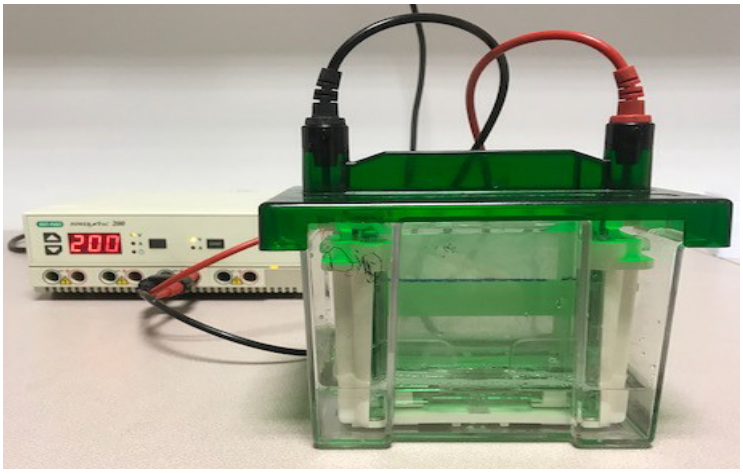

Figure 2.5 Gel electrophoresis equipment set-up.

2.7.3 Semi-dry transfer

Following electrophoresis, gels were carefully removed from between glass plates and placed in Dunn-carbonate semi-dry transfer buffer (20% methanol, 19mM $NaCHO_3$, 3mM $NaCO_3$) on a gentle shaker (Stovall Life Science, Inc) for 10 minutes. Nitrocellulose membrane and filter paper were soaked in the same buffer for 15 minutes prior to transfer. Filter paper was placed on the positive electrode plate of a Trans-Blot Semi Dry Transfer Cell (Bio-Rad, Hertfordshire, UK) followed by nitrocellulose membrane, the acrylamide gel and more filter paper. A sterile 15ml tube was used to gently roll out any air bubbles that might have formed at any of these layers. The negative electrode plate lid was placed over this sandwich arrangement and the unit was operated at 15V for 30 minutes. Resultant membranes were washed and stained with Ponceau S in 5% acetic acid to confirm the successful transfer of proteins and a digital image was taken to assess equal protein loading (Uvipro Digital Photographer).

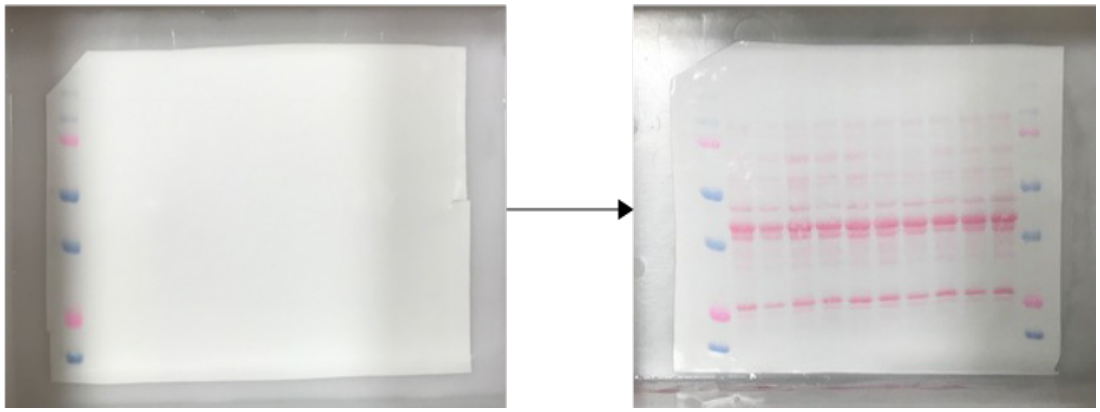

Figure 2.6 Protein transfer. Representative nitrocellulose membrane washed directly after protein transfer (left) and following Ponceau S staining (right), demonstrating successful protein transfer and relatively equal protein loading.

2.7.4. Immunostaining

Nitrocellulose membranes were blocked for 1 hour in TBST (20mM Tris-HCL, pH 7.6, 150mM NaCl, 0.15% tween) containing 5% non-fat dried milk. Primary antibodies of interest were diluted as per the manufacturer's instructions; anti-NOX2, anti-NOX4; 1:10000; 1:2000 (Abcam, Cambridge, UK) in 5% bovine serum albumin (BSA) / 5%

non-fat dried milk. Membranes were incubated in primary antibody solutions overnight with gentle shaking at 4°C and rinsed with TBST 5 times at 5-minute intervals the next day. Membranes were then incubated with a horse radish peroxidase (HRP) conjugated secondary antibody (anti-mouse, 1:2000 5% non-fat dried milk) specific for the primary antibody of interest. Following another 5 washes with TBST at 5-minute intervals, enhanced chemiluminescence (ECL) solution (GE Healthcare, UK) was added to the surface of membranes and they were incubated for 5 minutes at room temperature. Membranes were exposed to photosensitive film and developed using an automatic film processer (AGFA CP1000). Resultant films were imaged and densitometric analysis was performed on both Ponceau S and developed film images using Image J software (NIH Image) to determine relative band intensities. The band intensities generated for proteins of interest were normalised to corresponding Ponceau S band intensities to correct for any variations in the quantity of protein per well, thus allowing comparative analysis of results. Results are expressed as optical density (O.D)/Ponceau S (arbitrary units; a.u).

2.8 Spectrophotometric assays

2.8.1 Protein extraction and quantification

Sternohyoid and diaphragm muscles were homogenised, and protein was quantified using the protocol previously described in section 2.7.1.

2.8.2 NADPH oxidase activity

NOX enzyme activity was assessed in sternohyoid and diaphragm muscle homogenates from sham and CIH-exposed mice (n = 8 per group) using a cocktail mixture containing: nitroblue tetrazolium (NTB, 2.2mM in water), Tris-HCL pH8 (2.8mM) & diethylene-triamine-penta-acetic acid (1.3mM in Tris-HCL) and a fresh solution of NADPH (1mM). 20μl of muscle homogenate, 250μl of cocktail mixture and 30μl of NADPH was added per well in a black 96-well plate. The plate was gently shaken at room temperature for 2 minutes following which absorbance was measured in a SpectraMax-M3 spectrophotometer (Molecular Devices, Sunnyvale, California, USA) at 560nm at 1 min intervals for 30 minutes. NOX activity corresponded to the slope of the formation of formazan blue over time. Data were expressed as enzymatic activity per mg of protein in the sample, previously determined by BCA assay, per minute.

2.8.3 Citrate synthase activity

Citrate synthase is an enzyme that catalyses the reaction between acetyl coenzyme A (acetyl CoA) and oxaloacetic acid to produce citric acid. It is the initial enzyme of the tricarboxylic acid (TCA) cycle and is commonly used as a marker of mitochondrial integrity. Citrate synthase activity was examined in sternohyoid and diaphragm muscle homogenates from sham and CIH-exposed mice (n=8 per group). The experimental procedure for the citrate synthase activity assay was performed in accordance with the manufacturer's instructions (CS0720; Sigma-Aldrich). All assay solutions were warmed to 25°C in a water bath and a SpectraMax-M3 spectrophotometer (Molecular Devices, Sunnyvale, California, USA) was set to 412nm before beginning. 8μl of muscle homogenate was loaded per well in a black 96 well plate. A cocktail mixture containing 178μl assay buffer, 2μl acetyl CoA

(30mM) & 2μl DTNB (10mM) solution) was added to the sample in each well following which absorbance was immediately recorded for 1.5 mins to measure the baseline reaction or endogenous activity levels. 10μl of oxaloacetate (OAA, 10mM) was then added to each well and absorbance was recorded at 10 second intervals for another 1.5 mins to measure total activity. Data were expressed as enzymatic activity per μmole per min per mg protein in the sample, previously determined by BCA assay.

2.8.4 Thiobarbituric acid reactive substances

Thiobarbituric acid reactive substances (TBARS) are degradation products of fats which are routinely used as a marker of lipid peroxidation, an indirect measurement of oxidative stress. Levels of TBARS were examined in sternohyoid and diaphragm muscle homogenates from sham and CIH-exposed mice (n=8 per group). Malondialdehyde (MDA) of a known concentration was used to generate a standard curve. Next, 50μl of thiobarbituric acid (TBA, 50 mM) was added to 50μl of muscle homogenate and the solution was incubated for 60 minutes at 97°C on a dry heating block. Samples were subsequently cooled on ice, and 75μl of methanol: 1 mM NaOH (91: 9) was added to the solution. Samples were then centrifuged at 3000 RPM and 70μl of the resultant supernatant was added per well in a black 96-well plate. The plate was read in a SpectraMax-M3 spectrophotometer (Molecular Devices, USA) using 523/553 excitation/emission settings and data were compared with standards. Data are expressed as nM TBARS per mg of protein in the sample, previously determined by BCA assay.

2.9 Cell signalling assays

2.9.1 Protein extraction and quantification

Sternohyoid and diaphragm muscles were homogenised and prepared using the same protocol described in section 2.7.1 with some minor optimisation alterations. These included using a 2.5% w/v ratio of tissue to RIPA buffer, using twice the amount of phosphatase inhibitor and a 1:3 dilution of homogenates for the BCA assay. These modifications were made in order to maximise the protein yield for cell signalling assays discussed below.

2.9.2 MAP Kinase phosphoprotein assay

The MAP Kinase Phosphoprotein Assay quantifies the phosphoprotein content of the Mitogen-Activated Protein (MAP) kinases ERK1/2, p38 and JNK in a multiplex fashion. This assay was carried out on sternohyoid and diaphragm muscle homogenates (n = 8 per group) from mice exposed to 2 weeks of CIH or normoxia (sham). The Mesoscale multiplex format assay (Mesoscale Discovery, Gaithersburg, USA) allows the measurement of all three of these phospho-proteins in one well. A host of capture antibodies against various proteins of interest are pre-coated on distinct spots in each well of a 96-well plate. All wells of the plate were initially blocked for 1 hour and subsequently washed out 3 times. 25μg of sample was added per well in duplicate and the plate was sealed and incubated with vigorous shaking (300-1000 RPM) at room temperature for 3 hours. This enabled the analyte to be captured by the immoblilised capture antibodies on the surface of the electrodes on the bottom of the well. Following this, the wells were washed out again and an antibody detection solution containing antibodies for each protein of interest was added. These detection antibodies are bound to an electrochemiluminescent compound that acts as a tag. The detection antibody binds to the protein of interest which is already bound to the capture antibody on the surface of the well, thus creating a sandwich immunoassay. Following a 1-hour incubation the wells were washed again and read buffer was added to provide the correct chemical environment for electrochemiluminescence to occur. The plate was loaded into the MSD Sector Imager where a voltage is rapidly applied to the plate's electrodes resulting in the

labels attached to these electrodes emitting light. This system measures the intensity of emitted light in order to generate a quantitative measure of the protein within the sample. A plate blank was used to adjust for background signal. Values are expressed as signal/ug of total protein, previously determined by BCA assay.

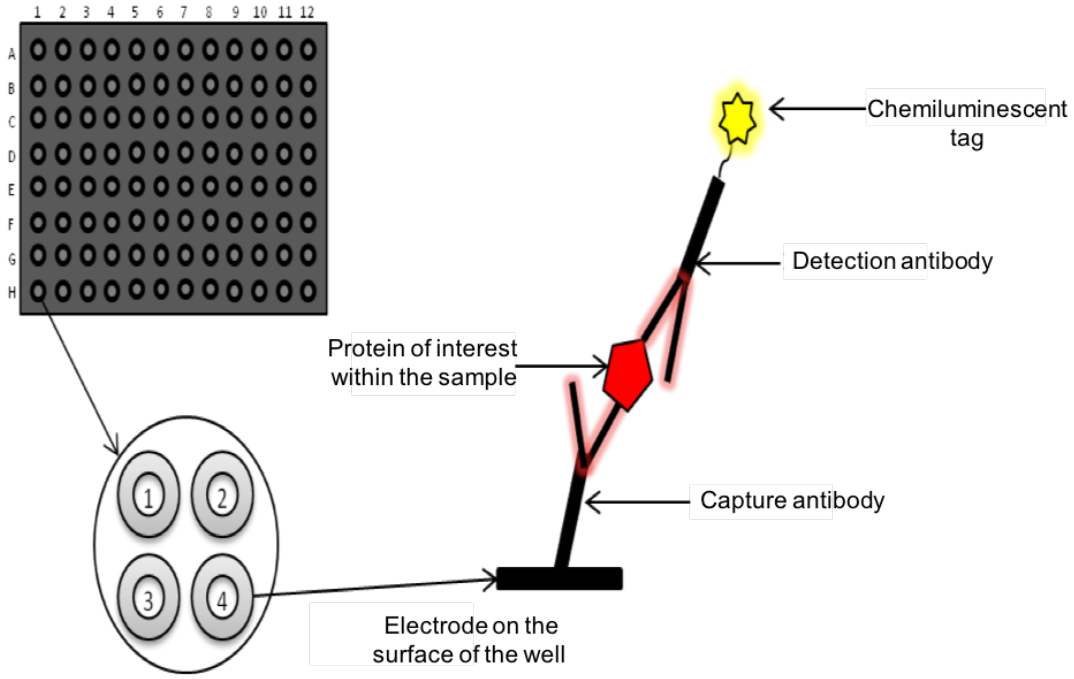

Figure 2.7 Schematic depicting the principle of the Mesoscale 96-well plate. Schematic illustrating a 96 well place with 4 distinct spots for proteins of interest within each well and how the antibody-protein-antibody sandwich is formed and subsequently detected (Image adapted from www.mesoscale.com).

2.9.3 Phospho-FOXO3a assay

The Phospho-FOXO3a Assay is a singleplex version of the assay described above, quantifying phosphorylated Forkhead box O3a (FOXO3a) only. This assay was carried out in the same manner as described in section 2.9.2 using sternohyoid and diaphragm muscle homogenates (n = 8 per group) from mice exposed to 2 weeks of CIH or normoxia (sham). A plate blank was used to adjust for background signal.

Values are expressed as signal/µg of total protein, previously determined by BCA assay

2.9.4 Total HIF-1α assay

The HIF-1α Assay examines the total Hypoxia-Inducible Factor (HIF)-1α protein content in samples. This assay was carried out in the same manner as described in section 2.9.2 using sternohyoid and diaphragm muscle homogenates (n = 8 per group) from mice exposed to 2 weeks of CIH or normoxia (sham). A plate blank was used to adjust for background signal. Values are expressed as signal/µg of total protein, previously determined by BCA assay.

2.10 Statistical analysis

Values are expressed as mean ± SD. Data were statistically compared using Prism 8.0 (Graphpad Software, San Diego, CA, USA). Data were tested for normal distribution and equal variances. Data sets which were normally distributed and of equal variance were statistically compared using unpaired two-tailed Student's *t* test. Welch's correction was applied in the case of unequal variance. Data which were not normally distributed were compared using Mann Whitney non-parametric tests. $P < 0.0125$ was considered statistically significant for Student's *t* test and Mann Whitney test on the basis of the multiple comparisons that were performed. $P < 0.05$ was considered statistically significant for Student's *t* test and Mann Whitney test when only one comparison was used. Data for isotonic muscle measurements over a range of load percentages were statistically compared by repeated measures two-way ANOVA (RMANOVA) with Bonferroni *post hoc* test; $P < 0.05$ was considered statistically significant.

2.11 References

BURNS, D. P., CANAVAN, L., ROWLAND, J., O'FLAHERTY, R., BRANNOCK, M., DRUMMOND, S. E., O'MALLEY, D., EDGE, D. & O'HALLORAN, K. D. 2018. Recovery of respiratory function in mdx mice co-treated with neutralizing interleukin-6 receptor antibodies and urocortin-2. *J Physiol,* 596**,** 5175-5197.

BURNS, D. P., DRUMMOND, S. E., BOLGER, D., COISCAUD, A., MURPHY, K. H., EDGE, D. & O'HALLORAN, K. D. 2019. N-acetylcysteine Decreases Fibrosis and Increases Force-Generating Capacity of mdx Diaphragm. *Antioxidants (Basel),* 8.

BURNS, D. P., ROY, A., LUCKING, E. F., MCDONALD, F. B., GRAY, S., WILSON, R. J., EDGE, D. & O'HALLORAN, K. D. 2017. Sensorimotor control of breathing in the mdx mouse model of Duchenne muscular dystrophy. *J Physiol,* 595**,** 6653-6672.

CLARKE, G., GRENHAM, S., SCULLY, P., FITZGERALD, P., MOLONEY, R. D., SHANAHAN, F., DINAN, T. G. & CRYAN, J. F. 2013. The microbiome-gut-brain axis during early life regulates the hippocampal serotonergic system in a sex-dependent manner. *Mol Psychiatry,* 18**,** 666-73.

EDGE, D., BRADFORD, A. & O'HALLORAN, K. D. 2012. Chronic intermittent hypoxia increases apnoea index in sleeping rats. *Adv Exp Med Biol,* 758**,** 359-63.

GRUNDY, D. 2015. Principles and standards for reporting animal experiments in The Journal of Physiology and Experimental Physiology. *The Journal of Physiology,* 593**,** 2547-2549.

LUCKING, E. F., O'HALLORAN, K. D. & JONES, J. F. 2014. Increased cardiac output contributes to the development of chronic intermittent hypoxia-induced hypertension. *Exp Physiol,* 99**,** 1312-24.

O'CONNOR, K. M., LUCKING, E. F., GOLUBEVA, A. V., STRAIN, C. R., FOUHY, F., CENIT, M. C., DHALIWAL, P., BASTIAANSSEN, T. F. S., BURNS, D. P., STANTON, C., CLARKE, G., CRYAN, J. F. & O'HALLORAN, K. D. 2019. Manipulation of gut microbiota blunts the ventilatory response to hypercapnia in adult rats. *EBioMedicine,* 44**,** 618-638.

O'LEARY, A. J., DRUMMOND, S. E., EDGE, D. & O'HALLORAN, K. D. 2018. Diaphragm Muscle Weakness Following Acute Sustained Hypoxic Stress in the Mouse Is Prevented by Pretreatment with N-Acetyl Cysteine. *Oxid Med Cell Longev,* 2018**,** 4805493.

O'LEARY, A. J. & O'HALLORAN, K. D. 2016. Diaphragm muscle weakness and increased UCP-3 gene expression following acute hypoxic stress in the mouse. *Respir Physiol Neurobiol,* 226**,** 76-80.

PENG, Y. J., NANDURI, J., KHAN, S. A., YUAN, G., WANG, N., KINSMAN, B., VADDI, D. R., KUMAR, G. K., GARCIA, J. A., SEMENZA, G. L. & PRABHAKAR, N. R. 2011. Hypoxia-inducible factor 2α (HIF-2α) heterozygous-null mice exhibit exaggerated carotid body sensitivity to hypoxia, breathing instability, and hypertension. *Proc Natl Acad Sci U S A,* 108**,** 3065-70.

SOUZA, G. M., BONAGAMBA, L. G., AMORIM, M. R., MORAES, D. J. & MACHADO, B. H. 2015. Cardiovascular and respiratory responses to chronic intermittent hypoxia in adult female rats. *Exp Physiol,* 100**,** 249-58.

Chapter 3. The role of NADPH oxidase-2 in chronic intermittent hypoxia-induced respiratory plasticity.

3.1 Aims and hypothesis

Study aims:

To determine the effects of exposure to CIH on ventilation and metabolism during baseline (normoxic) breathing in adult male mice.

To investigate ventilatory responsiveness to acute physiological challenges, namely hypoxia and hypercapnia, to assess the effects of exposure to CIH on peripheral and central chemoreceptor responsiveness.

To examine the effect of exposure to CIH on the propensity for apnoea and respiratory instability.

To assess the effect of exposure to CIH on brainstem 5HT and 5HIAA concentrations.

To assess the contribution of NOX2 to CIH-induced alterations in the respiratory control system using pharmacological and transgenic approaches.

Study hypothesis:

We hypothesised that 2 weeks of exposure to CIH would evoke mal-adaptation in respiratory control, which would manifest as enhanced normoxic ventilation, and altered chemoreflex responsiveness, together with the manifestation of respiratory instability and increased apnoeic index.

Furthermore, we postulated that these alterations would be dependent upon NOX2 derived ROS-dependent signalling, amenable to blockade by supplementation with apocynin (putative NOX2 inhibitor) and NOX2 genetic knock-out.

3.2 Materials and Methods

Respiratory recordings and metabolic measurements during quiet rest and in response to hypoxic and hypercapnic chemostimulation were assessed using whole body plethysmography (WBP), as described in Section 2.3.

5-HT and 5-HIAA, important in the neurochemical control of breathing, were analysed in brainstem samples using high performance liquid chromatography (HPLC), as described in Section 2.4.

3.3 Results

3.3.1 Organ and muscle mass

Comparisons of organ and muscle mass in all experimental groups are shown in Table 3.1. Haematocrit (Hct) was increased following exposure to CIH in wild-type (P = 0.0247) and NOX2 KO mice (P = 0.0167), but this did not reach the threshold for statistical significance when correction for multiple comparisons was applied. The administration of the putative NOX2 inhibitor, apocynin (2mM), in the drinking water during exposure to CIH, significantly reduced Hct compared with CIH-exposed mice (P = 0.0062). A similar trend towards a decrease in spleen mass following exposure to CIH was observed in wild-type (P = 0.0400) and NOX2 KO mice (P = 0.0839); apocynin treatment significantly increased spleen mass compared with exposure to CIH alone (P = 0.0017). Limb muscle mass was unchanged following exposure to CIH in wild-type (tibialis anterior (TA); P = 0.7304, extensor digitorum longus (EDL); P = 0.2972 , and soleus (Sol); P = 0.5435) and NOX2 KO mice (TA; P = 0.3474, EDL; P = 0.0424, Sol; P = 0.4236). Treatment with apocynin throughout the exposure to CIH significantly increased limb muscle mass compared to exposure to CIH alone (TA; P = 0.0868, EDL; P < 0.0001, Sol; P = 0.0435). Cardiac muscle mass was unaffected by exposure to CIH compared to sham (RV; P = 0.6306, LV; P = 0.2790, RV + LV; P = 0.1771, RV:LV; P = 0.9711); treatment with apocynin also had no effect on cardiac muscle mass. LV (P = 0.0048) and total ventricular mass (RV + LV; P = 0.0075) were significantly increased following exposure to CIH in NOX2 KO mice. The difference between wet and dry lung mass, an index of pulmonary oedema, showed a trend towards an increase in both wild-type (P = 0.0736) and NOX2 KO mice (P = 0.0449) exposed to CIH compared with sham. NOX2 KO had no effect on Hct, spleen mass, limb muscle mass, cardiac muscle mass or measures of pulmonary oedema compared to wild-type controls (sham).

	Sham (n = 9)	CIH (n = 9)	CIH + APO (n = 10)	NOX2 KO sham (n = 12)	NOX2 KO CIH (n = 12)	Sham *vs* CIH (P value)	CIH *vs* CIH + APO (P value)	NOX2 KO Sham vs NOX2 KO CIH (P value)	Sham *vs* NOX2 KO sham (P value)
Hct (%)	44.1 ± 1.0	46.9 ± 3.3	43.2 ± 2.0[#]	45.4 ± 2.2	47.6 ± 1.9	0.0247	**0.0062**[#]	0.0167	0.1050
Spleen (mg/g)	2.37 ±0.57	1.92 ± 0.37	2.63 ± 0.46[#]	2.70 ± 0.50	2.42 ± 0.20	0.0400	**0.0017**[#]	0.0839	0.1847
TA (mg/g)	1.47 ± 0.22	1.43 ± 0.10	1.56 ± 0.10	1.52 ± 0.21	1.60 ± 0.24	0.7304	0.0868	0.3474	0.5079
EDL (mg/g)	0.32 ± 0.06	0.29 ± 0.05	0.42 ± 0.04[#]	0.36 ± 0.04	0.40 ± 0.04	0.2972	**<0.0001**[#]	0.0424	0.0411
Sol (mg/g)	0.29 ± 0.07	0.27 ± 0.04	0.31 ± 0.05	0.30 ± 0.04	0.32 ± 0.04	0.5435	0.0435	0.4236	0.5186
RV (mg/g)	1.16 ± 0.26	1.21 ± 0.21	1.31 ± 0.25	0.99 ± 0.13	1.06 ± 0.20	0.6306	0.3910	0.3707	0.0888
LV (mg/g)	3.34 ± 0.35	3.50 ± 0.25	3.41 ± 0.40	3.21 ± 0.24	3.61 ± 0.35[$]	0.2790	0.5483	**0.0048**[$]	0.3584
RV + LV (mg/g)	4.49 ± 0.40	4.71 ± 0.18	4.71 ± 0.33	4.20 ± 0.25	4.67 ± 0.46[$]	0.1771	0.9991	**0.0075**[$]	0.0655
RV: LV	0.35 ± 0.11	0.35 ± 0.08	0.39 ± 0.11	0.31 ± 0.05	0.29 ± 0.06	0.9711	0.3479	0.4579	0.3316
Lung (Wet – Dry) (mg/g)	4.64 ± 0.34	5.14 ± 0.70	5.15 ± 0.37	4.29 ± 0.35	4.70 ± 0.44	0.0736	0.9596	0.0449	0.0342

Table 3.1 Organ and muscle mass. *Definition of abbreviations:* Hct, haematocrit; TA, tibialis anterior; EDL, extensor digitorum longus; sol, soleus; RV, right heart ventricle; LV, left heart ventricle; sham, normoxia (21% O_2) exposed; CIH, chronic intermittent hypoxia exposed; CIH + APO, Apocynin (2mM) given in the drinking water for the duration of CIH exposure; NOX2 KO, NADPH Oxidase 2 knock-out (B6.129S-Cybbtm1Din/J), sham or CIH exposed. Values are expressed as mean ± SD. Data sets which were normally distributed were statistically compared using unpaired two-tailed Student's *t* test. Welch's correction was applied in the case of unequal variance. Data which were not normally distributed were compared using Mann Whitney non-parametric tests. Bolded numbers indicate statistical significance ($P < 0.0125$) following correction for multiple comparisons. Relevant comparisons are denoted as follows: [#] APO + CIH significantly different from corresponding CIH values; [$] NOX2 KO CIH significantly different from corresponding NOX2 KO sham values.

3.3.2 Baseline ventilation and metabolism

Respiratory and metabolic parameters during baseline (normoxia) are shown in Table 3.2. Minute ventilation ($\dot{V}_I$) during baseline (combined periods of normoxia) was equivalent for sham and CIH groups (P = 0.0691). The administration of the putative NOX2 inhibitor, apocynin (2mM), in the drinking water during exposure to CIH, resulted in increased V_T (P = 0.0085) and $\dot{V}_I$ (P = 0.0188). $\dot{V}_I$ was significantly reduced in NOX2 KO sham compared with sham mice (P = 0.0018). The reduction in $\dot{V}_I$ during normoxia was the result of a lower V_T (P = 0.0029); f_R did not differ between NOX2 KO sham and sham groups (P = 0.3091). PIF (P = 0.9744) and PEF (P = 0.8016) were equivalent for sham and CIH groups. However, treatment with apocynin during exposure to CIH revealed an increase in both PIF (P = < 0.0001) and PEF (P < 0.0001). Exposure to CIH had no effect on PIF (P = 0.4580) or PEF (P = 0.9323) in NOX2 KO mice compared with the corresponding sham group. Additionally, PEF was reduced in NOX2 KO sham (P = 0.0120) compared with wild-type sham mice. Assessment of oxygen consumption ($\dot{V}O_2$) and carbon dioxide production ($\dot{V}CO_2$) revealed minimal differences between groups. Of note, $\dot{V}O_2$ and $\dot{V}CO_2$ were both increased for the CIH + APO group compared to exposure to CIH alone ($\dot{V}O_2$; P = 0.0046, $\dot{V}CO_2$; P = 0.0001). The ventilatory equivalent for carbon dioxide ($\dot{V}_I/\dot{V}CO_2$) did not differ between sham and CIH mice (P = 0.9338), while a significant reduction in $\dot{V}_I/\dot{V}CO_2$ was evident following treatment with apocynin during exposure to CIH (P = 0.0064). $\dot{V}_I/\dot{V}CO_2$ was significantly lower in NOX2 KO sham compared with sham mice (P = 0.0050), indicative of hypoventilation in mice deficient in the NOX2 enzyme. Body mass (g) was significantly decreased following exposure to CIH compared with sham (P = 0.0011); apocynin prevented this decrease (P = 0.0008). This well described decrease in body mass following exposure to CIH was also evident in NOX2 KO mice (P = 0.0042), reminiscent of that seen in C57BL/6J (wild-type) mice. Mice lacking the NOX2 enzyme were significantly heavier than their wild-type control counterparts (P < 0.0001). Inspiratory duration (T_i), expiratory duration (T_e), ventilatory equivalent for O_2 ($\dot{V}_I/\dot{V}O_2$) and the ratio of $\dot{V}CO_2$ to $\dot{V}O_2$ (respiratory exchange ratio) were unchanged between groups.

	Sham (n = 12)	CIH (n = 12)	CIH + APO (n = 11-12)	NOX2 KO sham (n = 12)	NOX2 KO CIH (n = 12)	Sham *vs* CIH (P value)	CIH *vs* CIH + APO (P value)	NOX2 KO sham vs NOX2 KO CIH (P value)	Sham *vs* NOX2 KO sham (P value)
f_R (bpm)	184.6 ± 12.0	182.8 ± 11.9	183.0 ± 20.5	190.7 ± 16.0	175.1 ± 18.1	0.7099	0.9780	0.0358	0.3091
V_T (ml/g)	0.0068 ±0.001	0.0073 ± 0.001	0.0084 ± 0.001$^{\#}$	0.0057 ± 0.001$^{£}$	0.0063 ± 0.001	0.0832	**0.0085**$^{\#}$	0.0332	**0.0029**$^{£}$
$\dot{V}_I$ (ml/min/g)	1.23 ± 0.13	1.32 ± 0.12	1.53 ± 0.25	1.05 ± 0.14$^{£}$	1.04 ± 0.15	0.0691	0.0188	>0.9999	**0.0018**$^{£}$
PIF (ml/s)	2.52 ± 0.29	2.52 ± 0.30	3.24 ± 0.42$^{\#}$	2.60 ± 0.27	2.67 ± 0.25	0.9774	<0.0001$^{\#}$	0.4580	0.5550
PEF (ml/s)	1.68 ± 0.20	1.70 ± 0.18	2.53 ± 0.29$^{\#}$	1.93 ± 0.24$^{£}$	1.92 ± 0.20	0.8016	<0.0001$^{\#}$	0.9323	0.0120$^{£}$
T_i (ms)	116.7 ± 4.0	119.5 ± 6.9	112.9 ± 8.5	116.0 ± 6.5	117.1 ± 6.9	0.2434	0.0513	0.6904	0.7566
T_e (ms)	225.4 ± 23.1	224.8 ± 21.6	227.8 ± 34.3	216.7 ± 31.1	254.5 ± 47.1	0.9489	0.8001	0.0301	0.4455
$\dot{V}O_2$ (ml/min/g)	0.038 ± 0.01	0.041 ± 0.01	0.059 ± 0.02$^{\#}$	0.040 ± 0.01	0.038 ± 0.01	0.2195	**0.0046**$^{\#}$	0.7982	0.6976
$\dot{V}CO_2$ (ml/min/g)	0.031 ± 0.01	0.033 ± 0.01	0.053 ± 0.01$^{\#}$	0.035 ± 0.01	0.033 ± 0.01	0.3229	**0.0001**$^{\#}$	0.4568	0.1726
$\dot{V}_I/\dot{V}O_2$	32.7 ± 5.3	32.8 ± 4.7	29.0 ± 13.9	29.3 ± 11.7	29.5 ± 8.5	0.9402	0.0512	0.7125	0.0780
$\dot{V}_I/\dot{V}CO_2$	40.6 ± 7.4	40.9 ± 8.9	29.9 ± 8.2$^{\#}$	31.3 ± 7.2$^{£}$	33.8 ± 9.9	0.9338	**0.0064**$^{\#}$	0.4703	**0.0050**$^{£}$
$\dot{V}CO_2/\dot{V}O_2$	0.82 ± 0.17	0.82 ± 0.19	0.94 ± 0.22	0.93 ± 0.21	0.89 ± 0.20	0.9138	0.1997	0.6563	0.1869
Body Mass (g)	23.6 ± 1.5	21.4 ± 0.7*	23.5 ± 1.6$^{\#}$	28.1 ± 2.6$^{£}$	25.4 ± 0.94$^{\$}$	**0.0011***	**0.0008**$^{\#}$	**0.0042**$^{\$}$	**<0.0001**$^{£}$

Table 3.2 Baseline breathing and metabolism measurements. *Definition of abbreviations*: f_R, breathing frequency; V_T, tidal volume; $\dot{V}_I$, minute ventilation; PIF, peak inspiratory flow; PEF, peak expiratory flow; T_i, inspiratory duration; T_e, expiratory duration; $\dot{V}O_2$, oxygen consumption; $\dot{V}CO_2$, carbon dioxide production; $\dot{V}_I/\dot{V}O_2$, ventilatory equivalent for oxygen; $\dot{V}_I/\dot{V}CO_2$, ventilatory equivalent for carbon dioxide; $\dot{V}CO_2/\dot{V}O_2$, respiratory exchange ratio (RER); sham, normoxia (21% O_2) exposed; CIH, chronic intermittent hypoxia exposed; CIH + APO, apocynin (2mM) given in the drinking water for the duration of CIH exposure; NOX2 KO, NADPH Oxidase 2 knock-out (B6.129S-Cybbtm1Din/J), sham- or CIH-exposed. Values are expressed as mean ± SD. Data sets which were normally distributed were statistically compared using unpaired two-tailed Student's *t* test. Welch's correction was applied in the case of unequal variance. Data which were not normally distributed were compared using Mann Whitney non-parametric tests. Bolded numbers indicate statistical significance (P < 0.0125) following correction for multiple comparisons. Relevant comparisons are denoted as follows: * CIH significantly different from corresponding sham values; $^{\#}$ APO + CIH significantly different from corresponding CIH values; $^{\$}$ NOX2 KO CIH significantly different from corresponding NOX2 KO sham values; $^{£}$ NOX2 KO sham significantly different from corresponding sham values.

3.3.3 Expression of sighs and apnoeas during normoxia

Figure 3.1 shows representative respiratory flow traces illustrating a sigh and post-sigh apnoea (A) and a spontaneous apnoea (B) in a wild-type sham mouse during normoxia. Analysis of sighs revealed that exposure to CIH had no effect on the frequency of sighs in both wild-type (P = 0.0364; Fig 3.1; C) and NOX2 KO (P = 0.2128; Fig 3.1; C) mice. A significant increase in the frequency of sighs was evident in NOX2 KO sham compared with wild-type sham mice (P = 0.0066; Fig 3.1; C). No difference was observed in the frequency of post-sigh apnoeas following exposure to CIH in wild-type (P = 0.1170; Fig 3.1; D) or NOX2 KO (P = 0.3872; Fig 3.1; D) mice. Frequency of post-sigh apnoeas was also equivalent following NOX2 blockade via apocynin administration (P = 0.1230; Fig 3.1; D) and genetic NOX2 knock-out (P = 0.0522; Fig 3.1; D). The duration of post-sigh apnoeas was significantly elevated in CIH-exposed compared to sham mice (P = 0.0053; Fig 3.1; E); the increase was entirely prevented by the administration of apocynin throughout the exposure to CIH (P = 0.0083; Fig 3.1 E). The increase in the duration of post-sigh apnoeas following exposure to CIH was not observed in mice lacking the NOX2 enzyme (P = 0.1651; Fig 3.1; E).

Analysis of spontaneous apnoeas revealed a significant increase in the frequency of spontaneous apnoeas in mice following exposure to CIH compared to the corresponding sham group (P < 0.0001; Fig 3.1; F); treatment with apocynin completely prevented the increase, with values comparable to those observed in sham mice (P < 0.0001; Fig 3.1; F). The frequency of spontaneous apnoeas was elevated following exposure to CIH in NOX2 KO mice (P = 0.0063; Fig 3.1; F), similar to that revealed in wild-type mice, suggesting a non-NOX2 dependent mechanism of action of ROS. The duration of spontaneous apnoeas was unaffected by exposure to CIH for both wild-type (P = 0.5125; Fig 3.1; G) and NOX2 KO (P = 0.6231; Fig 3.1; G) mice. Similarly, the duration of spontaneous apnoeas was not different following NOX2 blockade via apocynin treatment (P = 0.4007; Fig 3.1; G) and genetic NOX2 knock-out (P = 0.7386; Fig 3.1; G).

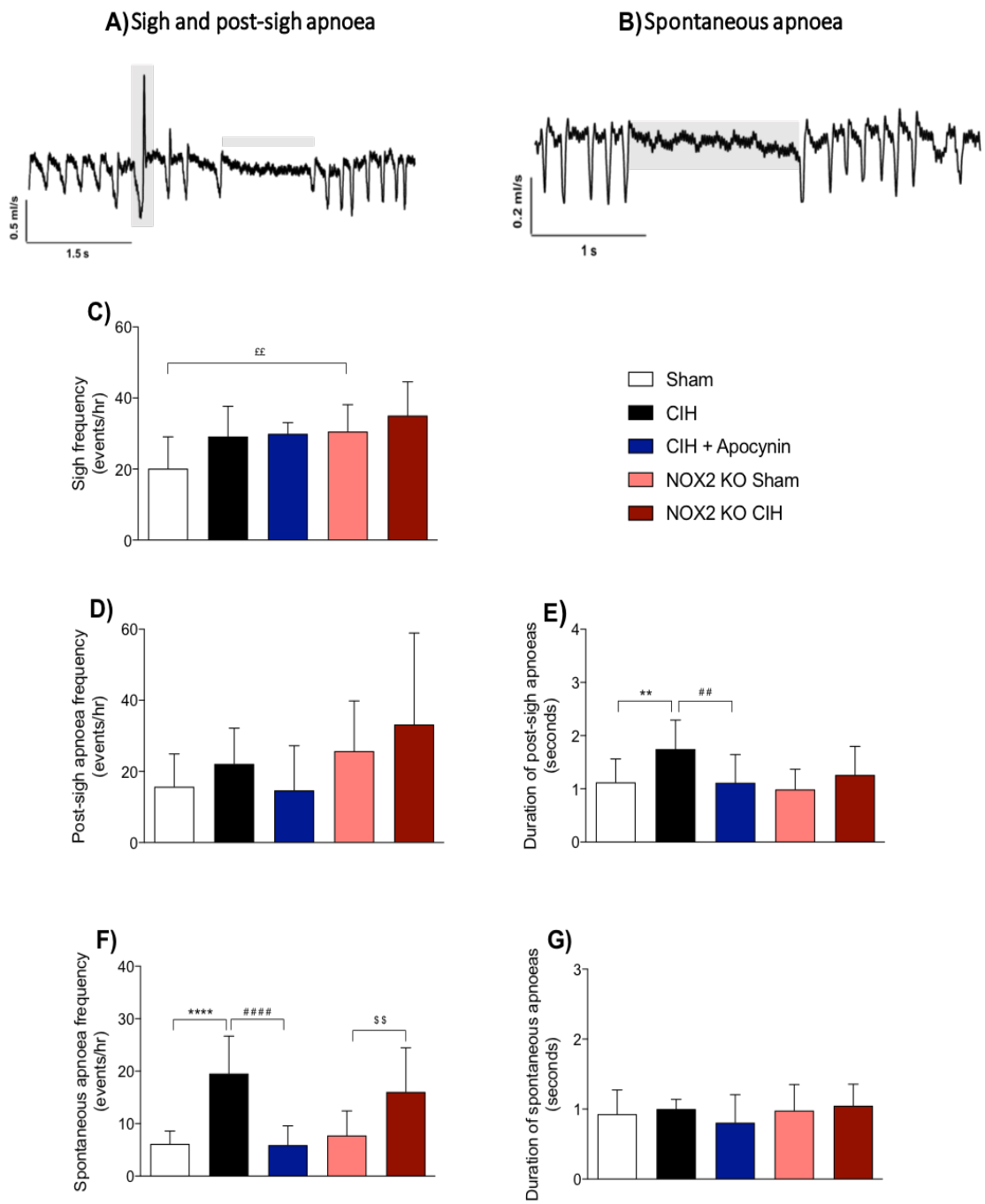

Figure 3.1 Expression of sighs and apnoeas in awake mice during normoxia. *A* and B, representative respiratory flow traces demonstrating an augmented breath or sigh (A; grey shading) and post-sigh apnoea (A; grey line) and a spontaneous apnoea (B; grey shading) in a sham mouse during normoxia. C, D, E, F, G, group data for sigh frequency (C), post-sigh apnoea frequency (D) and duration (E), and spontaneous apnoea frequency (F) and duration (G) occurring during normoxia for all groups. Sham, normoxia (21% O_2) exposed; CIH, chronic intermittent hypoxia exposed; CIH + APO, apocynin (2mM) given in the drinking water for the duration of CIH exposure; NOX2 KO, NADPH Oxidase 2 knock-out (B6.129S-Cybbtm1Din/J), sham- or CIH-exposed. Values are expressed as mean ± SD (n=12 per group).

Data sets which were normally distributed were statistically compared using unpaired two-tailed Student's *t* test. Welch's correction was applied in the case of unequal variance. Data which were not normally distributed were compared using Mann Whitney non-parametric tests. Statistical significance was taken at P < 0.0125. Relevant comparisons are denoted as follows: *denotes sham *vs*. CIH, ** *P* < 0.01, **** P < 0.0001; [#] denotes CIH *vs.* CIH + APO, [##] *P* < 0.01, [####] *P* < 0.0001; [£]denotes sham *vs.* NOX2 KO sham, [££] *P* < 0.01; [$] denotes NOX2 KO sham *vs.* NOX2 KO CIH, [$$] *P* < 0.01.

3.3.4 Respiratory timing measurements during normoxia

Figure 3.2 shows Poincaré plots of the breath-to-breath (BB_n) and subsequent interval (BB_{n+1}) of 200 consecutive breaths for expiratory duration (T_e; A- E) and total breath duration (T_{tot}; H-L) in sham (A and H; white), CIH (B and I; black), CIH + APO (C and J; blue), NOX2 KO sham (D and K; pink) and NOX2 KO CIH (E and L; red). Assessment of the short-term (SD1) and long-term (SD2) variability of breathing revealed no evidence for respiratory instability for T_e following exposure to CIH in either wild-type (SD1; *P* = 0.5875, SD2; *P* = 0.3474; Fig 3.2; F and G, respectively) or NOX2 KO (SD1; *P* = 0.1978, SD2; *P* = 0.2267; Fig 3.2; F and G, respectively) mice. However, treatment with apocynin throughout the exposure to CIH increased breathing stability as indicated by significantly lower short-term (SD1; *P* = 0.0032; Fig 3.2; F) and long-term (SD2; *P* = 0.0009; Fig 3.2; G) variability of breathing assessments. Similarly, SD1 and SD2 revealed no evidence for respiratory instability for T_{tot} following exposure to CIH in either wild-type (SD1; *P* = 0.3809, SD2; *P* = 0.0827; Fig 3.2; M and N, respectively) or NOX2 KO (SD1; *P* = 0.2155, SD2; *P* = 0.2854; Fig 3.2; M and N, respectively) mice. However, treatment with apocynin increased breathing stability as indicated by significantly lower SD1 compared to exposure to CIH alone (*P* = 0.0018; Fig 3.2; M) and SD2 (*P* = 0.0021; Fig 3.2; N).

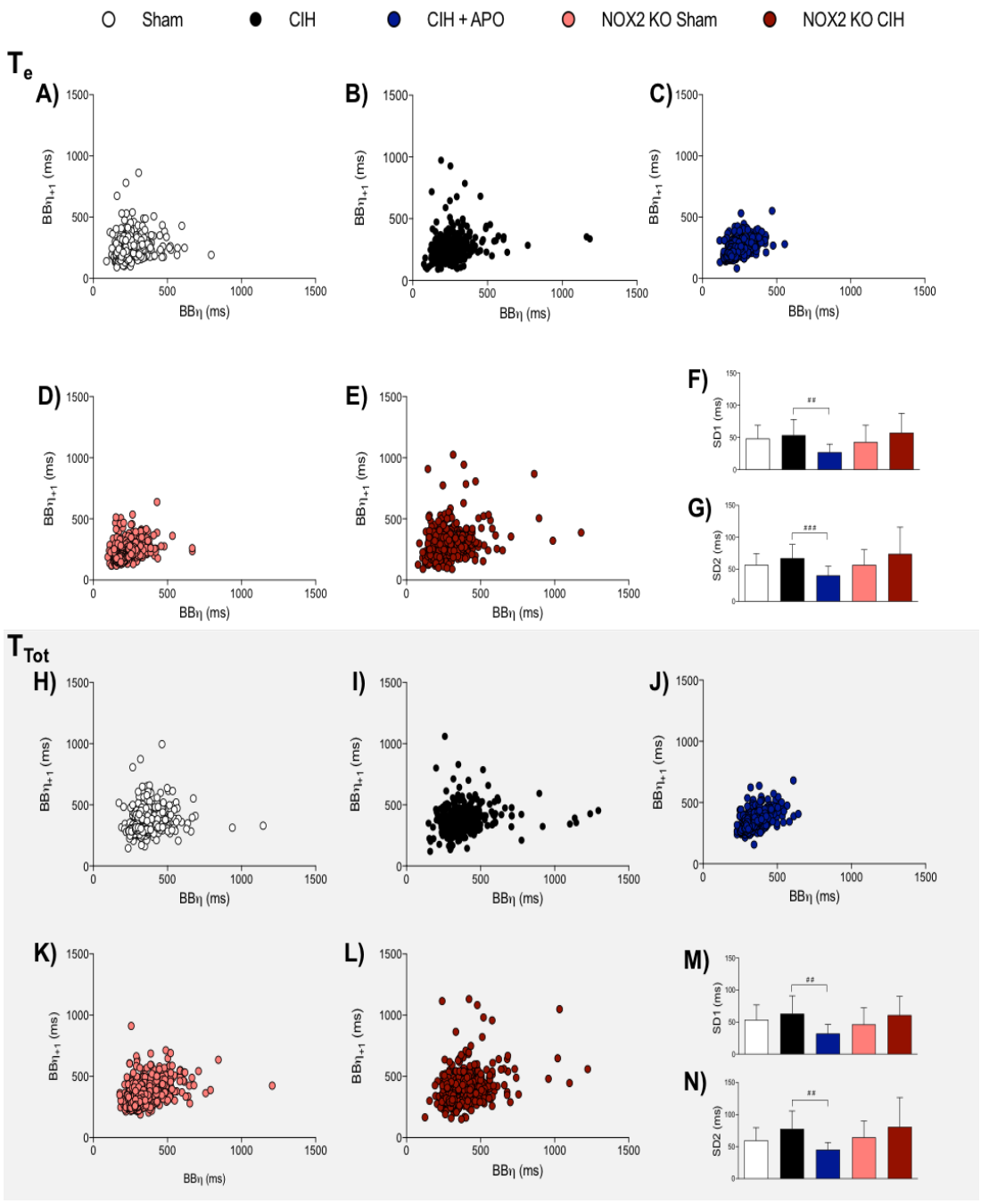

Figure 3.2 Respiratory timing measurements in awake mice during normoxia. A B, C, D and E, Poincaré plot of breath-to-breath (BB_n) and subsequent breath-to-breath (BB_{n+1}) interval of expiratory duration (T_e) over 200 consecutive breaths for sham (A), CIH (B), CIH + APO (C), NOX2 KO sham (D) and NOX2 KO CIH (E) groups. F and G, group data of short-term (F; SD1) and long-term (G; SD2) variability of breathing based on Te for all groups. H, I, J, K and L, Poincaré plots of BB_n and BB_{n+1} of total breath duration (T_{tot}) over 200 consecutive breaths for sham (H), CIH (I), CIH + APO (J), NOX2 KO sham (K) and NOX2 KO CIH (L) groups. M and N, group data of short-term (M; SD1) and long-term (N; SD2) variability of breathing based on T_{tot} for all groups. Values are expressed as mean ± SD (n=12 per group). Data sets which were

normally distributed were statistically compared using unpaired two-tailed Student's *t* test. Welch's correction was applied in the case of unequal variance. Data which were not normally distributed were compared using Mann Whitney non-parametric tests. Statistical significance was taken at $p < 0.0125$. Relevant comparisons denoted as follows; $^{\#}$denotes APO + CIH significantly different from corresponding CIH values, $^{\#\#}P < 0.01$, $^{\#\#\#}P < 0.001$.

3.3.5 Brainstem 5-HT and 5-HIAA concentrations

Concentrations of 5-HT and its metabolite 5-HIAA were quantified in brainstem samples of mice from all groups using HPLC. These and the ratio of 5-HIAA to 5-HT (index of serotonergic metabolism) is shown in Figure 3.3 A-C. The concentration of 5-HT was not different following exposure to CIH in wild-type ($P = 0.3160$; Fig 3.3; A) and NOX2 KO mice ($P = 0.1431$; Fig 3.3; A). Moreover, treatment with apocynin ($P = 0.1683$; Fig 3.3; A) or genetic knock-out of the NOX2 enzyme alone ($P = 0.0343$; Fig 3.3; A) did not significantly alter 5-HT concentration. Analysis of 5-HIAA revealed that its concentration was equivalent in the brainstem of both wild-type ($P = 0.0560$; Fig 3.3; B) and NOX2 KO mice ($P = 0.5288$; Fig 3.3; B) exposed to CIH, as well as mice treated with apocynin during the exposure to CIH ($P = 0.2930$; Fig 3.3; B). A significant decrease in the concentration of the metabolite 5-HIAA was observed in NOX2 KO sham mice compared to wild-type sham mice ($P = 0.0031$; Fig 3.3; B). The ratio of 5-HIAA to 5-HT, was significantly reduced in CIH-exposed mice compared to sham ($P < 0.0001$; Fig 3.3; C); apocynin treatment had no effect on 5-HIAA/5-HT ($P = 0.8676$; Fig 3.3; C). There was no difference in the ratio of 5-HIAA/5-HT between NOX2 KO mice exposed to CIH compared with NOX2 KO sham mice ($P = 0.3333$; Fig 3.3; C). Mice lacking the NOX2 enzyme had a significantly lower ratio of 5-HIAA/5HT within brainstem homogenates when compared to wild-type sham ($P < 0.0001$; Fig 3.3; C), suggesting reduced serotonergic metabolism.

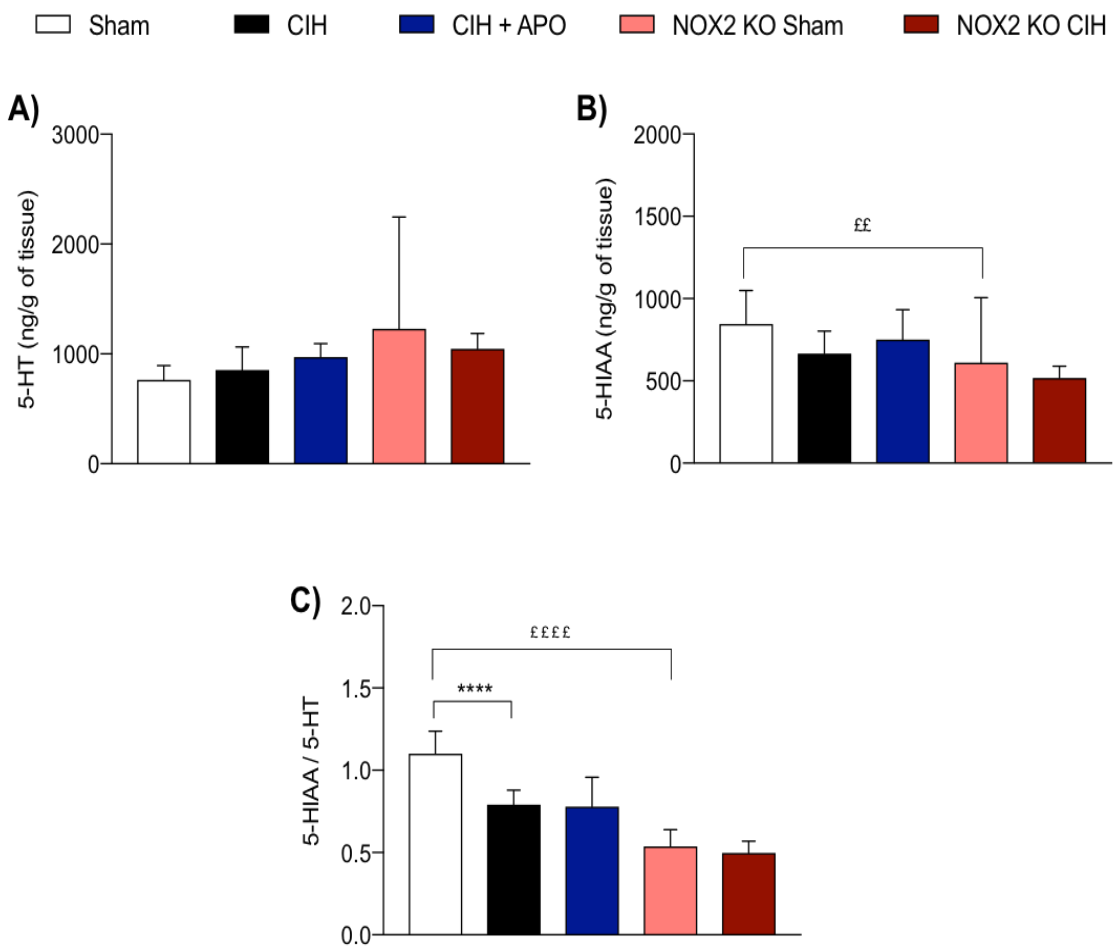

Figure 3.3 Brainstem monoamine analysis. *Definition of abbreviations*: 5-HT, serotonin; 5-HIAA, 5-hydroxyindole acetic acid. Group data for 5-HT concentration (A), 5-HIAA concentration (B) and 5-HIAA/5-HT ratio (C) for all groups. Sham, normoxia (21% O_2) exposed; CIH, chronic intermittent hypoxia exposed; CIH + APO, apocynin (2mM) given in the drinking water for the duration of CIH exposure; NOX2 KO, NADPH Oxidase 2 knock-out (B6.129S-Cybbtm1Din/J), sham- or CIH-exposed. Values are expressed as mean ± SD (n=8-10 per group). Data sets which were normally distributed were statistically compared using unpaired two-tailed Student's *t* test. Welch's correction was applied in the case of unequal variance. Data which were not normally distributed were compared using Mann Whitney non-parametric tests. Statistical significance was taken at $p < 0.0125$ to correct for multiple comparisons. *denotes sham *vs*. CIH,**** $P < 0.0001$; [£]denotes sham *vs.* NOX2 KO sham, [ff] $P < 0.01$, [ffff] $P < 0.0001$.

3.3.6 Ventilatory and metabolic responsiveness to hypoxia

Figure 3.4 shows the time course of the response of a range of ventilatory and metabolic parameters during a 10-minute exposure to hypoxic challenge (F_iO_2 = 0.1; balance N_2) for all groups. Minute ventilation increased rapidly across all groups at the onset of hypoxia compared to baseline ventilation values (Fig 3.4; G, H & I, respectively). Exposure to 2 weeks of CIH increased ventilation over the duration of the hypoxic challenge compared with sham (*P* = 0.0334; Fig 3.4; G), owing to a modest increase in breathing frequency (*P* = 0.0857; Fig 3.4; A). Apocynin treatment throughout the exposure to CIH did not ameliorate the increase in ventilation (*P* = 0.5349; Fig 3.4; G). Similarly, exposure to CIH increased hypoxic ventilation in NOX2 KO mice (*P* = 0.0032; Fig 3.4; H), owing to an increase in tidal volume (*P* = 0.0194; Fig 3.4; E). No effect of NOX2 KO alone was observed on ventilation in response to hypoxia compared to C57BL/6J (wild-type) mice (*P* = 0.1699; Fig 3.4; I). $\dot{V}_I/\dot{V}CO_2$ increased rapidly at the onset of hypoxia compared to baseline values (Fig 3.4; M, N & O, respectively). However, exposure to CIH had no effect on $\dot{V}_I/\dot{V}CO_2$ during the hypoxic challenge for wild type (*P* = 0.5221; Fig 3.4; M) or NOX2 KO mice (*P* = 0.7805; Fig 3.4; N) compared with corresponding sham exposures. Treatment with apocynin during exposure to CIH significantly reduced $\dot{V}_I/\dot{V}CO_2$ during hypoxic breathing (*P* = 0.0118; Fig 3.4; M) and the genetic deletion of NOX2 also reduced this parameter when compared to wild-type controls (*P* = 0.0036; Fig 3.4; O). The respiratory exchange ratio (RER) initially decreased at the onset of hypoxia for all groups, with the exception of the CIH + APO group (Fig 3.4; P, Q & R, respectively.) RER was equivalent for mice exposed to CIH compared with sham mice for both wild type (*P* = 0.9083; Fig 3.4; P) and NOX2 KO groups (*P* = 0.6242; Fig 3.4; Q). Treatment with apocynin during the exposure to CIH resulted in a significantly increased RER (*P* = <0.0001; Fig 3.4; P). The change in RER during the hypoxic challenge was equivalent in mice lacking the NOX2 enzyme compared with wild-type sham (*P* = 0.2479; Fig 3.4; R).

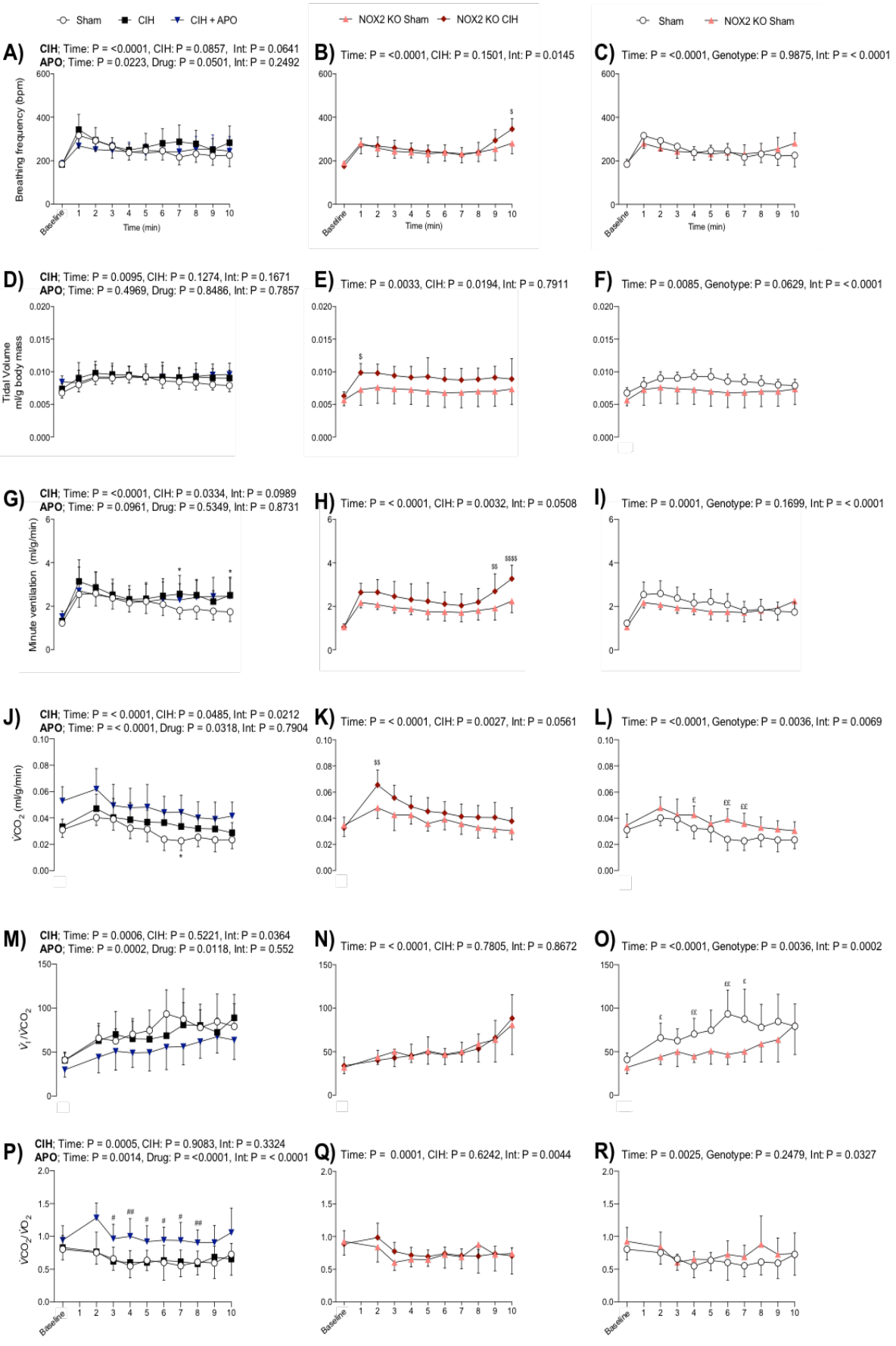
Sham
CIH
CIH + APO
NOX2 KO Sham
NOX2 KO CIH
A) CIH; Time: P = <0.0001, CIH: P = 0.0857, Int: P = 0.0641
APO; Time: P = 0.0223, Drug: P = 0.0501, Int: P = 0.2492
B) Time: P = <0.0001, CIH: P = 0.1501, Int: P = 0.0145
C) Time: P = <0.0001, Genotype: P = 0.9875, Int: P = < 0.0001
D) CIH; Time: P = 0.0095, CIH: P = 0.1274, Int: P = 0.1671
APO; Time: P = 0.4969, Drug: P = 0.8486, Int: P = 0.7857
E) Time: P = 0.0033, CIH: P = 0.0194, Int: P = 0.7911
F) Time: P = 0.0085, Genotype: P = 0.0629, Int: P = < 0.0001
G) CIH; Time: P = <0.0001, CIH: P = 0.0334, Int: P = 0.0989
APO; Time: P = 0.0961, Drug: P = 0.5349, Int: P = 0.8731
H) Time: P = < 0.0001, CIH: P = 0.0032, Int: P = 0.0508
I) Time: P = 0.0001, Genotype: P = 0.1699, Int: P = < 0.0001
J) CIH; Time: P = < 0.0001, CIH: P = 0.0485, Int: P = 0.0212
APO; Time: P = < 0.0001, Drug: P = 0.0318, Int: P = 0.7904
K) Time: P = < 0.0001, CIH: P = 0.0027, Int: P = 0.0561
L) Time: P = <0.0001, Genotype: P = 0.0036, Int: P = 0.0069
M) CIH; Time: P = 0.0006, CIH: P = 0.5221, Int: P = 0.0364
APO; Time: P = 0.0002, Drug: P = 0.0118, Int: P = 0.552
N) Time: P = < 0.0001, CIH: P = 0.7805, Int: P = 0.8672
O) Time: P = <0.0001, Genotype: P = 0.0036, Int: P = 0.0002
P) CIH; Time: P = 0.0005, CIH: P = 0.9083, Int: P = 0.3324
APO; Time: P = 0.0014, Drug: P = <0.0001, Int: P = < 0.0001
Q) Time: P = 0.0001, CIH: P = 0.6242, Int: P = 0.0044
R) Time: P = 0.0025, Genotype: P = 0.2479, Int: P = 0.0327
Breathing frequency (bpm)
Tidal Volume ml/g body mass
Minute ventilation (ml/g/min)
V̇CO2 (ml/g/min)
V̇I/V̇CO2
V̇CO2/V̇O2
Time (min)
Baseline

Figure 3.4 Ventilatory and metabolic responsiveness to hypoxia. Group data (mean ± SD; n=10-12 per group) for breathing frequency (A, B, C; f_R), tidal volume (D, E, F; V_T), minute ventilation (G, H ,I; V_I), carbon dioxide production (J, K ,L; $\dot{V}CO_2$), ventilatory equivalent for carbon dioxide (M, N, O; V_I/VCO_2) and respiratory exchange ratio (P, Q, R; VCO_2/VO_2) during baseline and 10 min of exposure to hypoxia (10% inspired oxygen; balance N_2) for sham, CIH, CIH + APO, NOX2 KO sham and NOX2 KO CIH groups. Sham, normoxia (21% O_2) exposed; CIH, chronic intermittent hypoxia exposed; CIH + APO, Apocynin (2mM) given in the drinking water for the duration of CIH exposure; NOX2 KO, NADPH Oxidase 2 knock-out (B6.129S-Cybbtm1Din/J), sham or CIH exposed. Data were statistically compared by repeated measures two-way ANOVA with Bonferroni *post hoc* test. For repeated measures two-way ANOVA; **CIH** denotes sham *vs*. CIH; **APO** denotes CIH *vs.* CIH + APO for A, D, G, J, M & P. Int denotes the interaction between two factors for A-R. For Bonferroni *post hoc* test; *denotes sham *vs*. CIH, *P < 0.05; #denotes CIH *vs*. CIH + APO, #P < 0.05, ## *P* < 0.01; $denotes NOX2 KO sham *vs.* NOX2 KO CIH, $ P < 0.05, $$ P < 0.01, $$$$ *P* < 0.0001; £ denotes sham *vs.* NOX2 KO sham, £ P < 0.05, ££ P < 0.01.

3.3.7 Ventilatory and metabolic responsiveness to hypercapnia

Fig 3.5 shows the time course of the response of a range of ventilatory and metabolic parameters to a 10-minute hypercapnic challenge (F_iCO_2 = 0.05, balance N_2) for all groups. Ventilation increased rapidly at the onset of hypercapnia for all groups and remained elevated for the duration of the challenge (Fig 3.5; G, H & I). Exposure to CIH had no effect on hypercapnic ventilation compared to sham-exposed mice (*P* = 0.3186; Fig 3.5; G); treatment with apocynin throughout the exposure to CIH also resulted in no difference in hypercapnic ventilation compared with exposure to CIH alone (*P* = 0.8206; Fig 3.5; G). In contrast, exposure to CIH significantly increased hypercapnic ventilation in NOX2 KO mice compared with NOX2 KO sham mice (*P* = 0.0007; Fig 3.5; H), an effect underpinned by an increase in tidal volume (*P* = 0.0001; Fig 3.5; E). Moreover, a significant increase in ventilation was observed in NOX2 KO mice compared with wild-type sham mice (*P* = 0.0029; Fig 3.5; I). The increase in ventilation in NOX2 KO mice in response to hypercapnia was due to a concomitant increase in breathing frequency (*P* = 0.0015; Fig 3.5; C) and tidal volume (*P* = 0.0150; Fig 3.5; C). $\dot{V}_I/\dot{V}CO_2$ also increased at the onset of hypercapnia compared to baseline values (Fig 3.5; M, N & O, respectively). However, exposure to CIH had no effect on $\dot{V}_I/\dot{V}CO_2$ during the hypercapnic challenge compared to sham mice (*P* = 0.2043; Fig 3.5; M); apocynin treatment had no significant effect on $\dot{V}_I/\dot{V}CO_2$ compared with

exposure to CIH alone (*P* = 0.384; Fig 3.5; M). However, $\dot{V}_I/\dot{V}CO_2$ was significantly elevated following exposure to CIH in mice lacking the NOX2 enzyme (*P* = 0.0352; Fig 3.5; N). When ventilation was normalised for CO_2 production, $\dot{V}_I/\dot{V}CO_2$ was equivalent in NOX2 KO and wild-type sham groups (*P* = 0.4357; Fig 3.5; O).

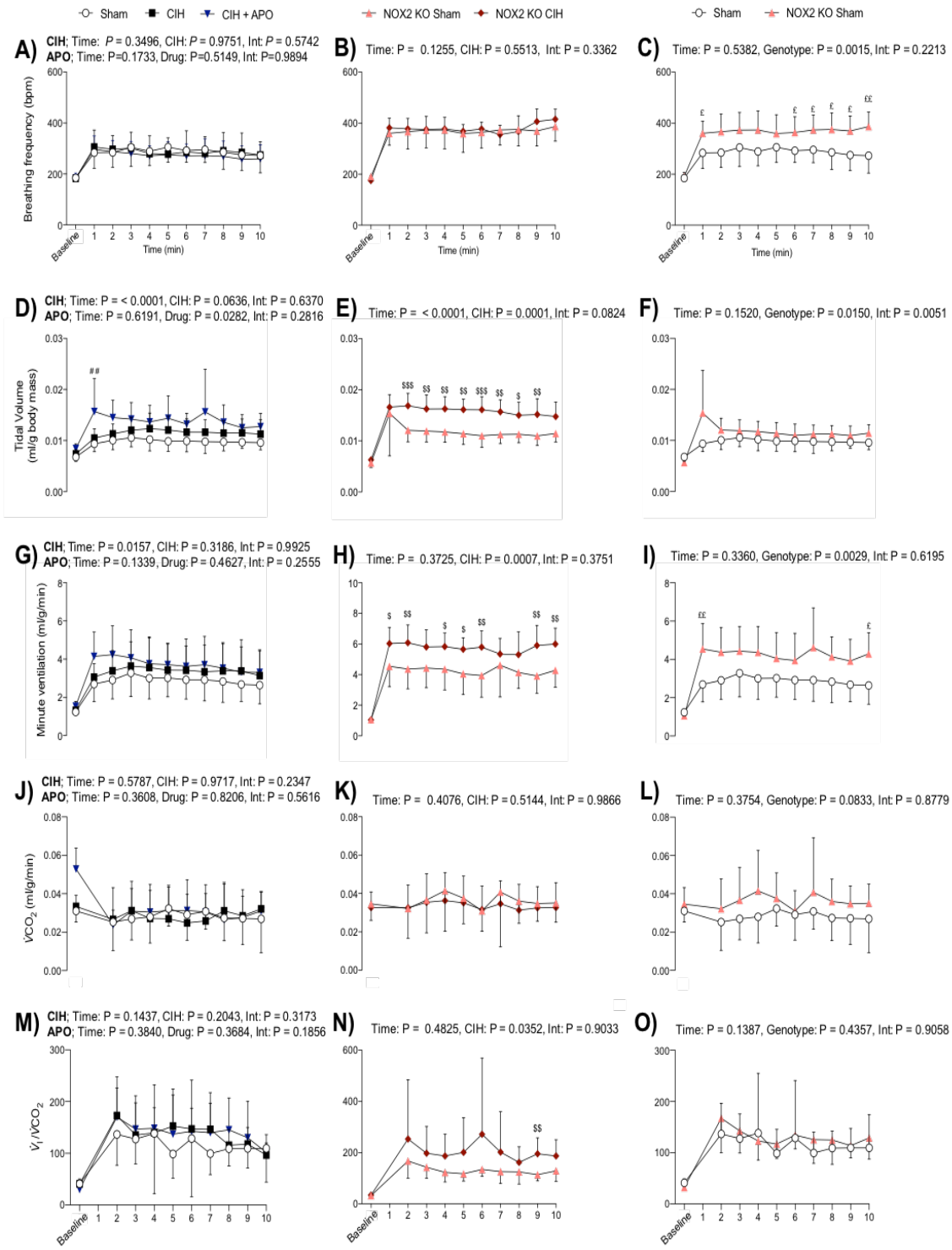

Figure 3.5 Ventilatory and metabolic responsiveness to hypercapnia. Group data (mean ± SD; n=10-12 per group) for breathing frequency (A, B, C; f_R), tidal volume (D, E, F; V_T), minute ventilation (G, H, I; V_I), carbon dioxide production (J, K, L; $\dot{V}CO_2$) and ventilatory equivalent for carbon dioxide (M, N, O; V_I/VCO_2) during baseline and 10 min of exposure to hypercapnia (5% inspired CO_2; balance O_2) for sham, CIH, CIH + APO, NOX2 KO sham and NOX2 KO CIH groups. Sham, normoxia (21% O_2) exposed; CIH, chronic intermittent hypoxia exposed; CIH + APO, apocynin (2mM) given in the drinking water for the duration of CIH exposure; NOX2 KO, NADPH Oxidase 2 knock-out (B6.129S-Cybbtm1Din/J), sham or CIH exposed. Data were statistically compared by repeated measures two-way ANOVA with Bonferroni *post hoc* test. For repeated measures two-way ANOVA; **CIH** denotes sham *vs*. CIH; **APO** denotes CIH *vs.* CIH + APO for A, D, G, J, & M. Int denotes the interaction between two factors for A-O. For Bonferroni *post hoc* test; $^{\#}$denotes CIH *vs.* CIH + APO, $^{\#\#}$ $P < 0.01$; $^{\$}$denotes NOX2 KO sham *vs.* NOX2 KO CIH, $^{\$}$ $P < 0.05$, $^{\$\$}$ $P < 0.01$; $^{£}$denotes sham *vs.* NOX2 KO sham, $^{£}$ $P < 0.05$, $^{££}$ P < 0.01.

3.3.8 Peak ventilatory responsiveness to hypoxia and hypercapnia

Figure 3.6 shows grouped ventilatory and metabolic data from all groups of mice in response to ventilatory challenge with hypoxia (10% O_2, balance N_2; Fig 3.5; A and B, respectively) and hypercapnia (5% CO_2, 95% O_2; Fig 3.5; C and D, respectively) in order to assess chemoreceptor responsiveness. The peak hypoxic ventilatory response (HVR; delta $\dot{V}_I$) was increased following exposure to CIH compared with sham-exposed mice ($P = 0.0341$; Fig 3.6; A), although this did not meet the threshold for statistical significance when correction for multiple comparisons was applied. Apocynin treatment throughout the exposure to CIH did not affect the ventilatory response to hypoxia ($P = 0.3989$; Fig 3.6 A). Peak HVR was significantly increased in NOX2 KO mice exposed to CIH compared with NOX2 KO sham mice ($P = 0.0003$, Fig 3.6; A). There was no difference in peak HVR in NOX2 KO mice compared with wild-type sham mice ($P = 0.4103$; Fig 3.6; A). The peak response for $\dot{V}_I/\dot{V}CO_2$ during hypoxic exposure is shown in Figure 3.6; B. Exposure to CIH increased the $\dot{V}_I/\dot{V}CO_2$ peak response to hypoxia in both wild-type ($P = 0.0633$; Fig 3.6; B) and NOX2 KO mice ($P = 0.2115$; Fig 3.6; B), evidenced by a notable effect size. NOX2 blockade using apocynin ($P = 0.6811$; Fig 3.6; B) or the genetic deletion of the NOX2 enzyme ($P = 0.8977$; Fig 3.6; B) had no effect on the peak $\dot{V}_I/\dot{V}CO_2$ response to hypoxia. The peak ventilatory response to hypercapnia (HCVR; delta $\dot{V}_I$) and the corresponding peak $\dot{V}_I/\dot{V}CO_2$ response are shown in Figure 3.6; C and D, respectively. Exposure to CIH had no significant effect on the peak HCVR compared with sham ($P = 0.4182$; Fig 3.6; C);

apocynin did not significantly alter the peak HCVR compared with exposure to CIH alone (P = 0.2661; Fig 3.6; C). Exposure to CIH resulted in a significant increase in the peak HVCR in mice lacking the NOX2 enzyme (P = 0.0016; Fig 3.6 C). A significant increase in the peak HCVR was also evident in NOX2 KO sham compared to wild-type sham mice (P = 0.0002; Fig 3.6 C). There was no significant difference in peak $\dot{V}_I/\dot{V}CO_2$ in response to acute hypercapnia following exposure to CIH in both wild-type (P = 0.7139; Fig 3.6; D) and NOX2 KO mice (P = 0.1161; Fig 3.6; D). NOX2 blockade had no effect on peak $\dot{V}_I/\dot{V}CO_2$, when examined after apocynin treatment during exposure to CIH (P = 0.0149; Fig 3.6; D) or after the genetic deletion of the NOX2 enzyme alone (P = 0.0371; Fig 3.6; D).

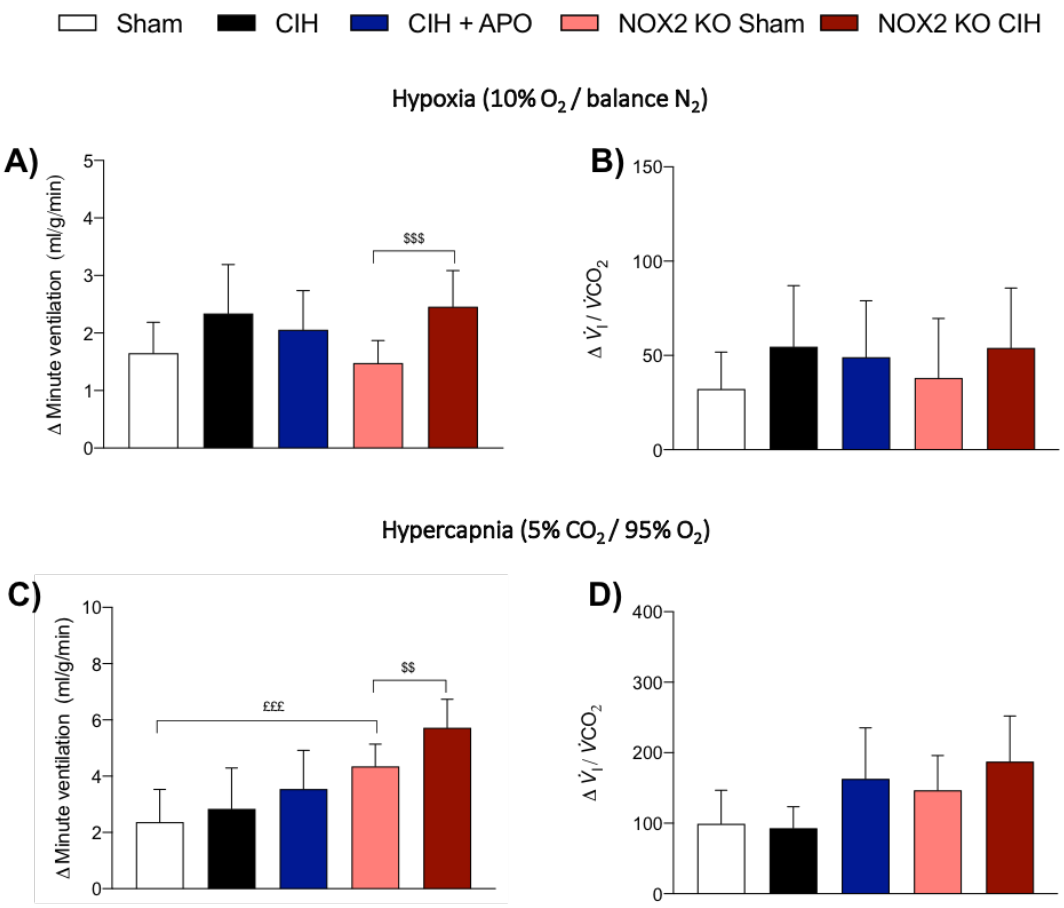

Figure 3.6 Peak ventilatory and metabolic responsiveness to hypoxia and hypercapnia. Group data for peak ventilatory responsiveness (expressed as Δ minute ventilation) to hypoxia (A) and hypercapnia (C) and the corresponding peak ventilatory equivalent for carbon dioxide (Δ $\dot{V}_I/\dot{V}CO_2$) to hypoxia (B) and hypercapnia (D) for sham, CIH, CIH + APO,

NOX2 KO sham and NOX2 KO CIH groups. Peak ventilatory responsiveness was taken as each individual animal's peak response to hypoxia or hypercapnia. The corresponding $\dot{V}CO_2$ value for each peak response was then used to calculate $\Delta \dot{V}_I / \dot{V}CO_2$. Values are expressed as mean ± SD (n=10-12 per group). Sham, normoxia (21% O_2)-exposed; CIH, chronic intermittent hypoxia-exposed; CIH + APO, Apocynin (2mM) given in the drinking water for the duration of CIH exposure; NOX2 KO, NADPH Oxidase 2 knock-out (B6.129S-Cybbtm1Din/J), sham- or CIH-exposed. Data sets which were normally distributed were statistically compared using unpaired two-tailed Student's *t* test. Welch's correction was applied in the case of unequal variance. Data which were not normally distributed were compared using Mann Whitney non-parametric tests. Statistical significance was taken at $p < 0.0125$. $^{\$}$ denotes NOX2 KO sham *vs.* NOX2 KO CIH, $^{\$\$}$ P < 0.01, $^{\$\$\$}$ P < 0.001; $^{£}$ denotes sham *vs.* NOX2 KO sham, $^{£££}$ P < 0.001.

3.4 Discussion

The major findings of this study are:

1) 2 weeks of exposure to CIH was not sufficient to elicit a persistent change in normoxic breathing in wild-type or NOX2 KO mice.

2) Mice lacking the NOX2 enzyme and mice administered apocynin during exposure to CIH hypoventilate during normoxic breathing, evidenced by a reduction in basal $\dot{V}_I/\dot{V}CO_2$.

3) Exposure to CIH increased the frequency of spontaneous apnoeas by a similar magnitude in wild-type and NOX2 KO mice during normoxia; the increase was blocked by the administration of apocynin in wild-type mice throughout the exposure to CIH.

4) Serotonergic activity, estimated by the ratio of 5-HIAA/5-HT, was reduced in NOX2 KO mice and following exposure to CIH in wild-type mice.

5) Both wild-type and NOX2 KO mice exposed to CIH display a modest increase in ventilatory responsiveness to hypoxia; apocynin significantly decreased the temporal $\dot{V}_I/\dot{V}CO_2$ response to hypoxia.

6) NOX2 KO results in a significantly decreased temporal ventilatory response to hypoxia; the peak ventilatory response to hypoxia remained unchanged.

7) Exposure to CIH had no effect on the hypercapnic ventilatory response in wild-type mice. NOX2 KO yields a potentiated hypercapnic ventilatory response, which was further enhanced following exposure to CIH.

OSAS is a highly prevalent sleep disorder, which harbours significant consequences for a range of integrative body systems, primarily that of cardio-respiratory control (Carlson et al., 1993, Leuenberger et al., 1995, Somers et al., 1995, Imadojemu et al., 2002, Del Rio et al., 2014a, Lucking et al., 2018). CIH is the classic hallmark feature of OSAS as a result of repeated obstruction of the pharyngeal airway leading to repeated arterial oxygen desaturation (White and Younes, 2012). OSAS is widely considered an oxidative stress disorder (Lavie, 2003). There is a remarkable capacity for plasticity within the respiratory control system and there is now a growing body of evidence indicating hypoxia-induced respiratory plasticity. A large body of evidence now points to exposure to CIH as driving force maintaining aberrant respiratory plasticity at multiple sites of the respiratory control network, which has the potential to contribute to, or exacerbate the severity of, OSAS. Varying intensities and durations of CIH have been shown to induce respiratory muscle weakness and fatigue in animal models of sleep-disordered breathing (McGuire et al., 2002a, McGuire et al., 2002b, Liu et al., 2005, Pae et al., 2005, Dunleavy et al., 2008, Liu et al., 2009, Jia and Liu, 2010, Skelly et al., 2012, Wang et al., 2013, Zhou and Liu, 2013, McDonald et al., 2015). Moreover, exposure to CIH can lead to impaired motor control of the upper airway (O'Halloran et al., 2002, Veasey et al., 2004, Ray et al., 2007), altered respiratory motor outflow (Moraes et al., 2013, Moraes and Machado, 2015) and discordant respiratory rhythm and pattern generation culminating in increased apnoea index (Edge et al., 2012, Donovan et al., 2014, Zanella et al., 2014, Souza et al., 2015, Elliot-Portal et al., 2018). Exposure to CIH can evoke sensory long-term facilitation within the carotid body (Peng et al., 2003), and induce facilitation of breathing and altered chemoreflex control of breathing (Reeves and Gozal, 2006, Skelly et al., 2012, Morgan et al., 2016b, Elliot-Portal et al., 2018). The precise mechanisms of respiratory system mal-adaptation following exposure to CIH remains unclear. Studies utilising pharmacological interventions now place CIH-induced ROS at the centre of this debate (Peng et al., 2003, Veasey et al., 2004, Dunleavy et al., 2008, Edge et al., 2012, Skelly et al., 2012). Furthermore, recent evidence highlights a role for the NOX2 enzymatic complex as a potential source of ROS underlying sensory and motor plasticity at multiple sites of the respiratory control network (Peng et al., 2006a, MacFarlane et al., 2009, Peng et al., 2009, Peng et al., 2011,

MacFarlane et al., 2014, Perim et al., 2018). Given the clinical implication of poor respiratory function in OSAS, the development of therapies targeting the specific source of CIH-induced ROS, postulated to be NOX2, may serve as an adjunct therapy for this debilitating disorder.

In the current study, we set out to examine the effect of exposure to CIH on ventilation in awake, unrestrained mice using WBP. We utilised an established rodent model of SDB with the CIH profile employed consisting of a 14-day treatment. Our CIH paradigm consisted of O_2 cycling from 21% for 210 seconds to 5% at the nadir for 90 seconds, 8 hours per day during light hours (Lucking et al., 2014). This CIH profile yielded 12 hypoxia-reoxygenation cycles per hour, reflective of that typically observed throughout the night cycle of an OSAS patient with a mild-to-moderate form of the disorder (Goyal and Johnson, 2017). We aimed to determine the effects of exposure to CIH on ventilation and metabolism during baseline (normoxic) breathing. It is well established that IH holds the capacity to induce plasticity at multiple levels of the respiratory control system, with the magnitude of this effect largely dependent on the time, intensity and duration of the IH stimulus (Navarrete-Opazo and Mitchell, 2014). Ventilatory adaptation following exposure to CIH, which can manifest as a progressive increase in normoxic ventilation following chronic exposure to IH, has previously been reported in rats (Reeves and Gozal, 2006, Skelly et al., 2012). We also aimed to investigate ventilatory responses to acute physiological challenges, namely hypoxia and hypercapnia, to assess the effects of exposure to CIH on peripheral and central chemoreceptor responsiveness. The functional significance of altered responses to these acute challenges is divergent. Respiratory mal-adaptation may present in an apnoeic patient when an inability to respond to a perturbation with an appropriate ventilatory response results in chemoreflexes not holding the essential capability to terminate apnoeic events. Conversely, an 'overshoot' or exaggerated ventilatory response may serve to create respiratory instability by excessively removing CO_2, thus reducing the CO_2 reserve toward the apnoeic threshold (Dempsey et al., 2010). We also sought to examine the effect of exposure to CIH on the propensity for apnoea in mice. Increased propensity for central apnoea has been reported in patients with OSAS (Salloum et al., 2010). In

light of this, it has been demonstrated that exposure to CIH results in central apnoea in neonatal rat pups (Julien et al., 2008), adult rats (Edge et al., 2012, Souza et al., 2015, Joseph et al., 2020) and mice (Elliot-Portal et al., 2018). Exposure to CIH has also been shown to increase the frequency of sighs and post-sigh apnoeas in rats (Edge et al., 2012, Souza et al., 2015, Joseph et al., 2020). Of interest, the administration of antioxidants has proven beneficial in ameliorating a range of IH-induced respiratory anomalies, highlighting the role of ROS in CIH-induced respiratory morbidity (Peng et al., 2003, Edge et al., 2012). Moreover, evidence suggests that NOX2 may be the source of CIH-induced ROS which may act to facilitate some of the mechanisms which underpin the alterations in respiratory control outlined above (Peng et al., 2009, Edge et al., 2012, Joseph et al., 2020). We hypothesised that 2 weeks of exposure to CIH would result in mal-adaptation in respiratory control which would manifest as enhanced normoxic ventilation, altered reflex chemoresponsiveness, and the manifestation of respiratory instability and increased apnoeic index. Furthermore, we postulated that these alterations would be underpinned by a NOX2-derived ROS-dependent mechanism, amenable to blockade by supplementation with apocynin (putative NOX2 inhibitor) and NOX2 knock-out.

Ventilatory adaptation is a form of respiratory plasticity described as a persistent increase in normoxic ventilation following exposure to CIH. This likely represents a chemoreflex driven increase in breathing potentially contributing to instability and sympathetic nervous activity that is recognised as contributing to systemic hypertension in OSAS patients (Marcus et al., 2010). In our model, normoxic ventilation and corresponding metabolic measurements were unaffected by 2 weeks of exposure to CIH in both wild-type and NOX2 KO mice. This lack of a CIH-induced effect on resting ventilation is in agreement with previous studies in guinea pigs (Lucking et al., 2018), rats (McGuire et al., 2003, Edge et al., 2012, Souza et al., 2015, Joseph et al., 2020) and mice (Elliot-Portal et al., 2018). However, previous research by our group demonstrates increased normoxic ventilation in male rats following 9 days of exposure to CIH (Skelly et al., 2012). This difference may be explained by the intensity of the IH stimulus, which was more severe in the latter study, as the CIH

profile utilised 20 hypoxia-reoxygenation cycles/hour compared with the 12 cycles/hour employed in the current study. Indeed, ventilatory adaptation to intermittent hypoxia (VAIH) has also been reported in rats following 30 days (Reeves and Gozal, 2006) and 21 days of exposure (Morgan et al., 2016a), with both groups highlighting that the duration and paradigm of IH exposure appears pivotal in determining the phenotypical respiratory response. Thus, we suggest that we did not observe evidence of enhanced normoxic ventilation due to the relatively mild and short duration of CIH used in this study. A CIH-induced decrease in metabolic rate has previously reported in rat models (Morgan et al., 2016a, Joseph et al., 2020). However, we report no alteration to $\dot{V}CO_2$ or $\dot{V}O_2$ following exposure to CIH in either wild-type or NOX2 KO mice, consistent with previous studies in mice (Elliot-Portal et al., 2018). Differences in metabolic responses during normoxic breathing following exposure to CIH are likely due to species differences between rat and mouse models, as differential metabolic responses to hypoxia between small and large mammals have been described (Haouzi et al., 2009).

Many forms of IH-induced plasticity are ROS-dependent (MacFarlane and Mitchell, 2008), and more specifically these ROS appear to be NOX2-derived (MacFarlane et al., 2009, Peng et al., 2009). In the current study, we report that mice administered with apocynin throughout the 2-week exposure to CIH hypoventilate during normoxic breathing. Moreover, mice deficient in the NOX2 enzyme also hypoventilate during normoxia. Both of these observations are reflected by a significantly reduced $\dot{V}_I/\dot{V}CO_2$, but appear to depend on different contributing factors. In apocynin-treated mice, there was a significant increase in metabolism that was only partially compensated for by increased ventilation. Ventilatory drive was increased in apocynin-treated mice, leading to decreased respiratory variability, but a relative hypoventilation persisted characterised by inadequate clearance of CO_2. Conversely, NOX2 deletion resulted in a reduction in basal ventilation (with no change in metabolism), suggesting a key role for NOX2 at one or more sites of the respiratory control network in facilitating adequate respiratory motor outflow. It remains to be elucidated the precise mechanism by which NOX2 blockade leads to hypoventilation. This could be the result of alterations at the carotid body, central

pattern-generating sites and/or respiratory motor neurons, wherein ROS have been shown to be pivotal. Interestingly, serotonergic turnover was decreased in NOX2 KO mice as evidenced by a reduced 5-HIAA/5-HT ratio. 5-HT neurons contribute to the regulation of ventilatory control by providing tonic, excitatory drive to multiple components of the respiratory network (Steinbusch, 1981, Connelly et al., 1989, Voss et al., 1990). 5-HT neurons also appropriately adjust ventilation through changes in neurotransmitter release to alter the level of tonic excitatory drive, in response to alterations in tissue pH/CO_2 (Richerson et al., 2001, Severson et al., 2003, Richerson, 2004, Richerson et al., 2005, Corcoran et al., 2009). Studies in transgenic mice, deficient in 5-HT neurons, demonstrate that ventilatory output in the neonatal period is critically dependent on serotonergic neurons, which provide excitatory drive to the respiratory network (Hodges et al., 2009). This culminates in severe disruption to eupnoeic respiratory rhythm and leads to high postnatal mortality in neonates, findings which provide an insight into the mechanisms underpinning sudden infant death syndrome (SIDS). Conversely, the deletion of 5-HT neurons does not decrease eupnoeic ventilation in adult mammals (Hodges et al., 2008). However, it has been suggested that divergent findings may be due to differential experimental approaches, and as such, the majority of the existing evidence is consistent with the concept that 5-HT neurons play an exclusively excitatory role at all postnatal ages (Hodges and Richerson, 2010). Neurotransmitter receptor activation may trigger ROS formation. Indeed, 5-HT receptor activation activates NOX in carotid bodies (Peng et al., 2006a) and phrenic motor neurons (MacFarlane et al., 2011), suggesting a serotonergic stimulus for NOX-dependent ROS formation which may underlie chemosensory and spinal respiratory plasticity. 5-HT receptors regulate NOX activity in the respiratory control system and ROS formation in cells is known to play a role in ventilatory control (MacFarlane et al., 2008). Our finding of reduced 5-HIAA/5-HT in NOX2 KO mice suggests that there may be changes in serotonergic modulation of respiratory motor function and chemoresponsiveness but this requires further investigation.

Whilst obstructive apnoeas are the predominant apnoea type in OSAS patients due to collapse of the upper airway, central or spontaneous apnoeas also occur in

patients due to respiratory control instability. This reveals a common overlap in obstructive and central sleep apnoea. OSAS patients receiving CPAP treatment regularly present with periodic breathing and central apnoeas, with some patients consequentially being diagnosed with complex apnoea (Morgenthaler et al., 2006). Complex apnoea in OSAS patients may be a result of CIH-induced remodelling in the central respiratory network governing respiration, serving to perpetuate the severity of OSAS (O'Halloran, 2016). A key finding in the current study is that exposure to CIH produced a significant increase in the frequency of spontaneous apnoeas in wild-type mice during resting ventilation. Studies in female rats (Souza et al., 2015, Joseph et al., 2020), male rats (Edge et al., 2012) and male mice (Elliot-Portal et al., 2018) have revealed similar CIH-induced increases in apnoea index. To determine if NOX2 was a potential source of ROS underlying increased apnoea index, we administered apocynin throughout the exposure to CIH. This was efficacious in preventing the CIH-induced increase in the frequency of spontaneous apnoeas to levels comparable to sham mice. This result is largely reminiscent of findings reported by (Edge et al., 2012), where 9 days of exposure to CIH induced a similar rise in the frequency of spontaneous apnoeas, an effect ameliorated by the same dose of apocynin (2mM) used in the current study. While apocynin is commonly used as a putative NOX2 inhibitor, evidence suggests that apocynin's pharmacological action may be through more general antioxidant action (Wind et al., 2010). To examine the specificity of the apocynin-induced effect, we utilised NOX2 KO mice which were exposed to CIH. Somewhat surprisingly, we observed a near identical increase in the frequency of spontaneous apnoeas following exposure to CIH in mice deficient in NOX2 compared to wild-type controls. These data reveal a non-NOX2 dependent source of ROS in the mechanism underlying the development of increased apnoea index following exposure to CIH. Multiple regions of the respiratory control network are affected by ROS as a result of exposure to CIH (Mifflin et al., 2015, Semenza and Prabhakar, 2015). Additionally, a wide range of signaling molecules including ROS, 5-HT, adenosine, HIF-1α and inflammatory cytokines are involved in the CIH-induced respiratory plasticity (Peng et al., 2006b, Pawar et al., 2009, Peng et al., 2009, Del Rio et al., 2011, Peng et al., 2013, Iturriaga et al., 2014, Sacramento et al., 2015, Morgan et al., 2016b, Moya et al., 2020). As these substances exhibit pro-oxidant properties

and/or are sensitive to ROS, oxidative stress may represent a common thread underpinning a complex mechanism that results in CIH-induced increase in apnoea index (Del Rio et al., 2010). The specific source of ROS warrants further experimentation.

While we report no alteration to the frequency of sighs or post-sigh apnoeas following exposure to CIH, the duration of post-sigh apnoeas was increased following exposure to CIH, which was ameliorated by apocynin administration. This suggests that CIH-exposed mice develop a delayed ability to create regular respiratory cycles following deep breaths, characterised by sighs or post-sigh apnoeas, similar to previous observations in female rats (Souza et al., 2015). Furthermore, our study implicates a role for NOX2-derived ROS, evidenced by the absence of this effect following treatment with apocynin and in CIH-exposed NOX2 KO mice. The frequency of spontaneous apnoeas was equivalent in wild-type and NOX2 KO mice. However, we observed a significant increase in sigh frequency in mice lacking the NOX2 enzyme during normoxic breathing. Sighs are reportedly generated in the preBötC (Nagel et al., 2001) and interestingly, the application of the dismutated form of O_2^-, H_2O_2, evokes a transient depression followed by an augmentation of neuronal activity in this region (Garcia et al., 2011). This suggests that ROS are capable of exerting an inhibitory effect at this level of the respiratory control network. The increase in sigh frequency in NOX2 KO mice suggests that these ROS may be NOX2 derived in nature, as the removal of NOX2 may function to remove this inhibition, thus increasing sigh frequency. Our results generally support the view that ROS exert a tonic inhibition, yet surprisingly, NOX2 KO mice hypoventilate, which reveals the complex role of NOX2-derived ROS in the integrative control of breathing.

We reasoned that there is a capacity for exposure to CIH to induce breathing instability, likely through alterations to the rhythm and pattern generation of respiration. However, assessments of respiratory stability through Poincaré plot analysis revealed no evidence for CIH-induced alterations to respiratory timing. This is in contrast to studies in adult female rats which suggest that exposure to CIH produces an increase in short- and long-term breathing variability, resulting in

changes in respiratory pattern (Souza et al., 2015). Conversely, studies in male guinea pigs, with hypoxia-insensitive carotid bodies, reveal a CIH-induced decrease in indices of breathing variability (Lucking et al., 2018). This apparent dichotomy in results may relate to differences in sex, species and IH intensity and duration between experimental approaches. In the current study, administration of apocynin throughout the exposure to CIH produced a significant decrease in breathing variability to levels below that of controls. This effect could be mal-adaptive as it is well established that an optimal level of ROS is necessary for numerous homeostatic processes, with alterations in the levels of ROS contributing to functional deficits in respiratory control (MacFarlane et al., 2008). A degree of breathing variability is normal (Wuyts et al., 2011). Sighs hold an essential function in the normal respiratory cycle through monitoring brain states, stimulating arousal and resetting breathing variability (Ramirez, 2014). An increase in sighs during respiratory perturbations such as hypoxia, stimulates an arousal which highlights their critical role in survival. Failure to sigh or arouse has been implicated in SIDS (Garcia et al., 2013). Therefore, an increase in breathing stability to the extent that apocynin produced in our study, may represent an over-scavenging of ROS at sites pivotal for rhythmogenesis. In turn, this could be mal-adaptive by reducing the capacity of the respiratory control system to adapt to various environmental and behavioural demands. However, the pronounced metabolic effect of apocynin, which resulted in a reflex increase in ventilatory drive, albeit inadequate resulting in a relative hypoventilation, likely resulted in decreased variability due to elevated $PaCO_2$.

Respiratory neurons at multiple brainstem sites are believed to have key roles in generating homeostatic respiratory rhythm with inspiratory neurons at the preBötC coming to the fore as key players in this process. Exposure to CIH has been shown to alter the electrophysiological properties of these neurons (Moraes et al., 2013) and respiratory circuits at the level of the preBötC, in turn affecting transmission to the hypoglossal motor nucleus leading to increased transmission failure to the hypoglossal nerve (Garcia et al., 2016). Furthermore, complete ablation of the preBötC increases the propensity for apnoea in sleeping rats (McKay and Feldman, 2008). ROS are implicated in multiple forms of IH-induced plasticity, with H_2O_2 shown

to be capable of modulating rhythmogenesis by the preBötC (Garcia et al., 2011). Furthermore, antioxidant therapy has been shown to successfully reduce CIH-mediated irregularities of the network rhythm improving transmission to the hypoglossal nerve (Garcia et al., 2016). Thus, in the current study we suggest that exposure to CIH may promote a pro-oxidant state which destabilises rhythmogenesis originating from the preBötC. This may represent part of a central mechanism that promotes apnoea and respiratory instability. Additionally, due to the similar effect of exposure to CIH on measures of respiratory stability in wild-type and NOX2 KO mice, it appears that apocynin functions as a non-specific antioxidant at higher centres of respiratory control in a similar manner to that previously shown in the vascular system (Heumüller et al., 2008). It is also plausible to suggest that increased propensity for apnoea arises from altered peripheral control of breathing. A CIH-induced enhancement of the hypoxic ventilatory response (HVR) (discussed below) may lead to ventilatory overshoot and in this way may destabilise breathing, providing the substrate for apnoea.

Ventilatory responsiveness to hypoxia following exposure to CIH varies greatly depending on the pattern and duration of hypoxic exposure. A diverse range of observations arise as a result of an intricate system of molecular mechanisms that underlie plasticity in the respiratory control reflex circuits and ultimately control the physiology of breathing in response to oxygen desaturation. Augmented HVRs and concomitant oxidative stress have been observed in healthy individuals following exposure to CIH (Pialoux et al., 2009) and in patients with OSAS (Narkiewicz et al., 1999). Exposure to CIH evokes carotid body sensory facilitation *ex vivo* and in anesthetised animals (Peng et al., 2001, Rey et al., 2004, Peng et al., 2006b). Carotid body responses to hypoxia are enhanced following exposure to CIH (Peng et al., 2001, Peng et al., 2003, Peng et al., 2009, Del Rio et al., 2010, Del Rio et al., 2012, Del Rio et al., 2014b). Nevertheless, an enhancement (Reeves et al., 2003, Reeves and Gozal, 2004, Peng et al., 2006b, Julien et al., 2008, Morgan et al., 2016a, Elliot-Portal et al., 2018), depression (Reeves et al., 2006, Gonzalez-Martín et al., 2011, Olea et al., 2014, Lucking et al., 2018) or unchanged (Edge et al., 2009, Skelly et al., 2012) HVR in intact animals has been reported across a range of species following treatment with a

variety of IH paradigms. In the current study, we report a modest CIH-induced increase in ventilation in wild-type mice over the time course of the hypoxia challenge. In a similar manner, we observed a small increase in the peak HVR following exposure to CIH, although this did not reach statistical significance taking multiple comparisons into account. The importance of assessing metabolic rate in concert with respiratory recordings has previously been emphasised (Morgan et al., 2016a), to account for the decrease in metabolic rate that occurs when small mammals are acutely exposed to hypoxia (Frappell et al., 1992). This is an especially crucial consideration in mouse models, such as that employed in the current study, as mice exhibit a greater hypometabolic response to hypoxia than rats (Jochmans-Lemoine et al., 2015). When ventilation is normalised for $\dot{V}CO_2$ production, the *a priori* index of metabolic function, the true hyperventilatory response to hypoxia in mice is revealed (i.e. an increase in $\dot{V}_I/\dot{V}CO2$). Failure to report on metabolic measures in several previous studies, limits the capacity to determine the true hyperventilatory response to hypoxia (Morgan et al., 2016a). In the current study, analysis of the delta $\dot{V}_I/\dot{V}CO2$ response to hypoxia revealed an increase in CIH-exposed mice compared with sham, which was largely unaffected by NOX2 deletion. Although the changes were not statistically significant, the effect size was notable (~100%).

There is increased interest in the role of oxidative stress in facilitating hypoxic chemosensitivity, but evidence surrounding the culpable source of ROS remains largely inconclusive. NOX subunits including p22phox, gp91phox, p47phox, and p67phox have been localised to type I cells of guinea pig, rat, and human carotid bodies (Kummer and Acker, 1995). Exposure to CIH significantly increases the mRNA expression of NOX1, NOX2 and NOX3 in peripheral chemoreceptors (Peng et al., 2009, Khan et al., 2011, Prabhakar et al., 2015). Moreover, there is ample evidence to suggest that CIH-induced sensory plasticity of the carotid body is NOX2-dependent (Peng et al., 2006a, Peng et al., 2009, Yuan et al., 2011, Nanduri et al., 2013, Nanduri et al., 2015). CIH-induced increases in ventilatory responsiveness to hypoxia are attenuated in rats treated with apocynin, as evidenced by a reduction in $\dot{V}_I/\dot{V}CO_2$ (Morgan et al., 2016b). This implicates ROS, which may be NOX2-derived (depending

on the specificity of apocynin), in altered chemoreflex sensitivity following exposure to CIH, possibly due to a reduction in nitrotyrosine production in the carotid body (Del Rio et al., 2010, Morgan et al., 2016b). Similarly, treatment with apocynin throughout the exposure to CIH significantly reduced the temporal $\dot{V}_I/\dot{V}CO_2$ response to acute hypoxia in the current study, further confirming that ROS are necessary for hypoxic chemosensitivity. However, reminiscent of findings in wild-type mice, the CIH-induced increase in minute ventilation in NOX2 KO mice during exposure to hypoxia was ameliorated when ventilation was normalised for metabolic rate. The equivalent magnitudes of the peak ventilatory responses to hypoxia in both wild-type and NOX2 KO suggests that NOX2-derived ROS do not play a role in CIH-induced augmentation of the chemoreflex response to acute hypoxia. p47phox, but not gp91phox knock-out, alters the O_2 sensing capability of the carotid body seen as a potentiated ventilatory and chemoreceptor response to hypoxia (Sanders et al., 2002). This suggests that NOX subunits significantly differ in their complex regulatory function of respiratory control. Patch-clamp studies have demonstrated that intact NEBs in lung slice preparations from mice deficient in gp91phox, failed to respond to a hypoxic stimulus (Fu et al., 2000). The latter study provides evidence indicating that the dysfunction of NOX disrupts the O_2 sensing capability of the NEBs. Interestingly, no difference in the response to hypoxia between wild-type and gp91phox mice has also been reported (Roy et al., 2000). This is attributed to no alteration in glomus cell functioning and a conclusion that although NOX is a major source of ROS, it does not function as an oxygen sensor in the carotid body. In our gp91phox (NOX2) knock-out mice, we observed a decrease in $\dot{V}_I/\dot{V}CO_2$ over ten minutes of exposure to acute hypoxia. However, gp91phox knock-out had no effect on the peak hypoxic ventilatory response.

Therefore, we conclude that exposure to CIH increases ventilatory sensitivity to hypoxia, which presumably is a carotid body-mediated effect (Peng et al., 2001, Peng et al., 2003, Peng et al., 2006b, Peng et al., 2009), but apparently not NOX2-dependent, which was surprising, given the finding that CIH-induced carotid body sensory long-term facilitation and potentiated chemosensory responsiveness to hypoxia is NOX2-dependent (Peng et al., 2009, Morgan et al., 2016b). Our results

suggest that there appear to be latent pathways, independent of NOX2 signalling, capable of driving enhanced hypoxic chemosensitivity in response to exposure to CIH. Whilst a wealth of studies have focussed on the role of the carotid bodies in hypoxic chemosensitivity, plasticity within other respiratory centres in the central nervous system (CNS) may play a role in the integrative response to hypoxia. It is likely that CIH-induced plasticity at the level of NTS neurons underpins enhanced hypoxic ventilatory drive following CIH (Moya et al., 2020). The NTS represents an important integrative centre in the brainstem where sensory cues relayed from peripheral chemoreceptors inform changes in respiratory motor output, culminating in altered ventilatory responses (Zoccal et al., 2014). HIF-1α deficiency has been shown to have a pivotal role in carotid body plasticity following exposure to hypoxia (Kline et al., 2002, Peng et al., 2006b). Additionally, selective HIF-1α deficiency in NTS neurons has been shown to prevent hypoxic sensitivity following exposure to chronic sustained hypoxia (Moya et al., 2020). Therefore, it is plausible to suggest a that a HIF-1α dependent mechanism within neurons of the NTS may underpin the increased HVR observed following exposure to CIH in the current study. The carotid body and CNS regions including the NTS, paraventricular nucleus of the hypothalamus (PVN) and rostral ventrolateral medulla (RVLM), which are important for the chemoreflex control of ventilation and sympathetic outflow, are all affected by increased ROS as a result of exposure to CIH (Mifflin et al., 2015, Semenza and Prabhakar, 2015). Additionally, it has been demonstrated that a range of signaling molecules including ROS, 5-HT, adenosine, HIF-1α and inflammatory cytokines are involved in the CIH-induced chemoreflex sensitization (Peng et al., 2006b, Pawar et al., 2009, Peng et al., 2009, Del Rio et al., 2011, Peng et al., 2013, Iturriaga et al., 2014, Sacramento et al., 2015, Morgan et al., 2016b, Moya et al., 2020). As these substances and processes exhibit pro-oxidant properties and/or are sensitive to ROS, oxidative stress may represent a common thread linking many drivers of CIH-induced hypoxic sensitivity, at multiple points throughout the chemoreflex loop (Del Rio et al., 2010). This highlights the complexity in understanding the precise mechanisms underlying CIH-induced ROS-dependent hypoxic sensitivity and as such, it warrants further attention.

Although CO_2 has a pivotal role in ventilatory control during sleep, there is a paucity of information examining the effects of exposure to CIH on hypercapnic sensitivity. Chemoreflexes are essential during sleep as a protective mechanism to stimulate arousal and terminate apnoeic events. Failure to do so may contribute to an increased propensity of apnoeic events, thus leading to an increased severity of OSAS. Conversely, an exaggerated response to CO_2 contributes to ventilatory instability by reducing the CO_2 reserve towards apnoeic threshold (Dempsey et al., 2010). An increase in the hypercapnic ventilatory response (HCVR) has been observed in OSAS patients, as a result of episodic hypoxia (Appelberg and Sundström, 1997, Khodadadeh et al., 2006). Consistent with this, a CIH-induced increase in the ventilatory response to hypercapnia has been reported in mice (Elliot-Portal et al., 2018) and dogs (Katayama et al., 2007). Conversely, evidence supports an unaltered HCVR following CIH exposure in a range of models including guinea pigs (Lucking et al., 2018) and rats (Greenberg et al., 1999, Edge et al., 2012). In the current study, we report no evidence in support of a CIH-induced augmentation to the chemoreflex response to hypercapnia in wild-type mice. However, mice lacking the NOX2 enzyme have an exaggerated response to CO_2 compared with wild-type controls. This ventilatory response was further enhanced following exposure to CIH in NOX2 KO mice. The increase in ventilation during hypercapnia is somewhat surprising given that NOX2-deficient mice exhibit evidence of hypoventilation (reduced $\dot{V}_I/\dot{V}CO_2$) and reduced excitatory input (reduced 5-HIAA/5-HT). Serotonergic neurons are thought to play a key role in pH/CO_2 sensing, as genetic deletion of 5-HT neurons prevents arousal from hypercapnia (Kaur et al., 2020). Therefore, the potentiated ventilatory response to hypercapnia in NOX2 KO mice suggests a very powerful suppression of hypercapnic drive by a NOX2-dependent mechanism. An exaggerated response to alterations in CO_2 may serve to destabilise breathing. Our results support the notion that NOX2-dependent ROS exert a tonic inhibition on sites important for central chemoreception such as the NTS, locus coeruleus and the retrotrapezoid nucleus (Nattie and Li, 2012), which functions to suppress hypercapnic drive. This NOX2-dependent inhibition may have a regulatory function in generating an appropriate ventilatory response to a perturbation in CO_2 levels, as exposure to CIH further exacerbates the chemoreflex response in NOX2 KO mice, whereas it was without

effect in wild-type animals. The mechanisms underpinning this response warrant further investigation.

Our results reveal the capacity for 2 weeks of exposure to a mild-to-moderate paradigm of CIH to evoke plasticity within the respiratory control system, predominantly evidenced by increased sensitization to hypoxia and increased apnoea index. Increased ventilatory responsiveness to hypoxia has been observed in patients with OSAS (Narkiewicz et al., 1999) and may represent an increase in sympathetic tone to drive a hypertensive phenotype (Narkiewicz et al., 1998, Imadojemu et al., 2007), while also contributing to the development of respiratory instability, culminating in increased apnoea index (Peng et al., 2003). Oxidative stress plays a causal role in the ventilatory mal-adaptations and sympathetic nervous system overactivity observed in animal models of OSAS, consistent with the human condition (Peng et al., 2009, Peng et al., 2013). Our results implicate ROS, which are not NOX2-derived, in the development of CIH-induced respiratory mal-adaptation, as we observe what we suggest are general antioxidant effects of apocynin ameliorating the CIH-induced increase in the temporal ventilatory response to hypoxia and increased apnoea index. Our results may have implications for OSAS patients diagnosed with complex apnoea (Morgenthaler et al., 2006). Patients with complex apnoea exhibit spontaneous or central apnoeas, in addition to obstructive apnoeas, which may be the result of CIH-induced remodeling with the central respiratory network (O'Halloran, 2016), such as the PreBötC (Garcia et al., 2016). Therefore, respiratory system mal-adaptation following exposure to CIH may exacerbate OSAS severity, serving to perpetuating a vicious cycle of respiratory morbidity. Our results reveal that antioxidant therapies may be a useful adjunctive therapy for the treatment of OSAS patients. However, further experimentation is necessary to delineate the source of ROS, mechanism of action and specific sites throughout the respiratory control network at which they exert their effects in order to develop precise therapeutic strategies.

3.5 References

APPELBERG, J. & SUNDSTRÖM, G. 1997. Ventilatory response to CO2 in patients with snoring, obstructive hypopnoea and obstructive apnoea. *Clin Physiol,* 17**,** 497-507.

CARLSON, J. T., HEDNER, J., ELAM, M., EJNELL, H., SELLGREN, J. & WALLIN, B. G. 1993. Augmented resting sympathetic activity in awake patients with obstructive sleep apnea. *Chest,* 103**,** 1763-8.

CONNELLY, C. A., ELLENBERGER, H. H. & FELDMAN, J. L. 1989. Are there serotonergic projections from raphe and retrotrapezoid nuclei to the ventral respiratory group in the rat? *Neurosci Lett,* 105**,** 34-40.

CORCORAN, A. E., HODGES, M. R., WU, Y., WANG, W., WYLIE, C. J., DENERIS, E. S. & RICHERSON, G. B. 2009. Medullary serotonin neurons and central CO2 chemoreception. *Respir Physiol Neurobiol,* 168**,** 49-58.

DEL RIO, R., MOYA, E. A. & ITURRIAGA, R. 2010. Carotid body and cardiorespiratory alterations in intermittent hypoxia: the oxidative link. *Eur Respir J,* 36**,** 143-50.

DEL RIO, R., MOYA, E. A. & ITURRIAGA, R. 2011. Differential expression of pro-inflammatory cytokines, endothelin-1 and nitric oxide synthases in the rat carotid body exposed to intermittent hypoxia. *Brain Res,* 1395**,** 74-85.

DEL RIO, R., MOYA, E. A. & ITURRIAGA, R. 2014a. Carotid body potentiation during chronic intermittent hypoxia: implication for hypertension. *Frontiers in Physiology,* 5.

DEL RIO, R., MOYA, E. A. & ITURRIAGA, R. 2014b. Carotid body potentiation during chronic intermittent hypoxia: implication for hypertension. *Front Physiol,* 5**,** 434.

DEL RIO, R., MOYA, E. A., PARGA, M. J., MADRID, C. & ITURRIAGA, R. 2012. Carotid body inflammation and cardiorespiratory alterations in intermittent hypoxia. *Eur Respir J,* 39**,** 1492-500.

DEMPSEY, J. A., VEASEY, S. C., MORGAN, B. J. & O'DONNELL, C. P. 2010. Pathophysiology of sleep apnea. *Physiol Rev,* 90**,** 47-112.

DONOVAN, L. M., LIU, Y. & WEISS, J. W. 2014. Effect of endothelin antagonism on apnea frequency following chronic intermittent hypoxia. *Respir Physiol Neurobiol,* 194**,** 6-8.

DUNLEAVY, M., BRADFORD, A. & O'HALLORAN, K. D. 2008. Oxidative stress impairs upper airway muscle endurance in an animal model of sleep-disordered breathing. *Adv Exp Med Biol,* 605**,** 458-62.

EDGE, D., BRADFORD, A. & O'HALLORAN, K. D. 2012. Chronic intermittent hypoxia increases apnoea index in sleeping rats. *Adv Exp Med Biol,* 758**,** 359-63.

EDGE, D., SKELLY, J. R., BRADFORD, A. & O'HALLORAN, K. D. 2009. Ventilatory drive is enhanced in male and female rats following chronic intermittent hypoxia. *Adv Exp Med Biol,* 648**,** 337-44.

ELLIOT-PORTAL, E., LAOUAFA, S., ARIAS-REYES, C., JANES, T. A., JOSEPH, V. & SOLIZ, J. 2018. Brain-derived erythropoietin protects from intermittent hypoxia-induced cardiorespiratory dysfunction and oxidative stress in mice. *Sleep,* 41.

FRAPPELL, P., LANTHIER, C., BAUDINETTE, R. V. & MORTOLA, J. P. 1992. Metabolism and ventilation in acute hypoxia: a comparative analysis in small mammalian species. *Am J Physiol,* 262**,** R1040-6.

FU, X. W., WANG, D., NURSE, C. A., DINAUER, M. C. & CUTZ, E. 2000. NADPH oxidase is an O2 sensor in airway chemoreceptors: evidence from K+ current modulation in wild-type and oxidase-deficient mice. *Proc Natl Acad Sci U S A,* 97**,** 4374-9.

GARCIA, A. J., 3RD, KHAN, S. A., KUMAR, G. K., PRABHAKAR, N. R. & RAMIREZ, J. M. 2011. Hydrogen peroxide differentially affects activity in the pre-Bötzinger complex and hippocampus. *J Neurophysiol,* 106**,** 3045-55.

GARCIA, A. J., 3RD, KOSCHNITZKY, J. E. & RAMIREZ, J. M. 2013. The physiological determinants of sudden infant death syndrome. *Respir Physiol Neurobiol,* 189**,** 288-300.

GARCIA, A. J., 3RD, ZANELLA, S., DASHEVSKIY, T., KHAN, S. A., KHUU, M. A., PRABHAKAR, N. R. & RAMIREZ, J. M. 2016. Chronic Intermittent Hypoxia Alters Local Respiratory Circuit Function at the Level of the preBötzinger Complex. *Front Neurosci,* 10**,** 4.

GONZALEZ-MARTÍN, M. C., VEGA-AGAPITO, M. V., CONDE, S. V., CASTAÑEDA, J., BUSTAMANTE, R., OLEA, E., PEREZ-VIZCAINO, F., GONZALEZ, C. & OBESO, A. 2011. Carotid body function and ventilatory responses in intermittent hypoxia. Evidence for anomalous brainstem integration of arterial chemoreceptor input. *J Cell Physiol,* 226**,** 1961-9.

GOYAL, M. & JOHNSON, J. 2017. Obstructive Sleep Apnea Diagnosis and Management. *Mo Med,* 114**,** 120-124.

GREENBERG, H. E., SICA, A., BATSON, D. & SCHARF, S. M. 1999. Chronic intermittent hypoxia increases sympathetic responsiveness to hypoxia and hypercapnia. *J Appl Physiol (1985),* 86**,** 298-305.

HAOUZI, P., BELL, H. J., NOTET, V. & BIHAIN, B. 2009. Comparison of the metabolic and ventilatory response to hypoxia and H2S in unsedated mice and rats. *Respir Physiol Neurobiol,* 167**,** 316-22.

HEUMÜLLER, S., WIND, S., BARBOSA-SICARD, E., SCHMIDT, H. H., BUSSE, R., SCHRÖDER, K. & BRANDES, R. P. 2008. Apocynin is not an inhibitor of vascular NADPH oxidases but an antioxidant. *Hypertension,* 51**,** 211-7.

HODGES, M. R. & RICHERSON, G. B. 2010. The role of medullary serotonin (5-HT) neurons in respiratory control: contributions to eupneic ventilation, CO2 chemoreception, and thermoregulation. *J Appl Physiol (1985),* 108**,** 1425-32.

HODGES, M. R., TATTERSALL, G. J., HARRIS, M. B., MCEVOY, S. D., RICHERSON, D. N., DENERIS, E. S., JOHNSON, R. L., CHEN, Z. F. & RICHERSON, G. B. 2008. Defects in breathing and thermoregulation in mice with near-complete absence of central serotonin neurons. *J Neurosci,* 28**,** 2495-505.

HODGES, M. R., WEHNER, M., AUNGST, J., SMITH, J. C. & RICHERSON, G. B. 2009. Transgenic mice lacking serotonin neurons have severe apnea and high mortality during development. *J Neurosci,* 29**,** 10341-9.

IMADOJEMU, V. A., GLEESON, K., GRAY, K. S., SINOWAY, L. I. & LEUENBERGER, U. A. 2002. Obstructive apnea during sleep is associated with peripheral vasoconstriction. *Am J Respir Crit Care Med,* 165**,** 61-6.

IMADOJEMU, V. A., MAWJI, Z., KUNSELMAN, A., GRAY, K. S., HOGEMAN, C. S. & LEUENBERGER, U. A. 2007. Sympathetic chemoreflex responses in obstructive sleep apnea and effects of continuous positive airway pressure therapy. *Chest,* 131**,** 1406-13.

ITURRIAGA, R., ANDRADE, D. C. & DEL RIO, R. 2014. Enhanced carotid body chemosensory activity and the cardiovascular alterations induced by intermittent hypoxia. *Front Physiol,* 5**,** 468.

JIA, S. S. & LIU, Y. H. 2010. Down-regulation of hypoxia inducible factor-1alpha: a possible explanation for the protective effects of estrogen on genioglossus fatigue resistance. *Eur J Oral Sci,* 118**,** 139-44.

JOCHMANS-LEMOINE, A., VILLALPANDO, G., GONZALES, M., VALVERDE, I., SORIA, R. & JOSEPH, V. 2015. Divergent physiological responses in laboratory rats and mice raised at high altitude. *J Exp Biol,* 218**,** 1035-43.

JOSEPH, V., LAOUAFA, S., MARCOUILLER, F., ROUSSEL, D., PIALOUX, V. & BAIRAM, A. 2020. Progesterone decreases apnoea and reduces oxidative stress induced by chronic intermittent hypoxia in ovariectomized female rats. *Exp Physiol,* 105**,** 1025-1034.

JULIEN, C., BAIRAM, A. & JOSEPH, V. 2008. Chronic intermittent hypoxia reduces ventilatory long-term facilitation and enhances apnea frequency in newborn rats. *Am J Physiol Regul Integr Comp Physiol,* 294**,** R1356-66.

KATAYAMA, K., SMITH, C. A., HENDERSON, K. S. & DEMPSEY, J. A. 2007. Chronic intermittent hypoxia increases the CO2 reserve in sleeping dogs. *J Appl Physiol (1985),* 103**,** 1942-9.

KAUR, S., DE LUCA, R., KHANDAY, M. A., BANDARU, S. S., THOMAS, R. C., BROADHURST, R. Y., VENNER, A., TODD, W. D., FULLER, P. M., ARRIGONI, E. & SAPER, C. B. 2020. Role of serotonergic dorsal raphe neurons in hypercapnia-induced arousals. *Nat Commun,* 11**,** 2769.

KHAN, S. A., NANDURI, J., YUAN, G., KINSMAN, B., KUMAR, G. K., JOSEPH, J., KALYANARAMAN, B. & PRABHAKAR, N. R. 2011. NADPH oxidase 2 mediates intermittent hypoxia-induced mitochondrial complex I inhibition: relevance to blood pressure changes in rats. *Antioxid Redox Signal,* 14**,** 533-42.

KHODADADEH, B., BADR, M. S. & MATEIKA, J. H. 2006. The ventilatory response to carbon dioxide and sustained hypoxia is enhanced after episodic hypoxia in OSA patients. *Respir Physiol Neurobiol,* 150**,** 122-34.

KLINE, D. D., PENG, Y. J., MANALO, D. J., SEMENZA, G. L. & PRABHAKAR, N. R. 2002. Defective carotid body function and impaired ventilatory responses to chronic hypoxia in mice partially deficient for hypoxia-inducible factor 1 alpha. *Proc Natl Acad Sci U S A,* 99**,** 821-6.

KUMMER, W. & ACKER, H. 1995. Immunohistochemical demonstration of four subunits of neutrophil NAD(P)H oxidase in type I cells of carotid body. *J Appl Physiol (1985),* 78**,** 1904-9.

LAVIE, L. 2003. Obstructive sleep apnoea syndrome--an oxidative stress disorder. *Sleep Med Rev,* 7**,** 35-51.

LEUENBERGER, U., JACOB, E., SWEER, L., WARAVDEKAR, N., ZWILLICH, C. & SINOWAY, L. 1995. Surges of muscle sympathetic nerve activity during obstructive apnea are linked to hypoxemia. *J Appl Physiol (1985),* 79**,** 581-8.

LIU, S. S., LIU, H. G., XIONG, S. D., NIU, R. J., XU, Y. J. & ZHANG, Z. X. 2005. [Effects of Shen-Mai injection on sternohyoid contractile properties in chronic intermittent hypoxia rat]. *Zhonghua Jie He He Hu Xi Za Zhi,* 28**,** 611-4.

LIU, Y. H., HUANG, Y. & SHAO, X. 2009. Effects of estrogen on genioglossal muscle contractile properties and fiber-type distribution in chronic intermittent hypoxia rats. *Eur J Oral Sci,* 117**,** 685-90.

LUCKING, E. F., O'CONNOR, K. M., STRAIN, C. R., FOUHY, F., BASTIAANSSEN, T. F. S., BURNS, D. P., GOLUBEVA, A. V., STANTON, C., CLARKE, G., CRYAN, J. F. & O'HALLORAN, K. D. 2018. Chronic intermittent hypoxia disrupts cardiorespiratory homeostasis and gut microbiota composition in adult male guinea-pigs. *EBioMedicine,* 38**,** 191-205.

LUCKING, E. F., O'HALLORAN, K. D. & JONES, J. F. 2014. Increased cardiac output contributes to the development of chronic intermittent hypoxia-induced hypertension. *Exp Physiol,* 99**,** 1312-24.

MACFARLANE, P. M. & MITCHELL, G. S. 2008. Respiratory long-term facilitation following intermittent hypoxia requires reactive oxygen species formation. *Neuroscience,* 152**,** 189-97.

MACFARLANE, P. M., SATRIOTOMO, I., WINDELBORN, J. A. & MITCHELL, G. S. 2009. NADPH oxidase activity is necessary for acute intermittent hypoxia-induced phrenic long-term facilitation. *J Physiol,* 587**,** 1931-42.

MACFARLANE, P. M., VINIT, S. & MITCHELL, G. S. 2011. Serotonin 2A and 2B receptor-induced phrenic motor facilitation: differential requirement for spinal NADPH oxidase activity. *Neuroscience,* 178**,** 45-55.

MACFARLANE, P. M., VINIT, S. & MITCHELL, G. S. 2014. Spinal nNOS regulates phrenic motor facilitation by a 5-HT2B receptor- and NADPH oxidase-dependent mechanism. *Neuroscience,* 269**,** 67-78.

MACFARLANE, P. M., WILKERSON, J. E., LOVETT-BARR, M. R. & MITCHELL, G. S. 2008. Reactive oxygen species and respiratory plasticity following intermittent hypoxia. *Respir Physiol Neurobiol,* 164**,** 263-71.

MARCUS, N. J., LI, Y. L., BIRD, C. E., SCHULTZ, H. D. & MORGAN, B. J. 2010. Chronic intermittent hypoxia augments chemoreflex control of sympathetic activity: role of the angiotensin II type 1 receptor. *Respir Physiol Neurobiol,* 171**,** 36-45.

MCDONALD, F. B., WILLIAMS, R., SHEEHAN, D. & O'HALLORAN, K. D. 2015. Early life exposure to chronic intermittent hypoxia causes upper airway dilator muscle weakness, which persists into young adulthood. *Exp Physiol,* 100**,** 947-66.

MCGUIRE, M., MACDERMOTT, M. & BRADFORD, A. 2002a. Effects of chronic episodic hypoxia on rat upper airway muscle contractile properties and fiber-type distribution. *Chest,* 122**,** 1012-7.

MCGUIRE, M., MACDERMOTT, M. & BRADFORD, A. 2002b. The effects of chronic episodic hypercapnic hypoxia on rat upper airway muscle contractile properties and fiber-type distribution. *Chest,* 122**,** 1400-6.

MCGUIRE, M., ZHANG, Y., WHITE, D. P. & LING, L. 2003. Chronic intermittent hypoxia enhances ventilatory long-term facilitation in awake rats. *J Appl Physiol (1985),* 95**,** 1499-508.

MCKAY, L. C. & FELDMAN, J. L. 2008. Unilateral ablation of pre-Botzinger complex disrupts breathing during sleep but not wakefulness. *Am J Respir Crit Care Med,* 178**,** 89-95.

MIFFLIN, S., CUNNINGHAM, J. T. & TONEY, G. M. 2015. Neurogenic mechanisms underlying the rapid onset of sympathetic responses to intermittent hypoxia. *J Appl Physiol (1985),* 119**,** 1441-8.

MORAES, D. J., DA SILVA, M. P., BONAGAMBA, L. G., MECAWI, A. S., ZOCCAL, D. B., ANTUNES-RODRIGUES, J., VARANDA, W. A. & MACHADO, B. H. 2013. Electrophysiological properties of rostral ventrolateral medulla presympathetic neurons modulated by the respiratory network in rats. *J Neurosci,* 33**,** 19223-37.

MORAES, D. J. & MACHADO, B. H. 2015. Electrophysiological properties of laryngeal motoneurones in rats submitted to chronic intermittent hypoxia. *J Physiol,* 593**,** 619-34.

MORGAN, B. J., ADRIAN, R., WANG, Z. Y., BATES, M. L. & DOPP, J. M. 2016a. Chronic intermittent hypoxia alters ventilatory and metabolic responses to acute hypoxia in rats. *J Appl Physiol (1985),* 120**,** 1186-95.

MORGAN, B. J., BATES, M. L., RIO, R. D., WANG, Z. & DOPP, J. M. 2016b. Oxidative stress augments chemoreflex sensitivity in rats exposed to chronic intermittent hypoxia. *Respir Physiol Neurobiol,* 234**,** 47-59.

MORGENTHALER, T. I., KAGRAMANOV, V., HANAK, V. & DECKER, P. A. 2006. Complex sleep apnea syndrome: is it a unique clinical syndrome? *Sleep,* 29**,** 1203-9.

MOYA, E. A., GO, A., KIM, C. B., FU, Z., SIMONSON, T. S. & POWELL, F. L. 2020. Neuronal HIF-1α in the nucleus tractus solitarius contributes to ventilatory acclimatization to hypoxia. *J Physiol,* 598**,** 2021-2034.

NAGEL, I. L., LIESKE SP, S. P., THOBY-BRISSON, M., TRYBA, A. K. & RAMIREZ, J. M. 2001. The neural mechanisms involved in the generation of three types of respiratory activities in the transverse slice preparation of mice. *Respiratory research,* 2**,** 2.7-2.7.

NANDURI, J., VADDI, D. R., KHAN, S. A., WANG, N., MAKARENKO, V., SEMENZA, G. L. & PRABHAKAR, N. R. 2015. HIF-1α activation by intermittent hypoxia requires NADPH oxidase stimulation by xanthine oxidase. *PLoS One,* 10**,** e0119762.

NANDURI, J., VADDI, D. R., KHAN, S. A., WANG, N., MAKERENKO, V. & PRABHAKAR, N. R. 2013. Xanthine oxidase mediates hypoxia-inducible factor-2α degradation by intermittent hypoxia. *PLoS One,* 8**,** e75838.

NARKIEWICZ, K., VAN DE BORNE, P. J., MONTANO, N., DYKEN, M. E., PHILLIPS, B. G. & SOMERS, V. K. 1998. Contribution of tonic chemoreflex activation to sympathetic activity and blood pressure in patients with obstructive sleep apnea. *Circulation,* 97**,** 943-5.

NARKIEWICZ, K., VAN DE BORNE, P. J., PESEK, C. A., DYKEN, M. E., MONTANO, N. & SOMERS, V. K. 1999. Selective potentiation of peripheral chemoreflex sensitivity in obstructive sleep apnea. *Circulation,* 99**,** 1183-9.

NATTIE, E. & LI, A. 2012. Central chemoreceptors: locations and functions. *Compr Physiol,* 2**,** 221-54.

NAVARRETE-OPAZO, A. & MITCHELL, G. S. 2014. Therapeutic potential of intermittent hypoxia: a matter of dose. *Am J Physiol Regul Integr Comp Physiol,* 307**,** R1181-97.

O'HALLORAN, K. D. 2016. Chronic intermittent hypoxia creates the perfect storm with calamitous consequences for respiratory control. *Respir Physiol Neurobiol,* 226**,** 63-7.

O'HALLORAN, K. D., MCGUIRE, M., O'HARE, T. & BRADFORD, A. 2002. Chronic intermittent asphyxia impairs rat upper airway muscle responses to acute hypoxia and asphyxia. *Chest,* 122**,** 269-75.

OLEA, E., AGAPITO, M. T., GALLEGO-MARTIN, T., ROCHER, A., GOMEZ-NIÑO, A., OBESO, A., GONZALEZ, C. & YUBERO, S. 2014. Intermittent hypoxia and diet-induced obesity: effects on oxidative

status, sympathetic tone, plasma glucose and insulin levels, and arterial pressure. *J Appl Physiol (1985),* 117**,** 706-19.

PAE, E. K., WU, J., NGUYEN, D., MONTI, R. & HARPER, R. M. 2005. Geniohyoid muscle properties and myosin heavy chain composition are altered after short-term intermittent hypoxic exposure. *J Appl Physiol (1985),* 98**,** 889-94.

PAWAR, A., NANDURI, J., YUAN, G., KHAN, S. A., WANG, N., KUMAR, G. K. & PRABHAKAR, N. R. 2009. Reactive oxygen species-dependent endothelin signaling is required for augmented hypoxic sensory response of the neonatal carotid body by intermittent hypoxia. *Am J Physiol Regul Integr Comp Physiol,* 296**,** R735-42.

PENG, Y., KLINE, D. D., DICK, T. E. & PRABHAKAR, N. R. 2001. Chronic intermittent hypoxia enhances carotid body chemoreceptor response to low oxygen. *Adv Exp Med Biol,* 499**,** 33-8.

PENG, Y. J., NANDURI, J., RAGHURAMAN, G., WANG, N., KUMAR, G. K. & PRABHAKAR, N. R. 2013. Role of oxidative stress-induced endothelin-converting enzyme activity in the alteration of carotid body function by chronic intermittent hypoxia. *Exp Physiol,* 98**,** 1620-30.

PENG, Y. J., NANDURI, J., YUAN, G., WANG, N., DENERIS, E., PENDYALA, S., NATARAJAN, V., KUMAR, G. K. & PRABHAKAR, N. R. 2009. NADPH oxidase is required for the sensory plasticity of the carotid body by chronic intermittent hypoxia. *J Neurosci,* 29**,** 4903-10.

PENG, Y. J., OVERHOLT, J. L., KLINE, D., KUMAR, G. K. & PRABHAKAR, N. R. 2003. Induction of sensory long-term facilitation in the carotid body by intermittent hypoxia: implications for recurrent apneas. *Proc Natl Acad Sci U S A,* 100**,** 10073-8.

PENG, Y. J., RAGHURAMAN, G., KHAN, S. A., KUMAR, G. K. & PRABHAKAR, N. R. 2011. Angiotensin II evokes sensory long-term facilitation of the carotid body via NADPH oxidase. *J Appl Physiol (1985),* 111**,** 964-70.

PENG, Y. J., YUAN, G., JACONO, F. J., KUMAR, G. K. & PRABHAKAR, N. R. 2006a. 5-HT evokes sensory long-term facilitation of rodent carotid body via activation of NADPH oxidase. *J Physiol,* 576**,** 289-95.

PENG, Y. J., YUAN, G., RAMAKRISHNAN, D., SHARMA, S. D., BOSCH-MARCE, M., KUMAR, G. K., SEMENZA, G. L. & PRABHAKAR, N. R. 2006b. Heterozygous HIF-1alpha deficiency impairs carotid body-mediated systemic responses and reactive oxygen species generation in mice exposed to intermittent hypoxia. *J Physiol,* 577**,** 705-16.

PERIM, R. R., FIELDS, D. P. & MITCHELL, G. S. 2018. Cross-talk inhibition between 5-HT(2B) and 5-HT(7) receptors in phrenic motor facilitation via NADPH oxidase and PKA. *Am J Physiol Regul Integr Comp Physiol,* 314**,** R709-r715.

PIALOUX, V., HANLY, P. J., FOSTER, G. E., BRUGNIAUX, J. V., BEAUDIN, A. E., HARTMANN, S. E., PUN, M., DUGGAN, C. T. & POULIN, M. J. 2009. Effects of exposure to intermittent hypoxia on oxidative stress and acute hypoxic ventilatory response in humans. *Am J Respir Crit Care Med,* 180**,** 1002-9.

PRABHAKAR, N. R., PENG, Y. J., KUMAR, G. K. & NANDURI, J. 2015. Peripheral chemoreception and arterial pressure responses to intermittent hypoxia. *Compr Physiol,* 5**,** 561-77.

RAMIREZ, J. M. 2014. The integrative role of the sigh in psychology, physiology, pathology, and neurobiology. *Prog Brain Res,* 209**,** 91-129.

RAY, A. D., MAGALANG, U. J., MICHLIN, C. P., OGASA, T., KRASNEY, J. A., GOSSELIN, L. E. & FARKAS, G. A. 2007. Intermittent hypoxia reduces upper airway stability in lean but not obese Zucker rats. *Am J Physiol Regul Integr Comp Physiol,* 293**,** R372-8.

REEVES, S. R. & GOZAL, D. 2004. Platelet-activating factor receptor modulates respiratory adaptation to long-term intermittent hypoxia in mice. *Am J Physiol Regul Integr Comp Physiol,* 287**,** R369-74.

REEVES, S. R. & GOZAL, D. 2006. Changes in ventilatory adaptations associated with long-term intermittent hypoxia across the age spectrum in the rat. *Respir Physiol Neurobiol,* 150**,** 135-43.

REEVES, S. R., GOZAL, E., GUO, S. Z., SACHLEBEN, L. R., JR., BRITTIAN, K. R., LIPTON, A. J. & GOZAL, D. 2003. Effect of long-term intermittent and sustained hypoxia on hypoxic ventilatory and metabolic responses in the adult rat. *J Appl Physiol (1985),* 95**,** 1767-74.

REEVES, S. R., MITCHELL, G. S. & GOZAL, D. 2006. Early postnatal chronic intermittent hypoxia modifies hypoxic respiratory responses and long-term phrenic facilitation in adult rats. *Am J Physiol Regul Integr Comp Physiol,* 290**,** R1664-71.

REY, S., DEL RIO, R., ALCAYAGA, J. & ITURRIAGA, R. 2004. Chronic intermittent hypoxia enhances cat chemosensory and ventilatory responses to hypoxia. *J Physiol,* 560**,** 577-86.

RICHERSON, G. B. 2004. Serotonergic neurons as carbon dioxide sensors that maintain pH homeostasis. *Nat Rev Neurosci,* 5**,** 449-61.

RICHERSON, G. B., WANG, W., HODGES, M. R., DOHLE, C. I. & DIEZ-SAMPEDRO, A. 2005. Homing in on the specific phenotype(s) of central respiratory chemoreceptors. *Exp Physiol,* 90**,** 259-66; discussion 266-9.

RICHERSON, G. B., WANG, W., TIWARI, J. & BRADLEY, S. R. 2001. Chemosensitivity of serotonergic neurons in the rostral ventral medulla. *Respir Physiol,* 129**,** 175-89.

ROY, A., ROZANOV, C., MOKASHI, A., DAUDU, P., AL-MEHDI, A. B., SHAMS, H. & LAHIRI, S. 2000. Mice lacking in gp91 phox subunit of NAD(P)H oxidase showed glomus cell [Ca(2+)](i) and respiratory responses to hypoxia. *Brain Res,* 872**,** 188-93.

SACRAMENTO, J. F., GONZALEZ, C., GONZALEZ-MARTIN, M. C. & CONDE, S. V. 2015. Adenosine Receptor Blockade by Caffeine Inhibits Carotid Sinus Nerve Chemosensory Activity in Chronic Intermittent Hypoxic Animals. *Adv Exp Med Biol,* 860**,** 133-7.

SALLOUM, A., ROWLEY, J. A., MATEIKA, J. H., CHOWDHURI, S., OMRAN, Q. & BADR, M. S. 2010. Increased propensity for central apnea in patients with obstructive sleep apnea: effect of nasal continuous positive airway pressure. *Am J Respir Crit Care Med,* 181**,** 189-93.

SANDERS, K. A., SUNDAR, K. M., HE, L., DINGER, B., FIDONE, S. & HOIDAL, J. R. 2002. Role of components of the phagocytic NADPH oxidase in oxygen sensing. *J Appl Physiol (1985),* 93**,** 1357-64.

SEMENZA, G. L. & PRABHAKAR, N. R. 2015. Neural regulation of hypoxia-inducible factors and redox state drives the pathogenesis of hypertension in a rodent model of sleep apnea. *J Appl Physiol (1985),* 119**,** 1152-6.

SEVERSON, C. A., WANG, W., PIERIBONE, V. A., DOHLE, C. I. & RICHERSON, G. B. 2003. Midbrain serotonergic neurons are central pH chemoreceptors. *Nat Neurosci,* 6**,** 1139-40.

SKELLY, J. R., EDGE, D., SHORTT, C. M., JONES, J. F., BRADFORD, A. & O'HALLORAN, K. D. 2012. Tempol ameliorates pharyngeal dilator muscle dysfunction in a rodent model of chronic intermittent hypoxia. *Am J Respir Cell Mol Biol,* 46**,** 139-48.

SOMERS, V. K., DYKEN, M. E., CLARY, M. P. & ABBOUD, F. M. 1995. Sympathetic neural mechanisms in obstructive sleep apnea. *J Clin Invest,* 96**,** 1897-904.

SOUZA, G. M., BONAGAMBA, L. G., AMORIM, M. R., MORAES, D. J. & MACHADO, B. H. 2015. Cardiovascular and respiratory responses to chronic intermittent hypoxia in adult female rats. *Exp Physiol,* 100**,** 249-58.

STEINBUSCH, H. W. 1981. Distribution of serotonin-immunoreactivity in the central nervous system of the rat-cell bodies and terminals. *Neuroscience,* 6**,** 557-618.

VEASEY, S. C., ZHAN, G., FENIK, P. & PRATICO, D. 2004. Long-term intermittent hypoxia: reduced excitatory hypoglossal nerve output. *Am J Respir Crit Care Med,* 170**,** 665-72.

VOSS, M. D., DE CASTRO, D., LIPSKI, J., PILOWSKY, P. M. & JIANG, C. 1990. Serotonin immunoreactive boutons form close appositions with respiratory neurons of the dorsal respiratory group in the cat. *J Comp Neurol,* 295**,** 208-18.

WANG, W. J., LU, G., DING, N., HUANG, H. P., DING, W. X. & ZHANG, X. L. 2013. Adiponectin alleviates contractile dysfunction of genioglossus in rats exposed to chronic intermittent hypoxia. *Chin Med J (Engl),* 126**,** 3259-63.

WHITE, D. P. & YOUNES, M. K. 2012. Obstructive sleep apnea. *Compr Physiol,* 2**,** 2541-94.

WIND, S., BEUERLEIN, K., EUCKER, T., MÜLLER, H., SCHEURER, P., ARMITAGE, M. E., HO, H., SCHMIDT, H. H. & WINGLER, K. 2010. Comparative pharmacology of chemically distinct NADPH oxidase inhibitors. *Br J Pharmacol,* 161**,** 885-98.

WUYTS, R., VLEMINCX, E., BOGAERTS, K., VAN DIEST, I. & VAN DEN BERGH, O. 2011. Sigh rate and respiratory variability during normal breathing and the role of negative affectivity. *Int J Psychophysiol,* 82**,** 175-9.

YUAN, G., KHAN, S. A., LUO, W., NANDURI, J., SEMENZA, G. L. & PRABHAKAR, N. R. 2011. Hypoxia-inducible factor 1 mediates increased expression of NADPH oxidase-2 in response to intermittent hypoxia. *J Cell Physiol,* 226**,** 2925-33.

ZANELLA, S., DOI, A., GARCIA, A. J., 3RD, ELSEN, F., KIRSCH, S., WEI, A. D. & RAMIREZ, J. M. 2014. When norepinephrine becomes a driver of breathing irregularities: how intermittent hypoxia fundamentally alters the modulatory response of the respiratory network. *J Neurosci,* 34**,** 36-50.

ZHOU, J. & LIU, Y. 2013. Effects of genistein and estrogen on the genioglossus in rats exposed to chronic intermittent hypoxia may be HIF-1α dependent. *Oral Dis,* 19**,** 702-11.

ZOCCAL, D. B., FURUYA, W. I., BASSI, M., COLOMBARI, D. S. & COLOMBARI, E. 2014. The nucleus of the solitary tract and the coordination of respiratory and sympathetic activities. *Front Physiol,* 5**,** 238.

Chapter 4. NADPH oxidase-2 is necessary for chronic intermittent hypoxia-induced sternohyoid muscle weakness.

4.1 Aims and hypothesis

Study aims:

To examine the effect of a 2-week exposure to CIH on the function of the sternohyoid (a representative upper airway dilator muscle) in adult male mice.

To characterise the effect of exposure to CIH on NOX enzymes in sternohyoid muscle at multiple levels of regulation: mRNA, protein and activity.

To examine the effect of exposure to CIH on indices of oxidative stress and antioxidant capacity in sternohyoid muscle.

To examine the effect of exposure to CIH on the mRNA expression of redox-sensitive genes pivotal in the regulation of skeletal muscle form and function.

To assess the contribution of NOX2 to CIH-induced alterations to upper airway muscle function using pharmacological and transgenic approaches.

Study hypothesis:

We hypothesised that 2 weeks of exposure to CIH would result in sternohyoid muscle mal-adaptation, which would manifest as muscle weakness, increased expression and/or activity of NOX enzymes, altered redox balance and a ROS-dependent alteration to the expression of genes important in skeletal muscle contractile performance.

Furthermore, we postulated that these alterations would be underpinned by a NOX2 derived ROS-dependent mechanism, amenable to blockade by supplementation with apocynin (putative NOX2 inhibitor) and NOX2 knock-out.

4.2 Materials and methods

Sternohyoid muscle function was examined *ex vivo*, as described in section 2.5.

The mRNA expression of NOX subunits and genes relating to the regulation of skeletal muscle form were assessed by qRT-PCR, as described in section 2.6.

The protein expression of NOX subunits was determined by Western blot, as described in section 2.7.

Spectrophotometric assays were used to measure levels of lipid peroxidation (TBARS), citrate synthase and NOX activity, as described in section 2.8.

Cell signalling assays were used to examine HIF-1α and proteins involved in the regulation of skeletal muscle mass, as described in section 2.9.

4.3. Results

4.3.1 Sternohyoid muscle contractile function ex vivo

Sternohyoid twitch kinetics (P_t, CT and ½ RT) and isotonic contractile parameters (Pmax, Wmax, Smax and Vmax) are shown in Table 4.1. Sternohyoid twitch force (P_t) was significantly depressed following 2 weeks of exposure to CIH compared to sham mice (*P* = 0.0067; Table 4.1); administration of apocynin (2mM) in the drinking water throughout the exposure to CIH completely prevented this decrease in twitch force (*P* = 0.0004; Table 4.1). Exposure to CIH had no effect on P_t in NOX2 KO mice compared to NOX2 KO sham mice (*P* = 0.3063; Table 4.1). NOX2 KO significantly increased P_t compared to wild-type sham mice (*P* = 0.0004; Table 4.1). Twitch contraction time (CT) and half-relaxation time (½ RT) were unaffected by exposure to CIH in both wild-type (sham *vs.* CIH; CT, *P* = 0.7466; ½ RT, *P* = 0.2463; Table 4.1) and NOX2 KO mice (NOX2 KO sham *vs.* NOX2 KO CIH; CT, *P* = 0.2891; ½ RT, P = 0.1371; Table 4.1). Similarly, the administration of apocynin during the exposure to CIH (CIH *vs.* CIH + APO; CT, *P* = 0.2891; ½ RT, *P* = 0.1371; Table 4.1) or NOX2 KO (sham *vs.* NOX2 KO sham; CT, *P* = 0.0723; ½ RT, *P* = 0.0772; Table 4.1) had no effect on these parameters.

	Sham (n = 8)	CIH (n = 8)	CIH + APO (n = 9)	NOX2 KO Sham (n = 8)	NOX2 KO CIH (n = 10)	Sham *vs* CIH (P value)	CIH *vs* CIH + APO (P value)	NOX2 KO Sham *vs* NOX2 KO CIH (P value)	Sham *vs* NOX2 KO Sham (P value)
P_t (N/cm^2)	1.61 ± 0.39	1.12 ± 0.26*	1.67 ± 0.26$^{\#}$	2.53 ± 0.46$^{£}$	2.81 ± 0.62	**0.0067***	**0.0004$^{\#}$**	0.3063	**0.0004$^{£}$**
CT (ms)	9.83 ± 1.03	10.17 ± 2.83	10.56 ± 1.72	10.94 ± 1.32	11.50 ± 0.85	0.7466	0.7292	0.2891	0.0723
½ RT (ms)	1.47 ± 0.22	1.43 ± 0.10	1.56 ± 0.10	1.52 ± 0.21	1.60 ± 0.24	0.2463	0.3058	0.1371	0.0772
Wmax (J/cm^2)	0.44 ± 0.17	0.25 ± 0.06	0.64 ± 0.24$^{\#}$	0.93 ± 0.33$^{£}$	1.03 ± 0.38	0.0157	**0.0009$^{\#}$**	0.5877	**0.0024$^{£}$**
Pmax (W/cm^2)	6.56 ± 2.61	4.36 ± 0.98	7.64 ± 2.28$^{\#}$	11.98 ± 3.01$^{£}$	14.07 ± 5.01	0.0527	**0.0023$^{\#}$**	0.3149	**0.0018$^{£}$**
Smax (L/L_o)	0.28 ± 0.12	0.23 ± 0.10	0.27 ± 0.05	0.25 ± 0.05	0.30 ± 0.06	0.3760	0.3468	0.0897	0.5789
Vmax (L_0/s)	4.07 ± 1.71	3.64 ± 1.59	4.01 ± 0.97	4.49 ± 0.70	5.35 ± 1.02	0.3823	0.3704	0.0598	0.5367

Table 4.1 *Ex vivo* sternohyoid muscle contractile parameters. *Definition of abbreviations*: P_t, isometric twitch force; CT, contraction time; 1⁄2 RT, half-relaxation time; Wmax, maximum mechanical work; Pmax, maximum mechanical power; Smax, maximum shortening; Vmax, maximum shortening velocity; L_o, optimum length. Values are expressed as mean ± SD. Data sets which were normally distributed and of equal variance were statistically compared using unpaired two-tailed Student's *t* test. Welch's correction was applied in the case of unequal variance. Data which were not normally distributed were compared using Mann Whitney non-parametric tests. Bolded numbers highlight statistical significance ($P < 0.0125$). Relevant comparisons are denoted as follows: * CIH significantly different from corresponding sham values; $^{\#}$ APO + CIH significantly different from corresponding CIH values; $^{£}$ NOX2 KO sham significantly different from corresponding sham values.

Figure 4.1 shows representative original traces for sham (grey), CIH (black), CIH + APO (blue), NOX2 KO sham (pink) and NOX2 KO CIH (red) tetanic contractions (A). 2 weeks of exposure to CIH significantly decreased the force-generating capacity of the sternohyoid compared to sham mice ($P < 0.0001$; Fig 4.1; B). Exposure to CIH resulted in a ~45% decrease in peak specific force of the sternohyoid compared to sham mice. Apocynin administration throughout the exposure to CIH successfully ameliorated CIH-induced muscle weakness ($P < 0.0001$; Fig 4.1; B). Moreover, there was no difference in the peak tetanic force produced by NOX2 KO mice exposed to CIH compared to NOX2 KO sham controls ($P = 0.1147$; Fig 4.1; B), revealing a specific role for NOX2 in CIH-induced sternohyoid muscle weakness. Tetanic force was increased by ~31% in NOX2 KO sham mice compared to wild-type sham mice, but this increase did not reach the threshold for statistical significance when correction for multiple comparisons was applied ($P = 0.0419$; Fig 4.1; B).

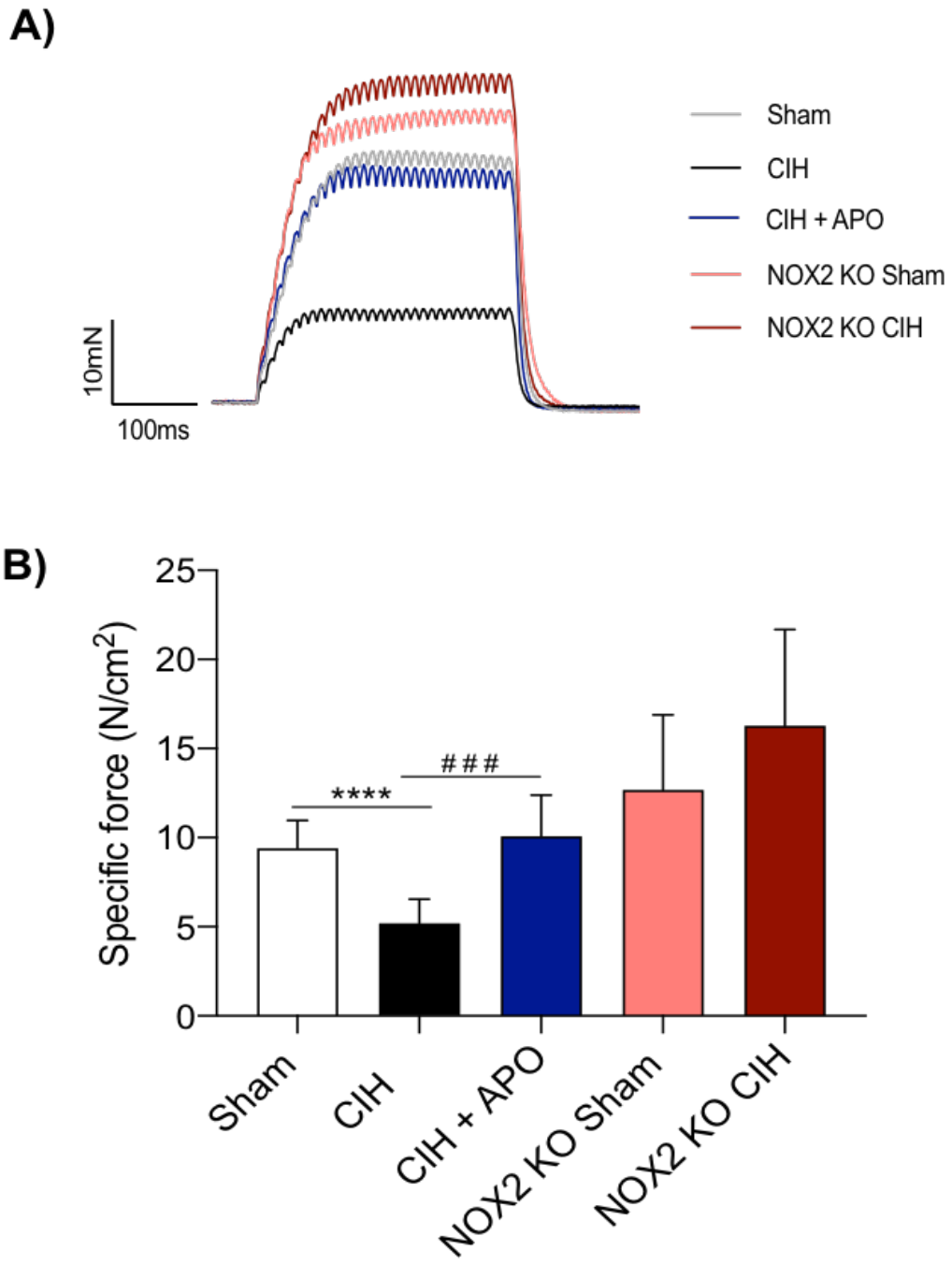

Figure 4.1 *Ex vivo* sternohyoid muscle peak tetanic force. A) Original traces of *ex vivo* sternohyoid muscle tetanic contractions for sham (grey), CIH (black), CIH + APO (blue), NOX2 KO Sham (pink) and NOX2 KO CIH (red) preparations. **B)** Group data for sternohyoid muscle tetanic force, normalised for muscle CSA, in sham (n = 8), CIH (n = 8), CIH + APO (n = 9), NOX2 KO sham (n = 8) and NOX2 KO CIH (n = 10) mice. Tetanic force was measured following stimulation at 100 Hz *ex vivo*. Values are expressed as mean ± SD. Data sets which were normally distributed and of equal variance were statistically compared using unpaired two-tailed Student's *t* test. Statistical significance was taken at P < 0.0125. Relevant comparisons are denoted as follows: * CIH *vs.* sham, **** $P < 0.0001$; $^{\#}$ APO + CIH *vs.* CIH, $^{\#\#\#}$ $P < 0.001$.

Figure 4.2 shows original traces of *ex vivo* sternohyoid muscle maximum unloaded shortening for sham (grey), CIH (black), CIH + APO (blue), NOX2 KO sham (pink) and NOX2 KO CIH (red) preparations (A). Figure 4.2; B, C and D show the sternohyoid power-load relationship. This is the power generated by the sternohyoid over a range of incremental loads on the muscle between 0-100% of the peak force-generating capacity (Fmax), determined at the beginning of the protocol. Exposure to CIH significantly decreased the power-generating capacity of the sternohyoid muscle over a range of loads compared to sham mice ($P < 0.0001$; repeated measures two-way ANOVA; Fig 4.2; B). *Post-hoc* analysis revealed a statistically significant decrease in the power-generating capacity of the sternohyoid following exposure to CIH at 30% (*$P < 0.05$) and 40% (**$P < 0.01$) of its peak force-generating capacity when compared to sham mice (Fig 4.2; B). The administration of apocynin throughout the exposure to CIH prevented the CIH-induced decrease in the power-generating capacity of the sternohyoid over a range of loads compared to mice exposed to CIH alone ($P < 0.0001$; Fig 4.2; B). *Post-hoc* analysis revealed a statistically significant increase in the power-generating capacity of the sternohyoid following treatment with apocynin throughout exposure to CIH at 20% - 80% of the peak force-generating capacity compared to CIH-exposed mice (Fig 4.2; B). Peak power (Pmax) was measured and typically occurred between 30 and 40% load. Exposure to CIH reduced Pmax compared to sham mice, although this did not reach the threshold for statistical significance ($P = 0.0527$; Table 4.1); Apocynin treatment throughout exposure to CIH significantly prevented this decrease ($P = 0.0023$; Table 4.1). Exposure to CIH had no effect on the power-generating capacity of the sternohyoid in NOX2 KO mice over the range of loads examined when compared to NOX2 KO sham controls ($P = 0.0575$; Fig 4.2; C). Similarly, Pmax was unaffected by exposure to CIH in NOX2 KO mice ($P = 0.3149$; Table 4.1). Genetic knock-out of NOX2 significantly increased the power-generating capacity of the sternohyoid over the range of loads examined compared to wild-type sham mice ($P < 0.0001$; Fig 4.2; D). *Post-hoc* analysis revealed a statistically significant increase in the power generated by the sternohyoid from NOX2 KO sham mice at 20%-80% load compared to wild-type sham mice (Fig 4.2; D). Pmax was also significantly increased in NOX2 KO sham mice compared to wild-type sham mice ($P = 0.0018$; Table 4.1).

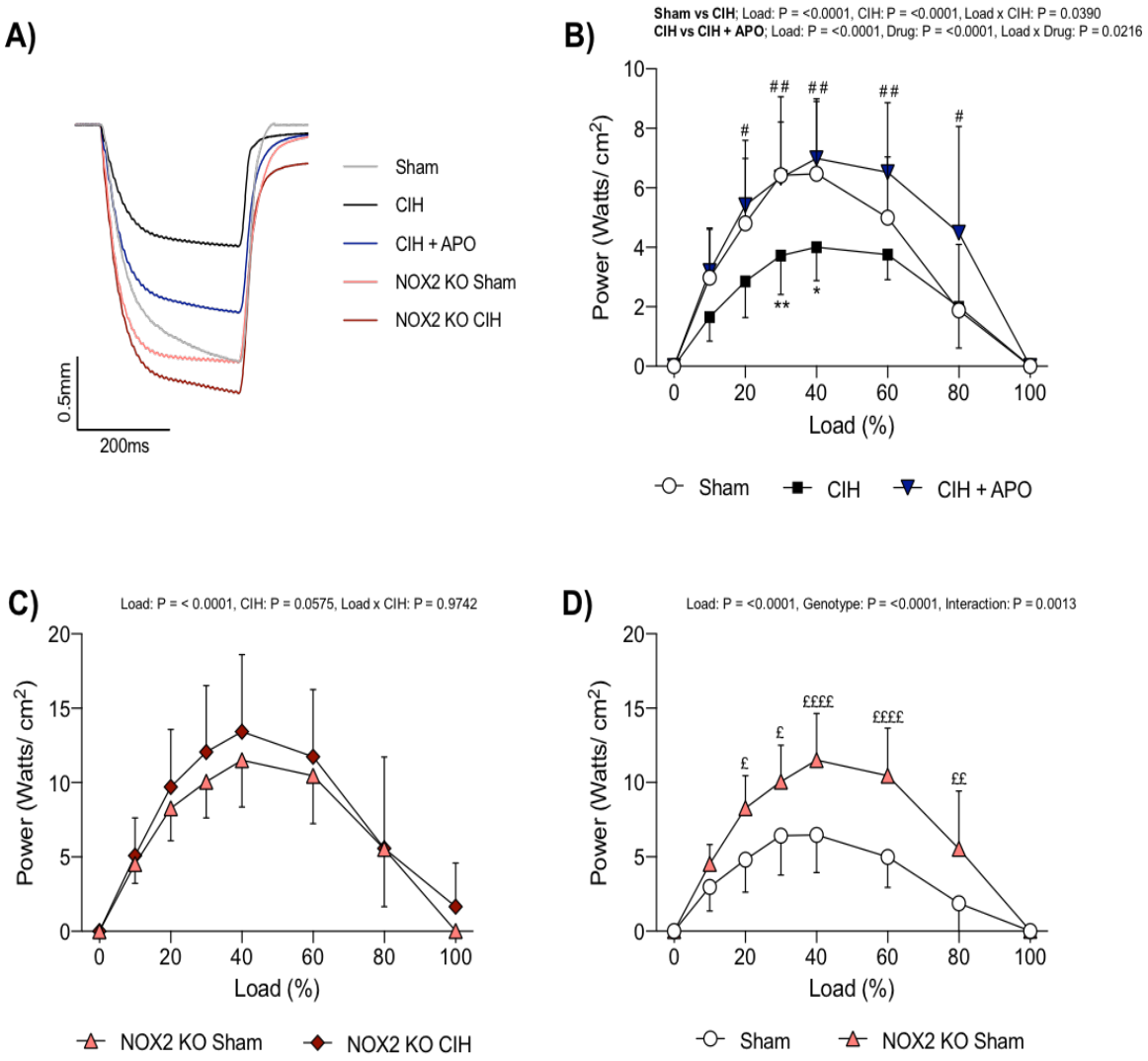

Figure 4.2: Sternohyoid muscle power–load relationship. A, original traces of *ex vivo* sternohyoid muscle maximum unloaded shortening for Sham (grey), CIH (black), CIH + APO (blue), NOX2 KO Sham (pink) and NOX2 KO CIH (red) preparations. B, C, D, group data for sternohyoid power shown as power per unit CSA (Watts/cm^2) as a function of the load on the muscle expressed as a percentage of peak tetanic force for Sham (n = 8), CIH (n = 8), CIH + APO (n = 9), NOX2 KO Sham (n = 8) and NOX2 KO CIH (n = 10) mice. Data are shown as mean ± SD and were statistically compared by repeated measures two-way ANOVA with Bonferroni's *post hoc* test. Relevant comparisons are denoted as follows: *denotes sham *vs*. CIH, *$P < 0.05$, **$P < 0.01$; $^{\#}$denotes CIH *vs*. CIH + APO, $^{\#}P < 0.05$, $^{\#\#}P < 0.01$; $^{£}$ denotes Sham *vs.* NOX2 KO Sham, $^{£}P < 0.05$, $^{££}P < 0.01$, $^{££££}P < 0.0001$.

Figure 4.3 shows original traces of *ex vivo* sternohyoid muscle maximum unloaded shortening for sham (grey), CIH (black), CIH + APO (blue), NOX2 KO sham (pink) and NOX2 KO CIH (red) preparations (A). Figure 4.3; B, C and D show the sternohyoid work-load relationship. This is the work produced by the sternohyoid over a range of incremental loads on the muscle between 0-100% of the peak force-generating capacity (Fmax), determined at the beginning of the protocol. Exposure to CIH significantly decreased the work produced by the sternohyoid muscle over a range of loads compared to sham mice ($P < 0.0001$; repeated measures two-way ANOVA; Fig 4.3; B). *Post-hoc* analysis revealed a statistically significant decrease in the power-generating capacity of the sternohyoid following exposure to CIH at 20% ($*P < 0.05$), 30% ($***P < 0.001$) and 40% ($**P < 0.01$) of the peak force-generating capacity compared to sham mice (Fig 4.3; B). The administration of apocynin throughout the exposure to CIH prevented the CIH-induced decrease in the work produced by the sternohyoid over a range of loads compared to mice exposed to CIH alone ($P < 0.0001$; Fig 4.3; B). *Post-hoc* analysis revealed a statistically significant increase in work produced by the sternohyoid following treatment with apocynin throughout CIH exposure at 20% ($^{\#} P < 0.05$), 30% ($^{\#} P < 0.05$), and 40% ($^{\#} P < 0.05$) of the peak force-generating capacity compared to CIH-exposed mice (Fig 4.3; B). Peak work (Wmax) was measured and typically occurred between 30% and 40% load. Wmax was reduced following 2 weeks of exposure to CIH compared to sham mice, but this did not meet the threshold for statistical significance ($P = 0.0157$; Table 4.1); apocynin administration completely prevented the CIH-induced decrease in Wmax ($P = 0.0009$; Table 4.3). Exposure to CIH had no effect on the work produced by the sternohyoid in NOX2 KO mice over the range of loads examined compared to NOX2 KO sham controls ($P = 0.2417$; Fig 4.3; C). Similarly, Wmax was unaffected by exposure to CIH in NOX2 KO mice ($P = 0.5877$; Table 4.1). Genetic knock-out of NOX2 significantly increased the work produced by the sternohyoid over the range of loads examined compared to wild-type sham mice ($P < 0.0001$; Fig 4.3 D). *Post-hoc* analysis revealed a statistically significant increase in the work generated by the sternohyoid from NOX2 KO sham mice at 30%-80% load compared to wild-type sham mice (Fig 4.3; D). Wmax was also significantly increased in mice lacking the NOX2 enzyme compared with wild-type controls ($P = 0.0024$; Table 4.1).

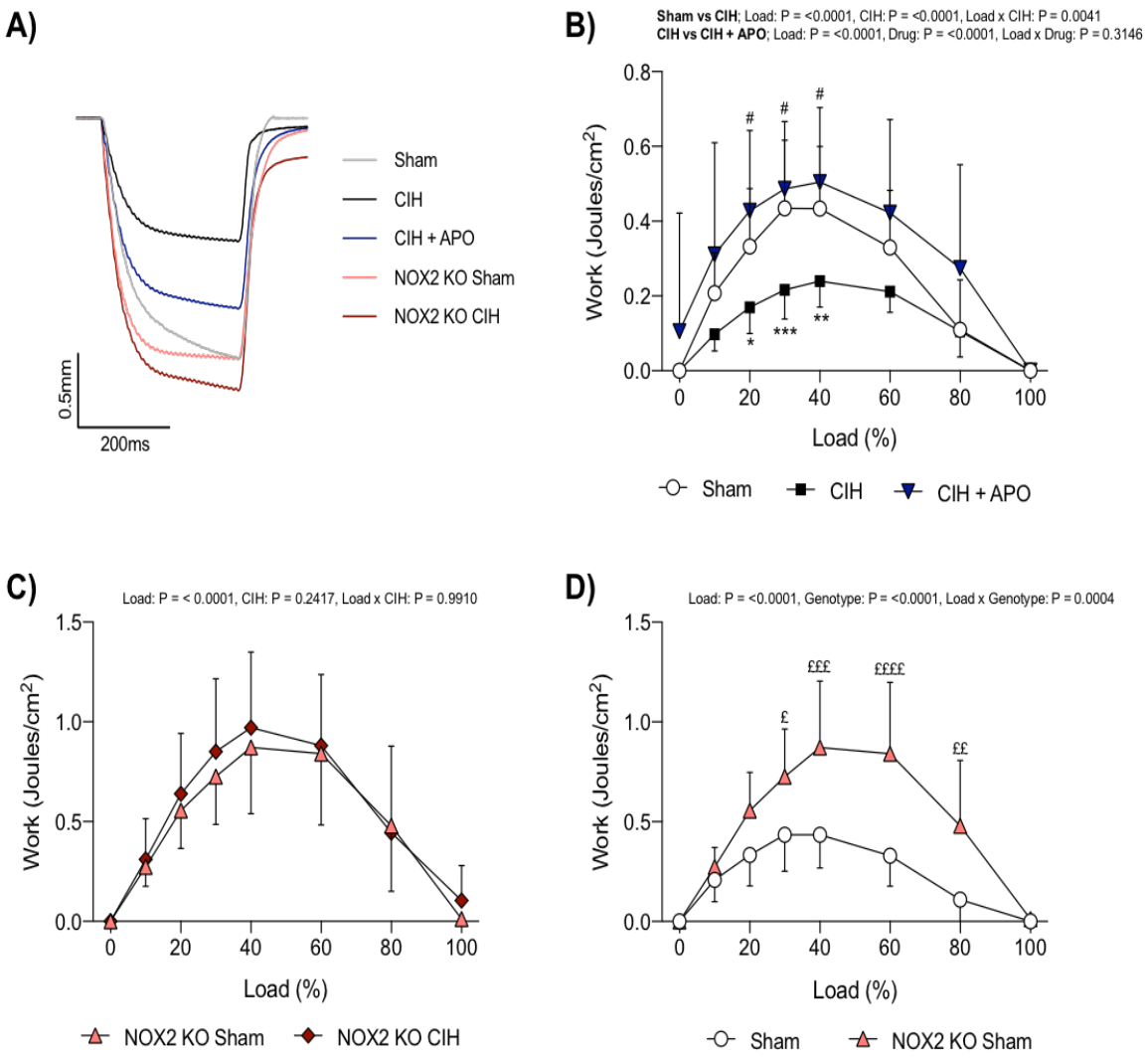

Figure 4.3 Sternohyoid muscle work–load relationship. A, original traces of *ex vivo* sternohyoid muscle maximum unloaded shortening for sham (grey), CIH (black), CIH + APO (blue), NOX2 KO sham (pink) and NOX2 KO CIH (red) preparations. B, C, D, group data for sternohyoid work (mean ± SD) shown as work per unit CSA (Joules/cm^2) as a function of the load on the muscle expressed as a percentage of peak tetanic force for sham (n = 8), CIH (n = 8), CIH + APO (n = 9), NOX2 KO sham (n = 8) and NOX2 KO CIH (n = 10) mice. Data were statistically compared by repeated measures two-way ANOVA with Bonferroni's *post hoc* test. Relevant comparisons are denoted as follows: *denotes sham *vs*. CIH, *$P < 0.05$, **$P < 0.01$, ***$P < 0.001$; $^{\#}$denotes CIH *vs*. CIH + APO, $^{\#}P < 0.05$; $^{£}$denotes sham *vs.* NOX2 KO sham, $^{£}P < 0.05$, $^{££}P < 0.01$, $^{£££}P < 0.001$, $^{££££}P < 0.0001$.

Figure 4.4 shows original traces of *ex vivo* sternohyoid muscle maximum unloaded shortening for sham (grey), CIH (black), CIH + APO (blue), NOX2 KO sham (pink) and NOX2 KO CIH (red) preparations (A). Figure 4.4; B, C and D show the sternohyoid shortening-load relationship. This is the distance of shortening of the sternohyoid over a range of incremental loads on the muscle between 0-100% of the peak force-generating capacity (Fmax), determined at the beginning of the protocol. 2 weeks of exposure to CIH had no effect on the distance of shortening of the sternohyoid muscle when compared to sham mice (P = 0.1429; repeated measures two-way ANOVA; Fig 4.4; B); apocynin treatment throughout the exposure to CIH significantly increased the distance of shortening of the sternohyoid over a range of loads examined compared with exposure to CIH alone (P = 0.0106; Fig 4.4; B). Peak shortening (Smax) was measured and occurred at 0% load, as expected. Smax was unaffected by exposure to CIH (P = 0.3760; Table 4.1) or apocynin treatment (P = 0.3468; Table 4.1) in wild-type mice. NOX2 KO mice exposed to CIH had a significantly increased distance of shortening over the range of loads examined compared to NOX2 KO sham controls (P = 0.0116; Fig 4.4; C). *Post hoc* analysis revealed that NOX2 KO CIH-exposed mice had a significantly increased distance of shortening at 0% of the peak force-generating capacity compared to NOX2 KO sham mice ($^{\$\$}P < 0.01$; Fig 4.4; C). Smax was unchanged following exposure to CIH in NOX2 KO mice (P = 0.0897; Table 4.1). Genetic knock-out of NOX2 had no effect on the distance of shortening of the sternohyoid over the range of loads examined compared to wild-type sham mice (P = 0.3413; Fig 4.4; D). Similarly, Smax was not different in NOX2 KO mice compared with wild-type controls (P = 0.5789; Table 4.1).

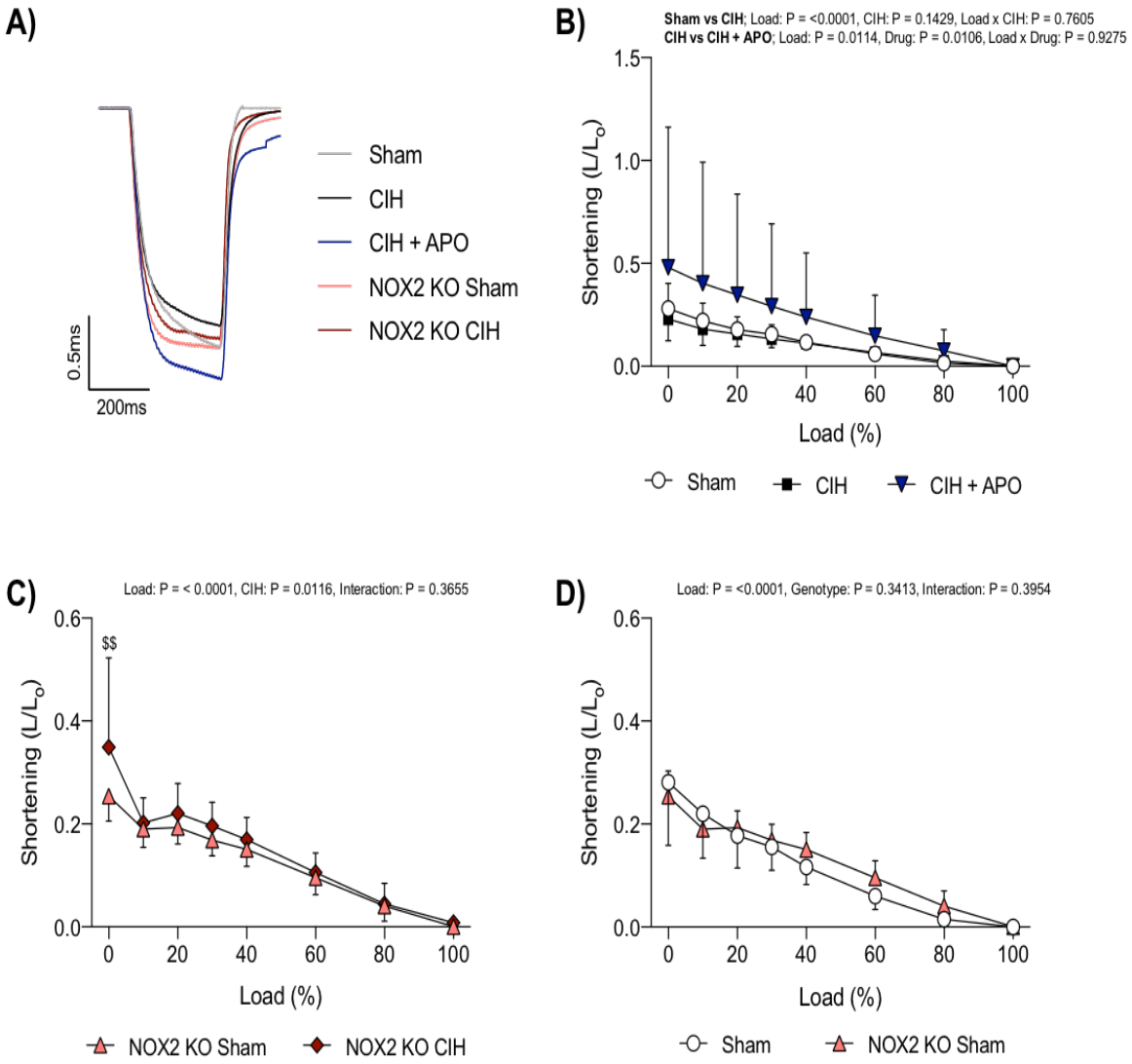

Figure 4.4 Sternohyoid muscle shortening–load relationship. A, original traces of *ex vivo* sternohyoid muscle maximum unloaded shortening for Sham (grey), CIH (black), CIH + APO (blue), NOX2 KO Sham (pink) and NOX2 KO CIH (red) preparations. B, C, D, group data for sternohyoid shortening (mean ± SD) shown as length per unit optimal length (L/L_o) as a function of the load on the muscle expressed as a percentage of peak tetanic force for Sham (n = 8), CIH (n = 8), CIH + APO (n = 9), NOX2 KO Sham (n = 8) and NOX2 KO CIH (n = 10) mice. Data were statistically compared by repeated measures two-way ANOVA with Bonferroni's *post hoc* test. Relevant comparisons are denoted as follows: $^{\$}$ denotes NOX2 KO sham *vs.* NOX2 KO CIH, $^{\$\$}$ $P < 0.01$.

Figure 4.5 shows original traces of *ex vivo* sternohyoid muscle maximum unloaded shortening velocity for sham (grey), CIH (black), CIH + APO (blue), NOX2 KO sham (pink) and NOX2 KO CIH (red) preparations (A). Figure 4.5; B, C and D show the sternohyoid shortening velocity-load relationship. This is the shortening velocity of the sternohyoid over a range of incremental loads on the muscle between 0-100% of the peak force-generating capacity (Fmax), determined at the beginning of the protocol. 2 weeks of exposure to CIH had no effect on the shortening velocity of the sternohyoid muscle compared to sham mice (P = 0.9398; repeated measures two-way ANOVA; Fig 4.5; B); apocynin treatment throughout the exposure to CIH also had no effect on the shortening velocity of the sternohyoid over a range of loads examined compared with exposure to CIH alone (P = 0.9289; Fig 4.5; B). The peak shortening velocity (Vmax) was measured and occurred at 0% load, as expected. Vmax was unaffected by exposure to CIH (P = 0.3823; Table 4.1) or treatment with apocynin (P = 0.3704; Table 4.1) in wild-type mice. NOX2 KO mice exposed to CIH had a significantly increased shortening velocity over the range of loads examined compared to NOX2 KO sham controls (P = 0.0005; Fig 4.5; C). *Post hoc* analysis revealed that NOX2 KO CIH mice had a significantly increased velocity of shortening at 0% of the peak force-generating capacity when compared to NOX2 KO sham mice ($^{\$}$ P < 0.05; Fig 4.5; C). Vmax was unaffected by exposure to CIH in NOX2 KO mice (P = 0.0598; Table 4.1). Genetic knock-out of NOX2 had no effect on the shortening velocity of the sternohyoid over the range of loads examined compared to wild-type sham mice (P = 0.0921; Fig 4.5; D). Similarly, Vmax was not different between NOX2 KO sham and sham mice (P = 0.5367: Table 4.1).

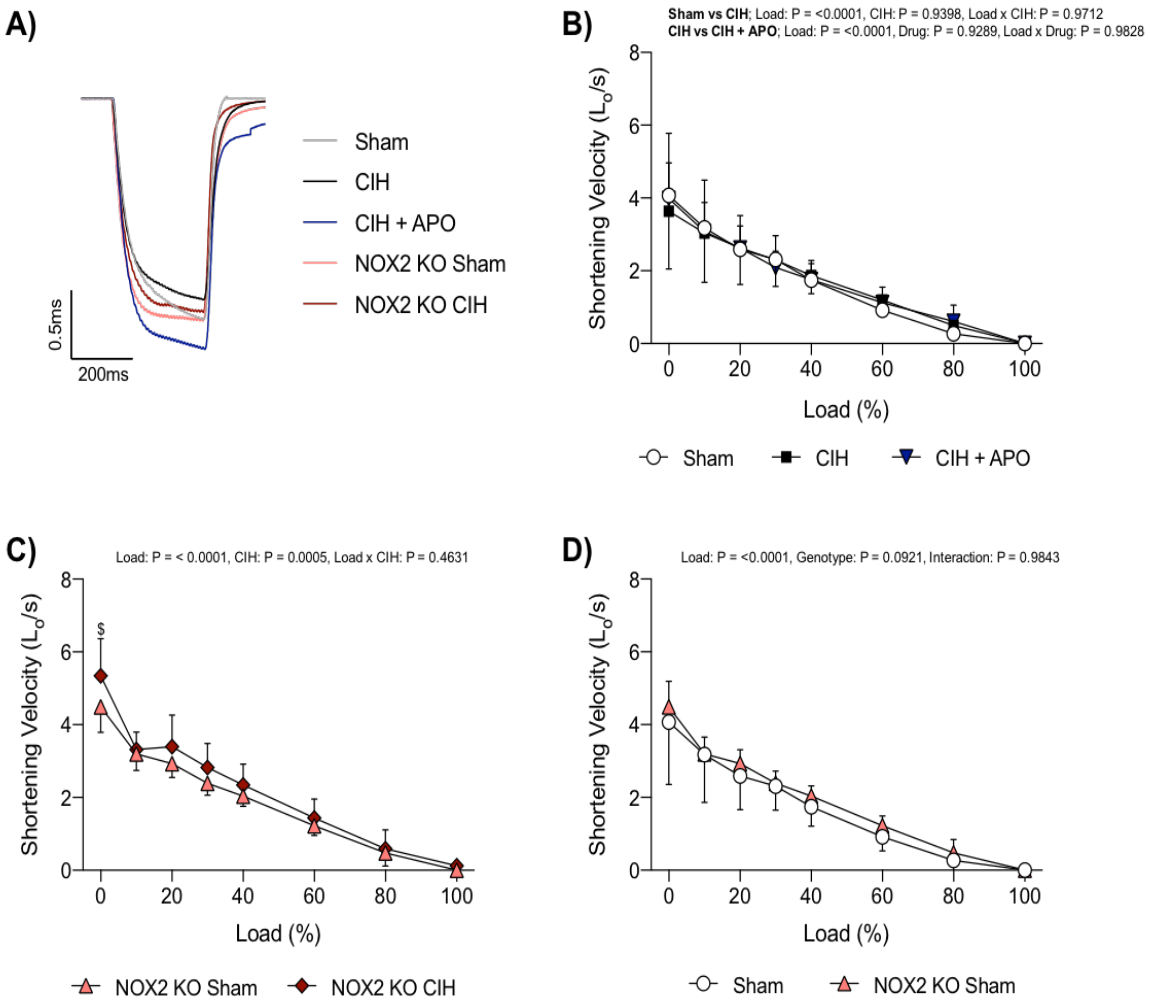

Figure 4.5 Sternohyoid muscle shortening velocity–load relationship. A, original traces of *ex vivo* sternohyoid muscle maximum unloaded shortening for sham (grey), CIH (black), CIH + APO (blue), NOX2 KO sham (pink) and NOX2 KO CIH (red) preparations. B, C, D, group data for sternohyoid shortening velocity (mean ± SD) shown as optimal length per unit time (Lo/s) as a function of the load on the muscle expressed as a percentage of peak tetanic force for sham (n = 8), CIH (n = 8), CIH + APO (n = 9), NOX2 KO sham (n = 8) and NOX2 KO CIH (n = 10) mice. Data were statistically compared by repeated measures two-way ANOVA with Bonferroni's *post hoc* test. Relevant comparisons are denoted as follows: $^{\$}$ denotes NOX2 KO sham *vs.* NOX2 KO CIH, $^{\$}$ $P < 0.05$.

4.3.2 Characterisation of NOX enzymes in sternohyoid muscle

Figure 4.6 shows the mRNA expression of the most predominant muscle-specific NOX isoforms in naïve wild-type mouse sternohyoid muscle. The mRNA expression of NOX1 in the sternohyoid was significantly lower than that of both NOX4 (Fig 4.6; P = 0.0002) and NOX2 (Fig 4.6; P = 0.0002). There was no difference in the mRNA expression of NOX4 compared with NOX2 (Fig 4.6; P = 0.5346).

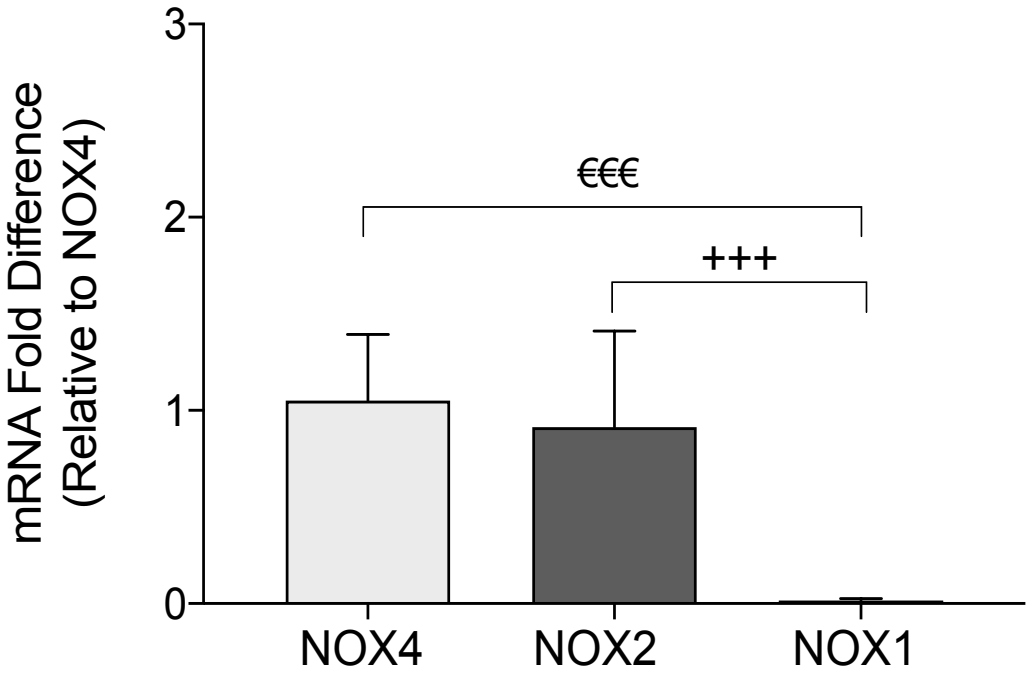

Figure 4.6 mRNA expression of the predominant muscle-specific NOX isoforms in naive wild-type mouse sternohyoid muscle. Group data (mean ± SD, n = 6-8 per group) expressed as a fold difference in messenger RNA (mRNA) expression (relative to NOX4) for naïve wild-type mouse sternohyoid muscle. Data sets, which were normally distributed and of equal variance, were statistically compared using unpaired two-tailed Student's *t* test. Welch's correction was applied in the case of unequal variance. Data, which were not normally distributed, were compared using Mann Whitney non-parametric tests. $^{€}$ denotes NOX4 *vs.* NOX1, $^{€€€}P < 0.001$; $^{+}$ denotes NOX2 *vs.* NOX1, $^{+++}P < 0.001$. *Definition of abbreviations:* NOX4, NADPH oxidase 4; NOX2, NADPH oxidase 2; NOX1, NADPH oxidase 1.

mRNA and protein expression of the NOX2 enzyme in mouse sternohyoid muscle is shown in Figure 4.7. There was no statistically significant difference in the mRNA expression of NOX2 following exposure to CIH compared with sham; apocynin treatment also had no effect on NOX2 mRNA levels (Fig 4.7; A). As expected, a significant decrease (97%) in the mRNA expression of NOX2 following NOX2 KO was observed compared with sham (Fig 4.7, A; $P = 0.0004$). Exposure to CIH had no effect on NOX2 mRNA expression in NOX2 KO mice (Fig 4.7; A). Western blot bands were detected at approximately 65kDa, corresponding to the predicted molecular weight (MW) of the NOX2 subunit (Fig 4.7; B). Fig. 4.7; C shows the corresponding Ponceau S-stained membrane, confirming relatively equal protein loading and electro-transfer. Densitometric analysis of NOX2 band intensities, normalised by the intensity of the corresponding Ponceau S-stained proteins, revealed no significant difference in the protein expression of the NOX2 subunit in the sternohyoid of mice exposed to CIH compared with sham (Fig 4.7, D; $P = 0.120$).

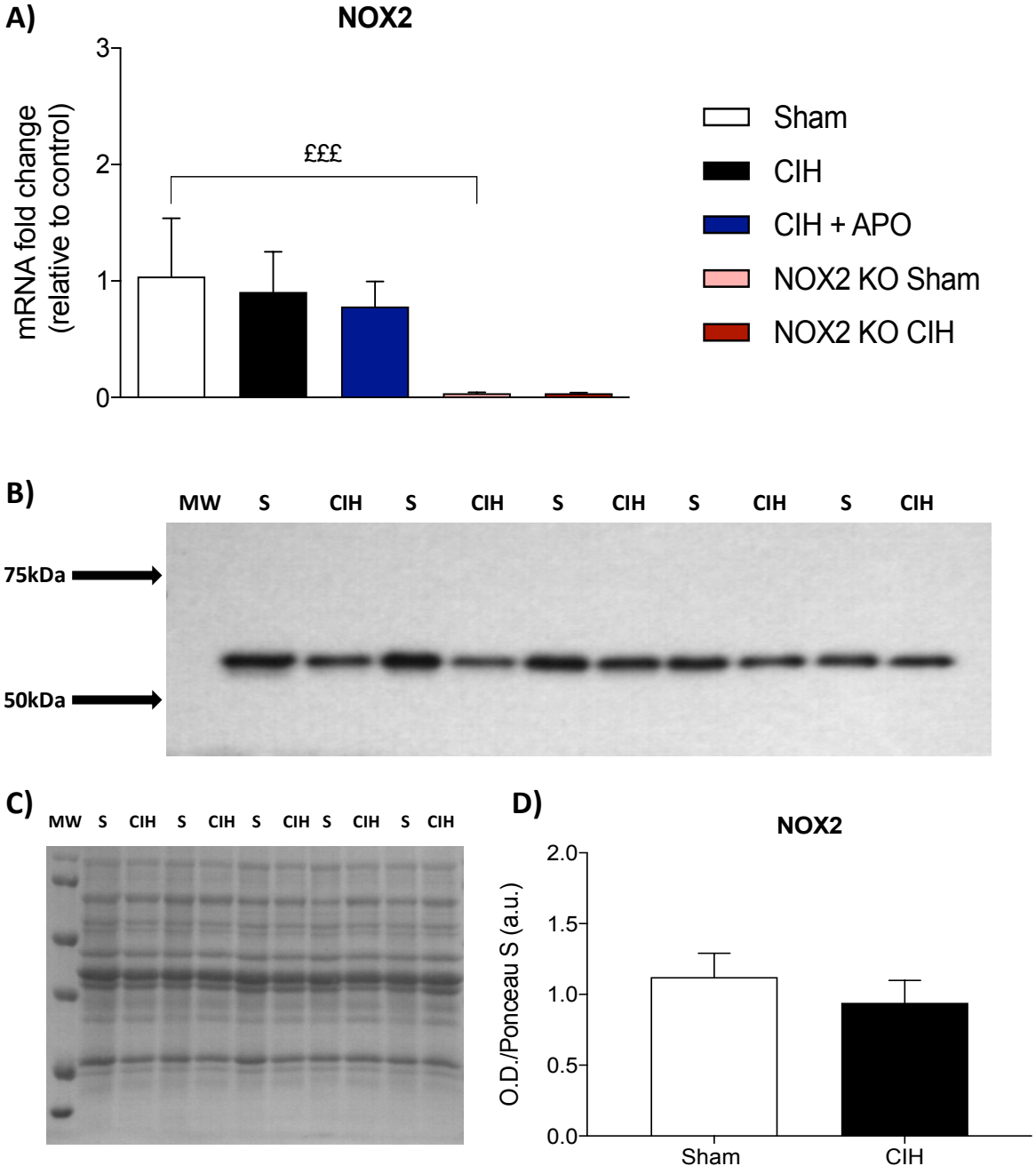

Figure 4.7 NOX2 mRNA and protein expression in sternohyoid muscle. A, Group data (mean ± SD, n = 6-8 per group) expressed as a fold change in messenger RNA (mRNA) expression (relative to the control (sham) group) for sham, CIH, CIH + APO, NOX2 KO sham and NOX2 KO CIH groups for A, NOX2. B, Western blot of NOX2 in 15μg of protein extracted from the sternohyoid of mice exposed to 2 weeks of normoxia (sham) or CIH. C, corresponding Ponceau S-stained membrane used for normalisation and compensation for protein loading and the electro-transfer of proteins. D**,** Group data (mean ± SD, n = 5 per group) for normalised NOX2 expression expressed as arbitrary units (a.u.). This is a product of the band intensity of the developed blot (B) / band intensity of the corresponding Ponceau S image (C), as determined by densitometry. Data sets, which were normally distributed and of equal variance, were statistically compared using unpaired two-tailed Student's *t* test. Welch's correction was applied in the case of unequal variance. Data, which were not normally distributed, were compared using Mann Whitney non-parametric tests. Statistical significance was taken at $P < 0.0125$ (A) or $P < 0.05$ (D). $^{£}$ denotes sham *vs.* NOX2 KO sham, $^{£££}P < 0.001$. *Definition of abbreviations:* MW, molecular weight marker; S. sham; NOX2, NADPH oxidase 2.

mRNA and protein expression of the NOX4 enzyme in mouse sternohyoid muscle is shown in Figure 4.8. There was no statistically significant difference in the mRNA expression of NOX4 following exposure to CIH compared with sham; apocynin treatment also had no effect on NOX4 mRNA levels (Fig 4.8; A). A trend towards an increase in the mRNA expression of NOX4 in NOX2 KO muscle was observed compared with sham (Fig 4.8, A; $P = 0.0327$). Exposure to CIH had no effect on NOX4 mRNA expression in NOX2 KO mice (Fig 4.8; A). Western blot bands were detected at approximately 63kDa, corresponding to the predicted MW of the NOX4 subunit (Fig 4.8; B). Fig. 4.8; C shows the corresponding Ponceau S-stained membrane, confirming relatively equal protein loading and electro-transfer. Densitometric analysis of NOX4 band intensities, normalised by the intensity of the corresponding Ponceau S-stained proteins, revealed no significant difference in the protein expression of the NOX4 subunit in the sternohyoid of mice exposed to CIH compared to sham (Fig 4.8, D; $P = 0.419$).

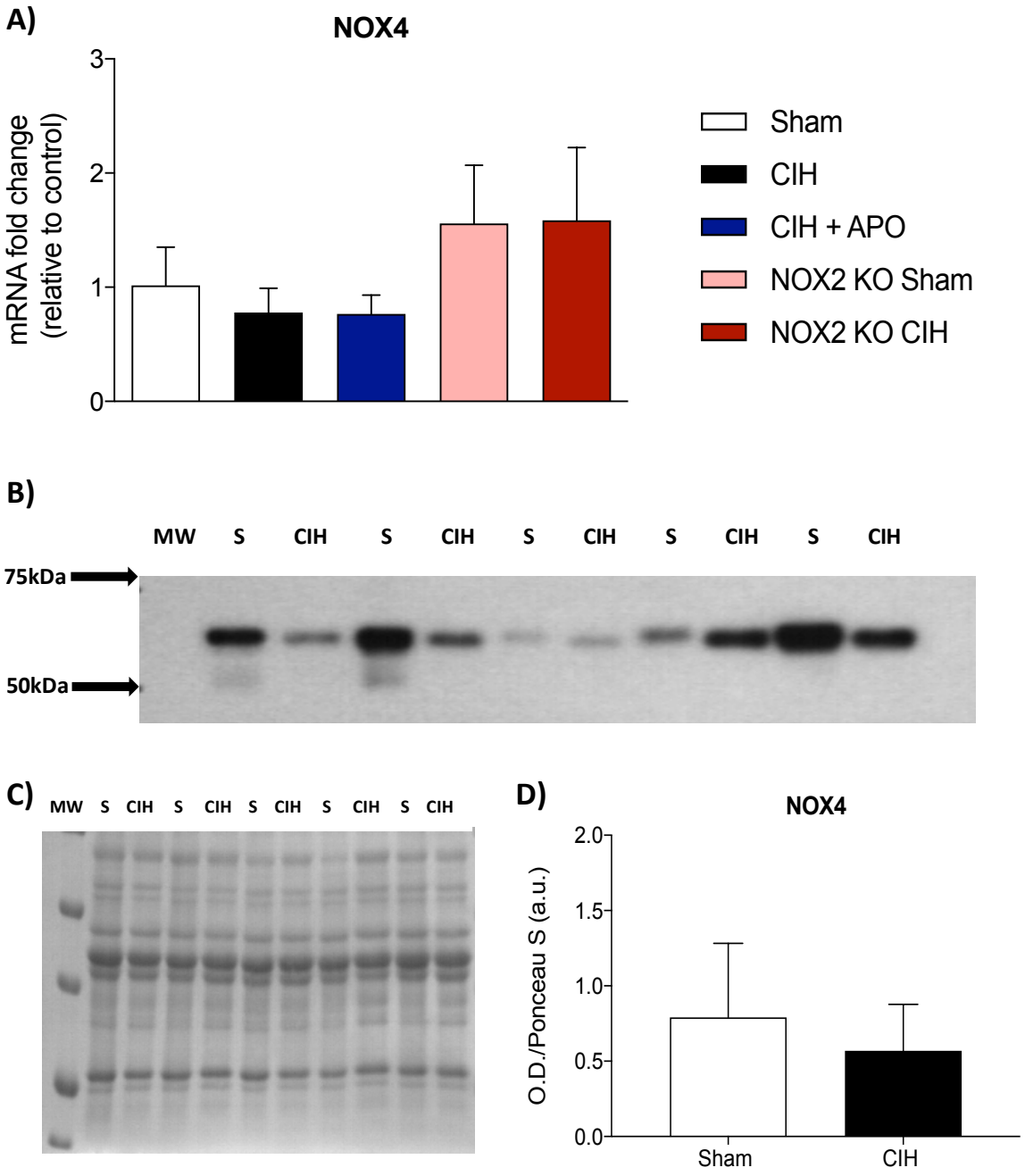

Figure 4.8 NOX4 mRNA and protein expression in sternohyoid muscle. A, Group data (mean ± SD, n = 6-8 per group) expressed as a fold change in messenger RNA (mRNA) expression (relative to the control (sham) group) for sham, CIH, CIH + APO, NOX2 KO sham and NOX2 KO CIH groups for, A, NOX4. B, Western blot of NOX4 in 15μg of protein extracted from the sternohyoid of mice exposed to 2 weeks of normoxia (sham) or CIH. C, corresponding Ponceau S-stained membrane used for normalisation and compensation for protein loading and the electro-transfer of proteins. D**,** Group data (mean ± SD, n = 5 per group) for normalised NOX4 expression expressed as arbitrary units (a.u.). This is a product of the band intensity of the developed blot (B) / band intensity of the corresponding Ponceau S image (C), as determined by densitometry. Data sets, which were normally distributed and of equal variance, were statistically compared using unpaired two-tailed Student's *t* test. Welch's correction was applied in the case of unequal variance. Data, which were not normally distributed, were compared using Mann Whitney non-parametric tests. Statistical significance was taken at $P < 0.0125$ (A) or $P < 0.05$ (D). *Definition of abbreviations:* MW, molecular weight marker; S. sham; NOX4, NADPH oxidase 4.

The mRNA expression of NOX catalytic and accessory subunits in sternohyoid muscle is show in Figure 4.9. There was no statistically significant difference in the mRNA expression of NOX1 (Fig 4.9; A), p22phox (Fig 4.9; B), p47phox (Fig 4.9; C), p67phox (Fig 4.9; D), Rac (Fig 4.9; E), DUOX1 (Fig 4.9; G) or DUOX2 (Fig 4.9; H) across all groups examined. 2 weeks of exposure to CIH caused a significant increase in NOX enzymatic activity in sternohyoid muscle compared with sham (Fig 4.9, I; $P = 0.0009$).

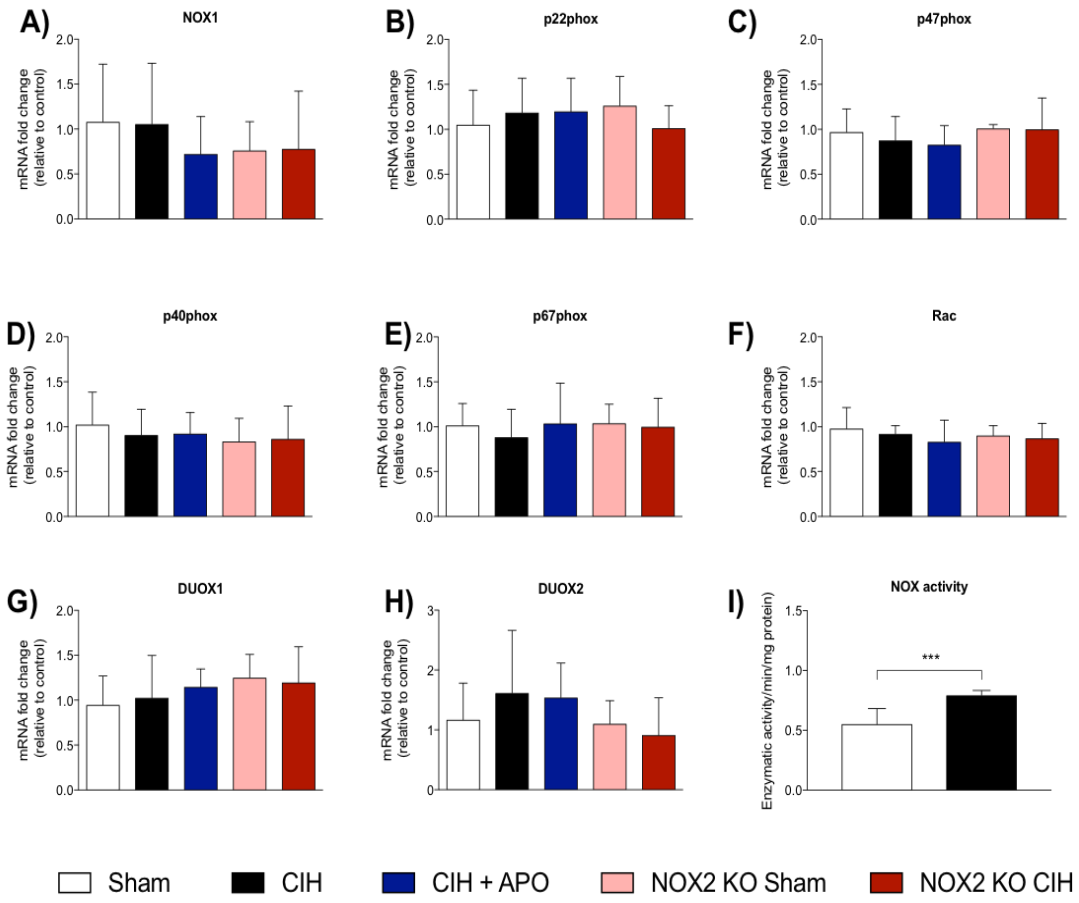

Figure 4.9 mRNA expression of NOX catalytic and accessory subunits in sternohyoid muscle. Group data (mean ± SD, n = 6-8 per group) expressed as a fold change in messenger RNA (mRNA) expression (relative to the control (sham) group) for sham, CIH, CIH + APO, NOX2 KO sham and NOX2 KO CIH groups for (A) NOX1; (B) p22phox; (C) p47phox; (D) p40phox; (E) p67phox; (F) Rac; (G) DUOX1 and (H) DUOX2. Group data (mean ± SD, n = 8 per group) for NOX enzymatic activity in sternohyoid muscle following 2 weeks of exposure to CIH or normoxia (sham), expressed as enzymatic activity per minute per mg protein (I). Data sets, which were normally distributed and of equal variance, were statistically compared using unpaired two-tailed Student's *t* test. Welch's correction was applied in the case of

unequal variance. Data, which were not normally distributed, were compared using Mann Whitney non-parametric tests. Statistical significance was taken at $P < 0.0125$ (A-H, inclusive) or $P < 0.05$ (I). Relevant comparisons are denoted as follows: * CIH *vs.* sham, *** $P < 0.001$. *Definition of abbreviations:* NOX1, NADPH oxidase 1.

4.3.3 Molecular analysis of redox sensitive indices of sternohyoid muscle form and function

Figure 4.10 shows the mRNA expression of genes relating to the muscle differentiation process in sternohyoid muscle. There were no statistically significant changes in the mRNA expression of Myogenin, Myostatin, MEF2C, MyoD, Sirtuin-1 or IGF-1 across all groups examined (Fig 4.10; A, B, C, D, E & F, respectively).

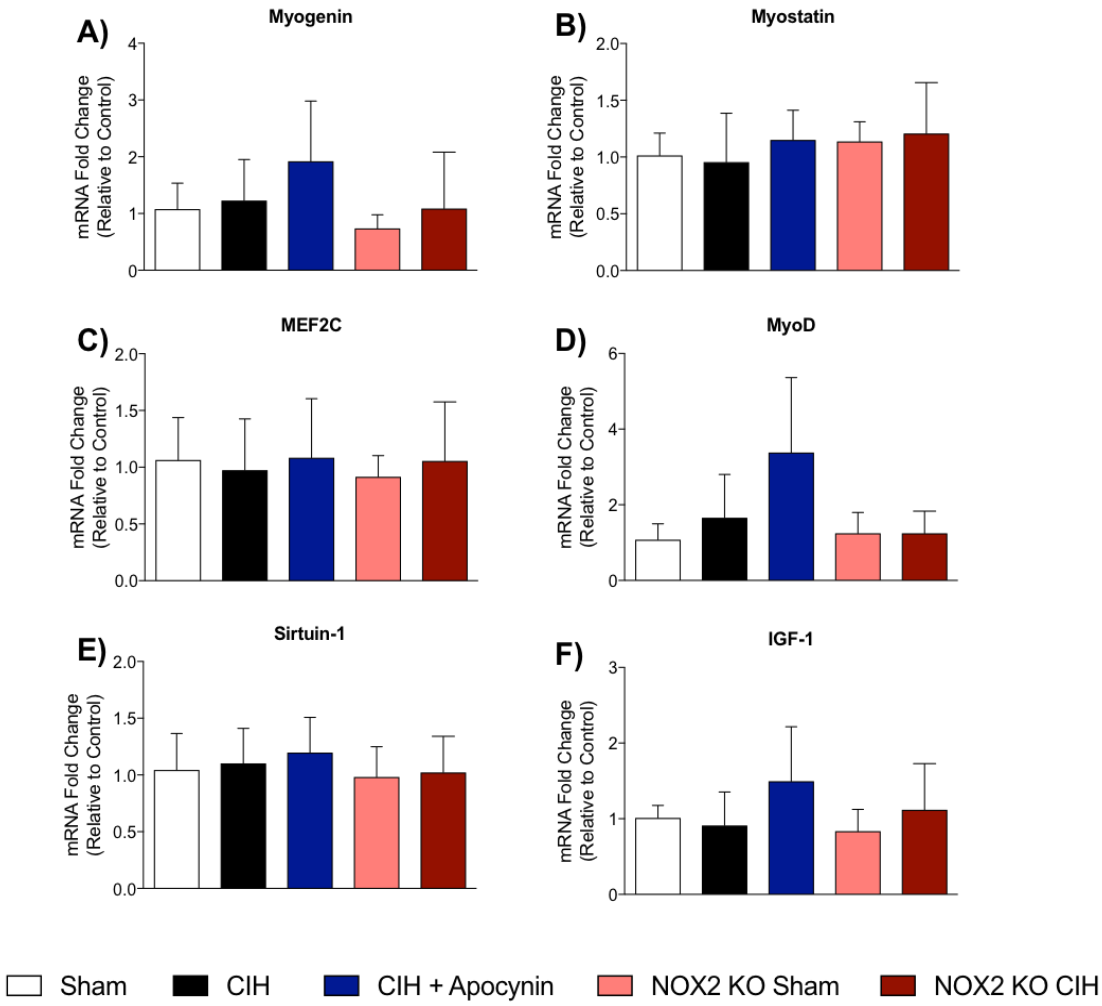

Figure 4.10 mRNA expression of genes related to muscle differentiation in sternohyoid muscle. Group data (mean ± SD, n = 6-8 per group) expressed as a fold change in messenger RNA (mRNA) expression (relative to the control (sham) group) for sham, CIH, CIH + APO, NOX2 KO sham and NOX2 KO CIH groups for (A) Myogenin; (B) Myostatin; (C) MEF2C; (D) MyoD; (E) Sirtuin-1; and (F) IGF-1. Data sets, which were normally distributed and of equal variance, were statistically compared using unpaired two-tailed Student's *t* test. Welch's

correction was applied in the case of unequal variance. Data, which were not normally distributed, were compared using Mann Whitney non-parametric tests. Statistical significance was taken at $P < 0.0125$. *Definition of abbreviations:* MyoD, muscle differentiation protein 1; MEF2C, myocyte-specific enhancer factor 2C; IGF-1, insulin-like growth factor 1.

Figure 4.11 shows the mRNA expression of genes relating to antioxidant status in sternohyoid muscle. There were no statistically significant differences in the mRNA expression of SOD1, SOD2, Catalase or NRF2 across all groups examined (Fig 4.11; A, B, C, & D, respectively). SOD1 and SOD2, pivotal endogenous antioxidants, displayed a trend towards a decrease in mRNA expression in NOX2 KO sham sternohyoid compared to sham ($P = 0.0478$; Fig 4.11, A & $P = 0.0452$; Fig 4.11, B, respectively), but this failed to reach the threshold for significance.

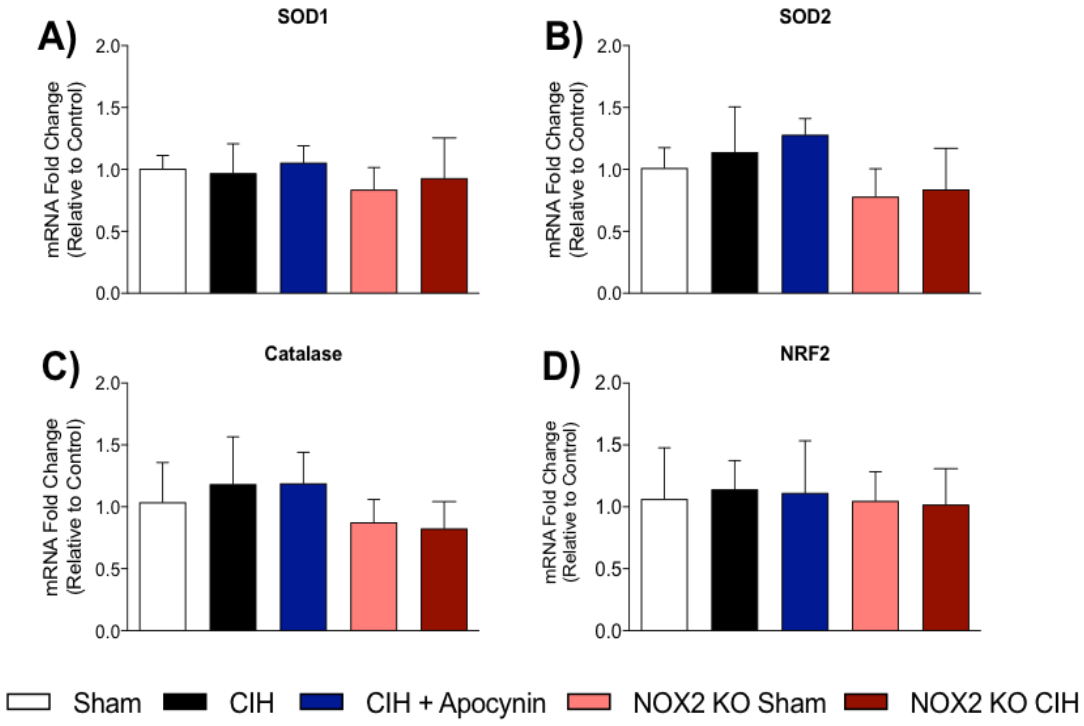

Figure 4.11 mRNA expression of genes related to antioxidant capacity in sternohyoid muscle. Group data (mean ± SD, n = 6-8 per group) expressed as a fold change in messenger RNA (mRNA) expression (relative to the control (sham) group) for sham, CIH, CIH + APO, NOX2 KO sham and NOX2 KO CIH groups for (A) SOD1; (B) SOD2; (C) Catalase; and (D) NRF2. Data sets, which were normally distributed and of equal variance, were statistically

compared using unpaired two-tailed Student's *t* test. Welch's correction was applied in the case of unequal variance. Data, which were not normally distributed, were compared using Mann Whitney non-parametric tests. Statistical significance was taken at $P < 0.0125$. *Definition of abbreviations:* SOD1, superoxide dismutase 1; SOD2, superoxide dismutase 2; NRF2, nuclear factor erythroid 2-related factor 2.

Figure 4.12 shows a range of indices relating to mitochondrial capacity in sternohyoid muscle. There was no significant difference in the mRNA expression of genes relating to mitophagy, PINK1 and PARK2, across all groups examined (Fig 4.12; A & B, respectively). Both PINK1 and PARK2 displayed non-significant trends toward an increase in mRNA expression following treatment with apocynin throughout the exposure to CIH, compared with exposure to CIH alone ($P = 0.0947$; Fig 4.12; A, $P = 0.0225$; Fig 4.12; B, respectively). Citrate synthase activity, commonly used as a quantitative enzyme marker for the presence of intact mitochondria, and hence aerobic capacity, was unchanged following 2 weeks of exposure to CIH (Fig 4.12; C).

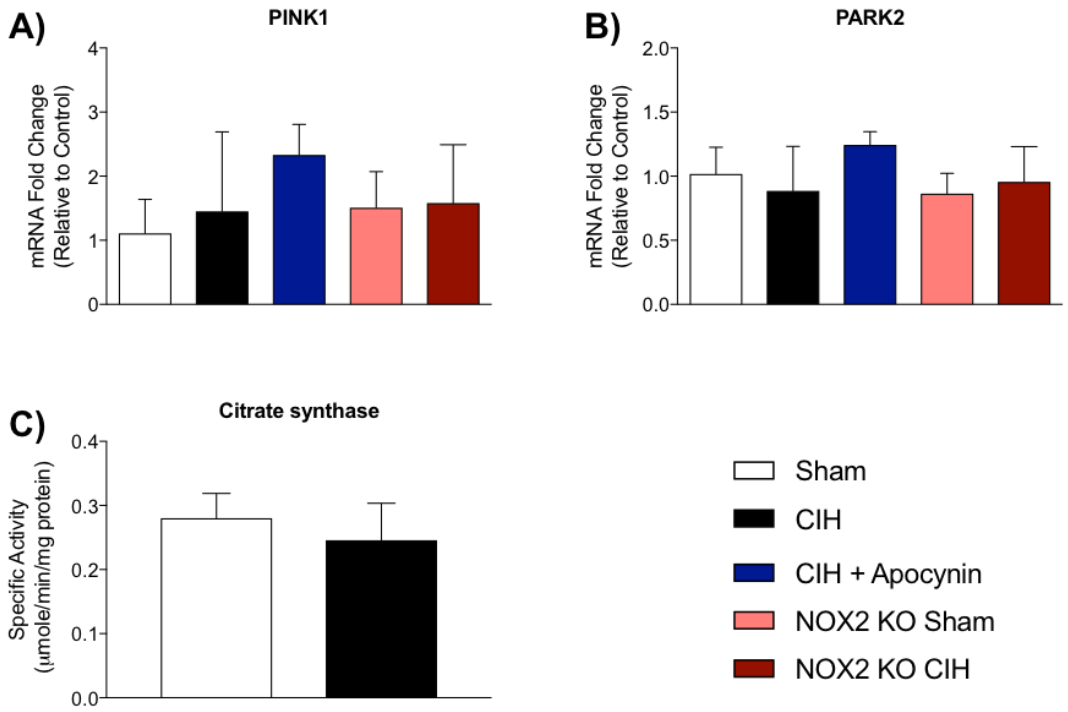

Figure 4.12 Indices relating to mitochondrial integrity in sternohyoid muscle. Group data (mean ± SD, n = 6-8 per group) expressed as fold changes in messenger RNA (mRNA) expression (relative to the control (sham) group) for Sham, CIH, CIH + APO, NOX2 KO Sham

and NOX2 KO CIH groups for A, PINK1; and B, PARK2. C, Citrate synthase activity following 2 weeks of exposure to CIH (mean ± SD, n = 8 per group). Data sets, which were normally distributed and of equal variance, were statistically compared using unpaired two-tailed Student's *t* test. Welch's correction was applied in the case of unequal variance. Data, which were not normally distributed, were compared using Mann Whitney non-parametric tests. Statistical significance was taken at $P < 0.0125$ (Fig _ A & B) or $P < 0.05$ (Fig _C). *Definition of abbreviations:* PINK1, PTEN-induced kinase 1; PARK2, parkin.

Figure 4.13 shows a range of measures relating to inflammation and redox balance in sternohyoid muscle. There was no statistically significant difference in the mRNA expression of the inflammatory transcription factor, NF-κB, across all groups examined (Fig 4.13; A). However, there was a non-significant increase in the mRNA expression of NF-κB following the administration of apocynin throughout the exposure to CIH, compared with exposure to CIH exposure ($P = 0.0939$; Fig 4.13; A). TBARS are formed as a by-product of lipid peroxidation and thus, are commonly used as an indirect measure of oxidative stress. Levels of TBARS in sternohyoid muscle were unchanged following 2 weeks of exposure to CIH compared to sham, although a trend toward an increase was observed ($P = 0.0962$; Fig 4.13; B). HIF-1α is considered a master transcriptional regulator during periods of hypoxia and mediates adaptive responses to oxidative stress. Protein expression of HIF-1α was unaltered following 2 weeks of exposure to CIH in sternohyoid muscle compared with sham (Fig 4.13; C).

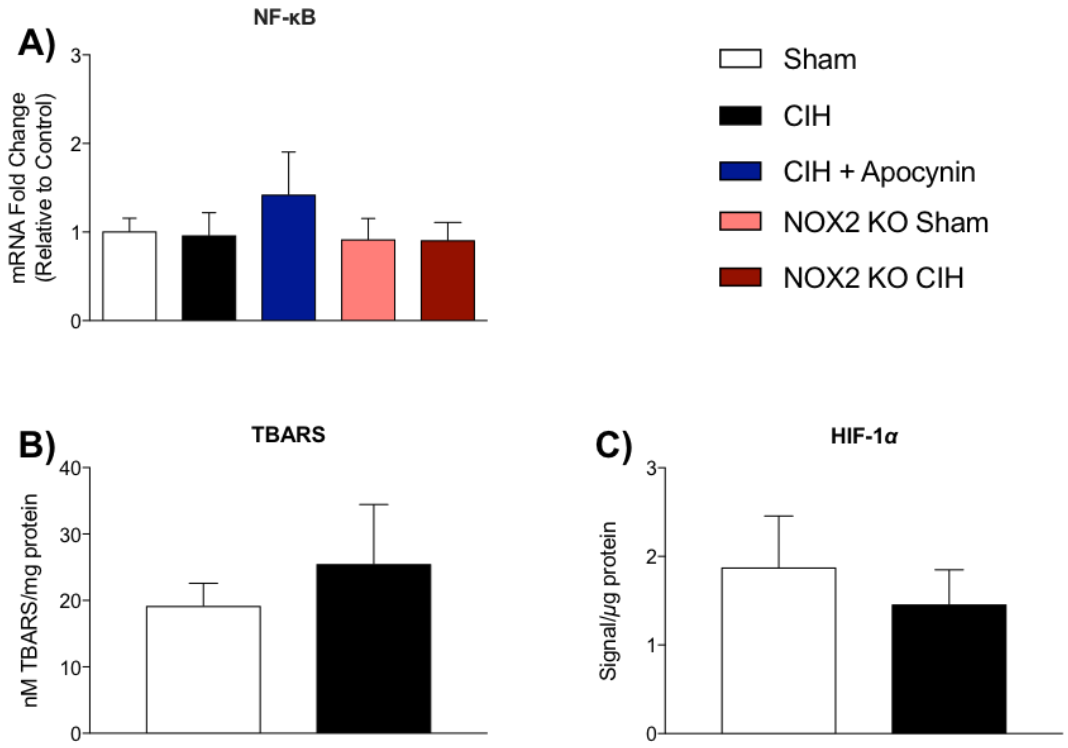

Figure 4.13 Inflammatory mediators and indirect measures of redox imbalance in sternohyoid muscle. Group data (mean ± SD, n = 6-8 per group) expressed as a fold change in messenger RNA (mRNA) expression (relative to the control (sham) group) for Sham, CIH, CIH + APO, NOX2 KO Sham and NOX2 KO CIH groups for A, NF-κB. B, TBARS and C, HIF-1α protein content in sternohyoid muscle following 2 weeks of exposure to CIH (mean ± SD, n = 8 per group). Data sets, which were normally distributed and of equal variance, were statistically compared using unpaired two-tailed Student's *t* test. Welch's correction was applied in the case of unequal variance. Data, which were not normally distributed, were compared using Mann Whitney non-parametric tests. Statistical significance was taken at $P < 0.0125$ (Fig _ A) or $P < 0.05$ (Fig _B & C). *Definition of abbreviations:* NF-κB, nuclear factor kappa-light-chain-enhancer of activated B cells; TBARS, thiobarbituric acid reactive substances; HIF1α, hypoxia-inducible factor 1-alpha.

Figure 4.14 shows the mRNA expression of genes relating to autophagy and atrophy in sternohyoid muscle. The mRNA expression of the autophagy-related gene, BNIP3, was significantly reduced in sternohyoid muscle following NOX2 KO compared to wild-type mice ($P = 0.0040$; Fig 4.14; A); there was no difference in the mRNA expression of BNIP3 across all other groups. There were no statistically significant differences in the mRNA expression of the atrophy-related gene, MuRF1 (Fig 4.14; E), across all groups. However non-significant trends towards a decreased mRNA

expression of MuRF1 were observed following exposure to CIH in wild-type mice (sham *vs.* CIH, *P* = 0.0150, Fig 4.14; E) and following NOX2 KO (sham *vs.* NOX2 KO sham, *P* = 0.127, Fig 4.14; E). The mRNA expression of GABARAPL1 (Fig 4.14; B), LC3B (Fig 4.14; C) and Atrogin-1 (Fig 4.14; D) were not different across all groups examined.

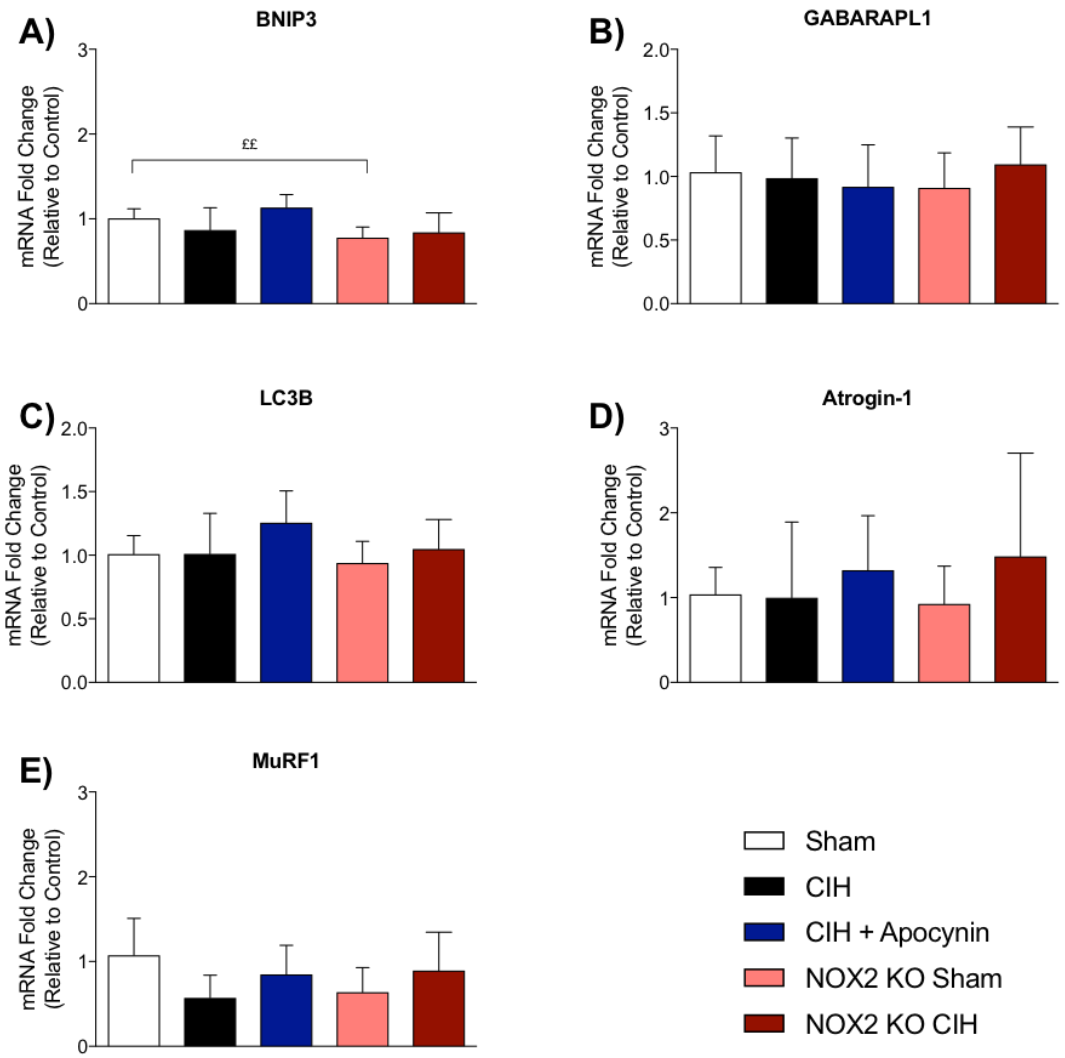

Figure 4.14 mRNA expression of genes relating to autophagy and atrophy in sternohyoid muscle. Group data (mean ± SD, n = 6-8 per group) expressed as a fold change in messenger RNA (mRNA) expression (relative to the control (sham) group) for sham, CIH, CIH + APO, NOX2 KO sham and NOX2 KO CIH groups for (A) BNIP3; (B) GABARAPL1; (C) LC3B; (D) Atrogin-1; and (E) MuRF1. Data sets, which were normally distributed and of equal variance, were statistically compared using unpaired two-tailed Student's *t* test. Welch's correction was applied in the case of unequal variance. Data, which were not normally distributed, were compared using Mann Whitney non-parametric tests. Statistical significance was taken at *P* < 0.0125. $^{£}$ denotes sham *vs.* NOX2 KO sham, $^{££}P$ < 0.01. *Definition of abbreviations:* BNIP3,

bcl-2 nineteen-kilodalton interacting protein 3; GABARAPL1, gamma-aminobutyric acid receptor-associated protein-like 1; LC3B, microtubule-associated proteins 1A/1B light chain 3B; MuRF1, muscle RING finger 1.

Figure 4.15 shows the phosphoprotein content of key proteins involved in protein synthesis and degradation signalling pathways in sternohyoid muscle. There was no alteration to the phosphoprotein content of Phospho-FOXO3a following 2 weeks of exposure to CIH compared with sham (Fig 4.15; A). Similarly, exposure to CIH resulted in no difference in the phosphoprotein content of components of the mitogen activated protein kinase (MAPK) pathway including Phospho-JNK, Phospho-p38 or Phospho-ERK 1/2 in the sternohyoid (Fig 4.15; B, C & D, respectively).

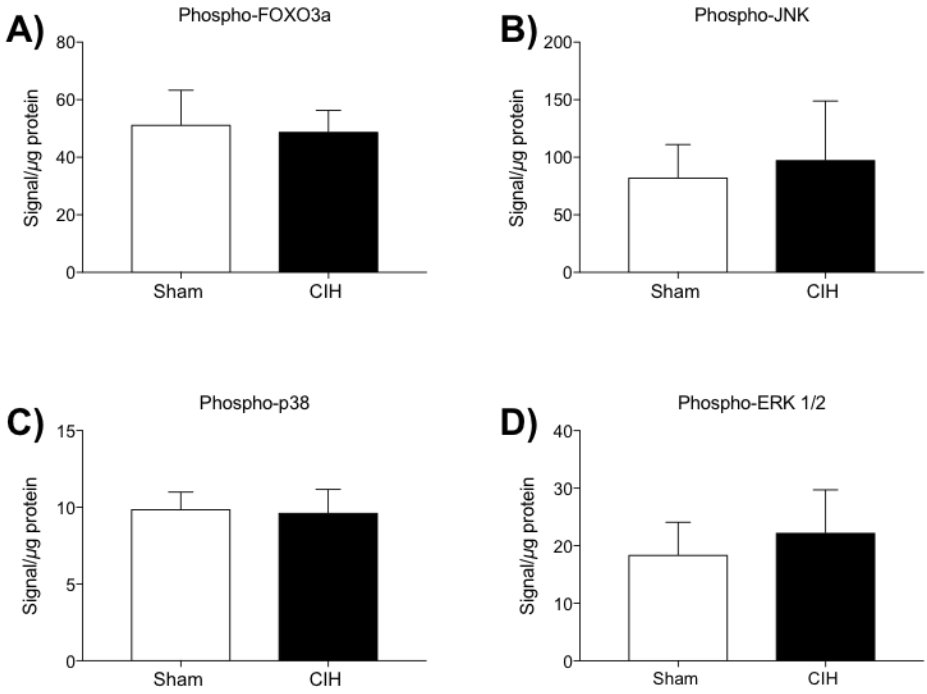

Figure 4.15 Phosphoprotein content relating to protein synthesis and degradation signalling in sternohyoid muscle. A, Phospho-FOXO3a; B, Phospho-JNK; C, Phospho-p38 protein content and D, sternohyoid phospho-ERK 1/2 (mean ± SD, n = 8 per group) from mice exposed to 2 weeks of CIH or normoxia (sham). Values are expressed as signal/µg of total protein (adjusted for background signal). Data sets, which were normally distributed and of equal variance, were statistically compared using unpaired two-tailed Student's *t* test. Welch's correction was applied in the case of unequal variance. Statistical significance was

taken at $P < 0.05$. *Definition of abbreviations:* FOXO3a, forkhead box O3a; JNK, c-Jun N-terminal kinase; ERK 1/2, extracellular-signal-regulated kinase 1/2.

4.4 Discussion

The key findings of this study are:

1) Exposure to CIH results in considerable sternohyoid muscle weakness, which is prevented by treatment with apocynin, and absent in NOX2 KO mice exposed to CIH.

2) NOX2 KO increases the force- and power-generating capacity of the sternohyoid muscle compared with wild-type controls (sham).

4) Exposure to CIH does not affect the mRNA or protein expression of the predominant NOX isoforms, NOX2 or NOX4, in skeletal muscle.

6) Exposure to CIH results in no alteration to the mRNA expression of NOX1, DUOX 1 & 2 or NOX accessory subunits in mouse sternohyoid. However, exposure to CIH increases NOX activity in wild-type mice, which appears to be independent of HIF-1α.

5) The mRNA expression of NOX2 is almost completely ablated in NOX2 KO mice; NOX2 KO increases the mRNA expression of NOX4 compared with wild-type controls (sham).

7) Indices of redox imbalance including levels of TBARS, citrate synthase activity and the mRNA expression of endogenous antioxidants are unaffected by exposure to CIH in mouse sternohyoid muscle.

8) The mRNA expression of genes relating to the regulation of skeletal muscle form and function including inflammation, autophagy, atrophy, mitophagy and muscle differentiation are unaffected by exposure to CIH in wild-type and NOX2 KO mice. Similarly, treatment with apocynin or NOX2 KO alone has no effect on the gene expression of these indices.

UA dilator muscles have a central role in the maintenance of airway patency. Impaired function of these striated muscles is a well-described contributor to respiratory pathology in OSAS by increasing the susceptibility to collapse and triggering a vicious cycle, which perpetuates obstructive airway events (Petrof et al., 1996, Bradford et al., 2005). The structure and function of UA muscles is altered in patients with OSAS, with these functional deficits subsequently contributing to upper airway collapse in patients with OSAS (Sérlès et al., 1996, Carrera et al., 1999). While the mechanisms underpinning aberrant UA muscle remodelling in OSAS are likely multifactorial, a wealth of research has implicated exposure to CIH as a major factor. CIH-induced UA muscle weakness and/or fatigue has been well described in animal models utilising a variety of IH paradigms (Pae et al., 2005, Liu et al., 2005, Dunleavy et al., 2008, Liu et al., 2009, Jia and Liu, 2010, Ding and Liu, 2011, Skelly et al., 2012b, Wang et al., 2013, Zhou and Liu, 2013, McDonald et al., 2015). Similarly, 2 weeks of exposure to CIH resulted in significant sternohyoid muscle weakness in our model, evidenced by a ~45% reduction in its peak force-generating capacity when compared with normoxic controls. This remarkable IH-induced sternohyoid weakness is far greater than that previously observed in rat models and in fact, is more reminiscent of the magnitude of UA muscle weakness observed in models utilising chronic sustained hypoxia (Lewis et al., 2015), associated with profound oxidative stress and muscle atrophy. When considering the sternohyoid and its physiological function, peak isometric force is arguably the most relevant parameter given that isometric contractions are most likely responsible for enabling the function of the sternohyoid in stabilising the hyoid bone and contributing to the maintenance of UA patency.

Exposure to CIH significantly decreased additional parameters including peak work (Wmax), peak power (Pmax) and the work and power produced over the range of loads examined *ex vivo*. We assume that the reduced power-generating capacity of the sternohyoid over physiological loads (predominantly due to decreased force-generating capacity) following exposure to CIH translates *in vivo* to a reduced capacity to preserve and maintain UA calibre, given that the sternohyoid is a recognised UA dilator muscle, and that the response is likely representative of changes in other important dilator muscles of the upper airway. OSAS is a neurogenic

phenomenon as state-dependent reductions in neural traffic to UA muscles predispose the occurrence of occlusions in patients with OSAS (Saboisky et al., 2012). However, resolving obstructive events requires forceful muscle activation to reopen the airway, such that weak dilator muscles may predispose to prolonged obstruction and perhaps increased frequency of obstructions, arising from the failure to defend airway calibre. Indeed, the current study demonstrates that exposure to CIH causes significant UA muscle weakness, which could subsequently put the intrinsically collapsible human airway at risk, and in particular, may put a patient with OSAS at risk of protracted apnoea, thus exacerbating the severity of OSAS pathology.

Alterations to Ca^{2+} signalling may contribute to skeletal muscle dysfunction in many muscular disorders such as myopathies, systemic disorders like hypoxia, sepsis, cachexia, sarcopenia, heart failure, and dystrophy (Agrawal et al., 2018). Reduced contractile kinetics (CT and ½ RT) have been observed in the genioglossus (principal airway dilator) of male rats following exposure to CIH (Wang et al., 2013). In contrast, exposure to CIH had no effect on the contractile kinetics (CT or ½ RT) of the sternohyoid muscle in the current study. The latter observations are consistent with previous findings from rat models of CIH (Skelly et al., 2012b, McDonald et al., 2016). The divergence in these findings may be explained by varying paradigms and durations of exposure to CIH as altered kinetics are observed following 5 weeks of exposure to CIH (Wang et al., 2013), but not the shorter duration of 2 weeks (Skelly et al., 2012b). The apparent lack of an alteration to contractile kinetics in the present study suggests that Ca^{2+} handling in the sternohyoid muscle, i.e. its release and re-uptake, at the SR is unaffected by exposure to CIH, thus dysregulated SR functioning is unlikely to underpin CIH-induced sternohyoid weakness. Alterations to the distance of shortening or velocity of shortening of pharyngeal airway muscles has previously been suggested to be indicative of poor mechanical efficiency, culminating in muscle dysfunction (Attal et al., 2000, Burns et al., 2017). However, we report no CIH-induced alterations to either of these contractile parameters in the sternohyoid over the load continuum in the current study.

OSAS is an oxidative stress disorder with the ROS produced as a result of recurrent hypoxia/reoxygenation cycles having devastating consequences for a range of integrative bodily systems, highlighting a therapeutic role for antioxidants (Lavie, 2003). Antioxidant supplementation has previously been shown to ameliorate or prevent UA muscle dysfunction following exposure to CIH in rat models (Liu et al., 2005, Dunleavy et al., 2008, Skelly et al., 2012b, Skelly et al., 2013). However, these studies have largely utilised superoxide scavengers which may over-scavenge ROS, resulting in an equally detrimental consequence for muscle force production as proposed by (Reid et al., 1992). NOX enzymes have been proposed as a source of ROS contributing skeletal muscle dysfunction in a range of models (Whitehead et al., 2010, Ahn et al., 2015, Williams et al., 2015b, Liu et al., 2017, Regan et al., 2017). In the current study, the administration of apocynin (NOX2 inhibitor), throughout the exposure to CIH, entirely prevented sternohyoid muscle weakness to levels comparable to sham animals. This extends previous work (Liu et al., 2005, Dunleavy et al., 2008, Skelly et al., 2012b, Skelly et al., 2013) and implicates NOX2 as the specific source of ROS underpinning CIH-induced muscle weakness in our model. However, while commonly used as a NOX2 inhibitor, apocynin is also reported to function as a general antioxidant (Altenhöfer et al., 2015). To account for this and ensure the specificity of our findings, transgenic NOX2 KO mice were employed. We demonstrated that CIH-induced muscle weakness is absent in NOX2 KO mice, as evidenced by an absence of deficits in the peak force-generating capacity, work or power produced by the sternohyoid following exposure to CIH, in mice lacking the NOX2 enzyme. This confirms that NOX2-derived ROS are entirely responsible and necessary for CIH-induced sternohyoid muscle weakness. Improved UA muscle performance during sleep in patients with OSAS may help reduce the incidence and severity of occlusive events, thus we posit that insights gleaned from our pharmacological and transgenic approaches may have implications for the human condition.

The homologues NOX1, 2 and 4 are the predominant NOX isoforms expressed in skeletal muscle cells in culture (Piao et al., 2005, Hutchinson et al., 2007, Sun et al., 2011, Handayaningsih et al., 2011, Hori et al., 2011). The relative abundance of these

isoforms, based on mRNA data in C2C12 cells, demonstrates that NOX4 is the most highly expressed, followed by NOX2 and subsequently NOX1 (Sun et al., 2011, Handayaningsih et al., 2011). Consistent with this, we have confirmed the mRNA expression of NOX1, NOX2 and NOX4, as well as their respective accessory subunits (p22phox, p40phox, p47phox, p67phox, Rac), in sternohyoid muscle from wild-type mice. We observed no difference between the mRNA expression of NOX2 and NOX4 in the sternohyoid, however, we report significantly lower levels of NOX1 mRNA. Myostatin upregulates NOX1 in C2C12 myoblasts (Sriram et al., 2011), but a further role for NOX1 in skeletal muscle has not yet been discerned. In the present study, we also demonstrate low mRNA levels of DUOX1 and DUOX2 in the sternohyoid, consistent with that previously reported in C2C12 muscle cells (Sandiford et al., 2014). Aside from this recent study highlighting the potential role of DUOX1 and DUOX2 in myogenesis, little is known about the physiological relevance of DUOX enzymes in skeletal muscle. NOX2- and NOX4-dependent ROS have been strongly implicated in muscle dysfunction in a variety of disease states (Spurney et al., 2008, Whitehead et al., 2010, Sullivan-Gunn and Lewandowski, 2013, Pal et al., 2014, Williams et al., 2015b, Henríquez-Olguín et al., 2015, Ahn et al., 2015, Yamada et al., 2015). Therefore, based on these observations, in conjunction with our mRNA data, we suggest that NOX2 and NOX4 isoforms hold the most relevance for respiratory muscle pathology in our model, and perhaps human OSAS.

CIH-induced increases in NOX enzyme expression and or/activity have been reported in a wide range of organs and tissues including, but not confined to, liver, cardiovascular system, brain, kidneys and the respiratory system (Zhan et al., 2005, Peng et al., 2006, Jun et al., 2008, Hayashi et al., 2008, Peng et al., 2009, Nisbet et al., 2009, Hui-guo et al., 2010, Peng et al., 2011, Gao et al., 2013, Williams et al., 2015b). This highlights a role for NOX-dependent ROS in CIH-induced alterations to homeostatic control. The regulation of NOX enzymes and their associated subunits is highly complex with evidence for the transient and sequential activation of NOX, such that understanding the patterns of NOX expression, activity and isoform cross-talk is a challenging task (Brandes et al., 2014). Two weeks of exposure to CIH has been shown to increase the protein expression of NOX2, and its activator subunit,

p47phox, in rat sternohyoid muscle (Williams et al., 2015b), suggestive of a role for NOX2-dependent ROS in CIH-induced UA muscle weakness (Skelly et al., 2012b). In contrast to this, we observed no alteration to the mRNA or protein expression of NOX2 or the mRNA expression of p47phox, p22phox, p67phox, p40phox or Rac in the sternohyoid muscle in the current study. While transcriptional regulation of NOX2 has been observed, NOX2 is thought to be predominantly acutely regulated by post-translational mechanisms such as the phosphorylation of regulatory cytosolic subunits, thus enabling the enzyme to assemble as a fully functioning complex (Lambeth, 2004). Under resting conditions, NOX2 and p22phox are complexed in the plasma membrane with accessory subunits unbound in the cytosol. Following stimulation by factors such as hypoxia or mechanical stress, including that of muscle contraction (Loureiro et al., 2016), cytosolic subunits are phosphorylated and translocated to the membrane to elicit the production of NOX2-derived ROS through the oxidation of NADPH. NOX2 is a major source of ROS production during exercise in human and mouse skeletal muscle with NOX2-dependent ROS production representing an important signal for increasing muscle glucose uptake during exercise (Henríquez-Olguin et al., 2019). Species differences between rat and mouse models may also represent a contributing factor to the divergent observations in NOX2 expression following exposure to CIH. Of interest, apocynin had no effect on NOX2 mRNA expression in the sternohyoid. Apocynin inhibits the generation of superoxide by NOX by blocking migration of p47phox to the membrane, thus interfering with assembly of the functional NOX complex (Touyz, 2008). Therefore, the lack of an effect of apocynin on NOX2 mRNA expression in the current study may be explained by the fact that apocynin acutely inhibits NOX activity, rather than its transcriptional expression.

NOX4 is a unique NOX isoform in that it is constitutively active, with its activity largely dependent upon its level of protein expression. Therefore, the ROS that NOX4 generates are driven at the level of gene transcription rather than through acute, post-translational mechanisms (Serrander et al., 2007). NOX4 is suggested to function as pivotal O_2 sensor, with a number of studies reporting an increase in NOX4 mRNA and protein expression following exposure to hypoxia (Nisbet et al., 2009,

Diebold et al., 2010). NOX4-dependent ROS have been implicated in poor skeletal muscle function as evidenced by increased NOX4 expression in models of disease characterised by skeletal muscle weakness (Ahn et al., Liu et al., 2017, Regan et al., 2017). Therefore, it is plausible that NOX4 could be implicated in CIH-induced muscle weakness. However, we report no alteration to the mRNA or protein expression of NOX4, nor to the mRNA of NOX4 accessory proteins, p22phox or Rac, in CIH-exposed sternohyoid muscle. This suggests that this paradigm of CIH exposure does not induce alterations to NOX4 at the transcriptional level.

Our findings point to an exclusive role for NOX2 in CIH-induced sternohyoid muscle weakness. Whereas gene and protein expression of NOX2 subunits were unaffected by exposure to CIH, a significant CIH-induced increase in NOX activity in the sternohyoid was evident in our model. We suggest that this increase in NOX activity may represent an increase in NOX-dependent ROS based on an acute process to increase enzymatic assembly and thus, ROS production. This is in contrast to an increase in NOX-dependent ROS production that occurs as a result of a transcriptional increase in the abundance of NOX enzymes. We have shown that NOX2 and NOX4 are the predominant NOX isoforms in sternohyoid muscle, consistent with previous findings in skeletal muscle cells (Sun et al., 2011, Handayaningsih et al., 2011). We rationalise that the increase in NOX activity in the sternohyoid following exposure to CIH in our model is NOX2-dependent given that 1) NOX2 is typically acutely regulated and 2) NOX2 KO prevents CIH-induced muscle weakness in our model. HIF-1α has been shown to mediate NOX activation in a range of organs and tissues (Diebold et al., 2010, Yuan et al., 2011, Diebold et al., 2012, Nanduri et al., 2015, Chen et al., 2018, Wang et al., 2020a). Interestingly, exposure to CIH has previously been shown to increase NOX2 expression in PC12 pheochromocytoma cells as well as mouse embryonic fibroblasts in a HIF-1α-dependent manner (Yuan et al., 2011). In the current study, we report no alteration to HIF-1α protein content in the sternohyoid following exposure to CIH, consistent with observations in rat models (Williams et al., 2015b). Therefore, we suggest that NOX activity is not increased in a HIF-1α dependent manner in our mouse model. However, we acknowledge that our results must be interpreted with caution as the

NOX activity assay utilised in the current study is not specific for any one isoform of NOX, rather it functions to assess the rate of NADPH consumption. NAD(P)H consumption assays have previously been used in the assessment of NOX activity in skeletal muscle (Javeshghani et al., 2002, Adams et al., 2005, Ahn et al., 2015, Bowen et al., 2015a, Bowen et al., 2015b). However, a recent study shows that these assays are not specific to NOX activity and, in several tissues and cell types, the signal generated was unchanged with a triple NOX1, NOX2, and NOX4 knockout (Rezende et al., 2016). Indeed, the lack of specific NOX activity measurements has been a major impediment in the field, and this warrants further attention. It is also important to consider that our assessment of muscle was performed on 'day 15', at least 15 hours following the final exposure to IH. As such, mice were normoxic for several hours before assessments were made. In this way, HIF-1α may have played a significant role in muscle (mal)-adaptation to CIH, in the course of exposure to CIH, but levels were likely restored to normal during return to normoxia. Therefore, we cannot discount a potential role for HIF-1α-dependent signalling in CIH-induced respiratory muscle weakness and this would be interesting to explore. Nevertheless, other models have demonstrated a stabilisation of HIF-1α mRNA and protein in the genioglossus following a 5-week exposure to CIH (Jia and Liu, 2010, Zhou and Liu, 2013). Indeed, it has been suggested that HIF-1α is regulated in a dose-dependent manner in response to IH (Martinez et al., 2019).

There is evidence of increased oxidative stress in a variety of tissues across animal models of CIH, consistent with the observation that human OSAS is an oxidative stress disorder (Lavie, 2003). However, despite the clear link between NOX2-dependent ROS and CIH-induced UA muscle weakness in our model, we report no evidence of concomitant overt oxidative stress in the sternohyoid following exposure to CIH. Oxidative stress may present due to an accumulation of ROS, a depletion of antioxidant defences, or a culmination of both. Skeletal muscle encompasses a robust antioxidant defence system, rendering it remarkably flexible in response to changes in the redox milieu that can occur in both health and disease (Kozakowska et al., 2015, Specht et al., 2021). Reduced levels of aconitase and GR activity, indicative of modest oxidative stress, have been demonstrated in the sternohyoid of

male rats following a 2 week exposure to CIH (Williams et al., 2015b). Similarly, reduced activity of GPX, CAT and SOD, with concomitant genioglossus fatigue, was observed in female rats following exposure to 5 weeks of CIH (Ding and Liu, 2011). In the present study, we report no alteration to the mRNA expression of the master cellular regulator of antioxidant response, NRF2, or the endogenous antioxidants, SOD1, SOD2 & catalase, in the sternohyoid following exposure to CIH. As a result, we suggest that any putative CIH-induced challenge to redox homeostasis does not manifest as a depletion of the antioxidant defence system (Ding and Liu, 2011, Williams et al., 2015b), nor does it evoke an adaptive response in the form of an increase in antioxidant enzyme expression. However, we acknowledge that our results only reflect changes at the transcriptional level of the antioxidant defence system and that CIH-induced alterations to antioxidant enzyme activity cannot be ruled out.

ROS have been shown to oxidise lipids as a function of the severity of OSAS (Hopps et al., 2014). TBARS are degradation products of fats routinely used as a marker of lipid peroxidation, as an indirect measurement of oxidative stress. Levels of TBARS show a positive correlation to OSAS severity as determined by increased apnoea index (Kent et al., 2011). 5 weeks of exposure to CIH has been shown to increase lipid peroxidation, evidenced by increased MDA levels in the genioglossus of female rats (Ding and Liu, 2011). Conversely, 2 weeks of exposure to CIH was insufficient to alter levels of lipid peroxidation, determined by levels of 4-HNE, in the sternohyoid in a rat model of CIH (Williams et al., 2015b). Consistent with the latter study, we report that 2 weeks of exposure to CIH had no effect on levels of TBARS in the sternohyoid and thus, oxidative stress in the form of lipid peroxidation appears to be absent in our model.

Mitochondria are an important source of ROS in skeletal muscle with ROS-dependent alterations to mitochondrial function and/or capacity proving consequential for skeletal muscle function (Hood et al., 2019). 5 weeks of exposure to CIH has been shown to cause genioglossus muscle fatigue and increased mitochondrial ROS production, suggesting a role for mitochondrial ROS in decreased genioglossus

endurance (Ding and Liu, 2011). Indeed, mal-adaptation of skeletal muscle to periods of hypoxia have been demonstrated as a loss of mitochondrial content, thus a reduced oxidative capacity and less endurant phenotype (Gamboa and Andrade, 2010). Given the pivotal role of O_2 as an electron acceptor in the ETC, hypoxia induces a build-up of electrons in this cycle, leading to an increased electron leakage and subsequent ROS formation. This increased ROS formation exacerbates mitochondrial dysfunction, yielding detrimental effects for muscle contractile performance. Citrate synthase activity is a routinely used marker of mitochondrial integrity and aerobic capacity, as it is the initial enzyme of the TCA cycle. Citrate synthase activity was unaffected by exposure to CIH in the sternohyoid in the current study, consistent with unaltered citrate synthase activity previously reported in a rat model of CIH (Williams et al., 2015a). Similarly, other metabolic markers, including SDH and GPDH activity, have been shown to be unaltered in rat sternohyoid following exposure to CIH (Skelly et al., 2012a, Skelly et al., 2012b).

Impaired mitochondria are removed or rejuvenated via autophagy (Kim et al., 2019). Mitochondria utilise a specialised form of autophagy, known as mitophagy, to protect against excessive ROS, such as that arising from exposure to CIH. Mitochondrial function has been shown to be essential for plasma membrane repair in skeletal muscle fibres, with mitochondrial ROS shown to be pivotal in facilitating this membrane repair (Horn et al., 2017). Inhibiting mitochondrial ROS in myofibres during eccentric exercise *ex vivo* increases myofibre damage with concomitant muscle force loss (Horn et al., 2017). This highlights the beneficial role of mitochondrial ROS in repair mechanisms in response to strain on skeletal muscle. An increase in key regulators of mitophagy has been observed in rat genioglossus following 2-3 weeks of exposure to CIH, with these markers of mitophagy subsequently decreasing for the remaining 2 weeks of exposure to CIH (Wang et al., 2020b). The initial increase in mitophagy is suggested to represent a protective mechanism against excessive ROS, with the persistent insult by exposure to CIH culminating in an increase in mitochondrial impairment and decrease in mitophagy. Thus, disturbances to genioglossus mitophagy may relate to impaired mitochondrial function and decreased contractile properties in rats induced by exposure to CIH. In

the current study, we examined the mRNA expression of the PINK1/PARK2 pathway, which has emerged as a principal regulator of mitochondrial degradation in a range of biological systems (Narendra and Youle, 2011). However, we found that exposure to CIH had no effect on the mRNA expression of PINK1 or PARK2 in the sternohyoid. Our data suggest that overt oxidative stress and subsequent mitochondrial dysfunction are not likely to underlie the CIH-induced alteration to sternohyoid muscle function observed in the current study.

Initially, the lack of evidence for CIH-induced oxidative stress could be considered surprising given the remarkable efficacy of antioxidants (Liu et al., 2005, Dunleavy et al., 2008, Skelly et al., 2012b, Skelly et al., 2013) and NOX2 KO (this study), in preventing CIH-induced muscle weakness. It has been well described that the elaboration of adaptive or mal-adaptive outcomes in response to CIH is largely determined by the pattern, intensity and duration of hypoxic exposure. IH models produce different degrees of hypoxia severity, yielding dose-dependent effects (Lim et al., 2016, Gallego-Martin et al., 2017, Docio et al., 2018). The CIH paradigm utilised in this study is sufficient to cause respiratory muscle dysfunction, hypertension (Lucking et al., 2014) and increased propensity for apnoea, characteristic of OSAS. However, it is considered quite a modest CIH exposure. Previous studies have suggested that short bouts of IH (15 s hypoxia; 5 min normoxia) produce higher levels of ROS compared with longer bouts of IH (Raghuraman et al., 2009), such as those used in the current study. Therefore, our paradigm may not be expected to produce overt oxidative stress. A study by our group has demonstrated that in addition to antioxidants proving efficacious in preventing CIH induced UA muscle dysfunction, they also hold the capacity, following acute administration, to reverse muscle weakness due to CIH (Skelly et al., 2012b). This finding is pivotal in our understanding of the mechanisms underpinning CIH-induced muscle weakness as it strongly suggests that exposure to CIH does not result in irreversible oxidative damage to muscle *per se*. This is consistent with the lack of evidence for increased lipid peroxidation or alterations to mitochondrial content and or/function in CIH-exposed muscle reported in the current study. Rather, we suggest that CIH-induced sternohyoid muscle weakness is a dynamic NOX2 derived ROS-dependent process

that serves to powerfully suppress muscle contractile function, independent of muscle damage, such that it is entirely reversible. This is important in the context of potential therapeutic targeting for human OSAS, recognising the considerable challenge of oxidative modifications contributing to muscle injury in the context of chronic disease.

Structural alterations in the form of slow-to-fast fibre-type transitions are observed in the UA musculature of humans with OSAS (Smirne et al., 1991, Carrera et al., 1999) as well as in the English bulldog model (Petrof et al., 1994). Consistent with this, a range of studies have demonstrated CIH-induced fibre-type transitions in UA muscles, which serve to promote a more fatigable phenotype (McGuire et al., 2002a; Liu et al., 2009). However, the development of UA muscle dysfunction does not require structural remodelling in the form of atrophy and/or fibre-type transitions in rat models (Skelly et al., 2012b, McDonald et al., 2015). Given the magnitude of UA muscle weakness observed following exposure to CIH in the current study, it is plausible to suggest that structural alterations may underpin muscle dysfunction. However, we report no indication of muscle atrophy in the sternohyoid following exposure to CIH in the current study, as evidenced by the unchanged mRNA expression of key muscle-specific ubiquitin ligases; MurF-1 and Atrogin-1. Similarly, key cell signalling pathways pivotal in maintaining the balance between atrophy and hypertrophy in skeletal muscle, including MAPK and FOXO-3a, appear unaltered by exposure to CIH. Basal levels of autophagy are necessary for the homeostatic maintenance of muscle mass. However, an interplay between atrophy and autophagy has been demonstrated to underlie a loss of muscle mass and resultant weakness in skeletal muscle (Dobrowolny et al., 2008). Consistent with a lack of evidence for CIH-induced muscle atrophy in the sternohyoid, we also report unaltered mRNA levels of key autophagy markers: GABARAPL1, LC3B and BNIP3.

Skeletal muscle has an exceptional capacity to regenerate and re-establish homeostatic contractile and metabolic properties in response to severe damage. However, successive rounds of muscle degeneration and regeneration can result in the incomplete remodelling of the ECM. This results in the generation of large

amounts of fibrosis and scar tissue rather than contractile tissue, thus yielding a muscle with a lower force-generating capacity (Smith and Barton, 2018). It has been demonstrated that physiological hypoxia e.g. exercise results in muscle cell proliferation and myogenesis, whereas pathological hypoxia, e.g. CIH, inhibits myogenesis (Yun et al., 2005). 5 weeks of exposure to CIH has been shown to decrease the expression of key MRFs, MyoD and myogenin, in the genioglossus of rats (Zhou and Liu, 2013). The authors suggest that exposure to CIH damaged genioglossus regenerative properties, which may have implications for the observed decrease in genioglossus fatigue resistance. In the present study, we report no alterations to the mRNA expression of key MRFs including MyoD, myostatin, myogenin, sirtuin-1 or MEF2C in the sternohyoid following exposure to CIH. These gene expression data, in conjunction with our functional results demonstrating that exposure to CIH does not affect the distance or velocity of shortening in the sternohyoid muscle, suggests that CIH-induced NOX2-dependent alterations to UA muscle performance are not likely to be underpinned by structural remodelling.

In view of the collective data described above, our results are consistent with previous views (Williams et al., 2015b) that CIH-induced sternohyoid muscle weakness may be mediated by altered redox signalling, perhaps within microdomains of the muscle, evidently with no widespread cellular stress or structural alterations. All NOX2-related subunits have been identified in skeletal muscle (Javeshghani et al., 2002). An increase in NOX2 activity and/or expression has been demonstrated in isolated SRs (Xia et al., 2003), as well as in intact and isolated t-tubules and triads of mammalian skeletal muscle (Hidalgo et al., 2006). Similarly, NOX4 expression has been shown in the mitochondria (Sakellariou et al., 2013), SR and t-tubules of skeletal muscle (Loureiro et al., 2016). The localisation of NOX enzymes juxtaposed to the contractile apparatus in skeletal muscle highlights the possibility of their role in ROS-dependent alterations to EC coupling mechanisms. Studies examining the underlying mechanisms pertaining to ROS-dependent alterations to muscle function have largely suggested that ROS elicit complex redox alterations to the Ca^{2+} release apparatus. ROS have been shown to activate RyR1s via s-glutathionylation of cysteine residues producing an increase in calcium induced

calcium release (CICR) in the t-tubules of skeletal muscle (Hidalgo et al., 2006). It has also been demonstrated that thiol groups on the SR are a critical target of oxidative modification by O_2^-, culminating in an increase in Ca^{2+} release, with thiol reducing agents successfully closing the channel (Abramson and Salamaz, 1988). In contrast, various studies have reported a down regulation and impaired Ca^{2+} channel functioning in skeletal muscle upon exposure to ROS (Guerra et al., 1996). This apparent dichotomy may be attributed to varying levels of ROS, which are known to have divergent effects in skeletal muscle. NOX4 expression has been shown to be positively regulated by O_2 tension. Interestingly, an increase in NOX4-derived H_2O_2 has been shown to be coupled to an increased oxidation of cysteine residues of RyRs in isolated SRs, cultured myofibres and intact muscle. This produced an increase in Ca^{2+} release and enhanced muscle contraction, implicating NOX-derived ROS in alterations to muscle performance in response to changes in PO_2 (Sun et al., 2011). Our functional data revealed no change in muscle contractile kinetics, suggesting no major redox modulation of Ca^{2+} handling. This suggests that muscle weakness in CIH-induced sternohyoid may be an effect of redox modulation at the level of the myofilaments influencing cross-bridge cycling or Ca^{2+} sensitivity of the contractile apparatus through redox modulation of troponin (de Paula Brotto et al., 2001, Ottenheijm et al., 2005, Ottenheijm et al., 2006, Coirault et al., 2007, Degens et al., 2010, Smuder et al., 2010, Pinto et al., 2011, McDonagh et al., 2014). Therefore, we speculate that CIH-induced NOX-dependent ROS may impair muscle force-generating capacity without concomitant widespread oxidative damage or structural (fibre-type transition and/or atrophy) alterations.

The specific mechanism by which NOX2-derived ROS underlie CIH-induced UA muscle weakness still remains elusive. It has been well described that ROS hold the capacity to modulate skeletal muscle performance, with the contractile apparatus of muscle fibres proving highly sensitive to alterations in cellular redox state (Reid et al., 1992). Previous studies by our group have demonstrated that incubation with a superoxide scavenger, tempol, yields a powerful inotropic effect on the sternohyoid muscle (Skelly et al., 2010, Skelly et al., 2012b). This suggests that under basal conditions, ROS exert a tonic inhibition on UA muscle force production. Furthermore, it is

suggested that NOX2 is the culpable source of these ROS as incubation of the sternohyoid with apocynin results in a significant increase in its force- and power-generating capacity (Williams et al., 2015b). However, studies utilising p47phox deficient mice report no inotropic effect of NOX2 knockout, evidenced by an unaltered force-generating capacity of the diaphragm muscle compared with wild-type controls (Ahn et al., 2015). Consistent with the former findings, we report a ~30% increase in the peak force-generating capacity of the sternohyoid in NOX2 KO mice, compared with wild-type controls. Similarly, we observed a significant increase in the power and work produced by the sternohyoid in NOX2 KO mice across the load continuum examined. Our findings extend previous work (Skelly et al., 2010, Skelly et al., 2012b, Williams et al., 2015b) to suggest that NOX2 is an important source of basal ROS production in mouse sternohyoid muscle. Our novel data highlight that NOX2-derived ROS are powerful inhibitors of sternohyoid force and power, and by extension it is therefore plausible to suggest that increased ROS associated with exposure to CIH directly impairs sternohyoid muscle function**.**

We demonstrate an almost complete ablation of NOX2 mRNA in the sternohyoid of NOX2 KO mice. A recent study utilising commercial NOX2 KO mice showed that NOX2 mRNA and protein expression was still detectable in various tissues using standard primers and antibodies (Göllner et al., 2020). Further analysis using RNA sequencing revealed a modified NOX2 mRNA in the KO mice that is subsequently translated to a truncated inactive mutant enzyme, as these KO mice displayed no considerable enzymatic NOX2 activity. Therefore, while we observe trace amounts of NOX2 mRNA in the sternohyoid of NOX2 KO mice, that is not attributable to non-specific PCR amplification, we suggest that this does not translate into a functional NOX2 protein that would contribute to significant ROS generation in our model. Additionally, we observed an increase in NOX4 mRNA in the sternohyoid of NOX2 KO mice. Studies in human pulmonary artery endothelial cells (HPAECs) demonstrate that either NOX2 or NOX4 knockdown using siRNA results in an upregulation of the other enzyme, suggesting a compensatory mechanism for basal ROS production (Pendyala et al., 2009). Indeed, a marked compensatory upregulation of NOX4 has been exhibited in NOX2 KO models of diabetic kidney disease (You et al., 2013) and ageing brains (Fan

et al., 2019). Moreover, an inhibition of NOX2 increases NOX4 expression in *mdx* limb muscle, suggesting that NOX enzymes are an important source of ROS in skeletal muscle (Cully and Rodney, 2020). It has been suggested that adaptations that occur with embryonic deficiency of a protein might affect redox balance in knockout animals as respiratory muscle from mice lacking the p47phox subunit exhibit a downregulation of the antioxidant enzymes SOD1 and CAT (Bost et al., 2015) and an upregulation of NOX4 protein levels (Ferreira and Laitano, 2016). Consistent with this, we suggest that the increase in NOX4 mRNA in the sternohyoid and a trend towards a decrease in the mRNA of antioxidant enzymes in NOX2 KO mice observed in the present study represents a compensatory mechanism to regulate a homeostatic redox state in the sternohyoid muscle, in the absence of NOX2.

In the current model, we reveal that NOX2 is essential for CIH-induced sternohyoid muscle weakness. Based on our data and previous observations in rats (Williams et al., 2015b), CIH-induced muscle weakness occurs in the absence of overt oxidative stress or structural remodelling that could explain diminished muscle function. Additionally, we demonstrate that NOX2-derived ROS are capable of affecting sternohyoid muscle performance. Therefore, it is plausible to suggest that NOX2-derived ROS may exert their effects on contractile function through actions at one or more sites critical for EC coupling (Geiszt et al., 1997, Kawakami and Okabe, 1998, Hidalgo et al., 2006, Espinosa et al., 2006, van der Poel et al., 2007, Sun et al., 2011, Lamb and Westerblad, 2011, Liu et al., 2012, Cully and Rodney, 2020). We speculate that the inotropic effects of NOX2 KO and thus, NOX2-dependent CIH-induced muscle weakness, may relate to redox modulation of Ca^{2+} sensitivity of the contractile filaments (Westerblad and Allen, 1991, Edwards et al., 2007, Murphy et al., 2008, Dutka et al., 2017).

The significance of our findings is that exposure to CIH, a hallmark feature of human OSAS, is detrimental to the maintenance of UA patency, potentially increasing the risk of obstructive airway events throughout the night cycle. Therefore, exposure to CIH could establish a vicious cycle serving to exacerbate respiratory morbidity in human OSAS. Therapeutic strategies to improve UA muscle performance may

function as an adjunct therapy to reduce OSAS severity in human OSAS. Our data suggest that NOX2 is a viable target for pharmacotherapeutic intervention.

4.5 References

ABRAMSON, J. J. & SALAMAZ, G. 1988. Sulfhydryl oxidation and Ca2+ release from sarcoplasmic reticulum. *Molecular and Cellular Biochemistry,* 82**,** 81-84.

ADAMS, V., LINKE, A., KRÄNKEL, N., ERBS, S., GIELEN, S., MÖBIUS-WINKLER, S., GUMMERT, J. F., MOHR, F. W., SCHULER, G. & HAMBRECHT, R. 2005. Impact of regular physical activity on the NAD(P)H oxidase and angiotensin receptor system in patients with coronary artery disease. *Circulation,* 111**,** 555-62.

AGRAWAL, A., SURYAKUMAR, G. & RATHOR, R. 2018. Role of defective Ca(2+) signaling in skeletal muscle weakness: Pharmacological implications. *J Cell Commun Signal,* 12**,** 645-659.

AHN, B., BEHARRY, A. W., COBLENTZ, P. D., PATEL, N., JUDGE, A. R., BONNELL, M. R. & HOOPES, C. W. Diaphragm Abnormalities in Heart Failure Patients: Upregulation of NAD(P)H Oxidase Subunits and Heightened Protein Oxidation. *C73. OXIDANTS.*

AHN, B., BEHARRY, A. W., FRYE, G. S., JUDGE, A. R. & FERREIRA, L. F. 2015. NAD(P)H oxidase subunit p47phox is elevated, and p47phox knockout prevents diaphragm contractile dysfunction in heart failure. *Am J Physiol Lung Cell Mol Physiol,* 309**,** L497-505.

ALTENHÖFER, S., RADERMACHER, K. A., KLEIKERS, P. W., WINGLER, K. & SCHMIDT, H. H. 2015. Evolution of NADPH Oxidase Inhibitors: Selectivity and Mechanisms for Target Engagement. *Antioxid Redox Signal,* 23**,** 406-27.

ATTAL, P., LAMBERT, F., MARCHAND-ADAM, S., BOBIN, S., POURNY, J. C., CHEMLA, D., LECARPENTIER, Y. & COIRAULT, C. 2000. Severe mechanical dysfunction in pharyngeal muscle from adult mdx mice. *Am J Respir Crit Care Med,* 162**,** 278-81.

BOST, E. R., FRYE, G. S., AHN, B. & FERREIRA, L. F. 2015. Diaphragm dysfunction caused by sphingomyelinase requires the p47(phox) subunit of NADPH oxidase. *Respir Physiol Neurobiol,* 205**,** 47-52.

BOWEN, T. S., MANGNER, N., WERNER, S., GLASER, S., KULLNICK, Y., SCHREPPER, A., DOENST, T., OBERBACH, A., LINKE, A., STEIL, L., SCHULER, G. & ADAMS, V. 2015a. Diaphragm muscle weakness in mice is early-onset post-myocardial infarction and associated with elevated protein oxidation. *J Appl Physiol (1985),* 118**,** 11-9.

BOWEN, T. S., ROLIM, N. P., FISCHER, T., BAEKKERUD, F. H., MEDEIROS, A., WERNER, S., BRØNSTAD, E., ROGNMO, O., MANGNER, N., LINKE, A., SCHULER, G., SILVA, G. J., WISLØFF, U. & ADAMS, V. 2015b. Heart failure with preserved ejection fraction induces molecular, mitochondrial, histological, and functional alterations in rat respiratory and limb skeletal muscle. *Eur J Heart Fail,* 17**,** 263-72.

BRADFORD, A., MCGUIRE, M. & O'HALLORAN, K. D. 2005. Does episodic hypoxia affect upper airway dilator muscle function? Implications for the pathophysiology of obstructive sleep apnoea. *Respir Physiol Neurobiol,* 147**,** 223-34.

BRANDES, R. P., WEISSMANN, N. & SCHRODER, K. 2014. Nox family NADPH oxidases: Molecular mechanisms of activation. *Free Radic Biol Med,* 76**,** 208-26.

BURNS, D. P., ROWLAND, J., CANAVAN, L., MURPHY, K. H., BRANNOCK, M., O'MALLEY, D., O'HALLORAN, K. D. & EDGE, D. 2017. Restoration of pharyngeal dilator muscle force in dystrophin-deficient (mdx) mice following co-treatment with neutralizing interleukin-6 receptor antibodies and urocortin 2. *Exp Physiol,* 102**,** 1177-1193.

CARRERA, M., BARBÉ, F., SAULEDA, J., TOMÁS, M., GÓMEZ, C. & AGUSTÍ, A. G. 1999. Patients with obstructive sleep apnea exhibit genioglossus dysfunction that is normalized after treatment with continuous positive airway pressure. *Am J Respir Crit Care Med,* 159**,** 1960-6.

CHEN, R., LAI, U. H., ZHU, L., SINGH, A., AHMED, M. & FORSYTH, N. R. 2018. Reactive Oxygen Species Formation in the Brain at Different Oxygen Levels: The Role of Hypoxia Inducible Factors. *Front Cell Dev Biol,* 6**,** 132.

COIRAULT, C., GUELLICH, A., BARBRY, T., SAMUEL, J. L., RIOU, B. & LECARPENTIER, Y. 2007. Oxidative stress of myosin contributes to skeletal muscle dysfunction in rats with chronic heart failure. *Am J Physiol Heart Circ Physiol,* 292**,** H1009-17.

CULLY, T. R. & RODNEY, G. G. 2020. Nox4 - RyR1 - Nox2: Regulators of micro-domain signaling in skeletal muscle. *Redox Biol,* 36**,** 101557.

DE PAULA BROTTO, M., VAN LEYEN, S. A., BROTTO, L. S., JIN, J. P., NOSEK, C. M. & NOSEK, T. M. 2001. Hypoxia/fatigue-induced degradation of troponin I and troponin C: new insights into physiologic muscle fatigue. *Pflugers Arch,* 442**,** 738-44.

DEGENS, H., BOSUTTI, A., GILLIVER, S. F., SLEVIN, M., VAN HEIJST, A. & WÜST, R. C. 2010. Changes in contractile properties of skinned single rat soleus and diaphragm fibres after chronic hypoxia. *Pflugers Arch,* 460**,** 863-73.

DIEBOLD, I., PETRY, A., HESS, J. & GORLACH, A. 2010. The NADPH oxidase subunit NOX4 is a new target gene of the hypoxia-inducible factor-1. *Mol Biol Cell,* 21**,** 2087-96.

DIEBOLD, I., PETRY, A., SABRANE, K., DJORDJEVIC, T., HESS, J. & GÖRLACH, A. 2012. The HIF1 target gene NOX2 promotes angiogenesis through urotensin-II. *J Cell Sci,* 125**,** 956-64.

DING, W. & LIU, Y. 2011. Genistein attenuates genioglossus muscle fatigue under chronic intermittent hypoxia by down-regulation of oxidative stress level and up-regulation of antioxidant enzyme activity through ERK1/2 signaling pathway. *Oral Dis,* 17**,** 677-84.

DOBROWOLNY, G., AUCELLO, M., RIZZUTO, E., BECCAFICO, S., MAMMUCARI, C., BONCOMPAGNI, S., BELIA, S., WANNENES, F., NICOLETTI, C., DEL PRETE, Z., ROSENTHAL, N., MOLINARO, M., PROTASI, F., FANÒ, G., SANDRI, M. & MUSARÒ, A. 2008. Skeletal muscle is a primary target of SOD1G93A-mediated toxicity. *Cell Metab,* 8**,** 425-36.

DOCIO, I., OLEA, E., PRIETO, L. J., GALLEGO-MARTIN, T., OBESO, A., GOMEZ-NIÑO, A. & ROCHER, A. 2018. Guinea Pig as a Model to Study the Carotid Body Mediated Chronic Intermittent Hypoxia Effects. *Front Physiol,* 9**,** 694.

DUNLEAVY, M., BRADFORD, A. & O'HALLORAN, K. D. 2008. Oxidative stress impairs upper airway muscle endurance in an animal model of sleep-disordered breathing. *Adv Exp Med Biol,* 605**,** 458-62.

DUTKA, T. L., MOLLICA, J. P., LAMBOLEY, C. R., WEERAKKODY, V. C., GREENING, D. W., POSTERINO, G. S., MURPHY, R. M. & LAMB, G. D. 2017. S-nitrosylation and S-glutathionylation of Cys134 on troponin I have opposing competitive actions on Ca(2+) sensitivity in rat fast-twitch muscle fibers. *Am J Physiol Cell Physiol,* 312**,** C316-c327.

EDWARDS, J. N., MACDONALD, W. A., VAN DER POEL, C. & STEPHENSON, D. G. 2007. O2(*-) production at 37 degrees C plays a critical role in depressing tetanic force of isolated rat and mouse skeletal muscle. *Am J Physiol Cell Physiol,* 293**,** C650-60.

ESPINOSA, A., LEIVA, A., PEÑA, M., MÜLLER, M., DEBANDI, A., HIDALGO, C., CARRASCO, M. A. & JAIMOVICH, E. 2006. Myotube depolarization generates reactive oxygen species through

NAD(P)H oxidase; ROS-elicited Ca2+ stimulates ERK, CREB, early genes. *J Cell Physiol,* 209**,** 379-88.

FAN, L. M., GENG, L., CAHILL-SMITH, S., LIU, F., DOUGLAS, G., MCKENZIE, C. A., SMITH, C., BROOKS, G., CHANNON, K. M. & LI, J. M. 2019. Nox2 contributes to age-related oxidative damage to neurons and the cerebral vasculature. *J Clin Invest,* 129**,** 3374-3386.

FERREIRA, L. F. & LAITANO, O. 2016. Regulation of NADPH oxidases in skeletal muscle. *Free Radic Biol Med,* 98**,** 18-28.

GALLEGO-MARTIN, T., FARRÉ, R., ALMENDROS, I., GONZALEZ-OBESO, E. & OBESO, A. 2017. Chronic intermittent hypoxia mimicking sleep apnoea increases spontaneous tumorigenesis in mice. *Eur Respir J,* 49.

GAMBOA, J. L. & ANDRADE, F. H. 2010. Mitochondrial content and distribution changes specific to mouse diaphragm after chronic normobaric hypoxia. *Am J Physiol Regul Integr Comp Physiol,* 298**,** R575-83.

GAO, J., DING, X. S., ZHANG, Y. M., DAI, D. Z., LIU, M., ZHANG, C. & DAI, Y. 2013. Hypoxia/oxidative stress alters the pharmacokinetics of CPU86017-RS through mitochondrial dysfunction and NADPH oxidase activation. *Acta Pharmacol Sin,* 34**,** 1575-84.

GEISZT, M., KAPUS, A., NÉMET, K., FARKAS, L. & LIGETI, E. 1997. Regulation of capacitative Ca2+ influx in human neutrophil granulocytes. Alterations in chronic granulomatous disease. *J Biol Chem,* 272**,** 26471-8.

GUERRA, L., CERBAI, E., GESSI, S., BOREA, P. A. & MUGELLI, A. 1996. The effect of oxygen free radicals on calcium current and dihydropyridine binding sites in guinea-pig ventricular myocytes. *British Journal of Pharmacology,* 118**,** 1278-1284.

GÖLLNER, M., IHRIG-BIEDERT, I., PETERMANN, V., SAURIN, S., OELZE, M., KRÖLLER-SCHÖN, S., VUJACIC-MIRSKI, K., KUNTIC, M., PAUTZ, A., DAIBER, A. & KLEINERT, H. 2020. NOX2ko Mice Show Largely Increased Expression of a Mutated NOX2 mRNA Encoding an Inactive NOX2 Protein. *Antioxidants (Basel),* 9.

HANDAYANINGSIH, A. E., IGUCHI, G., FUKUOKA, H., NISHIZAWA, H., TAKAHASHI, M., YAMAMOTO, M., HERNINGTYAS, E. H., OKIMURA, Y., KAJI, H., CHIHARA, K., SEINO, S. & TAKAHASHI, Y. 2011. Reactive oxygen species play an essential role in IGF-I signaling and IGF-I-induced myocyte hypertrophy in C2C12 myocytes. *Endocrinology,* 152**,** 912-21.

HAYASHI, T., YAMASHITA, C., MATSUMOTO, C., KWAK, C. J., FUJII, K., HIRATA, T., MIYAMURA, M., MORI, T., UKIMURA, A., OKADA, Y., MATSUMURA, Y. & KITAURA, Y. 2008. Role of gp91phox-containing NADPH oxidase in left ventricular remodeling induced by intermittent hypoxic stress. *Am J Physiol Heart Circ Physiol,* 294**,** H2197-203.

HENRÍQUEZ-OLGUIN, C., KNUDSEN, J. R., RAUN, S. H., LI, Z., DALBRAM, E., TREEBAK, J. T., SYLOW, L., HOLMDAHL, R., RICHTER, E. A., JAIMOVICH, E. & JENSEN, T. E. 2019. Cytosolic ROS production by NADPH oxidase 2 regulates muscle glucose uptake during exercise. *Nat Commun,* 10**,** 4623.

HENRÍQUEZ-OLGUÍN, C., ALTAMIRANO, F., VALLADARES, D., LÓPEZ, J. R., ALLEN, P. D. & JAIMOVICH, E. 2015. Altered ROS production, NF-κB activation and interleukin-6 gene expression induced by electrical stimulation in dystrophic mdx skeletal muscle cells. *Biochim Biophys Acta,* 1852**,** 1410-9.

HIDALGO, C., SANCHEZ, G., BARRIENTOS, G. & ARACENA-PARKS, P. 2006. A transverse tubule NADPH oxidase activity stimulates calcium release from isolated triads via ryanodine receptor type 1 S -glutathionylation. *J Biol Chem,* 281**,** 26473-82.

HOOD, D. A., MEMME, J. M., OLIVEIRA, A. N. & TRIOLO, M. 2019. Maintenance of Skeletal Muscle Mitochondria in Health, Exercise, and Aging. *Annu Rev Physiol,* 81**,** 19-41.

HOPPS, E., CANINO, B., CALANDRINO, V., MONTANA, M., LO PRESTI, R. & CAIMI, G. 2014. Lipid peroxidation and protein oxidation are related to the severity of OSAS. *Eur Rev Med Pharmacol Sci,* 18**,** 3773-8.

HORI, Y. S., KUNO, A., HOSODA, R., TANNO, M., MIURA, T., SHIMAMOTO, K. & HORIO, Y. 2011. Resveratrol ameliorates muscular pathology in the dystrophic mdx mouse, a model for Duchenne muscular dystrophy. *J Pharmacol Exp Ther,* 338**,** 784-94.

HORN, A., VAN DER MEULEN, J. H., DEFOUR, A., HOGARTH, M., SREETAMA, S. C., REED, A., SCHEFFER, L., CHANDEL, N. S. & JAISWAL, J. K. 2017. Mitochondrial redox signaling enables repair of injured skeletal muscle cells. *Sci Signal,* 10.

HUI-GUO, L., KUI, L., YAN-NING, Z. & YONG-JIAN, X. 2010. Apocynin attenuate spatial learning deficits and oxidative responses to intermittent hypoxia. *Sleep Med,* 11**,** 205-12.

HUTCHINSON, D. S., CSIKASZ, R. I., YAMAMOTO, D. L., SHABALINA, I. G., WIKSTRÖM, P., WILCKE, M. & BENGTSSON, T. 2007. Diphenylene iodonium stimulates glucose uptake in skeletal muscle cells through mitochondrial complex I inhibition and activation of AMP-activated protein kinase. *Cell Signal,* 19**,** 1610-20.

JAVESHGHANI, D., MAGDER, S. A., BARREIRO, E., QUINN, M. T. & HUSSAIN, S. N. 2002. Molecular characterization of a superoxide-generating NAD(P)H oxidase in the ventilatory muscles. *Am J Respir Crit Care Med,* 165**,** 412-8.

JIA, S. S. & LIU, Y. H. 2010. Down-regulation of hypoxia inducible factor-1alpha: a possible explanation for the protective effects of estrogen on genioglossus fatigue resistance. *Eur J Oral Sci,* 118**,** 139-44.

JUN, J., SAVRANSKY, V., NANAYAKKARA, A., BEVANS, S., LI, J., SMITH, P. L. & POLOTSKY, V. Y. 2008. Intermittent hypoxia has organ-specific effects on oxidative stress. *Am J Physiol Regul Integr Comp Physiol,* 295**,** R1274-81.

KAWAKAMI, M. & OKABE, E. 1998. Superoxide anion radical-triggered Ca2+ release from cardiac sarcoplasmic reticulum through ryanodine receptor Ca2+ channel. *Mol Pharmacol,* 53**,** 497-503.

KENT, B. D., RYAN, S. & MCNICHOLAS, W. T. 2011. Obstructive sleep apnea and inflammation: relationship to cardiovascular co-morbidity. *Respir Physiol Neurobiol,* 178**,** 475-81.

KIM, Y., TRIOLO, M., ERLICH, A. T. & HOOD, D. A. 2019. Regulation of autophagic and mitophagic flux during chronic contractile activity-induced muscle adaptations. *Pflugers Arch,* 471**,** 431-440.

KOZAKOWSKA, M., PIETRASZEK-GREMPLEWICZ, K., JOZKOWICZ, A. & DULAK, J. 2015. The role of oxidative stress in skeletal muscle injury and regeneration: focus on antioxidant enzymes. *Journal of Muscle Research and Cell Motility,* 36**,** 377-393.

LAMB, G. D. & WESTERBLAD, H. 2011. Acute effects of reactive oxygen and nitrogen species on the contractile function of skeletal muscle. *J Physiol,* 589**,** 2119-27.

LAMBETH, J. D. 2004. NOX enzymes and the biology of reactive oxygen. *Nat Rev Immunol,* 4**,** 181-189.

LAVIE, L. 2003. Obstructive sleep apnoea syndrome--an oxidative stress disorder. *Sleep Med Rev,* 7**,** 35-51.

LEWIS, P., SHEEHAN, D., SOARES, R., VARELA COELHO, A. & O'HALLORAN, K. D. 2015. Chronic sustained hypoxia-induced redox remodeling causes contractile dysfunction in mouse sternohyoid muscle. *Frontiers in Physiology,* 6.

LIM, D. C., BRADY, D. C., SOANS, R., KIM, E. Y., VALVERDE, L., KEENAN, B. T., GUO, X., KIM, W. Y., PARK, M. J., GALANTE, R., SHACKLEFORD, J. A. & PACK, A. I. 2016. Different cyclical intermittent hypoxia severities have different effects on hippocampal microvasculature. *J Appl Physiol (1985),* 121**,** 78-88.

LIU, S. S., LIU, H. G., XIONG, S. D., NIU, R. J., XU, Y. J. & ZHANG, Z. X. 2005. [Effects of Shen-Mai injection on sternohyoid contractile properties in chronic intermittent hypoxia rat]. *Zhonghua Jie He He Hu Xi Za Zhi,* 28**,** 611-4.

LIU, X. H., HARLOW, L., GRAHAM, Z. A., BAUMAN, W. A. & CARDOZO, C. 2017. Spinal Cord Injury Leads to Hyperoxidation and Nitrosylation of Skeletal Muscle Ryanodine Receptor-1 Associated with Upregulation of Nicotinamide Adenine Dinucleotide Phosphate Oxidase 4. *J Neurotrauma,* 34**,** 2069-2074.

LIU, Y., HERNÁNDEZ-OCHOA, E. O., RANDALL, W. R. & SCHNEIDER, M. F. 2012. NOX2-dependent ROS is required for HDAC5 nuclear efflux and contributes to HDAC4 nuclear efflux during intense repetitive activity of fast skeletal muscle fibers. *Am J Physiol Cell Physiol,* 303**,** C334-47.

LIU, Y. H., HUANG, Y. & SHAO, X. 2009. Effects of estrogen on genioglossal muscle contractile properties and fiber-type distribution in chronic intermittent hypoxia rats. *Eur J Oral Sci,* 117**,** 685-90.

LOUREIRO, A. C. C., DO RÊGO-MONTEIRO, I. C., LOUZADA, R. A., ORTENZI, V. H., DE AGUIAR, A. P., DE ABREU, E. S., CAVALCANTI-DE-ALBUQUERQUE, J. P. A., HECHT, F., DE OLIVEIRA, A. C., CECCATTO, V. M., FORTUNATO, R. S. & CARVALHO, D. P. 2016. Differential Expression of NADPH Oxidases Depends on Skeletal Muscle Fiber Type in Rats. *Oxidative Medicine and Cellular Longevity,* 2016**,** 6738701.

LUCKING, E. F., O'HALLORAN, K. D. & JONES, J. F. 2014. Increased cardiac output contributes to the development of chronic intermittent hypoxia-induced hypertension. *Exp Physiol,* 99**,** 1312-24.

MARTINEZ, C. A., KERR, B., JIN, C., CISTULLI, P. A. & COOK, K. M. 2019. Obstructive Sleep Apnea Activates HIF-1 in a Hypoxia Dose-Dependent Manner in HCT116 Colorectal Carcinoma Cells. *Int J Mol Sci,* 20.

MCDONAGH, B., SAKELLARIOU, G. K., SMITH, N. T., BROWNRIDGE, P. & JACKSON, M. J. 2014. Differential cysteine labeling and global label-free proteomics reveals an altered metabolic state in skeletal muscle aging. *J Proteome Res,* 13**,** 5008-21.

MCDONALD, F. B., DEMPSEY, E. M. & O'HALLORAN, K. D. 2016. Early Life Exposure to Chronic Intermittent Hypoxia Primes Increased Susceptibility to Hypoxia-Induced Weakness in Rat Sternohyoid Muscle during Adulthood. *Frontiers in Physiology,* 7**,** 69.

MCDONALD, F. B., WILLIAMS, R., SHEEHAN, D. & O'HALLORAN, K. D. 2015. Early life exposure to chronic intermittent hypoxia causes upper airway dilator muscle weakness, which persists into young adulthood. *Exp Physiol,* 100**,** 947-66.

MURPHY, R. M., DUTKA, T. L. & LAMB, G. D. 2008. Hydroxyl radical and glutathione interactions alter calcium sensitivity and maximum force of the contractile apparatus in rat skeletal muscle fibres. *J Physiol,* 586**,** 2203-16.

NANDURI, J., VADDI, D. R., KHAN, S. A., WANG, N., MAKARENKO, V., SEMENZA, G. L. & PRABHAKAR, N. R. 2015. HIF-1α activation by intermittent hypoxia requires NADPH oxidase stimulation by xanthine oxidase. *PLoS One,* 10**,** e0119762.

NARENDRA, D. P. & YOULE, R. J. 2011. Targeting mitochondrial dysfunction: role for PINK1 and Parkin in mitochondrial quality control. *Antioxid Redox Signal,* 14**,** 1929-38.

NISBET, R. E., GRAVES, A. S., KLEINHENZ, D. J., RUPNOW, H. L., REED, A. L., FAN, T. H., MITCHELL, P. O., SUTLIFF, R. L. & HART, C. M. 2009. The role of NADPH oxidase in chronic intermittent hypoxia-induced pulmonary hypertension in mice. *Am J Respir Cell Mol Biol,* 40**,** 601-9.

OTTENHEIJM, C. A., HEUNKS, L. M., GERAEDTS, M. C. & DEKHUIJZEN, P. N. 2006. Hypoxia-induced skeletal muscle fiber dysfunction: role for reactive nitrogen species. *Am J Physiol Lung Cell Mol Physiol,* 290**,** L127-35.

OTTENHEIJM, C. A., HEUNKS, L. M., SIECK, G. C., ZHAN, W. Z., JANSEN, S. M., DEGENS, H., DE BOO, T. & DEKHUIJZEN, P. N. 2005. Diaphragm dysfunction in chronic obstructive pulmonary disease. *Am J Respir Crit Care Med,* 172**,** 200-5.

PAE, E. K., WU, J., NGUYEN, D., MONTI, R. & HARPER, R. M. 2005. Geniohyoid muscle properties and myosin heavy chain composition are altered after short-term intermittent hypoxic exposure. *J Appl Physiol (1985),* 98**,** 889-94.

PAL, R., PALMIERI, M., LOEHR, J. A., LI, S., ABO-ZAHRAH, R., MONROE, T. O., THAKUR, P. B., SARDIELLO, M. & RODNEY, G. G. 2014. Src-dependent impairment of autophagy by oxidative stress in a mouse model of Duchenne muscular dystrophy. *Nat Commun,* 5**,** 4425.

PENDYALA, S., GORSHKOVA, I. A., USATYUK, P. V., HE, D., PENNATHUR, A., LAMBETH, J. D., THANNICKAL, V. J. & NATARAJAN, V. 2009. Role of Nox4 and Nox2 in hyperoxia-induced reactive oxygen species generation and migration of human lung endothelial cells. *Antioxid Redox Signal,* 11**,** 747-64.

PENG, Y. J., NANDURI, J., YUAN, G., WANG, N., DENERIS, E., PENDYALA, S., NATARAJAN, V., KUMAR, G. K. & PRABHAKAR, N. R. 2009. NADPH oxidase is required for the sensory plasticity of the carotid body by chronic intermittent hypoxia. *J Neurosci,* 29**,** 4903-10.

PENG, Y. J., RAGHURAMAN, G., KHAN, S. A., KUMAR, G. K. & PRABHAKAR, N. R. 2011. Angiotensin II evokes sensory long-term facilitation of the carotid body via NADPH oxidase. *J Appl Physiol (1985),* 111**,** 964-70.

PENG, Y. J., YUAN, G., JACONO, F. J., KUMAR, G. K. & PRABHAKAR, N. R. 2006. 5-HT evokes sensory long-term facilitation of rodent carotid body via activation of NADPH oxidase. *J Physiol,* 576**,** 289-95.

PETROF, B. J., HENDRICKS, J. C. & PACK, A. I. 1996. Does upper airway muscle injury trigger a vicious cycle in obstructive sleep apnea? A hypothesis. *Sleep,* 19**,** 465-71.

PETROF, B. J., PACK, A. I., KELLY, A. M., EBY, J. & HENDRICKS, J. C. 1994. Pharyngeal myopathy of loaded upper airway in dogs with sleep apnea. *J Appl Physiol (1985),* 76**,** 1746-52.

PIAO, Y. J., SEO, Y. H., HONG, F., KIM, J. H., KIM, Y. J., KANG, M. H., KIM, B. S., JO, S. A., JO, I., JUE, D. M., KANG, I., HA, J. & KIM, S. S. 2005. Nox 2 stimulates muscle differentiation via NF-kappaB/iNOS pathway. *Free Radic Biol Med,* 38**,** 989-1001.

PINTO, J. R., DE SOUSA, V. P. & SORENSON, M. M. 2011. Redox state of troponin C cysteine in the D/E helix alters the C-domain affinity for the thin filament of vertebrate striated muscle. *Biochim Biophys Acta,* 1810**,** 391-7.

RAGHURAMAN, G., RAI, V., PENG, Y. J., PRABHAKAR, N. R. & KUMAR, G. K. 2009. Pattern-specific sustained activation of tyrosine hydroxylase by intermittent hypoxia: role of reactive oxygen species-dependent downregulation of protein phosphatase 2A and upregulation of protein kinases. *Antioxid Redox Signal,* 11**,** 1777-89.

REGAN, J. N., MIKESELL, C., REIKEN, S., XU, H., MARKS, A. R., MOHAMMAD, K. S., GUISE, T. A. & WANING, D. L. 2017. Osteolytic Breast Cancer Causes Skeletal Muscle Weakness in an Immunocompetent Syngeneic Mouse Model. *Frontiers in Endocrinology,* 8.

REID, M. B., HAACK, K. E., FRANCHEK, K. M., VALBERG, P. A., KOBZIK, L. & WEST, M. S. 1992. Reactive oxygen in skeletal muscle. I. Intracellular oxidant kinetics and fatigue in vitro. *J Appl Physiol (1985),* 73**,** 1797-804.

REZENDE, F., LÖWE, O., HELFINGER, V., PRIOR, K. K., WALTER, M., ZUKUNFT, S., FLEMING, I., WEISSMANN, N., BRANDES, R. P. & SCHRÖDER, K. 2016. Unchanged NADPH Oxidase Activity in Nox1-Nox2-Nox4 Triple Knockout Mice: What Do NADPH-Stimulated Chemiluminescence Assays Really Detect? *Antioxid Redox Signal,* 24**,** 392-9.

SABOISKY, J. P., STASHUK, D. W., HAMILTON-WRIGHT, A., CARUSONA, A. L., CAMPANA, L. M., TRINDER, J., ECKERT, D. J., JORDAN, A. S., MCSHARRY, D. G., WHITE, D. P., NANDEDKAR, S., DAVID, W. S. & MALHOTRA, A. 2012. Neurogenic changes in the upper airway of patients with obstructive sleep apnea. *Am J Respir Crit Care Med,* 185**,** 322-9.

SAKELLARIOU, G. K., VASILAKI, A., PALOMERO, J., KAYANI, A., ZIBRIK, L., MCARDLE, A. & JACKSON, M. J. 2013. Studies of mitochondrial and nonmitochondrial sources implicate nicotinamide adenine dinucleotide phosphate oxidase(s) in the increased skeletal muscle superoxide generation that occurs during contractile activity. *Antioxid Redox Signal,* 18**,** 603-21.

SANDIFORD, S. D., KENNEDY, K. A., XIE, X., PICKERING, J. G. & LI, S. S. 2014. Dual oxidase maturation factor 1 (DUOXA1) overexpression increases reactive oxygen species production and inhibits murine muscle satellite cell differentiation. *Cell Commun Signal,* 12**,** 5.

SERRANDER, L., CARTIER, L., BEDARD, K., BANFI, B., LARDY, B., PLASTRE, O., SIENKIEWICZ, A., FÓRRÓ, L., SCHLEGEL, W. & KRAUSE, K.-H. 2007. NOX4 activity is determined by mRNA levels and reveals a unique pattern of ROS generation. *Biochemical Journal,* 406**,** 105-114.

SKELLY, J. R., BRADFORD, A., JONES, J. F. & O'HALLORAN, K. D. 2010. Superoxide scavengers improve rat pharyngeal dilator muscle performance. *Am J Respir Cell Mol Biol,* 42**,** 725-31.

SKELLY, J. R., EDGE, D., SHORTT, C. M., JONES, J. F., BRADFORD, A. & O'HALLORAN, K. D. 2012a. Respiratory control and sternohyoid muscle structure and function in aged male rats: decreased susceptibility to chronic intermittent hypoxia. *Respir Physiol Neurobiol,* 180**,** 175-82.

SKELLY, J. R., EDGE, D., SHORTT, C. M., JONES, J. F., BRADFORD, A. & O'HALLORAN, K. D. 2012b. Tempol ameliorates pharyngeal dilator muscle dysfunction in a rodent model of chronic intermittent hypoxia. *Am J Respir Cell Mol Biol,* 46**,** 139-48.

SKELLY, J. R., ROWAN, S. C., JONES, J. F. & O'HALLORAN, K. D. 2013. Upper airway dilator muscle weakness following intermittent and sustained hypoxia in the rat: effects of a superoxide scavenger. *Physiol Res,* 62**,** 187-96.

SMIRNE, S., IANNACCONE, S., FERINI-STRAMBI, L., COMOLA, M., COLOMBO, E. & NEMNI, R. 1991. Muscle fibre type and habitual snoring. *Lancet,* 337**,** 597-9.

SMITH, L. R. & BARTON, E. R. 2018. Regulation of fibrosis in muscular dystrophy. *Matrix Biol,* 68-69**,** 602-615.

SMUDER, A. J., KAVAZIS, A. N., HUDSON, M. B., NELSON, W. B. & POWERS, S. K. 2010. Oxidation enhances myofibrillar protein degradation via calpain and caspase-3. *Free Radic Biol Med,* 49**,** 1152-60.

SPECHT, K. S., KANT, S., ADDINGTON, A. K., MCMILLAN, R. P., HULVER, M. W., LEARNARD, H., CAMPBELL, M., DONNELLY, S. R., CALIZ, A. D., PEI, Y., REIF, M. M., BOND, J. M., DEMARCO, A., CRAIGE, B., KEANEY, J. F., JR. & CRAIGE, S. M. 2021. Nox4 mediates skeletal muscle metabolic responses to exercise. *Mol Metab,* 45**,** 101160.

SPURNEY, C. F., KNOBLACH, S., PISTILLI, E. E., NAGARAJU, K., MARTIN, G. R. & HOFFMAN, E. P. 2008. Dystrophin-deficient cardiomyopathy in mouse: expression of Nox4 and Lox are associated with fibrosis and altered functional parameters in the heart. *Neuromuscul Disord,* 18**,** 371-81.

SRIRAM, S., SUBRAMANIAN, S., SATHIAKUMAR, D., VENKATESH, R., SALERNO, M. S., MCFARLANE, C. D., KAMBADUR, R. & SHARMA, M. 2011. Modulation of reactive oxygen species in skeletal muscle by myostatin is mediated through NF-κB. *Aging Cell,* 10**,** 931-48.

SULLIVAN-GUNN, M. J. & LEWANDOWSKI, P. A. 2013. Elevated hydrogen peroxide and decreased catalase and glutathione peroxidase protection are associated with aging sarcopenia. *BMC Geriatr,* 13**,** 104.

SUN, Q. A., HESS, D. T., NOGUEIRA, L., YONG, S., BOWLES, D. E., EU, J., LAURITA, K. R., MEISSNER, G. & STAMLER, J. S. 2011. Oxygen-coupled redox regulation of the skeletal muscle ryanodine receptor-Ca2+ release channel by NADPH oxidase 4. *Proc Natl Acad Sci U S A,* 108**,** 16098-103.

SÉRLÈS, F., CÔTÉ, C., SIMONEAU, J.-A., PIERRE, S. S. & MARC, I. 1996. Upper airway collapsibility, and contractile and metabolic characteristics of musculus uvulae. *The FASEB Journal,* 10**,** 897-904.

TOUYZ, R. M. 2008. Apocynin, NADPH oxidase, and vascular cells: a complex matter. *Hypertension.* United States.

VAN DER POEL, C., EDWARDS, J. N., MACDONALD, W. A. & STEPHENSON, D. G. 2007. Mitochondrial superoxide production in skeletal muscle fibers of the rat and decreased fiber excitability. *Am J Physiol Cell Physiol,* 292**,** C1353-60.

WANG, N., SHI, X. F., KHAN, S. A., WANG, B., SEMENZA, G. L., PRABHAKAR, N. R. & NANDURI, J. 2020a. Hypoxia-inducible factor-1 mediates pancreatic β-cell dysfunction by intermittent hypoxia. *Am J Physiol Cell Physiol,* 319**,** C922-c932.

WANG, W., DING, W., HUANG, H., ZHU, Y., DING, N., FENG, G. & ZHANG, X. 2020b. The role of mitophagy in the mechanism of genioglossal dysfunction caused by chronic intermittent hypoxia and the protective effect of adiponectin. *Sleep Breath*.

WANG, W. J., LU, G., DING, N., HUANG, H. P., DING, W. X. & ZHANG, X. L. 2013. Adiponectin alleviates contractile dysfunction of genioglossus in rats exposed to chronic intermittent hypoxia. *Chin Med J (Engl),* 126**,** 3259-63.

WESTERBLAD, H. & ALLEN, D. G. 1991. Changes of myoplasmic calcium concentration during fatigue in single mouse muscle fibers. *J Gen Physiol,* 98**,** 615-35.

WHITEHEAD, N. P., YEUNG, E. W., FROEHNER, S. C. & ALLEN, D. G. 2010. Skeletal muscle NADPH oxidase is increased and triggers stretch-induced damage in the mdx mouse. *PLoS One,* 5**,** e15354.

WILLIAMS, R., LEMAIRE, P., LEWIS, P., MCDONALD, F. B., LUCKING, E., HOGAN, S., SHEEHAN, D., HEALY, V. & O'HALLORAN, K. D. 2015a. Chronic intermittent hypoxia increases rat sternohyoid muscle NADPH oxidase expression with attendant modest oxidative stress. *Front Physiol,* 6**,** 15.

WILLIAMS, R., LEMAIRE, P., LEWIS, P., MCDONALD, F. B., LUCKING, E., HOGAN, S., SHEEHAN, D., HEALY, V. & O'HALLORAN, K. D. 2015b. Chronic intermittent hypoxia increases rat sternohyoid muscle NADPH oxidase expression with attendant modest oxidative stress. *Frontiers in Physiology,* 6.

XIA, R., WEBB, J. A., GNALL, L. L., CUTLER, K. & ABRAMSON, J. J. 2003. Skeletal muscle sarcoplasmic reticulum contains a NADH-dependent oxidase that generates superoxide. *Am J Physiol Cell Physiol,* 285**,** C215-21.

YAMADA, T., ABE, M., LEE, J., TATEBAYASHI, D., HIMORI, K., KANZAKI, K., WADA, M., BRUTON, J. D., WESTERBLAD, H. & LANNER, J. T. 2015. Muscle dysfunction associated with adjuvant-induced arthritis is prevented by antioxidant treatment. *Skelet Muscle,* 5**,** 20.

YOU, Y. H., OKADA, S., LY, S., JANDELEIT-DAHM, K., BARIT, D., NAMIKOSHI, T. & SHARMA, K. 2013. Role of Nox2 in diabetic kidney disease. *Am J Physiol Renal Physiol,* 304**,** F840-8.

YUAN, G., KHAN, S. A., LUO, W., NANDURI, J., SEMENZA, G. L. & PRABHAKAR, N. R. 2011. Hypoxia-inducible factor 1 mediates increased expression of NADPH oxidase-2 in response to intermittent hypoxia. *J Cell Physiol,* 226**,** 2925-33.

YUN, Z., LIN, Q. & GIACCIA, A. J. 2005. Adaptive myogenesis under hypoxia. *Mol Cell Biol,* 25**,** 3040-55.

ZHAN, G., SERRANO, F., FENIK, P., HSU, R., KONG, L., PRATICO, D., KLANN, E. & VEASEY, S. C. 2005. NADPH oxidase mediates hypersomnolence and brain oxidative injury in a murine model of sleep apnea. *Am J Respir Crit Care Med,* 172**,** 921-9.

ZHOU, J. & LIU, Y. 2013. Effects of genistein and estrogen on the genioglossus in rats exposed to chronic intermittent hypoxia may be HIF-1α dependent. *Oral Dis,* 19**,** 702-11.

Chapter 5. NADPH oxidase-2 is necessary for chronic intermittent hypoxia-induced diaphragm muscle weakness.

5.1 Aims and hypothesis

Study aims:

To examine the effect of a 2-week exposure to CIH on diaphragm muscle function in adult male mice.

To characterise the effect of exposure to CIH on NOX enzymes in diaphragm muscle at multiple levels of regulation: mRNA, protein and activity.

To examine the effect of exposure to CIH on indices of oxidative stress and antioxidant capacity in diaphragm muscle.

To examine the effect of exposure to CIH on the mRNA expression of redox-sensitive genes pivotal in the regulation of skeletal muscle form and function.

To assess the contribution of NOX2 to CIH-induced alterations to diaphragm muscle function using pharmacological and transgenic approaches.

Study hypothesis:

We hypothesised that 2 weeks of exposure to CIH would result in diaphragm muscle mal-adaptation, which would manifest as muscle weakness, increased expression and/or activity of NOX enzymes, altered redox balance and a ROS-dependent alteration to the expression of genes important in skeletal muscle contractile performance.

Furthermore, we postulated that these alterations would be underpinned by a NOX2-derived ROS-dependent mechanism, amenable to blockade by supplementation with apocynin (putative NOX2 inhibitor) and NOX2 knock-out.

5.2 Materials and methods

Diaphragm muscle function was examined *ex vivo*, as described in section 2.5.

mRNA expression was assessed by qRT-PCR, as described in section 2.6.

Protein expression of NOX subunits was determined by Western blot, as described in section 2.7.

Spectrophotometric assays were used to measure the levels of lipid peroxidation (TBARS), and citrate synthase and NOX enzyme activities, as described in section 2.8.

Cell signalling assays were used to examine key pathways involved in the regulation of skeletal muscle form and function, as described in section 2.9.

5.3. Results

5.3.1 Diaphragm muscle contractile function ex vivo

Diaphragm twitch kinetics (P_t, CT and ½ RT) and isotonic contractile parameters (Pmax, Wmax, Smax and Vmax) are shown in Table 5.1. Diaphragm twitch force (P_t) was reduced following 2 weeks of exposure to CIH compared to sham mice (*P* = 0.0173; Table 5.1), however this did not reach the threshold for statistical significance. The administration of apocynin (2mM) in the drinking water throughout the exposure to CIH prevented the CIH-induced decrease in twitch force (*P* = 0.0043; Table 5.1). Exposure to CIH had no effect on P_t in NOX2 KO mice exposed to CIH compared to NOX2 KO sham mice (*P* = 0.1107; Table 5.1). Similarly, genetic knock-out of NOX2 resulted in no difference in P_t compared to wild-type sham mice (*P* = 0.3106; Table 5.1). Twitch contraction time (CT) and half-relaxation time (½ RT) were unaffected by exposure to CIH in both wild-type (Sham *vs.* CIH; CT, *P* = 0.0.4989; ½ RT, *P* = 0.9863; Table 5.1) and NOX2 KO mice (NOX2 KO sham *vs.* NOX2 KO CIH; CT, *P* = 0.8502; ½ RT, P = 0.8482; Table 5.1). Similarly, the administration of apocynin during the exposure to CIH resulted in no significant difference in these parameters (CIH *vs.* CIH + APO; CT, *P* = 0.3984; ½ RT, *P* = 0.4109; Table 5.1). CT was significantly decreased in NOX2 KO sham mice compared to wild-type sham mice (*P* = 0.0005; Table 5.1); ½ RT remained unchanged (*P* = 0.0246; Table 5.1).

	Sham (n = 8)	CIH (n = 8)	CIH + APO (n = 9)	NOX2 KO sham (n = 9)	NOX2 KO CIH (n = 9)	Sham *vs* CIH (P value)	CIH *vs* CIH + APO (P value)	NOX2 KO sham *vs* NOX2 KO CIH (P value)	Sham *vs* NOX2 KO sham (P value)
P_t (N/cm^2)	2.62 ± 0.89	1.63 ± 0.31	4.06 ± 1.89$^{\#}$	3.50 ± 2.30	5.52 ± 2.75	0.0173	**0.0043$^{\#}$**	0.1107	0.3106
CT (ms)	15.69 ±0.96	16.69 ± 3.87	18.17 ± 3.14	12.28 ± 2.00$^{£}$	12.44 ± 1.67	0.4989	0.3984	0.8502	**0.0005$^{£}$**
½ RT (ms)	19.69 ± 7.82	19.63 ± 6.39	17.50 ± 3.79	13.39 ± 5.41	12.56 ± 5.04	0.9863	0.4109	0.8482	0.0246
Wmax (J/cm^2)	1.60 ± 0.85	0.63 ± 0.21*	1.69 ± 0.84$^{\#}$	2.42 ± 0.67	2.16 ± 0.60	**0.0006***	**0.0052$^{\#}$**	0.3923	0.0927
Pmax (W/cm^2)	12.20 ± 3.49	6.57 ± 2.35*	13.60 ± 4.55$^{\#}$	18.74 ± 4.61$^{£}$	15.57 ± 5.02	**0.0020***	**0.0014$^{\#}$**	0.1821	**0.0053$^{£}$**
Smax (L/L_o)	1.16 ± 0.26	1.21 ± 0.21	1.31 ± 0.25	0.99 ± 0.13	1.06 ± 0.20	0.1417	0.0828	0.1148	0.1343
Vmax (L/L_0)	4.78 ± 1.57	3.59 ± 1.19	4.51 ± 0.95	4.53 ± 1.40	3.98 ± 1.27	0.1304	0.0745	0.3958	0.7291

Table 5.1 *Ex vivo* diaphragm muscle contractile parameters. *Definition of abbreviations*: P_t, isometric twitch force; CT, contraction time; 1⁄2 RT, half-relaxation time; Wmax, maximum mechanical work; Pmax, maximum mechanical power; Smax, maximum shortening; Vmax, maximum shortening velocity; L_o, optimum length. Values are expressed as mean ± SD. Data sets which were normally distributed and of equal variance were statistically compared using unpaired two-tailed Student's *t* test. Welch's correction was applied in the case of unequal variance. Data, which were not normally distributed, were compared using Mann Whitney non-parametric tests. Bolded numbers highlight statistical significance ($P < 0.0125$). Relevant comparisons are denoted as follows: * CIH significantly different from corresponding sham values; $^{\#}$ APO + CIH significantly different from corresponding CIH values; $^{£}$ NOX2 KO sham significantly different from corresponding sham values.

Figure 5.1 shows representative original traces for sham (grey), CIH (black), CIH + APO (blue), NOX2 KO sham (pink) and NOX2 KO CIH (red) tetanic contractions (A). 2 weeks of exposure to CIH significantly decreased the force-generating capacity of the diaphragm compared to sham mice (P = 0.0002; Fig 5.1; B). Exposure to CIH resulted in a ~45% decrease in peak specific force of the diaphragm compared to sham mice. Apocynin administration throughout the exposure to CIH successfully ameliorated CIH-induced muscle weakness (P = 0.0003; Fig 5.1; B). Moreover, there was no difference in the tetanic force produced by NOX2 KO mice exposed to CIH compared to NOX2 KO sham controls (P = 0.4613; Fig 5.1; B), revealing a specific role for NOX2 in CIH-induced diaphragm muscle weakness. Tetanic force was increased by ~47% in NOX2 KO sham mice compared to wild-type sham mice, although this increase did not reach the threshold for statistical significance when corrections for multiple comparisons was applied (P = 0.0111; Fig 5.1; B).

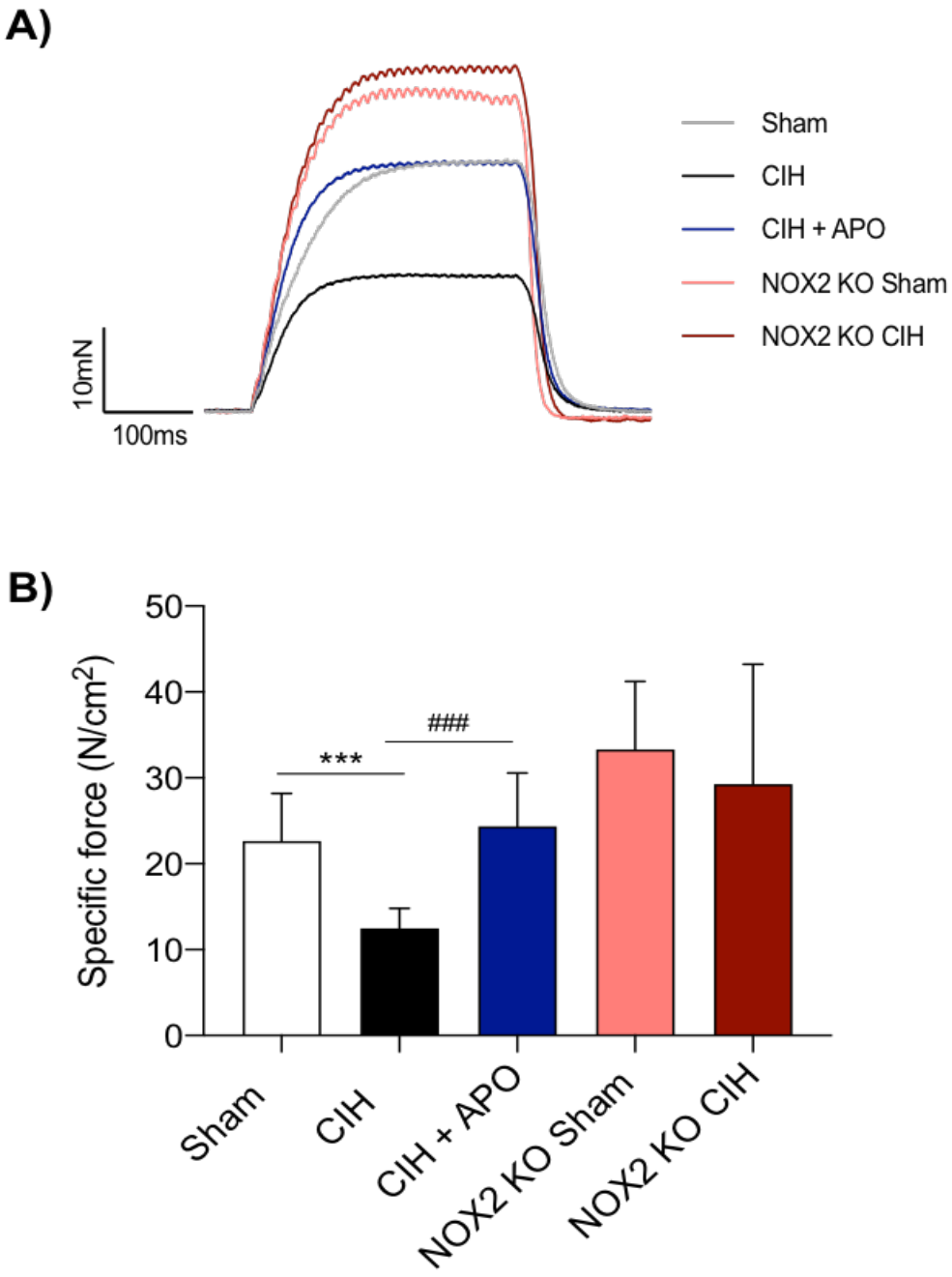

Figure 5.1 *Ex vivo* diaphragm muscle contractile force. A) Original traces of *ex vivo* diaphragm muscle tetanic contractions for sham (grey), CIH (black), CIH + APO (blue), NOX2 KO sham (pink) and NOX2 KO CIH (red) preparations. **B)** Group data for diaphragm muscle tetanic force, normalised for muscle CSA, in sham (n = 8), CIH (n = 8), CIH + APO (n = 9), NOX2 KO Sham (n = 9) and NOX2 KO CIH (n = 9) mice. Tetanic force was measured following stimulation at 100 Hz *ex vivo*. Values are expressed as mean ± SD. Data sets which were normally distributed and of equal variance were statistically compared using unpaired two-tailed Student's *t* test. Welch's correction was applied in the case of unequal variance. Data, which were not normally distributed, were compared using Mann Whitney non-parametric tests. Statistical significance was taken at $P < 0.0125$. Relevant comparisons are denoted as follows: * CIH *vs.* sham, *** $P < 0.001$; $^{\#}$ APO + CIH *vs.* CIH, $^{\#\#\#}$ $P <$ 0.001.

Figure 5.2 shows original traces of *ex vivo* diaphragm muscle maximum unloaded shortening for sham (grey), CIH (black), CIH + APO (blue), NOX2 KO sham (pink) and NOX2 KO CIH (red) preparations (A). Figure 5.2; B, C and D show the diaphragm power-load relationship. This is the power generated by the diaphragm over a range of incremental loads on the muscle between 0-100% of the peak force-generating capacity (Fmax), determined at the beginning of the protocol. Exposure to CIH significantly decreased the power-generating capacity of the diaphragm muscle over a range of loads compared to sham mice ($P < 0.0001$; repeated measures two-way ANOVA; Fig 5.2; B). *Post-hoc* analysis revealed a statistically significant decrease in the power-generating capacity of the diaphragm following exposure to CIH at 20% (*$P < 0.05$), 30% (**$P < 0.01$), 40% (**$P < 0.01$) and 60% (*$P < 0.05$) load compared to sham mice (Fig 5.2; B). The administration of apocynin throughout the exposure to CIH prevented the CIH-induced decrease in the power-generating capacity of the diaphragm over a range of loads compared to mice exposed to CIH alone ($P < 0.0001$; Fig 5.2; B). *Post-hoc* analysis revealed a statistically significant increase in the power-generating capacity of the diaphragm following treatment with apocynin throughout the exposure to CIH at 10% - 60% load compared to CIH-exposed mice (Fig 5.2; B). Peak power (Pmax) was measured and typically occurred between 30% and 40% load. Pmax was reduced following exposure to CIH compared to sham mice ($P = 0.0020$; Table 5.1); apocynin administration significantly prevented the CIH-induced decrease in Pmax ($P = 0.0014$; Table 5.1). Exposure to CIH reduced the power-generating capacity of the diaphragm in NOX2 KO mice over the range of loads examined compared to NOX2 KO sham controls ($P = 0.0020$; Fig 5.2; C). Pmax was unaffected by exposure to CIH in NOX2 KO mice ($P = 0.1821$; Table 5.1). Genetic knock-out of NOX2 significantly increased the power-generating capacity of the diaphragm over the range of loads examined compared to wild-type sham mice ($P = 0.0271$; Fig 5.2; D). Pmax was significantly increased in NOX2 KO sham compared with wild-type sham mice ($P = 0.0053$; Table 5.1).

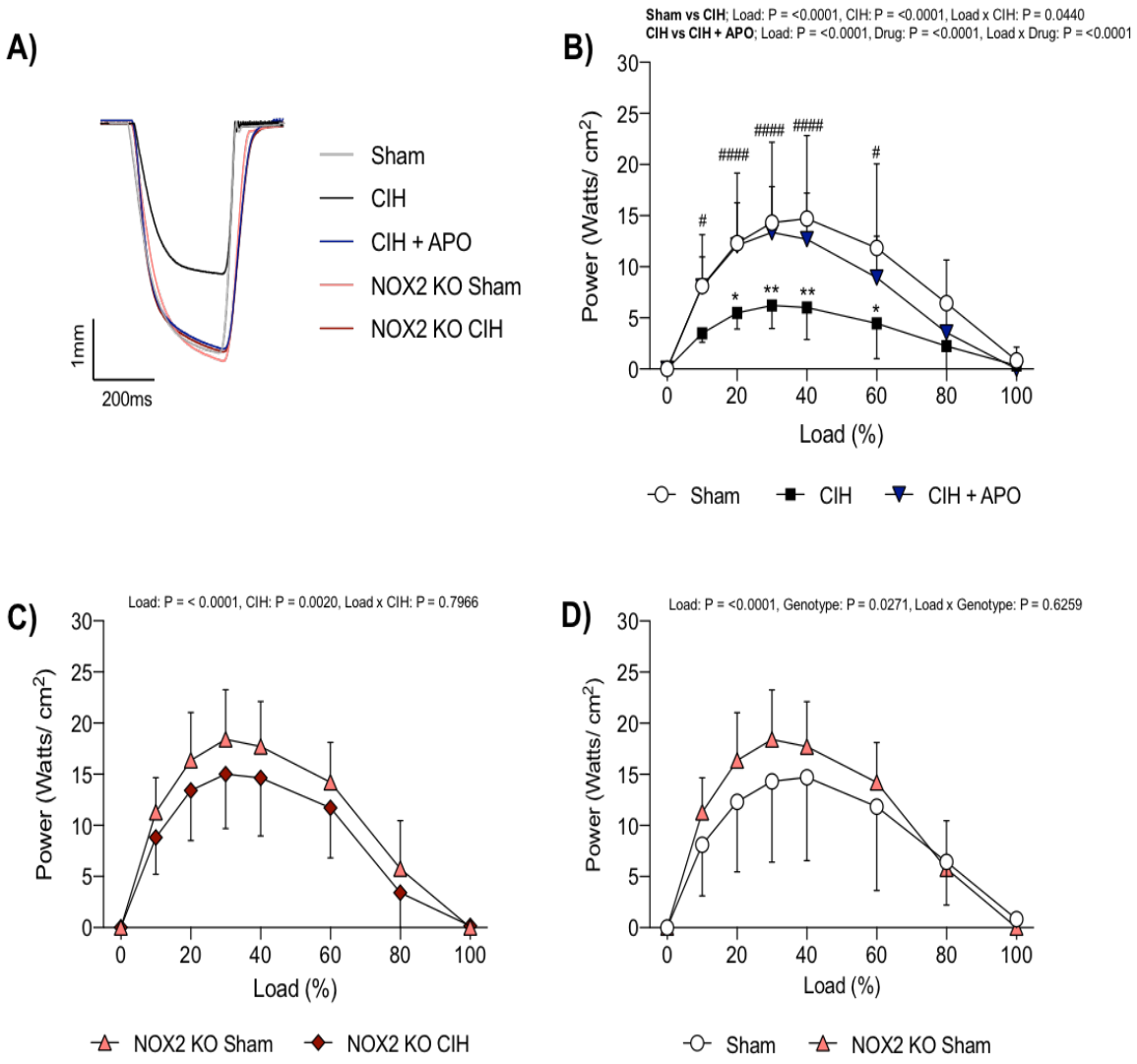

Figure 5.2 Diaphragm muscle power–load relationship. A, original traces of *ex vivo* diaphragm muscle maximum unloaded shortening for sham (grey), CIH (black), CIH + APO (blue), NOX2 KO sham (pink) and NOX2 KO CIH (red) preparations. B, C, D, group data for diaphragm power (mean ± SD) shown as power per unit CSA (Watts/cm^2) as a function of the load on the muscle expressed as a percentage of peak tetanic force for sham (n = 8), CIH (n = 8), CIH + APO (n = 9), NOX2 KO sham (n = 9) and NOX2 KO CIH (n = 9) mice. Data were statistically compared by repeated measures two-way ANOVA with Bonferroni's *post hoc* test. Relevant comparisons are denoted as follows: *denotes sham *vs*. CIH, *$P < 0.05$, **$P < 0.01$; $^{\#}$denotes CIH *vs*. CIH + APO, $^{\#}P < 0.05$, $^{\#\#\#\#}P < 0.0001$.

Figure 5.3 shows original traces of *ex vivo* diaphragm muscle maximum unloaded shortening for sham (grey), CIH (black), CIH + APO (blue), NOX2 KO sham (pink) and NOX2 KO CIH (red) preparations (A). Figure 5.3; B, C and D show the diaphragm work-load relationship. This is the work produced by the diaphragm over a range of incremental loads on the muscle between 0-100% of the peak force-generating capacity (Fmax), determined at the beginning of the protocol. Exposure to CIH significantly decreased the work produced by the diaphragm muscle over a range of loads compared to sham mice ($P < 0.0001$; repeated measures two-way ANOVA; Fig 5.3; B). *Post-hoc* analysis revealed a statistically significant decrease in the power-generating capacity of the diaphragm following exposure to CIH at 20% (*$P < 0.05$), 30% (***$P < 0.001$) 40% (****$P < 0.0001$) and 60% (****$P < 0.0001$) load compared to sham mice (Fig 5.3; B). The administration of apocynin throughout the exposure to CIH prevented the CIH-induced decrease in the work produced by the diaphragm over a range of loads compared to mice exposed to CIH alone ($P < 0.0001$; Fig 5.3; B). *Post-hoc* analysis revealed a statistically significant increase in work produced by the diaphragm following treatment with apocynin throughout the exposure to CIH at 20% - 60% load compared to CIH-exposed mice (Fig 5.3; B). Peak work (Wmax) was measured and typically occurred between 30% and 40% load. Exposure to CIH for 2 weeks significantly decreased Wmax compared to sham controls ($P = 0.0006$; Table 5.1); Apocynin treatment completely prevented the CIH-induced decrease in Wmax ($P = 0.0052$; Table 5.1). Exposure to CIH decreased the work produced by the diaphragm in NOX2 KO mice over the range of loads examined compared to NOX2 KO sham controls ($P = 0.0305$; Fig 5.3; C). Wmax was unaffected by exposure to CIH in NOX2 KO mice ($P = 0.3923$; Table 5.1). Genetic knock-out of NOX2 significantly increased the work produced by the diaphragm over the range of loads examined compared to wild-type sham mice ($P < 0.0001$; Fig 5.; D). *Post-hoc* analysis revealed a statistically significant increase in the power generated by the diaphragm of NOX2 KO sham mice at 20%-40% load compared to wild-type sham mice (Fig 5.3; D). NOX2 KO had no significant effect on Wmax compared to wild-type controls ($P = 0.0927$; Table 5.1).

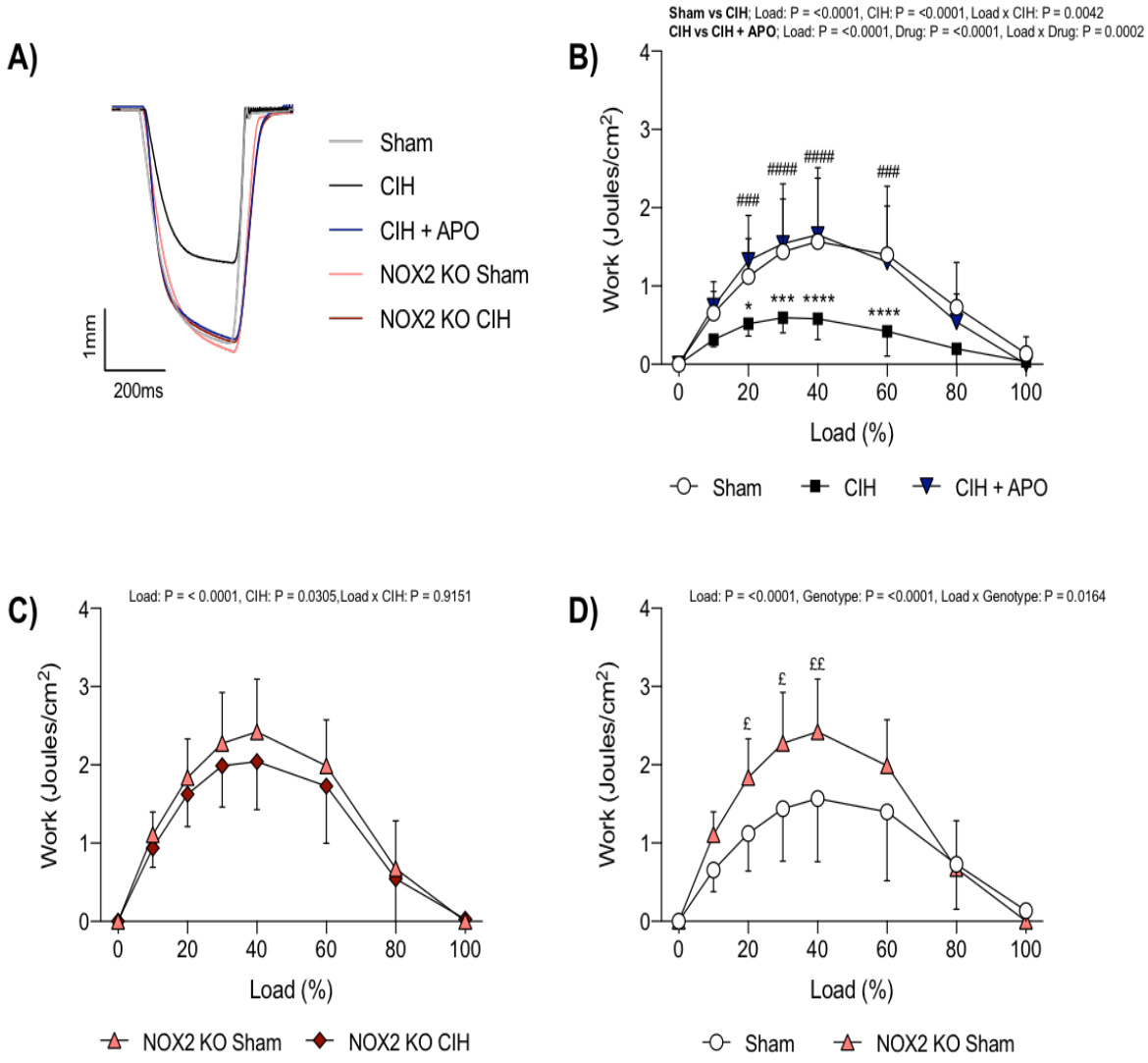

Figure 5.3 Diaphragm muscle work–load relationship. A, original traces of *ex vivo* diaphragm muscle maximum unloaded shortening for sham (grey), CIH (black), CIH + APO (blue), NOX2 KO sham (pink) and NOX2 KO CIH (red) preparations. B, C, D, group data for diaphragm work (mean ± SD) shown as work per unit CSA (Joules/cm^2) as a function of the load on the muscle expressed as a percentage of peak tetanic force for sham (n = 8), CIH (n = 8), CIH + APO (n = 9), NOX2 KO sham (n = 9) and NOX2 KO CIH (n = 9) mice. Data were statistically compared by repeated measures two-way ANOVA with Bonferroni's *post hoc* test. Relevant comparisons are denoted as follows: *denotes sham *vs*. CIH, *$P < 0.05$, ***$P < 0.001$, ****$P < 0.0001$; $^{\#}$ denotes CIH *vs*. CIH + APO, $^{\#\#\#}$ $P < 0.001$, $^{\#\#\#\#}$ $P < 0.0001$; $^{£}$ denotes sham *vs.* NOX2 KO sham, $^{£}$ $P < 0.05$, $^{££}$ $P < 0.01$.

Figure 5.4 shows original traces of *ex vivo* diaphragm muscle maximum unloaded shortening for sham (grey), CIH (black), CIH + APO (blue), NOX2 KO sham (pink) and NOX2 KO CIH (red) preparations (A). Figure 5.4; B, C and D show the diaphragm shortening-load relationship. This is the distance of shortening of the diaphragm over a range of incremental loads on the muscle between 0-100% of its peak force-generating capacity (Fmax), determined at the beginning of the protocol. 2 weeks of exposure to CIH significantly decreased the distance of shortening of the diaphragm muscle compared to sham mice ($P < 0.0001$; repeated measures two-way ANOVA; Fig 5.4; B); Apocynin treatment throughout the exposure to CIH prevented the CIH-induced decrease in the distance of shortening of the diaphragm over a range of loads examined compared with mice exposed to CIH alone ($P < 0.0001$; Fig 5.4; B). *Post hoc* analysis revealed that apocynin treatment significantly increased the distance of shortening at 0% of the peak force-generating capacity compared to CIH exposed mice ($^{\#}P < 0.05$). Peak shortening (Smax) was measured and occurred at 0% load, as expected. Smax was not different following exposure to CIH ($P = 0.1417$; Table 5.1) or apocynin treatment ($P = 0.0828$; Table 5.1) in wild-type mice. There was no difference in the distance of shortening between NOX2 KO sham and NOX2 KO CIH groups over the range of loads examined ($P = 0.3893$; Fig 5.4; C). Similarly, Smax was not different following exposure to CIH in NOX2 KO mice ($P = 0.1148$; Table 5.1). Genetic knock-out of NOX2 had no effect on the distance of shortening of the diaphragm over the range of loads examined compared to wild-type sham mice ($P = 0.3655$; Fig 5.4; D); Smax was also not different between these groups ($P = 0.1343$; Table 5.1).

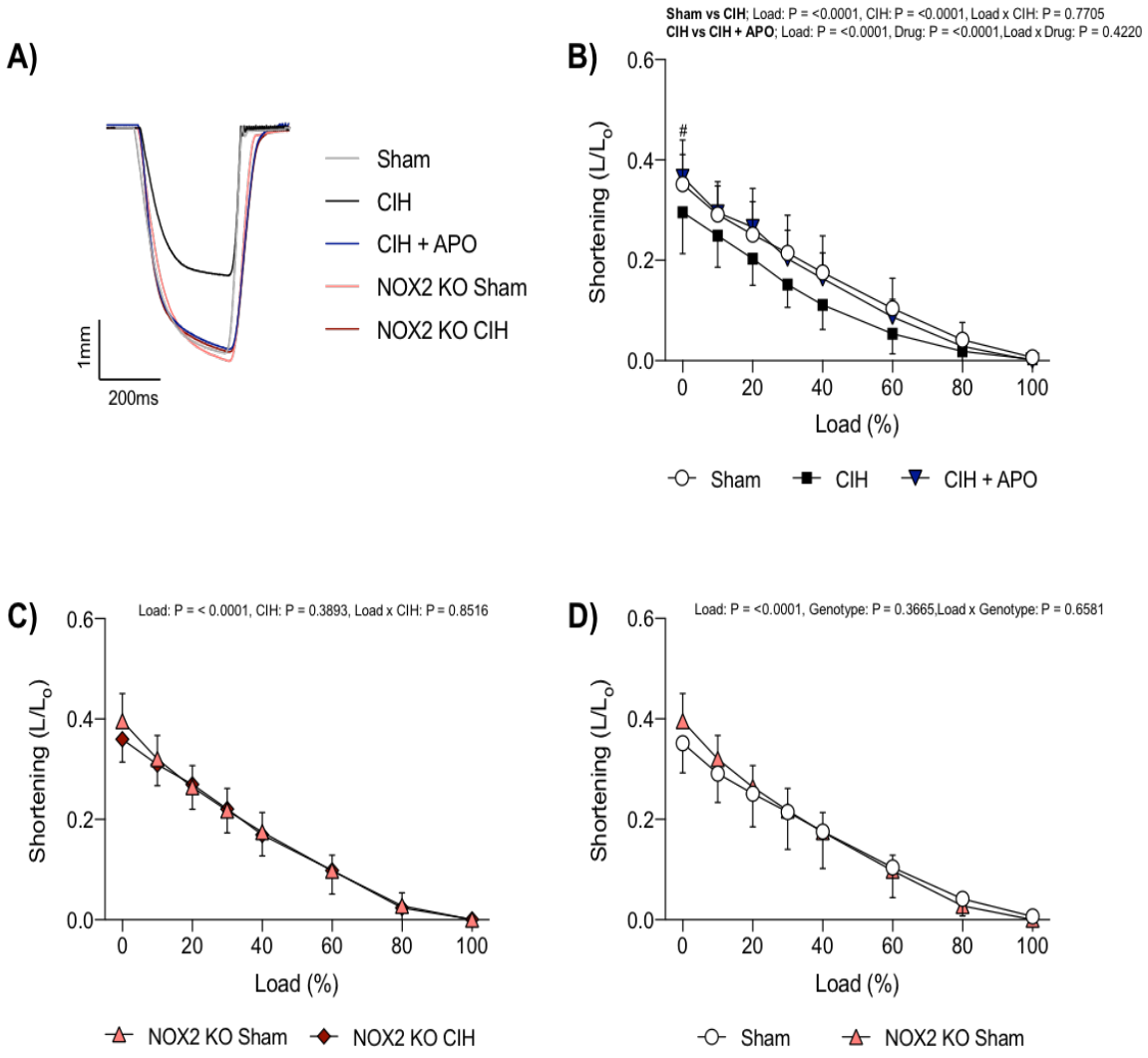

Figure 5.4 Diaphragm muscle shortening–load relationship. A, original traces of *ex vivo* diaphragm muscle maximum unloaded shortening for sham (grey), CIH (black), CIH + APO (blue), NOX2 KO sham (pink) and NOX2 KO CIH (red) preparations. B, C, D, group data for diaphragm shortening (mean ± SD) shown as length per unit optimal length (L/L_o) as a function of the load on the muscle expressed as a percentage of peak tetanic force for sham (n = 8), CIH (n = 8), CIH + APO (n = 9), NOX2 KO sham (n = 9) and NOX2 KO CIH (n = 9) mice. Data were statistically compared by repeated measures two-way ANOVA with Bonferroni's *post hoc* test. Relevant comparisons are denoted as follows: $^{\#}$ denotes CIH *vs*. CIH + APO, $^{\#}P < 0.05$.

Figure 5.5 shows original traces of *ex vivo* diaphragm muscle maximum unloaded shortening for sham (grey), CIH (black), CIH + APO (blue), NOX2 KO sham (pink) and NOX2 KO CIH (red) preparations (A). Figure 5.5; B, C and D show the diaphragm shortening velocity-load relationship. This is the shortening velocity of the diaphragm over a range of incremental loads on the muscle between 0-100% of the peak force-generating capacity (Fmax), determined at the beginning of the protocol. 2 weeks of exposure to CIH significantly decreased the shortening velocity of the diaphragm muscle compared to sham mice ($P = 0.0006$; repeated measures two-way ANOVA; Fig 5.5; B). *Post hoc* analysis revealed that exposure to CIH significantly decreased the shortening velocity of the diaphragm at 0% load compared to sham mice (*P = 0.05; Fig 5.5; B). Apocynin treatment throughout the exposure to CIH prevented the decrease in shortening velocity of the diaphragm over a range of loads examined compared to exposure to CIH alone ($P = 0.0123$; Fig 5.5; B). Peak shortening velocity (Vmax) was measured and occurred at 0% load, as expected. Vmax was unaffected by exposure to CIH ($P = 0.1304$; Table 5.1) or apocynin treatment ($P = 0.0745$; Table 5.1) in wild-type mice. There was no difference in the shortening velocity between NOX2 KO sham and NOX2 KO CIH groups ($P = 0.0754$; Fig 5.5; C); Vmax was also not different between these groups ($P = 0.3958$; Table 5.1). Similarly, genetic knock-out of NOX2 had no effect on the shortening velocity of the diaphragm over the range of loads examined compared to wild-type sham mice ($P = 0.0930$; Fig 5.5; D); Vmax was not different between NOX2 KO sham and wild-type sham mice ($P = 0.7291$; Table 5.1).

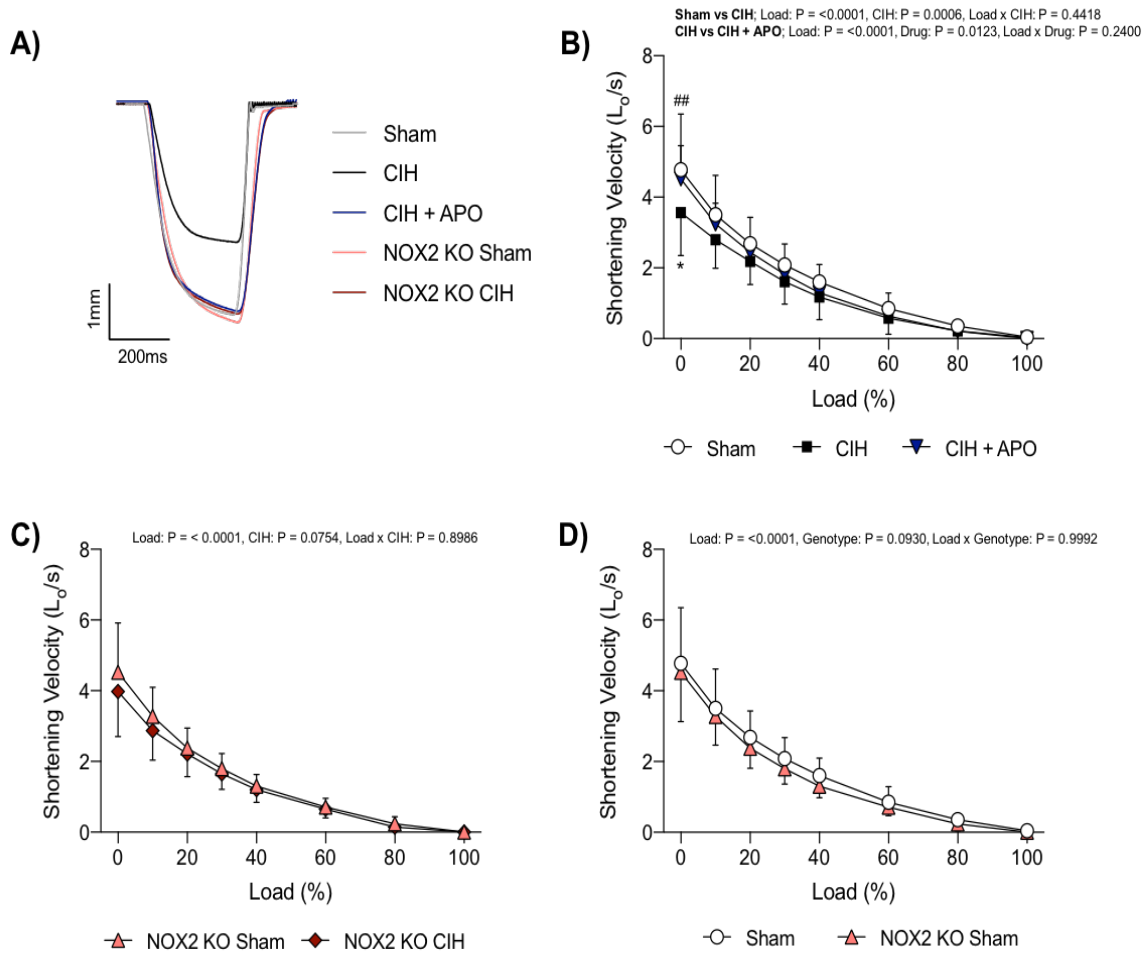

Figure 5.5 Diaphragm muscle shortening velocity–load relationship. A, original traces of *ex vivo* diaphragm muscle maximum unloaded shortening for sham (grey), CIH (black), CIH + APO (blue), NOX2 KO sham (pink) and NOX2 KO CIH (red) preparations. B, C, D, group data for diaphragm shortening velocity (mean ± SD) shown as optimal length per unit time (Lo/s) as a function of the load on the muscle expressed as a percentage of peak tetanic force for sham (n = 8), CIH (n = 8), CIH + APO (n = 9), NOX2 KO sham (n = 9) and NOX2 KO CIH (n = 9) mice. Data were statistically compared by repeated measures two-way ANOVA with Bonferroni's *post hoc* test. Relevant comparisons are denoted as follows: $^{\#\#}$denotes CIH *vs*. CIH + APO, $^{\#\#}P < 0.01$.

5.3.2 Characterisation of NOX enzymes in diaphragm muscle

Figure 5.6 shows the mRNA expression of the most predominant muscle-specific NOX isoforms in naïve wild-type mouse diaphragm muscle. The mRNA expression of NOX1 in the diaphragm was found to be significantly lower than that of both NOX4 (Fig 5.6; $P < 0.0001$) and NOX2 (Fig 5.6; $P < 0.0001$). There was no difference in the mRNA expression of NOX4 compared with NOX2 (Fig 5.6; $P = 0.9709$).

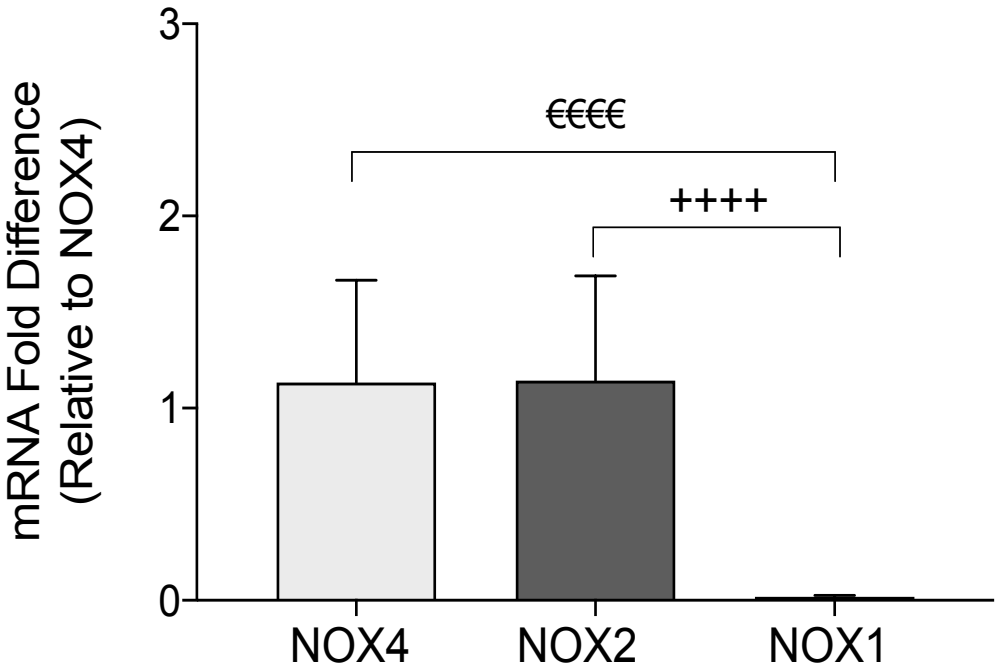

Figure 5.6 mRNA expression of the predominant muscle-specific NOX isoforms in naive wild-type mouse diaphragm muscle. Group data (mean ± SD, n = 8-9 per group) expressed as a fold difference in messenger RNA (mRNA) expression (relative to NOX4) for naïve wild-type mouse diaphragm muscle. Data sets, which were normally distributed and of equal variance, were statistically compared using unpaired two-tailed Student's *t* test. Welch's correction was applied in the case of unequal variance. Data, which were not normally distributed, were compared using Mann Whitney non-parametric tests. $^{€}$ denotes NOX4 *vs.* NOX1, $^{€€€€}P < 0.0001$; $^{+}$ denotes NOX2 *vs.* NOX1, $^{++++}P < 0.0001$. *Definition of abbreviations:* NOX4, NADPH oxidase 4; NOX2, NADPH oxidase 2; NOX1, NADPH oxidase 1.

mRNA and protein expression of the NOX2 enzyme in mouse diaphragm muscle is shown in Figure 5.7. There was no statistically significant difference in the mRNA expression of NOX2 following exposure to CIH compared with sham; a trend towards a lower mRNA expression of NOX2 was observed following treatment with apocynin throughout the exposure to CIH, however this did not reach the threshold for statistical significance (Fig 5.7; A, $P = 0.0136$). Similarly, exposure to CIH had no effect on NOX2 mRNA expression in NOX2 KO mice (Fig 5.7; A). As expected, a significant decrease (97%) in the mRNA expression of NOX2 following NOX2 KO was observed, compared with sham (Fig 5.7; A, $P = 0.0002$). Western blot bands were detected at approximately 65kDa, corresponding to the predicted MW of the NOX2 subunit (Fig 5.7; B). Fig 5.7; C shows the corresponding Ponceau S-stained membrane, confirming relatively equal protein loading and electro-transfer. Densitometric analysis of NOX2 band intensities, normalised by the intensity of the corresponding Ponceau S-stained proteins, revealed no significant difference in the protein expression of the NOX2 subunit in the diaphragm of mice exposed to CIH compared with sham (Fig 5.7; D, $P = 0.3806$).

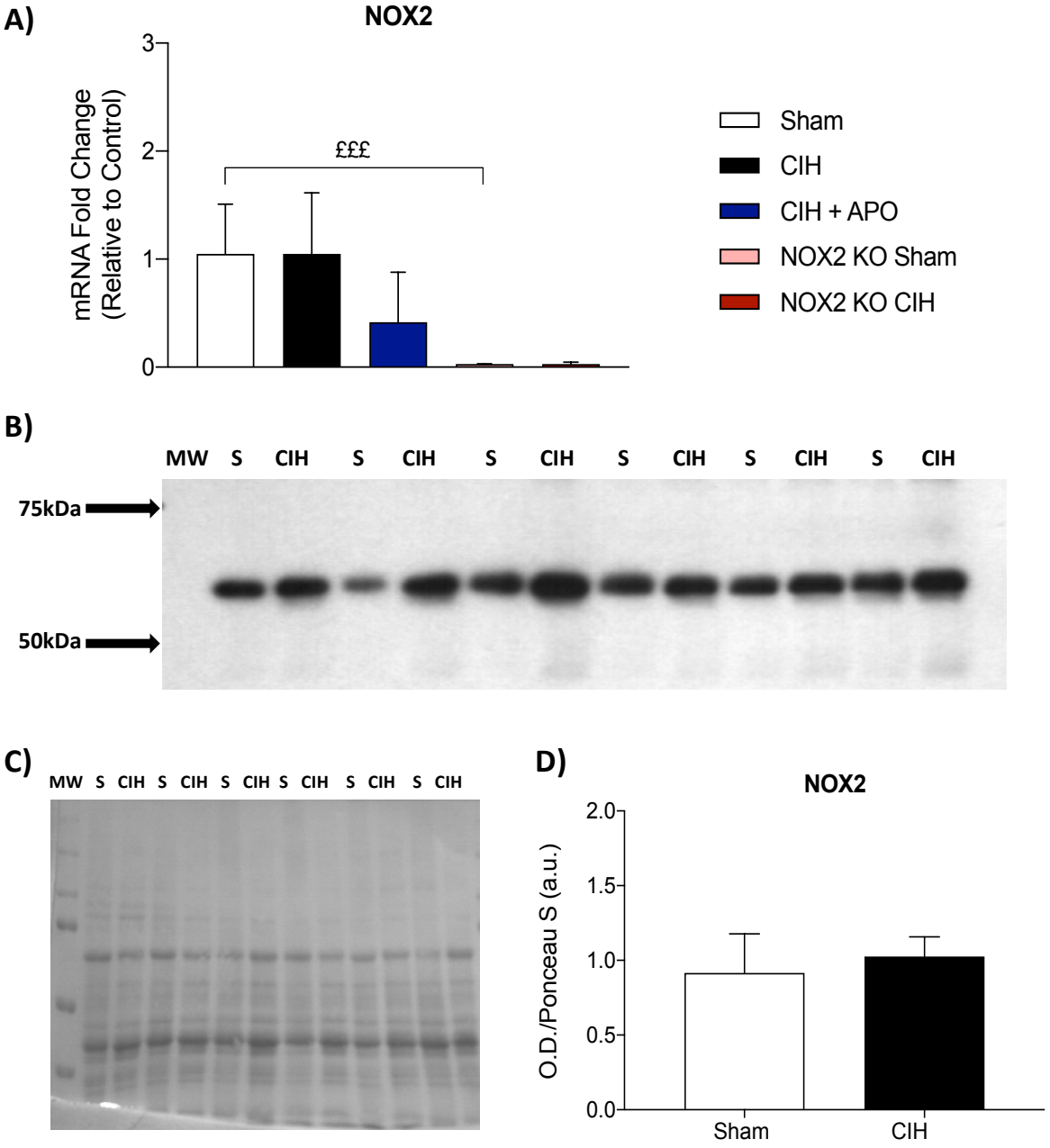

Figure 5.7 NOX2 mRNA and protein expression in diaphragm muscle. A, Group data (mean ± SD, n = 8-9 per group) expressed as a fold change in messenger RNA (mRNA) expression (relative to the control (sham) group) for sham, CIH, CIH + APO, NOX2 KO sham and NOX2 KO CIH groups for A, NOX2. B, Western blot of NOX2 in 20μg of protein extracted from the diaphragm of mice exposed to 2 weeks of normoxia (sham) or CIH. C, corresponding Ponceau S-stained membrane used for normalisation and compensation for protein loading and the electro-transfer of proteins. D**,** Group data (mean ± SD, n = 6 per group) for normalised NOX2 expression expressed as arbitrary units (a.u.). This is a product of the band intensity of the developed blot (B) / band intensity of the corresponding Ponceau S image (C), as determined by densitometry. Data sets, which were normally distributed and of equal variance, were statistically compared using unpaired two-tailed Student's *t* test. Welch's correction was applied in the case of unequal variance. Data, which were not normally distributed, were compared using Mann Whitney non-parametric tests. Statistical significance was taken at $P < 0.0125$ (Fig 5.7; A) or $P < 0.05$ (Fig 5.7; D). Comparisons are denoted as follows: $^{£}$ denotes sham *vs.* NOX2 KO sham, $^{£££}P < 0.001$. *Definition of abbreviations:* MW, molecular weight marker; S. Sham; NOX2, NADPH oxidase 2.

mRNA and protein expression of the NOX4 enzyme in mouse diaphragm muscle is shown in Figure 5.8. Exposure to CIH increased the mRNA expression of NOX4 compared with sham, although this did not reach the threshold for statistical significance when correction for multiple comparisons was applied (Fig 5.8; A, P = 0.0157); apocynin treatment throughout the exposure to CIH significantly decreased NOX4 mRNA levels in diaphragm muscle compared with exposure to CIH alone (Fig 5.8; A, P = 0.0040). NOX4 mRNA expression was significantly increased in NOX2 KO mice following exposure to CIH, with the size of this effect similar to that observed in wild-type mice (Fig 5.8; A, P = 0.0040). Western blot bands were detected at approximately 63kDa, corresponding to the predicted MW of the NOX4 subunit (Fig 5.8; B). Fig 5.8; C shows the corresponding Ponceau S-stained membrane, confirming relatively equal protein loading and electro-transfer. Densitometric analysis of NOX4 band intensities, normalised by the intensity of the corresponding Ponceau S-stained proteins, revealed a significant near two-fold increase in the protein expression of the NOX4 subunit in the diaphragm of mice exposed to CIH compared with sham controls (Fig 5.8; D, P = 0.0014).

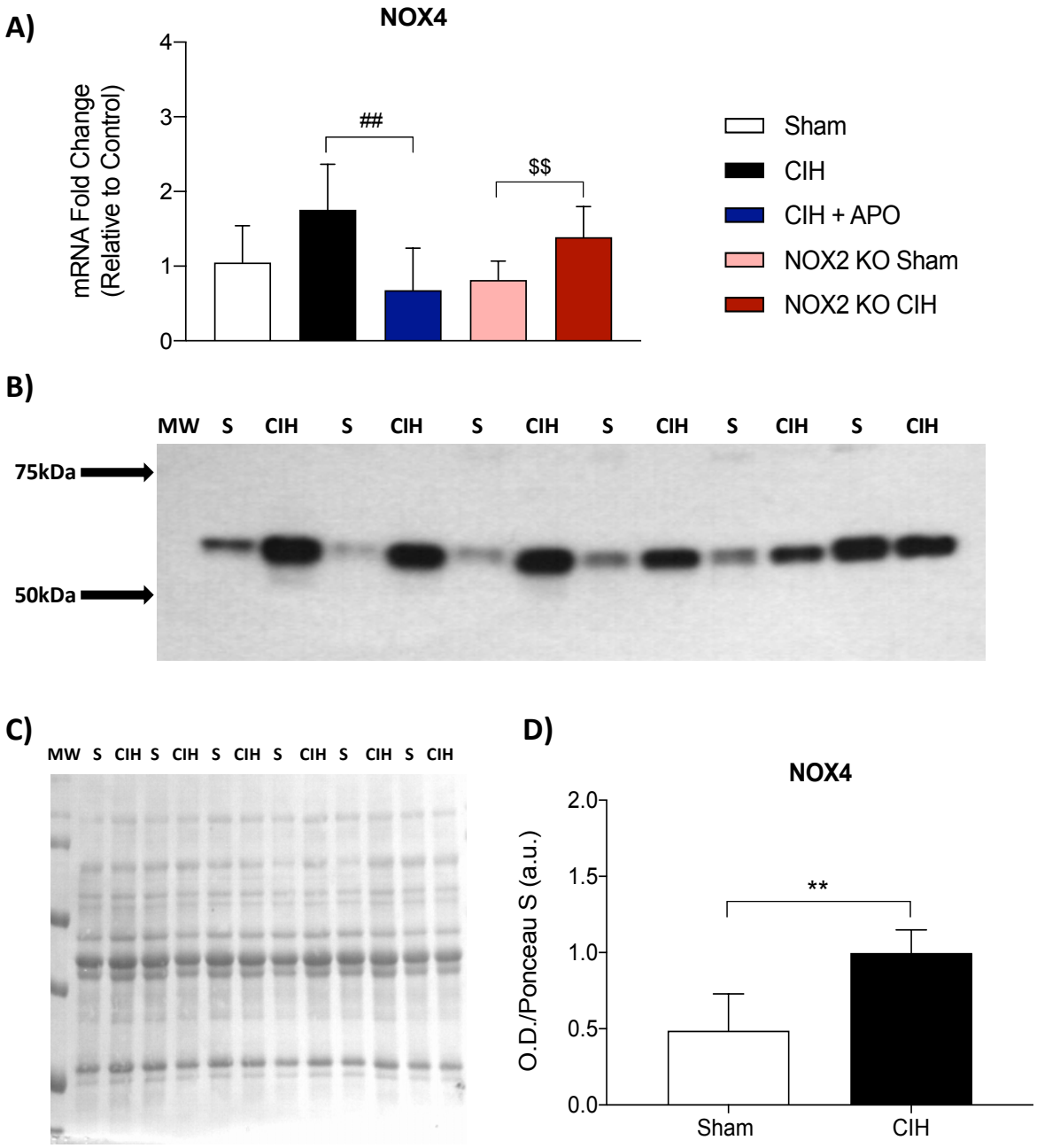

Figure 5.8 NOX4 mRNA and protein expression in diaphragm muscle. A, Group data (mean ± SD, n = 8-9 per group) expressed as a fold change in messenger RNA (mRNA) expression (relative to the control (sham) group) for sham, CIH, CIH + APO, NOX2 KO sham and NOX2 KO CIH groups for A, NOX4. B, Western blot of NOX4 in 20μg of protein extracted from the diaphragm of mice exposed to 2 weeks of normoxia (sham) or CIH. C, corresponding Ponceau S-stained membrane used for normalisation and compensation for protein loading and the electro-transfer of proteins. D**,** Group data (mean ± SD, n = 6 per group) for normalised NOX4 expression expressed as arbitrary units (a.u.). This is a product of the band intensity of the developed blot (B) / band intensity of the corresponding Ponceau S image (C), as determined by densitometry. Data sets, which were normally distributed and of equal variance, were statistically compared using unpaired two-tailed Student's *t* test. Welch's correction was applied in the case of unequal variance. Data, which were not normally distributed, were compared using Mann Whitney non-parametric tests. Statistical significance was taken at $P < 0.0125$ (Fig 5.8; A) or $P < 0.05$ (Fig 5.8; D). Comparisons are denoted as follows: *denotes sham *vs*. CIH, **$P < 0.01$, $^{\#}$denotes CIH *vs*. CIH + APO, $^{\#\#}$ $P < 0.01$, $^{\$}$denotes CIH *vs*. CIH + APO, $^{\$\$}$ $P < 0.01$. *Definition of abbreviations:* MW, molecular weight marker; S. Sham; NOX4, NADPH oxidase 4.

The mRNA expression of NOX catalytic and accessory subunits in diaphragm muscle is show in Figure 5.9. A trend towards a decrease in the mRNA expression of the accessory subunit, p22phox, was observed following 2 weeks of exposure to CIH in the diaphragm, but this did not reach the threshold for statistical significance (Fig 5.9; B, P = 0.0264); apocynin treatment throughout the exposure to CIH prevented the decrease in p22phox to levels equivalent to sham (Fig 5.9; B). The mRNA expression of p22phox was not different in NOX2 KO mice following exposure to CIH compared to NOX2 KO sham mice (Fig 5.9; B). Similarly, exposure to CIH resulted in a decrease in the mRNA expression of the small GTPase, Rac, compared with sham mice (Fig 5.9; F, P = 0.0543), but this failed to reach the threshold for statistical significance; apocynin administration prevented the decrease in the mRNA expression of Rac compared to exposure to CIH alone. There was no difference in the mRNA expression of Rac in NOX2 KO mice following exposure to CIH compared with NOX2 KO sham mice (Fig 5.9; F). There was no difference in the mRNA expression of NOX1 (Fig 5.9; A), p47phox (Fig 5.9; C), p40phox (Fig 5.9; D), p67phox (Fig 5.9; E), DUOX1 (Fig 5.9; G) or DUOX2 (Fig 5.9; H) across all groups examined. 2 weeks of exposure to CIH had no effect on NOX activity in the diaphragm compared with sham (Fig 5.9; I).

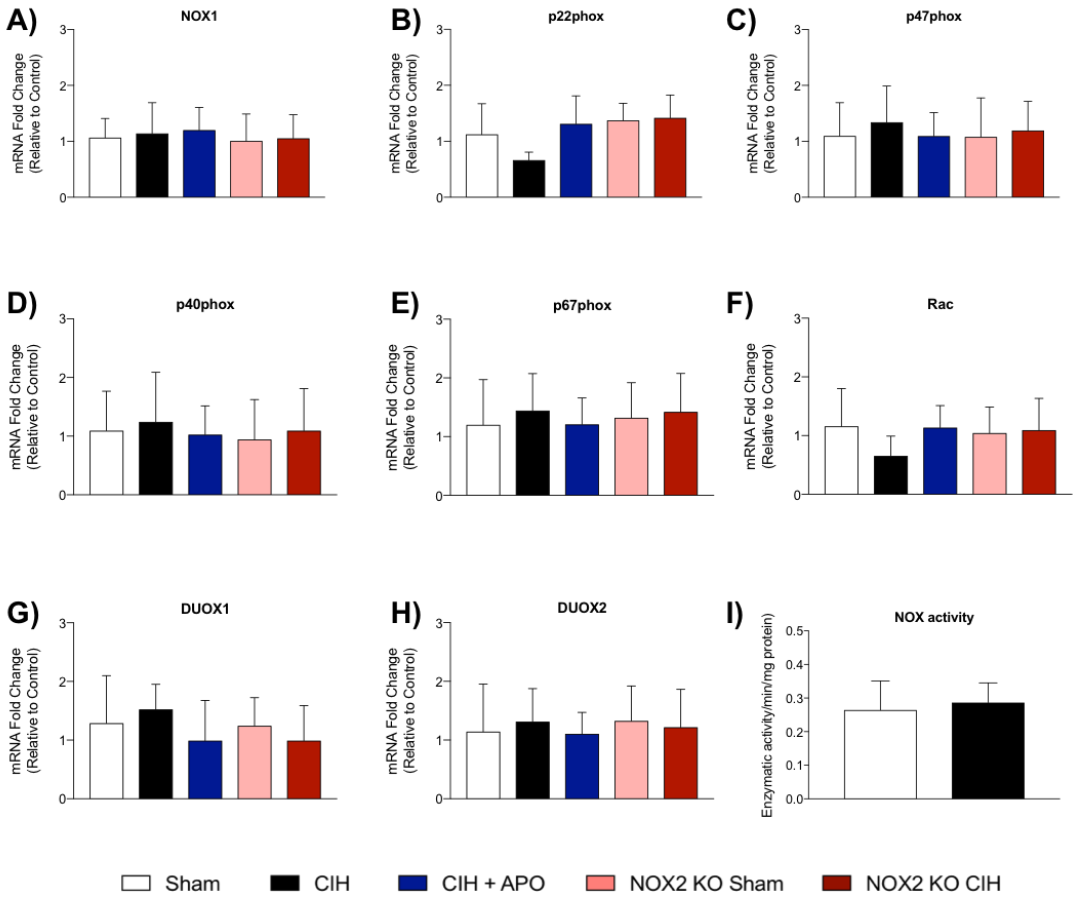

Figure 5.9 mRNA expression of NOX catalytic and accessory subunits in diaphragm muscle. Group data (mean ± SD, n = 8-9 per group) expressed as a fold change in messenger RNA (mRNA) expression (relative to the control (sham) group) for sham, CIH, CIH + APO, NOX2 KO sham and NOX2 KO CIH groups for (A) NOX1; (B) p22phox; (C) p47phox; (D) p40phox; (E) p67phox; (F) Rac; (G) DUOX1 and (H) DUOX2. Group data (mean ± SD, n = 8 per group) for NOX enzymatic activity in diaphragm muscle following 2 weeks of CIH or normoxia (sham), expressed as enzymatic activity per minute per mg protein (I). Data sets, which were normally distributed and of equal variance, were statistically compared using unpaired two-tailed Student's *t* test. Welch's correction was applied in the case of unequal variance. Data, which were not normally distributed, were compared using Mann Whitney non-parametric tests. Statistical significance was taken at $P < 0.0125$ (A-H, inclusive) or $P < 0.05$ (I). *Definition of abbreviations:* NOX1, NADPH oxidase 1.

5.3.3 Molecular analysis of redox sensitive indices of diaphragm muscle form and function

Figure 5.10 shows the mRNA expression of genes relating to the muscle differentiation process in diaphragm muscle. Exposure to CIH increased the mRNA expression of the transcriptional activator of muscle differentiation, myogenin, but this did not reach the threshold for statistical significance (P = 0.0132; Fig 5.10; A); treatment with apocynin throughout the exposure to CIH significantly prevented the increase in myogenin (P < 0.0001; Fig 5.10; A). A trend towards a decrease in the mRNA expression of myogenin was observed in NOX2 KO sham mice when compared with sham (P = 0.0703; Fig 5.10; A). Exposure to CIH had no effect on the mRNA expression of myogenin in NOX2 KO mice. Exposure to CIH significantly increased the mRNA expression of the myogenesis inhibitor, myostatin (P = 0.0041; Fig 5.10; B); apocynin treatment throughout the exposure to CIH reduced the increase in myostatin compared to exposure to CIH alone, but this did not reach statistical significance (P = 0.0512; Fig 5.10; B). Exposure to CIH had no effect on the mRNA expression of myostatin in NOX2 KO mice compared with NOX2 KO sham mice. NOX2 KO resulted in a significant increase in the mRNA expression of myostatin compared with wild-type sham mice (P = 0.0052; Fig 5.10; B). The mRNA expression of the muscle differentiation regulator, MyoD, was increased following exposure to CIH, but this did not meet the threshold for statistical significance (P = 0.0128; Fig 5.10; C); treatment with apocynin throughout the exposure to CIH prevented the increase compared with exposure to CIH alone (P = 0.0003; Fig 5.10; C). Exposure to CIH resulted in no difference in the mRNA expression of MyoD in NOX2 KO mice. A trend towards a decrease in the mRNA expression of MyoD was observed in mice lacking the NOX2 enzyme compared with wild-type controls (P = 0.0703; Fig 5.10; C). There was a trend towards an increase in mRNA for the transcription factor, MEF2C, following exposure to CIH compared with sham (P = 0.0215; Fig 5.10; D); administration of apocynin throughout the exposure to CIH prevented the increase compared with exposure to CIH alone (P = 0.0028; Fig 5.10; D). There was no difference in the mRNA expression of MEF2C in NOX2 KO mice exposed to CIH compared with NOX2 KO sham mice. A trend towards a decrease in the mRNA

expression of MEF2C was observed in mice lacking the NOX2 enzyme when compared with wild-type mice (*P* = 0.0253; Fig 5.10; D). Exposure to CIH increased the mRNA expression of sirtuin-1 compared with sham, but this did not reach statistical significance (*P* = 0.0355; Fig 5.10; E); treatment with apocynin ameliorated the increase compared with exposure to CIH alone (P = 0.0005; Fig 5.10; E). There was no difference in the mRNA expression of sirtuin-1 between NOX2 KO CIH and sham mice. The mRNA expression of IGF-1 was unchanged across all groups (Fig 5.10; F).

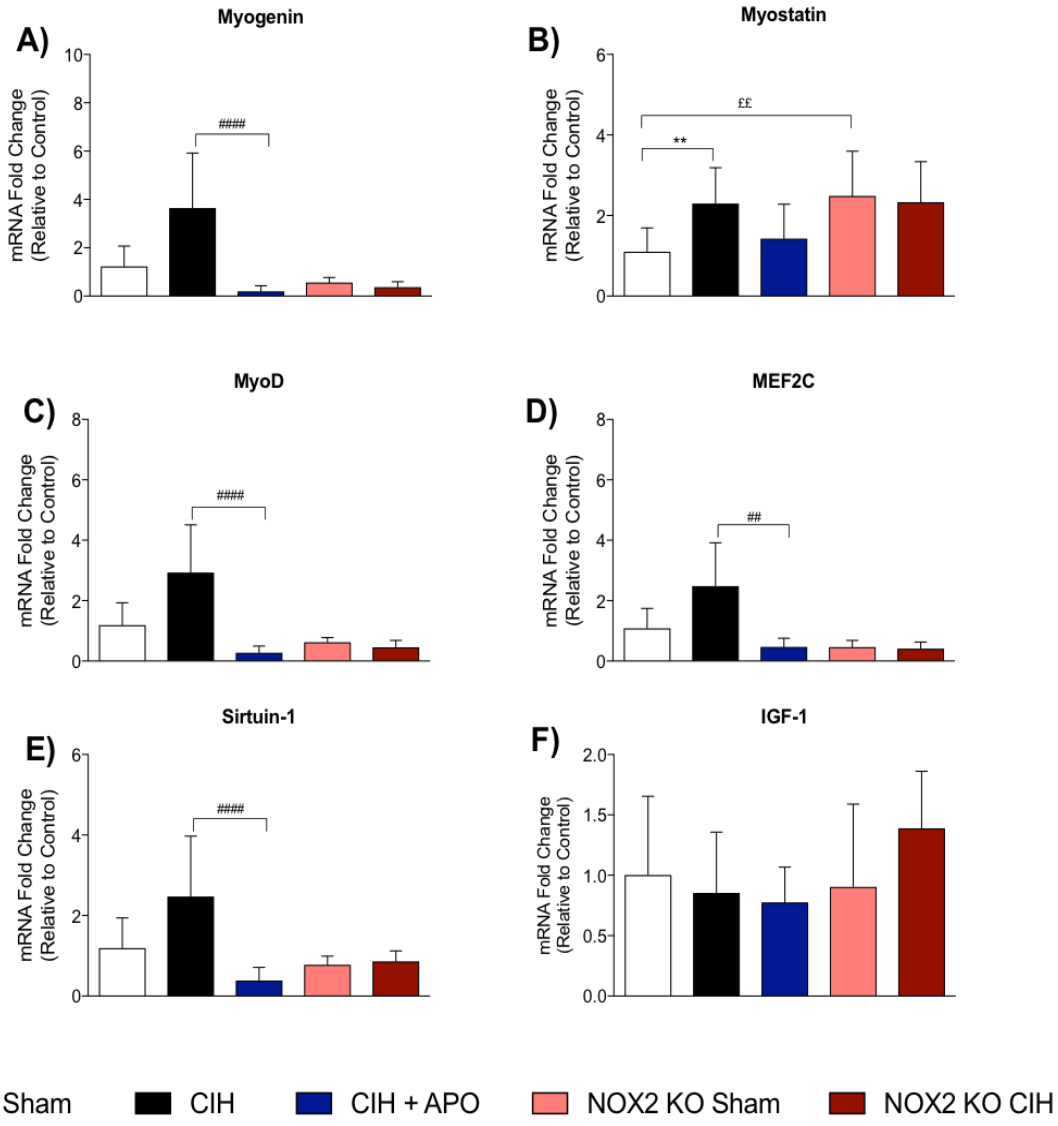

Figure 5.10 mRNA expression of genes related to muscle differentiation in diaphragm muscle. Group data (mean ± SD, n = 8-9 per group) expressed as a fold change in messenger RNA (mRNA) expression (relative to the control (sham) group) for Sham, CIH, CIH + APO,

NOX2 KO Sham and NOX2 KO CIH groups for (A) Myogenin; (B) Myostatin; (C) MyoD; (D) MEF2C; (E) Sirtuin-1; and (F) IGF-1. Data sets, which were normally distributed and of equal variance, were statistically compared using unpaired two-tailed Student's *t* test. Welch's correction was applied in the case of unequal variance. Data, which were not normally distributed, were compared using Mann Whitney non-parametric tests. Statistical significance was taken at $P < 0.0125$. Relevant comparisons are denoted as follows: *denotes sham *vs*. CIH, ** $P < 0.01$; $^{\#}$ denotes CIH *vs*. CIH + APO, $^{\#\#}$ $P < 0.01$, $^{\#\#\#\#}$ $P < 0.0001$; $^{£}$ denotes Sham *vs.* NOX2 KO Sham, $^{££}$ $P < 0.01$. *Definition of abbreviations:* MyoD, muscle differentiation protein 1; MEF2C, myocyte-specific enhancer factor 2C; IGF-1, insulin-like growth factor 1.

Figure 5.11 shows the mRNA expression of genes relating to antioxidant status in diaphragm muscle. There were no statistically significant differences in the mRNA expression of SOD1, SOD2 or catalase across all groups examined (Fig 5.11; A, B and C, respectively). However, exposure to CIH significantly increased the mRNA expression of NRF2 (transcription factor involved in the regulation of antioxidant proteins) compared with sham ($P = 0.0098$; Fig 5.11; D); administration of apocynin throughout the exposure to CIH prevented the increase in NRF2 mRNA compared to exposure to CIH alone ($P = 0.0005$; Fig 5.11; D). There was no difference in the mRNA expression of NRF2 in NOX2 KO mice following exposure to CIH compared with sham controls. There was a trend towards a decrease in the mRNA expression of NRF2 in NOX2 KO sham mice compared with wild-type controls (sham), however this did not reach the threshold for statistical significance when correction for multiple comparisons was applied ($P = 0.0334$; Fig 5.11; D).

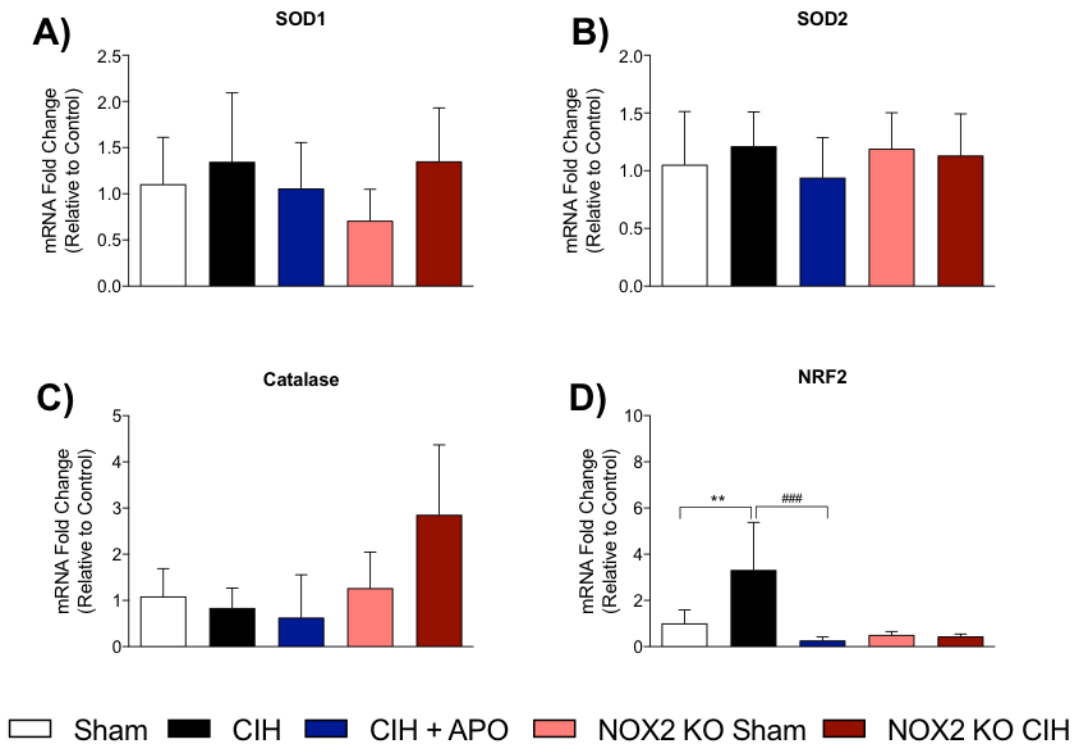

Figure 5.11 mRNA expression of genes related to antioxidant capacity in diaphragm muscle. Group data (mean ± SD, n = 8-9 per group) expressed as a fold change in messenger RNA (mRNA) expression (relative to the control (sham) group) for sham, CIH, CIH + APO, NOX2 KO sham and NOX2 KO CIH groups for (A) SOD1; (B) SOD2; (C) Catalase; and (D) NRF2. Data sets, which were normally distributed and of equal variance, were statistically compared using unpaired two-tailed Student's *t* test. Welch's correction was applied in the case of unequal variance. Data, which were not normally distributed, were compared using Mann Whitney non-parametric tests. Statistical significance was taken at $P < 0.0125$. Relevant comparisons are denoted as follows: *denotes sham *vs*. CIH, **$P < 0.01$; $^{\#}$denotes CIH *vs*. CIH + APO,$^{\#\#\#}$ $P < 0.001$. *Definition of abbreviations:* SOD1, superoxide dismutase 1 ; SOD2, superoxide dismutase 2; NRF2, nuclear factor erythroid 2-related factor 2.

Figure 5.12 shows a range of indices relating to mitochondrial capacity in diaphragm muscle. Exposure to CIH (both in wild-type and NOX2 KO mice) or treatment with apocynin had no effect on the mRNA expression of the mitophagy-related gene, PINK1, in diaphragm muscle (Fig 5.12; A). However, genetic knock-out of the NOX2 enzyme resulted in a significant increase in the mRNA expression of PINK1 in the diaphragm compared to sham ($P = 0.0003$; Fig 5.12; A). Exposure to CIH increased the mRNA expression of another mitophagy-related gene, PARK2, compared with sham, but this did not reach the threshold for statistical significance ($P = 0.0208$; Fig

5.12; B); treatment with apocynin significantly prevented the CIH-induced increase in PARK2 compared with exposure to CIH alone (P = 0.0006; Fig 5.12; B). There was no alteration to the mRNA expression of PARK2 in NOX2 KO mice following exposure to CIH. Citrate synthase activity, commonly used as a quantitative enzyme marker for the presence of intact mitochondria, and hence aerobic capacity, was unchanged following 2 weeks of exposure to CIH Fig 5.12; C).

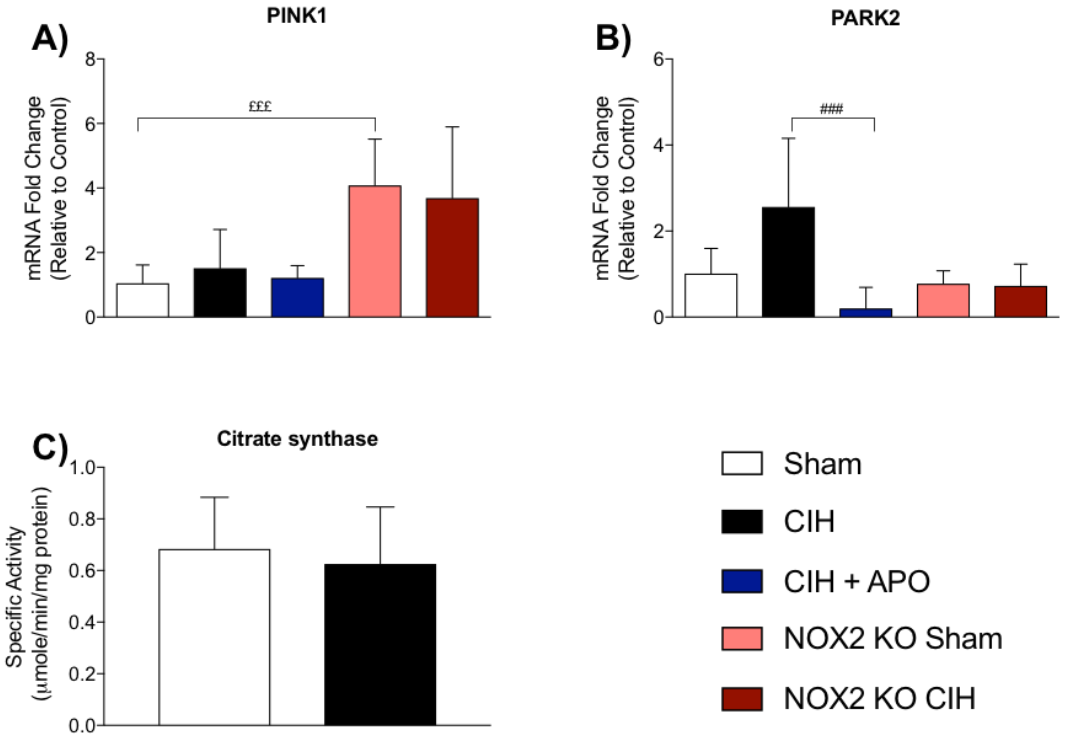

Figure 5.12 Indices relating to mitochondrial integrity in diaphragm muscle. Group data (mean ± SD, n = 8-9 per group) expressed as fold changes in messenger RNA (mRNA) expression (relative to the control group) for sham, CIH, CIH + APO, NOX2 KO sham and NOX2 KO CIH groups for A, PINK1; and B, PARK2. C, citrate synthase activity following 2 weeks of CIH exposure (mean ± SD, n = 8 per group). Data sets, which were normally distributed and of equal variance, were statistically compared using unpaired two-tailed Student's *t* test. Welch's correction was applied in the case of unequal variance. Data, which were not normally distributed, were compared using Mann Whitney non-parametric tests. Statistical significance was taken at $P < 0.0125$ (Fig 5.12; A & B) or $P < 0.05$ (Fig 5.12; C). Relevant comparisons are denoted as follows: $^{\#}$ denotes CIH *vs*. CIH + APO, $^{\#\#\#}$ $P < 0.001$; $^{£}$ denotes sham *vs.* NOX2 KO sham, $^{£££}P < 0.001$. *Definition of abbreviations:* PINK1, PTEN-induced kinase 1; PARK2, parkin.

Figure 5.13 shows a range of measures relating to inflammation and redox balance in diaphragm muscle. A trend towards an increase in the expression of the inflammatory transcription factor, NF-κB, was observed following exposure to CIH compared with sham (P = 0.0742; Fig 5.13; A); administration of apocynin throughout the exposure to CIH prevented the CIH-induced increase in NF-κB mRNA compared with exposure to CIH alone (P = 0.0012; Fig 5.13; A). There was no difference in the mRNA expression of NF-κB in NOX2 KO mice following exposure to CIH. Levels of TBARS (indirect measure of oxidative stress) and protein expression of HIF-1α (mediator of adaptive responses to oxidative stress during hypoxia) were unaltered following 2 weeks of exposure to CIH (Fig 5.13; B & C, respectively).

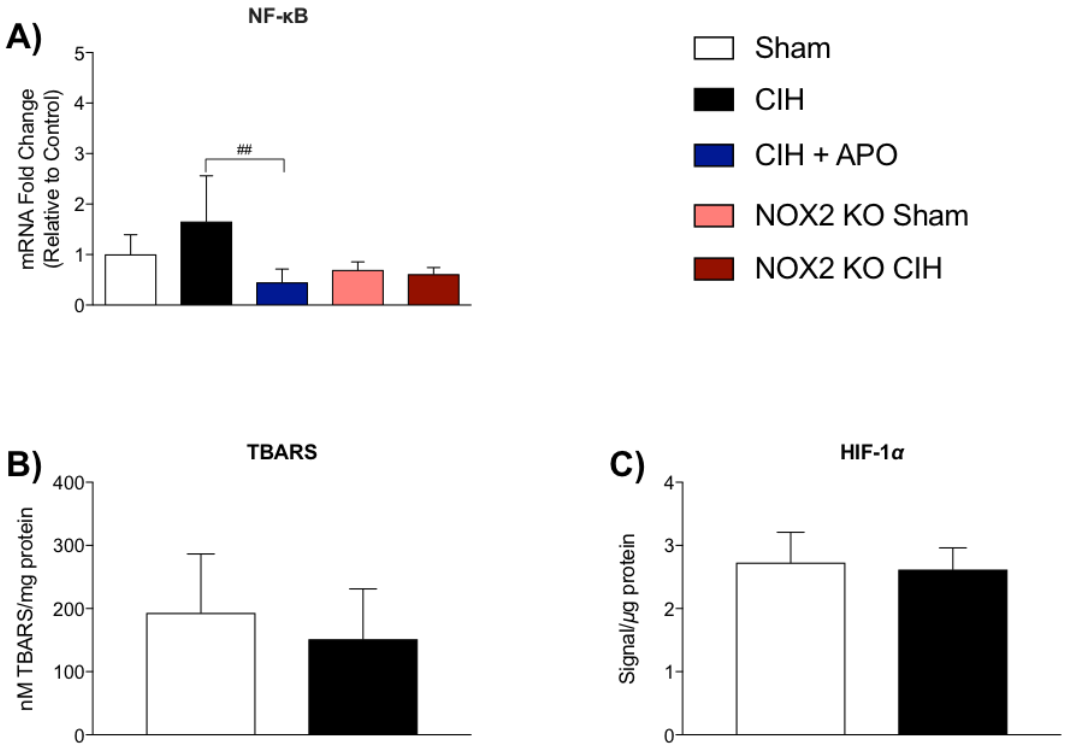

Figure 5.13 Inflammatory mediators and indirect measures of redox imbalance in diaphragm muscle. Group data (mean ± SD, n = 8-9 per group) expressed as a fold change in messenger RNA (mRNA) expression (relative to the control (sham) group) for sham, CIH, CIH + APO, NOX2 KO sham and NOX2 KO CIH groups for A, NF-κB. B, TBARS and C, HIF-1α protein content in sternohyoid muscle following 2 weeks of CIH (mean ± SD, n = 8 per group). Data sets, which were normally distributed and of equal variance, were statistically compared using unpaired two-tailed Student's *t* test. Welch's correction was applied in the case of

unequal variance. Data, which were not normally distributed, were compared using Mann Whitney non-parametric tests. Statistical significance was taken at $P < 0.0125$ (Fig 5.13; A) or $P < 0.05$ (Fig 5.13; B & C). Relevant comparisons are denoted as follows: $^{\#}$ denotes CIH *vs*. CIH + APO, $^{\#\#}$ $P < 0.01$. *Definition of abbreviations:* NF-κB, nuclear factor kappa-light-chain-enhancer of activated B cells; TBARS, thiobarbituric acid reactive substances; HIF-1α, hypoxia-inducible factor 1-alpha.

Figure 5.14 shows the mRNA expression of genes relating to autophagy and atrophy in diaphragm muscle. There was a trend towards an increase in the mRNA expression of the autophagy-related gene, BNIP3, following exposure to CIH compared to sham ($P = 0.0245$; Fig 5.14; A); treatment with apocynin throughout the exposure to CIH significantly ameliorated the increase in BNIP3 ($P = 0.0026$; Fig 5.14; A). There was no difference in the mRNA expression of BNIP3 in NOX2 KO mice following exposure to CIH. Similarly, there was a trend towards an increase in the mRNA expression of another autophagy-related gene, LC3B, following exposure to CIH compared to sham mice ($P = 0.0263$; Fig 5.14; C); treatment with apocynin significantly ameliorated the increase in LC3B compared to exposure to CIH alone ($P = 0.0066$; Fig 5.14; C). There was no difference in the mRNA expression of LC3B in NOX2 KO mice following exposure to CIH. Exposure to CIH had no effect on the mRNA expression of the atrophy-related gene, atrogin-1, in wild-type or NOX2 KO mice (Fig 5.14; D). However, treatment with apocynin throughout the exposure to CIH significantly decreased the mRNA expression of atrogin-1 compared to exposure to CIH alone ($P = 0.0056$; Fig 5.14; D). Exposure to CIH increased the mRNA expression of another atrophy related gene, MuRF1, compared to sham, but this did not reach statistical significance ($P = 0.0371$; Fig 5.14; E; apocynin administration throughout the exposure to CIH prevented the CIH induced increase in MuRF1 ($P = 0.0050$; Fig 5.14; E). The mRNA expression of MuRF1 was not different in NOX2 KO mice following exposure to CIH compared to NOX2 KO sham mice. There was no difference in the mRNA expression of GAPARAPL1 across all groups (Fig 5.14; B).

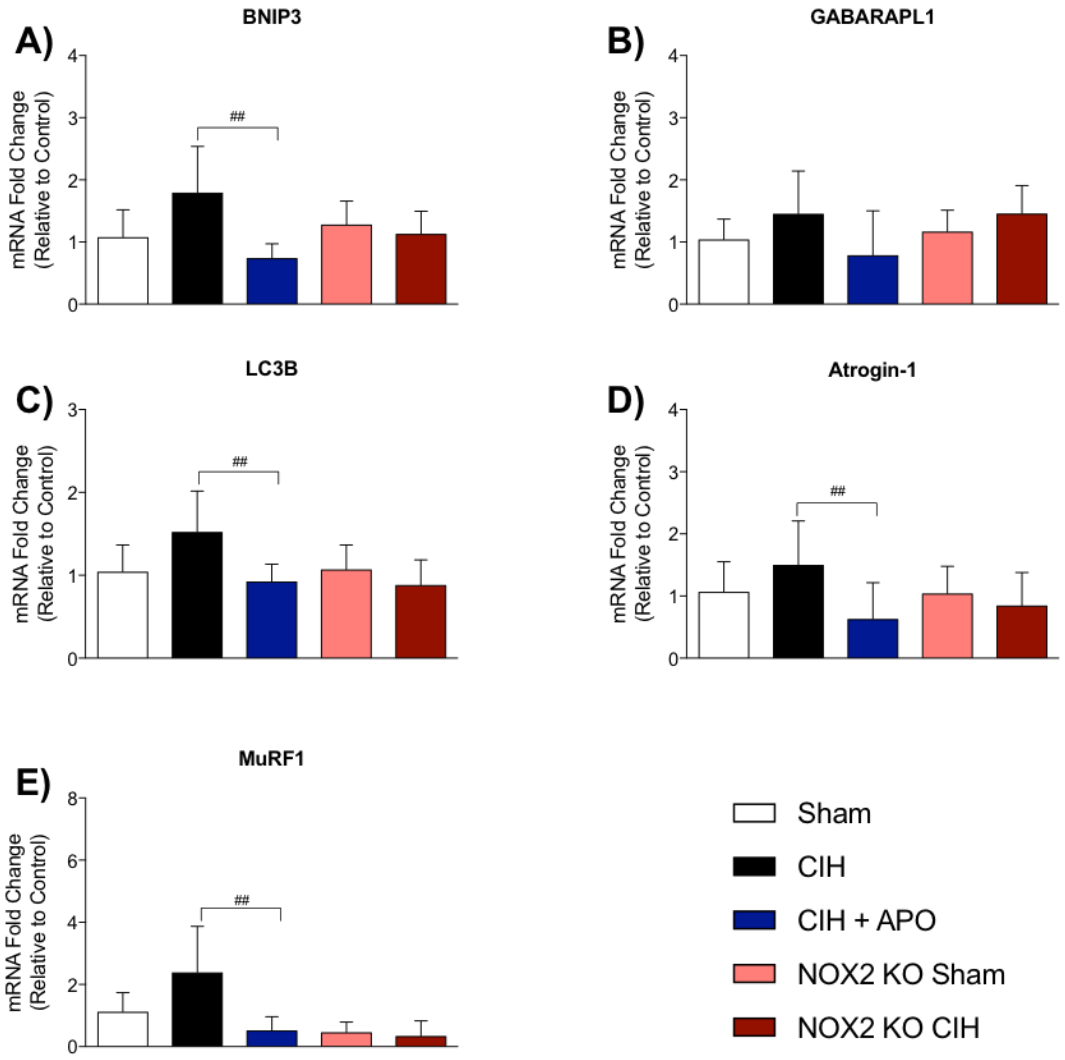

Fig 5.14 mRNA expression of genes relating to autophagy and atrophy in diaphragm muscle. Group data (mean ± SD, n = 8-9 per group) expressed as a fold change in messenger RNA (mRNA) expression (relative to the control (sham) group) for sham, CIH, CIH + APO, NOX2 KO sham and NOX2 KO CIH groups for (A) BNIP3; (B) GABARAPL1; (C) LC3B; (D) Atrogin-1; and (E) MuRF1. Data sets, which were normally distributed and of equal variance, were statistically compared using unpaired two-tailed Student's *t* test. Welch's correction was applied in the case of unequal variance. Data, which were not normally distributed, were compared using Mann Whitney non-parametric tests. Statistical significance was taken at $P < 0.0125$. Relevant comparisons are denoted as follows: $^{\#}$ denotes CIH *vs*. CIH + APO, $^{\#\#}$ $P < 0.01$. *Definition of abbreviations:* BNIP3, bcl-2 nineteen-kilodalton interacting protein 3; GABARAPL1, gamma-aminobutyric acid receptor-associated protein-like 1; LC3B, microtubule-associated proteins 1A/1B light chain 3B; MuRF1, muscle RING finger 1.

Figure 5.15 shows the phosphoprotein content of key proteins involved in protein synthesis and degradation signalling pathways in diaphragm muscle. The phospho – JNK (*P* = 0.0287; Fig 5.15; B), phospho - p38 (*P* = 0.0007; Fig 5.15; C) and phospho - ERK 1/2 (*P* = 0.0379; Fig 5.15; D) protein content of these arms of the mitogen activated protein kinase (MAPK) pathway were significantly decreased in diaphragm muscle following 2 weeks of exposure to CIH compared to sham mice. There was no alteration to the phosphoprotein content of phospho-FOXO3a in the diaphragm following 2 weeks of exposure to CIH compared with sham (Fig 5.15; A).

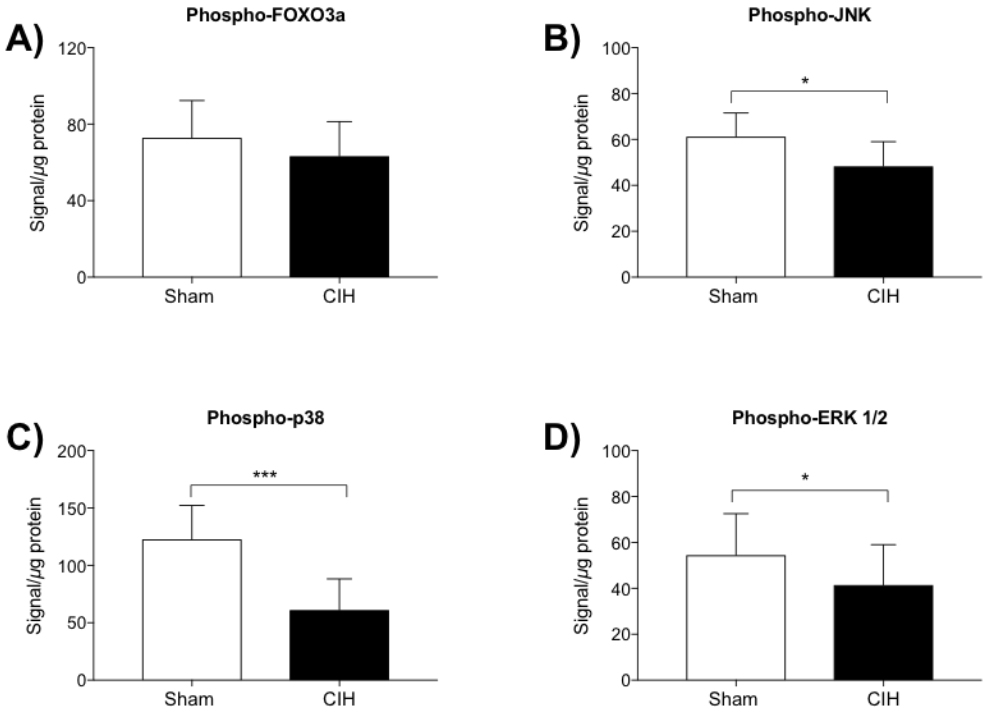

Figure 5.15 Phosphoprotein content relating to protein synthesis and degradation signalling in diaphragm muscle. A, Phospho-FOXO3a; B, Phospho-JNK; C, Phospho-p38 protein content and D, Phospho-ERK 1/2 (mean ± SD, n = 8 per group) from mice exposed to 2 weeks of CIH or normoxia (sham)**.** Values are expressed as signal/µg of total protein (adjusted for background signal). Data sets, which were normally distributed and of equal variance, were statistically compared using unpaired two-tailed Student's *t* test. Welch's correction was applied in the case of unequal variance. Statistical significance was taken at $P < 0.05$. Relevant comparisons are denoted as follows: * denotes sham *vs*. CIH, *P < 0.05, ***P < 0.001. *Definition of abbreviations:* FOXO3a, forkhead box O3a; JNK, c-Jun N-terminal kinase; ERK 1/2, extracellular-signal-regulated kinase 1/2.

5.3.4 Comparison of the molecular profile of sternohyoid and diaphragm muscle

Figure 5.16 compares the mRNA expression of the most predominant NOX isoforms in skeletal muscle between the sternohyoid and diaphragm muscle. The mRNA expression of NOX2 was significantly lower in the sternohyoid compared with the diaphragm muscle (Fig 5.16; A; $P = 0.0223$). NOX4 mRNA expression was lower in the sternohyoid compared with diaphragm, however this did not reach the threshold for statistical significance (Fig 5.16; B; $P = 0.0519$). There was no difference in the mRNA expression of NOX1 in the diaphragm compared with the sternohyoid (Fig 5.16; C; $P = 0.1947$).

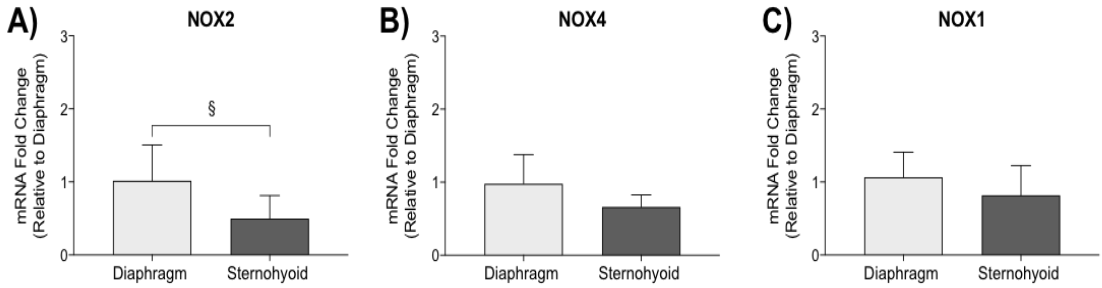

Figure 5.16 Comparison of the mRNA expression of the predominant muscle-specific NOX isoforms in naive wild-type sternohyoid and diaphragm muscle. Group data (mean ± SD, n = 6-9 per group) expressed as a fold change in messenger RNA (mRNA) expression (relative to diaphragm) for A, NOX2, B, NOX4 & C, NOX1 for sham (naïve wild-type) sternohyoid and diaphragm muscle. Data sets, which were normally distributed and of equal variance, were statistically compared using unpaired two-tailed Student's *t* test. Welch's correction was applied in the case of unequal variance. Data, which were not normally distributed, were compared using Mann Whitney non-parametric tests. Statistical significance was taken at $P < 0.05$. § denotes diaphragm *vs.* sternohyoid, $^{\S}P < 0.05$. *Definition of abbreviations:* NOX4, NADPH oxidase 4; NOX2, NADPH oxidase 2; NOX1, NADPH oxidase 1.

Figure 5.17 is a heat map summarising the sternohyoid (A) and diaphragm (B) NOX enzyme mRNA expression data for all genes examined. Figure 5.18 is a heat map summarising the sternohyoid (A) and diaphragm (B) mRNA expression data for all other genes examined.

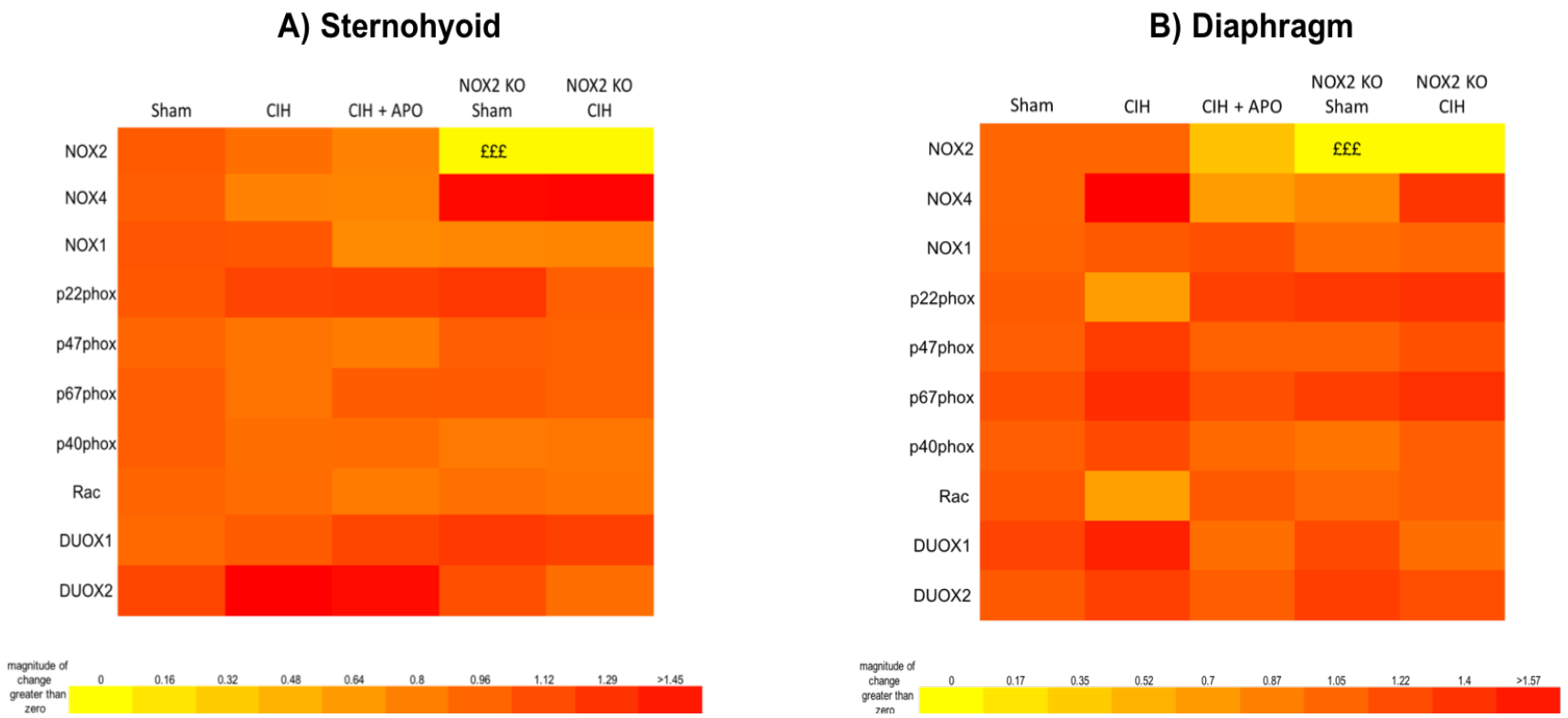

Figure 5.17 Muscle gene expression data expressed in a heat map. Heat map depicting the fold changes in mRNA expression relative to the control (sham) group (mean ± SD, n = 6-8 per group) for NOX enzyme catalytic and accessory subunits for sham, CIH, CIH + APO, NOX2 KO sham and NOX2 KO CIH groups in A) sternohyoid and B) diaphragm muscle. Red represents an increase in expression. $^{£}$ denotes sham *vs.* NOX2 KO sham, $^{£££}P < 0.001$.

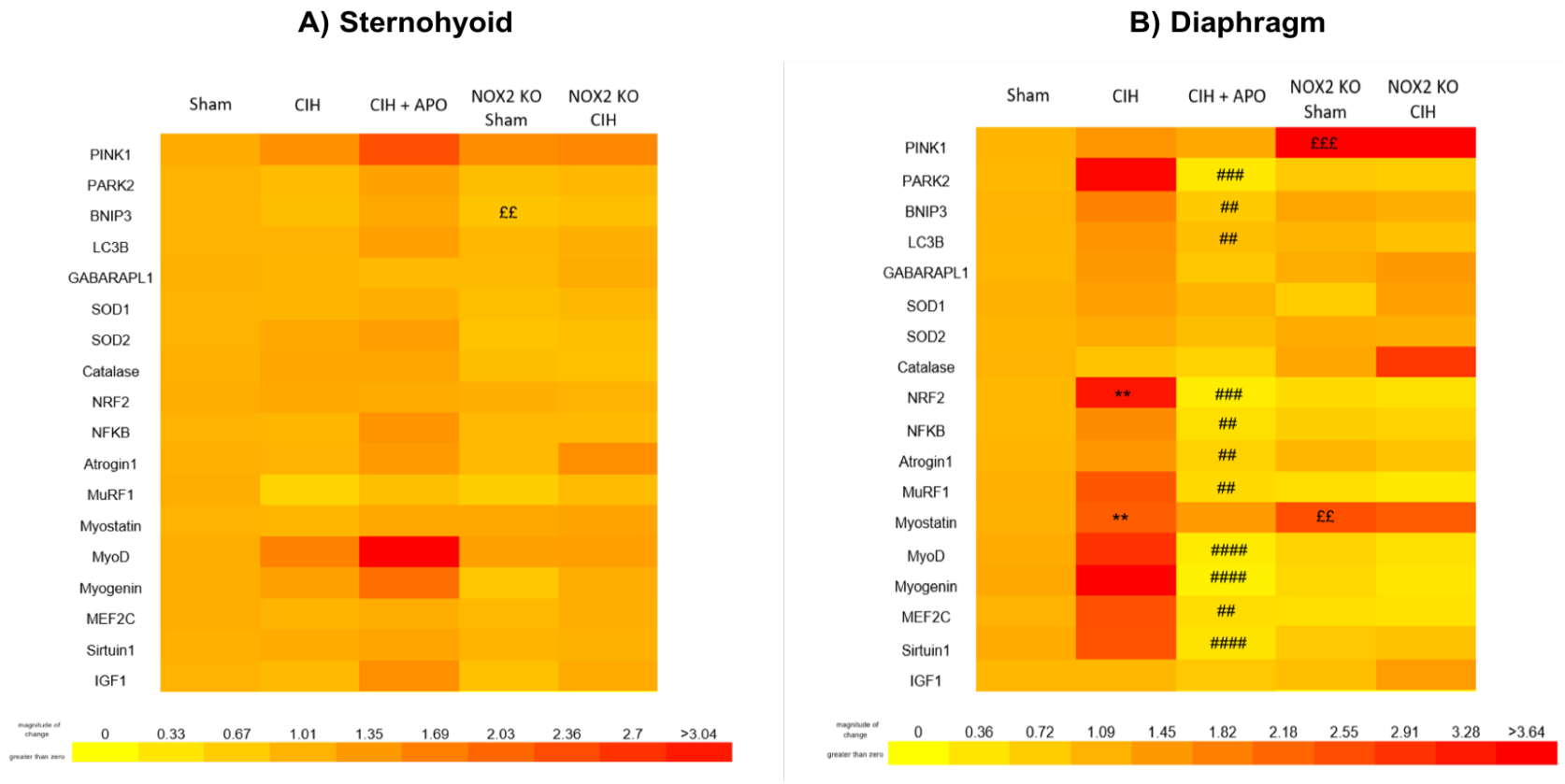

Figure 5.18 Muscle gene expression data expressed in a heat map. Heat map depicting the fold changes in mRNA expression relative to the control (sham) group (mean ± SD, n = 6-8 per group) for genes related to mitochondrial function, autophagy, antioxidant capacity, inflammation, atrophy and muscle differentiation for Sham, CIH, CIH + APO, NOX2 KO Sham and NOX2 KO CIH groups in A) sternohyoid and B) diaphragm muscle. Red represents an increase in expression. Relevant comparisons are denoted as follows: *denotes sham *vs*. CIH, ***P* < 0.01; $^{\#}$ denotes CIH *vs*. CIH + APO, $^{\#\#}$ *P* < 0.01, $^{\#\#\#}$ *P* < 0.001, $^{\#\#\#\#}$ *P* < 0.0001; $^{£}$ denotes Sham *vs.* NOX2 KO Sham, $^{££}$ *P* < 0.01, $^{£££}$ *P* < 0.001.

5.4. Discussion

The key findings of this study are:

1) Exposure to CIH results in considerable diaphragm muscle weakness, which is prevented by treatment with apocynin, and absent in NOX2 KO mice exposed to CIH.

2) NOX2 KO increases the force-generating capacity of the diaphragm muscle compared with wild-type controls (sham).

4) Exposure to CIH does not affect the mRNA or protein expression of NOX2 in diaphragm muscle. However, exposure to CIH increases the mRNA expression and protein expression of NOX4; NOX activity remained unchanged following exposure to CIH.

5) Indices of oxidative stress including levels of TBARS and citrate synthase activity remain unchanged in diaphragm following exposure to CIH. The mRNA expression of NRF2 is increased following exposure to CIH in wild-type mice only.

6) The mRNA expression of genes relating to the regulation of skeletal muscle form and function including autophagy, atrophy, mitophagy and muscle differentiation are increased following exposure to CIH in wild-type mice. The increase is prevented by treatment with apocynin and is absent in NOX2 KO mice following exposure to CIH.

7) Whilst the magnitude of muscle weakness observed in sternohyoid and diaphragm muscle is similar, differences in molecular responses following exposure to CIH highlight the possibility of muscle-specific mechanisms underpinning respiratory muscle dysfunction. Nevertheless, in both muscles, NOX2 is pivotal to CIH-induced muscle weakness.

The diaphragm muscle displays remarkable adaptability and plasticity owing to its mixed fibre-type composition. Diaphragm muscle dysfunction has been reported in OSAS patients (Griggs et al., 1989, Chien et al., 2010), and animals exposed to tracheal occlusion (Smith et al., 2012). Conversely, there is also evidence that diaphragm dysfunction does not present in OSAS patients (Montserrat et al., 1997), revealing considerable heterogeneity in the respiratory consequences of OSAS. A fine balance between the dilating and stabilizing forces produced by UA muscles and the sub-atmospheric collapsing pressure of the diaphragm ensures that UA calibre remains patent (Brouillette and Thach, 1979). During OSAS, the diaphragm is under considerable stress as a consequence of heavy and prolonged contractions during hypoxic periods. This may culminate in tissue hypoxia and disordered energy balance, rendering it more susceptible to further damage, stress and dysfunction (Clanton et al., 2001). It has also been suggested that the diaphragm is susceptible to fatigue during apnoeic episodes in OSAS patients (Vincken et al., 1987). Diaphragm fatigue may represent a reduction in the collapsing force during apnoeas, thereby functioning to offset the effect of UA muscle dysfunction on OSAS pathology. Conversely, weakness and fatigue may also contribute to a reduced ability to generate large powerful manoeuvres necessary for non-ventilatory functions such as airway clearance and cough, which is associated with increased morbidity. CIH-induced muscle plasticity has been shown to extend to the diaphragm, however the underlying mechanisms are largely underexplored.

The effects of exposure to CIH are largely reliant on the duration and intensity of exposure and as a result of this, varied effects of IH on diaphragm muscle function have been reported (Clanton et al., 2001, McGuire et al., 2003, Pae et al., 2005, Shortt et al., 2014, Giordano et al., 2015). In the current study, 2 weeks of exposure to CIH significantly reduced the peak force-generating capacity of the diaphragm by ~45% compared with sham controls. This is consistent with diaphragm dysfunction observed following 2 weeks (Shortt et al., 2014) and 5 weeks (McGuire et al., 2003) of exposure to CIH in rat models. Of note, the degree of diaphragm weakness observed in the current study is greater than that previously reported in rat models following a 2-week exposure to CIH (Shortt et al., 2014) and in fact, is more

reminiscent of diaphragm weakness observed following 6 weeks of exposure to chronic sustained hypoxia (Lewis et al., 2016), associated with profound oxidative stress. Additional measures, including peak work (Wmax), peak power (Pmax) and the work and power produced over the range of loads examined *ex vivo*, were significantly reduced following 2 weeks of exposure to CIH in the diaphragm. We posit that if the reduced power-generating capacity of the diaphragm over physiological loads following exposure to CIH (predominantly due to decreased force-generating capacity) translates *in vivo*, then it would have implications for human OSAS, and diseases characterised by exposure to CIH.

Alterations to Ca^{2+} signalling may contribute to skeletal muscle dysfunction in many muscular disorders such as myopathies, systemic disorders like hypoxia, sepsis, cachexia, sarcopenia, heart failure, and dystrophy (Agrawal et al., 2018). Similar to our observations in the sternohyoid (Chapter 4), exposure to CIH had no effect on the contractile kinetics (CT and ½ RT) of the diaphragm when compared with sham controls. This is consistent with a number of other studies examining diaphragm contractile kinetics in rat models following exposure to varying durations and paradigms of exposure to CIH (McGuire et al., 2003, McDonald et al., 2016). This finding suggests that Ca^{2+} handling in the diaphragm muscle, i.e. its release and re-uptake, at the SR is unaffected by exposure to CIH, thus dysregulated SR functioning is unlikely to underpin CIH-induced diaphragm weakness. Alterations to the distance of shortening or velocity of shortening of respiratory muscles has previously been suggested to be indicative of poor mechanical efficiency, culminating in muscle dysfunction (Attal et al., 2000, Burns et al., 2017). Exposure to CIH results in a decrease in both the distance and velocity of shortening of the diaphragm muscle across a range of physiological loads in the current study. A decrease in these parameters is suggestive of an increased load on the muscle, thereby contributing to a reduced capacity to contract and produce optimal force. We suggest that the reduction in the shortening of the diaphragm observed may have implications in the mechanism underlying CIH-induced diaphragm muscle dysfunction, due to a reduced capacity to contract optimally.

OSAS is an oxidative stress disorder with the ROS produced as a result of recurrent hypoxia/reoxygenation cycles having devasting consequences for a range of integrative bodily systems, highlighting a therapeutic role for antioxidants (Lavie, 2003). Similar to studies in UA musculature (Liu et al., 2005, Dunleavy et al., 2008, Skelly et al., 2012, Skelly et al., 2013) increased ROS production has been implicated in diaphragm muscle dysfunction and indeed, antioxidants have been efficacious in preventing diaphragm weakness and fatigue (Shortt et al., 2014). Administration of tempol, apocynin and NAC each prevented CIH-induced diaphragm muscle fatigue, with NAC proving most efficacious since it also prevented CIH-induced muscle weakness. In the current study, the administration of the NOX2 inhibitor, apocynin, throughout the exposure to CIH, entirely prevented diaphragm muscle weakness, restoring force to levels comparable to controls (sham). Apocynin prevented CIH-induced decreases in diaphragm work and power produced across a range of physiological loads, and also prevented CIH-induced decreases in diaphragm shortening kinetics. These findings are consistent with previous studies, which demonstrate that apocynin successfully ameliorates diaphragmatic contractile dysfunction (Supinski et al., 1999, McClung et al., 2009, Shortt et al., 2014). Moreover, we confirmed these results utilising transgenic NOX2 KO mice, which suggests a key role for NOX2-derived ROS in CIH-induced diaphragm dysfunction. The pronounced CIH-induced diaphragm muscle weakness observed in wild-type mice was entirely absent in NOX2 KO mice, confirming a specific obligatory role for NOX2-derived ROS. Our data are consistent with other studies in mouse models of DMD (Loehr et al., 2018) and CHF (Ahn et al., 2015), which implicate a fundamental role for NOX2 in disease-related diaphragm dysfunction. Our results may have implications for human OSAS. Additionally, our results may have relevance to other disorders characterised by oxidative stress and diaphragm muscle weakness.

It has been well described that ROS hold the capacity to modulate skeletal muscle performance, with the contractile apparatus of muscle fibres proving highly sensitive to alterations in cellular redox state (Reid et al., 1992). Previous studies suggest that under basal conditions, ROS exert a tonic inhibition on UA muscle force production (Skelly et al., 2010, Skelly et al., 2012, Williams et al., 2015). Consistent with this, we

have demonstrated that NOX2 is a culpable source of these ROS in sternohyoid muscle (Chapter 4). Similarly, we demonstrate that NOX2 knock-out results in a ~47% increase in the peak force-generating capacity of the diaphragm compared to wild-type sham mice. This reveals for the first time that the powerful inhibition of NOX2-dependent ROS on muscle force under basal conditions extends to the diaphragm muscle. The power and work produced by the diaphragm over the load continuum examined was increased following NOX2 KO, with no alteration to diaphragm shortening kinetics, indicative of no structural changes which may underlie the increase in force observed. However, reduced contractile kinetics (CT & ½ RT) were observed following NOX2 KO, suggesting an increase in Ca^{2+} release and re-uptake, which may have implications in the mechanism underpinning the increased force-generating capacity of the diaphragm in NOX2 KO mice. An increase in myoplasmic Ca^{2+}or an increase in the sensitivity of myofibrillar proteins to Ca^{2+} in the absence of NOX2 may underlie, or contribute to, the increased force-generating capacity of the diaphragm observed following NOX2 KO. In contrast to our findings, force production has been shown to be normal in the diaphragm of p47phox KO mice, suggesting that NOX2-derived ROS do not exert a tonic inhibition on muscle force under basal conditions (Ahn et al., 2015, Bost et al., 2015). The varied muscle phenotypes between these models may be due to the differential contribution of NOX2 subunits to ROS generation, as we utilise a gp91phox KO model in the current study. The phosphorylation of p47phox is largely considered essential in the production of NOX2-dependent ROS and as such, we would expect to observe the same inotropic effect in the diaphragm following p47phox or gp91phox KO, if NOX2-derived ROS underlies this effect. However, p47phox, but not gp91phox knock-out, has been shown to alter the O_2 sensing capability of the carotid body, exemplified as a potentiated ventilatory and chemoreceptor response to hypoxia (Sanders et al., 2002). This highlights that NOX subunits may differ in their complex regulatory function and contribution to NOX2-dependent ROS within the respiratory system, and therefore this may also extend to the muscles of respiration.

The homologues NOX1, 2 and 4 are the predominant NOX isoforms expressed in skeletal muscle cells in culture (Piao et al., 2005, Sun et al., 2011, Hutchinson et al.,

2007, Handayaningsih et al., 2011, Hori et al., 2011). The relative abundance of these isoforms, based on mRNA data in C2C12 cells, demonstrates that NOX4 is the most highly expressed, followed by NOX2 and subsequently NOX1 (Sun et al., 2011, Handayaningsih et al., 2011). Consistent with this, we have confirmed the mRNA expression of NOX1, 2 and 4, as well as their respective accessory subunits (p22phox, p40phox, p47phox, p67phox, Rac), in diaphragm muscle from wild-type mice. Similar to the sternohyoid (Chapter 4), we observed no difference between the mRNA expression of NOX2 and NOX4 in the diaphragm, however we report significantly lower levels of NOX1 mRNA. In the present study, we also demonstrate low mRNA levels of DUOX1 and DUOX2 in the diaphragm, consistent with that previously reported in C2C12 muscle cells (Sandiford et al., 2014). NOX2- and NOX4-dependent ROS have been strongly implicated in muscle dysfunction in a variety of disease states (Spurney et al., 2008, Whitehead et al., 2010, Sullivan-Gunn and Lewandowski, 2013, Pal et al., 2014, Williams et al., 2015, Henríquez-Olguín et al., 2015, Ahn et al., 2015, Yamada et al., 2015). Therefore, based on these observations in conjunction with our mRNA data, we suggest that NOX2 and NOX4 isoforms hold the most relevance for respiratory muscle pathology in our model.

CIH-induced increases in NOX enzyme expression and/or activity have been reported in a range of organs and tissues (Zhan et al., 2005, Peng et al., 2006, Jun et al., 2008, Hayashi et al., 2008, Nisbet et al., 2009, Peng et al., 2009, Hui-guo et al., 2010, Peng et al., 2011, Gao et al., 2013, Williams et al., 2015). This highlights a role for NOX-dependent ROS in CIH-induced alterations to homeostatic control. We observed no alteration to the mRNA or protein expression of NOX2 in the diaphragm muscle following exposure to CIH in the current study. While transcriptional regulation of NOX2 has been observed, NOX2 is thought to be predominantly acutely regulated by post-translational mechanisms such as the phosphorylation of regulatory cytosolic subunits, thus enabling the enzyme to assemble as a fully functioning complex (Lambeth, 2004). Under resting conditions, NOX2 and p22phox are complexed in the plasma membrane with accessory subunits unbound in the cytosol. Following stimulation by factors such as hypoxia or mechanical stress, including that of muscle contraction (Loureiro et al., 2016), cytosolic subunits are phosphorylated and

translocated to the membrane to elicit the production of NOX2-derived ROS through the oxidation of NADPH. Increases in NOX2 and its accessory subunits have been implicated in diaphragm muscle dysfunction in DMD (Loehr et al., 2018) and CHF (Ahn et al., 2015), evidenced by NOX2 pharmacological blockade and genetic KO ameliorating diaphragm weakness in these models. The pattern, duration and intensity of IH is pivotal in determining a phenotypical response and therefore we suggest that the paradigm of CIH used in this study was not sufficient to induce a transcriptional change in NOX2, but rather may induce an increase in NOX2 assembly and thus, enzymatic activity.

Interestingly, we observed an increase in NOX4 mRNA in the diaphragm of both wild-type and NOX2 KO mice following exposure to CIH. The protein expression of NOX4 was also nearly doubled following exposure to CIH in the diaphragm of wild-type mice. NOX4 is a unique NOX isoform in that it is constitutively active, with its activity largely dependent on its level of protein expression. Therefore, the ROS that NOX4 generates are inducible at the level of gene transcription rather than through acute, post-translational mechanisms (Serrander et al., 2007). NOX4 has been suggested to function as pivotal O_2 sensor, with a number of studies reporting an increase in NOX4 mRNA and protein expression following exposure to hypoxia (Nisbet et al., 2009, Diebold et al., 2010). Thus, we suggest that our results are consistent with these observations based on the transcriptional activation of NOX4 by exposure to CIH in the diaphragm. A decrease in the NOX4 accessory subunits, p22phox and Rac, was observed in the diaphragm of wild-type mice following exposure to CIH. Similar to NOX2, NOX4 requires an association with p22phox to generate ROS, with the mRNA expression of this subunit significantly decreased in the diaphragm following exposure to CIH. While the contribution of Rac to the function of NOX4 is unsettled in the literature, its inhibition has been shown to prevent NOX4-derived H_2O_2 production (Gorin et al., 2003, Meng et al., 2008). Negative feedback mechanisms to prevent against damage through excessive NOX4-derived ROS have previously been demonstrated (Kovac et al., 2015, Matsushima et al., 2016). Rac-induced superoxide production through NOX is connected to a negative feedback loop whereby Rac turnover is accelerated through its increased degradation by the ubiquitin-

proteasome system (Kovacic et al., 2001). This negative feedback loop is thought to represent a switch-off mechanism for the Rac-induced activation of NOX, which controls excessive ROS production in the cell. Therefore, we suggest that the decrease in Rac, and by extension p22phox, observed in the CIH-exposed diaphragm may represent a protective mechanism against NOX4-induced oxidative damage, based on the upregulation of NOX4 mRNA and protein following exposure to CIH. NOX4-dependent ROS have been implicated in poor skeletal muscle function as evidenced by increased NOX4 expression in models of disease characterised by skeletal muscle weakness (Ahn et al., Liu et al., 2017, Regan et al., 2017) and CIH-induced NOX4 expression has also been demonstrated in lung tissue (Nisbet et al., 2009). Therefore, we speculate that our data highlights a role for CIH-induced NOX4 derived ROS in diaphragm muscle dysfunction.

It remains to be elucidated as to how diaphragm muscle weakness is prevented following exposure to CIH in NOX2 KO mice, given the apparent lack of an alteration to NOX2 expression and activity, and the concomitant increase in the abundance of NOX4. Cross-talk between NOX4- and NOX2-dependent ROS has been demonstrated in skeletal muscle, whereby NOX4-derived ROS induce RyR Ca^{2+} leakage, with the increase in Ca^{2+} in the junctional space serving to exacerbate NOX2-derived ROS, which otherwise have little effect on RyR function (Cully and Rodney, 2020). The cumulative effect of this cascade is proposed to manifest as a disruption to downstream cellular processes that contribute to reduced muscle performance. We suggest that NOX4-derived ROS may function through a similar sequential mechanism to contribute to diaphragm muscle weakness through the end effector, NOX2. We observe an increase in NOX4 mRNA in NOX2 KO mice following exposure to CIH, reminiscent of that observed in wild-type mice following exposure to CIH. We suggest that diaphragm muscle weakness is absent in NOX2 KO mice following exposure to CIH because the cumulative production of ROS necessary for muscle weakness, possibly due to cross-talk between NOX4 and NOX2, is absent in NOX2 KO mice. Surprisingly, we observed no CIH-induced increase in NOX enzyme activity in the light of a significant increase in NOX4 expression and our hypothesis that NOX2-dependent CIH-induced diaphragm dysfunction is based on the acute regulation of

NOX2, and the observation of increased NOX2 activity in CIH-induced sternohyoid (Chapter 4). We suggest that this may relate to the NOX activity assay utilised in the current study. NAD(P)H consumption assays have previously been used in the assessment of NOX activity in skeletal muscle (Javeshghani et al., 2002, Adams et al., 2005, Ahn et al., 2015, Bowen et al., 2015a, Bowen et al., 2015b). However, a recent study shows that these assays are not specific to NOX activity and, in several tissues and cell types, the signal generated was unchanged with a triple NOX1, NOX2, and NOX4 knock-out (Rezende et al., 2016). While all NOX enzymes utilise NADPH as an electron donor to reduce O_2 to produce ROS, reports suggest that NOX4 preferentially utilises NADH as an electron donor and so the assay employed in this study may not be suitable to detect changes in NOX4 activity (Shiose et al., 2001). Additionally, NOX activity has been shown in microdomains of skeletal muscle (Cully and Rodney, 2020), therefore the analysis of NOX activity in whole diaphragm muscle homogenates used in the current study may not have been adequately sensitive to detect changes in NOX activity in this instance.

There is evidence of increased oxidative stress in a variety of tissues across animal models of CIH, consistent with the observation that human OSAS is an oxidative stress disorder (Lavie, 2003). However, despite NOX-dependent ROS evidently underpinning CIH-induced diaphragm muscle weakness in our model, we report no evidence of concomitant overt oxidative stress in the diaphragm following exposure to CIH. Oxidative stress may present due to an accumulation of ROS, a depletion of antioxidant defences, or a culmination of both. Skeletal muscle encompasses a robust antioxidant defence system, rendering it remarkably flexible in response to changes in the redox milieu that can occur both in health and disease (Kozakowska et al., 2015). A reduction in the GSSG/GSH ratio, indicative of modest oxidative stress due to the depletion in levels of the endogenous antioxidant GSH, has been reported following exposure to CIH in rat diaphragm muscle (Shortt et al., 2014). CIH-induced diaphragm muscle weakness and a restoration of the GSH system to homeostatic levels was demonstrated following the administration of NAC throughout the exposure to CIH, highlighting the pivotal role of redox homeostasis in muscle contractile function (Shortt et al., 2014). NRF2 is a transcription factor pivotal in

controlling the expression of genes whose protein products are responsible for the elimination of reactive oxidants by enhancing cellular antioxidant capacity (Nguyen et al., 2009). The mRNA expression of NRF2 is significantly increased in the diaphragm following exposure to CIH, with the increase ameliorated in mice administered apocynin and NOX2 KO. This suggests that the production of NOX2-derived ROS following exposure to CIH disrupts redox balance in the diaphragm, with the increase in NRF2 potentially representing an adaptive mechanism to up-regulate antioxidant defences and protect against oxidative injury. Indeed, CIH-induced increases in NRF2 have been observed in renal and cardiac tissue (Sun et al., 2012, Zhou et al., 2017). Surprisingly, we did not observe a subsequent increase in the predominant antioxidants in skeletal muscle; SOD1, SOD2 or catalase. The effects of IH on diaphragm muscle function are time-dependent (Shortt et al., 2014) and therefore it is plausible to suggest that accompanying IH-induced alterations to cell signalling pathways are also transient and complex and warrant further attention. NOX2-derived ROS have previously been shown to activate NRF2 (Chandran et al., 2018). Moreover, combinational antioxidant therapy inhibiting NOX2, while concomitantly activating NRF2, has been utilised in a model of traumatic brain injury (Chandran et al., 2018). We suggest that the CIH-induced NOX2-dependent increase in the mRNA expression of NRF2 may point to an early adaptive response, ultimately serving to increase antioxidant status in the diaphragm as a defence against CIH-induced NOX2-derived ROS. The specificity of the NRF2 response further highlights that a redox signature underpins respiratory muscle dysfunction following exposure to CIH.

ROS have been shown to oxidise lipids as a function of the severity of OSAS (Hopps et al., 2014). TBARS are degradation products of fats routinely used as a marker of lipid peroxidation, as an indirect measurement of oxidative stress. Levels of TBARS show a positive correlation to OSAS severity as determined by increased apnoea index (Kent et al., 2011). We report no evidence of lipid peroxidation in the diaphragm following exposure to CIH, as evidenced by unchanged levels of TBARS. This is consistent with previous observations in rat models that report unaltered levels of MDA and 4-HNE in the diaphragm following a 2-week exposure to CIH (Shortt et al., 2014). We suggest that the relatively moderate paradigm of CIH utilised

in the current study was not sufficient to cause oxidative stress, in the form of lipid peroxidation, similar to our observations in the sternohyoid muscle (Chapter 4).

Mitochondria are an important source of ROS in skeletal muscle with ROS-dependent alterations to mitochondrial function and/or capacity proving consequential for skeletal muscle function (Hood et al., 2019). Mal-adaptation of skeletal muscle to periods of hypoxia have been demonstrated as a loss of mitochondrial content, thus a reduced oxidative capacity and less endurant phenotype (Gamboa and Andrade, 2010). Citrate synthase activity is a routinely used marker of mitochondrial integrity and thus, aerobic capacity as it is the initial enzyme of the tricarboxylic acid (TCA) cycle. Citrate synthase activity has been shown to be reduced following 10 days of intermittent hypoxia in rat diaphragm, suggestive of shift away from mitochondrial respiration towards glycolysis (Clanton et al., 2001). In contrast, we observed no alteration to citrate synthase activity in the CIH-exposed diaphragm, which may relate to differences in the intensity of IH used between these studies. Similarly, other metabolic markers, including SDH and GPDH activity, have been shown to be unaltered in rat diaphragm following exposure to CIH (Shortt et al., 2013, Shortt et al., 2014), indicating that alterations to skeletal muscle metabolism are not likely to underlie the altered contractile function of the diaphragm following exposure to CIH. Mitochondria utilise a specialised form of autophagy, known as mitophagy, to protect against excessive ROS. Given the pivotal role of O_2 as an electron acceptor in the ETC, hypoxia induces a build-up of electrons in this cycle, leading to an increased electron leakage and subsequent ROS formation. The increased ROS formation exacerbates mitochondrial dysfunction, yielding detrimental effects for muscle contractile performance. Additionally, mitochondrial function has been shown to be essential for plasma membrane repair in skeletal muscle fibres, with mitochondrial ROS shown to be pivotal in facilitating this membrane repair (Horn et al., 2017). Inhibiting mitochondrial ROS in myofibres during eccentric exercise *ex vivo* increases myofibre damage with concomitant muscle force loss (Horn et al., 2017). This highlights the beneficial role of mitochondrial ROS in repair mechanisms in response to strain on skeletal muscle. In the current study, we examined the mRNA expression of the PINK1/PARK2 pathway which has emerged as a principal regulator of

mitochondrial degradation in a range of biological systems (Narendra and Youle, 2011). PARK2 mRNA expression was increased in the diaphragm following exposure to CIH, with apocynin treatment and NOX2 KO each efficacious in preventing the increase. An increase in mitophagy as a protective mechanism has previously been demonstrated in platelets, cardiomyocytes and models of cerebral ischaemia (Lee et al., 2016, Tang et al., 2016, Nah et al., 2017, Tan et al., 2019). On the contrary, an over-activation of mitophagy due to a persistent stimulus may result in the degradation of essential mitochondrial machinery, which would similarly have unfavourable consequences for skeletal muscle function (Borgia et al., 2017, Sato et al., 2018). Cross-talk between NOX and the mitochondria has been demonstrated, as NOX-derived ROS increase mitochondrial ROS (Dikalov, 2011, Kim et al., 2017). If the CIH-induced increase in PARK2 mRNA observed in the current study translates to an increase in mitophagy, it may represent a protective mechanism against excessive NOX2-derived ROS-induced mitochondrial stress, which would otherwise have detrimental effects on skeletal muscle performance. However, further experimentation to measure mitophagic flux and/or dynamics is necessary to confirm the implications of the observed CIH-induced increase in PARK2 mRNA. However, since citrate synthase activity was unchanged, it is likely that the mitochondrial density in CIH-exposed diaphragm is normal.

Structural alterations in the form of muscle atrophy are unaltered following a 2-week exposure to CIH in the diaphragm in rat models, however, an increase in type 2B fibres has been observed suggestive of a switch towards a more fatigable muscle phenotype (Shortt et al., 2013, Shortt et al., 2014). In contrast, 4 days of IH has been shown to result in a fibre-type switch towards type-1 fibres, representing a compensatory metabolic switch associated with fatigue resistance (Giordano et al., 2015). Divergent responses between these studies may be due to the duration of IH with resultant adaptive and mal-adaptive responses in fibre-type transitions. In the current study, we observed a trend towards a pro-atrophic (atrogin-1 & MuRF1) and pro-autophagic (LC3B, GABARAPL1 & BNIP3) response in the diaphragm following exposure to CIH at the mRNA level, which was ameliorated by treatment with apocynin and was absent in mice lacking the NOX2 enzyme. This is consistent with

studies reporting an increase in the mRNA of autophagy markers (LC3B, GABARAPL1 & BNIP3) with concomitant diaphragm atrophy following 4 days of IH exposure (Giordano et al., 2015). Indeed, an interplay between atrophy and autophagy has been demonstrated to underlie a loss of muscle mass and resultant weakness in skeletal muscle (Dobrowolny et al., 2008). Additionally, a decrease in phospho-JNK and phospho-p38 observed in the diaphragm following exposure to CIH in the current study is suggestive of decreased protein synthesis, perhaps via the mTOR pathway. An increase in NOX4 expression with concomitant skeletal muscle atrophy has been demonstrated in rat models of SCI (Liu et al., 2017). Similarly, the deletion of NOX2 has been shown to prevent Ang-II induced skeletal muscle atrophy (Kadoguchi et al.). Consistent with these observations, our results suggest that NOX2-derived ROS may promote diaphragm muscle atrophy following exposure to CIH, which may subsequently decrease muscle mass and contribute to a reduced force-generating capacity of the diaphragm.

Studies have shown that physiological hypoxia tends to result in muscle cell proliferation and myogenesis, whereas pathological hypoxia is largely mal-adaptive and inhibits myogenesis (Yun et al., 2005). Indeed, the intensity of the hypoxic stimulus appears to be paramount in determining the myogenic response (Sakushima et al., 2020). Skeletal muscle has a large capacity to regenerate and re-establish homeostatic contractile and metabolic properties in response to severe damage. NOX2 has been shown to stimulate muscle differentiation, with the increase prevented by treatment with DPI and apocynin in C2C12 myoblasts (Piao et al., 2005). Consistent with this, we observed an increase in the mRNA of key MRFs (Myogenin, MyoD & MEF2C) in the diaphragm following exposure to CIH, with the increase absent following treatment with apocynin and NOX2 KO. Successive rounds of muscle degeneration and regeneration can result in the incomplete remodelling of the ECM. This leads to the generation of large amounts of fibrosis and scar tissue rather than contractile tissue, thus yielding a muscle with a lower force-generating capacity (Smith and Barton, 2018). CIH-induced fibrosis has been reported in a range of organs and tissues (Didier et al., Kang et al., 2017, Kang et al., 2018, Wang et al., 2018, Zhang et al., 2019). Earlier, we reported a modest decrease in the shortening

velocity and distance of shortening in the diaphragm following exposure to CIH, which is not present following apocynin treatment or NOX2 KO. Therefore, it is plausible to suggest that CIH-induced fibrosis, as a result of dysregulated myogenesis, may inhibit its optimal contraction. However, we also report a concomitant increase in the negative regulator of myogenesis, myostatin, suggestive of increased myogenesis being a regulated and adaptive response to muscle damage elicited by exposure to CIH. Further work is warranted to assess the effects of these changes at the mRNA level on the structure of the diaphragm to delineate whether this myogenic signal translates to a structural alteration in the diaphragm muscle and if so, whether this culminates as adaptive or mal-adaptive, and whether NOX2 is obligatory for the outcome.

We demonstrate that NOX2-derived ROS underlie CIH-induced diaphragm muscle weakness. A complex interplay between increased NOX4 and NOX2 expression and/or activity appears to culminate in a sufficient level of ROS necessary to induce diaphragm muscle weakness. Oxidative stress *per se* is absent in the diaphragm following the paradigm of exposure to CIH utilised in the current study. However, an increase in the antioxidant defence system may represent an early adaptive response to protect against excessive NOX2-derived ROS, perhaps indicative of a modest (and localised) disruption to redox balance. NOX2-derived ROS appear to underlie CIH-induced increases in the mRNA expression of genes relating to mitophagy, autophagy, atrophy and myogenesis. We acknowledge that these changes are determined only at the level of transcription and a comprehensive understanding of whether these alterations represent adaptive or mal-adaptive responses for muscle structure, and thus function, following exposure to CIH remains to be elucidated. Additionally, these processes do not appear to be HIF-1α-dependent. As previously mentioned in Chapter 4, mice were normoxic for several hours following the last exposure to CIH. Therefore, HIF-1α-dependent signalling may have a role in CIH-induced respiratory muscle remodelling, but it may not be obligatory in the persistent expression of respiratory muscle weakness. We also speculate that NOX-derived ROS may also affect muscle contractile performance through alterations to Ca^{2+} sensitivity of myofilaments influencing cross-bridge cycling or through

alterations to Ca^{2+} sensitivity of the contractile apparatus through redox modulation of troponin (de Paula Brotto et al., 2001, Ottenheijm et al., 2005, Ottenheijm et al., 2006, Coirault et al., 2007, Degens et al., 2010, Smuder et al., 2010, Pinto et al., 2011, McDonagh et al., 2014). Alternatively, or concurrently, NOX-derived ROS may elicit their effects through downstream signalling processes that regulate the structure and hence functional capacity of skeletal muscle.

We have demonstrated that CIH-induced muscle weakness is entirely prevented by NOX2 KO in sternohyoid (Chapter 4) and diaphragm muscle. However, the mechanisms underpinning respiratory muscle weakness are likely to be muscle fibre-type specific, as evidenced by varied molecular responses to exposure to CIH between respiratory muscles revealed in the current study. Skeletal muscles are made up of heterogeneous fibre types that display distinct metabolic and contractile properties corresponding to the specific function of that muscle. Skeletal muscle fibres have different properties with respect to force, shortening velocity, time of relaxation, fatigability, and metabolic capacities. Skeletal muscle has a remarkable ability to modify its size and adjust its metabolic and contractile properties to a variety of stimuli including endogenous and exogenous stimuli, including mechanical stress and neuronal activity (i.e. contractile activity) as well as environmental stimuli (i.e. hypoxia) (Flück, 2006). Consistent with this, the specialisation of respiratory muscles appears to derive from the characteristics of the fibres from which they are composed. The diaphragm encompasses a mixture of all 4 myosin isoform subtypes. Type 1 and type 2a (oxidative) fibres support the diaphragm's primary function as an inspiratory pump muscle through the preservation of a high degree of endurance. Additionally, the diaphragm exhibits a large force reserve capacity owing to type 2x/2b (glycolytic) fibres. These fibres generate large amounts of force to facilitate non-respiratory functions such as airway clearance manoeuvres (Gransee et al., 2012). The sternohyoid is structurally composed of mainly type 2b fibres, enabling large force generation, which is essential in the negative pressure reflex activation of UA muscles to defend airway patency and associated functions in swallowing.

Diaphragm muscle remodelling and dysfunction presents in several diseases characterised by respiratory disturbances. Sarcopenia, an age-related disorder of skeletal muscle, is associated with a loss of muscle mass and function (Fielding et al., 2011). In murine models, the diaphragm muscle of older mice exhibit a ~35% decrease in force compared with younger mice, with a concomitant reduction in the size of the type 2x and/or 2b fibres (Greising et al., 2013, Greising et al., 2015). This is expected to impact on the ability of the diaphragm to perform non-ventilatory function, such as airway clearance. Cancer associated muscle dysfunction is a major syndrome, with the spectrum ranging from muscle weakness in the absence of weight loss to profound muscle wasting and cachexia (Fearon et al., 2013). Persistent oxidative stress (Giordano et al., 2003), atrophy and resultant muscle weakness of the diaphragm (Roberts et al., 2013) are associated with respiratory failure, a major cause of death in cancer patients. Indeed, animal models demonstrate a 30% reduction in respiratory muscle force production, atrophy and dysfunction across all fibre types, culminating in significantly impaired ventilation (Roberts et al., 2013). CHF causes diaphragm muscle weakness and fatigue that contributes to dyspnoea and limited physical capacity in patients (Empinado et al., 2014). Studies in mouse models of CHF display a 35% reduction in the force-generating capacity of the diaphragm, with an attendant increase in oxidative stress markers (Ahn et al., 2015), highlighting that diaphragm abnormalities contribute to the pathophysiology of CHF. Patients with COPD display reduced maximal inspiratory and expiratory pressures and the endurance of respiratory muscles is often reduced. Respiratory muscle dysfunction in COPD patients imposes ventilatory constraints, which may serve to perpetuate respiratory failure already present in patients. Animal models utilising chronic sustained hypoxia to mimic COPD display diaphragm weakness evidenced by a 35% reduction in the force-generating capacity (Lewis et al., 2016). Structural alterations in the form of type 2B fibre atrophy, oxidative stress and increased proteolysis are features of diaphragm muscle in COPD patients and animal models of the disease (Barreiro and Gea, 2015). Respiratory failure is a leading cause of mortality in patients with DMD. Profound diaphragm muscle weakness demonstrated by a 50% reduction in the force generated by *mdx* mice has previously been demonstrated (Burns et al., 2019). Dystrophic diaphragm muscle weakness is

associated with fibre remodelling, fibrosis, inflammation and oxidative stress resulting in a severe mechanical disadvantage. Therefore, the respiratory muscle weakness we observed in the current study following a relatively modest exposure to CIH is quite remarkable when compared to other models that display severe respiratory deficits with lesser or similar magnitudes of weakness. Our model exemplifies the powerful inhibitory effect of NOX-2 derived ROS in suppressing muscle function, in the absence of overt oxidative stress. OSAS is a common disorder and it presents as a co-morbidity in many other respiratory conditions such as COPD and DMD. Our study draws focus to the potential role of exposure to CIH on diaphragm dysfunction in a range of disorders. Moreover, our study reveals NOX2 as a potential target in the treatment of diaphragm dysfunction.

NOX expression has previously been shown to be higher in oxidative fibres compared with glycolytic fibres in limb muscle, with differences in the expression of NOX in fibre types possibly relating to the contractile characteristics of each fibre (Loureiro et al., 2016). It has been suggested that NOX enzymes have a role in skeletal muscle contraction through alterations to EC coupling and that higher NOX activity in muscles with a high density of oxidative fibres could be related to higher intracellular Ca^{2+} availability during contractions, crucial for sustaining muscle contractions for longer periods of time, which is characteristic of slow-twitch fibres (Loureiro et al., 2016). Consistent with this, we show a greater mRNA expression of NOX enzymes (NOX2 & NOX4) in the diaphragm compared with the sternohyoid muscle. However, we report higher NOX activity in the sternohyoid muscle compared with the diaphragm. This discrepancy may be due to the differential regulation of NOX isoforms (i.e. regulated transcriptionally or post translationally), the muscle-specific regulation and contribution of NOX-derived ROS to cellular processes, or perhaps may relate to the NOX activity assay we utilised. While NOX2 is essential for CIH-induced muscle weakness in both the sternohyoid and diaphragm muscle, we observed a CIH-induced increase in NOX4 in the diaphragm only. Owing to its oxidative phenotype, the diaphragm encompasses a greater density of mitochondria than the sternohyoid and indeed, NOX4 contains a mitochondria localisation sequence in its n-terminal and as such has been identified in the mitochondria of

cardiac (Ago et al., 2010) and skeletal muscle (Sakellariou et al., 2013). Moreover, a sequential pathway whereby NOX4-derived H_2O_2 activate NOX2 which then evokes an increase in mitochondrial ROS has been demonstrated in endothelial cells (Kim et al., 2017). This may represent a feed-forward mechanism of ROS-induced ROS release orchestrated by NOX2 and NOX4. This increase in ROS may subsequently affect downstream signalling pathways important in the form and function of skeletal muscle. Therefore, it is plausible to suggest that this may explain, in part, the NOX2-dependent CIH-induced increase in the mRNA expression of genes relating to atrophy, mitophagy, autophagy and muscle differentiation in the diaphragm compared with the sternohyoid. Additionally, oxidative and glycolytic fibres differ in their contractile response, in that increased tension during contraction reaches a peak and declines faster in glycolytic than in oxidative fibres (Polla et al., 2004), determined by Ca^{2+} release and re-uptake at the SR, the sensitivity of the myofibrils to Ca^{2+}, and the rate at which myosin forms cross bridges with actin. The density of Ca^{2+} release units and Ca^{2+} pumps are higher in fast fibres than in slow fibres (Franzini-Armstrong et al., 1999) and different specific isoforms of SERCA are expressed in slow and in fast fibres (Lytton et al., 1992). Therefore, glycolytic fibres may be more susceptible to alterations to these elements of muscle contractile performance which would alter the capacity to produce fast, forceful manoeuvres such as those produced by the sternohyoid in the maintenance of airway patency. Similarly, this is also applicable to glycolytic fibres of the diaphragm, which are pivotal in high force-dependent manoeuvres.

The significance of our findings is that exposure to CIH, a hallmark feature of human OSAS, is detrimental to the function of the diaphragm, potentially affecting ventilatory and non-ventilatory performance of the respiratory system. Combined with upper airway muscle dysfunction (Chapter 4), exposure to CIH could establish a vicious cycle serving to exacerbate respiratory morbidity in human OSAS. Therapeutic strategies to improve diaphragm muscle performance, through NOX2 blockade, may function as an adjunctive therapy to reduce disease burden in human OSAS. Our results may also have relevance to other diseases characterised by diaphragm muscle weakness.

5.6 References

ADAMS, V., LINKE, A., KRÄNKEL, N., ERBS, S., GIELEN, S., MÖBIUS-WINKLER, S., GUMMERT, J. F., MOHR, F. W., SCHULER, G. & HAMBRECHT, R. 2005. Impact of regular physical activity on the NAD(P)H oxidase and angiotensin receptor system in patients with coronary artery disease. *Circulation,* 111**,** 555-62.

AGO, T., KURODA, J., PAIN, J., FU, C., LI, H. & SADOSHIMA, J. 2010. Upregulation of Nox4 by hypertrophic stimuli promotes apoptosis and mitochondrial dysfunction in cardiac myocytes. *Circ Res,* 106**,** 1253-64.

AGRAWAL, A., SURYAKUMAR, G. & RATHOR, R. 2018. Role of defective Ca(2+) signaling in skeletal muscle weakness: Pharmacological implications. *J Cell Commun Signal,* 12**,** 645-659.

AHN, B., BEHARRY, A. W., COBLENTZ, P. D., PATEL, N., JUDGE, A. R., BONNELL, M. R. & HOOPES, C. W. Diaphragm Abnormalities in Heart Failure Patients: Upregulation of NAD(P)H Oxidase Subunits and Heightened Protein Oxidation. *C73. OXIDANTS.*

AHN, B., BEHARRY, A. W., FRYE, G. S., JUDGE, A. R. & FERREIRA, L. F. 2015. NAD(P)H oxidase subunit p47phox is elevated, and p47phox knockout prevents diaphragm contractile dysfunction in heart failure. *Am J Physiol Lung Cell Mol Physiol,* 309**,** L497-505.

ATTAL, P., LAMBERT, F., MARCHAND-ADAM, S., BOBIN, S., POURNY, J. C., CHEMLA, D., LECARPENTIER, Y. & COIRAULT, C. 2000. Severe mechanical dysfunction in pharyngeal muscle from adult mdx mice. *Am J Respir Crit Care Med,* 162**,** 278-81.

BARREIRO, E. & GEA, J. 2015. Respiratory and Limb Muscle Dysfunction in COPD. *Copd,* 12**,** 413-26.

BORGIA, D., MALENA, A., SPINAZZI, M., DESBATS, M. A., SALVIATI, L., RUSSELL, A. P., MIOTTO, G., TOSATTO, L., PEGORARO, E., SORARÙ, G., PENNUTO, M. & VERGANI, L. 2017. Increased mitophagy in the skeletal muscle of spinal and bulbar muscular atrophy patients. *Hum Mol Genet,* 26**,** 1087-1103.

BOST, E. R., FRYE, G. S., AHN, B. & FERREIRA, L. F. 2015. Diaphragm dysfunction caused by sphingomyelinase requires the p47(phox) subunit of NADPH oxidase. *Respir Physiol Neurobiol,* 205**,** 47-52.

BOWEN, T. S., MANGNER, N., WERNER, S., GLASER, S., KULLNICK, Y., SCHREPPER, A., DOENST, T., OBERBACH, A., LINKE, A., STEIL, L., SCHULER, G. & ADAMS, V. 2015a. Diaphragm muscle weakness in mice is early-onset post-myocardial infarction and associated with elevated protein oxidation. *J Appl Physiol (1985),* 118**,** 11-9.

BOWEN, T. S., ROLIM, N. P., FISCHER, T., BAEKKERUD, F. H., MEDEIROS, A., WERNER, S., BRØNSTAD, E., ROGNMO, O., MANGNER, N., LINKE, A., SCHULER, G., SILVA, G. J., WISLØFF, U. & ADAMS, V. 2015b. Heart failure with preserved ejection fraction induces molecular, mitochondrial, histological, and functional alterations in rat respiratory and limb skeletal muscle. *Eur J Heart Fail,* 17**,** 263-72.

BROUILLETTE, R. T. & THACH, B. T. 1979. A neuromuscular mechanism maintaining extrathoracic airway patency. *J Appl Physiol Respir Environ Exerc Physiol,* 46**,** 772-9.

BURNS, D. P., DRUMMOND, S. E., BOLGER, D., COISCAUD, A., MURPHY, K. H., EDGE, D. & O'HALLORAN, K. D. 2019. N-acetylcysteine Decreases Fibrosis and Increases Force-Generating Capacity of mdx Diaphragm. *Antioxidants (Basel),* 8.

BURNS, D. P., ROWLAND, J., CANAVAN, L., MURPHY, K. H., BRANNOCK, M., O'MALLEY, D., O'HALLORAN, K. D. & EDGE, D. 2017. Restoration of pharyngeal dilator muscle force in dystrophin-deficient (mdx) mice following co-treatment with neutralizing interleukin-6 receptor antibodies and urocortin 2. *Exp Physiol,* 102**,** 1177-1193.

CHANDRAN, R., KIM, T., MEHTA, S. L., UDHO, E., CHANANA, V., CENGIZ, P., KIM, H., KIM, C. & VEMUGANTI, R. 2018. A combination antioxidant therapy to inhibit NOX2 and activate Nrf2 decreases secondary brain damage and improves functional recovery after traumatic brain injury. *J Cereb Blood Flow Metab,* 38**,** 1818-1827.

CHIEN, M. Y., WU, Y. T., LEE, P. L., CHANG, Y. J. & YANG, P. C. 2010. Inspiratory muscle dysfunction in patients with severe obstructive sleep apnoea. *Eur Respir J,* 35**,** 373-80.

CLANTON, T. L., WRIGHT, V. P., REISER, P. J., KLAWITTER, P. F. & PRABHAKAR, N. R. 2001. Selected Contribution: Improved anoxic tolerance in rat diaphragm following intermittent hypoxia. *Journal of Applied Physiology,* 90**,** 2508-2513.

COIRAULT, C., GUELLICH, A., BARBRY, T., SAMUEL, J. L., RIOU, B. & LECARPENTIER, Y. 2007. Oxidative stress of myosin contributes to skeletal muscle dysfunction in rats with chronic heart failure. *Am J Physiol Heart Circ Physiol,* 292**,** H1009-17.

CULLY, T. R. & RODNEY, G. G. 2020. Nox4 - RyR1 - Nox2: Regulators of micro-domain signaling in skeletal muscle. *Redox Biol,* 36**,** 101557.

DE PAULA BROTTO, M., VAN LEYEN, S. A., BROTTO, L. S., JIN, J. P., NOSEK, C. M. & NOSEK, T. M. 2001. Hypoxia/fatigue-induced degradation of troponin I and troponin C: new insights into physiologic muscle fatigue. *Pflugers Arch,* 442**,** 738-44.

DEGENS, H., BOSUTTI, A., GILLIVER, S. F., SLEVIN, M., VAN HEIJST, A. & WÜST, R. C. 2010. Changes in contractile properties of skinned single rat soleus and diaphragm fibres after chronic hypoxia. *Pflugers Arch,* 460**,** 863-73.

DIDIER, M., ROTENBERG, C., MARCHANT, D., SUTTON, A., VALEYRE, D., NUNES, H., BONCOEUR, E. & PLANES, C. Effect of Chronic Intermittent Hypoxia in a Murine Model of Bleomycin-Induced Pulmonary Fibrosis. *B57. FIBROSIS BIOLOGY.*

DIEBOLD, I., PETRY, A., HESS, J. & GORLACH, A. 2010. The NADPH oxidase subunit NOX4 is a new target gene of the hypoxia-inducible factor-1. *Mol Biol Cell,* 21**,** 2087-96.

DIKALOV, S. 2011. Cross talk between mitochondria and NADPH oxidases. *Free Radic Biol Med,* 51**,** 1289-301.

DOBROWOLNY, G., AUCELLO, M., RIZZUTO, E., BECCAFICO, S., MAMMUCARI, C., BONCOMPAGNI, S., BELIA, S., WANNENES, F., NICOLETTI, C., DEL PRETE, Z., ROSENTHAL, N., MOLINARO, M., PROTASI, F., FANÒ, G., SANDRI, M. & MUSARÒ, A. 2008. Skeletal muscle is a primary target of SOD1G93A-mediated toxicity. *Cell Metab,* 8**,** 425-36.

DUNLEAVY, M., BRADFORD, A. & O'HALLORAN, K. D. 2008. Oxidative stress impairs upper airway muscle endurance in an animal model of sleep-disordered breathing. *Adv Exp Med Biol,* 605**,** 458-62.

EMPINADO, H. M., DEEVSKA, G. M., NIKOLOVA-KARAKASHIAN, M., YOO, J. K., CHRISTOU, D. D. & FERREIRA, L. F. 2014. Diaphragm dysfunction in heart failure is accompanied by increases in neutral sphingomyelinase activity and ceramide content. *Eur J Heart Fail,* 16**,** 519-25.

FEARON, K., ARENDS, J. & BARACOS, V. 2013. Understanding the mechanisms and treatment options in cancer cachexia. *Nat Rev Clin Oncol,* 10**,** 90-9.

FIELDING, R. A., VELLAS, B., EVANS, W. J., BHASIN, S., MORLEY, J. E., NEWMAN, A. B., ABELLAN VAN KAN, G., ANDRIEU, S., BAUER, J., BREUILLE, D., CEDERHOLM, T., CHANDLER, J., DE MEYNARD, C., DONINI, L., HARRIS, T., KANNT, A., KEIME GUIBERT, F., ONDER, G., PAPANICOLAOU, D., ROLLAND, Y., ROOKS, D., SIEBER, C., SOUHAMI, E., VERLAAN, S. & ZAMBONI, M. 2011. Sarcopenia: an undiagnosed condition in older adults. Current consensus definition: prevalence, etiology, and consequences. International working group on sarcopenia. *J Am Med Dir Assoc,* 12**,** 249-56.

FLÜCK, M. 2006. Functional, structural and molecular plasticity of mammalian skeletal muscle in response to exercise stimuli. *J Exp Biol,* 209**,** 2239-48.

FRANZINI-ARMSTRONG, C., PROTASI, F. & RAMESH, V. 1999. Shape, size, and distribution of Ca(2+) release units and couplons in skeletal and cardiac muscles. *Biophys J,* 77**,** 1528-39.

GAMBOA, J. L. & ANDRADE, F. H. 2010. Mitochondrial content and distribution changes specific to mouse diaphragm after chronic normobaric hypoxia. *Am J Physiol Regul Integr Comp Physiol,* 298**,** R575-83.

GAO, J., DING, X. S., ZHANG, Y. M., DAI, D. Z., LIU, M., ZHANG, C. & DAI, Y. 2013. Hypoxia/oxidative stress alters the pharmacokinetics of CPU86017-RS through mitochondrial dysfunction and NADPH oxidase activation. *Acta Pharmacol Sin,* 34**,** 1575-84.

GIORDANO, A., CALVANI, M., PETILLO, O., CARTENI, M., MELONE, M. R. & PELUSO, G. 2003. Skeletal muscle metabolism in physiology and in cancer disease. *J Cell Biochem,* 90**,** 170-86.

GIORDANO, C., LEMAIRE, C., LI, T., KIMOFF, R. J. & PETROF, B. J. 2015. Autophagy-associated atrophy and metabolic remodeling of the mouse diaphragm after short-term intermittent hypoxia. *PLoS One,* 10**,** e0131068.

GORIN, Y., RICONO, J. M., KIM, N. H., BHANDARI, B., CHOUDHURY, G. G. & ABBOUD, H. E. 2003. Nox4 mediates angiotensin II-induced activation of Akt/protein kinase B in mesangial cells. *Am J Physiol Renal Physiol,* 285**,** F219-29.

GRANSEE, H. M., MANTILLA, C. B. & SIECK, G. C. 2012. Respiratory muscle plasticity. *Compr Physiol,* 2**,** 1441-62.

GREISING, S. M., MANTILLA, C. B., GORMAN, B. A., ERMILOV, L. G. & SIECK, G. C. 2013. Diaphragm muscle sarcopenia in aging mice. *Exp Gerontol,* 48**,** 881-7.

GREISING, S. M., MEDINA-MARTÍNEZ, J. S., VASDEV, A. K., SIECK, G. C. & MANTILLA, C. B. 2015. Analysis of muscle fiber clustering in the diaphragm muscle of sarcopenic mice. *Muscle Nerve,* 52**,** 76-82.

GRIGGS, G. A., FINDLEY, L. J., SURATT, P. M., ESAU, S. A., WILHOIT, S. C. & ROCHESTER, D. F. 1989. Prolonged relaxation rate of inspiratory muscles in patients with sleep apnea. *Am Rev Respir Dis,* 140**,** 706-10.

HANDAYANINGSIH, A. E., IGUCHI, G., FUKUOKA, H., NISHIZAWA, H., TAKAHASHI, M., YAMAMOTO, M., HERNINGTYAS, E. H., OKIMURA, Y., KAJI, H., CHIHARA, K., SEINO, S. & TAKAHASHI, Y. 2011. Reactive oxygen species play an essential role in IGF-I signaling and IGF-I-induced myocyte hypertrophy in C2C12 myocytes. *Endocrinology,* 152**,** 912-21.

HAYASHI, T., YAMASHITA, C., MATSUMOTO, C., KWAK, C. J., FUJII, K., HIRATA, T., MIYAMURA, M., MORI, T., UKIMURA, A., OKADA, Y., MATSUMURA, Y. & KITAURA, Y. 2008. Role of gp91phox-containing NADPH oxidase in left ventricular remodeling induced by intermittent hypoxic stress. *Am J Physiol Heart Circ Physiol,* 294**,** H2197-203.

HENRÍQUEZ-OLGUÍN, C., ALTAMIRANO, F., VALLADARES, D., LÓPEZ, J. R., ALLEN, P. D. & JAIMOVICH, E. 2015. Altered ROS production, NF-κB activation and interleukin-6 gene expression induced by electrical stimulation in dystrophic mdx skeletal muscle cells. *Biochim Biophys Acta,* 1852**,** 1410-9.

HOOD, D. A., MEMME, J. M., OLIVEIRA, A. N. & TRIOLO, M. 2019. Maintenance of Skeletal Muscle Mitochondria in Health, Exercise, and Aging. *Annu Rev Physiol,* 81**,** 19-41.

HOPPS, E., CANINO, B., CALANDRINO, V., MONTANA, M., LO PRESTI, R. & CAIMI, G. 2014. Lipid peroxidation and protein oxidation are related to the severity of OSAS. *Eur Rev Med Pharmacol Sci,* 18**,** 3773-8.

HORI, Y. S., KUNO, A., HOSODA, R., TANNO, M., MIURA, T., SHIMAMOTO, K. & HORIO, Y. 2011. Resveratrol ameliorates muscular pathology in the dystrophic mdx mouse, a model for Duchenne muscular dystrophy. *J Pharmacol Exp Ther,* 338**,** 784-94.

HORN, A., VAN DER MEULEN, J. H., DEFOUR, A., HOGARTH, M., SREETAMA, S. C., REED, A., SCHEFFER, L., CHANDEL, N. S. & JAISWAL, J. K. 2017. Mitochondrial redox signaling enables repair of injured skeletal muscle cells. *Sci Signal,* 10.

HUI-GUO, L., KUI, L., YAN-NING, Z. & YONG-JIAN, X. 2010. Apocynin attenuate spatial learning deficits and oxidative responses to intermittent hypoxia. *Sleep Med,* 11**,** 205-12.

HUTCHINSON, D. S., CSIKASZ, R. I., YAMAMOTO, D. L., SHABALINA, I. G., WIKSTRÖM, P., WILCKE, M. & BENGTSSON, T. 2007. Diphenylene iodonium stimulates glucose uptake in skeletal muscle cells through mitochondrial complex I inhibition and activation of AMP-activated protein kinase. *Cell Signal,* 19**,** 1610-20.

JAVESHGHANI, D., MAGDER, S. A., BARREIRO, E., QUINN, M. T. & HUSSAIN, S. N. 2002. Molecular characterization of a superoxide-generating NAD(P)H oxidase in the ventilatory muscles. *Am J Respir Crit Care Med,* 165**,** 412-8.

JUN, J., SAVRANSKY, V., NANAYAKKARA, A., BEVANS, S., LI, J., SMITH, P. L. & POLOTSKY, V. Y. 2008. Intermittent hypoxia has organ-specific effects on oxidative stress. *Am J Physiol Regul Integr Comp Physiol,* 295**,** R1274-81.

KADOGUCHI, T., TAKADA, S., YOKOTA, T., FURIHATA, T., MATSUMOTO, J., TSUDA, M., MIZUSHIMA, W., FUKUSHIMA, A., OKITA, K. & KINUGAWA, S. Deletion of NAD(P)H Oxidase 2 Prevents Angiotensin II-Induced Skeletal Muscle Atrophy.

KANG, H. H., KIM, I. K., LEE, H. I., JOO, H., LIM, J. U., LEE, J., LEE, S. H. & MOON, H. S. 2017. Chronic intermittent hypoxia induces liver fibrosis in mice with diet-induced obesity via TLR4/MyD88/MAPK/NF-kB signaling pathways. *Biochem Biophys Res Commun,* 490**,** 349-355.

KANG, H. H., KIM, I. K. & LEE, S. H. 2018. Chronic intermittent hypoxia exacerbates lung fibrosis in bleomycin-induced lung injury mouse model. *European Respiratory Journal,* 52**,** PA428.

KENT, B. D., RYAN, S. & MCNICHOLAS, W. T. 2011. Obstructive sleep apnea and inflammation: relationship to cardiovascular co-morbidity. *Respir Physiol Neurobiol,* 178**,** 475-81.

KIM, Y. M., KIM, S. J., TATSUNAMI, R., YAMAMURA, H., FUKAI, T. & USHIO-FUKAI, M. 2017. ROS-induced ROS release orchestrated by Nox4, Nox2, and mitochondria in VEGF signaling and angiogenesis. *Am J Physiol Cell Physiol,* 312**,** C749-c764.

KOVAC, S., ANGELOVA, P. R., HOLMSTRÖM, K. M., ZHANG, Y., DINKOVA-KOSTOVA, A. T. & ABRAMOV, A. Y. 2015. Nrf2 regulates ROS production by mitochondria and NADPH oxidase. *Biochim Biophys Acta,* 1850**,** 794-801.

KOVACIC, H. N., IRANI, K. & GOLDSCHMIDT-CLERMONT, P. J. 2001. Redox regulation of human Rac1 stability by the proteasome in human aortic endothelial cells. *J Biol Chem,* 276**,** 45856-61.

KOZAKOWSKA, M., PIETRASZEK-GREMPLEWICZ, K., JOZKOWICZ, A. & DULAK, J. 2015. The role of oxidative stress in skeletal muscle injury and regeneration: focus on antioxidant enzymes. *Journal of Muscle Research and Cell Motility,* 36**,** 377-393.

LAMBETH, J. D. 2004. NOX enzymes and the biology of reactive oxygen. *Nat Rev Immunol,* 4**,** 181-189.

LAVIE, L. 2003. Obstructive sleep apnoea syndrome--an oxidative stress disorder. *Sleep Med Rev,* 7**,** 35-51.

LEE, S. H., DU, J., STITHAM, J., ATTEYA, G., LEE, S., XIANG, Y., WANG, D., JIN, Y., LESLIE, K. L., SPOLLETT, G., SRIVASTAVA, A., MANNAM, P., OSTRIKER, A., MARTIN, K. A., TANG, W. H. & HWA, J. 2016. Inducing mitophagy in diabetic platelets protects against severe oxidative stress. *EMBO Mol Med,* 8**,** 779-95.

LEWIS, P., SHEEHAN, D., SOARES, R., COELHO, A. V. & O'HALLORAN, K. D. 2016. Redox Remodeling Is Pivotal in Murine Diaphragm Muscle Adaptation to Chronic Sustained Hypoxia. *Am J Respir Cell Mol Biol,* 55**,** 12-23.

LIU, S. S., LIU, H. G., XIONG, S. D., NIU, R. J., XU, Y. J. & ZHANG, Z. X. 2005. [Effects of Shen-Mai injection on sternohyoid contractile properties in chronic intermittent hypoxia rat]. *Zhonghua Jie He He Hu Xi Za Zhi,* 28**,** 611-4.

LIU, X. H., HARLOW, L., GRAHAM, Z. A., BAUMAN, W. A. & CARDOZO, C. 2017. Spinal Cord Injury Leads to Hyperoxidation and Nitrosylation of Skeletal Muscle Ryanodine Receptor-1 Associated with Upregulation of Nicotinamide Adenine Dinucleotide Phosphate Oxidase 4. *J Neurotrauma,* 34**,** 2069-2074.

LOEHR, J. A., WANG, S., CULLY, T. R., PAL, R., LARINA, I. V., LARIN, K. V. & RODNEY, G. G. 2018. NADPH oxidase mediates microtubule alterations and diaphragm dysfunction in dystrophic mice. *Elife,* 7.

LOUREIRO, A. C. C., DO RÊGO-MONTEIRO, I. C., LOUZADA, R. A., ORTENZI, V. H., DE AGUIAR, A. P., DE ABREU, E. S., CAVALCANTI-DE-ALBUQUERQUE, J. P. A., HECHT, F., DE OLIVEIRA, A. C., CECCATTO, V. M., FORTUNATO, R. S. & CARVALHO, D. P. 2016. Differential Expression of NADPH Oxidases Depends on Skeletal Muscle Fiber Type in Rats. *Oxidative Medicine and Cellular Longevity,* 2016**,** 6738701.

LYTTON, J., WESTLIN, M., BURK, S. E., SHULL, G. E. & MACLENNAN, D. H. 1992. Functional comparisons between isoforms of the sarcoplasmic or endoplasmic reticulum family of calcium pumps. *J Biol Chem,* 267**,** 14483-9.

MATSUSHIMA, S., KURODA, J., ZHAI, P., LIU, T., IKEDA, S., NAGARAJAN, N., OKA, S., YOKOTA, T., KINUGAWA, S., HSU, C. P., LI, H., TSUTSUI, H. & SADOSHIMA, J. 2016. Tyrosine kinase FYN negatively regulates NOX4 in cardiac remodeling. *J Clin Invest,* 126**,** 3403-16.

MCCLUNG, J. M., VAN GAMMEREN, D., WHIDDEN, M. A., FALK, D. J., KAVAZIS, A. N., HUDSON, M. B., GAYAN-RAMIREZ, G., DECRAMER, M., DERUISSEAU, K. C. & POWERS, S. K. 2009. Apocynin attenuates diaphragm oxidative stress and protease activation during prolonged mechanical ventilation. *Crit Care Med,* 37**,** 1373-9.

MCDONAGH, B., SAKELLARIOU, G. K., SMITH, N. T., BROWNRIDGE, P. & JACKSON, M. J. 2014. Differential cysteine labeling and global label-free proteomics reveals an altered metabolic state in skeletal muscle aging. *J Proteome Res,* 13**,** 5008-21.

MCDONALD, F. B., DEMPSEY, E. M. & O'HALLORAN, K. D. 2016. Effects of Gestational and Postnatal Exposure to Chronic Intermittent Hypoxia on Diaphragm Muscle Contractile Function in the Rat. *Frontiers in Physiology,* 7**,** 276.

MCGUIRE, M., MACDERMOTT, M. & BRADFORD, A. 2003. Effects of chronic intermittent asphyxia on rat diaphragm and limb muscle contractility. *Chest,* 123**,** 875-81.

MENG, D., LV, D. D. & FANG, J. 2008. Insulin-like growth factor-I induces reactive oxygen species production and cell migration through Nox4 and Rac1 in vascular smooth muscle cells. *Cardiovasc Res,* 80**,** 299-308.

MONTSERRAT, J. M., KOSMAS, E. N., COSIO, M. G. & KIMOFF, R. J. 1997. Lack of evidence for diaphragmatic fatigue over the course of the night in obstructive sleep apnoea. *Eur Respir J,* 10**,** 133-8.

NAH, J., MIYAMOTO, S. & SADOSHIMA, J. 2017. Mitophagy as a Protective Mechanism against Myocardial Stress. *Compr Physiol,* 7**,** 1407-1424.

NARENDRA, D. P. & YOULE, R. J. 2011. Targeting mitochondrial dysfunction: role for PINK1 and Parkin in mitochondrial quality control. *Antioxid Redox Signal,* 14**,** 1929-38.

NGUYEN, T., NIOI, P. & PICKETT, C. B. 2009. The Nrf2-antioxidant response element signaling pathway and its activation by oxidative stress. *J Biol Chem,* 284**,** 13291-5.

NISBET, R. E., GRAVES, A. S., KLEINHENZ, D. J., RUPNOW, H. L., REED, A. L., FAN, T. H., MITCHELL, P. O., SUTLIFF, R. L. & HART, C. M. 2009. The role of NADPH oxidase in chronic intermittent hypoxia-induced pulmonary hypertension in mice. *Am J Respir Cell Mol Biol,* 40**,** 601-9.

OTTENHEIJM, C. A., HEUNKS, L. M., GERAEDTS, M. C. & DEKHUIJZEN, P. N. 2006. Hypoxia-induced skeletal muscle fiber dysfunction: role for reactive nitrogen species. *Am J Physiol Lung Cell Mol Physiol,* 290**,** L127-35.

OTTENHEIJM, C. A., HEUNKS, L. M., SIECK, G. C., ZHAN, W. Z., JANSEN, S. M., DEGENS, H., DE BOO, T. & DEKHUIJZEN, P. N. 2005. Diaphragm dysfunction in chronic obstructive pulmonary disease. *Am J Respir Crit Care Med,* 172**,** 200-5.

PAE, E. K., WU, J., NGUYEN, D., MONTI, R. & HARPER, R. M. 2005. Geniohyoid muscle properties and myosin heavy chain composition are altered after short-term intermittent hypoxic exposure. *J Appl Physiol (1985),* 98**,** 889-94.

PAL, R., PALMIERI, M., LOEHR, J. A., LI, S., ABO-ZAHRAH, R., MONROE, T. O., THAKUR, P. B., SARDIELLO, M. & RODNEY, G. G. 2014. Src-dependent impairment of autophagy by oxidative stress in a mouse model of Duchenne muscular dystrophy. *Nat Commun,* 5**,** 4425.

PENG, Y. J., NANDURI, J., YUAN, G., WANG, N., DENERIS, E., PENDYALA, S., NATARAJAN, V., KUMAR, G. K. & PRABHAKAR, N. R. 2009. NADPH oxidase is required for the sensory plasticity of the carotid body by chronic intermittent hypoxia. *J Neurosci,* 29**,** 4903-10.

PENG, Y. J., RAGHURAMAN, G., KHAN, S. A., KUMAR, G. K. & PRABHAKAR, N. R. 2011. Angiotensin II evokes sensory long-term facilitation of the carotid body via NADPH oxidase. *J Appl Physiol (1985),* 111**,** 964-70.

PENG, Y. J., YUAN, G., JACONO, F. J., KUMAR, G. K. & PRABHAKAR, N. R. 2006. 5-HT evokes sensory long-term facilitation of rodent carotid body via activation of NADPH oxidase. *J Physiol,* 576**,** 289-95.

PIAO, Y. J., SEO, Y. H., HONG, F., KIM, J. H., KIM, Y. J., KANG, M. H., KIM, B. S., JO, S. A., JO, I., JUE, D. M., KANG, I., HA, J. & KIM, S. S. 2005. Nox 2 stimulates muscle differentiation via NF-kappaB/iNOS pathway. *Free Radic Biol Med,* 38**,** 989-1001.

PINTO, J. R., DE SOUSA, V. P. & SORENSON, M. M. 2011. Redox state of troponin C cysteine in the D/E helix alters the C-domain affinity for the thin filament of vertebrate striated muscle. *Biochim Biophys Acta,* 1810**,** 391-7.

POLLA, B., D'ANTONA, G., BOTTINELLI, R. & REGGIANI, C. 2004. Respiratory muscle fibres: specialisation and plasticity. *Thorax,* 59**,** 808-17.

REGAN, J. N., MIKESELL, C., REIKEN, S., XU, H., MARKS, A. R., MOHAMMAD, K. S., GUISE, T. A. & WANING, D. L. 2017. Osteolytic Breast Cancer Causes Skeletal Muscle Weakness in an Immunocompetent Syngeneic Mouse Model. *Frontiers in Endocrinology,* 8.

REID, M. B., HAACK, K. E., FRANCHEK, K. M., VALBERG, P. A., KOBZIK, L. & WEST, M. S. 1992. Reactive oxygen in skeletal muscle. I. Intracellular oxidant kinetics and fatigue in vitro. *J Appl Physiol (1985),* 73**,** 1797-804.

REZENDE, F., LÖWE, O., HELFINGER, V., PRIOR, K. K., WALTER, M., ZUKUNFT, S., FLEMING, I., WEISSMANN, N., BRANDES, R. P. & SCHRÖDER, K. 2016. Unchanged NADPH Oxidase Activity in Nox1-Nox2-Nox4 Triple Knockout Mice: What Do NADPH-Stimulated Chemiluminescence Assays Really Detect? *Antioxid Redox Signal,* 24**,** 392-9.

ROBERTS, B. M., AHN, B., SMUDER, A. J., AL-RAJHI, M., GILL, L. C., BEHARRY, A. W., POWERS, S. K., FULLER, D. D., FERREIRA, L. F. & JUDGE, A. R. 2013. Diaphragm and ventilatory dysfunction during cancer cachexia. *Faseb j,* 27**,** 2600-10.

SAKELLARIOU, G. K., VASILAKI, A., PALOMERO, J., KAYANI, A., ZIBRIK, L., MCARDLE, A. & JACKSON, M. J. 2013. Studies of mitochondrial and nonmitochondrial sources implicate nicotinamide adenine dinucleotide phosphate oxidase(s) in the increased skeletal muscle superoxide generation that occurs during contractile activity. *Antioxid Redox Signal,* 18**,** 603-21.

SAKUSHIMA, K., YOSHIKAWA, M., OSAKI, T., MIYAMOTO, N. & HASHIMOTO, T. 2020. Moderate hypoxia promotes skeletal muscle cell growth and hypertrophy in C2C12 cells. *Biochem Biophys Res Commun,* 525**,** 921-927.

SANDERS, K. A., SUNDAR, K. M., HE, L., DINGER, B., FIDONE, S. & HOIDAL, J. R. 2002. Role of components of the phagocytic NADPH oxidase in oxygen sensing. *J Appl Physiol (1985),* 93**,** 1357-64.

SANDIFORD, S. D., KENNEDY, K. A., XIE, X., PICKERING, J. G. & LI, S. S. 2014. Dual oxidase maturation factor 1 (DUOXA1) overexpression increases reactive oxygen species production and inhibits murine muscle satellite cell differentiation. *Cell Commun Signal,* 12**,** 5.

SATO, Y., OHTSUBO, H., NIHEI, N., KANEKO, T., ADACHI, S. I., KONDO, S., NAKAMURA, M., MIZUNOYA, W., IIDA, H., TATSUMI, R., RADA, C. & YOSHIZAWA, F. 2018. Apobec2 deficiency causes mitochondrial defects and mitophagy in skeletal muscle. *Faseb j,* 32**,** 1428-1439.

SERRANDER, L., CARTIER, L., BEDARD, K., BANFI, B., LARDY, B., PLASTRE, O., SIENKIEWICZ, A., FÓRRÓ, L., SCHLEGEL, W. & KRAUSE, K.-H. 2007. NOX4 activity is determined by mRNA levels and reveals a unique pattern of ROS generation. *Biochemical Journal,* 406**,** 105-114.

SHIOSE, A., KURODA, J., TSURUYA, K., HIRAI, M., HIRAKATA, H., NAITO, S., HATTORI, M., SAKAKI, Y. & SUMIMOTO, H. 2001. A Novel Superoxide-producing NAD(P)H Oxidase in Kidney. *Journal of Biological Chemistry,* 276**,** 1417-1423.

SHORTT, C. M., FREDSTED, A., BRADFORD, A. & O'HALLORAN, K. D. 2013. Diaphragm muscle remodeling in a rat model of chronic intermittent hypoxia. *J Histochem Cytochem,* 61**,** 487-99.

SHORTT, C. M., FREDSTED, A., CHOW, H. B., WILLIAMS, R., SKELLY, J. R., EDGE, D., BRADFORD, A. & O'HALLORAN, K. D. 2014. Reactive oxygen species mediated diaphragm fatigue in a rat model of chronic intermittent hypoxia. *Exp Physiol,* 99**,** 688-700.

SKELLY, J. R., BRADFORD, A., JONES, J. F. & O'HALLORAN, K. D. 2010. Superoxide scavengers improve rat pharyngeal dilator muscle performance. *Am J Respir Cell Mol Biol,* 42**,** 725-31.

SKELLY, J. R., EDGE, D., SHORTT, C. M., JONES, J. F., BRADFORD, A. & O'HALLORAN, K. D. 2012. Tempol ameliorates pharyngeal dilator muscle dysfunction in a rodent model of chronic intermittent hypoxia. *Am J Respir Cell Mol Biol,* 46**,** 139-48.

SKELLY, J. R., ROWAN, S. C., JONES, J. F. & O'HALLORAN, K. D. 2013. Upper airway dilator muscle weakness following intermittent and sustained hypoxia in the rat: effects of a superoxide scavenger. *Physiol Res,* 62**,** 187-96.

SMITH, B. K., MARTIN, A. D., VANDENBORNE, K., DARRAGH, B. D. & DAVENPORT, P. W. 2012. Chronic intrinsic transient tracheal occlusion elicits diaphragmatic muscle fiber remodeling in conscious rodents. *PLoS One,* 7**,** e49264.

SMITH, L. R. & BARTON, E. R. 2018. Regulation of fibrosis in muscular dystrophy. *Matrix Biol,* 68-69**,** 602-615.

SMUDER, A. J., KAVAZIS, A. N., HUDSON, M. B., NELSON, W. B. & POWERS, S. K. 2010. Oxidation enhances myofibrillar protein degradation via calpain and caspase-3. *Free Radic Biol Med,* 49**,** 1152-60.

SPURNEY, C. F., KNOBLACH, S., PISTILLI, E. E., NAGARAJU, K., MARTIN, G. R. & HOFFMAN, E. P. 2008. Dystrophin-deficient cardiomyopathy in mouse: expression of Nox4 and Lox are associated with fibrosis and altered functional parameters in the heart. *Neuromuscul Disord,* 18**,** 371-81.

SULLIVAN-GUNN, M. J. & LEWANDOWSKI, P. A. 2013. Elevated hydrogen peroxide and decreased catalase and glutathione peroxidase protection are associated with aging sarcopenia. *BMC Geriatr,* 13**,** 104.

SUN, Q. A., HESS, D. T., NOGUEIRA, L., YONG, S., BOWLES, D. E., EU, J., LAURITA, K. R., MEISSNER, G. & STAMLER, J. S. 2011. Oxygen-coupled redox regulation of the skeletal muscle ryanodine receptor-Ca2+ release channel by NADPH oxidase 4. *Proc Natl Acad Sci U S A,* 108**,** 16098-103.

SUN, W., YIN, X., WANG, Y., TAN, Y., CAI, L., WANG, B., CAI, J. & FU, Y. 2012. Intermittent hypoxia-induced renal antioxidants and oxidative damage in male mice: hormetic dose response. *Dose Response,* 11**,** 385-400.

SUPINSKI, G., STOFAN, D., NETHERY, D., SZWEDA, L. & DIMARCO, A. 1999. Apocynin improves diaphragmatic function after endotoxin administration. *J Appl Physiol (1985),* 87**,** 776-82.

TAN, V. P., SMITH, J. M., TU, M., YU, J. D., DING, E. Y. & MIYAMOTO, S. 2019. Dissociation of mitochondrial HK-II elicits mitophagy and confers cardioprotection against ischemia. *Cell Death Dis,* 10**,** 730.

TANG, Y. C., TIAN, H. X., YI, T. & CHEN, H. B. 2016. The critical roles of mitophagy in cerebral ischemia. *Protein Cell,* 7**,** 699-713.

VINCKEN, W., GUILLEMINAULT, C., SILVESTRI, L., COSIO, M. & GRASSINO, A. 1987. Inspiratory muscle activity as a trigger causing the airways to open in obstructive sleep apnea. *Am Rev Respir Dis,* 135**,** 372-7.

WANG, W., ZHANG, K., LI, X., MA, Z., ZHANG, Y., YUAN, M., SUO, Y., LIANG, X., TSE, G., GOUDIS, C. A., LIU, T. & LI, G. 2018. Doxycycline attenuates chronic intermittent hypoxia-induced atrial fibrosis in rats. *Cardiovasc Ther,* 36**,** e12321.

WHITEHEAD, N. P., YEUNG, E. W., FROEHNER, S. C. & ALLEN, D. G. 2010. Skeletal muscle NADPH oxidase is increased and triggers stretch-induced damage in the mdx mouse. *PLoS One,* 5**,** e15354.

WILLIAMS, R., LEMAIRE, P., LEWIS, P., MCDONALD, F. B., LUCKING, E., HOGAN, S., SHEEHAN, D., HEALY, V. & O'HALLORAN, K. D. 2015. Chronic intermittent hypoxia increases rat sternohyoid muscle NADPH oxidase expression with attendant modest oxidative stress. *Frontiers in Physiology,* 6.

YAMADA, T., ABE, M., LEE, J., TATEBAYASHI, D., HIMORI, K., KANZAKI, K., WADA, M., BRUTON, J. D., WESTERBLAD, H. & LANNER, J. T. 2015. Muscle dysfunction associated with adjuvant-induced arthritis is prevented by antioxidant treatment. *Skelet Muscle,* 5**,** 20.

YUN, Z., LIN, Q. & GIACCIA, A. J. 2005. Adaptive myogenesis under hypoxia. *Mol Cell Biol,* 25**,** 3040-55.

ZHAN, G., SERRANO, F., FENIK, P., HSU, R., KONG, L., PRATICO, D., KLANN, E. & VEASEY, S. C. 2005. NADPH oxidase mediates hypersomnolence and brain oxidative injury in a murine model of sleep apnea. *Am J Respir Crit Care Med,* 172**,** 921-9.

ZHANG, Y., SU, X., ZOU, F., XU, T., PAN, P. & HU, C. 2019. Toll-like receptor-4 deficiency alleviates chronic intermittent hypoxia-induced renal injury, inflammation, and fibrosis. *Sleep Breath,* 23**,** 503-513.

ZHOU, S., YIN, X., JIN, J., TAN, Y., CONKLIN, D. J., XIN, Y., ZHANG, Z., SUN, W., CUI, T., CAI, J., ZHENG, Y. & CAI, L. 2017. Intermittent hypoxia-induced cardiomyopathy and its prevention by Nrf2 and metallothionein. *Free Radic Biol Med,* 112**,** 224-239.

Chapter 6. Summary and Conclusions.

6.1 Limitations

6.1.1 Animal model of OSAS

When conducting any scientific experiment, it must be acknowledged that certain limitations exist. Possibly the most important limitation in the current study is the use of a mouse model to research the human condition, OSAS. OSAS is a multi-factorial and complex disease (Casale et al., 2009). We acknowledge the fact that no animal model of a disorder can fully recapitulate the human scenario and so similar to other models, we chose to focus on a subset of events characteristic of the disorder, with resultant limitations. Like many others, we utilised IH as a central feature of OSAS in our mouse model due to previous evidence supporting its central role in driving pathology throughout the respiratory system (Edge et al., 2012, Shortt et al., 2014, Skelly et al., 2012, Peng et al., 2001, Peng et al., 2003, Morgan et al., 2016a, Morgan et al., 2016b) as well as in a wide range of other organs and tissues (Dumitrascu et al., 2013, Al Lawati et al., 2009, Drager et al., 2011b, Torres et al., 2014a, Wang et al., 2013b, Wang et al., 2018, Savransky et al., 2007, Rosas, 2011). This implicates IH in the exacerbation of OSAS severity as well as in the development of multiple co-morbidities of OSAS. It must be appreciated that other risk factors for the development of OSAS, such as obesity (Romero-Corral et al., 2010), genetic predisposition, or smoking (Lin et al., 2012) are not represented in this model.

The cyclical sinusoidal pattern of IH in our model does not aim to model the IH pattern experienced by OSAS patients, but more specifically, it models the intermittent cycling of hypoxia-reoxygenation and arterial oxygen desaturations, thus allowing us to examine the effects of IH on multiple levels of the respiratory system. We acknowledge that IH is only one aspect of the disorder as concomitant airway collapse with mechanical trauma and hypercapnia are also experienced by OSAS patients throughout the night cycle. While hypercapnia is a key ventilatory stimulant, data from models of intermittent hypercapnic hypoxia (asphyxia) have highlighted that IH appears to be the dominant injurious feature of the model (O'Halloran et al., 2002, McGuire et al., 2003, McGuire et al., 2002b). Another important point worth noting is the duration of IH chosen. The effects of CIH are

largely time-, intensity-, duration- i.e. pattern-dependent with alterations in any of these factors significantly affecting the experimental outcome. While 2 weeks seems like a relatively short period of time, considering that OSAS patients are subject to apnoeic events over a much longer period of time, exposure to CIH for 2 weeks has been shown to be sufficient to result in a number of hallmark features of OSAS including respiratory muscle weakness, increased apnoea index, hypertension and markers of oxidative stress (Shortt et al., 2014, Lucking et al., 2014, Skelly et al., 2012, Edge et al., 2012). We reasoned that this paradigm of CIH, while modest, represents an early time point where we could delineate key mechanisms underpinning the development of respiratory mal-adaptation. Nevertheless, a temporal study of exposure to CIH would be extremely interesting to gain a better understanding of the time frames wherein adaptive and mal-adaptive responses occur.

6.1.2 Strain difference between wild-type and NOX2 null mice

The specific role of NOX2 in CIH-induced respiratory system mal-adaptation was examined in the current study by utilising NOX2 null mice. NOX2 null male mice (B6.129S-Cybb^{tm1Din}/J) were purchased from the Jackson Laboratory (Bar Harbor, ME, USA) for this purpose. The appropriate control for these mice, as suggested by the Jackson Laboratory, are C57BL/6J male mice. Indeed, C57BL/6J mice have previously been used as a control for this particular NOX2 null model (You et al., 2013, Costford et al., 2014, Aydin et al., 2017). Thus, male C57BL/6J controls were purchased from Envigo, UK and used in the current study. However, we acknowledge that there are strain differences between the wild-type and NOX2 null mice employed. NOX2 null mice (B6.129S-Cybb^{tm1Din}/J) were produced by backcrossing the disrupted 129S strain to the C57BL/6J strain, compared to wild-type, C57BL/6J mice. This difference in the genetic background may have implications in differential physiological and neurochemical phenotypes between groups. We acknowledge this as a potential limitation in the current study and as a result, cautiously compare differences between wild-type and NOX2 null groups.

6.1.3 Whole body plethysmography

We studied breathing, without the confounding effects of anaesthesia, in awake and unrestrained mice by means of WBP. WBP is an attractive experimental approach, especially for extended periods of recording that were applied throughout our studies. However, we are aware that calculations using WBP are based on a number of assumptions for the volume-based parameters (tidal volume), notably chamber temperature and humidity and animal airway temperature (Mortola and Frappell, 1998, Stephenson and Gucciardi, 2002). Chamber temperature was measured and remained at ~21°C. However, body temperature was not measured, but rather assumed to be 37.5 °C for all groups examined for the calculation of tidal volume. We address this as a limitation as the decrease in ventilation in NOX2 KO mice compared with wild-type controls in the current study was as a result of a lower tidal volume. While we acknowledge that errors based on this assumption of body temperature may have contributed to differences between NOX2 KO mice and wild-type mice, we also note that basal CO_2 production was not different between groups, strongly suggestive of an unaltered metabolic rate, which suggests no difference in core temperature.

6.1.4 Ex vivo muscle function tests

Sternohyoid and diaphragm muscle contractile properties were examined *ex vivo* under hyperoxic conditions in a water-jacketed muscle bath maintained at 35°C. This was to allow for assessment of intrinsic muscle performance under these conditions which maintained muscle viability for the duration of muscle function tests. However, these conditions are not physiological, and it is noteworthy that muscle performance in this situation may not be the same as it would be *in vivo.* While these experiments are certainly valuable for assessing a muscle's intrinsic contractile activity, they do not account for a muscle's activity in the presence of its natural support system (other upper airway muscles and intercostal muscles) and innervation systems (hypoglossal and phrenic nerves) that would be present *in situ.* Future experiments to assess UA and diaphragm muscle function *in vivo* would be of great interest and is discussed in more detail below.

6.1.5 Measurement of NOX activity

The lack of a specific measurement for NOX activity has proven to be a significant challenge in the field. Lucigenin-enhanced chemiluminescence is an approach that has routinely been used for the measurement of NOX activity. Lucigenin, which is a fluorescent chloride indicator, reacts with superoxide to produce light. The lucigenin signal stimulated by addition of NAD(P)H to the reaction buffer is considered a measurement of NOX-derived superoxide. A conceptually similar approach involves the utilisation of NAD(P)H consumption by muscle homogenates. Lucigenin and NAD(P)H consumption assays have been used in the assessment of NOX activity in skeletal muscle (Javeshghani et al., 2002, Ahn et al., 2015, Adams et al., 2005, Bowen et al., 2015a, Bowen et al., 2015b). However, a recent study shows that these assays are not specific to NOX activity and in several tissues and cell types, the signal generated was unchanged in a triple NOX1, NOX2, and NOX4 knock-out (Rezende et al., 2016). We used a NADPH consumption assay in the current study and therefore, we acknowledge the limitations of this approach. In the light of findings by (Rezende et al., 2016), we cautiously report that the increase in NOX activity in the sternohyoid muscle following exposure to CIH is specific to NOX. Similarly, we acknowledge the discrepancy in the findings of an increase in the mRNA and protein expression of NOX4 in the diaphragm failing to translate to increased NOX activity.

While we used NADPH as a substrate for NOX in the assay in the current study, it has been shown that a range of other systems in skeletal muscle utilise NADPH as a substrate (Maghzal et al., 2012). Therefore, we cannot rule out that the signal generated may be related to biological factors other than NOX. While NADPH is considered the primary substrate for NOX in non-muscle cells (Bedard and Krause, 2007), the use of NADH as a substrate appears to elicit a three-to-five fold higher NOX activity than NADPH in adult skeletal muscle (Javeshghani et al., 2002). Additionally, some studies report that it is specifically NOX4 that preferentially uses NADH as an electron donor (Shiose et al., 2001), which may provide insight into why we observed no increase in NOX activity in the diaphragm muscle following exposure to CIH. Nevertheless, NADH consumption assays face the same issues with deciphering signal specificity between NOX and other biological factors. We and

others (Loureiro et al., 2016) have shown that NOX expression appears to be fibre-type specific. Moreover, NOX enzyme expression and/or activity has been shown to be localised to microdomains within skeletal muscle (Cully and Rodney, 2020). Taking these findings into consideration, it is reasonable to suggest that a NOX activity assay performed on a muscle homogenate may not have had the sensitivity to detect NOX activation in different sub-cellular compartments of skeletal muscle. Additionally, the signal may be diluted in whole muscle homogenates by areas of muscle in which NOX activity is unchanged.

Phosphorylation of p47phox is reportedly necessary for NOX2 activation and as such, immunoprecipitation and immunoblot to determine levels of serine phosphorylation of p47phox has been utilised as a surrogate measure of NOX2 activity in skeletal muscle (Ahn et al., 2015). Additionally, genetically-encoded redox probes have shown significant potential for the dynamic and site-specific assessment of redox potential (Meyer and Dick, 2010). These genetically-encoded biosensors have the capacity to be targeted to specific sub-cellular compartments, including the mitochondria, endoplasmic reticulum, and plasma membrane. Perhaps the most promising advancement in the search for a specific tool to measure NOX activity has been the development of a redox-sensitive protein (p47-roGFP) that specifically assesses NOX activity by linking redox-sensitive GFP (roGFP) to the NOX organiser protein, p47phox (Pal et al., 2013). The authors demonstrate that this probe is sensitive to NOX-derived ROS and allows for real-time assessment of NOX activity in living cells in response to exogenously applied agents as well as physiological conditions associated with increased skeletal muscle activity. p47-roGFP is extremely advantageous as it exhibits rapid oxidation and reduction, the capacity to be directed to the source of ROS and subcellular microdomains where NOX enzymes reside as well as conferring specificity towards NOX2. Recommendations by experts in the field of NOX enzymes have highlighted that it would be more beneficial to measure ROS formation in intact tissue rather than boosting their signal with NADPH or using homogenates, when addressing ROS production by NOX enzymes (Rezende et al., 2016). p47-roGFP appears to hold significant potential in this regard.

6.1.6 Extrapolation of molecular results

We acknowledge that some of our results pertaining to the mechanisms underpinning respiratory muscle weakness are only at the mRNA level. Therefore, we cannot presume that changes at the transcriptional level translate directly to changes in protein, in turn affecting cellular function. Similarly, we cannot presume that further downstream signalling pathways, in terms of protein expression or activity, are unaltered on the basis of unchanged observations in mRNA expression. For example, we measure the mRNA expression of LC3B in the current study as a marker of autophagy. However, studies suggest that LC3B may predominantly be regulated at the protein level (Jia and Bonifacino, 2020). Therefore, we acknowledge the limitations of our mRNA data and appreciate that measuring the ratio of LC3B II/I may be a more appropriate indicator of autophagy induction that should be considered for future studies (Kadowaki and Karim, 2009).

It would be inappropriate to assume that the behaviour of a single measurement at a single point in time is representative of an entire organelle, process or pathway as a whole. This highlights the necessity to examine cellular processes at all levels of regulation in order to gain a comprehensive insight into the molecular processes underlying pathological features of disease. This represents an important factor in the development of targeted treatments for disease, with the benefit of fewer side effects. Moreover, this is an especially important consideration when there is more than one stimulus, such as in our study, where IH, contractile activity and redox imbalance can each affect cellular processes. Exposure to IH culminates in a diverse range of observations that arise as a result of an intricate system of molecular mechanisms that underlie adaptive and mal-adaptive responses to oxygen desaturation, thus further experimentation is warranted to characterise these responses.

6.2 Future directions

6.2.1 Examination of skeletal muscle contractile apparatus function

Muscle force is generated by cross-bridges, formed by myosin heavy chains that attach to actin filaments (Huxley and Simmons, 1971). The force-generating capacity of single fibres is dependent upon the contractile protein content of that fibre (Brenner, 1988). Ca^{2+} sensitivity of force generation is determined by binding of Ca^{2+} to troponin C, which in turn affects cross-bridge formation, through myosin binding to actin. Skinned fibre studies provide an excellent model for the direct evaluation of contractile protein function in fibres as exposure of the skinned fibres to Ca^{2+} enables the evaluation of contractile protein function.

While a loss of contractile proteins may underlie skeletal muscle weakness, dysfunction of the remaining myofibrillar proteins may also contribute to poor muscle contractile performance. Altered cross-bridge kinetics have been described in skinned muscle fibres following acute exposure to hypoxia (de Paula Brotto et al., 2001, Ottenheijm et al., 2006) and in muscle biopsies of COPD patients (Ottenheijm et al., 2005), possibly due to alterations related to myosin and troponin. Ca^{2+} sensitisation stabilises the conformation of the troponin complex, which functions to trigger muscle contraction. Ca^{2+} sensitivity of force generation has been shown to be impaired in skinned muscle fibres from diaphragm muscle biopsies from COPD patients, possibly contributing to the reduced force generation observed (Ottenheijm et al., 2005).

Ca^{2+}sensitisers, such as levosimendan, have been shown to increase force generation in the diaphragm muscle of COPD patients by enhancing the binding of Ca^{2+} to regulatory proteins of the contractile apparatus, such as troponin C (van Hees et al., 2009). This in turn improves the responsiveness of myofilaments to Ca^{2+}, yielding greater amount of force, for the same amount of cytosolic Ca^{2+}. Troponin activators have also been shown to increase muscle contractility in critically-ill patients by restoring Ca^{2+}sensitivity back to control values (Russell et al., 2012). These studies may represent an approach to improve muscle function in diseases characterised by

respiratory muscle weakness. For future studies, it would be most interesting to examine the Ca^{2+} sensitivity of myofilaments following exposure to CIH to assess whether hypoxia-induced alterations occur at this level of the muscle.

6.2.2 Examination of redox-dependent alterations to skeletal muscle contractile proteins

ROS hold the capacity to alter myofilament structure and function (Smuder et al., 2010). Additionally, several myofibrillar proteins including troponin C (Pinto et al., 2011), actin (Coirault et al., 2007), alpha-actinin (McDonagh et al., 2014, Smuder et al., 2010) and myosin heavy chains are susceptible to oxidative modifications. These oxidative modifications affect Ca^{2+} sensitivity and cross-bridge cycling (discussed above), potentially culminating in contractile dysfunction. Modifications of myofibrillar proteins have been demonstrated as s-nitrosylation (de Paula Brotto et al., 2001), due to hypoxia-induced ROS. The complexity of redox-dependent alterations can be appreciated by divergent effects of oxidative modifications, evidenced by an increase or decrease in the sensitivity of contractile apparatus to Ca^{2+} (Hidalgo et al., 2006, Guerra et al., 1996). Indeed, studies in mechanically skinned fibres have demonstrated that *S*-nitrosylation and *S*-glutathionylation exert opposing effects on Ca^{2+} sensitivity in mammalian fast-twitch muscle fibres, mediated by competitive actions on Cys134 of troponin I (Dutka et al., 2017).

Previous studies by our group (Lewis et al., 2015, Lewis et al., 2016) have demonstrated a redox-dependent modulation of key proteins involved muscle contractile performance, following exposure to chronic sustained hypoxia. Using 2D redox proteomics and mass spectrometry, hypoxia-induced oxidation of metabolic markers and proteins at the level of cross bridge cycling were observed in weakened respiratory muscles (Lewis et al., 2015, Lewis et al., 2016), consistent with that of COPD patients. While this technique is a relatively crude measure for the presence of oxidative proteins, site-specific identification of the redox modification and quantification of site occupancy in the context of protein abundance remains a crucial concept for redox proteomic approaches (Cobley et al., 2019).

New strategies include the development of a label-free quantitative proteomic approach (McDonagh et al., 2014). This proteomic approach includes a differential cysteine labelling step to enable the simultaneous identification of up- and downregulated proteins between samples, in addition to the identification and relative quantification of the reversible oxidation state of susceptible redox cysteine residues. It would be extremely interesting to assess whether CIH-induced ROS act in a reversible manner through the transient oxidation of cysteine residues on key contractile proteins in respiratory muscle, especially since we observe no overt oxidative damage in our model and CIH-induced UA weakness has previously been shown to be reversible (Skelly et al., 2012). A co-assessment of the oxidation state of cysteine residues in key myofibrillar proteins as well as quantification of protein abundance would be interesting to assess in our model, as changes in redox state and/or changes in protein abundance have the capacity to underpin alterations to skeletal muscle contraction.

6.2.3 Examination of respiratory muscle structure

There is a need to assess whether structural alterations underlie, or in part contribute to NOX2-dependent CIH-induced respiratory muscle dysfunction and increased respiratory muscle force generation following NOX2 KO. We observed an increase in the mRNA expression of pro-autophagic, atrophic and myogenic genes in the diaphragm following exposure to CIH, which is prevented by treatment with apocynin and NOX2 KO. Further experimentation is warranted to assess whether these changes at the transcriptional level translate into structural alterations, which may hold consequences for the force-generating capacity of the muscle.

While muscle fibre atrophy is most consistently observed with chronic sustained hypoxia (McMorrow et al., 2011, Gamboa and Andrade, 2012), a decrease in myofibre size has also been observed following exposure to IH (Giordano et al., 2015). Immunohistochemical studies examining the cross-sectional area (CSA) and minimal Feret's diameter would be most interesting, to assess whether myofibre atrophy occurs and thus has a role in CIH-induced respiratory muscle weakness. A

reduction in myofibre size would be consistent with muscle weakness, as muscle strength is proportional to muscle area (Rospars and Meyer-Vernet, 2016).

Respiratory muscle structure encompasses a high degree of sophistication as it comprises a variety of different fibre types, enabling different functional properties. Immunohistochemical studies, such as those previously employed by our group (Skelly et al., 2012, McDonald et al., 2015, Shortt et al., 2013, Shortt et al., 2014, Burns et al., 2018), to assess the proportion and area of myosin heavy chain fibre types (type 1, type 2a, type 2x or type 2b) would be interesting to examine to determine whether alterations to the composition and size of fibre types in the sternohyoid or diaphragm underpin changes in their contractile characteristics following exposure to CIH, treatment with apocynin or NOX2 KO. A slow-to-fast fibre-type transition would suggest a more powerful, but more fatigable muscle. Whereas the converse, fast-to-slow fibre-type transition would yield a more endurant, but less powerful muscle.

CIH-induced fibrosis has been reported in a range of organs and tissues (Kang et al., 2018, Didier et al., Kang et al., 2017, Zhang et al., 2019, Wang et al., 2018). An assessment of muscle fibrosis, utilising Sirius Red staining, would be interesting to assess whether an increase in collagen infiltrate contributes to the deficits in muscle contractile performance following exposure to CIH, and indeed whether NOX2-derived ROS play a role in this. We suggest this in particular, as we observed a modest decrease in the capacity of the diaphragm muscle to shorten which may be indicative of CIH-induced structural alteration, such as fibrosis.

6.2.4 Examination of key structures in the respiratory control network

In the current study, we report CIH-induced ROS dependent alterations to respiratory function in mice. We report a CIH-induced increase in apnoea index in wild-type mice that is prevented by treatment with apocynin, but not NOX2 deletion (Chapter 3). This implicates another source of ROS in the manifestation of increased apnoea index which would be most interesting to investigate further. Similarly, we observe altered hypoxic and hypercapnic responses following exposure to CIH among groups, both

of which implicate ROS and/or NOX2 (Chapter 3). The carotid body and CNS regions including the nucleus tractus solitarius (NTS), paraventricular nucleus of the hypothalamus (PVN), rostral ventrolateral medulla (RVLM) and retrotrapezoid nucleus (RTN), which are important for the control of ventilation and sympathetic outflow, are all affected by increased ROS as a result of exposure to CIH (Mifflin et al., 2015, Semenza and Prabhakar, 2015). Additionally, it has been demonstrated that a range of signaling molecules including ROS, 5-HT, adenosine, HIF-1α and inflammatory cytokines are involved in the CIH-induced respiratory plasticity (Peng et al., 2006, Pawar et al., 2009, Peng et al., 2009, Del Rio et al., 2011, Peng et al., 2013, Iturriaga et al., 2014, Sacramento et al., 2015, Morgan et al., 2016b, Moya et al., 2020). As these substances and processes exhibit pro-oxidant properties and/or are sensitive to ROS, oxidative stress may represent a common thread linking many drivers of CIH-induced mal-adaptation, at multiple points throughout the respiratory control network (Del Rio et al., 2010). Thus, a direct examination of markers of oxidative stress, antioxidant capacity and inflammation in structures pivotal to respiratory control following exposure to CIH, treatment with apocynin and NOX2 knock-out would be most interesting in future studies to delineate the precise mechanisms underpinning CIH induced respiratory system mal-adaptation.

6.2.5 Assessment of respiratory muscle function in vivo

Dysfunctional UA muscles promote an unstable airway, rendering it more prone to collapse (Remmers et al., 1978). We and others (Liu et al., 2005, Liu et al., 2009, McDonald et al., 2015, Dunleavy et al., 2008, Jia and Liu, 2010, Ding and Liu, 2011, Wang et al., 2013c, Zhou and Liu, 2013, Skelly et al., 2012, Pae et al., 2005) have demonstrated that exposure to IH results in significant UA muscle weakness and/or fatigue. While we examined the contractile characteristics of a representative UA muscle (sternohyoid) *ex vivo*, there is a need to address the functional impact of the CIH-induced weakness we observed on airway stability in mice. The gold standard measurement of UA collapsibility during sleep is the pharyngeal critical closing pressure (Pcrit) (Carberry et al., 2016). Studies in rats have demonstrated that exposure to IH significantly elevated Pcrit under unstimulated conditions, resulting in a more collapsible airway (Ray et al., 2007). We acknowledge that OSAS is primarily

a neurogenic disorder. However, UA collapse can occur (and be exacerbated by) a lack of neural drive, UA muscle weakness or a culmination of both. In the current study, we show that CIH-induced UA muscle weakness is entirely prevented by NOX2 KO. In the light of this, it would be extremely interesting to assess whether an IH-induced increase in Pcrit, that may present in our model, would also be prevented by NOX2 KO.

Similarly, there is a need to assess the functional relevance of the CIH-induced diaphragm weakness observed *ex vivo* in the current study. An assessment of transdiaphragmatic pressure (Pdi) during ventilatory (i.e. eupnoea) and non-ventilatory behaviours (e.g. airway obstruction) is essential in understanding the implication of diaphragm muscle weakness in physiological responses (Mantilla et al., 2010, Greising et al., 2016). While we observe a ~45% decrease in the force-generating capacity of the diaphragm *ex vivo* following exposure to CIH in the current study, previous studies have shown that a similar magnitude of diaphragm weakness results in no perturbation to ventilatory behaviours, due to the large force reserve capacity of the diaphragm muscle (Greising et al., 2015). Indeed, there was no impairment in basal minute ventilation in CIH-exposed mice in the current study (Chapter 3). However, deficits may be revealed during high force-dependent manoeuvres, necessitating up to 100% of diaphragm peak force-generating capacity. Remarkably, peak inspiratory pressure-generating capacity is preserved during both ventilatory and non-ventilatory behaviours in the *mdx* mouse model of DMD, even with significant diaphragm muscle weakness (Burns et al., 2019). The latter observation reveals the capacity for accessory muscles to compensate for profound diaphragm weakness in at least some circumstances. Therefore, an assessment of Pdi and peak inspiratory pressure-generating capacity *in vivo* would be an essential step in determining the relevance of CIH-induced diaphragm weakness in ventilatory and non-ventilatory functions, and to determine the capacity for NOX2 blockade to prevent potentially mal-adaptive effects, similar to that observed in diaphragm muscle *ex vivo*.

6.2.6 Utilisation of a conditional NOX2 KO model

The transgenic NOX2 KO mouse model we utilised in the current study was a conventional KO, in that the NOX2 gene was eliminated in all tissues from early development. However, the study of gene function in adult mice in selected cells and tissues has been significantly enhanced by the development of conditional gene KO technology developed by Tsien and colleagues in the 1990s (Tsien et al., 1996). With a conditional KO, gene inactivation can occur in a certain tissue type or at a specific time point by crossing a loxP mouse with a specific Cre transgenic line, such that the target gene becomes inactivated *in vivo* within the expression domain of Cre (Friedel et al., 2011). Therefore, conditional KO models have allowed researchers to target genes in specific tissues, thus eliminating the drawbacks and confounders of traditional KO processes that eliminate genes from all tissues. For example, a gene may be essential for the proper development of an organism before birth and during postnatal development, and then later in life can encompass a different function, which may influence an individual's susceptibility towards a disease.

NOX2-derived ROS have a central role in innate immunity (Rada and Leto, 2008). NOX2 deficiency results in the development of chronic granulomatous disease (CGD), a primary immunodeficiency characterised by life-threatening bacterial and fungal infections (Segal et al., 2011). While there were no observable defects in mice lacking the NOX2 enzyme in the current study, we cannot rule out that NOX2 blockade would have unfavourable consequences for the immune system in humans. In the current study, we demonstrate that NOX2 is necessary for CIH-induced respiratory muscle weakness. However, a muscle-specific conditional NOX2 KO would be most interesting to confirm that muscle weakness was prevented due to the absence of NOX2 intrinsic to the muscle, and not due to extrinsic factors such as innervation or blood infiltrate. Comparisons between whole-body and muscle-specific SOD1 KO mouse models have shown that neuromuscular integrity and redox mechanisms are differentially affected, which may have implications in understanding the mechanism driving muscle loss during ageing (Sakellariou et al., 2018). These sophisticated, refined experimental approaches allow for a better understanding of the

pathophysiological processes that give rise to disease, providing a basis for targeted therapies.

6.3 Conclusion and Implications

OSAS occurs as a result of a reduction in neural outflow to the UA, resulting in repetitive airway collapse throughout the night cycle. However, several other factors may contribute to an increase in the severity of OSAS pathology. The striated muscles of breathing, including the diaphragm and pharyngeal dilator muscles, play a pivotal role in maintaining respiratory homeostasis. The negative pressure reflex activation of the pharyngeal dilator muscles serves to maintain UA patency on a breath-by-breath basis and crucially, is important in re-establishing airway patency following obstructive events. The co-ordinated activity of the diaphragm and UA dilator muscles is thereby essential for the maintenance of airway patency and thus, effective pulmonary ventilation. Potentially mal-adaptive alterations to UA (Sérlès et al., 1996, Carrera et al., 1999) and diaphragm muscles have been observed in OSAS patients (Griggs et al., 1989, Chien et al., 2010). Additionally, OSAS patients exhibit central apnoeas during CPAP treatment (Morgenthaler et al., 2006), which further serves to promote respiratory instability. Indeed, our results demonstrate that exposure to CIH for 2 weeks, mimicking mild-to-moderate OSAS, culminates in increased apnoea index (Chapter 3), and profound UA (Chapter 4) and diaphragm (Chapter 5) muscle weakness. If our study translates to the human condition, then each of these findings individually and moreover, combined, may contribute to respiratory system impairment that would ultimately serve to exacerbate the severity of OSAS and perpetuate a vicious cycle of events.

Patients with OSAS exhibit a derangement in the oxidant-antioxidant balance with a shift towards the former and as such, OSAS is widely considered an oxidative stress disorder (Lavie, 2003). CIH-induced ROS, as a consequence of repetitive UA collapse and re-opening, are implicated in impaired motor control of the UA (O'Halloran et al., 2002, Veasey et al., 2004, Ray et al., 2007), UA and diaphragm muscle dysfunction (Clanton et al., 2001, McGuire et al., 2002a, McGuire et al., 2002b, McGuire et al., 2003, Liu et al., 2005, Pae et al., 2005, Liu et al., 2009, Skelly et al., 2012, Skelly et al., 2013, Shortt et al., 2014, Shortt and O'Halloran, 2014, McDonald et al., 2015) and discordant rhythm and pattern generation (Peng et al., 2003, Reeves and Gozal,

2006, Edge et al., 2012, Moraes et al., 2013, Donovan et al., 2014, Souza et al., 2015, Elliot-Portal et al., 2018, Joseph et al., 2020). Therapies to improve any of these deficits individually, or moreover collectively, serves to reduce instability within the respiratory system contributing to a lower probability of airway collapse and thus, a reduced severity of OSAS pathology. Beyond the respiratory system, CIH-induced ROS drive a wide range of maladies with evidence for neurocognitive (Al Lawati et al., 2009), metabolic (Drager et al., 2011a), cardiovascular (Dumitrascu et al., 2013), testicular (Torres et al., 2014b), hepatic (Savransky et al., 2007), renal (Rosas, 2011) and pancreatic (Wang et al., 2013a) disorders. This highlights the devastating consequences that CIH-induced ROS have for integrative body systems as a whole, elevating the status of OSAS to that of a major public health disorder (Lavie, 2009). The application of CPAP is the first line of treatment for OSAS which functions to mechanically stabilise the UA in OSAS patients during sleep. CPAP has been shown to be efficacious in reducing several cardiovascular risk factors of OSAS (Hedner et al., 1995), but studies also suggest that this line of treatment does not entirely restore redox imbalance to homeostatic levels (Barceló et al., 2006, Phillips et al., 2007). Worryingly, the failure rate of CPAP treatment exceeds 50% (Stepnowsky and Moore, 2003) due to poor patient compliance with frequent reports of claustrophobia, facial discomfort, throat dryness, nasal and eye pain (Wolkove et al., 2008). Poor adherence to CPAP treatment may in part explain why the full benefits of this treatment are often not observed in OSAS patients and therefore, there is an urgent need for the development of new therapeutic strategies.

Interestingly, antioxidants have already shown efficacy as an adjunct therapy in the treatment of OSAS. Treatment of OSAS patients with the antioxidants, vitamin E and C, reduced lipid peroxidation and restored glutathione levels to levels similar to healthy controls, demonstrating their efficacy in preventing OSAS-associated oxidative stress (Singh et al., 2009). Moreover, this combinational antioxidant treatment improved SDB, indicated by a reduction in apnoea index, as well as decreasing excessive day-time sleepiness, the most common symptom of OSAS which has a hugely negative impact on quality of life in OSAS patients (Singh et al., 2009). Similarly, the administration of NAC to OSAS patients decreased lipid

peroxidation and increased levels of glutathione (Sadasivam et al., 2011). OSAS patients treated with NAC display significant improvements in sleep and respiratory parameters observed as reduced apnoea index, apnoea related-arousals, oxygen desaturations per hour and Epworth sleepiness score (Sadasivam et al., 2011). Additionally, snore characteristics were significantly decreased following NAC treatment, indicative of a reduction in airway narrowing and turbulent airflow in OSAS patients. It is suggested that long-term treatment with NAC may serve to reduce patient dependency on CPAP therapy (Sadasivam et al., 2011). Oral carbocysteine treatment has also been shown to improve the Epworth sleepiness score, apnoea index and time and percentage of oxygen desaturation, all of which are indicative of a less severe OSAS phenotype (Wu et al., 2016). Similar to the antioxidants above, carbocysteine reduced markers of oxidative stress in OSAS patients, demonstrated as decreased levels of MDA and increased levels of SOD (Wu et al., 2016). While CPAP treatment resulted in much of the same beneficial effects as carbocysteine, patient compliance was significantly higher in OSAS patients treated with carbocysteine compared with CPAP (Wu et al., 2016). This highlights that antioxidant treatment is a promising approach for the treatment of OSAS patients who cannot tolerate CPAP. Additionally, long term treatment with antioxidants may subsequently reduce patient dependency on CPAP treatment.

Although, exposure to CIH was not associated with overt oxidative stress in our model, we conclude that ROS, potentially derived from NOX2, are pivotal to CIH-induced respiratory mal-adaptation. We demonstrate that treatment with apocynin entirely prevents the CIH-induced increase in apnoea index (independent of NOX2) in our murine model of OSAS (Chapter 3), implicating ROS in the manifestation of respiratory instability following exposure to CIH. Additionally, treatment with apocynin and NOX2 KO entirely prevents the profound CIH-induced UA (Chapter 4) and diaphragm (Chapter 5) muscles weakness observed in our model, confirming that NOX2-derived ROS are entirely necessary for respiratory muscle dysfunction following exposure to CIH. If our pre-clinical study translates to the human condition, antioxidants targeting NOX2 (or possibly NOX4) may hold therapeutic potential in reducing the severity of OSAS pathology, in a similar manner to that observed in the

antioxidant studies in OSAS patients (Wu et al., 2016, Singh et al., 2009, Sadasivam et al., 2011). NOX2 blockade may represent a specific therapeutic target for improving UA and diaphragm muscle function in OSAS, thereby contributing to a reduction in respiratory perturbations.

Targeting NOX2 is particularly complex as it holds a pivotal role in host defence, yet it is also implicated in the pathogenesis of a wide range of diseases including cardiovascular disease (Liu et al., 2011, Nisbet et al., 2009), DMD (Pal et al., 2014) , COPD (Lagente et al., 2008), Cystic Fibrosis (Hayes et al., 2011), CHF (Ahn et al., 2015), Alzheimer's disease (Park et al., 2005), PD (Wu et al., 2003), ALS (Wu et al., 2006), traumatic brain injury (Dohi et al., 2010) and schizophrenia (Sorce et al., 2010) to name a few. Research has primarily focused on NOX4 and NOX1, due to concerns about the immunosuppressive effects of NOX2 blockade. Nevertheless, NOX2 clearly contributes to the pathogenesis of many diseases, and its inhibition is predicted to provide a novel therapeutic approach in the context of diseases characterised by oxidative stress. The World Health Organisation (WHO) has recently recognised NOX inhibitors as a new therapeutic class, which hold significant potential for the treatment of fibrotic, inflammatory, neurodegenerative and oncological disorders. GKT137831 (setanaxib or GKT-831), claimed to be a NOX1/4 dual inhibitor, was the first NOX inhibitor to reach the clinical trial stage (Wiesel et al., 2012). Phase II clinical trials using GKT137831 are ongoing for the treatment of idiopathic pulmonary fibrosis and kidney disease in patients with type 1 diabetes. Ewha-18278 (APX-115) has been shown to inhibit NOX1, NOX2, and NOX4 in pre-clinical studies (Cha et al., 2017). Moreover, this NOX inhibitor is currently moving from Phase I to II in clinical trials for patients with diabetic kidney disease (Lee et al., 2020). Studies demonstrating the efficacy of specific NOX2 blockade with minimal side effects are necessary to encourage future development of NOX2 inhibitors. In addition to the multitude of integrative systems that have previously been shown to succumb to the mal-adaptive tendencies of NOX2-derived ROS, our results reveal that respiratory muscle weakness in a murine model of OSAS is also NOX2-dependent. We suggest that this may have relevance for respiratory morbidity in the human condition of OSAS and potentially other disorders characterised by skeletal muscle weakness.

Overall, our study demonstrates that exposure to CIH, a fundamental feature of OSAS, is capable of inducing mal-adaptation within the respiratory control system through an increase in the incidence of central apnoeas and the development of severe respiratory muscle weakness. CPAP is the gold standard treatment for OSAS patients, beneficial in alleviating and preventing obstructive events. However, if reconfiguration throughout the respiratory control network has already occurred as a result of repetitive exposure to IH during obstructive events, OSAS patients are also susceptible to central apnoeic events during CPAP treatment. Indeed, many OSAS patients present with complex apnoea, suggesting that CIH-induced ROS drive an underlying central pathology which accelerates the progression of the severity of OSAS (i.e. mild-to-moderate-to-severe). If complex apnoea is CIH-dependent, then early treatment strategies are warranted to prevent these perturbations to respiratory control. Our results suggest a therapeutic role for antioxidant strategies that may intervene before long-lasting modifications ensue and CIH-induced increases in apnoea index develop. Moreover, a culmination of the profound UA and diaphragm muscle weakness observed following exposure to CIH in the current study is likely to increase the probability of airway collapse and impede the re-establishment of airway calibre following obstruction, potentially exacerbating existing respiratory morbidity in OSAS patients, perpetuating a vicious cycle of events. Our results suggest that CIH-induced respiratory muscle weakness is entirely amenable to NOX2 blockade, highlighting specific therapeutic potential in human OSAS and other diseases characterised by skeletal muscle weakness. Our study in a murine model of OSAS offers further evidence to support the use of antioxidants as an adjunct therapy to CPAP in human OSAS.

6.4 References

ADAMS, V., LINKE, A., KRÄNKEL, N., ERBS, S., GIELEN, S., MÖBIUS-WINKLER, S., GUMMERT, J. F., MOHR, F. W., SCHULER, G. & HAMBRECHT, R. 2005. Impact of regular physical activity on the NAD(P)H oxidase and angiotensin receptor system in patients with coronary artery disease. *Circulation,* 111**,** 555-62.

AHN, B., BEHARRY, A. W., FRYE, G. S., JUDGE, A. R. & FERREIRA, L. F. 2015. NAD(P)H oxidase subunit p47phox is elevated, and p47phox knockout prevents diaphragm contractile dysfunction in heart failure. *Am J Physiol Lung Cell Mol Physiol,* 309**,** L497-505.

AL LAWATI, N. M., PATEL, S. R. & AYAS, N. T. 2009. Epidemiology, risk factors, and consequences of obstructive sleep apnea and short sleep duration. *Prog Cardiovasc Dis,* 51**,** 285-93.

AYDIN, E., JOHANSSON, J., NAZIR, F. H., HELLSTRAND, K. & MARTNER, A. 2017. Role of NOX2-Derived Reactive Oxygen Species in NK Cell-Mediated Control of Murine Melanoma Metastasis. *Cancer Immunol Res,* 5**,** 804-811.

BARCELÓ, A., BARBÉ, F., DE LA PEÑA, M., VILA, M., PÉREZ, G., PIÉROLA, J., DURÁN, J. & AGUSTÍ, A. G. 2006. Antioxidant status in patients with sleep apnoea and impact of continuous positive airway pressure treatment. *Eur Respir J,* 27**,** 756-60.

BEDARD, K. & KRAUSE, K. H. 2007. The NOX family of ROS-generating NADPH oxidases: physiology and pathophysiology. *Physiol Rev,* 87**,** 245-313.

BOWEN, T. S., MANGNER, N., WERNER, S., GLASER, S., KULLNICK, Y., SCHREPPER, A., DOENST, T., OBERBACH, A., LINKE, A., STEIL, L., SCHULER, G. & ADAMS, V. 2015a. Diaphragm muscle weakness in mice is early-onset post-myocardial infarction and associated with elevated protein oxidation. *J Appl Physiol (1985),* 118**,** 11-9.

BOWEN, T. S., ROLIM, N. P., FISCHER, T., BAEKKERUD, F. H., MEDEIROS, A., WERNER, S., BRØNSTAD, E., ROGNMO, O., MANGNER, N., LINKE, A., SCHULER, G., SILVA, G. J., WISLØFF, U. & ADAMS, V. 2015b. Heart failure with preserved ejection fraction induces molecular, mitochondrial, histological, and functional alterations in rat respiratory and limb skeletal muscle. *Eur J Heart Fail,* 17**,** 263-72.

BRENNER, B. 1988. Effect of Ca2+ on cross-bridge turnover kinetics in skinned single rabbit psoas fibers: implications for regulation of muscle contraction. *Proc Natl Acad Sci U S A,* 85**,** 3265-9.

BURNS, D. P., CANAVAN, L., ROWLAND, J., O'FLAHERTY, R., BRANNOCK, M., DRUMMOND, S. E., O'MALLEY, D., EDGE, D. & O'HALLORAN, K. D. 2018. Recovery of respiratory function in mdx mice co-treated with neutralizing interleukin-6 receptor antibodies and urocortin-2. *J Physiol,* 596**,** 5175-5197.

BURNS, D. P., MURPHY, K. H., LUCKING, E. F. & O'HALLORAN, K. D. 2019. Inspiratory pressure-generating capacity is preserved during ventilatory and non-ventilatory behaviours in young dystrophic mdx mice despite profound diaphragm muscle weakness. *J Physiol,* 597**,** 831-848.

CARBERRY, J. C., JORDAN, A. S., WHITE, D. P., WELLMAN, A. & ECKERT, D. J. 2016. Upper Airway Collapsibility (Pcrit) and Pharyngeal Dilator Muscle Activity are Sleep Stage Dependent. *Sleep,* 39**,** 511-21.

CARRERA, M., BARBÉ, F., SAULEDA, J., TOMÁS, M., GÓMEZ, C. & AGUSTÍ, A. G. 1999. Patients with obstructive sleep apnea exhibit genioglossus dysfunction that is normalized after treatment with continuous positive airway pressure. *Am J Respir Crit Care Med,* 159**,** 1960-6.

CASALE, M., PAPPACENA, M., RINALDI, V., BRESSI, F., BAPTISTA, P. & SALVINELLI, F. 2009. Obstructive sleep apnea syndrome: from phenotype to genetic basis. *Curr Genomics,* 10**,** 119-26.

CHA, J. J., MIN, H. S., KIM, K. T., KIM, J. E., GHEE, J. Y., KIM, H. W., LEE, J. E., HAN, J. Y., LEE, G., HA, H. J., BAE, Y. S., LEE, S. R., MOON, S. H., LEE, S. C., KIM, G., KANG, Y. S. & CHA, D. R. 2017. APX-115, a first-in-class pan-NADPH oxidase (Nox) inhibitor, protects db/db mice from renal injury. *Lab Invest,* 97**,** 419-431.

CHIEN, M. Y., WU, Y. T., LEE, P. L., CHANG, Y. J. & YANG, P. C. 2010. Inspiratory muscle dysfunction in patients with severe obstructive sleep apnoea. *Eur Respir J,* 35**,** 373-80.

CLANTON, T. L., WRIGHT, V. P., REISER, P. J., KLAWITTER, P. F. & PRABHAKAR, N. R. 2001. Selected Contribution: Improved anoxic tolerance in rat diaphragm following intermittent hypoxia. *Journal of Applied Physiology,* 90**,** 2508-2513.

COBLEY, J. N., SAKELLARIOU, G. K., HUSI, H. & MCDONAGH, B. 2019. Proteomic strategies to unravel age-related redox signalling defects in skeletal muscle. *Free Radic Biol Med,* 132**,** 24-32.

COIRAULT, C., GUELLICH, A., BARBRY, T., SAMUEL, J. L., RIOU, B. & LECARPENTIER, Y. 2007. Oxidative stress of myosin contributes to skeletal muscle dysfunction in rats with chronic heart failure. *Am J Physiol Heart Circ Physiol,* 292**,** H1009-17.

COSTFORD, S. R., CASTRO-ALVES, J., CHAN, K. L., BAILEY, L. J., WOO, M., BELSHAM, D. D., BRUMELL, J. H. & KLIP, A. 2014. Mice lacking NOX2 are hyperphagic and store fat preferentially in the liver. *Am J Physiol Endocrinol Metab,* 306**,** E1341-53.

CULLY, T. R. & RODNEY, G. G. 2020. Nox4 - RyR1 - Nox2: Regulators of micro-domain signaling in skeletal muscle. *Redox Biol,* 36**,** 101557.

DE PAULA BROTTO, M., VAN LEYEN, S. A., BROTTO, L. S., JIN, J. P., NOSEK, C. M. & NOSEK, T. M. 2001. Hypoxia/fatigue-induced degradation of troponin I and troponin C: new insights into physiologic muscle fatigue. *Pflugers Arch,* 442**,** 738-44.

DEL RIO, R., MOYA, E. A. & ITURRIAGA, R. 2010. Carotid body and cardiorespiratory alterations in intermittent hypoxia: the oxidative link. *Eur Respir J,* 36**,** 143-50.

DEL RIO, R., MOYA, E. A. & ITURRIAGA, R. 2011. Differential expression of pro-inflammatory cytokines, endothelin-1 and nitric oxide synthases in the rat carotid body exposed to intermittent hypoxia. *Brain Res,* 1395**,** 74-85.

DIDIER, M., ROTENBERG, C., MARCHANT, D., SUTTON, A., VALEYRE, D., NUNES, H., BONCOEUR, E. & PLANES, C. Effect of Chronic Intermittent Hypoxia in a Murine Model of Bleomycin-Induced Pulmonary Fibrosis. *B57. FIBROSIS BIOLOGY.*

DING, W. & LIU, Y. 2011. Genistein attenuates genioglossus muscle fatigue under chronic intermittent hypoxia by down-regulation of oxidative stress level and up-regulation of antioxidant enzyme activity through ERK1/2 signaling pathway. *Oral Dis,* 17**,** 677-84.

\

DOHI, K., OHTAKI, H., NAKAMACHI, T., YOFU, S., SATOH, K., MIYAMOTO, K., SONG, D., TSUNAWAKI, S., SHIODA, S. & ARUGA, T. 2010. Gp91phox (NOX2) in classically activated microglia exacerbates traumatic brain injury. *J Neuroinflammation,* 7**,** 41.

DONOVAN, L. M., LIU, Y. & WEISS, J. W. 2014. Effect of endothelin antagonism on apnea frequency following chronic intermittent hypoxia. *Respir Physiol Neurobiol,* 194**,** 6-8.

DRAGER, L. F., LI, J., REINKE, C., BEVANS-FONTI, S., JUN, J. C. & POLOTSKY, V. Y. 2011a. Intermittent Hypoxia Exacerbates Metabolic Effects of Diet-Induced Obesity. *Obesity (Silver Spring, Md.),* 19**,** 2167-2174.

DRAGER, L. F., LI, J., REINKE, C., BEVANS-FONTI, S., JUN, J. C. & POLOTSKY, V. Y. 2011b. Intermittent hypoxia exacerbates metabolic effects of diet-induced obesity. *Obesity (Silver Spring),* 19**,** 2167-74.

DUMITRASCU, R., HEITMANN, J., SEEGER, W., WEISSMANN, N. & SCHULZ, R. 2013. Obstructive sleep apnea, oxidative stress and cardiovascular disease: lessons from animal studies. *Oxid Med Cell Longev,* 2013**,** 234631.

DUNLEAVY, M., BRADFORD, A. & O'HALLORAN, K. D. 2008. Oxidative stress impairs upper airway muscle endurance in an animal model of sleep-disordered breathing. *Adv Exp Med Biol,* 605**,** 458-62.

DUTKA, T. L., MOLLICA, J. P., LAMBOLEY, C. R., WEERAKKODY, V. C., GREENING, D. W., POSTERINO, G. S., MURPHY, R. M. & LAMB, G. D. 2017. S-nitrosylation and S-glutathionylation of Cys134 on troponin I have opposing competitive actions on Ca(2+) sensitivity in rat fast-twitch muscle fibers. *Am J Physiol Cell Physiol,* 312**,** C316-c327.

EDGE, D., BRADFORD, A. & O'HALLORAN, K. D. 2012. Chronic intermittent hypoxia increases apnoea index in sleeping rats. *Adv Exp Med Biol,* 758**,** 359-63.

ELLIOT-PORTAL, E., LAOUAFA, S., ARIAS-REYES, C., JANES, T. A., JOSEPH, V. & SOLIZ, J. 2018. Brain-derived erythropoietin protects from intermittent hypoxia-induced cardiorespiratory dysfunction and oxidative stress in mice. *Sleep,* 41.

FRIEDEL, R. H., WURST, W., WEFERS, B. & KÜHN, R. 2011. Generating conditional knockout mice. *Methods Mol Biol,* 693**,** 205-31.

GAMBOA, J. L. & ANDRADE, F. H. 2012. Muscle endurance and mitochondrial function after chronic normobaric hypoxia: contrast of respiratory and limb muscles. *Pflugers Arch,* 463**,** 327-38.

GIORDANO, C., LEMAIRE, C., LI, T., KIMOFF, R. J. & PETROF, B. J. 2015. Autophagy-associated atrophy and metabolic remodeling of the mouse diaphragm after short-term intermittent hypoxia. *PLoS One,* 10**,** e0131068.

GREISING, S. M., MANTILLA, C. B., MEDINA-MARTÍNEZ, J. S., STOWE, J. M. & SIECK, G. C. 2015. Functional impact of diaphragm muscle sarcopenia in both male and female mice. *Am J Physiol Lung Cell Mol Physiol,* 309**,** L46-52.

GREISING, S. M., MANTILLA, C. B. & SIECK, G. C. 2016. Functional Measurement of Respiratory Muscle Motor Behaviors Using Transdiaphragmatic Pressure. *Methods Mol Biol,* 1460**,** 309-19.

GRIGGS, G. A., FINDLEY, L. J., SURATT, P. M., ESAU, S. A., WILHOIT, S. C. & ROCHESTER, D. F. 1989. Prolonged relaxation rate of inspiratory muscles in patients with sleep apnea. *Am Rev Respir Dis,* 140**,** 706-10.

GUERRA, L., CERBAI, E., GESSI, S., BOREA, P. A. & MUGELLI, A. 1996. The effect of oxygen free radicals on calcium current and dihydropyridine binding sites in guinea-pig ventricular myocytes. *British Journal of Pharmacology,* 118**,** 1278-1284.

HAYES, E., POHL, K., MCELVANEY, N. G. & REEVES, E. P. 2011. The cystic fibrosis neutrophil: a specialized yet potentially defective cell. *Arch Immunol Ther Exp (Warsz),* 59**,** 97-112.

HEDNER, J., DARPÖ, B., EJNELL, H., CARLSON, J. & CAIDAHL, K. 1995. Reduction in sympathetic activity after long-term CPAP treatment in sleep apnoea: cardiovascular implications. *Eur Respir J,* 8**,** 222-9.

HIDALGO, C., SANCHEZ, G., BARRIENTOS, G. & ARACENA-PARKS, P. 2006. A transverse tubule NADPH oxidase activity stimulates calcium release from isolated triads via ryanodine receptor type 1 S -glutathionylation. *J Biol Chem,* 281**,** 26473-82.

HUXLEY, A. F. & SIMMONS, R. M. 1971. Proposed mechanism of force generation in striated muscle. *Nature,* 233**,** 533-8.

ITURRIAGA, R., ANDRADE, D. C. & DEL RIO, R. 2014. Enhanced carotid body chemosensory activity and the cardiovascular alterations induced by intermittent hypoxia. *Front Physiol,* 5**,** 468.

JAVESHGHANI, D., MAGDER, S. A., BARREIRO, E., QUINN, M. T. & HUSSAIN, S. N. 2002. Molecular characterization of a superoxide-generating NAD(P)H oxidase in the ventilatory muscles. *Am J Respir Crit Care Med,* 165**,** 412-8.

JIA, R. & BONIFACINO, J. S. 2020. Regulation of LC3B levels by ubiquitination and proteasomal degradation. *Autophagy,* 16**,** 382-384.

JIA, S. S. & LIU, Y. H. 2010. Down-regulation of hypoxia inducible factor-1alpha: a possible explanation for the protective effects of estrogen on genioglossus fatigue resistance. *Eur J Oral Sci,* 118**,** 139-44.

JOSEPH, V., LAOUAFA, S., MARCOUILLER, F., ROUSSEL, D., PIALOUX, V. & BAIRAM, A. 2020. Progesterone decreases apnoea and reduces oxidative stress induced by chronic intermittent hypoxia in ovariectomized female rats. *Exp Physiol,* 105**,** 1025-1034.

KADOWAKI, M. & KARIM, M. R. 2009. Cytosolic LC3 ratio as a quantitative index of macroautophagy. *Methods Enzymol,* 452**,** 199-213.

KANG, H. H., KIM, I. K., LEE, H. I., JOO, H., LIM, J. U., LEE, J., LEE, S. H. & MOON, H. S. 2017. Chronic intermittent hypoxia induces liver fibrosis in mice with diet-induced obesity via TLR4/MyD88/MAPK/NF-kB signaling pathways. *Biochem Biophys Res Commun,* 490**,** 349-355.

KANG, H. H., KIM, I. K. & LEE, S. H. 2018. Chronic intermittent hypoxia exacerbates lung fibrosis in bleomycin-induced lung injury mouse model. *European Respiratory Journal,* 52**,** PA428.

LAGENTE, V., PLANQUOIS, J. M., LECLERC, O., SCHMIDLIN, F. & BERTRAND, C. P. 2008. Oxidative stress is an important component of airway inflammation in mice exposed to cigarette smoke or lipopolysaccharide. *Clin Exp Pharmacol Physiol,* 35**,** 601-5.

LAVIE, L. 2003. Obstructive sleep apnoea syndrome--an oxidative stress disorder. *Sleep Med Rev,* 7**,** 35-51.

LAVIE, L. 2009. Oxidative stress--a unifying paradigm in obstructive sleep apnea and comorbidities. *Prog Cardiovasc Dis,* 51**,** 303-12.

LEE, S. R., AN, E. J., KIM, J. & BAE, Y. S. 2020. Function of NADPH Oxidases in Diabetic Nephropathy and Development of Nox Inhibitors. *Biomol Ther (Seoul),* 28**,** 25-33.

LEWIS, P., SHEEHAN, D., SOARES, R., COELHO, A. V. & O'HALLORAN, K. D. 2016. Redox Remodeling Is Pivotal in Murine Diaphragm Muscle Adaptation to Chronic Sustained Hypoxia. *Am J Respir Cell Mol Biol,* 55**,** 12-23.

LEWIS, P., SHEEHAN, D., SOARES, R., VARELA COELHO, A. & O'HALLORAN, K. D. 2015. Chronic sustained hypoxia-induced redox remodeling causes contractile dysfunction in mouse sternohyoid muscle. *Front Physiol,* 6**,** 122.

LIN, Y. N., LI, Q. Y. & ZHANG, X. J. 2012. Interaction between smoking and obstructive sleep apnea: not just participants. *Chin Med J (Engl),* 125**,** 3150-6.

LIU, S. S., LIU, H. G., XIONG, S. D., NIU, R. J., XU, Y. J. & ZHANG, Z. X. 2005. [Effects of Shen-Mai injection on sternohyoid contractile properties in chronic intermittent hypoxia rat]. *Zhonghua Jie He He Hu Xi Za Zhi,* 28**,** 611-4.

LIU, W., CHEN, Q., LIU, J. & LIU, K. J. 2011. Normobaric hyperoxia protects the blood brain barrier through inhibiting Nox2 containing NADPH oxidase in ischemic stroke. *Med Gas Res,* 1**,** 22.

LIU, Y. H., HUANG, Y. & SHAO, X. 2009. Effects of estrogen on genioglossal muscle contractile properties and fiber-type distribution in chronic intermittent hypoxia rats. *Eur J Oral Sci,* 117**,** 685-90.

LOUREIRO, A. C. C., DO RÊGO-MONTEIRO, I. C., LOUZADA, R. A., ORTENZI, V. H., DE AGUIAR, A. P., DE ABREU, E. S., CAVALCANTI-DE-ALBUQUERQUE, J. P. A., HECHT, F., DE OLIVEIRA, A. C., CECCATTO, V. M., FORTUNATO, R. S. & CARVALHO, D. P. 2016. Differential Expression of NADPH Oxidases Depends on Skeletal Muscle Fiber Type in Rats. *Oxidative Medicine and Cellular Longevity,* 2016**,** 6738701.

LUCKING, E. F., O'HALLORAN, K. D. & JONES, J. F. 2014. Increased cardiac output contributes to the development of chronic intermittent hypoxia-induced hypertension. *Exp Physiol,* 99**,** 1312-24.

MAGHZAL, G. J., KRAUSE, K. H., STOCKER, R. & JAQUET, V. 2012. Detection of reactive oxygen species derived from the family of NOX NADPH oxidases. *Free Radic Biol Med,* 53**,** 1903-18.

MANTILLA, C. B., SEVEN, Y. B., ZHAN, W. Z. & SIECK, G. C. 2010. Diaphragm motor unit recruitment in rats. *Respir Physiol Neurobiol,* 173**,** 101-6.

MCDONAGH, B., SAKELLARIOU, G. K., SMITH, N. T., BROWNRIDGE, P. & JACKSON, M. J. 2014. Differential cysteine labeling and global label-free proteomics reveals an altered metabolic state in skeletal muscle aging. *J Proteome Res,* 13**,** 5008-21.

MCDONALD, F. B., WILLIAMS, R., SHEEHAN, D. & O'HALLORAN, K. D. 2015. Early life exposure to chronic intermittent hypoxia causes upper airway dilator muscle weakness, which persists into young adulthood. *Exp Physiol,* 100**,** 947-66.

MCGUIRE, M., MACDERMOTT, M. & BRADFORD, A. 2002a. Effects of chronic episodic hypoxia on rat upper airway muscle contractile properties and fiber-type distribution. *Chest,* 122**,** 1012-7.

MCGUIRE, M., MACDERMOTT, M. & BRADFORD, A. 2002b. The effects of chronic episodic hypercapnic hypoxia on rat upper airway muscle contractile properties and fiber-type distribution. *Chest,* 122**,** 1400-6.

MCGUIRE, M., MACDERMOTT, M. & BRADFORD, A. 2003. Effects of chronic intermittent asphyxia on rat diaphragm and limb muscle contractility. *Chest,* 123**,** 875-81.

MCMORROW, C., FREDSTED, A., CARBERRY, J., O'CONNELL, R. A., BRADFORD, A., JONES, J. F. & O'HALLORAN, K. D. 2011. Chronic hypoxia increases rat diaphragm muscle endurance and sodium-potassium ATPase pump content. *Eur Respir J.* England.

MEYER, A. J. & DICK, T. P. 2010. Fluorescent protein-based redox probes. *Antioxid Redox Signal,* 13**,** 621-50.

MIFFLIN, S., CUNNINGHAM, J. T. & TONEY, G. M. 2015. Neurogenic mechanisms underlying the rapid onset of sympathetic responses to intermittent hypoxia. *J Appl Physiol (1985),* 119**,** 1441-8.

MORAES, D. J., DA SILVA, M. P., BONAGAMBA, L. G., MECAWI, A. S., ZOCCAL, D. B., ANTUNES-RODRIGUES, J., VARANDA, W. A. & MACHADO, B. H. 2013. Electrophysiological properties of rostral ventrolateral medulla presympathetic neurons modulated by the respiratory network in rats. *J Neurosci,* 33**,** 19223-37.

MORGAN, B. J., ADRIAN, R., WANG, Z. Y., BATES, M. L. & DOPP, J. M. 2016a. Chronic intermittent hypoxia alters ventilatory and metabolic responses to acute hypoxia in rats. *J Appl Physiol (1985),* 120**,** 1186-95.

MORGAN, B. J., BATES, M. L., RIO, R. D., WANG, Z. & DOPP, J. M. 2016b. Oxidative stress augments chemoreflex sensitivity in rats exposed to chronic intermittent hypoxia. *Respir Physiol Neurobiol,* 234**,** 47-59.

MORGENTHALER, T. I., KAGRAMANOV, V., HANAK, V. & DECKER, P. A. 2006. Complex sleep apnea syndrome: is it a unique clinical syndrome? *Sleep,* 29**,** 1203-9.

MORTOLA, J. P. & FRAPPELL, P. B. 1998. On the barometric method for measurements of ventilation, and its use in small animals. *Can J Physiol Pharmacol,* 76**,** 937-44.

MOYA, E. A., GO, A., KIM, C. B., FU, Z., SIMONSON, T. S. & POWELL, F. L. 2020. Neuronal HIF-1α in the nucleus tractus solitarius contributes to ventilatory acclimatization to hypoxia. *J Physiol,* 598**,** 2021-2034.

NISBET, R. E., GRAVES, A. S., KLEINHENZ, D. J., RUPNOW, H. L., REED, A. L., FAN, T. H., MITCHELL, P. O., SUTLIFF, R. L. & HART, C. M. 2009. The role of NADPH oxidase in chronic intermittent hypoxia-induced pulmonary hypertension in mice. *Am J Respir Cell Mol Biol,* 40**,** 601-9.

O'HALLORAN, K. D., MCGUIRE, M., O'HARE, T. & BRADFORD, A. 2002. Chronic intermittent asphyxia impairs rat upper airway muscle responses to acute hypoxia and asphyxia. *Chest,* 122**,** 269-75.

OTTENHEIJM, C. A., HEUNKS, L. M., GERAEDTS, M. C. & DEKHUIJZEN, P. N. 2006. Hypoxia-induced skeletal muscle fiber dysfunction: role for reactive nitrogen species. *Am J Physiol Lung Cell Mol Physiol,* 290**,** L127-35.

OTTENHEIJM, C. A., HEUNKS, L. M., SIECK, G. C., ZHAN, W. Z., JANSEN, S. M., DEGENS, H., DE BOO, T. & DEKHUIJZEN, P. N. 2005. Diaphragm dysfunction in chronic obstructive pulmonary disease. *Am J Respir Crit Care Med,* 172**,** 200-5.

PAE, E. K., WU, J., NGUYEN, D., MONTI, R. & HARPER, R. M. 2005. Geniohyoid muscle properties and myosin heavy chain composition are altered after short-term intermittent hypoxic exposure. *J Appl Physiol (1985),* 98**,** 889-94.

PAL, R., BASU THAKUR, P., LI, S., MINARD, C. & RODNEY, G. G. 2013. Real-time imaging of NADPH oxidase activity in living cells using a novel fluorescent protein reporter. *PLoS One,* 8**,** e63989.

PAL, R., PALMIERI, M., LOEHR, J. A., LI, S., ABO-ZAHRAH, R., MONROE, T. O., THAKUR, P. B., SARDIELLO, M. & RODNEY, G. G. 2014. Src-dependent impairment of autophagy by oxidative stress in a mouse model of Duchenne muscular dystrophy. *Nature communications,* 5**,** 4425-4425.

PARK, L., ANRATHER, J., ZHOU, P., FRYS, K., PITSTICK, R., YOUNKIN, S., CARLSON, G. A. & IADECOLA, C. 2005. NADPH-oxidase-derived reactive oxygen species mediate the cerebrovascular dysfunction induced by the amyloid beta peptide. *J Neurosci,* 25**,** 1769-77.

PAWAR, A., NANDURI, J., YUAN, G., KHAN, S. A., WANG, N., KUMAR, G. K. & PRABHAKAR, N. R. 2009. Reactive oxygen species-dependent endothelin signaling is required for augmented hypoxic sensory response of the neonatal carotid body by intermittent hypoxia. *Am J Physiol Regul Integr Comp Physiol,* 296**,** R735-42.

PENG, Y., KLINE, D. D., DICK, T. E. & PRABHAKAR, N. R. 2001. Chronic intermittent hypoxia enhances carotid body chemoreceptor response to low oxygen. *Adv Exp Med Biol,* 499**,** 33-8.

PENG, Y. J., NANDURI, J., RAGHURAMAN, G., WANG, N., KUMAR, G. K. & PRABHAKAR, N. R. 2013. Role of oxidative stress-induced endothelin-converting enzyme activity in the alteration of carotid body function by chronic intermittent hypoxia. *Exp Physiol,* 98**,** 1620-30.

PENG, Y. J., NANDURI, J., YUAN, G., WANG, N., DENERIS, E., PENDYALA, S., NATARAJAN, V., KUMAR, G. K. & PRABHAKAR, N. R. 2009. NADPH oxidase is required for the sensory plasticity of the carotid body by chronic intermittent hypoxia. *J Neurosci,* 29**,** 4903-10.

PENG, Y. J., OVERHOLT, J. L., KLINE, D., KUMAR, G. K. & PRABHAKAR, N. R. 2003. Induction of sensory long-term facilitation in the carotid body by intermittent hypoxia: implications for recurrent apneas. *Proc Natl Acad Sci U S A,* 100**,** 10073-8.

PENG, Y. J., YUAN, G., RAMAKRISHNAN, D., SHARMA, S. D., BOSCH-MARCE, M., KUMAR, G. K., SEMENZA, G. L. & PRABHAKAR, N. R. 2006. Heterozygous HIF-1alpha deficiency impairs carotid body-mediated systemic responses and reactive oxygen species generation in mice exposed to intermittent hypoxia. *J Physiol,* 577**,** 705-16.

PHILLIPS, C. L., YANG, Q., WILLIAMS, A., ROTH, M., YEE, B. J., HEDNER, J. A., BEREND, N. & GRUNSTEIN, R. R. 2007. The effect of short-term withdrawal from continuous positive airway pressure therapy on sympathetic activity and markers of vascular inflammation in subjects with obstructive sleep apnoea. *J Sleep Res,* 16**,** 217-25.

PINTO, J. R., DE SOUSA, V. P. & SORENSON, M. M. 2011. Redox state of troponin C cysteine in the D/E helix alters the C-domain affinity for the thin filament of vertebrate striated muscle. *Biochim Biophys Acta,* 1810**,** 391-7.

RADA, B. & LETO, T. L. 2008. Oxidative innate immune defenses by Nox/Duox family NADPH oxidases. *Contrib Microbiol,* 15**,** 164-187.

RAY, A. D., MAGALANG, U. J., MICHLIN, C. P., OGASA, T., KRASNEY, J. A., GOSSELIN, L. E. & FARKAS, G. A. 2007. Intermittent hypoxia reduces upper airway stability in lean but not obese Zucker rats. *Am J Physiol Regul Integr Comp Physiol,* 293**,** R372-8.

REEVES, S. R. & GOZAL, D. 2006. Changes in ventilatory adaptations associated with long-term intermittent hypoxia across the age spectrum in the rat. *Respir Physiol Neurobiol,* 150**,** 135-43.

REMMERS, J. E., DEGROOT, W. J., SAUERLAND, E. K. & ANCH, A. M. 1978. Pathogenesis of upper airway occlusion during sleep. *J Appl Physiol Respir Environ Exerc Physiol,* 44**,** 931-8.

REZENDE, F., LÖWE, O., HELFINGER, V., PRIOR, K. K., WALTER, M., ZUKUNFT, S., FLEMING, I., WEISSMANN, N., BRANDES, R. P. & SCHRÖDER, K. 2016. Unchanged NADPH Oxidase Activity in Nox1-Nox2-Nox4 Triple Knockout Mice: What Do NADPH-Stimulated Chemiluminescence Assays Really Detect? *Antioxid Redox Signal,* 24**,** 392-9.

ROMERO-CORRAL, A., CAPLES, S. M., LOPEZ-JIMENEZ, F. & SOMERS, V. K. 2010. Interactions Between Obesity and Obstructive Sleep Apnea: Implications for Treatment. *Chest,* 137**,** 711-9.

ROSAS, S. E. 2011. Sleep apnea in individuals with chronic kidney disease: a wake-up call. *Clin J Am Soc Nephrol,* 6**,** 954-6.

ROSPARS, J. P. & MEYER-VERNET, N. 2016. Force per cross-sectional area from molecules to muscles: a general property of biological motors. *R Soc Open Sci,* 3**,** 160313.

RUSSELL, A. J., HARTMAN, J. J., HINKEN, A. C., MUCI, A. R., KAWAS, R., DRISCOLL, L., GODINEZ, G., LEE, K. H., MARQUEZ, D., BROWNE, W. F. T., CHEN, M. M., CLARKE, D., COLLIBEE, S. E., GARARD, M., HANSEN, R., JIA, Z., LU, P. P., RODRIGUEZ, H., SAIKALI, K. G., SCHALETZKY, J., VIJAYAKUMAR, V., ALBERTUS, D. L., CLAFLIN, D. R., MORGANS, D. J., MORGAN, B. P. & MALIK, F. I. 2012. Activation of fast skeletal muscle troponin as a potential therapeutic approach for treating neuromuscular diseases. *Nat Med,* 18**,** 452-5.

SACRAMENTO, J. F., GONZALEZ, C., GONZALEZ-MARTIN, M. C. & CONDE, S. V. 2015. Adenosine Receptor Blockade by Caffeine Inhibits Carotid Sinus Nerve Chemosensory Activity in Chronic Intermittent Hypoxic Animals. *Adv Exp Med Biol,* 860**,** 133-7.

SADASIVAM, K., PATIAL, K., VIJAYAN, V. K. & RAVI, K. 2011. Anti-oxidant treatment in obstructive sleep apnoea syndrome. *Indian J Chest Dis Allied Sci,* 53**,** 153-62.

SAKELLARIOU, G. K., MCDONAGH, B., PORTER, H., GIAKOUMAKI, II, EARL, K. E., NYE, G. A., VASILAKI, A., BROOKS, S. V., RICHARDSON, A., VAN REMMEN, H., MCARDLE, A. & JACKSON, M. J. 2018. Comparison of Whole Body SOD1 Knockout with Muscle-Specific SOD1 Knockout Mice Reveals a Role for Nerve Redox Signaling in Regulation of Degenerative Pathways in Skeletal Muscle. *Antioxid Redox Signal,* 28**,** 275-295.

SAVRANSKY, V., NANAYAKKARA, A., VIVERO, A., LI, J., BEVANS, S., SMITH, P. L., TORBENSON, M. S. & POLOTSKY, V. Y. 2007. Chronic intermittent hypoxia predisposes to liver injury. *Hepatology,* 45**,** 1007-13.

SEGAL, B. H., VEYS, P., MALECH, H. & COWAN, M. J. 2011. Chronic granulomatous disease: lessons from a rare disorder. *Biol Blood Marrow Transplant,* 17**,** S123-31.

SEMENZA, G. L. & PRABHAKAR, N. R. 2015. Neural regulation of hypoxia-inducible factors and redox state drives the pathogenesis of hypertension in a rodent model of sleep apnea. *J Appl Physiol (1985),* 119**,** 1152-6.

SHIOSE, A., KURODA, J., TSURUYA, K., HIRAI, M., HIRAKATA, H., NAITO, S., HATTORI, M., SAKAKI, Y. & SUMIMOTO, H. 2001. A Novel Superoxide-producing NAD(P)H Oxidase in Kidney. *Journal of Biological Chemistry,* 276**,** 1417-1423.

SHORTT, C. M., FREDSTED, A., BRADFORD, A. & O'HALLORAN, K. D. 2013. Diaphragm muscle remodeling in a rat model of chronic intermittent hypoxia. *J Histochem Cytochem,* 61**,** 487-99.

SHORTT, C. M., FREDSTED, A., CHOW, H. B., WILLIAMS, R., SKELLY, J. R., EDGE, D., BRADFORD, A. & O'HALLORAN, K. D. 2014. Reactive oxygen species mediated diaphragm fatigue in a rat model of chronic intermittent hypoxia. *Exp Physiol,* 99**,** 688-700.

SHORTT, C. M. & O'HALLORAN, K. D. 2014. Hydrogen peroxide alters sternohyoid muscle function. *Oral Dis,* 20**,** 162-70.

SINGH, T. D., PATIAL, K., VIJAYAN, V. K. & RAVI, K. 2009. Oxidative stress and obstructive sleep apnoea syndrome. *Indian J Chest Dis Allied Sci,* 51**,** 217-24.

SKELLY, J. R., EDGE, D., SHORTT, C. M., JONES, J. F., BRADFORD, A. & O'HALLORAN, K. D. 2012. Tempol ameliorates pharyngeal dilator muscle dysfunction in a rodent model of chronic intermittent hypoxia. *Am J Respir Cell Mol Biol,* 46**,** 139-48.

SKELLY, J. R., ROWAN, S. C., JONES, J. F. & O'HALLORAN, K. D. 2013. Upper airway dilator muscle weakness following intermittent and sustained hypoxia in the rat: effects of a superoxide scavenger. *Physiol Res,* 62**,** 187-96.

SMUDER, A. J., KAVAZIS, A. N., HUDSON, M. B., NELSON, W. B. & POWERS, S. K. 2010. Oxidation enhances myofibrillar protein degradation via calpain and caspase-3. *Free Radic Biol Med,* 49**,** 1152-60.

SORCE, S., SCHIAVONE, S., TUCCI, P., COLAIANNA, M., JAQUET, V., CUOMO, V., DUBOIS-DAUPHIN, M., TRABACE, L. & KRAUSE, K. H. 2010. The NADPH oxidase NOX2 controls glutamate release: a novel mechanism involved in psychosis-like ketamine responses. *J Neurosci,* 30**,** 11317-25.

SOUZA, G. M., BONAGAMBA, L. G., AMORIM, M. R., MORAES, D. J. & MACHADO, B. H. 2015. Cardiovascular and respiratory responses to chronic intermittent hypoxia in adult female rats. *Exp Physiol,* 100**,** 249-58.

STEPHENSON, R. & GUCCIARDI, E. J. 2002. Theoretical and practical considerations in the application of whole body plethysmography to sleep research. *Eur J Appl Physiol,* 87**,** 207-19.

STEPNOWSKY, C. J., JR. & MOORE, P. J. 2003. Nasal CPAP treatment for obstructive sleep apnea: developing a new perspective on dosing strategies and compliance. *J Psychosom Res,* 54**,** 599-605.

SÉRLÈS, F., CÔTÉ, C., SIMONEAU, J.-A., PIERRE, S. S. & MARC, I. 1996. Upper airway collapsibility, and contractile and metabolic characteristics of musculus uvulae. *The FASEB Journal,* 10**,** 897-904.

TORRES, M., LAGUNA-BARRAZA, R., DALMASES, M., CALLE, A., PERICUESTA, E., MONTSERRAT, J. M., NAVAJAS, D., GUTIERREZ-ADAN, A. & FARRÉ, R. 2014a. Male fertility is reduced by chronic intermittent hypoxia mimicking sleep apnea in mice. *Sleep,* 37**,** 1757-65.

TORRES, M., LAGUNA-BARRAZA, R., DALMASES, M., CALLE, A., PERICUESTA, E., MONTSERRAT, J. M., NAVAJAS, D., GUTIERREZ-ADAN, A. & FARRÉ, R. 2014b. Male Fertility Is Reduced by Chronic Intermittent Hypoxia Mimicking Sleep Apnea in Mice. *Sleep,* 37**,** 1757-1765.

TSIEN, J. Z., CHEN, D. F., GERBER, D., TOM, C., MERCER, E. H., ANDERSON, D. J., MAYFORD, M., KANDEL, E. R. & TONEGAWA, S. 1996. Subregion- and cell type-restricted gene knockout in mouse brain. *Cell,* 87**,** 1317-26.

VAN HEES, H. W., DEKHUIJZEN, P. N. & HEUNKS, L. M. 2009. Levosimendan enhances force generation of diaphragm muscle from patients with chronic obstructive pulmonary disease. *Am J Respir Crit Care Med,* 179**,** 41-7.

VEASEY, S. C., ZHAN, G., FENIK, P. & PRATICO, D. 2004. Long-term intermittent hypoxia: reduced excitatory hypoglossal nerve output. *Am J Respir Crit Care Med,* 170**,** 665-72.

WANG, N., KHAN, S. A., PRABHAKAR, N. R. & NANDURI, J. 2013a. Impairment of pancreatic beta-cell function by chronic intermittent hypoxia. *Exp Physiol,* 98**,** 1376-85.

WANG, N., KHAN, S. A., PRABHAKAR, N. R. & NANDURI, J. 2013b. Impairment of pancreatic β-cell function by chronic intermittent hypoxia. *Exp Physiol,* 98**,** 1376-85.

WANG, W., ZHANG, K., LI, X., MA, Z., ZHANG, Y., YUAN, M., SUO, Y., LIANG, X., TSE, G., GOUDIS, C. A., LIU, T. & LI, G. 2018. Doxycycline attenuates chronic intermittent hypoxia-induced atrial fibrosis in rats. *Cardiovasc Ther,* 36**,** e12321.

WANG, W. J., LU, G., DING, N., HUANG, H. P., DING, W. X. & ZHANG, X. L. 2013c. Adiponectin alleviates contractile dysfunction of genioglossus in rats exposed to chronic intermittent hypoxia. *Chin Med J (Engl),* 126**,** 3259-63.

WOLKOVE, N., BALTZAN, M., KAMEL, H., DABRUSIN, R. & PALAYEW, M. 2008. Long-term compliance with continuous positive airway pressure in patients with obstructive sleep apnea. *Canadian Respiratory Journal : Journal of the Canadian Thoracic Society,* 15**,** 365-369.

WU, D. C., RÉ, D. B., NAGAI, M., ISCHIROPOULOS, H. & PRZEDBORSKI, S. 2006. The inflammatory NADPH oxidase enzyme modulates motor neuron degeneration in amyotrophic lateral sclerosis mice. *Proc Natl Acad Sci U S A,* 103**,** 12132-7.

WU, D. C., TEISMANN, P., TIEU, K., VILA, M., JACKSON-LEWIS, V., ISCHIROPOULOS, H. & PRZEDBORSKI, S. 2003. NADPH oxidase mediates oxidative stress in the 1-methyl-4-phenyl-1,2,3,6-tetrahydropyridine model of Parkinson's disease. *Proc Natl Acad Sci U S A,* 100**,** 6145-50.

WU, K., SU, X., LI, G. & ZHANG, N. 2016. Antioxidant Carbocysteine Treatment in Obstructive Sleep Apnea Syndrome: A Randomized Clinical Trial. *PLoS One,* 11**,** e0148519.

YOU, Y. H., OKADA, S., LY, S., JANDELEIT-DAHM, K., BARIT, D., NAMIKOSHI, T. & SHARMA, K. 2013. Role of Nox2 in diabetic kidney disease. *Am J Physiol Renal Physiol,* 304**,** F840-8.

ZHANG, Y., SU, X., ZOU, F., XU, T., PAN, P. & HU, C. 2019. Toll-like receptor-4 deficiency alleviates chronic intermittent hypoxia-induced renal injury, inflammation, and fibrosis. *Sleep Breath,* 23**,** 503-513.

ZHOU, J. & LIU, Y. 2013. Effects of genistein and estrogen on the genioglossus in rats exposed to chronic intermittent hypoxia may be HIF-1α dependent. *Oral Dis,* 19**,** 702-11.